Dissertation zur Erlangung des Doktorgrades

der Fakultät für Chemie und Pharmazie

der Ludwig-Maximilians-Universität München

# Bioorthogonal reactions of heterodienes: synthesis, reactivity and fluorogenic bioimaging applications

Sebastian Josef Siegl

aus

Furth im Wald, Deutschland

2020

## Erklärung

Diese Dissertation wurde im Sinne von § 7 der Promotionsordnung vom 28. November 2011 von Herrn Prof. Dr. Thomas Carell betreut.

## Eidesstattliche Versicherung

Diese Dissertation wurde eigenständig und ohne unerlaubte Hilfe erarbeitet.

München, 08.04.2021

_____

(Sebastian Siegl)


| | |
|---|---|
| Dissertation eingereicht am: | 28.05.2020 |
| 1. Gutachter: | Prof. Dr. Thomas Carell |
| 2. Gutachter: | Prof. Dr. Konstantin Karaghiosoff |
| Mündliche Prüfung am: | 24.06.2020 |

# List of Publications

Parts of this PhD thesis were already published or presented on scientific conferences.

## Publications:

- S.J. Siegl, R. Dzijak, A. Vázquez, R. Pohl, M. Vrabel, *Chem. Sci.* **2017**, 8, 3593-3598.
  "The discovery of pyridinium 1,2,4-triazines with enhanced performance in bioconjugation reactions", https://doi.org/10.1039/C6SC05442K.

- S.J. Siegl*, A. Vázquez*, R. Dzijak, M. Dračínský, J. Galeta, R. Rampmaier, B. Klepetářová, M. Vrabel, *Chem. Eur. J.* **2018**, 24, 2426-2432.
  "Design and Synthesis of Aza-Bicyclononene Dienophiles for Rapid Fluorogenic Ligations", https://doi.org/10.1002/chem.201705188.
  *: These authors contributed equally to this work.

- S.J. Siegl, M. Vrabel, *Eur. J. Org. Chem.* **2018**, 5081–5085.
  "Probing the Scope of the Amidine–1,2,3-triazine Cycloaddition as a Prospective Click Ligation Method", https://doi.org/10.1002/ejoc.201800530.

- S.J. Siegl, J. Galeta, R. Dzijak, A. Vázquez, M. Del Río-Villanueva, M. Dračínský, M. Vrabel, *ChemBioChem* **2019**, 20, 886– 890.
  "An Extended Approach for the Development of Fluorogenic *trans*-Cyclooctene-Tetrazine Cycloadditions",
  https://doi.org/10.1002/cbic.201800711.

- S.J. Siegl, J. Galeta, R. Dzijak, M. Dračínský, M. Vrabel, *ChemPlusChem* **2019**, 84, 493-497.
  "Bioorthogonal Fluorescence Turn-On Labeling Based on Bicyclononyne–Tetrazine Cycloaddition Reactions that Form Pyridazine Products",
  https://doi.org/10.1002/cplu.201900176.

## Conferences:

- **Poster presentation:** S.J. Siegl, M. Vrabel, *EMBO Conference Chemical Biology* **2016**, Heidelberg, Germany.
  "Systematic study on the reactivity of 1,2,4-triazines with trans-cyclooctenes"

- **Poster presentation:** S.J. Siegl, R. Dzijak, A. Vázquez, R. Pohl, M. Vrabel, *6th Conference of the ICBS* **2017**, Shanghai, China.
  "The discovery of pyridinium 1,2,4-triazines with enhanced performance in bioconjugation reactions"

## Further publications:

- A. Vázquez, R. Dzijak, M. Dračínský, R. Rampmaier, S.J. Siegl, M. Vrabel, *Angew. Chem. Int. Ed.* **2017**, 56, 1334 –1337.
  "Mechanism-Based Fluorogenic *trans*-Cyclooctene–Tetrazine Cycloaddition"

# Danksagung

An dieser Stelle möchte ich mich bei zahlreichen Personen für ihre Hilfe und Unterstützung während meiner Promotion bedanken.

Zunächst geht ein großer Dank an *Prof. Dr. Thomas Carell* für sein Vertrauen und seine Bereitschaft die Betreuung meiner Promotion zu übernehmen. Dadurch war es mir möglich eine äußerst interessante und lehrreiche Stelle für meine Promotion anzunehmen und auf eine etwas ungewöhnliche Weise durchzuführen, vielen Dank dafür.
Ein genauso großer Dank geht an *Dr. Milan Vrábel* für die freundliche Aufnahme in seine Arbeitsgruppe und die spannenden Forschungsprojekte, an denen ich arbeiten durfte. Vielen Dank sowohl für die hervorragende fachliche Betreuung und Arbeitsbedingungen in den letzten Jahren als auch für die große Unterstützung außerhalb des Labors.
Des Weiteren bedanke ich mich bei *Prof. Dr. Konstantin Karaghiosoff* für die Übernahme des Zweitgutachtens und bei allen weiteren Mitgliedern der Prüfungskommission: *Dr. Sabine Schneider, Dr. Stefanie Kellner, Prof. Dr. Franz Bracher* und *Prof. Dr. Oliver Trapp*.
*Dr. Markus Müller* danke ich für seine große Hilfsbereitschaft bei allen bürokratischen Fragen bezüglich des Verfassens und der Abgabe meiner Arbeit.

Als Nächstes möchte ich mich bei allen derzeitigen und ehemaligen Laborkollegen und bei den Mitarbeitern der Arbeitsgruppe von *Miloslav Polášek* für die angenehme und freundschaftliche Arbeitsatmosphäre bedanken: *Arcadio Vázquez Alvarez, Robert Rampmaier, Tereza Schröpferová, Rastislav Dzijak, Anna Kovalová, Anna Beránková, Juraj Galeta, Miloslav Polášek, David Tomáš* und *Jan Kretschmer*. Ein großer Dank geht dabei an *Arcadio Vázquez Alvarez* für die freundschaftliche Zusammenarbeit sowohl im als auch außerhalb des Labors, von dem ich noch einiges lernen konnte. Bei *Tereza Schröpferová* möchte ich mich für ihre Hilfe bei allen bürokratischen Angelegenheiten bedanken. Bei *Rastislav Dzijak* bedanke ich mich für die schnelle und gewissenhafte Durchführung sämtlicher Zellexperimente. An *Robert Rampmaier* geht ein Dank für die oftmals eher weniger fachlichen Gespräche, so dass auch in stressigeren Zeiten meine Motivation am Arbeiten nicht verloren ging.
Für das schnelle und gewissenhafte Korrekturlesen meiner Arbeit bedanke ich mich herzlichst bei *Dr. Milan Vrábel, Kseniia Afitska, Dr. Dmytro Sysoiev, Dr. Markus Müller, Robert Rampmaier* und *Tobias Winklmüller*.

Ich möchte mich zudem bei allen weiteren Bekannten und Freunden, die ich in den letzten Jahren am IOCB und in Prag gewinnen konnte, für die großartige Zeit bedanken. Ein großer Dank geht im Besonderen an unsere Brettspiel-Gruppe für die zahlreichen schönen Abende und Ausflüge.
Auch alle Freunde außerhalb des Studiums möchte ich hier erwähnen. Vielen Dank für eure Geduld und eure Bereitschaft kurzfristig was zu unternehmen, wenn ich mal wieder für längere Zeit nichts von mir hören hab lassen!

Zuletzt geht mein größter Dank an meine Familie. Durch die bedingungslose Unterstützung, all die Ratschläge und die Geduld insbesondere meiner Eltern und meiner Schwester ist all dies erst möglich geworden. Vielen Dank, dass ihr immer an mich geglaubt habt! Meiner Freundin *Kseniia* danke ich für die großartige Zeit zusammen und den stetigen Rückhalt, falls mal etwas nicht nach Plan verlaufen ist. Du bist das Beste was mir während meiner Zeit hier in Prag passiert ist. Ich bin euch allen unendlich dankbar für all eure Unterstützung!

# Table of Contents

# Abstract

Over the past decades a variety of different strategies for the study of biomolecules and their biological functions have been developed. One of the latest and increasingly popular option for this purpose are so-called bioorthogonal reactions, a set of highly selective chemical reactions that should neither interfere with other biological components nor be affected by biological processes. Besides that, potential bioorthogonal reactions have to fulfil several requirements such as high biocompatibility, rather small size of reagents and high reaction rate. Over the past years, numerous research groups have already reported about various functional groups and reactions as suitable candidates for the use in bioorthogonal labeling.
However, there is still space for expanding this set of tools by developing new bioorthogonal reactions or improving already known ones. Our group recently developed a novel type of fluorogenic inverse-electron-demand Diels-Alder (iEDDA) cycloaddition between a *trans*-cyclooctene (TCO) dienophile and various 1,2,4,5-tetrazines. This type of reaction directly leads to the formation of fluorescent products. Therefore, the presence of an additional pre-fluorophore or quenching moiety in the structure of one of the reagents is not required.

In the present thesis, this newly developed fluorogenic bioorthogonal reaction was further improved. In the initial work, axTCO-ol was the only TCO dienophile that resulted in the formation of fluorescent 1,4-dihydropyridazine products upon reaction with tetrazines. Therefore, the main goal of the first part of the thesis was to extend the range of dienophiles showing this fluorogenic behavior.
First, a novel type of TCOs that contain an aziridine moiety fused to the TCO core (aza-TCO) was designed and synthesized for this purpose. These TCOs form fluorescent 1,4-dihydropyridazines upon cycloaddition with various 1,2,4,5-tetrazines and, unlike the axTCO-ol, maintain their fluorescent nature even when modified with different functional groups. Furthermore, it was demonstrated that the cycloaddition between aza-TCOs and 1,2,4,5-tetrazines belongs to the fastest bioorthogonal reactions known to date and at the same time features high biocompatibility.
Additionally, the concept of an iEDDA reaction between 1,2,4,5-tetrazines and TCOs, which directly results in the formation of a fluorophore, was next extended to other known TCO derivatives by developing an alternative and more general strategy. For this purpose, specific tetrazines bearing an electron-donating dimethylamino or azetidine moiety were synthesized. These tetrazines form fluorescent 4,5-dihydropyridazine intermediates in reactions with

various TCOs, even with those, which did not show any fluorogenic properties in reactions with other tetrazines in the previous studies. Further experiments revealed that such 1,2,4,5-tetrazines containing specific electron-donating substituents also form fluorescent products in reactions with bicyclo[6.1.0]nonyne (BCN) derivatives. In addition, one of these particular tetrazines was successfully employed for simultaneous two-color labeling of a BCN derivative and a TCO derivative.

Furthermore, by labeling of model biomolecules and labeling of different compartments in live cells, it was demonstrated that the fluorogenic nature of all these novel tetrazine ligation reactions is well preserved under biological conditions.

With these results the fluorogenic tetrazine ligation recently discovered in our group was further improved so that it is now more suitable for fluorogenic bioorthogonal ligation applications. In addition, the development of aza-TCOs added a new and potent type of strained TCOs to the set of dienophiles commonly used in bioorthogonal iEDDA reactions with 1,2,4,5-tetrazines.

Recently, 1,2,4- as well as 1,2,3-triazines were described as potential alternatives to 1,2,4,5-tetrazines for the use in bioorthogonal reactions. Based on that, the second part of this thesis was focused on the evaluation of these alternative heterodienes for the cycloaddition with various strained dienophiles.

Herein, kinetic studies were performed to gain a deeper insight into the reactivity of 1,2,4-triazines with various TCOs. These studies showed that the reaction rates can vary by orders of magnitude strongly depending on the structure of both starting materials. During these kinetic studies a new class of cationic pyridinium 1,2,4-triazines was discovered. These cationic triazines feature several interesting properties for the use in bioorthogonal labeling applications, including increased reactivity, enhanced water solubility and remarkable biocompatibility. However, their most fascinating feature is the unprecedented formation of fluorescent dihydropyridine products through reaction with various TCOs, which was successfully applied to labeling of different compartments in live cells. Additionally, an efficient method for the late-stage functionalization of the pyridinium triazines was developed. This allows for the easy synthesis of various useful heterobifunctional pyridinium triazines.

The study of 1,2,3-triazines first led to the development of an optimized protocol for their iEDDA cycloadditions with amidines. Amidines are prone to degradation and therefore are usually stored as salts, which do not react with triazines efficiently enough. Thus, it is

necessary to prepare the free amidine base directly before the cycloaddition reaction. Unlike standard procedures, the newly designed protocol allows for the *in situ* formation of the free amidine base under mild reaction conditions. Despite limitations to non-aqueous systems due to an observed sensitivity of 1,2,3-triazines toward water, the 1,2,3-triazine-amidine cycloaddition still shows great potential for various applications because of its remarkable chemo- and regioselectivity. It was demonstrated, for example, that this reaction is orthogonal to some of the most popular bioorthogonal reactions, which makes it especially useful for simultaneous labeling of multiple tags on more complex systems.

With this study, it was shown that the novel pyridinium 1,2,4-triazines are suitable and versatile candidates for the use in bioorthogonal reactions and that their fluorogenic cycloadditions with various TCOs possess great potential for bioimaging. The reported data about 1,2,3-triazines and their cycloadditions with amidines should serve as a valuable guideline for future studies of this reaction and for further evaluation of its use in various labeling applications.

# Zusammenfassung

In den letzten Jahrzehnten wurde eine Vielzahl unterschiedlicher Strategien für die Untersuchung von Biomolekülen und deren biologischen Funktionen entwickelt. Eine relativ neue und zunehmend verbreitete Option dafür sind sogenannte bioorthogonale Reaktionen. Dabei handelt es sich um äußerst selektive chemische Reaktionen, die weder andere biologische Bestandteile beeinflussen noch von biologischen Prozessen beeinträchtigt werden dürfen. Abgesehen davon müssen potenzielle bioorthogonale Reaktionen mehrere Bedingungen wie eine hohe Biokompatibilität, eine eher geringe Größe der Reaktionspartner und eine hohe Reaktionsgeschwindigkeit erfüllen. In den letzten Jahren berichteten bereits zahlreiche Arbeitsgruppen über verschiedene funktionelle Gruppen und Reaktionen, die sich für die bioorthogonale Markierung eignen.
Allerdings besteht weiterhin Bedarf neue bioorthogonale Reaktionen zu entwickeln oder bereits existierende zu verbessern, um eine größere Auswahl an Methoden zur Verfügung zu haben. In unserer Gruppe wurde vor Kurzem eine neuartige fluorogene Variante der Diels-Alder-Reaktion mit inversem Elektronenbedarf (iEDDA) zwischen einem *trans*-Cycloocten (TCO) und verschiedenen 1,2,4,5-Tetrazinen entwickelt. Durch diese Art von Tetrazin-Ligation werden direkt fluoreszierende Produkte gebildet, wodurch weder ein zusätzlicher Fluorophor noch quenchende Gruppen in der Struktur eines der Reaktionspartner benötigt werden.

In der vorliegenden Dissertation wurde diese neu entwickelte fluorogene bioorthogonale Reaktion weiter verbessert. In der ursprünglichen Arbeit führte axTCO-ol als einziges TCO-Dienophil in Reaktionen mit Tetrazinen zur Bildung von fluoreszierenden 1,4-Dihydropyridazinen. Daher war das Hauptziel des ersten Teils dieser Doktorarbeit die Auswahl an Dienophilen, die dieses fluorogene Verhalten aufweisen, zu vergrößern.
Zunächst wurde eine neue Art von TCOs entworfen und synthetisiert, bei denen eine Aziridin-Gruppe an der TCO Struktur (aza-TCO) angebracht wurde. Solche TCOs bilden in Cycloadditionen mit 1,2,4,5-Tetrazinen fluoreszierende 1,4-Dihydropyridazine und behalten diesen fluorogenen Charakter anders als axTCO-ol auch nach Anbringen verschiedener funktioneller Gruppen bei. Zudem wurde gezeigt, dass die Cycloaddition zwischen aza-TCOs und 1,2,4,5-Tetrazinen zu den bisher schnellsten bekannten bioorthogonalen Reaktionen gehört und gleichzeitig eine hohe Biokompatibilität aufweist.

Als Nächstes wurde eine alternative und allgemeingültigere Strategie entwickelt, um das Konzept einer Fluorophor-erzeugenden iEDDA-Reaktion zwischen 1,2,4,5-Tetrazinen und TCOs auf weitere bekannte TCO Derivate auszuweiten. Dies wurde mit Hilfe spezieller Tetrazine mit elektronenschiebenden Dimethylamino- oder Azetidin-Gruppen erreicht, welche in Reaktionen mit verschiedenen TCOs fluoreszierende 4,5-Dihydropyridazine bilden. Solche fluoreszierenden Zwischenprodukte wurden dabei sogar mit TCOs erhalten, welche in Reaktionen mit anderen Tetrazinen in den vorherigen Studien noch keine fluorogenen Eigenschaften zeigten. Weiterführende Experimente deckten zudem auf, dass 1,2,4,5-Tetrazine mit solch elektronenschiebenden Substituenten auch in Reaktionen mit Bicyclo[6.1.0]nonin (BCN) Derivaten fluoreszierende Produkte formen. Zusätzlich wurde mit Hilfe eines dieser Tetrazine gleichzeitig ein BCN- und ein TCO-Derivat erfolgreich mit zwei unterschiedlichen Farben markiert.
Weiterhin wurde durch die Markierung von Modell-Biomolekülen und von verschiedenen Kompartimenten in lebenden Zellen gezeigt, dass der fluorogene Charakter dieser neuartigen Tetrazin-Ligationen unter biologischen Bedingungen bestehen bleibt.
Durch diese Ergebnisse wurde die kürzlich in unserer Gruppe entdeckte fluorogene Tetrazin-Ligation weiter verbessert und ist nun besser für den Einsatz in bioorthogonalen Markierungen geeignet. Außerdem wurde durch Entwicklung des aza-TCOs ein neues und vielversprechendes TCO-Derivat zur Auswahl an gespannten Dienophilen für bioorthogonale iEDDA-Reaktionen mit 1,2,4,5-Tetrazinen hinzugefügt.

Kürzlich wurden sowohl 1,2,4- als auch 1,2,3-Triazine als potenzielle Alternativen zu 1,2,4,5-Tetrazinen für den Einsatz in bioorthogonalen Reaktionen entdeckt. Der Schwerpunkt des zweiten Teils dieser Arbeit lag daher in der Untersuchung dieser alternativen Heterodiene und deren Verwendung in Cycloadditionen mit gespannten Dienophilen.
Zunächst wurden kinetische Studien durchgeführt, um einen besseren Einblick in die Reaktivität von 1,2,4-Triazinen gegenüber TCOs zu erhalten. Diese zeigten, dass sich die Reaktionsgeschwindigkeiten abhängig von den Strukturen beider Startmaterialien um mehrere Größenordnungen unterscheiden können. Im Laufe dieser kinetischen Studien wurden zudem neuartige kationische Pyridinium-1,2,4-Triazine entwickelt. Diese positiv-geladenen Triazine zeichnen sich durch mehrere für die Verwendung in bioorthogonalen Markierungen interessante Eigenschaften aus. Neben erhöhter Reaktivität, verbesserter Wasserlöslichkeit und bemerkenswerter Biokompatibilität, sticht vor allem die beispiellose Bildung von fluoreszierenden Dihydropyridinen in Reaktionen mit verschiedenen TCOs heraus. Diese

fluorogene Reaktion wurde bereits erfolgreich für die Markierung verschiedener Kompartimente in lebenden Zellen verwendet. Zusätzlich wurde eine effiziente Methode für die nachträgliche Funktionalisierung der Pyridinium-Triazine entwickelt, so dass verschiedene nützliche hetero-bifunktionelle Derivate auf einfache Weise synthetisierbar sind.
Bei der Untersuchung der 1,2,3-Triazine wurde zunächst ein optimiertes Protokoll für deren iEDDA-Reaktion mit Amidinen entwickelt. Aus Stabilitätsgründen werden Amidine für gewöhnlich als Salze gelagert, welche allerdings wenig effizient mit Triazinen reagieren. Daher muss die freie Amidin-Base unmittelbar vor der Cycloaddition hergestellt werden. Das neu entworfene Protokoll ermöglicht dabei, anders als bisherige Standardverfahren, die *in situ* Bildung der freien Amidin-Base unter milden Reaktionsbedingungen. Leider wurde eine Empfindlichkeit der 1,2,3-Triazine gegenüber Wasser beobachtet, was zur Beschränkung auf wasserfreie Systeme führt. Dennoch besitzt die 1,2,3-Triazin-Amidin-Cycloaddition großes Potential für verschiedene Anwendungen aufgrund ihrer bemerkenswerten Chemo- und Regioselektivität. So konnte beispielsweise gezeigt werden, dass diese Reaktion orthogonal zu einigen der weitverbreitetsten bioorthogonalen Reaktionen ist. Dies ist besonders für die gleichzeitige Markierung mehrerer Tags in komplexeren Systemen von Vorteil.
In dieser Arbeit wurde gezeigt, dass die neu entwickelten Pyridinium-1,2,4-Triazine vielseitig in bioorthogonalen Reaktionen verwendbar sind und deren fluorogene Cycloadditionen mit TCOs großes Potential für die Markierung von Biomolekülen besitzen. Die gesammelten Daten über 1,2,3-Triazine und deren Cycloadditionen mit Amidinen sollten zudem als nützlicher Leitfaden für weitere Untersuchungen dieser Reaktion und ihres Nutzens für verschiedene Markierungsanwendungen dienen.

# 1. Introduction

## 1.1 Bioconjugation reactions

In 2003 *Bertozzi* and co-workers[1] introduced the term “bioorthogonal”, which refers to a set of chemical transformations compatible with biological systems enabling the labeling and study of biomolecules in their native environment. These chemical modifications allow for the attachment of various functional groups to biomolecules. The attached moieties can then be used for different applications. The attachment of small fluorescent dyes, for instance, is a common method for the visualization of the studied biomolecules or biological processes inside cells. As there was always great interest in the study of biological processes and of the distribution and biological functions of biomolecules, it is not surprising that this new discovery attracted a lot of attention. Over the past decades, many research groups worked in this new scientific field, so that nowadays numerous types of bioorthogonal reactions exist, which have become an essential tool in biological research.[2] However, already before the term “bioorthogonal” was introduced, several reactions and methods were established as bioconjugation reactions. These methods were mainly employed for the labeling of proteins through targeting of naturally occurring functional groups, the termini of proteins or unique amino acid sequences.

### 1.1.1 Traditional protein modification methods

Proteins have been the target of chemical modifications for a long time, originally in order to define their structure and study macromolecular interactions.[3] Classic bioconjugation of proteins is usually done through selective chemical modifications of the various functionalities in the side chains of the canonical amino acids.[4] Among these the thiol group of cysteine is one of the most popular targets for labeling due to its relatively low natural occurrence[5] and highly nucleophilic character compared to other functional groups present in amino acids.[6] By careful control of pH and reaction time, relatively high chemoselectivity can be achieved even in the presence of other nucleophilic residues such as lysine or histidine.[6a, 7] Nowadays, numerous cysteine-specific reagents exist.[6a, 8] Common techniques for cysteine modification encompass alkylation with various electrophiles and formation of disulfides.

$\alpha$-Halocarbonyls, such as iodoacetamides, were among the first electrophiles used for the alkylation of cysteines (Figure 1A).[9] Although undesired alkylation of other nucleophiles like the lysine side chain is known,[10] it can be overcome by the use of chloroacetamide or similar derivatives, which show higher selectivity toward cysteine and similar alkylation efficiency.[11] Alkylation of cysteines by α-halocarbonyls was already successfully employed for numerous biological applications.[12]

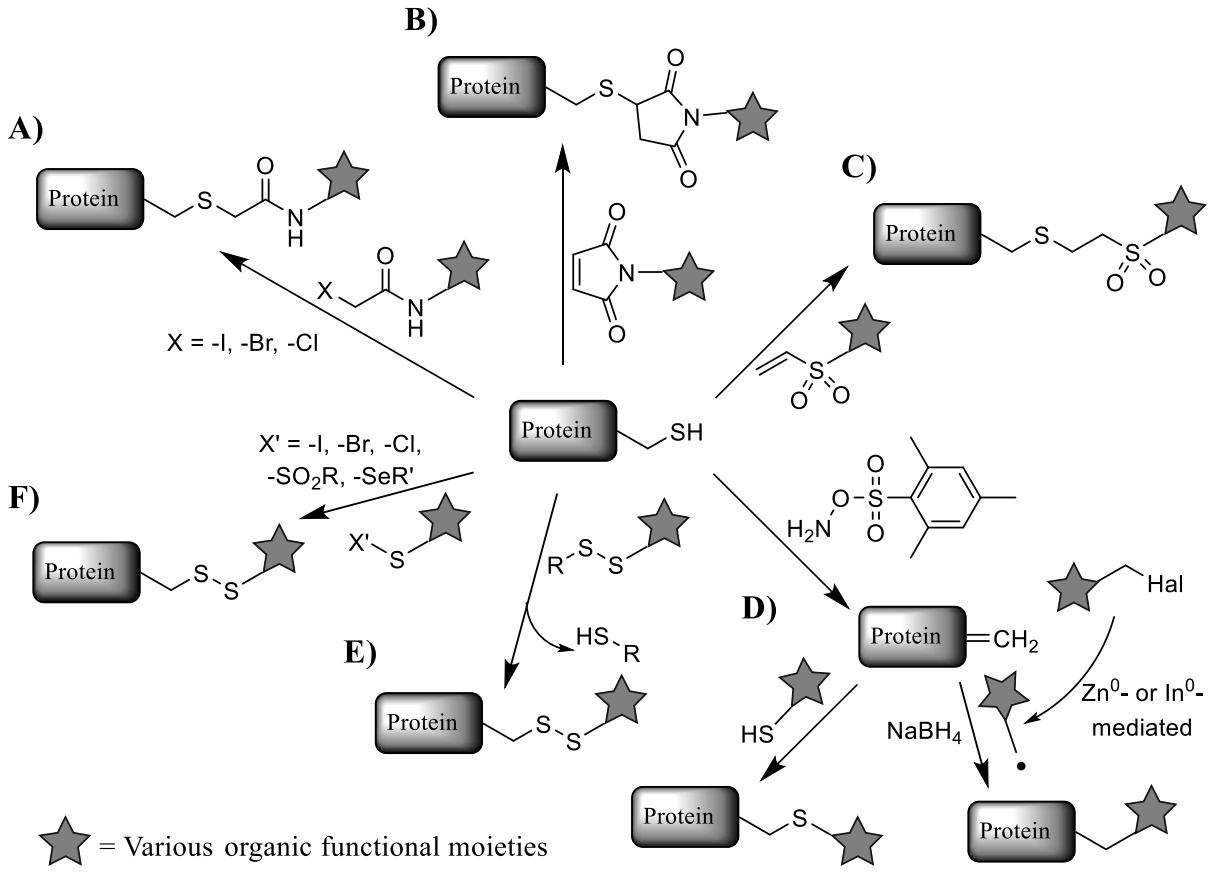


**Figure 1:** Examples of traditional bioconjugation reactions used for the labeling of natural cysteine residues. The thiol group of cysteine can be modified by alkylation with $\alpha$-halocarbonyls (A), Michael addition with maleimides (B) and vinyl sulfones (C), a two-step method which involves formation of a dehydroalanine and subsequent Michael addition with thiol reagents or radical chemistry with halide precursors (D), and disulfide formation through disulfide exchange (E) or use of activated thiol reagents (F).

Another versatile tool for selective alkylation of thiols is the addition to Michael acceptors (Figure 1B and 1C). For the bioconjugation of cysteines mainly maleimides[7, 13] and vinyl sulfones[14] are used. Although the alkylation with maleimides shows high reactivity and forms a stable succinimide thioether bond, it was reported that the Michael addition is reversible under physiological conditions. In the presence of other thiols this may result in thiol-exchange and reduced efficiency of the bioconjugation.[15] However, this problem can be overcome by hydrolysis and opening of the succinimide ring, which increases the stability of

the product toward retro reaction.[15b, 15c] Using vinyl sulfones instead of maleimides as Michael acceptors results in decreased reversibility of the Michael addition, however, due to their less electrophilic character vinyl sulfones are less reactive than maleimides.[16] Furthermore, *Davis* and co-workers developed a two-step method including the transformation of cysteine to dehydroalanine with *O*-mesitylenesulfonylhydroxylamine and subsequent Michael addition with thiol reagents (Figure 1D).[17] Recently, the dehydroalanine moiety was also used for the introduction of various natural and unnatural functional groups through a radical-mediated reaction with halide precursors (Figure 1D).[18]

The easiest way for disulfide formation is air oxidation by simply mixing the cysteine residue with a thiol in the presence of air. As this method suffers from low reaction rates and low selectivity due to the formation of dimers,[6a] disulfide exchange reactions[19] or the use of activated reagents like sulfenyl halides,[20] thiosulfonates[21] or selenenyl sulfides[22] are usually favored (Figure 1E and 1F).

Another widely used alternative is the modification of the ε-amino group of lysine. Despite the often rather low chemoselectivity of such modifications in the presence of stronger nucleophiles like cysteine and the relatively high occurrence of lysine in proteins, the variety of possible reactions for primary amines still makes lysine a common target for bioconjugation of proteins.[4b] Common reagents for bioconjugation of lysine are isocyanates, isothiocyanates, activated esters, aldehydes, sulfonyl halides and imidoesters.

In early studies, isocyanates were already successfully used for the conjugation to different proteins by forming ureas with the amino group of lysine (Figure 2A).[23] Nowadays, due to their low stability and the difficulties in preparation and storage, isocyanates are mostly replaced by isothiocyanates yielding thioureas (Figure 2A).[23b, 24] However, *Podhradský et al.* showed that isothiocyanates also reversibly react with various thiol-containing residues yielding dithiocarbamates.[25] Fortunately, the formation of thioureas with amino groups is irreversible, shifting the equilibrium toward the conjugation product with amines. Nevertheless, these side reactions with thiols can reduce the efficiency and reaction rates of amine conjugations.

Although conjugation of lysine residues with isothiocyanates is easier to control, the use of *N*-hydroxysuccinimide (NHS) activated esters (Figure 2B) is often favored due to higher reaction rates and stability of the formed amide-linked conjugates.[26] Unfortunately, several studies reported about a competing reactivity of NHS-activated esters with the hydroxyl-containing side chains of several other amino acids like serine, tyrosine and threonine.[27]

However, these potential side reactions occur with considerably lower reaction rates and strongly depend on the reaction conditions and thus usually do not interfere with the amine conjugation. As the activation with NHS usually results in rather hydrophobic activated esters with reduced water solubility, the more water-soluble sulfo-NHS-activated esters are often used as an alternative in bioconjugations due to their more hydrophilic character.[28]

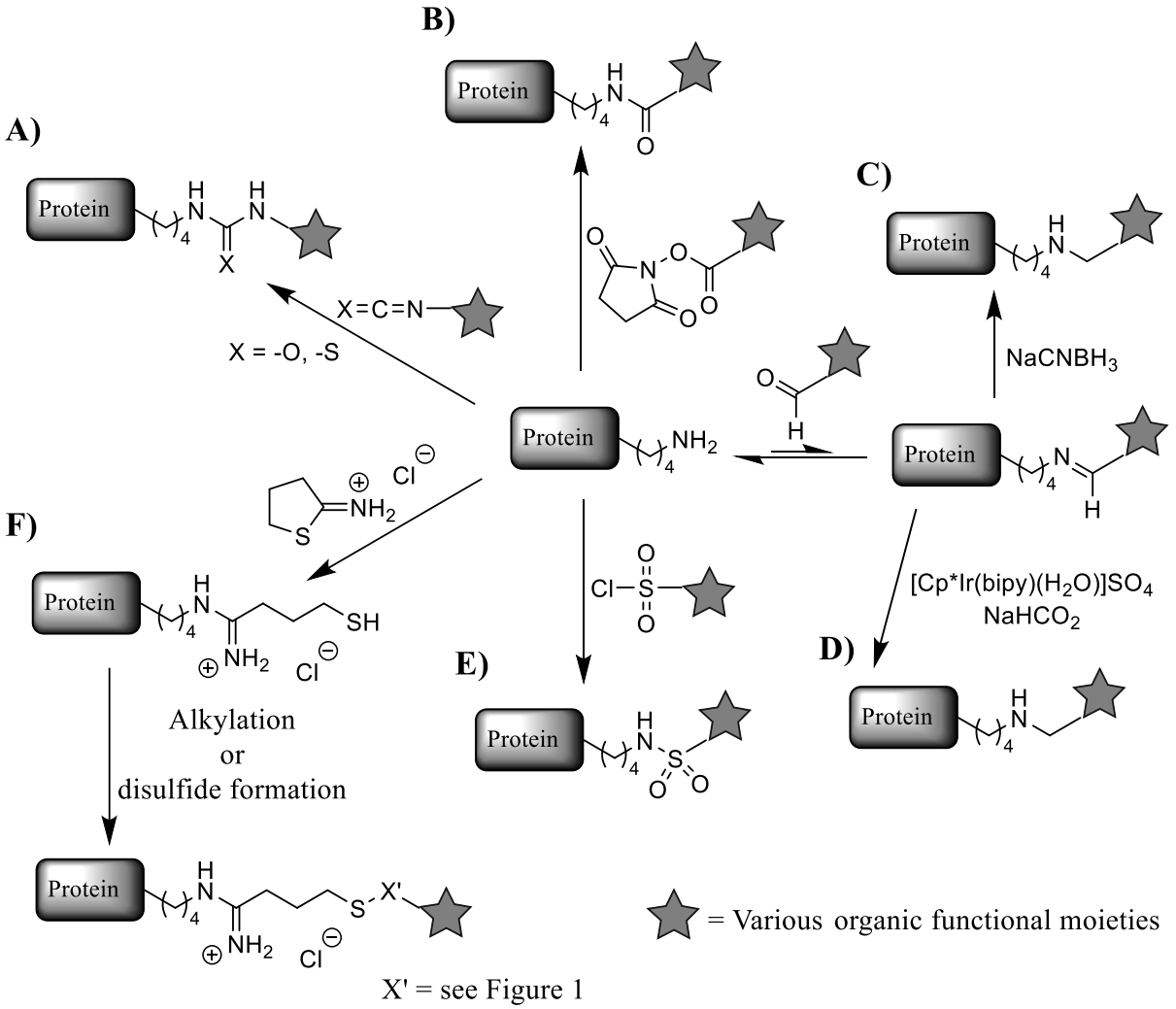


**Figure 2:** Example of traditional bioconjugation reactions used for the labeling of natural lysine residues. The ε-amino group of lysine can be modified by using various chemical reagents such as isocyanates or isothiocyanates (A), NHS-activated esters (B) and sulfonyl halides (E), $NaCNBH_3$-based (C) or iridium-catalyzed (D) reductive alkylation and reaction with Traut's reagent (F) which involves formation of a reactive thiol group and subsequent thiol-selective labeling (see Figure 1).

A less frequently used method for amine conjugation is the reductive amination. Amines can reversibly react with aldehyde groups forming imines. In the presence of sodium cyanoborohydride, a mild reducing agent, the imine can then be irreversibly reduced to the corresponding secondary amine (Figure 2C).[29] *MaFarland* and *Francis* reported an alternative method using an iridium-catalyzed reductive alkylation, which is less pH-dependent and water-sensitive (Figure 2D).[30]

By fluorescent labelling of proteins with dansyl chloride (DNSC) *Weber* introduced sulfonyl halides as another option for protein modification (Figure 2E).[31] Sulfonyl halides show high reactivity, but are quite unstable under aqueous conditions and prone to hydrolysis during conjugation reactions when compared to, for example, NHS-activated esters.[32] Nevertheless, sulfonyl chlorides were already successfully used for the labeling and study of peptides and different proteins.[33]

*Hunter* and *Ludwig* investigated the modification of protein amino groups by imidoesters.[34] Later, *Traut et al.* described 2-iminothiolane, the so-called *Traut's* reagent, as a cleavable cross-linking reagent for proteins. It enables the introduction of a reactive thiol group to α- or ε-amino groups of proteins and their subsequent modification by thiol group-selective methods like alkylation or disulfide bond formation (Figure 2F).[35]

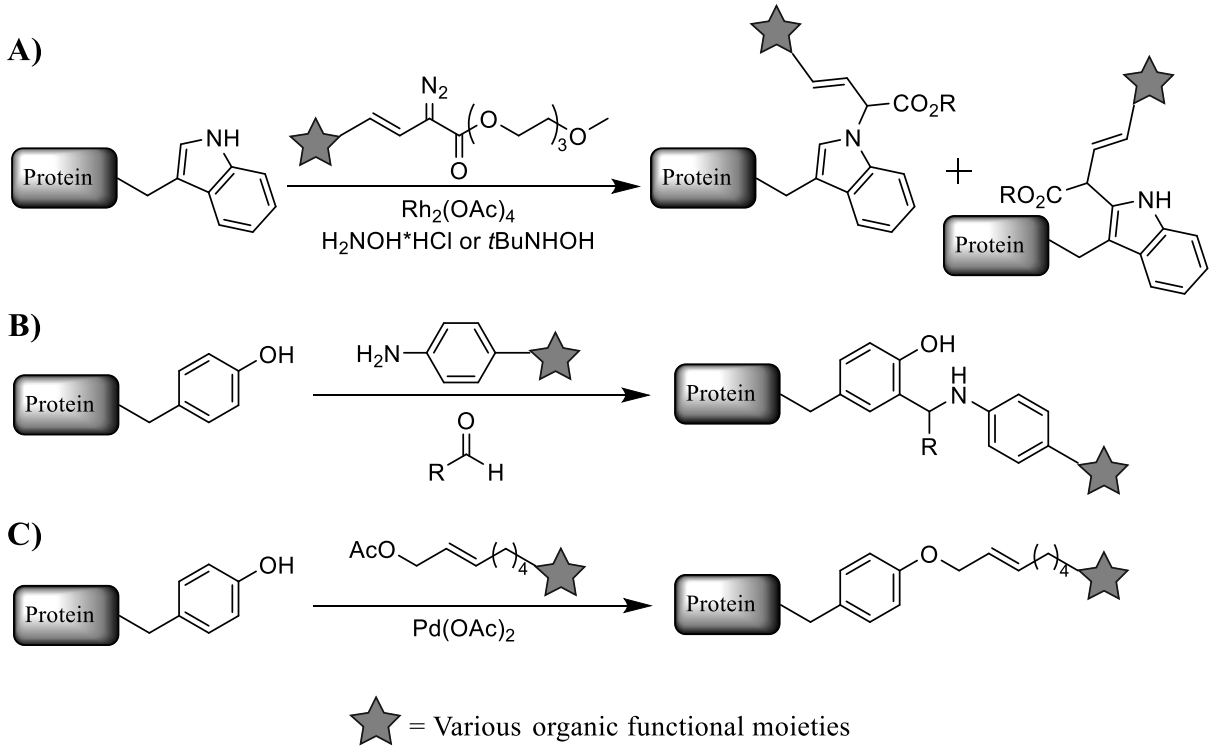


**Figure 3:** Bioconjugation reactions used for the labeling of natural tryptophan or tyrosine residues. The indole group of tryptophan can be modified by an *in situ* generated rhodium carbenoid (A) and the tyrosyl group by a three-component Mannich reaction (B) or palladium-catalyzed π-allylation (C).

Apart from cysteine and lysine, other proteogenic amino acids are much less used, and developed methods for their modification quite often suffer from rather low selectivity or reactivity.[4a] Successful applications include, for example, the selective modification of tryptophan by a diazo compound, which is catalyzed by a rhodium carbenoid generated *in situ* from rhodium acetate (Figure 3A).[36] Furthermore, *Francis* and co-workers developed

methods for tyrosine modification through a three-component Mannich reaction using an aldehyde and an aniline (Figure 3B)[37] as well as through alkylation with π-allyl palladium complexes (Figure 3C).[38]

### 1.1.2 Protein labeling with fluorescent proteins

While the above-mentioned methods for the bioconjugation of proteins are indeed quite useful for *in vitro* applications, their use in more complex biological systems is quite challenging. The naturally occurring amino acids, which are used as targets for the conjugation, are also present in virtually every other non-target protein within the system. Thus, labeling of only a specific protein in the presence of other non-target proteins and reactive biomolecules is quite difficult, if not impossible. An elegant alternative strategy enabling site-specific fluorescent tagging of proteins became available through the introduction of naturally occurring fluorescent proteins (FP) and their mutated versions.

Already in 1962 *Shimomura et al.* discovered the green fluorescent protein (GFP) as a companion molecule to aequorin, a chemiluminescent protein from the jelly fish *Aequorea Victoria*.[39] Decades later after successful cloning of the gene,[40] it was demonstrated that expression of this protein in other organisms results in a fluorescent product.[41] The discovery that the formation of the chromophore and thus also of the fluorescence does not require any other substrates or cofactors made GFP a promising tool for fluorescent protein tagging and for the study of proteins and their functions in general.[42] A fluorescent protein like GFP can be fused to basically every protein of interest enabling quite precise targeting. Since then, a lot of research and effort has been put into the development of new or enhanced fluorescent proteins with improved brightness, photostability, sensitivity, expression efficiency and reduced tendency toward oligomerization. Despite all these advances, the enhanced version of the wild-type GFP (EGFP) with red-shifted excitation maximum and improved brightness and photostability is still among the most popular options.[43] Furthermore, the available spectral range of FPs was expanded to the blue,[44] cyan[44a, 45] and yellow regions[46] by other modified versions of the wild-type GFP (wtGFP) and to the orange and red regions through the discovery of an orange-red FP from a non-bioluminescent reef coral[47] and its mutated versions.[48]

Another promising step in the design of new FPs was the discovery of photoactivatable or photoconvertible versions. Such FPs create chromophores, which can be activated either to

initiate fluorescence emission[49] or to convert it to a different bandwidth[50] after irradiation at a special wavelength. This strategy allows the activation or conversion of only a limited amount of FPs within the cell. Activated and thus fluorescent proteins can then be tracked independently of other newly formed (and therefore still dark) proteins. Such an approach is especially useful for studying dynamics of proteins, for example their lifetimes, trafficking and turnover rates.[42b, 42c] This class of FPs was further improved by introducing photoswitchable FPs, which can be reversibly switched on or off by irradiation at a special wavelength.[51]

### 1.1.3 Short peptide tags for the labeling of proteins

Fluorescent proteins (FP) have emerged as an essential tool for studying proteins and their behavior within live cells and even organisms. Nevertheless, all FPs suffer from the same common drawback, their large size (more than 200 amino acid residues) and thus possible interference with the folding and function of the proteins fused to them.[52] This is especially crucial if the target protein is smaller than the FP.[53]

This problem prompted *Tsien* and co-workers to develop an alternative labeling strategy based on the genetic modification of the protein of interest with a short peptide tag, which can selectively bind a specific small molecule. In their pioneering work they showed that fluorogenic biarsenical compounds such as FlAsH, a green-emitting fluorescein derivative, or ReAsH, a red-emitting resorufin derivative, selectively react with a tetracysteine-motif CCXXCC (Figure 4A and 4B).[54] The advantages of this strategy are the relatively small size of the tetracysteine tag (only six amino acid residues)[52] and a quite low background fluorescence due to a significant increase in fluorescence of the biarsenical dyes after binding to the tetracysteine-tag.[54] Unfortunately, the cytotoxicity of the arsenic moiety limits the use of these approaches in live cell imaging.[55]

In a similar approach *Schepartz* and co-workers used RhoBo, a rhodamine-based bisboronic acid, which binds selectively to a linear tetraserine-motif SSPGSS (Figure 4C).[56] Like FlAsH or ReAsH, RhoBo is fluorogenic and cell-permeable, but additionally it does not contain the cytotoxic arsenic moiety and shows lower background fluorescence as well as increased brightness. However, unlike the tetracysteine-motif, the tetraserine-tag is present in several human proteins that could cause off-target labeling.

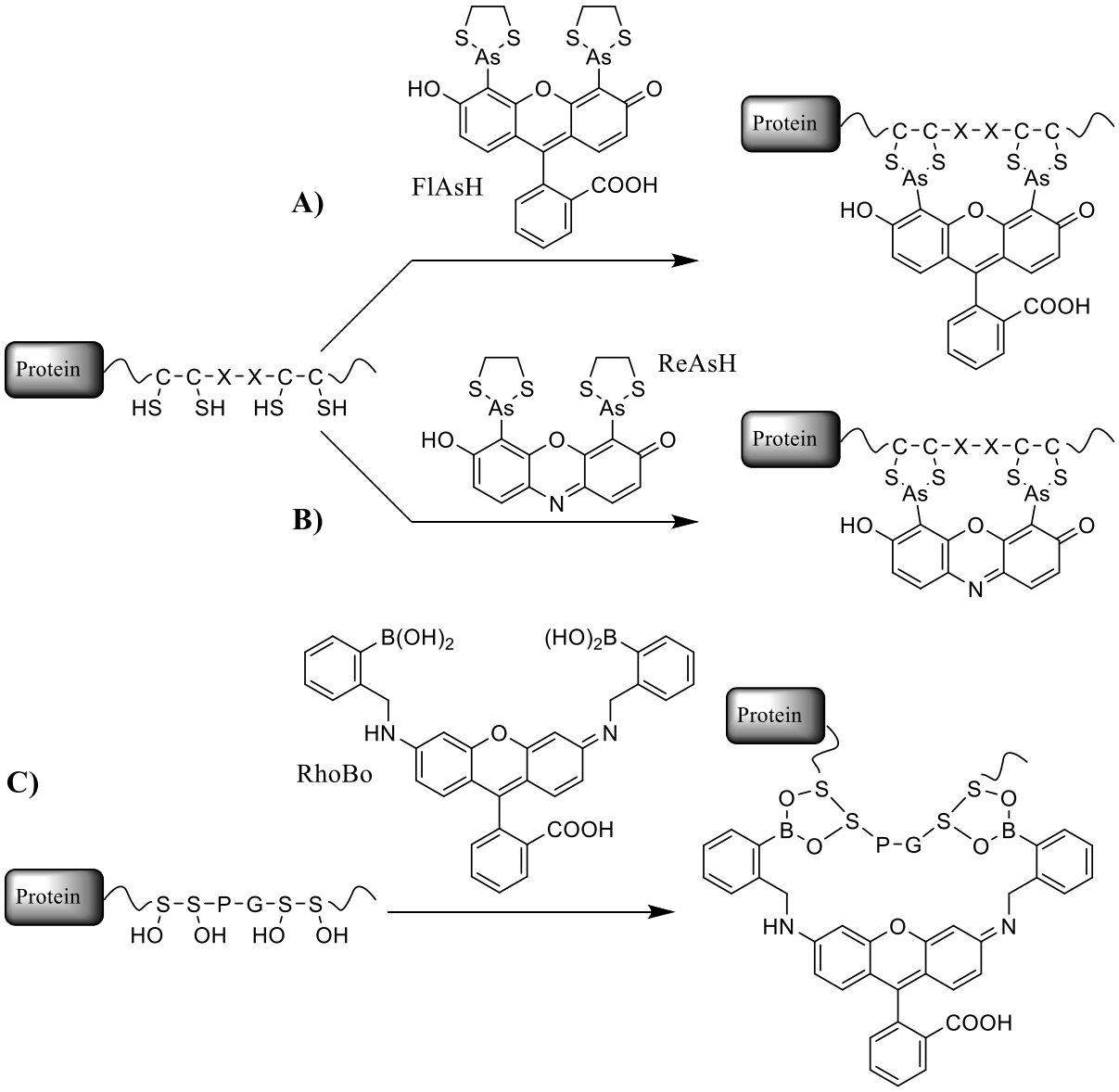


**Figure 4:** Labeling of proteins fused to specific short peptide tags with fluorogenic small molecules. The biarsenical compounds FlAsH (A) and ReAsH (B) bind selectively tetracysteine-motifs and the bisboronic acid RohBo binds selectively a tetraserine-motif.

A different strategy for the labeling of small peptide tags is based on chelation of transition metals (Figure 5). Various short peptide sequences like oligohistidine tags or oligoaspartate tags were already successfully fused to proteins and labeled with small molecules mediated by chelation of different metal ions like $Ni^{2+}$, $Zn^{2+}$ or $Tb^{3+}$.[57]

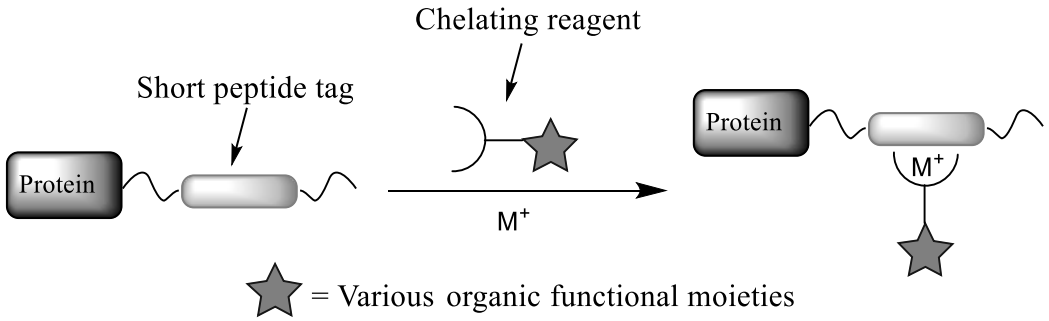


**Figure 5:** Labeling of proteins fused to short peptide tags with small molecules mediated by chelation of different metals.

### 1.1.4 Enzyme-mediated labeling of proteins

Another option for labeling proteins with small molecules are enzyme-mediated modifications. *Johnsson* and co-workers used the human DNA repair protein $O^6$-alkylguanine-DNA alkyl transferase (hAGT) as an enzyme tag, called SNAP-tag, for this purpose (Figure 6A).[58] hAGT usually repairs guanosines, which are alkylated at the 6-oxo position, by transferring the alkyl group to a reactive cysteine of the enzyme.[59] Thus, if the enzyme is fused to target proteins, those proteins can be specifically labeled with various $O^6$-benzylguanine derivatives by transferring the benzyl group irreversibly to the fused hAGT. The benzyl group can be modified with various labels without significantly affecting the reaction with hAGT, making the SNAP-tag a versatile tool for various biological applications.[58, 60] Mutagenesis of eight amino acids in the SNAP-tag led to the creation of CLIP-tag, which reacts selectively and irreversibly with different fluorescent $O^2$-benzylcytosine derivatives.[61] As labeling of the CLIP-tag is orthogonal to labeling of the SNAP-tag, simultaneous and specific labeling of two different proteins in living cells is possible by combining both approaches.

At the *Promega Corporation*, a modified bacterial haloalkane dehalogenase (DhaA) tag (HaloTag) was designed to specifically bind to chloroalkane derivatives (Figure 6B). After formation of a covalent ester bond between the chloroalkane and an aspartate in the enzyme, wild-type DhaA subsequently releases the hydrocarbon again as an alcohol by base-catalyzed hydrolysis. The introduced mutations in HaloTag prevent this hydrolysis and lead to the formation of a stable ester bond, thus irreversibly trapping the intermediate.[62] A variety of useful moieties such as fluorescent dyes, affinity handles or solid surfaces can be attached to the chloroalkane linker enabling a broad spectrum of applications.[62-63]

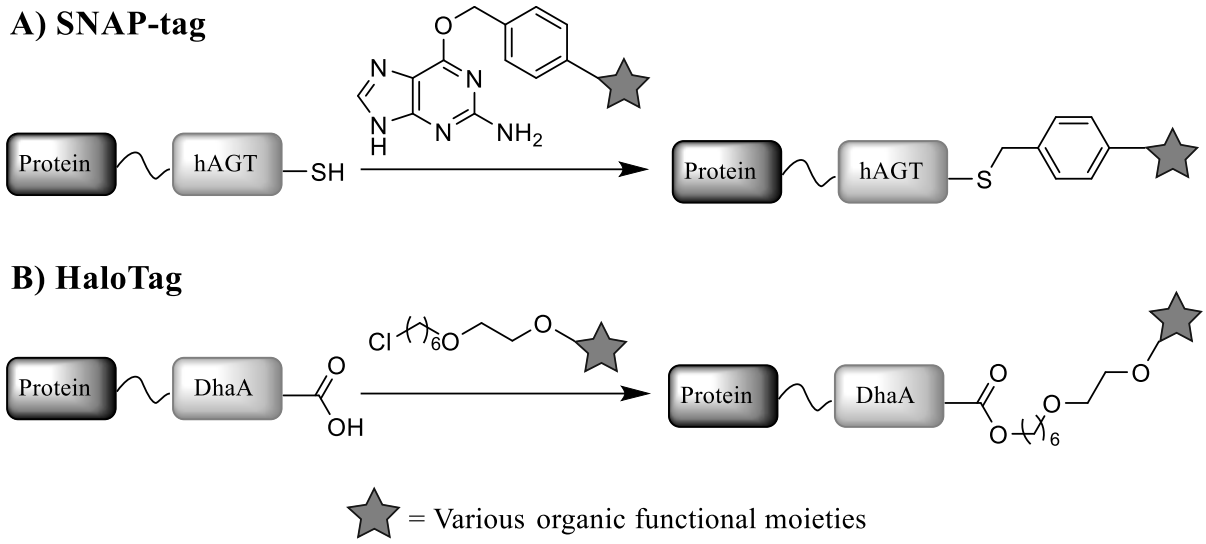


**Figure 6:** Labeling of proteins fused to enzyme tags with small molecules. hAGT-fused proteins can be enzymatically labelled with $O^6$-benzylguanine derivatives (A) and proteins fused to a mutated DhaA with chloroalkanes (B).

Despite the numerous successful applications of these enzyme tags, there is the same potential drawback as for the use of fluorescent proteins. Enzyme tags can negatively influence the functions of the proteins of interest due to their rather large size, which is comparable to the size of FPs. This problem can be overcome by using enzymes that recognize short peptide sequences, which can be genetically attached to proteins of interest. In such cases, the enzymes can modify these peptide sequences without being directly fused to the target protein (Figure 7). Over the past decades, several enzyme-mediated strategies for the covalent labeling of proteins have been developed. Successful applications include the usage of the biotin ligase (BirA) from different species,[64] the guinea pig liver trans-glutaminase (TGase),[65] a modified lipoic acid ligase (LplA) from *E. coli*,[66] the formylglycine-generating enzyme (FGE) from different species,[67] the transpeptidase Sortase A (SrtA) from *S. aureus*[68] and the phosphopantetheine transferases (PPTase) from *E. coli* (AcpS) and from *B. subtilis* (Sfp).[69]

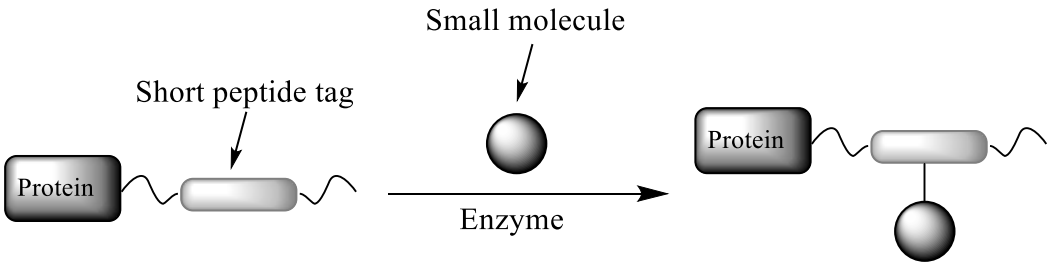


**Figure 7:** Labeling of proteins fused to short peptide tags with small molecules mediated by different enzymatic reactions.

## 1.2 Bioorthogonal reactions for the labeling of biomolecules

Over the past decades, the discovery and development of various strategies for labeling of proteins through genetically encoded tags like the use of fluorescent proteins, short peptide tags and enzyme-mediated methods led already to a much more detailed understanding of the structure and biological functions of many proteins. However, none of these techniques is a universal tool and all they suffer from one or another drawback or limitation like the big size of FPs and some enzyme tags, which can affect the function or structure of the target protein. Other approaches offer rather low selectivity or efficiency and thus suffer from unspecific labeling of undesired residues or high background fluorescence. Yet other strategies are limited to certain applications or are restricted to specific cell lines or parts of the cells.
Furthermore, the usage of genetically encoded tags is limited to proteins and is hence not applicable to other classes of biomolecules such as glycans, lipids, nucleic acids and some metabolites as well as various post-translational modifications.[2a, 2c] Therefore, there is still need for the development of novel methods to expand the set of tools for bioconjugation applications.

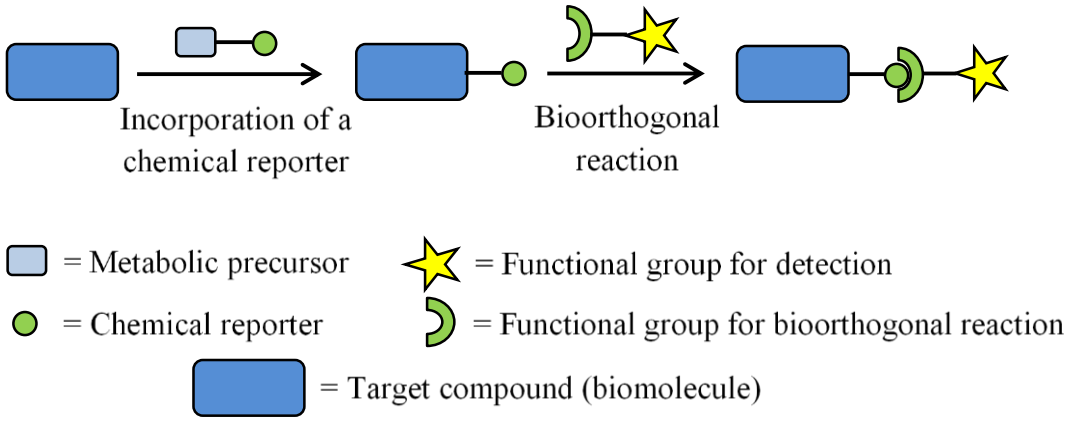


**Figure 8:** Schematic representation of the labeling of biomolecules by bioorthogonal reactions. A chemical reporter (green circle) is introduced into the target compound (dark blue) through a metabolic precursor (light blue). In a subsequent step the chemical reporter is labeled (yellow star) through a bioorthogonal reaction with a complementary functional group (green half ring).

An alternative strategy, which is suitable for all biomolecules, is based on the introduction of a specific functional group, the so-called chemical reporter, into the target compound (Figure 8).[2b] This is usually done by attachment of the chemical reporter to a metabolic precursor of the target biomolecule, such as monosaccharides in the case of glycans,[70] nucleosides for DNA,[71] amino acids for proteins[72] and fatty acids for lipids.[73] Alternatively, there exist fully synthetic approaches for the incorporation of the unnatural reporter moiety into the

structure of the biomolecule. In a subsequent step this chemical reporter can be labeled with various probes through a selective reaction with a complementary functional group.

Such reactions are called bioorthogonal reactions and come along with several prerequisites for the reagents and reaction conditions. First, starting materials as well as products of the reaction have to be biologically as well as chemically inert. They may neither interfere with surrounding biological components nor be affected by biological processes. Furthermore, the reactions should be highly selective to avoid side reactions with the myriad of functional groups present in biological systems. Bioorthogonal reactions also have to be biocompatible. They should not contain cytotoxic components and should be carried out under physiological conditions that is aqueous milieu at 37 °C and pH 6-8. Additionally, in case of using metabolic incorporation, the chemical reporter has to be small enough to be accepted by the biosynthetic machinery of the cell or organism. Last but not least, rather high reaction rates are favored in order to follow rapid biological processes, to enable the use of low nano- to micromolar concentrations of the reagents and to avoid excretion of the labeling probe from the biological system before labeling could take place.[2b, 2d]

Nowadays, numerous chemical reactions are known that fulfill these strict requirements for bioorthogonality. Besides others, condensation reactions of carbonyl-containing compounds with hydroxylamine- or hydrazine-based reagents as well as cycloadditions of various dipoles and heterodienes with unsaturated dienophiles have proven to be among the most promising candidates.[2b-e]

### 1.2.1 Bioorthogonal labeling with carbonyl-containing compounds

In 1986, in an effort to improve cancer therapeutics, *Rideout* reported about the selective *in vitro* formation of hydrazones between the carbonyl group of decanal and *N*-amino-*N'*-octylguanidine.[74] Since then, several compounds bearing an amine functionality with $\alpha$-effect were applied to protein labeling and used for targeting metabolically introduced aldehyde or ketone tags. These methods include amongst others the formation of stable hydrazones (Figure 9A) or oximes (Figure 9B) by using the corresponding hydrazines/hydrazides or *O*-hydroxylamines.[67a, 75] Furthermore, a modified Pictet-Spengler reaction (Figure 9C)[76] and an aminobenzamidoxime (ABAO)-based methodology were developed (Figure 9D) providing products, which are more stable toward hydrolysis.[77] The carbonyl tags can also react with biological nucleophiles such as amines, thiols or alcohols,

but unlike the above-mentioned labeling reactions, these reactions are reversible favoring the equilibrium toward the free carbonyl group under aqueous conditions.[75c, 78]

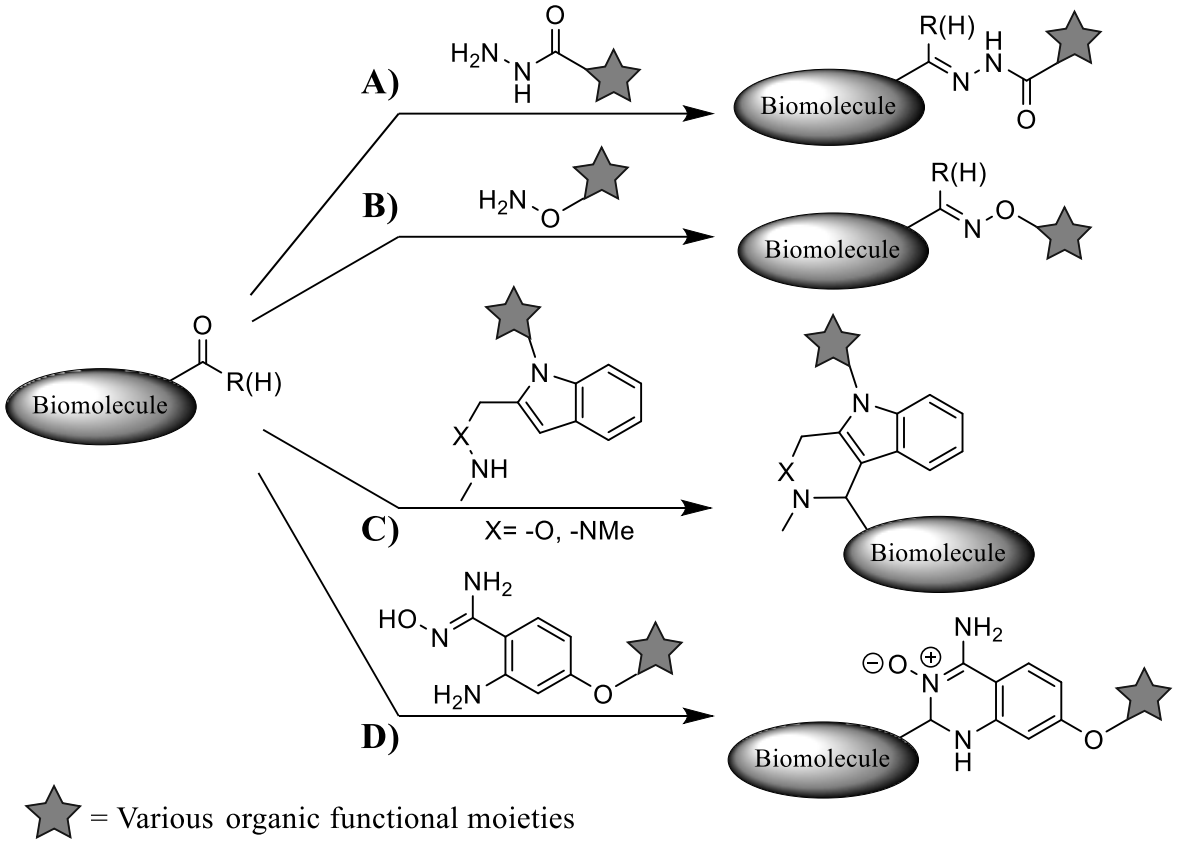


**Figure 9:** Carbonyl group-based bioorthogonal labeling methods. Carbonyl tags such as aldehyde or ketone groups can be modified with hydrazides (A), *O*-hydroxylamines (B), by a modified Pictet-Spengler-reaction (C) or with aminobenzamidoximes (D).

Unfortunately, carbonyl-based ligations are best performed under slightly acidic conditions. Thus, physiological conditions significantly reduce the reaction rates, which often have to be improved by using nucleophilic catalysts such as aniline[79] or better performing alternatives like anthranilic, aminobenzoic[80] and 2-aminobenzenephosphonic acids.[81] The reduced stability of the products (especially hydrazones) is another important factor that must be considered when using this type of chemical labeling strategy.[78] However, kinetic studies on the formation of hydrazones and oximes at pH 7.4 revealed that the structure of both carbonyl compound and $\alpha$-effect nucleophile strongly affects the reaction rates.[82] By careful choice of the reagents, rate constants that compete with those of common cycloadditions (see chapter 1.2.2 and 1.2.3) can be achieved at biological pH without the need for a catalyst. In general, electron-deficient carbonyl compounds are more reactive than electron-rich derivatives, and alkyl substituents in their structure were found to increase reaction rates more than aryl ones.[82a] Additionally, the authors demonstrated that very high reaction rates can be reached

using aldehydes and ketones with acid/base groups like hydroxy, carboxy, imino or pyridine groups near the reactive center. This was explained by a catalytic intramolecular proton transfer between the acid/base group and the leaving hydroxy group of the tetrahedral intermediate, which is reversibly formed during the condensation reaction. The subsequent elimination of water from the intermediate to form the final hydrazone product is usually the rate limiting step,[83] which is accelerated by this acidic/basic intramolecular catalysis. Addressing the structure of $\alpha$-effect nucleophiles, the studies showed that in general electron-rich derivatives react faster than electron-poor ones.[82b] Additionally, as in case of the carbonyl compounds, the presence of a neighboring acid/base group in the structure of the nucleophile significantly accelerates the hydrazone/oxime formation by catalyzing the elimination of water in the second step.

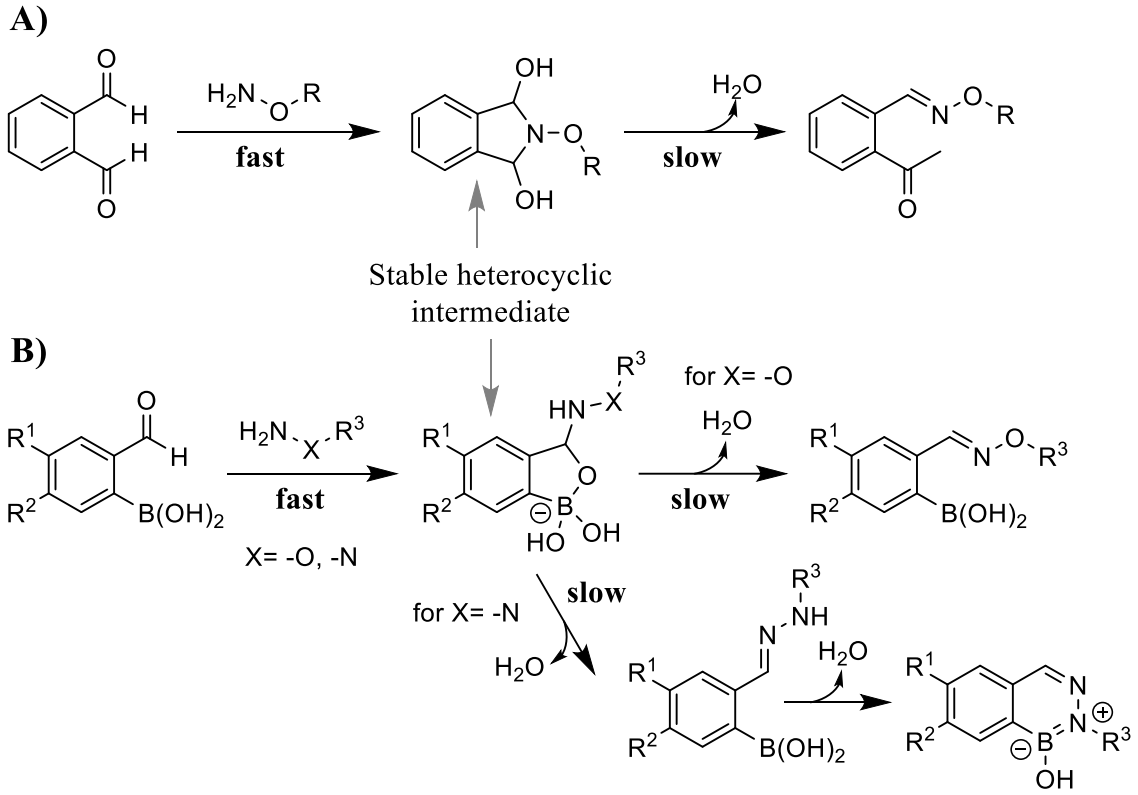


**Figure 10:** Improved carbonyl group-based bioorthogonal labeling methods. Introduction of a second aldehyde group (A) or a boronic acid moiety (B) in *ortho*-position to the reactive aldehyde group of the carbonyl compound participating in the condensation reaction with $\alpha$-effect nucleophiles leads to the fast formation of unusually stable heterocyclic intermediates.

A different concept was developed by *Gillingham* and co-workers, who used a dialdehyde together with *O*-hydroxylamines to form oximes (Figure 10A).[84] Unlike in classic condensation reactions forming oximes, their approach generates an unusually stable heterocyclic intermediate, which can be considered as the ligation step. This strategy was further improved by replacing the second aldehyde group in the dialdehyde with a boronic

acid, which again leads to the fast formation of a stable heterocyclic intermediate (Figure 10B).[85] Additionally, using hydrazines instead of *O*-hydroxylamines in this strategy leads not to the expected hydrazones as final products, but to the irreversible formation of more stable aromatic boron-substituted benzodiazaborines.[85b]

However, the presence of endogenous aldehyde or ketone groups can result in side reactions that limit the applicability of the labeling with carbonyl tags, when working in more complex biological systems.[75b] Luckily, carbonyl groups are absent at the cell surface and hence carbonyl tags were already successfully used for the labeling of membrane proteins and glycans.[79c, 86]

### 1.2.2 Bioorthogonal labeling with azides and alternative 1,3-dipoles

Another widely used chemical reporter is the azide group. Azides are almost absent in biological systems[87] and hardly react with other biological nucleophiles such as amines or alcohols. Thus, azide-based labeling is quite selective and the azide group is inert toward most biological functional groups. Furthermore, organic azides are quite stabile under physiological conditions and non-cytotoxic. Finally, their small size facilitates the introduction into biomolecules through metabolic pathways.[88]

Azide groups were used for the first time in a bioorthogonal reaction through a modified Staudinger reaction developed by *Saxon* and *Bertozzi*.[89] The classic Staudinger reaction between an azide and a triphenylphosphine ($PPh_3$) includes a hydrolytic cleavage of the initially formed aza-ylide intermediate into a phosphine oxide and an amine in the end.[90] In a bioorthogonal labeling reaction, this hydrolytic cleavage would cause the removal of an introduced label. By connecting an ester group to one of the aryl substituents of $PPh_3$ at *ortho*-position, *Saxon* and *Bertozzi* were able to avoid this consequential removal.[89] This so-called Staudinger ligation leads to the formation of a stable amide bond during the hydrolysis through an intramolecular rearrangement (Figure 11A). By using an inverted ester or thioester group in the starting $PPh_3$, *Bertozzi* and co-workers[91] as well as *Raines* and co-workers[92] were even able to remove the formed phosphine oxide moiety during the hydrolysis step (Figure 11B). This enhanced version is now known as the traceless Staudinger ligation. Furthermore, *Bertozzi* and co-workers developed fluorogenic phosphines, which become fluorescent upon the Staudinger ligation.[93]

However, there are also drawbacks to the Staudinger ligation. Phosphines are prone to oxidation on air and could potentially oxidize already before the ligation takes place. Additionally, the first reaction step, the nucleophilic attack of the phosphine to the azide, is quite slow under physiological conditions and thus requires rather high concentrations of the phosphine.[94] Nevertheless, nowadays the different versions of the Staudinger ligation are a powerful and wide-spread tool for bioconjugation and were used in various applications such as labeling of azidosugars, glycans and glycoproteins *in vitro* as well as *in vivo*,[89, 95] protein enrichment,[96] functionalization of recombinant proteins[97] and detection of posttranslational modifications of proteins[98].

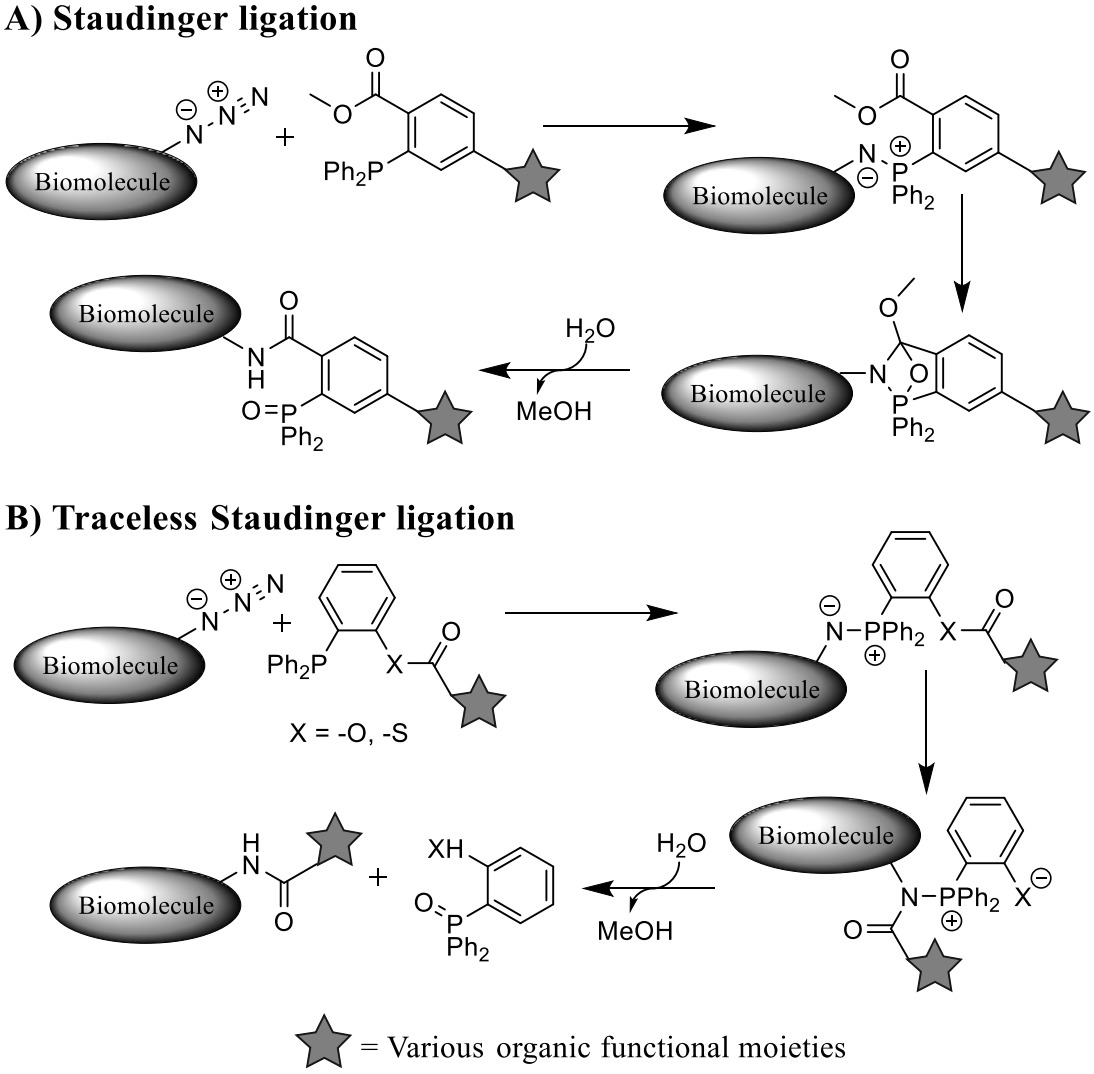


**Figure 11:** Reaction scheme for the "classic" (A) and "traceless" (B) Staudinger ligation.

Another suitable reaction for bioorthogonal labeling based on azides is the copper-catalyzed variant of the azide-alkyne [3+2] cycloaddition (CuAAC), which forms 1,2,3-triazoles and was developed independently by the research groups of *Sharpless*[99] and *Meldal*.[100] This

reaction is a prime example of the so-called “click chemistry”, which was introduced by *Kolb, Finn* and *Sharpless* in 2001 and requires criteria similar to bioorthogonal labeling.[101] The classical, non-catalyzed version of this 1,3-dipolar cycloaddition developed by *Huisgen* and co-workers[102] was less suitable for biological applications due to the requirement of rather high temperature or pressure to overcome the initial activation barrier. However, addition of a Cu(I)-catalyst and consequential formation of a copper acetylide intermediate, which activates the alkyne for reaction with the azide, significantly improves the reaction kinetics, so that the reaction proceeds readily at room temperature (Figure 12).[99-100]

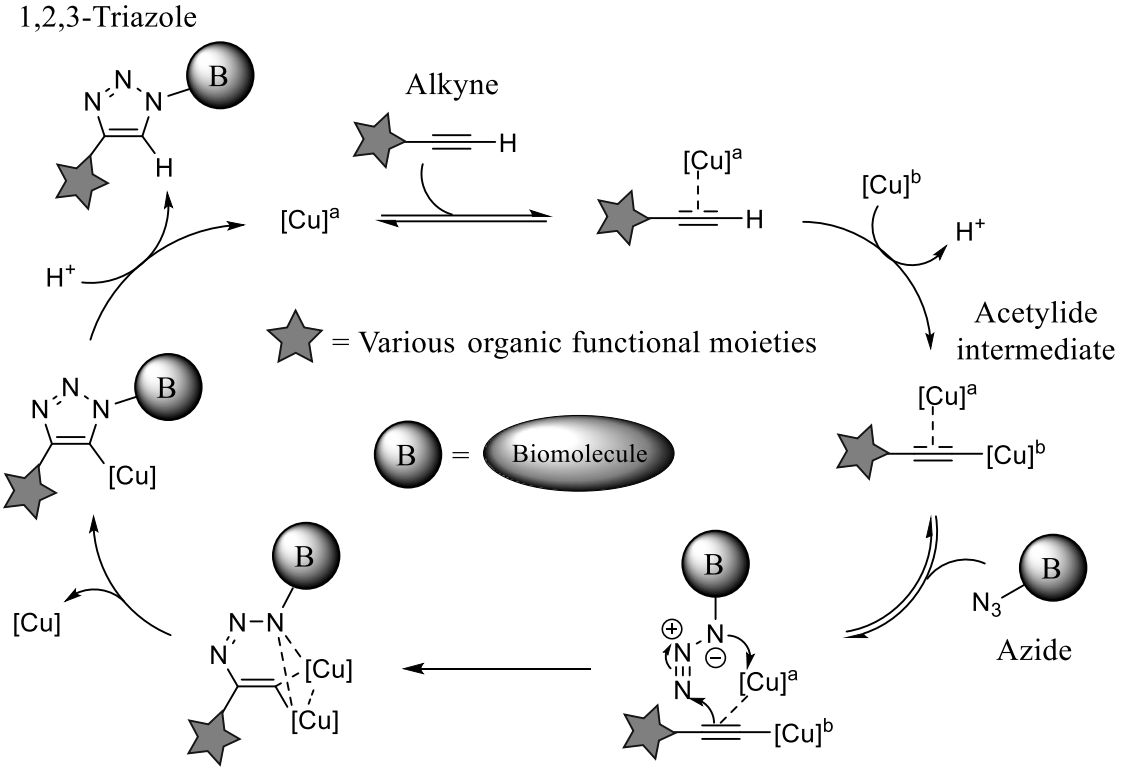


**Figure 12:** Reaction scheme of the CuAAC through a copper acetylide intermediate.

The main disadvantage of CuAAC for *in vivo* applications is the potential cytotoxicity of the copper catalyst.[103] Although several Cu(I)-chelating ligands exist, whose addition to the cycloaddition increases the reaction kinetics, reduces the cytotoxic effects and stabilizes the catalyst toward oxidation,[103a, 104] new strategies allowing the reaction to proceed without additional metal catalysis were desired.

Based on the work on cyclooctyne and its fast 1,3-dipolar cycloaddition reaction with phenylazide,[105] *Agard et al.* developed a copper-free variant of the azide-alkyne cycloaddition, the so-called strain-promoted azide-alkyne cycloaddition (SPAAC, Figure 13A).[106] By using strained cyclic alkyne derivatives like a biotinylated cyclooctyne, they

were able to reach rate constants similar to the Staudinger ligation without addition of a copper-catalyst and to avoid the sensitivity of phosphines to oxidation. This discovery led to numerous attempts to develop new strained alkynes with enhanced performance in bioorthogonal labeling.[107] One of the most widely used derivative among those is the bicyclo[6.1.0]nonyne (BCN) with a cyclopropyl ring fused to the cyclooctyne moiety. This structural modification increases the ring tension and further enhances the reaction rate of the cycloaddition.[107f]

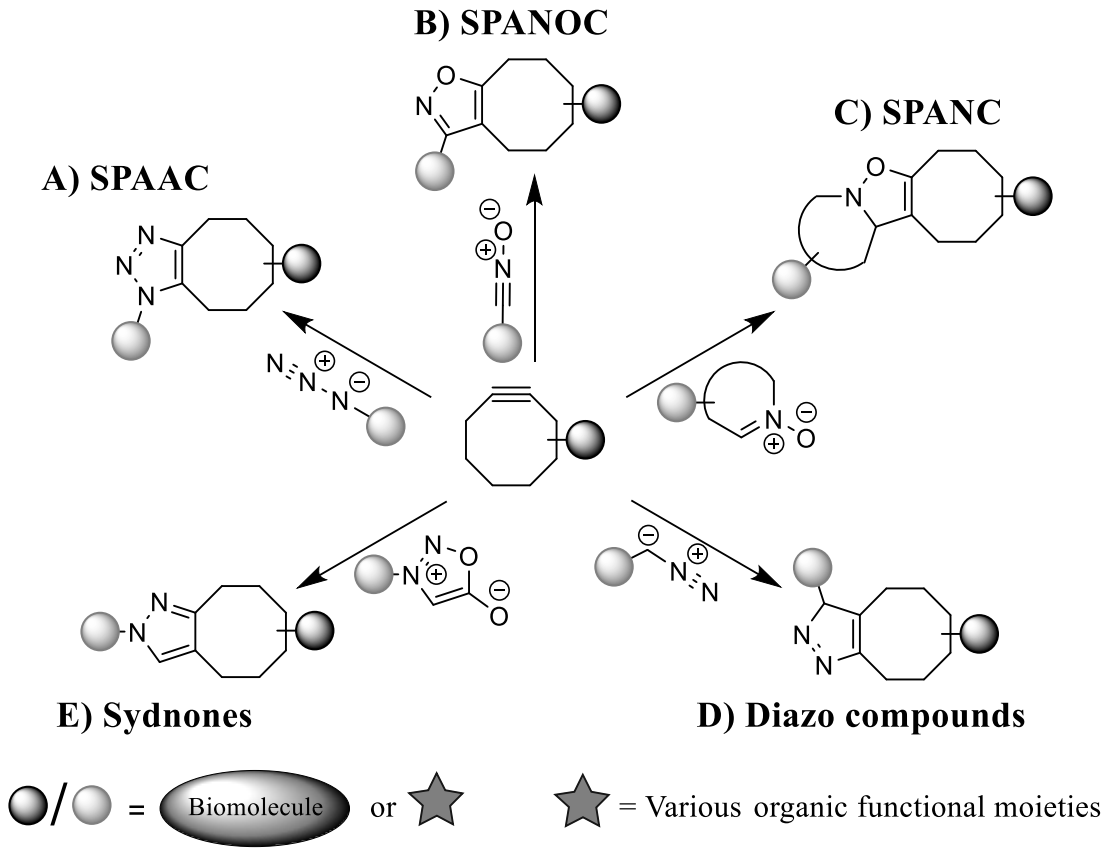


**Figure 13:** Overview of different copper-free 1,3-dipolar cycloadditions. Strained cycloalkynes can react with azides (SPAAC, A), nitrile oxides (SPANOC, B), nitrones (SPANC, C), diazo compounds (D) or sydnones (E).

Inspired by the success of cyclooctynes and their application in SPAAC reactions, several other 1,3-dipoles were developed as an alternative to azides in [3+2] cycloadditions. For example, nitrile oxides and nitrones undergo quite fast cycloadditions with alkynes or alkenes forming isoxazoles (SPANOC, Figure 13B)[108] and isoxazolines (SPANC, Figure 13C),[109] respectively. These types of 1,3-dipolar cycloadditions show even higher reaction rates than SPAAC. However, the high reactivity of nitrile oxides and nitrones comes along with relatively low stability and tendency for dimerization. Thus, *in situ* preparation of the reagents before performing the actual bioorthogonal labeling is required, especially when using the

more reactive but also less stable nitrile oxides.[108b] Furthermore, diazo compounds (Figure 13D)[110] as well as sydnones (Figure 13E)[111] were already successfully applied to cycloadditions with cyclooctynes.

### 1.2.3 Bioorthogonal labeling using iEDDA cycloadditions between alkenes/ alkynes and heterodienes

Another promising candidate for bioorthogonal labeling is the inverse-electron-demand Diels-Alder (iEDDA) cycloaddition. Unlike the classical Diels-Alder reaction, this [4+2]-cycloaddition takes place between the lowest unoccupied molecular orbital (LUMO) of an electron-poor diene and the highest occupied molecular orbital (HOMO) of an electron-rich dienophile. In particular, the iEDDA reaction of 1,2,4,5-tetrazines with various dienophiles has attracted significant interest over the last years due to remarkable kinetics and biocompatibility. From a mechanistic point of view, this reaction involves the initial inverse-electron Diels-Alder reaction between the electron-poor tetrazine and an alkene or alkyne dienophile, followed by a retro Diels-Alder reaction leading to the release of molecular nitrogen and yielding the corresponding dihydropyridazines or pyridazines (Figure 14).[112] Even though the reaction itself was known for decades, it was only in 2008, when two groups independently demonstrated that these tetrazine-based iEDDA reactions are suitable for bioorthogonal labeling.[113] *Devaraj et al.* showed the successful labeling of receptors on live human breast cancer cells via an iEDDA reaction between tetrazine and norbornene.[113a] *Blackman et al.* instead labeled the protein thioredoxin through an iEDDA reaction between tetrazine and *trans*-cyclooctene (TCO).[113b]

The reaction rates of tetrazine ligations strongly depend on the structure of both the tetrazine and the dienophile. Over the last years, the development of new methodologies gave access to various 1,2,4,5-tetrazine derivatives, which were evaluated in iEDDA reactions with different dienophiles.[114] In general, electron-deficient heteroaryl substituents such as pyridyl or pyrimidyl groups at position C3 or C6 significantly increase the reactivity of tetrazines, while electron-donating substituents like amino groups decrease it. Unfortunately, the increased reactivity usually correlates with decreased stability of the tetrazine and increased tendency to side reactions, especially *in vivo*.

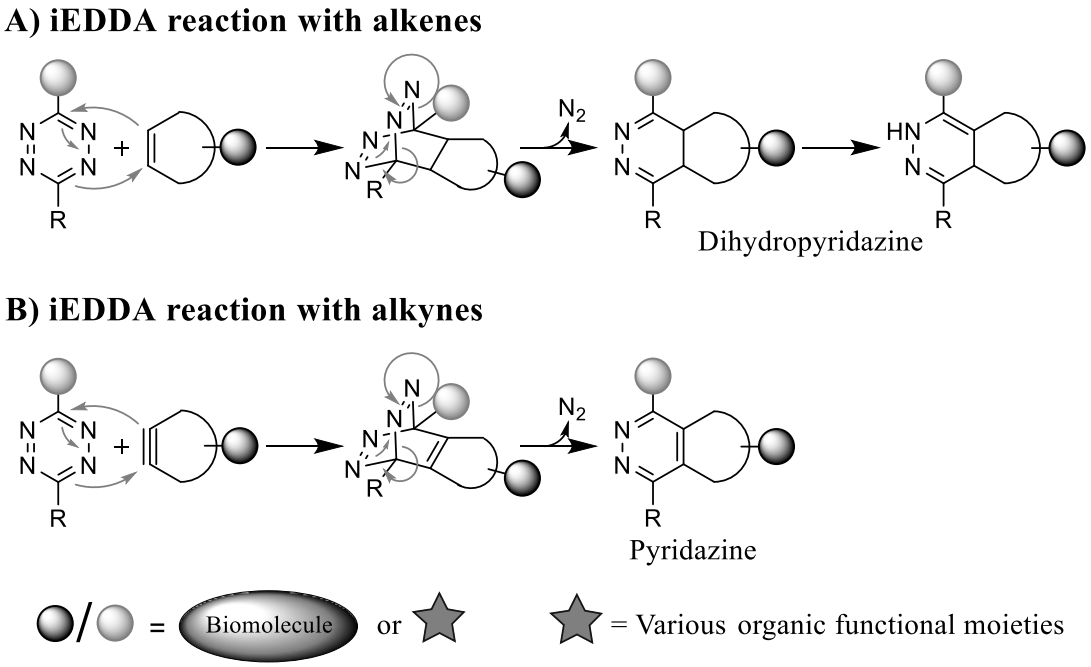


**Figure 14:** Reaction scheme showing the tetrazine ligation between 1,2,4,5-tetrazines and alkene (A) or alkyne (B) dienophiles leading to the formation of dihydropyridazines (A) or pyridazines (B) through an iEDDA cycloaddition and subsequent retro Diels-Alder reaction.

Similar effort has been put into the development of new dienophiles as reaction partners in bioorthogonal tetrazine ligations. Increased ring strain in the structure of the dienophile seems to be essential for high reaction rates. Suitable dienophiles range from strained alkenes like TCOs,[113b, 114b, 115] *trans*-cycloheptenes,[116] cyclopropenes,[117] norbornenes[113a, 118] and azetines[119] to cyclooctynes[114b, 120] like BCN. The highest reactivity is usually obtained in iEDDA reactions of tetrazines with strained TCOs resulting in reaction rates orders of magnitudes higher compared to other dienophiles. Among those, cyclopropyl-fused TCO (s-TCO) shows by far the best kinetics due to a highly strained "half-chair" conformation of the cyclooctene moiety.[114b, 115a] However, s-TCO is prone to isomerization to the less reactive *cis*-conformer during longer incubations *in vivo*.[114b] Unlike the s-TCO, a dioxolane ring-fused TCO (d-TCO) is more stable under physiological conditions, while providing almost comparable reaction rates.[115b]

Since its discovery as a bioorthogonal labeling method, tetrazine ligation already found widespread use in biological research. Bioorthogonal reactions of genetically encoded amino acids containing norbornene, cyclooctyne or TCO moieties with different 1,2,4,5-tetrazine derivatives were used for selective labeling of isolated proteins[121] and proteins on the surface[118a] as well as in[114b, 122] live mammalian cells. Tetrazine-bearing amino acids were also genetically encoded into proteins and successfully labeled with TCO derivatives both

*in vitro* and *in vivo*.[123] Furthermore, iEDDA reactions between tetrazines and norbornenes or TCOs were used to image live cancer cells with quantum dots[124] and diagnostic nanomaterials,[125] respectively. Due to its fast kinetics, the iEDDA cycloaddition between tetrazines and TCOs is also an ideal candidate for tumor imaging in live mice with radionuclides $^{111}$In[126] and $^{18}$F.[127] Additionally, tetrazine ligations were also applied to labeling of glycans both *in vitro*[117b, 128] and *in vivo*,[129] of lipids in live cells[117a, 130] and of synthetic[131] and cellular[132] DNA as well as synthetic RNA[133] and RNA in live cells.[134]
Furthermore, due to the remarkable selectivity, the iEDDA reaction of 1,2,4,5-tetrazines is a suitable candidate for the so-called orthogonal bioorthogonal reactions. This term refers to a pair of two different bioorthogonal reactions, which are additionally orthogonal to each other. This means that the reagents of one reaction should be inert to the reagents of the other reaction and thus should not react or interfere with those. This strategy allows site-selective double labeling of either two different targets or the same target in more complex multicomponent systems. Tetrazine ligations with various strained dienophiles were already successfully used in combination with CuAAC, SPAAC or the Staudinger ligation for two-step[135] or even single-step[131b, 136] double labeling of proteins, glycans and DNA *in vitro* and *in vivo*.
Another noteworthy application of tetrazine-TCO cycloadditions is the recently developed decaging strategy. Unlike usual bioorthogonal reactions that employ the formation of a new stable and covalent bond in order to connect two different moieties, this concept triggers a bond-cleavage through the iEDDA reaction. *Robillard* and co-workers used this strategy in an elegant prodrug activation approach, in which caged doxorubicin was released by iEDDA reaction between tetrazine and TCO both *in vitro* and in tumor-bearing mice.[137] *Chen* and co-workers utilized the decaging mechanism for activation and manipulation of the activity of different enzymes in living systems.[138] Enzymes, which are caged and deactivated by TCO derivatives attached to their active site, can be reactivated through cleavage of the TCO moiety triggered by an iEDDA reaction with tetrazines.

Recently, 1,2,4-triazines were identified as alternative heterodienes for iEDDA reactions with strained dienophiles like TCOs[139] and BCNs (Figure 15).[140] While the reactivity of 1,2,4-triazines is significantly lower compared to 1,2,4,5-tetrazines, their remarkable stability under physiological conditions and in the presence of biological nucleophiles makes them a promising candidate for bioorthogonal labeling. Although several new approaches for the synthesis of 1,2,4-triazines from the last years gave already access to a broader spectrum of

different triazine derivatives,[141] more research is needed in the following years to reveal the full potential of 1,2,4-triazines for bioorthogonal applications.

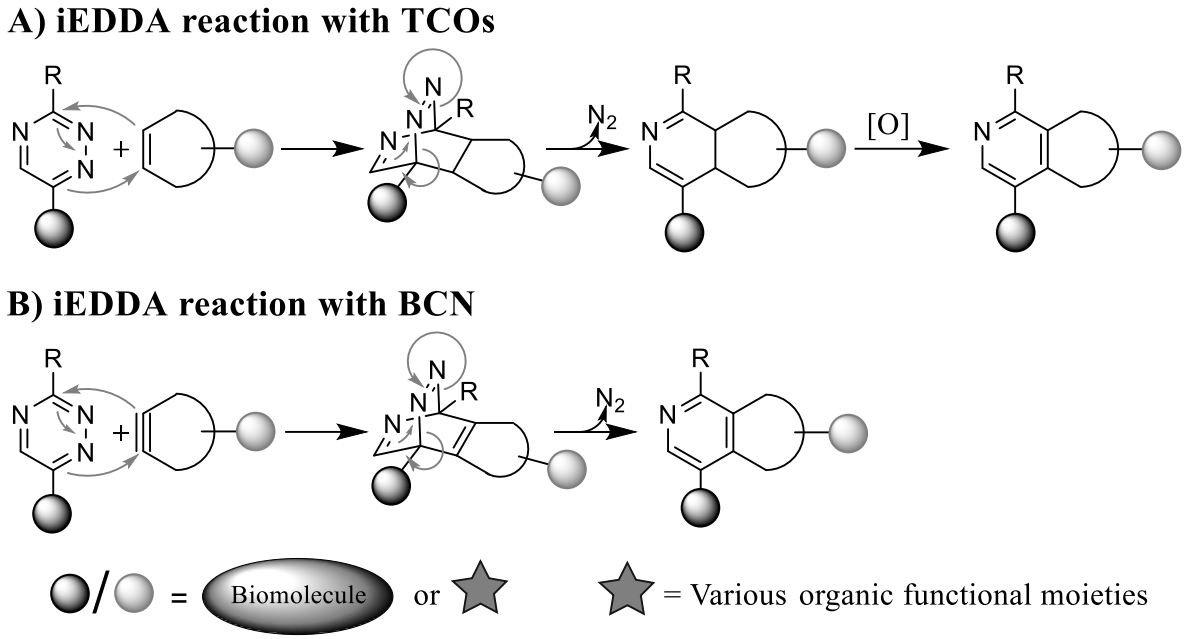


**Figure 15:** Reaction scheme of iEDDA cycloaddition and subsequent retro Diels-Alder reaction between 1,2,4-triazines and TCOs (A) or BCN (B). The initially formed dihydropyridine in reactions with TCOs oxidizes to the pyridine product over time (A).

In addition to 1,2,4-triazines, *Boger* and co-workers recently reported about the exquisite reactivity of 1,2,3-triazines with various dienophiles (Figure 16).[142] The [4+2]-cycloaddition between 1,2,3-triazines and dienophiles like alkynes or amidines yields pyridine and pyrimidine products, respectively. The reaction proceeds under mild reaction conditions and with fascinating regioselectivity. However, similarly to the 1,2,4-triazines, the 1,2,3-triazines need further investigation concerning their potential use as efficient bioorthogonal reagents.

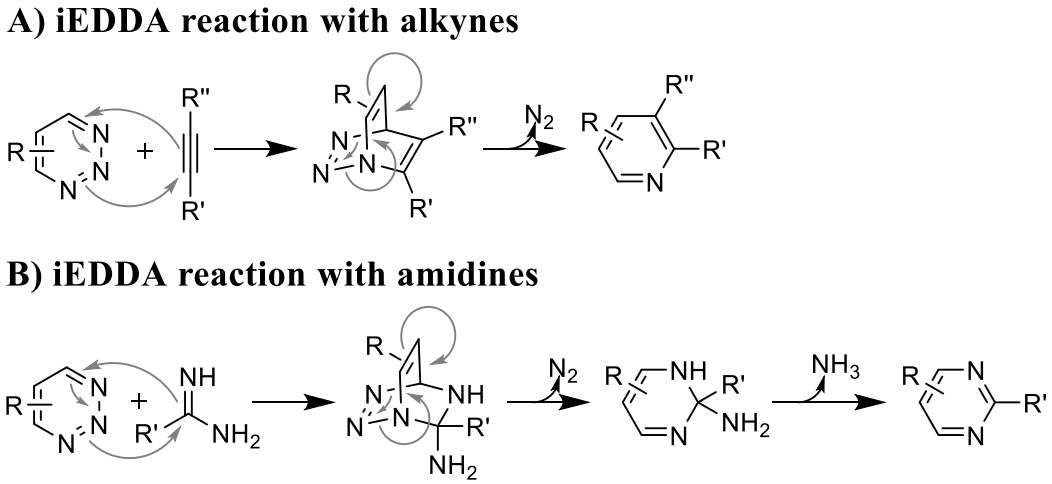


**Figure 16:** Reaction scheme of iEDDA cycloaddition and subsequent retro Diels-Alder reaction between 1,2,3-triazines and alkynes (A) or amidines (B). In iEDDA reactions with amidines, the final pyrimidine product is obtained after a subsequent elimination of $NH_3$.

### 1.2.4 Fluorogenic bioorthogonal reactions

Besides the genetically encodable fluorescent proteins described in chapter 1.1.2, small fluorescent dyes are a common tool for tagging and visualizing biomolecules involved in biological processes. In experiments based on the detection of a fluorescent signal, the signal-to-noise ratio plays a crucial role. Therefore, no fluorescent signal at the beginning and a large increase in the signal after the reaction is beneficial. For this reason, the so-called fluorogenic probes are of special interest in bioorthogonal labeling.[143] Ideally, such fluorogenic reactions allow the generation of a fluorescent product from non-fluorescent starting materials and create the fluorescent signal only when the bioorthogonal reaction takes place. This strategy results in excellent signal-to-noise ratio and fast imaging without the need for washing steps or removal of excess fluorescent labeling reagent.

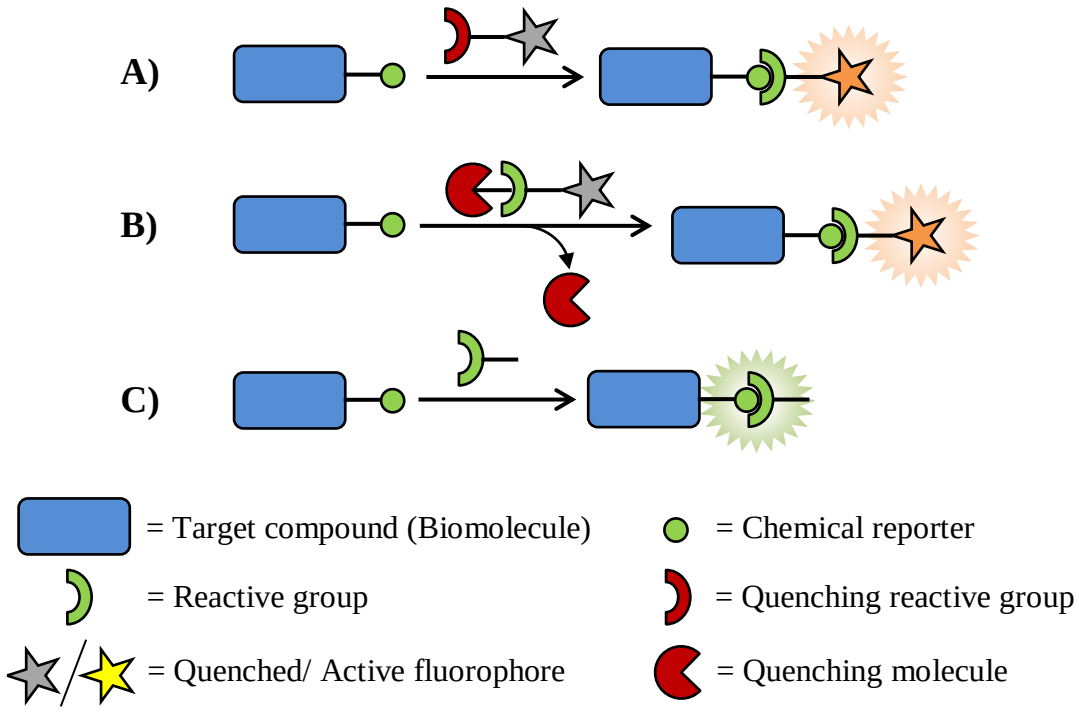


**Figure 17:** Schematic representation of different strategies for fluorogenic bioorthogonal labeling. The fluorophore is quenched before the labeling reaction either by one of the reactive groups (A) or by an additional quenching molecule (B) and then restored during the bioorthogonal reaction. Alternatively, it can directly be formed through the bioorthogonal reaction without the need for an extra fluorophore (C).

The concept of fluorogenicity was already successfully applied to various bioorthogonal reactions such as Staudinger ligation,[93] both copper-mediated[144] and copper-free[145] azide-alkyne cycloaddition and tetrazine ligation.[114d, 117a, 146] The most commonly used strategy utilizes quenching of the fluorescence via intramolecular energy transfer from the functional group, which directly participates in the bioorthogonal reaction, to the attached dye. The

structural changes due to the subsequent bioorthogonal reaction then lead to restoration of the fluorescence in the product (Figure 17A). This principle is used in for example FlAsH- and ReAsH-based labeling of short peptide tags as mentioned in chapter 1.1.3.[54] An alternative strategy employs an additional quenching molecule attached to the bioorthogonal fluorophore conjugate. This quenching moiety is removed through the labeling reaction, resulting in restoration of the fluorescence of the fluorophore (Figure 17B). This approach is for example used in the aforementioned SNAP-tag and CLIP-tag strategies (see chapter 1.1.2), in which enzyme-tagged proteins are labeled with $O^6$-benzylguanine and $O^2$-benzylcytosine derivatives, respectively.[58, 61, 147]

Much less common is the formation of the fluorophore as an inherent result of the bioorthogonal reaction of two non-fluorescent reagents (Figure 17C). Such approaches do not require the presence of an extra fluorophore moiety in the structure of one of the starting materials and therefore benefit from less complex syntheses of the reagents and the absence of virtually any background fluorescence. To this class of fluorogenic reactions belongs, for example, the 1,3-dipolar cycloaddition between nitrile imines and various dipolarophiles.[148] The suitability of this cycloaddition for bioorthogonal applications was first reported by *Lin* and co-workers, who generated the nitrile imine *in situ* through photoirradiation of a tetrazole and subsequently reacted it with suitable alkenes in a 1,3-dipolar cycloaddition to form fluorescent pyrazolines (Figure 18A).[149] The authors applied this approach to *in vivo* protein labeling in *E. coli*[150] and mammalian cells.[151] In a following study, the rate of the photo-induced cycloaddition was then further increased by using strained cyclopropenes as the dipolarophile.[152] Additionally, it was shown that nitrile imines can also be generated from corresponding hydrazonoyl chlorides without the need for photoactivation (Figure 18B)[121, 153]

*Shang et al.* recently described another example of a fluorophore-forming bioorthogonal reaction.[154] They reported about the formation of fluorescent dihydropyridazines through iEDDA reaction between an 1,2,4,5-tetrazine and styrene derivatives (Figure 18C). This approach was applied to both *in vivo* and *in vitro* labeling of proteins via a genetically incorporated unnatural amino acid containing the styrene moiety.

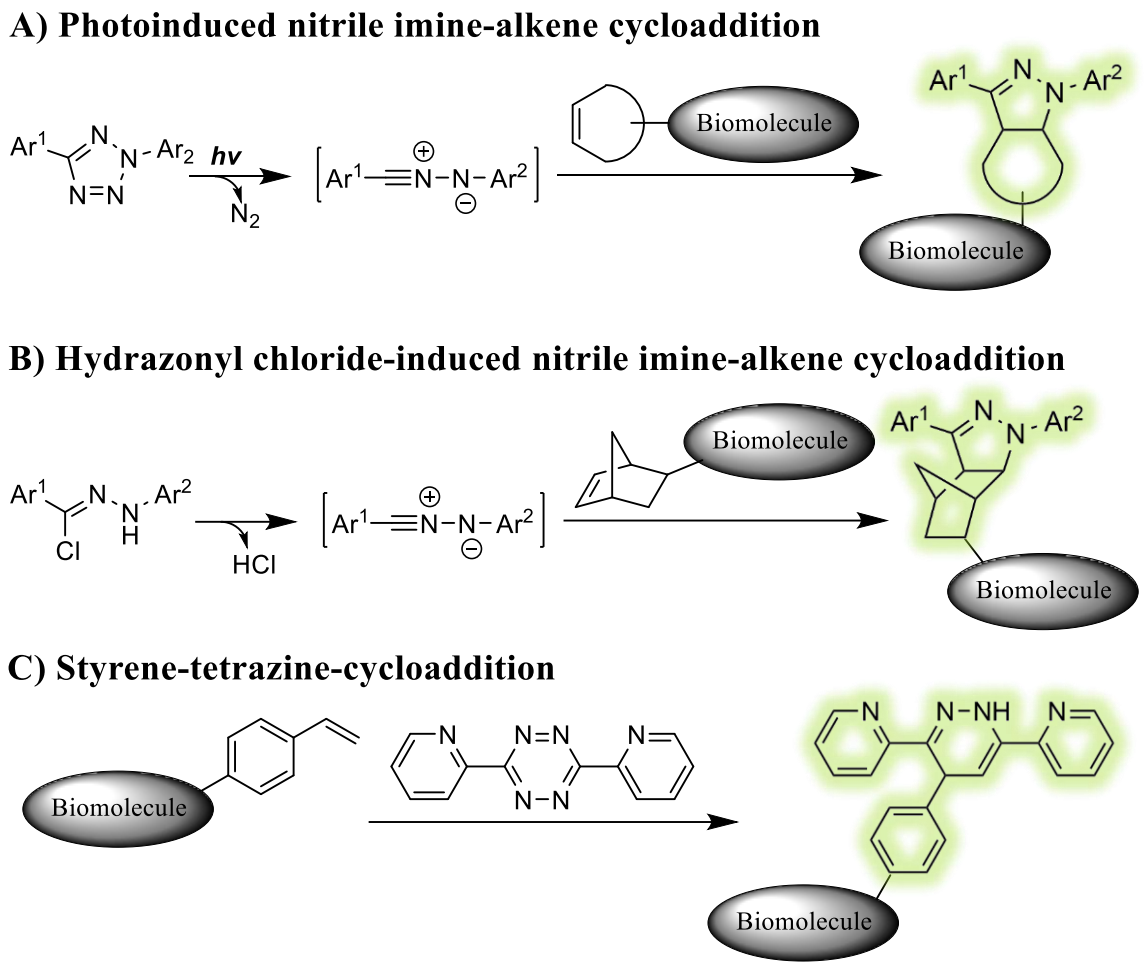


**Figure 18:** Fluorogenic bioorthogonal reactions, in which the fluorophore is formed during the reaction. Nitrile imines created *in situ* by photoirradiation of tetrazoles (A) or HCl elimination of corresponding hydrazonyl chlorides (B) form fluorescent pyrazolines via 1,3-dipolar cycloaddition with various dipolarophiles. Styrene derivatives lead via cycloaddition with 1,2,4,5-tetrazines to fluorescent dihydropyridazines (C).

At the same time, our group was able to show that also iEDDA reactions between various 1,2,4,5-tetrazines and particular TCOs lead to direct formation of fluorophores with tunable photophysical properties.[155] We found that the conformation of the *trans*-cyclooctene-5-ol (TCO-ol) directly influences the outcome of iEDDA reactions with 1,2,4,5-tetrazines (Figure 19A). When the axial isomer of TCO-ol (axTCO-ol) was used for the cycloaddition, fluorescent products were formed, while the use of the equatorial isomer (eqTCO-ol) led to the formation of non-fluorescent products. We explained this unusual behavior by different mechanisms of the isomerization of the 4,5-dihydropyridazine intermediate to the 1,4-dihydropyridazine product (Figure 19B). Detailed NMR and DFT calculation studies revealed that using axTCO-ol provides directly the fluorescent 1,4-dihydropyridazines, while the equatorial isomer first yields non-fluorescent 4,5-dihydropyridazines, which only very slowly isomerize to 1,4-dihydropyridazines. The difference in the formation of the products is

the result of an intramolecular-promoted hydrogen migration from the bridgehead carbon atom to the hydroxyl group, which was only observed in the axial position. The photophysical properties of this new type of fluorophores can be easily tuned by changing the substitution pattern of the starting tetrazine.

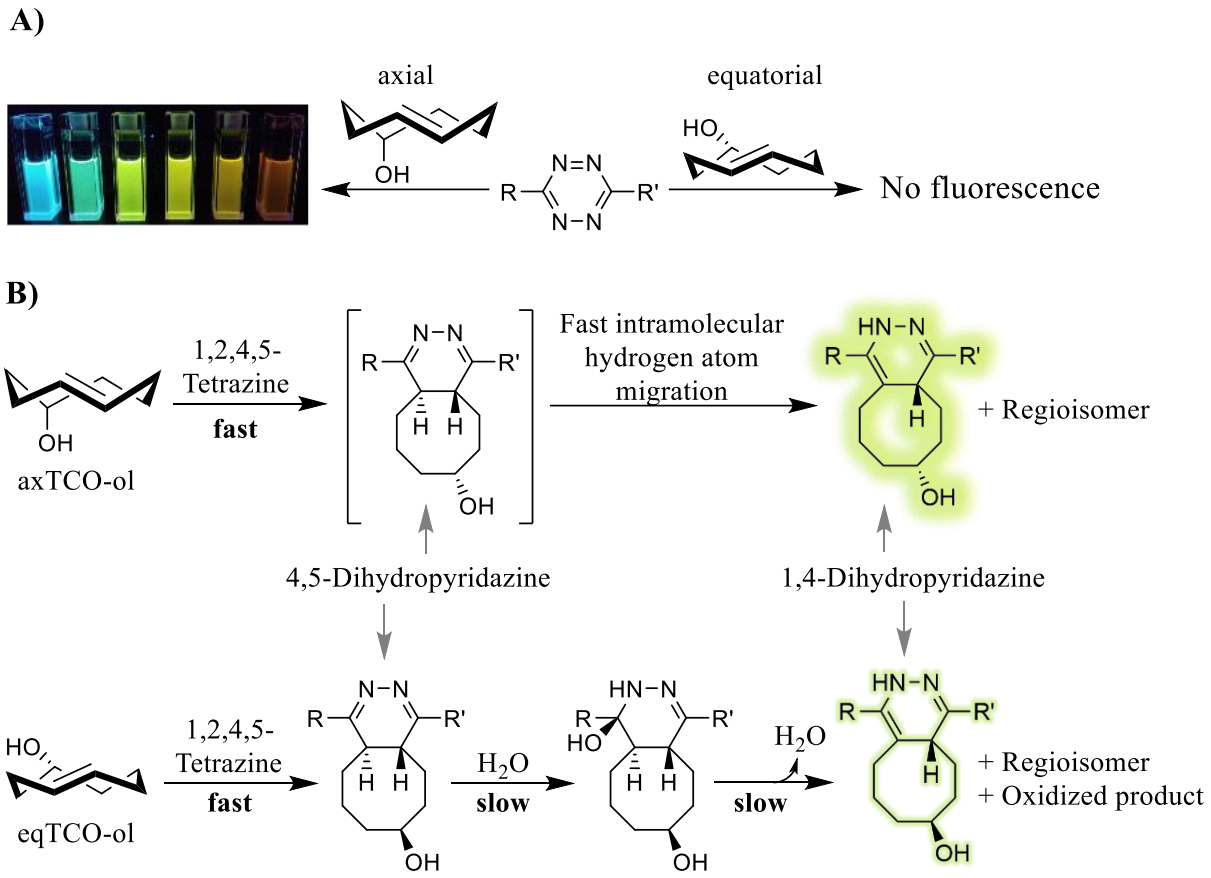


**Figure 19:** Fluorogenic iEDDA reaction between various 1,2,4,5-tetrazines and axTCO-ol and the corresponding non-fluorogenic cycloaddition with eqTCO-ol (A). The emission wavelength of the fluorescent products depends on the substitution pattern (R and R') of the starting tetrazine. Scheme of the corresponding different mechanisms for the isomerization of the 4,5-dihydropyridazine intermediates to the 1,4-dihydropyridazine products (B). When using eqTCO-ol, the 1,4-dihydropyridazine product shows only a weak fluorescent signal due to concomitant formation of the corresponding non-fluorescent oxidized pyridazine product.

The applicability of this approach for bioimaging was successfully demonstrated by labeling intracellular compartments or small biologically active molecules in live cancer cells. For the cell labeling experiments we synthesized two different 1,2,4,5-tetrazine derivatives with specific moieties, which target the tetrazines to different subcellular compartments. One tetrazine was modified with a taxol moiety (taxol-Tet), which binds to and stabilizes microtubules. The attachment of a triphenylphosphonium group to the other tetrazine derivative (TTP-Tet) targets it to mitochondria. After incubation of live cancer cells with either taxol-Tet or TTP-Tet, addition of axTCO-ol resulted in efficient and rapid labeling of

the cellular compartments (Figure 20), which was demonstrated by co-localization experiments with Tubulin tracker and Mitotracker, respectively.

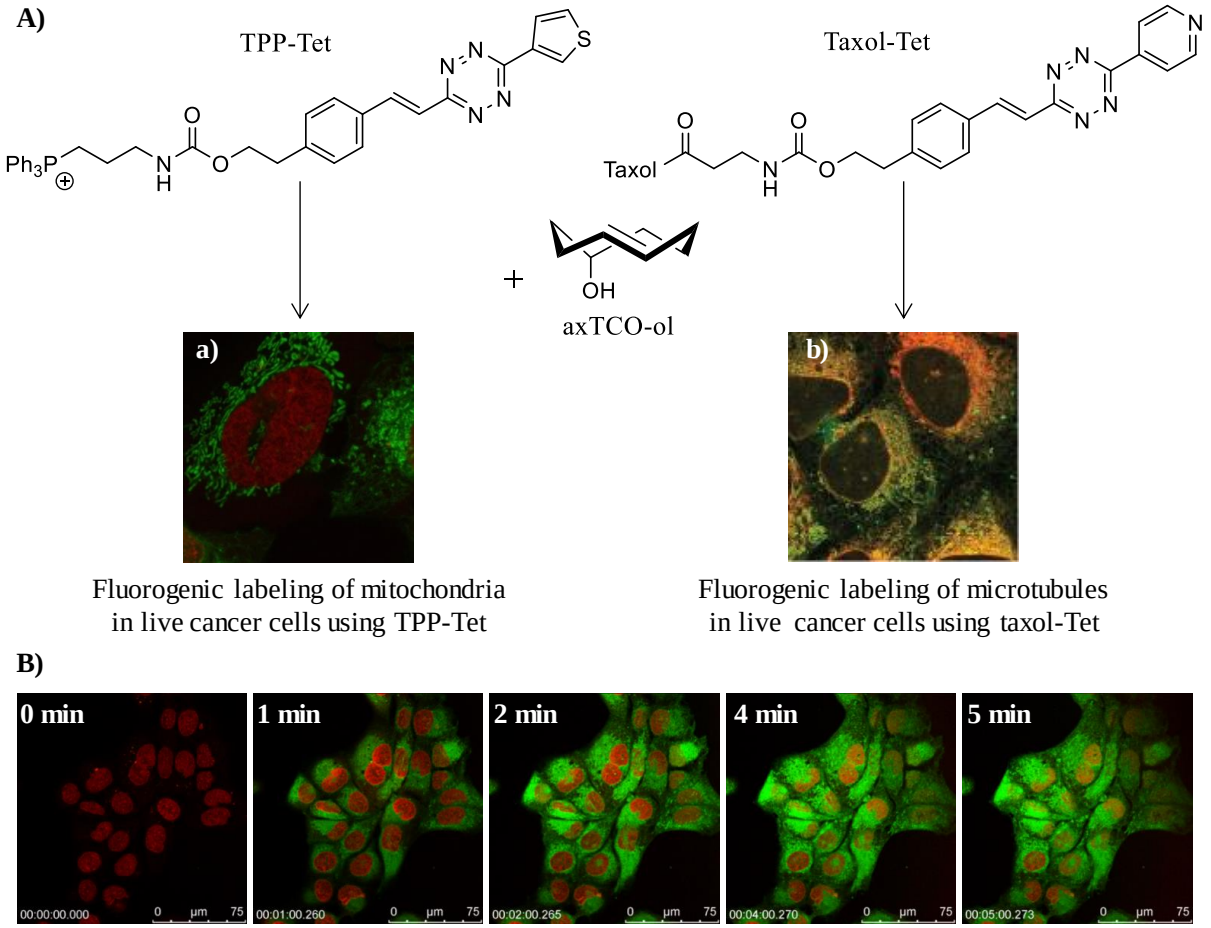


**Figure 20:** Live cell labeling experiments in U2OS cells. A) Confocal microscope images of U2OS cells treated with mitochondrion-selective TPP-Tet or microtubule-selective taxol-Tet after subsequent addition of axTCO-ol; a) Merged channel image with TPP-Tet after co-staining of the nucleus. The nucleus was stained with DRAQ5 dye; b) Image of the co-localization experiment with Taxol-Tet using Tubulin tracker. B) Time-lapse of the TPP-Tet-based live cell labeling. Pictures of the time-lapse experiment were taken at indicated time points after addition of axTCO-ol.

# 2. Aim of the thesis

Recently, our group developed a novel type of fluorogenic tetrazine cycloadditions between various 1,2,4,5-tetrazines and particular *trans*-cyclooctene dienophiles.[155] The formation of the fluorophores is an inherent result of this chemical reaction so that attachment of additional fluorophores to the reagents is not needed. Based on this discovery, the main goal of the present thesis is to enhance this methodology by expanding it to other TCOs and heterodienes and thus to establish a more general approach for fluorogenic labeling based on this concept.

In our initial work we showed that the cycloaddition between axTCO-ol and various 1,2,4,5-tetrazines leads to the direct formation of fluorescent 1,4-dihydropyridazine products. However, the fluorogenic character of the reaction was observed only when the unmodified axial isomer of TCO-ol was used as dienophile. Addition of other substituents or functionalization of the hydroxy group of axTCO-ol resulted in decrease or even complete loss of the fluorogenicity. Therefore, the first aim of this thesis is to design and synthesize new TCO derivatives that are amenable to further derivatization, while preserving the fluorogenic properties of the reaction. We intend to address it by fusing an aziridine ring to the TCO structure (aza-TCO). Based on our previous observation that the presence of a heteroatom in the right conformation is responsible and therefore essential for the formation of the fluorescent product, we expect the introduced nitrogen atom of the aziridine to ensure the fluorogenicity in cycloadditions with tetrazines.[155] In addition, aza-TCOs are speculated to adopt a highly strained “half-chair” conformation, which is known to significantly increase the reactivity of TCOs in iEDDA reactions with tetrazines.[115]
Since a variety of other TCO derivatives exist and are nowadays even commercially available, the next goal of this work is to develop an alternative and more general strategy, which extends the range of applicable dienophiles for this type of fluorogenic tetrazine ligations. For this purpose, we decided to screen a series of 1,2,4,5-tetrazines bearing various substituents in order to find derivatives leading to fluorescent compounds in reactions with virtually any strained dienophile.

Another aim of this thesis is to evaluate other heterodienes, namely 1,2,3-[142a, 142b] and 1,2,4-triazines,[139-140] as potential reaction partners for cycloadditions with strained dienophiles. Although both types of triazines are reported to be less reactive in cycloaddition reactions when compared to 1,2,4,5-tetrazines, they exhibit other interesting characteristics

such as increased stability and biocompatibility and excellent chemo- and regio-selectivity. In order to explore the potential use of these types of triazines in bioorthogonal labeling applications, systematic studies of the influence of their structure on the performance in cycloadditions with various dienophiles should be performed. Furthermore, it is planned to evaluate optimal reaction conditions and the biocompatibility of reagents as well as of the products.

# 3. Results and publications

## 3.1 Design and Synthesis of Aza-Bicyclononene Dienophiles for Rapid Fluorogenic Ligations

S.J. Siegl*, A. Vázquez*, R. Dzijak, M. Dračínský, J. Galeta, R. Rampmaier, B. Klepetářová, M. Vrabel, *Chem. Eur. J.* **2018**, 24, 2426-2432.

*: These authors contributed equally to this work.



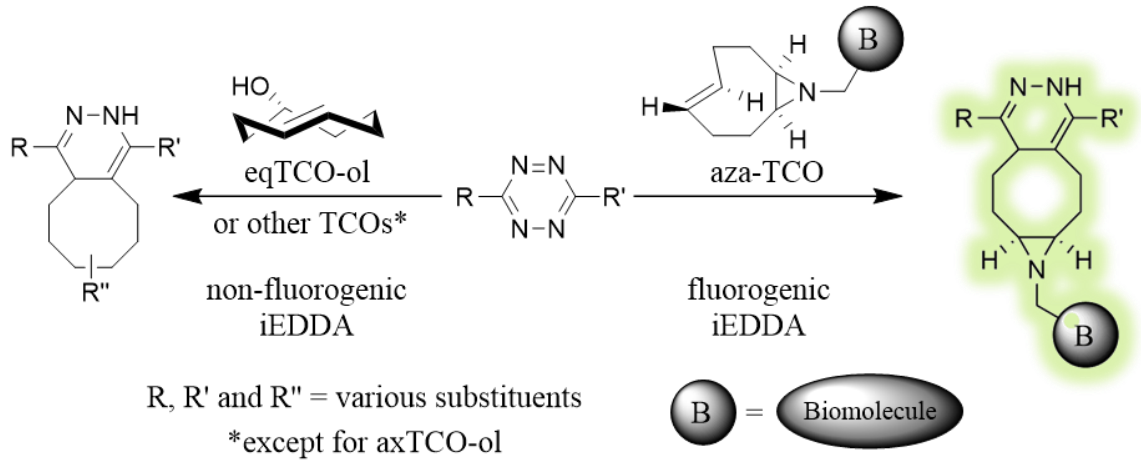


### 3.1.1 Background

Although we were able to successfully apply our recently discovered fluorogenic tetrazine ligation to bioimaging, its broader utility was limited to the use of unmodified axTCO-ol as the dienophile.[155] Therefore, the goal of this study was to design new TCO derivatives featuring such fluorogenicity even when modified with various functional groups. During our previous study of the iEDDA reactions between tetrazines and both TCO-ol isomers, we performed detailed NMR and DFT calculation analyses of the transition state structures of these tetrazine ligations. The data showed that the presence of a heteroatom in the right conformation is responsible and hence crucial for the formation of the fluorescent product.[155] Based on these results, we developed herein new TCO derivatives bearing an additional aziridine ring (aza-TCO), which is fused to the cyclooctene moiety, as alternative dienophiles for fluorogenic tetrazine ligations. We demonstrated that the nitrogen atom in the aziridine

moiety indeed ensures the fluorogenic properties even when the TCO is modified with different functional groups.

### 3.1.2 Declaration of contribution

In the course of my master thesis, I started with the design and synthesis of the novel aziridine-fused TCO derivatives, which I finished together with *Dr. Arcadio Vázquez* and *Dr. Milan Vrábel* during this PhD project. Other known TCOs, tetrazines and triazines used during this work were prepared by *Dr. Arcadio Vázquez*, *Dr. Milan Vrábel* and me. Computational studies as well as detailed NMR experiments for the theoretical design of aza-TCO and analysis of its fluorescent product with di-phenyl-*s*-tetrazine were carried out by *Dr. Martin Dračínský*. X-ray analysis of the *N*-tosylated aza-TCO crystals was done by *Dr. Blanka Klepetářová*. I performed all cycloaddition reactions between the various TCOs and 1,2,4,5-tetrazines or 1,2,4-triazines and verified the formation of the corresponding click products by HPLC-MS measurements. I further measured the photophysical properties of the products and performed the kinetic studies in order to determine the second-order rate constants. Stability studies of aza-TCO as well as its click products with diphenyl-*s*-tetrazine and dipyridyl-*s*-tetrazine by NMR and HPLC-MS analysis were performed in collaboration with *Dr. Martin Dračínský* and *Dr. Milan Vrábel*. Furthermore, I carried out the fluorogenic labeling experiments on the model peptide and model proteins. The model peptide was synthesized by *Robert Rampmaier* and the two model proteins were kindly provided by *Dr. Pavlína Řezáčová* (hCAII) and *Dr. Dominika Chalupská* (Arf1). The cell labeling experiments were performed by *Dr. Rastislav Dzijak*. Together with *Dr. Juraj Galeta*, I synthesized the functionalized aza-TCO and 1,2,4,5-tetrazine derivatives for all fluorogenic labeling experiments. I actively participated in writing the manuscript.

ChemPubSoc Europe

DOI: 10.1002/chem.201705188

CHEMISTRY A European Journal Full Paper

Biological Chemistry

# Design and Synthesis of Aza-Bicyclononene Dienophiles for Rapid Fluorogenic Ligations

Sebastian J. Siegl[+], Arcadio Vázquez[+], Rastislav Dzijak, Martin Dračínský, Juraj Galeta, Robert Rampmaier, Blanka Klepetářová, and Milan Vrabel*[a]

**Abstract:** Fluorogenic bioorthogonal reactions enable visualization of biomolecules under native conditions with excellent signal-to-noise ratio. Here, we present the design and synthesis of conformationally-strained aziridine-fused *trans*-cyclooctene (aza-TCO) dienophiles, which lead to the formation of fluorescent products in tetrazine ligations without the need for attachment of an extra fluorophore moiety. The presented aza-TCOs adopt the highly strained "half-chair" conformation, which was predicted computationally and confirmed by NMR measurements and X-ray crystallography. Kinetic studies revealed that the aza-TCOs belong to the most reactive dienophiles known to date. The potential of the newly developed aza-TCO probes for bioimaging applications is demonstrated by protein labeling experiments, imaging of cellular glycoconjugates and peptidoglycan imaging of live bacteria.

## Introduction

Fluorogenic bioorthogonal reactions have emerged as a powerful tool for bioimaging because they offer an excellent signal-to-noise ratio without the need to use extensive washing steps.[1] Significant progress has been made in the development of probes which can be activated by means of a selective chemical reaction in a complex biological environment. These include Staudinger ligation,[2] azide-alkyne cycloadditions,[3] light-triggered nitrilimine-alkene cycloadditions[4] and tetrazine ligations.[5] In most cases, the fluorogenic probe contains an appropriately modified fluorophore moiety with its fluorescence being quenched through energy transfer and being restored upon the bioorthogonal chemical reaction. A much less common situation represents fluorogenic ligations in which the formation of the fluorophore is an inherent result of the chemical reaction. One particular advantage of these types of probes is the absence of virtually any background fluorescence signal because no real pre-fluorophore (or any quenched fluorophore moiety) is present in the structure of reagents before the reaction takes place. One of the prominent examples of this type of reaction is the formation of pyrazolines upon cycloaddition of nitrilimines with alkenes.[6] Shang et al. recently reported a conceptually similar styrene-tetrazine cycloaddition leading to fluorescent dihydropyridazines.[7] In parallel to the later study, we have shown that the inverse electron-demand Diels–Alder reaction (IEDDA) of 1,2,4,5-tetrazines with *trans*-cyclooctene (TCO) dienophiles can also directly lead to the formation of fluorescent products. In particular, we found that the axial *trans*-cyclooctene-5-ol (ax-TCO-ol) upon reaction with various tetrazines leads to the formation of fluorescent dihydropyridazines with tuneable photophysical properties.[8] Although we could demonstrate the power of this chemistry for bioimaging, we also found that by modifying the hydroxyl group of the ax-TCO-ol, the fluorogenic properties of the reaction alter or even completely disappear. For many reasons, it would be advantageous to maintain the fluorogenic nature of the reaction while enabling attachment of various useful functional groups to, for example, biomolecules. The aim of the present study was to design new TCO derivatives, which would fulfill these criteria. Here, we show that by *cis*-fusion of an aziridine ring to the *trans*-cyclooctene skeleton a new type of highly reactive dienophiles are formed, which produce fluorescent products in IEDDA reaction with tetrazines. In addition, our kinetic measurements show that these strained alkenes belong to the most reactive bioorthogonal probes known to date. Their excellent reactivity is a result of the highly strained "half-chair" conformation, which was confirmed by NMR measurements and, to the best of our knowledge, for the first time also by X-ray crystallography.

## Results and Discussion

### Rational design of aza-TCOs and computational methods

Our previous in silico conformational analysis and DFT modelling of transition state structures of the reaction between ax-TCO-ol and diphenyl-*s*-tetrazine showed that the hydroxyl oxygen atom of TCO is very close to one of the bridgehead hydrogen atoms in a low energy conformer of the IEDDA prod-

[a] S. J. Siegl,[+] Dr. A. Vázquez,[+] Dr. R. Dzijak, Dr. M. Dračínský, Dr. J. Galeta, R. Rampmaier, Dr. B. Klepetářová, Dr. M. Vrabel
Institute of Organic Chemistry and Biochemistry of the Czech Academy of Sciences, Flemingovo nám. 2, 16610, Prague 6 (Czech Republic)
E-mail: vrabel@uochb.cas.cz

[+] These authors contributed equally to this work.

Supporting information and the ORCID number(s) for the author(s) of this article can be found under https://doi.org/10.1002/chem.201705188.

uct.[8] These calculations show that the conformation of the intermediate 4,5-dihydropyridazine promotes hydrogen migration to the hydroxyl oxygen, which results in the formation of the final 1,4-dihydropyridazine fluorophore. This means that the presence of a heteroatom in the right conformation is responsible for the rapid tautomerization of the dihydropyridazine and for the formation of fluorescent products. We therefore speculated that fusion of an aziridine ring to *trans*-cyclooctene would ensure the fluorogenicity of the reaction by introducing the required heteroatom in the right position. In addition, this should also force the *trans*-cyclooctene ring to adopt the highly strained "half-chair" conformation, which is known to enhance the rate of the IEDDA reaction dramatically.[9] With this hypothesis in mind, we performed a computational study with two aims: 1) to predict the most favourable conformation of aza-TCO compound **1 a** and 2) to predict the propensity of aza-TCO to form fluorescent products. The conformational analysis of compound **1 a** was performed with 100 molecular-mechanics simulated annealings. In 97 out of the 100 simulations, the resulting structure had the desired "half-chair" conformation depicted in Figure 1 A. The "half-chair" conformation of **1 a** was also retained after geometry optimization by the DFT method (Figure 1 A and the Supporting Information).

The expected first step in the reaction sequence of compound **1 a** with 1,2,4,5-tetrazines is the IEDDA reaction followed by nitrogen elimination, which provides 4,5-dihydropyridazine intermediate **1 a-II** (Figure 1 C). The transition state structures were predicted by DFT computations for both of these reactions starting from compound **1 a** and diphenyl-*s*-tetrazine and the energy barriers toward intermediates **1 a-I** and **1 a-II** were found to be 12.1 and 8.3 kcal mol$^{-1}$, respectively. The key reaction step found previously for the formation of a 1,4-dihydropyridazine fluorophore involved a hydrogen atom transfer from one of the bridgehead carbon atoms to a heteroatom. This hydrogen atom transfer was only possible for conformations with short distances between the hydrogen atom and the heteroatom. Therefore, we performed conformational analysis of compound **1 a-II** by simulated annealing followed by DFT geometry optimization, which revealed that a low-energy conformer of **1 a-II** has the bridgehead hydrogen-aziridine nitrogen distance of 2.29 Å, which is suitable for the hydrogen atom migration to take place. The transition-state structure and a modest energy barrier (10 kcal mol$^{-1}$ from the suitable conformation, 16 kcal mol$^{-1}$ from the lowest-energy conformation of **1 a-II**) for the hydrogen atom migration to the nitrogen atom were found by DFT calculations. Compound **1 a-II** protonated at one of the pyridazine nitrogen atoms was considered in the transition-state search. The hydrogen atom migration step is possible also for neutral compound **1 a-II**; however, the reaction barrier is higher by 18 kcal mol$^{-1}$ (see details in the Supporting Information). The computational study thus corroborates our presumption of both the "half-chair" conformation of **1 a** and its tendency to promote the formation of fluorescent 1,4-dihydropyridazines in reaction with 1,2,4,5-tetrazines. For comparison, we also performed the transition-state search for the hydrogen atom migration reaction for dioxolane fused TCO (d-TCO), which also contains a heteroatom and adopts the highly strained "half-chair" conformation as reported previously.[9d] The calculated reaction barrier was found to be significantly higher (28 kcal mol$^{-1}$) than for compound **1 a-II** (see the Supporting Information) showing that it is the unique structure of aza-TCOs, which leads to the formation of fluorescent products by promoting the dihydropyridazine tautomerization. This unique behavior of aza-TCO was confirmed also experimentally (Figure S8 in the Supporting Information).

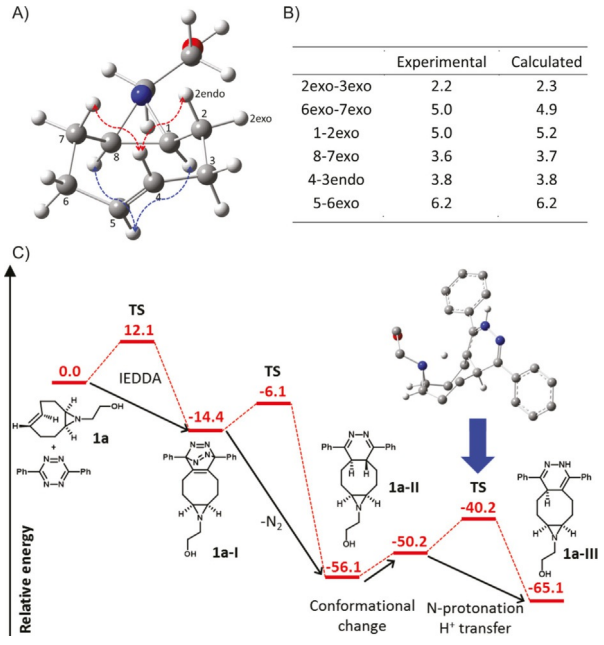


**Figure 1.** A) Lowest-energy conformation found by molecular modelling together with the most important experimental NOE contacts (indicated by arrows) confirming the half-chair conformation of **1 a**. B) Selected experimental and calculated (B3LYP/6–31 + g(d,p)/PCM) vicinal coupling constants (Hz) between hydrogen atoms in **1 a**. C) The proposed reaction pathway for the reaction of **1 a** with diphenyl-*s*-tetrazine leading to fluorescent product **1 a-III** and the transition-state structure.

## Synthesis of aza-TCOs

Encouraged by these computational results, we next focused on the synthesis of the aziridine-fused *trans*-cyclooctene. In our initial synthesis, we utilized Sharpless aziridination,[10a] which yielded the desired *N*-tosyl-protected aziridine **3** in a single step (Scheme 1).[10b] Compound **3** was then conveniently converted to the corresponding *trans*-isomer **4** by the continuous flow-photoisomerization protocol developed by Fox and co-workers.[11] Unfortunately, our attempts to efficiently remove the tosyl group using sodium naphthalenide[12] were unsuccessful and led only to concomitant *trans*-to-*cis* isomerization of (1*R*,8*S*,*E*)-9-azabicyclo[6.1.0]non-4-ene **5**. We therefore used a different strategy and started the synthesis from known (*Z*)-9-oxabicyclo[6.1.0]non-4-ene **6**. Opening of the epoxide afforded azido alcohol **7**, which was converted to the corresponding aziridine **8** by the Staudinger reduction-cyclization reaction using triphenylphosphine.[13] This sequence of reaction steps leads to *cis*-ring fusion, which is known to induce the "half-

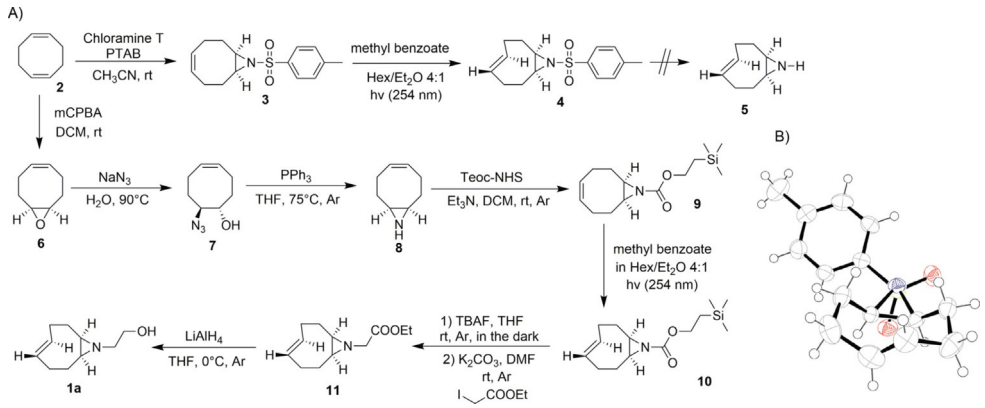


**Scheme 1.** A) Synthesis of aza-TCOs. B) An ORTEP view of the major enantiomer of compound **4** (displacement ellipsoids shown with 50% probability; CCDC 1553867).[10b]

chair" conformation in bicyclononenes.[9a,c] The next crucial step in the synthesis was the protection of the aziridine nitrogen atom. After extensive experimentation, we found that the trimethylsilylethoxycarbonyl (Teoc) protecting group enables efficient photoisomerization and subsequent mild deprotection to yield compound **5**. Alkylation of the aziridine nitrogen afforded ethyl ester **11**, which was reduced by $LiAlH_4$ to the desired 2-((1*R*,8*S*,*E*)-9-azabicyclo[6.1.0]non-4-en-9-yl)ethan-1-ol **1a**. Considering that the conformation of the *trans*-cyclooctene ring is crucial for its reactivity, we performed conformational analysis of compound **1a** by NMR spectroscopy. All proton and carbon NMR signals were assigned by a combination of 1D and 2D NMR experiments and all observable proton-proton spin-spin coupling constants were determined. The experimental coupling constants are in excellent agreement with those calculated by using the DFT method for the lowest-energy (half-chair) conformer of **1a** (Figure 1B). The "half-chair" conformation of **1a** was further confirmed by nuclear Overhauser effect spectroscopy (NOESY); the most important NOE contacts for the determination of the conformation are depicted in Figure 1A. In addition, *N*-tosylated bicyclononene **4** was a crystalline compound which afforded crystals suitable for X-ray analysis and further confirmed the "half-chair" conformation. The compound crystalized as a mixture of two enantiomers in a 6:4 ratio (Scheme 1B and the Supporting Information, Figure S2).

## Reactivity of aza-TCOs and photophysical properties of the click products after reaction with 1,2,4,5-tetrazines

As already predicted by the computations, the new aza-TCO dienophile **1a** yields fluorescent products in the IEDDA reaction with tetrazines similarly to the previously reported ax-TCO-ol.[8] A series of experiments and calculations confirmed the identity of 1,4-dihydropyridazines as the actual fluorescent species formed during the reaction (see the Supporting Information). We determined the photophysical properties of the corresponding click products, which are summarized in Table 1. The dihydropyridazine products **13a–e** have large Stokes shifts and tunable emission maxima depending on the substitution pattern of the starting tetrazine (Figure S7 in the Supporting Information). The fluorescence enhancement upon the reaction ranges from 20- to an excellent 70-fold. The fluorescence quantum yields are relatively low when compared to the more commonly used fluorophores (e.g., fluorescein $\phi_{fl}=$ ca. 0.9 in 0.1 M NaOH)[14] however, still sufficient for bioimaging applications as we show below.

The second order rate constants of the reaction between **1a** and tetrazines **12a–e** were determined. The kinetic measurements were performed under pseudo first-order conditions using an excess of the dienophile. The decrease in concentration of the starting tetrazine was followed in time by measuring the decrease in its absorbance by UV/Vis spectroscopy. All measurements were carried out at least in triplicate and the average rate constants are summarized in Table 1 (for details, see the Supporting Information). The second order rate constants range from 250 $M^{-1}s^{-1}$ to more than 6000 $M^{-1}s^{-1}$ (in MeOH at 21 °C), highlighting the exceptional reactivity of **1a**. The aza-TCO showed good reactivity toward 1,2,4-triazines as well, which were recently shown to be a good alternative to the more commonly used 1,2,4,5-tetrazines (Table S10 in the Supporting Information).[15]

Furthermore, we used some of the known TCO derivatives to directly compare their reactivity with **1a**. We used diphenyl-*s*-tetrazine as the heterodiene in this case (Figure 2). Our data show that **1a** reacts about 20 times faster than simple ax-TCO-ol (Table S9 in the Supporting Information), which we have used previously in fluorogenic cell labeling experiments.[8]

Compound **1a** reacts about 1.5 times faster than the dioxolane-fused TCO (d-TCO) reported by Fox and co-workers.[9d] The only derivative, which exceeded **1a** in reactivity (about 3 times), was the cyclopropyl-fused *trans*-cyclooctene (s-TCO) developed by the same group.[9c] These data clearly show that fusion of an aziridine ring to *trans*-cyclooctenes yields highly reactive dienophiles belonging to the fastest reacting bioorthogonal probes known to date.

## Stability of aza-TCOs and the click products under biologically relevant conditions

We then studied the stability of the newly developed dienophile under various conditions. Compound **1a** showed excel-

**Table 1.** Photophysical properties of click products and second-order rate constants of the reaction between 1,2,4,5-tetrazines and aza-TCO **1a**.

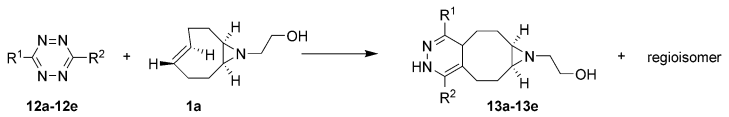


| Entry | Tetrazine | Click product | $R^1$ | $R^2$ | Fluorescence of the click product[a] | $\lambda_{Abs}/\lambda_{Em}$[b] | Stokes shift[b] | $\phi_{fl}/\varepsilon_{max}$[c] | Intensity increase | $k_2$ ($M^{-1}$ $s^{-1}$)[d] |
|---|---|---|---|---|---|---|---|---|---|---|
| 1 | **12a** | **13a** |  |  |  | 317/478 | 161 | 0.06/12 | 20-fold | 6360 ± 90 |
| 2 | **12b** | **13b** |  | 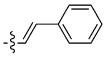 | 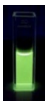 | 333/501 | 168 | 0.07/21 | 60-fold | 318 ± 3 |
| 3 | **12c** | **13c** |  | 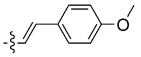 |  | 321/475 | 154 | 0.15/16 | 55-fold | 255 ± 7 |
| 4 | **12d** | **13d** |  | 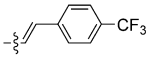 |  | 337/540 | 203 | 0.04/23 | 40-fold | 316 ± 2 |
| 5 | **12e** | **13e** |  | 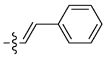 | 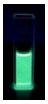 | 335/489 | 154 | 0.11/17 | 70-fold | 740 ± 25 |

[a] Pictures were captured in quartz cuvettes using a hand-held UV lamp (365 nm), [b] given in nm, [c] extinction coefficients $\varepsilon_{max}$ are in $10^3$ $M^{-1}$ $cm^{-1}$, quantum yields were determined using quinine sulfate in 0.5 M $H_2SO_4$ as standard, [d] kinetic measurements were performed in MeOH at room temperature under pseudo first-order conditions using an excess of **1a** (for details, see the Supporting Information).

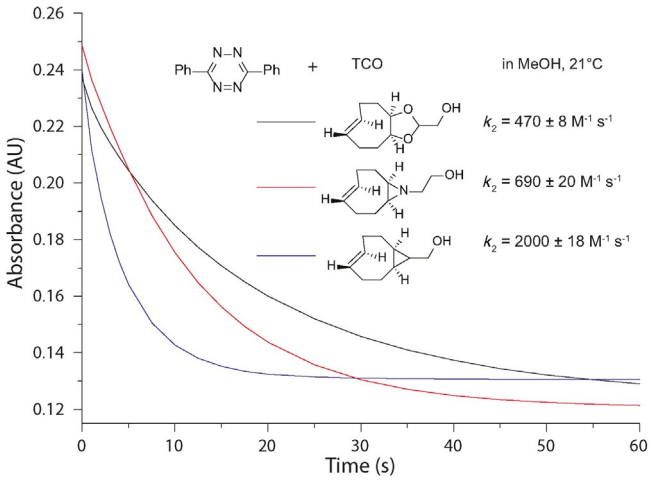


**Figure 2.** Comparison of the reactivity of various TCOs in reaction with diphenyl-*s*-tetrazine measured in MeOH at 21 °C using manual stopped-flow device connected to the UV/Vis spectrophotometer.

lent stability when stored in the dark at room temperature as a solution in $CD_3OD$ (Figure S9 in the Supporting Information). The stability of the compound in the presence of L-cysteine, which is known to promote the *trans*-to-*cis* isomerization of TCOs,[9d,16] was also very good. A 1:1 mixture of *cis* and *trans* isomers was obtained in 7 days after subjecting compound **1a** to 3.5 equivalents of L-cysteine at neutral pH in deuterated phosphate buffer (Figure S10 in the Supporting Information). We also examined the stability of the click products. The 1,4-dihydropyridazines formed upon reaction of **1a** with diphenyl-*s*-tetrazine or dipyridyl-*s*-tetrazine are stable under various conditions (e.g., phosphate buffered saline, fetal bovine serum) for several days. HPLC-MS analysis showed that the corresponding fully aromatic pyridazines are formed as major "side" products in this case. Our data show that the click product of diphenyl-*s*-tetrazine oxidizes faster than the click product of dipyridyl-*s*-tetrazine (Figure S11 in the Supporting Information).

## Fluorogenic labeling of peptides

To evaluate the performance of **1a** as a bioorthogonal handle for fluorogenic biomolecule tagging, we first performed labeling experiments on a model peptide. Our attempts to prepare the active ester directly from **1a** failed, giving under various reaction conditions a mixture of products. Similarly, the hydrolysis of ethyl ester **11** also did not afford the desired carboxylic acid derivative. Fortunately, the structural features of aza-bicyclononene **5** enable a straightforward synthesis of its derivatives by simple alkylation of the free aziridine nitrogen atom. After optimization, we prepared the active ester of aza-TCO using methyl 4-(bromomethyl)benzoate as the alkylating agent followed by reduction of the ester to the corresponding alco-

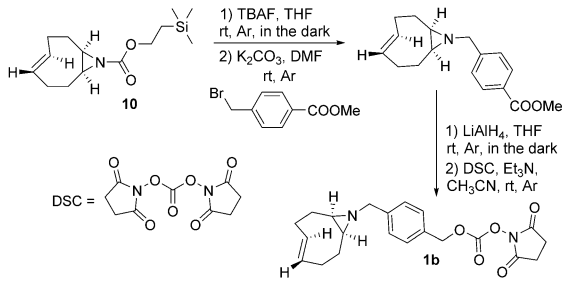


**Scheme 2.** Synthesis of aza-TCO active ester **1 b**.

hol and finally by reaction with *N*,*N*′-disuccinimidyl carbonate (Scheme 2 and the Supporting Information). Active ester **1 b** was first reacted with the model peptide (KYHWYGYTPQNVI) containing an N-terminal lysine. The final aza-TCO-modified peptide, still attached to the resin (Tentagel-OH), was treated with various tetrazines (**12 b**, **c** and **e**) and the formation of fluorescent products was verified using fluorescence microscopy (Figure 3 and Figure S12 in the Supporting Information). We observed the successful formation of the desired click products in all cases, which was also confirmed by HPLC-MS analysis (Figure S13–S17). Our previous experiments with the ax-TCO-ol showed that the fluorogenic properties of the reaction under these conditions alter or even completely disappear.[8] Aza-TCOs are therefore superior compounds for fluorescent peptide labeling applications.

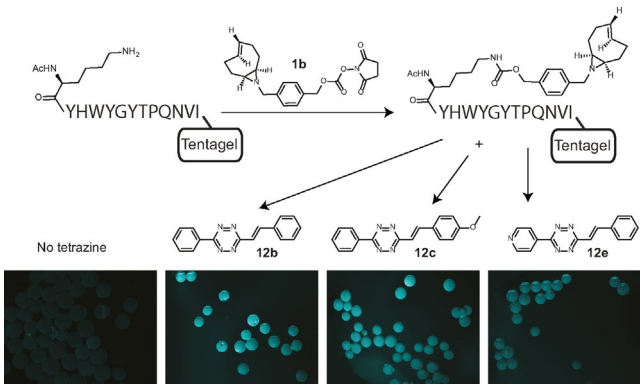


**Figure 3.** The fluorogenic click reaction was performed on a model peptide modified with aza-TCO **1 b** using various tetrazine probes. Pictures were captured under a fluorescence stereomicroscope at 350 nm irradiation using CoolLED p*E*-300 light source and the following setup in each case: Exposure time 300 ms, IL light intensity 1000 and objective 1x/0.08. Colors were finally adjusted using LAS AF Lite program.

## Fluorogenic labeling of proteins

The active ester-mediated protein modification still belongs to the most frequently applied methodology for covalent protein modification.[17] Alternatively, a cysteine-maleimide reaction can be used for this purpose.[18] We performed a series of experiments to probe aza-TCO derivatives for the fluorogenic labeling of proteins. We first modified human carbonic anhydrase II (hCAII) with the active ester **1 b** under standard conditions and added tetrazine **12 c** to the protein (Figure 4 and Figure S18 in the Supporting Information). We also used a biotin-conjugated tetrazine probe **12 f**, which enables double detection after the reaction, namely by spectrophotometry, based on the formation of the fluorescent dihydropyridazine, and by western blot analysis due to the presence of the biotin moiety. SDS-PAGE analysis of the reaction mixtures showed that the reaction proceeded efficiently and the fluorescently-labeled products were clearly visible after UV irradiation of the gel (Figure 4 A). The presence of the biotin was successfully confirmed by western blot analysis using fluorescein-conjugated streptavidin. The fluorogenicity, which is an intrinsic property of the chemical reaction, thus facilitates straightforward detection of the reaction products and should enable the development of for example, multimodal detection probes similar to **12 f**.

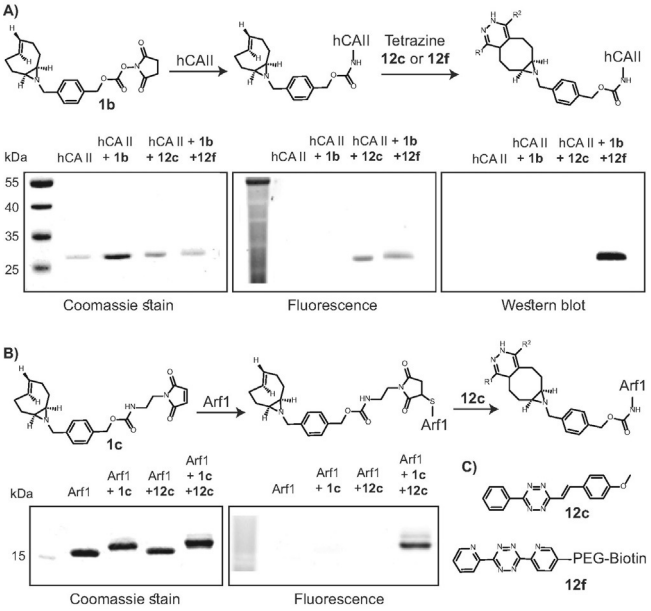


**Figure 4.** Fluorogenic labeling of A) aza-TCO-modified hCAII using tetrazine **12 c** and **12 f**; and B) Arf1 protein using maleimide and subsequent reaction with tetrazine **12 c**. C) Tetrazines **12 c** and **12 f**.

We then used ADP-ribosylation factor 1 protein (Arf1), which was prepared using standard recombinant techniques.[19] Arf1 contains a single cysteine residue, which was used for the attachment of aza-TCO using maleimide **1 c**. The success of the reaction after addition of **12 c** was evident from the shift of the protein band on SDS-PAGE gel as well as after spectrophotometric imaging (Figure 4 B and Figure S19 in the Supporting Information). These experiments manifest that aza-TCOs are useful bioconjugation reagents enabling efficient fluorogenic tagging of proteins.

## Fluorogenic labeling of glycoconjugates on U2OS cancer cells

We next turned our attention to cell labeling experiments to further demonstrate the potential of aza-TCOs for bioimaging applications. First, we attached the aza-TCO moiety to concanavalin A (ConA). ConA is a lectin which shows high specificity for α-D-mannose- and α-D-glucose-containing glycoconjugates

and is useful in carbohydrate studies.[20] To compare the performance of aza-TCO with the previously reported ax-TCO-ol, we also conjugated two different axial TCOs to ConA. Derivative **1d** is attached to ConA through a carbamate linker, in difference to the peptide bond of **1e**. We next separately added the three TCO-modified ConAs to fixed and permeabilized U2OS cancer cells to enable intracellular glycoconjugate staining after addition of **12c**.

We used fluorescein-tagged tetrazine **12g** as a positive control in this experiment as this compound yields fluorescent products in each case. The formation of fluorescent products was verified by inspecting the cells under a confocal microscope (Figure 5 and Figure S21 in the Supporting Information). Our experiment confirmed the superior performance of the newly developed aza-TCO. ConA modified with **1b** gave the most intensive labeling when compared to ConA modified with either **1d** or **e**, although a weak staining of glycoconjugates was visible in these cases as well. On the other hand, equal staining of the cells was observed when we used FITC-tetrazine derivative **12g** under the same conditions (Figure 5B and Figure S21 in the Supporting Information).

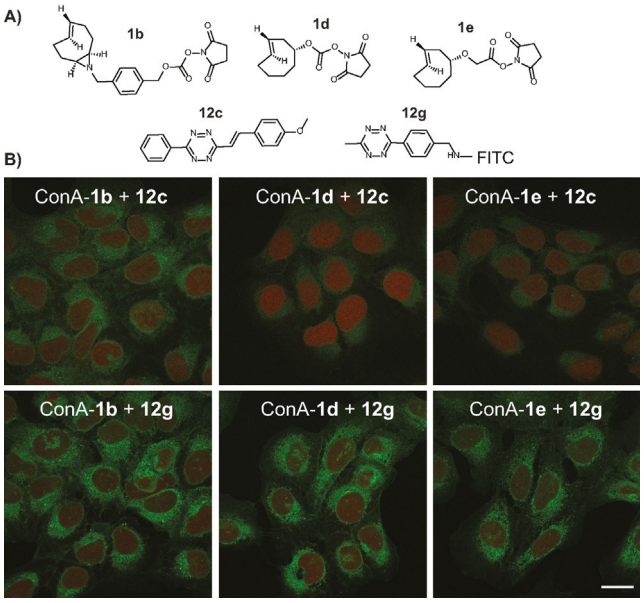


**Figure 5.** A) Structures of active esters used to modify ConA and structure of tetrazines **12c** and **12g** used for labeling. B) Confocal microscope images of fluorogenic U2OS cell labeling using ConA modified with TCOs **1b**, **d**, **e** and tetrazine **12c** or FITC-conjugated tetrazine **12g**. Conditions: The cells were fixed, permeabilized and incubated for 1 hour with the respective TCO-modified ConA (0.25 $\mu g\,\mu L^{-1}$). After washing, the cells were incubated with 0.25 mM tetrazine and 5 μM DRAQ5 for 10 min and imaged under confocal microscope. Click product (ex.: 405 nm, em.: 560–666 nm); FITC channel (ex.: 458 nm, em.: 490–552 nm); the nucleus was stained with DRAQ5 (ex.: 633 nm, em.: 653–732 nm). Scale bar: 20 μm.

### Fluorogenic imaging of peptidoglycans in live bacteria

Various derivatives of D-amino acids can be incorporated into the peptidoglycans (PGs) of diverse bacterial species and can be used as valuable chemical probes providing information about dynamics, synthesis and maturation of PGs.[21] To test if our aza-TCOs could serve as a reporter molecule for similar application, we prepared the aza-TCO modified D-amino acid **1f** (see the Supporting Information). The gram-positive Bacillus subtilis were first grown in the presence of **1f** for 2 hours. Similarly, gram-negative *E. coli* cells were grown in the presence of **1f** for different period of time (2, 6 or 12 hours). Incorporation of the amino acid into PGs was subsequently validated under confocal microscope after labeling with the fluorogenic BODIPY-tetrazine probe **12h**. We observed a fluorescent signal on the surface of the bacteria after incubation with **1f** and labeling with **12h**, whereas no fluorescence formed in cells incubated only with the amino acid **1f** or tetrazine **12h** under the same conditions (Figure 6B–C and Figures S22 and S23 in the Supporting Information). Weak fluorescent signal formed in *E. coli* cells even after 12 hours of incubation with **1f** and subsequent labeling with **12h** shows that at least part of the modified amino acid remains in the highly reactive *trans*-conformation within this time period. These experiments further demonstrate that the aza-TCO moiety can serve as valuable reporter group for various bioimaging applications. The high reactivity accompanied with good stability favors aza-TCOs for experiments in which both of these attributes are important and desirable.

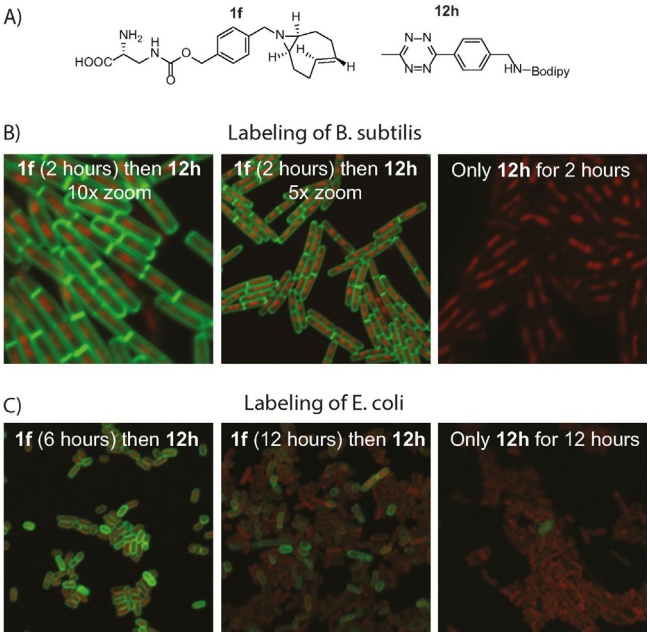


**Figure 6.** A) Structure of D-amino acid **1f** and tetrazine-bodipy **12h**. B, C) confocal microscope images of fluorogenic bacterial cell wall labeling using **1f** and **12h**. Conditions: Live B. subtilis or *E. coli* cells were incubated with **1f** (1 mM) for the indicated time. After washing, the cells were incubated for 15 min with **12h** (25 μM) and 50 μM DRAQ5. The cells were then inspected under confocal microscope using the following set up: nucleus was stained with DRAQ5 (ex.: 633 nm, em.: 653–732 nm) and click product resulting from the reaction (ex.: 458 nm, em.: 499–569 nm). 5x and 10x zoom for B. subtilis, 10x zoom for E.coli.

## Conclusion

In this study, we present the design and synthesis of aziridine-fused *trans*-cyclooctene derivatives, which produce fluorescent

products in reaction with 1,2,4,5-tetrazines. The newly developed dienophiles adopt the "half-chair" conformation as a result of the *cis*-ring fusion of the aziridine moiety. This highly strained conformation leads to remarkable reactivity in the IEDDA reactions making these compounds one of the most reactive bioorthogonal probes known to date. Despite their high reactivity, these compounds show good stability under various conditions. Stability of the corresponding click products was found to be excellent as well. We demonstrate the potential of aza-TCOs in fluorogenic ligation reactions by the labeling of model biomolecules and by cell imaging experiments. The exceptional reactivity together with the intrinsic formation of fluorescent products upon reaction with simple tetrazines make aza-TCO dienophiles attractive candidates for fluorogenic biomolecule tagging and bioimaging applications.

## *Acknowledgements*

This work was supported by the Czech Science Foundation (P207/15-06020Y, for M.V.), Ministry of Education, Youth and Sports of the Czech Republic (project LO1304, program "NPU-I", for M. D.) and by the European Research Council (ERC) under the European Union's Horizon 2020 research and innovation programme (grants agreement No 677465, for M.V.). We thank A. M. Downey for critical reading of the manuscript. We acknowledge the kind donation of hCAII (P. Řezáčová), Arf1 (D. Chalupská) used in model protein labeling experiments and B.subtilis provided by K. Stříšovský lab.

## Conflict of interest

The authors declare no conflict of interest.

**Keywords:** cell labeling · Diels–Alder reaction · fluorogenic · tetrazines · *trans*-cyclooctene

[1] a) A. Nadler, C. Schultz, *Angew. Chem. Int. Ed.* **2013**, *52*, 2408 – 2410; *Angew. Chem.* **2013**, *125*, 2466 – 2469; b) G. B. Cserép, A. Herner, P. Kele, *Methods Appl. Fluoresc.* **2015**, *3*, 042001.

[2] a) M. J. Hangauer, C. R. Bertozzi, *Angew. Chem. Int. Ed.* **2008**, *47*, 2394 – 2397; *Angew. Chem.* **2008**, *120*, 2428 – 2431; b) G. A. Lemieux, C. L. De Graffenried, C. R. Bertozzi, *J. Am. Chem. Soc.* **2003**, *125*, 4708 – 4709.

[3] a) F. Friscourt, C. J. Fahrni, G. J. Boons, *J. Am. Chem. Soc.* **2012**, *134*, 18809 – 18815; b) A. Herner, I. Nikic, M. Kallay, E. A. Lemke, P. Kele, *Org. Biomol. Chem.* **2013**, *11*, 3297 – 3306; c) C. Le Droumaguet, C. Wang, Q. Wang, *Chem. Soc. Rev.* **2010**, *39*, 1233 – 1239; d) J. Li, M. Hu, S. Q. Yao, *Org. Lett.* **2009**, *11*, 3008 – 3011; e) J. Qi, M. S. Han, Y. C. Chang, C. H. Tung, *Bioconjugate Chem.* **2011**, *22*, 1758 – 1762; f) P. Shieh, M. S. Siegrist, A. J. Cullen, C. R. Bertozzi, *Proc. Natl. Acad. Sci. USA* **2014**, *111*, 5456 – 5461; g) K. Sivakumar, F. Xie, B. M. Cash, S. Long, H. N. Barnhill, Q. Wang, *Org. Lett.* **2004**, *6*, 4603 – 4606; h) Z. Zhou, C. J. Fahrni, *J. Am. Chem. Soc.* **2004**, *126*, 8862 – 8863; i) O. Demeter, A. Kormos, C. Koehler, G. Mező, K. Németh, E. Kozma, L. B. Takács, E. A. Lemke, P. Kele, *Bioconjugate Chem.* **2017**, *28*, 1552 – 1559.

[4] a) Y. Wang, C. I. Vera, Q. Lin, *Org. Lett.* **2007**, *9*, 4155 – 4158; b) W. Song, Y. Wang, J. Qu, Q. Lin, *J. Am. Chem. Soc.* **2008**, *130*, 9654 – 9655; c) W. Song, Y. Wang, J. Qu, M. M. Madden, Q. Lin, *Angew. Chem. Int. Ed.* **2008**, *47*, 2832 – 2835; *Angew. Chem.* **2008**, *120*, 2874 – 2877; d) Z. Yu, L. Y. Ho, Q. Lin, *J. Am. Chem. Soc.* **2011**, *133*, 11912 – 11915; e) E. Kaya, M. Vrabel, C. Deiml, S. Prill, V. S. Fluxa, T. Carell, *Angew. Chem. Int. Ed.* **2012**, *51*, 4466 – 4469; *Angew. Chem.* **2012**, *124*, 4542 – 4545; f) Z. Yu, T. Y. Ohulchanskyy, P. An, P. N. Prasad, Q. Lin, *J. Am. Chem. Soc.* **2013**, *135*, 16766 – 16769; g) X. S. Wang, Y. J. Lee, W. R. Liu, *Chem. Commun.* **2014**, *50*, 3176 – 3179.

[5] a) N. K. Devaraj, S. Hilderbrand, R. Upadhyay, R. Mazitschek, R. Weissleder, *Angew. Chem. Int. Ed.* **2010**, *49*, 2869 – 2872; *Angew. Chem.* **2010**, *122*, 2931 – 2934; b) J. Yang, J. Seckute, C. M. Cole, N. K. Devaraj, *Angew. Chem. Int. Ed.* **2012**, *51*, 7476 – 7479; *Angew. Chem.* **2012**, *124*, 7594 – 7597; c) L. G. Meimetis, J. C. Carlson, R. J. Giedt, R. H. Kohler, R. Weissleder, *Angew. Chem. Int. Ed.* **2014**, *53*, 7531 – 7534; *Angew. Chem.* **2014**, *126*, 7661 – 7664; d) A. Wieczorek, T. Buckup, R. Wombacher, *Org. Biomol. Chem.* **2014**, *12*, 4177 – 4185; e) H. Wu, J. Yang, J. Seckute, N. K. Devaraj, *Angew. Chem. Int. Ed.* **2014**, *53*, 5805 – 5809; *Angew. Chem.* **2014**, *126*, 5915 – 5919; f) E. Kozma, O. Demeter, P. Kele, *ChemBioChem* **2017**, *18*, 486 – 501; g) A. Wieczorek, P. Werther, J. Euchner, R. Wombacher, *Chem. Sci.* **2017**, *8*, 1506 – 1510; h) E. Kozma, G. Estrada Girona, G. Paci, E. A. Lemke, P. Kele, *Chem. Commun.* **2017**, *53*, 6696 – 6699.

[6] C. P. Ramil, Q. Lin, *Curr. Opin. Chem. Biol.* **2014**, *21*, 89 – 95.

[7] X. Shang, X. Song, C. Faller, R. Lai, H. Li, R. Cerny, W. Niu, J. Guo, *Chem. Sci.* **2017**, *8*, 1141 – 1145.

[8] A. Vázquez, R. Dzijak, M. Dracinsky, R. Rampmaier, S. J. Siegl, M. Vrabel, *Angew. Chem. Int. Ed.* **2017**, *56*, 1334 – 1337; *Angew. Chem.* **2017**, *129*, 1354 – 1357.

[9] a) R. D. Bach, *J. Am. Chem. Soc.* **2009**, *131*, 5233 – 5243; b) J. Dommerholt, S. Schmidt, R. Temming, L. J. Hendriks, F. P. Rutjes, J. C. van Hest, D. J. Lefeber, P. Friedl, F. L. van Delft, *Angew. Chem. Int. Ed.* **2010**, *49*, 9422 – 9425; *Angew. Chem.* **2010**, *122*, 9612 – 9615; c) M. T. Taylor, M. L. Blackman, O. Dmitrenko, J. M. Fox, *J. Am. Chem. Soc.* **2011**, *133*, 9646 – 9649; d) A. Darko, S. Wallace, O. Dmitrenko, M. M. Machovina, R. A. Mehl, J. W. Chin, J. M. Fox, *Chem. Sci.* **2014**, *5*, 3770 – 3776.

[10] a) J. U. Jeong, B. Tao, I. Sagasser, H. Henniges, K. B. Sharpless, *J. Am. Chem. Soc.* **1998**, *120*, 6844 – 6845; b) CCDC 1553867 (**4**) contains the supplementary crystallographic data for this paper. These data are provided free of charge by The Cambridge Crystallographic Data Centre.

[11] M. Royzen, G. P. Yap, J. M. Fox, *J. Am. Chem. Soc.* **2008**, *130*, 3760 – 3761.

[12] S. C. Bergmeier, P. P. Seth, *Tetrahedron Lett.* **1999**, *40*, 6181 – 6184.

[13] Y. Ittah, Y. Sasson, I. Shahak, S. Tsaroom, J. Blum, *J. Org. Chem.* **1978**, *43*, 4271 – 4273.

[14] A. M. Brouwer, *Pure Appl. Chem.* **2011**, *83*, 2213 – 2228.

[15] a) K. A. Horner, N. M. Valette, M. E. Webb, *Chem. Eur. J.* **2015**, *21*, 14376 – 14381; b) D. N. Kamber, Y. Liang, R. J. Blizzard, F. Liu, R. A. Mehl, K. N. Houk, J. A. Prescher, *J. Am. Chem. Soc.* **2015**, *137*, 8388 – 8391; c) S. J. Siegl, R. Dzijak, A. Vazquez, R. Pohl, M. Vrabel, *Chem. Sci.* **2017**, *8*, 3593 – 3598.

[16] R. Rossin, S. M. van den Bosch, W. Ten Hoeve, M. Carvelli, R. M. Versteegen, J. Lub, M. S. Robillard, *Bioconjugate Chem.* **2013**, *24*, 1210 – 1217.

[17] a) E. Baslé, N. Joubert, M. Pucheault, *Chem. Biol.* **2010**, *17*, 213 – 227; b) O. Koniev, A. Wagner, *Chem. Soc. Rev.* **2015**, *44*, 5495 – 5551.

[18] S. B. Gunnoo, A. Madder, *ChemBioChem* **2016**, *17*, 529 – 553.

[19] A. Baumlova, D. Chalupska, B. Różycki, M. Jovic, E. Wisniewski, M. Klima, A. Dubankova, D. P. Kloer, R. Nencka, T. Balla, E. Boura, *EMBO Rep.* **2014**, *15*, 1085 – 1092.

[20] I. J. Goldstein, R. D. Poretz, in *The Lectins. Properties, Functions, and Applications in Biology and Medicine., Vol. 32* (Eds.: I. E. Liener, N. Sharon, I. J. Goldstein), Elsevier, **1986**, pp. 33 – 247.

[21] a) M. S. Siegrist, S. Whiteside, J. C. Jewett, A. Aditham, F. Cava, C. R. Bertozzi, *ACS Chem. Biol.* **2013**, *8*, 500 – 505; b) E. Kuru, S. Tekkam, E. Hall, Y. V. Brun, M. S. Van Nieuwenhze, *Nat. Protoc.* **2014**, *10*, 33 – 52.

Manuscript received: November 1, 2017
Accepted manuscript online: December 15, 2017
Version of record online: January 25, 2018

## 3.2 An Extended Approach for the Development of Fluorogenic *trans*-Cyclooctene-Tetrazine Cycloadditions

S.J. Siegl, J. Galeta, R. Dzijak, A. Vázquez, M. Del Río-Villanueva, M. Dračínský, M. Vrabel, *ChemBioChem* **2019**, 20, 886– 890.



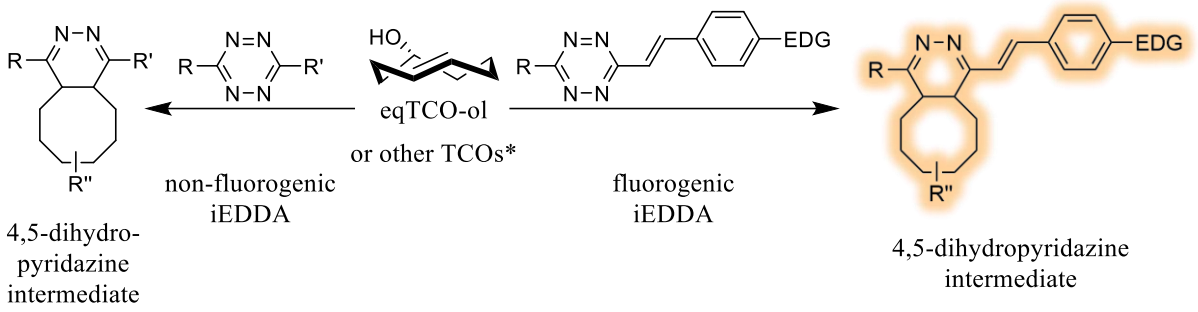


### 3.2.1 Background

Previously we showed that only axTCO-ol and the novel aza-TCO produce fluorescent products directly through iEDDA reaction with 1,2,4,5-tetrazines.[155-156] In order to find an alternative and more general approach for such fluorogenic tetrazine ligations, we searched for 1,2,4,5-tetrazine derivatives yielding fluorescent compounds in reactions with a bigger range of TCOs. We speculated that the initially formed 4,5-dihydropyridazine intermediate, which is formed upon reaction between tetrazines and all TCO derivatives, offers a unique π-conjugated system suitable for the potential formation of fluorophores. Indeed, our experiments with various 1,2,4,5-tetrazines showed that tetrazines containing an electron-donating dimethylamino or azetidine moiety form fluorescent 4,5-dihydropyridazine intermediates through cycloaddition with various TCO derivatives. We even demonstrated that also TCOs, which did not show any fluorogenic properties in our previous studies, create such fluorescent compounds upon reaction with these particular 1,2,4,5-tetrazines.

## 3.2.2 Declaration of contribution

Together with *Dr. Juraj Galeta*, *Dr. Arcadio Vázquez* and *Miguel Del Río-Villanueva*, I prepared the 1,2,4,5-tetrazines and TCOs used in this study. HPLC-MS and NMR measurements for monitoring and analyzing the formation of the fluorescent 4,5-dihydropyridazine intermediates by tetrazine ligation with eqTCO-ol and specific 1,2,4,5-tetrazines were performed by *Dr. Martin Dračínský* and *Dr. Milan Vrábel*. I determined the second-order rate constants of the click reactions between the 1,2,4,5-tetrazines and various TCOs and measured the photophysical properties of all formed fluorescent intermediates. Furthermore, I carried out the time-dependent fluorescence measurements to evaluate the decay of the fluorescence intensity of the 4,5-dihydropyridazine intermediates and to estimate their half-life. Cell labeling experiments were performed by *Dr. Rastislav Dzijak*. I also actively participated in writing the manuscript.

ChemPubSoc Europe

DOI: 10.1002/cbic.201800711

CHEMBIOCHEM Communications

VIP *Very Important Paper*

# An Extended Approach for the Development of Fluorogenic *trans*-Cyclooctene–Tetrazine Cycloadditions

Sebastian J. Siegl, Juraj Galeta, Rastislav Dzijak, Arcadio Vázquez, Miguel Del Río-Villanueva, Martin Dračínský, and Milan Vrabel*[a]

Inverse-electron-demand Diels–Alder (iEDDA) cycloaddition between 1,2,4,5-tetrazines and strained dienophiles belongs among the most popular bioconjugation reactions. In addition to its fast kinetics, this cycloaddition can be tailored to produce fluorescent products from non-fluorescent starting materials. Here we show that even the reaction intermediates formed in iEDDA cycloaddition can lead to the formation of new types of fluorophores. The influence of various substituents on their photophysical properties and the generality of the approach with use of various *trans*-cyclooctene derivatives were studied. Model bioimaging experiments demonstrate the application potential of fluorogenic iEDDA cycloaddition.

Bioorthogonal reactions are a set of chemical transformations that enable labeling and study of biomolecules under native biological conditions.[1] The properties of these reactions include, among other beneficial factors, high degrees of selectivity, fast kinetics, formation of stable covalent products, and compatibility with strict biological conditions. A number of reactions featuring these attributes are currently available and they have been developed into valuable tools in biology, chemical biology, materials sciences, and biomedical research.[2]

One especially useful property of bioorthogonal reactions is fluorogenicity. This attribute is based on the production of fluorescent products from nonfluorescent starting materials, thus providing a convenient means of detection through the production of a fluorescent signal.[3] There are several ways in which this can be achieved. One is based on quenching of fluorescence through intramolecular energy transfer in bioorthogonal fluorophore conjugates. The subsequent reaction provides products as different chemical species, and this leads to restoration of the fluorescence of the attached fluorophore. One prominent example of a class of reagents of this type is that of 1,2,4,5-tetrazines.[4]

Another, comparably rare, example of a fluorogenic reaction is based on the formation of a fluorophore as a result of reaction between two non-fluorescent bioorthogonal reagents. An example belonging to this class of fluorogenic reactions is the formation of fluorescent pyrazolines through reaction between nitrile imines and various dipolarophiles.[5]

We recently discovered that pyridinium 1,2,4-triazines containing a push–pull substitution pattern also form fluorescent products in reaction with strained *trans*-cyclooctenes (TCOs).[6] In addition, we and others have reported that reactions between 1,2,4,5-tetrazines and particular dienophiles also lead to fluorescent products without the need for attachment of an extra fluorophore moiety.[7] Despite successful application of this chemistry for bioimaging, we found that only the axially substituted hydroxy *trans*-cyclooctene and azabicyclononene[8] dienophiles afforded fluorescent dihydropyridazine products. This limited scope of dienophiles suitable for fluorogenic labeling hampers broader utility of the methodology. An alternative and more general approach is hence desirable. In continuation of our work in this direction we show here that by using 1,2,4,5-tetrazines containing specific electron-donating substituents it is possible to extend the fluorogenic tetrazine cycloaddition to other dienophiles. We have characterized the photophysical properties of the reaction products and in this sense evaluated the effects of various substituents on the tetrazine core, as well as the influence of the TCO structure. In addition, we show that the inherent fluorogenic nature of the chemistry is also operative under biological conditions and can be applied for bioimaging.

The first reaction step of inverse-electron-demand Diels–Alder (iEDDA) cycloaddition between a 1,2,4,5-tetrazine and a dienophile involves the formation of a tetraazabicyclic system, which, after a retro-Diels–Alder reaction and extrusion of molecular nitrogen, is transformed into a 4,5-dihydropyridazine (Figure 1 A). This can further isomerize to the corresponding 1,4-dihydropyridazine through, for example, addition and elimination of a water molecule or alternatively through intramolecular interaction with an appropriately placed heteroatom substituent on the TCO.[7b,9] The initially formed 4,5-dihydropyridazine heterocyclic core is a unique π-conjugated system formed upon reaction between tetrazines and all TCO derivatives. Therefore, we thought that it offers an exclusive opportunity to be used for potential formation of fluorophores. Indeed, during experimentation with various 1,2,4,5-tetrazines we

[a] S. J. Siegl, Dr. J. Galeta, Dr. R. Dzijak, Dr. A. Vázquez, M. Del Río-Villanueva, Dr. M. Dračínský, Dr. M. Vrabel
Institute of Organic Chemistry and Biochemistry of the Czech Academy of Sciences
Flemingovo nám. 2, 166 10, Prague (Czech Republic)
E-mail: vrabel@uochb.cas.cz

Supporting information and the ORCID identification numbers for the authors of this article can be found under https://doi.org/10.1002/cbic.201800711.



This article is part of the young researchers' issue ChemBioTalents. To view the complete issue, visit http://chembiochem.org/chembiotalents

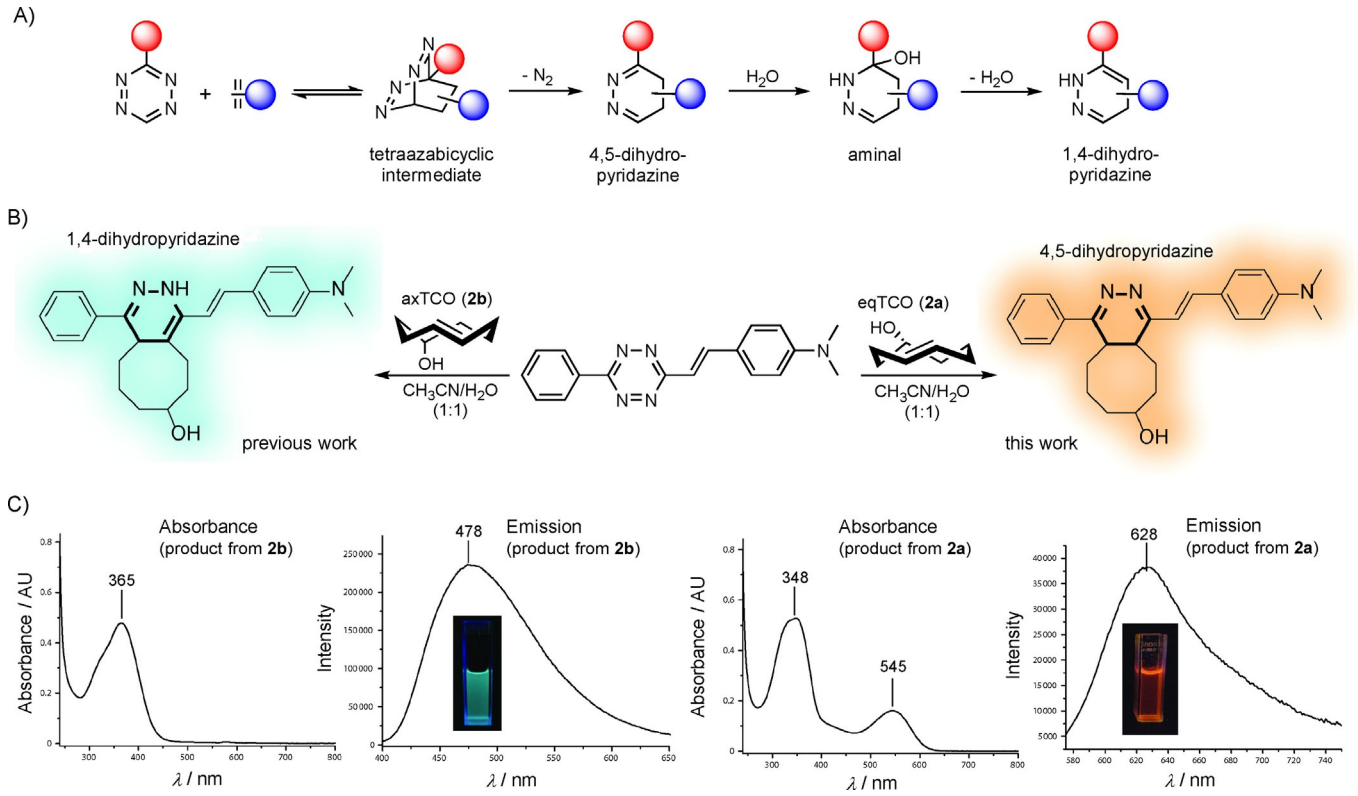


**Figure 1.** A) General mechanism of iEDDA cycloaddition between a 1,2,4,5-tetrazine and an alkene dienophile. B) Scheme showing formation of two different products in the reactions between tetrazine **1a** and different TCO isomers. The dihydropyridazine core is highlighted in bold. For clarity only one regioisomer of each product is shown. C) Absorption and emission spectra of products formed in the reactions between **1a** and **2a** or **2b**.

found that tetrazine derivative **1a**, bearing a *p*-dimethylamino substituent, forms a fluorescent product when combined with equatorially hydroxy-substituted TCO **2a** (eqTCO). As we have previously reported,[7b] the same derivative leads to fluorescent products, with different photophysical properties, upon reaction with the corresponding axially hydroxy-substituted TCO **2b** (axTCO, Figure 1 B and C). We ascribed the formation of the two different fluorescent species to the production of different tautomers of the dihydropyridazine core (Figures S1 and S2 in the Supporting Information). The structure of the central dihydropyridazine heterocycle thus influences the photophysical properties of the products, enabling control over the outcome of the reaction by simply changing the configuration of the starting TCO. This interesting behavior prompted us to explore the phenomenon in more detail.

We first synthesized a series of tetrazine derivatives by the Heck cross-coupling methodology developed by Devaraj and co-workers[4b] and measured the photophysical properties of the products formed after reaction with eqTCO (Table 1).

The derivative formed from the tetrazine **1b**, bearing a methoxy substituent, was found to be non-fluorescent. This indicates that the weaker electron-donating ability of the methoxy group is not sufficient to promote formation of the fluorophore. On the other hand, the presence of a phenyl or thiophene moiety at position 6 in the tetrazine structure, in combination with a dimethylamino substituent (tetrazines **1a** and **1c**), led to the formation of fluorophores with higher fluores-

**Table 1.** Photophysical properties of 4,5-dihydropyridazine products.

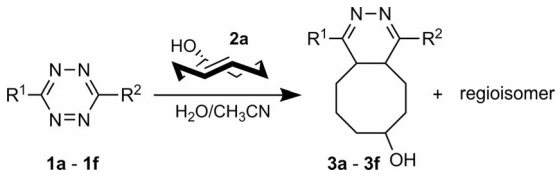


| | R¹ | R² | $\lambda_{abs}/\lambda_{em}$ [a] [nm] | Stokes shift [nm] | $\Phi_{fl}$ [b] [%] | Intensity increase |
|---|---|---|---|---|---|---|
| **a** | 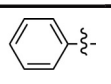 | 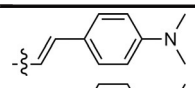 | 545/628 | 83 | 0.55 | 13-fold |
| **b** | 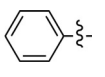 | 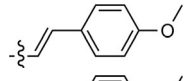 | 295/– | – | – | – |
| **c** | 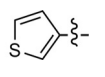 | 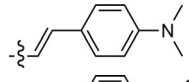 | 546/626 | 80 | 0.52 | 18-fold |
| **d** | 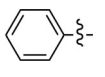 | 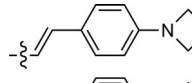 | 546/626 | 80 | 0.45 | 10-fold |
| **e** | 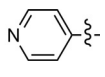 | 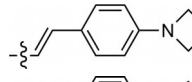 | 566/643 | 77 | 0.21 | threefold |
| **f** | 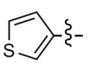 | 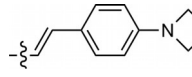 | 549/626 | 77 | 0.47 | 12-fold |

[a] Absorption and emission maxima were measured in $CH_3CN/H_2O$ 1:1. [b] Relative fluorescence quantum yields were determined by using Nile Red in methanol as standard.

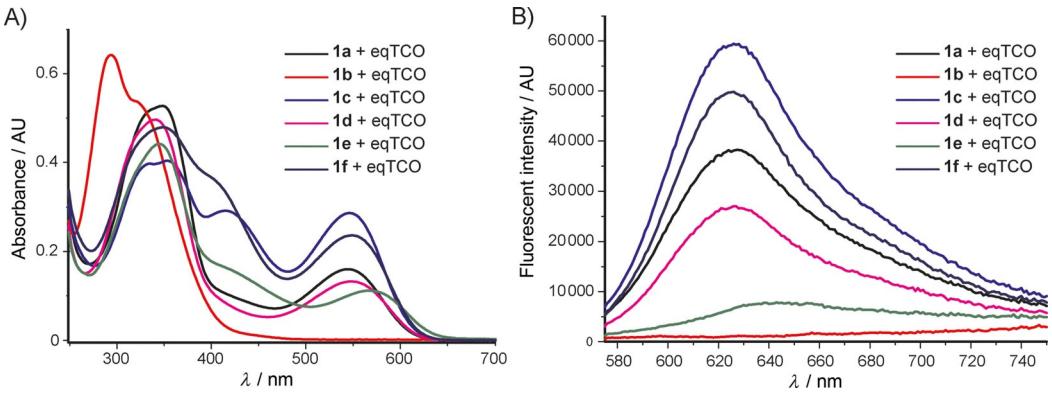


**Figure 2.** Summary of A) absorption, and B) emission spectra of the products formed in the reactions between tetrazines **1a–f** and eqTCO.

cence quantum yields. The enhancement of the fluorescence signals after the iEDDA click cycloaddition reached 13- and 18-fold for the phenyl- and the thiophene-substituted tetrazines, respectively (Figures 2 and S3–S8, Tables 1 and S2).

A recent literature example prompted us to explore the possibility of introducing an azetidine moiety as an alternative electron-donating substituent; this had been shown to improve the photophysical properties of some xanthene dyes.[10] We also varied the substituent on the other side of the tetrazine and introduced phenyl, thiophene, and pyridyl groups at position 6. Surprisingly the iEDDA cycloaddition between the pyridyl-substituted tetrazine **1e** and eqTCO provided only modestly increased fluorescence (Table 1). Possibly, the presence of an electron-withdrawing substituent (pyridyl) at this position is not beneficial for fluorescence generation and/or other quenching mechanisms are responsible for the observed lower fluorescence. By comparing the absorption and emission maxima of all derivatives it can be concluded that none of these substituents influence the absorption and emission maxima to any great extent. Although the fluorescence quantum yields of the fluorophores formed in the reactions are rather low, their photophysical properties enabled successful use in bioimaging application, as we show below.

An important aspect of bioconjugation reactions is the reactivity of the reagents, which are usually used at low-micromolar concentrations. Accordingly, we determined the second-order rate constants of iEDDA cycloaddition between tetrazines **1a–f** and the eqTCO **2a** (Table S1). All of the tetrazines reacted with this dienophile, displaying second-order rate constants of approximately 7 $M^{-1}s^{-1}$ in a 1:1 mixture of $CH_3CN$ and $H_2O$ at room temperature. For purposes of comparison, we also determined the second-order rate constants of cycloaddition between the same tetrazines and the axTCO **2b**. Our data are in good agreement with previous observations in which the equatorial isomer was found to react four to five times more slowly than the corresponding axial isomer (Table S1).[11]

As mentioned above, the 4,5-dihydropyridazine system is an intermediate in the iEDDA reaction. Depending on the TCO structure and the environment (e.g., presence of water), it can further isomerize to the corresponding 1,4-dihydropyridazine (Figure 1A). This means that the fluorescence of the initially formed 4,5-dihydropyridazine should decrease over time as the tautomerization proceeds. This decrease in fluorescence is an important factor for potential application in, for example, bioimaging. Consequently, we measured the decay in the fluorescent signal over time for tetrazine derivatives **1c** and **1f** (Figures 3, S9, and S10).

Our data show that the fluorescence of the click products persists over hours with a half-life of about two hours, almost completely disappearing within one day. Concomitant appearance of the fluorescence of the newly formed 1,4-dihydropyridazine tautomer was detected after this time period (Figures S9 and S10). In addition, formation of a small amount of the fully oxidized pyridazine product was observed by HPLC-MS analysis (Figure S1). This product can also partially contribute to the observed decay in the fluorescent signal. Although

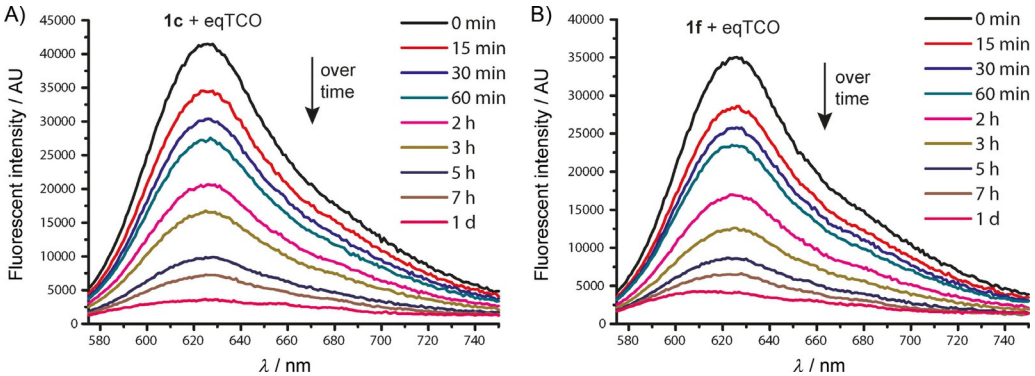


**Figure 3.** The decay in fluorescence signals over time for the click products formed from eqTCO **2a** and tetrazines **1c** and **1f**.

 

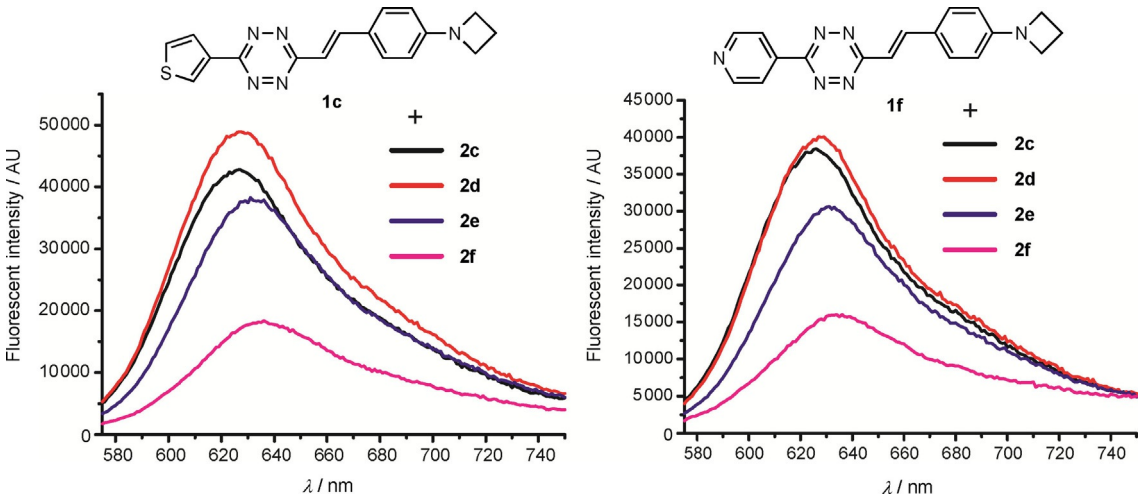


**Figure 4.** Fluorescence enhancement of the reaction between tetrazines **1 c**/**1 f** and different TCOs.

this enables only temporary labeling, the timescale is sufficient for bioimaging applications (see below).

To study the scope of the fluorogenic reaction we tested a series of TCOs[12]—**2 c** to **2 f**—for their propensity to form fluorescent products with tetrazines **1 c** and **1 f** (Figures 4, S11, and S12, Tables 2, S3, and S4). We found that all TCOs tested gave rise to the formation of fluorophores with similar photophysical properties to those observed with the eqTCO **2 a**. The only exception was the dioxolane-fused TCO **2 f**, which provided a less pronounced fluorescence enhancement of only sixfold. The absorption and emission maxima of all derivatives were similar, being centered around 550 nm and 630 nm, respectively. These data demonstrate that the formation of 4,5-dihydropyridazines in cycloadditions between tetrazines and TCOs can be considered a more general approach for the development of fluorogenic reactions based on this type of chemistry.

**Table 2.** Absorption and emission maxima [nm] and fluorescence enhancement of the products formed in reaction of **1 c**/**1 f** with different TCOs.

| Tetrazine | 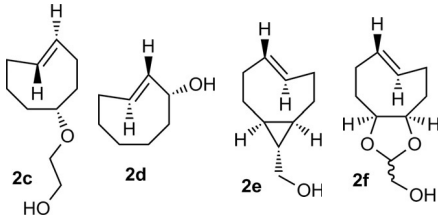 | | | |
|---|---|---|---|---|
| | **2c** | **2d** | **2e** | **2f** |
| **1 c** | 547/627 | 550/627 | 547/631 | 558/638 |
| Fl. intensity increase | 13-fold | 14-fold | 11-fold | sixfold |
| **1 f** | 550/627 | 550/627 | 550/631 | 551/631 |
| Fl. intensity increase | ninefold | ninefold | eightfold | fourfold |

We next performed a series of experiments to test whether we could apply these fluorogenic reactions for bioimaging. We first prepared triphenylphosphonium-functionalized TCO (TPP-TCO). The TPP moiety is known to target various cargoes to mitochondria[13] and thus enables organelle-specific intracellular labeling. We incubated live HeLa cells with 5 μM TPP-TCO for 15 min, then washed the cells to remove any excess of the probe, and finally added 5 μM tetrazine **1 c** to initiate the fluorogenic reaction. We observed the formation of a marked fluorescence signal inside the cells after only 5 min incubation, thus indicating good cell permeability of probe **1 c** and confirming successful reaction. Co-staining with commercially available mitochondrion-specific MitoTracker Deep Red dye further confirmed specific labeling of this organelle (Figures 5 A and S13). The fluorescent signal was still detectable even after 2 h, in good agreement with our previous time-lapse fluorescence-decay experiments.

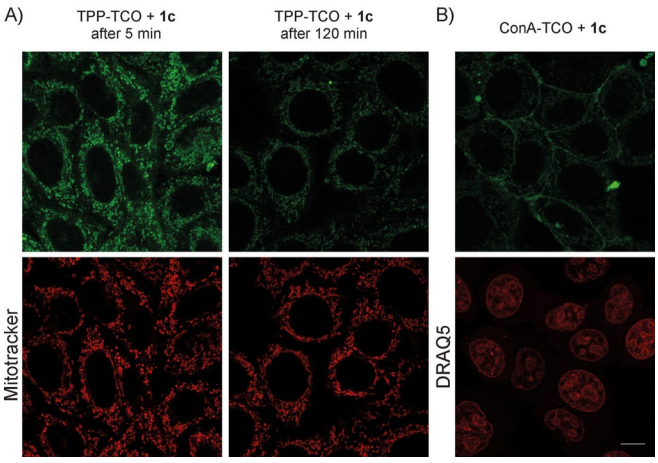


**Figure 5.** Confocal microscope images from fluorogenic live cell labeling. A) Live HeLa cells were incubated with the mitochondrion-selective TPP-TCO probe followed by incubation with **1 c**. Mitochondrial labeling was confirmed by co-staining with Mitotracker Deep Red. B) Labeling of glycoconjugates with ConA-TCO and **1 c**. Excitation for the click product: $\lambda = 561$ nm (intensity 50 %). Emission was collected in the $\lambda = 568$–620 nm window. MitoTracker Deep Red and DRAQ5 were excited with a $\lambda = 633$ nm laser, intensity 20 % and 25 %, respectively. Emission was collected in the $\lambda = 643$–703 nm window. Scale bar: 10 μm.

To examine the potential of the fluorogenic reaction for bioimaging further, we also conjugated the TCO moiety to concanavalin A (ConA-TCO). Concanavalin A is a lectin with high specificity for α-D-mannose- and α-D-glucose-containing glycoconjugates.[14] After incubation of live HeLa cells with ConA-TCO and addition of tetrazine **1 c**, specific cell membrane labeling was observed by confocal fluorescence microscopy, whereas cells treated only with ConA-TCO were not fluorescent (Figures 5 B and S14). These experiments demonstrate that the fluorogenic nature of the cycloaddition is well preserved under biological conditions and can be used for intracellular labeling as well as for fluorescent labeling of cell membrane compartments.

In conclusion, we have shown that the 4,5-dihydropyridazine reaction intermediate is a unique structural motif that can be utilized for the formation of fluorescent products in iEDDA cycloaddition between 1,2,4,5-tetrazines and *trans*-cyclooctenes. Tetrazines containing electron-donating dimethylamino or azetidine groups form fluorescent products upon treatment with various TCOs. The fluorogenic nature of the cycloaddition enables application for bioimaging, as we have shown by fluorogenic labeling of intracellular compartments and cell membrane glycoconjugates.

## Acknowledgements

*This work was supported by the European Research Council (ERC) under the European Union's Horizon 2020 research and innovation programme (grant agreement no. 677465). We acknowledge the Light Microscopy Facility at the Institute of Molecular Genetics AS CR supported by the Czech-BioImaging large RI project (LM2015062 funded by MEYS CR) and by European Regional Development Fund-Project "National infrastructure for biological and medical imaging" (no. CZ.02.1.01/0.0/0.0/16_013/0001775) for their support with obtaining scientific data presented in this paper. We thank Michael Downey for critical reading of the manuscript.*

## Conflict of Interest

*The authors declare no conflict of interest.*

**Keywords:** bioorthogonal chemistry · click chemistry · cycloaddition · heterocycles · tetrazines

[1] a) J. M. Baskin, C. R. Bertozzi, *QSAR Comb. Sci.* **2007**, *26*, 1211 – 1219; b) M. F. Debets, J. C. M. van Hest, F. P. J. T. Rutjes, *Org. Biomol. Chem.* **2013**, *11*, 6439 – 6455; c) M. King, A. Wagner, *Bioconjugate Chem.* **2014**, *25*, 825 – 839; d) R. K. V. Lim, Q. Lin, *Chem. Commun.* **2010**, *46*, 1589 – 1600; e) E. M. Sletten, C. R. Bertozzi, *Angew. Chem. Int. Ed.* **2009**, *48*, 6974 – 6998; *Angew. Chem.* **2009**, *121*, 7108 – 7133.

[2] a) R. Kluger, *J. Am. Chem. Soc.* **2010**, *132*, 6611 – 6612; b) K. Nwe, M. W. Brechbiel, *Cancer Biother. Radiopharm.* **2009**, *24*, 289 – 302; c) C. D. Spicer, B. G. Davis, *Nat. Commun.* **2014**, *5*, 4740; d) C. D. Spicer, E. T. Pashuck, M. M. Stevens, *Chem. Rev.* **2018**, *118*, 7702 – 7743; e) W. Xi, T. F. Scott, C. J. Kloxin, C. N. Bowman, *Adv. Funct. Mater.* **2014**, *24*, 2572 – 2590; f) *Topics in Current Chemistry, Vol. 374: Cycloadditions in Bioorthogonal Chemistry* (Eds.: M. Vrabel, T. Carell), Springer, Switzerland, **2016**.

[3] a) C. Le Droumaguet, C. Wang, Q. Wang, *Chem. Soc. Rev.* **2010**, *39*, 1233 – 1239; b) A. Nadler, C. Schultz, *Angew. Chem. Int. Ed.* **2013**, *52*, 2408 – 2410; *Angew. Chem.* **2013**, *125*, 2466 – 2469.

[4] a) N. K. Devaraj, S. Hilderbrand, R. Upadhyay, R. Mazitschek, R. Weissleder, *Angew. Chem. Int. Ed.* **2010**, *49*, 2869 – 2872; *Angew. Chem.* **2010**, *122*, 2931 – 2934; b) H. X. Wu, J. Yang, J. Seckute, N. K. Devaraj, *Angew. Chem. Int. Ed.* **2014**, *53*, 5805 – 5809; *Angew. Chem.* **2014**, *126*, 5915 – 5919; c) A. Wieczorek, P. Werther, J. Euchner, R. Wombacher, *Chem. Sci.* **2017**, *8*, 1506 – 1510; d) E. Kozma, G. E. Girona, G. Paci, E. A. Lemke, P. Kele, *Chem. Commun.* **2017**, *53*, 6696 – 6699; e) E. Kozma, O. Demeter, P. Kele, *ChemBioChem* **2017**, *18*, 486 – 501; f) G. Knorr, E. Kozma, J. M. Schaart, K. Nemeth, G. Torok, P. Kele, *Bioconjugate Chem.* **2018**, *29*, 1312 – 1318.

[5] a) Z. Yu, T. Y. Ohulchanskyy, P. An, P. N. Prasad, Q. Lin, *J. Am. Chem. Soc.* **2013**, *135*, 16766 – 16769; b) E. Kaya, M. Vrabel, C. Deiml, S. Prill, V. S. Fluxa, T. Carell, *Angew. Chem. Int. Ed.* **2012**, *51*, 4466 – 4469; *Angew. Chem.* **2012**, *124*, 4542 – 4545; c) W. Song, Y. Wang, J. Qu, M. M. Madden, Q. Lin, *Angew. Chem. Int. Ed.* **2008**, *47*, 2832 – 2835; *Angew. Chem.* **2008**, *120*, 2874 – 2877; d) W. Song, Y. Wang, J. Qu, Q. Lin, *J. Am. Chem. Soc.* **2008**, *130*, 9654 – 9655.

[6] S. J. Siegl, R. Dzijak, A. Vázquez, R. Pohl, M. Vrabel, *Chem. Sci.* **2017**, *8*, 3593 – 3598.

[7] a) X. Shang, X. Song, C. Faller, R. Lai, H. Li, R. Cerny, W. Niu, J. Guo, *Chem. Sci.* **2017**, *8*, 1141 – 1145; b) A. Vázquez, R. Dzijak, M. Dracinsky, R. Rampmaier, S. J. Siegl, M. Vrabel, *Angew. Chem. Int. Ed.* **2017**, *56*, 1334 – 1337; *Angew. Chem.* **2017**, *129*, 1354 – 1357.

[8] S. J. Siegl, A. Vázquez, R. Dzijak, M. Dračínský, J. Galeta, R. Rampmaier, B. Klepetářová, M. Vrabel, *Chem. Eur. J.* **2018**, *24*, 2426 – 2432.

[9] M. L. Blackman, M. Royzen, J. M. Fox, *J. Am. Chem. Soc.* **2008**, *130*, 13518 – 13519.

[10] a) J. B. Grimm, A. K. Muthusamy, Y. J. Liang, T. A. Brown, W. C. Lemon, R. Patel, R. W. Lu, J. J. Macklin, P. J. Keller, N. Ji, L. D. Lavis, *Nat. Methods* **2017**, *14*, 987 – 994; b) J. B. Grimm, B. P. English, J. J. Chen, J. P. Slaughter, Z. J. Zhang, A. Revyakin, R. Patel, J. J. Macklin, D. Normanno, R. H. Singer, T. Lionnet, L. D. Lavis, *Nat. Methods* **2015**, *12*, 244 – 250.

[11] R. Rossin, S. M. van den Bosch, W. ten Hoeve, M. Carvelli, R. M. Versteegen, J. Lub, M. S. Robillard, *Bioconjugate Chem.* **2013**, *24*, 1210 – 1217.

[12] a) M. T. Taylor, M. L. Blackman, O. Dmitrenko, J. M. Fox, *J. Am. Chem. Soc.* **2011**, *133*, 9646 – 9649; b) A. Darko, S. Wallace, O. Dmitrenko, M. M. Machovina, R. A. Mehl, J. W. Chin, J. M. Fox, *Chem. Sci.* **2014**, *5*, 3770 – 3776; c) R. M. Versteegen, R. Rossin, W. ten Hoeve, H. M. Janssen, M. S. Robillard, *Angew. Chem. Int. Ed.* **2013**, *52*, 14112 – 14116; *Angew. Chem.* **2013**, *125*, 14362 – 14366.

[13] J. Zielonka, J. Joseph, A. Sikora, M. Hardy, O. Ouari, J. Vasquez-Vivar, G. Cheng, M. Lopez, B. Kalyanaraman, *Chem. Rev.* **2017**, *117*, 10043 – 10120.

[14] I. J. Goldstein, R. D. Poretz in *The Lectins: Properties, Functions, and Applications in Biology and Medicine., Vol. 32* (Eds.: I. E. Liener, N. Sharon, I. J. Goldstein), Academic Press, Orlando, **1986**, pp. 33 – 247.

Manuscript received: November 19, 2018

Accepted manuscript online: December 18, 2018

Version of record online: March 7, 2019

 

## 3.3 Bioorthogonal Fluorescence Turn-On Labeling Based on Bicyclononyne–Tetrazine Cycloaddition Reactions that Form Pyridazine Products

S.J. Siegl, J. Galeta, R. Dzijak, M. Dračínský, M. Vrabel, *ChemPlusChem* **2019**, 84, 493-497. Copy of the publication with permission of the publisher; Published by Wiley-VCH Verlag GmbH & Co. KGaA.

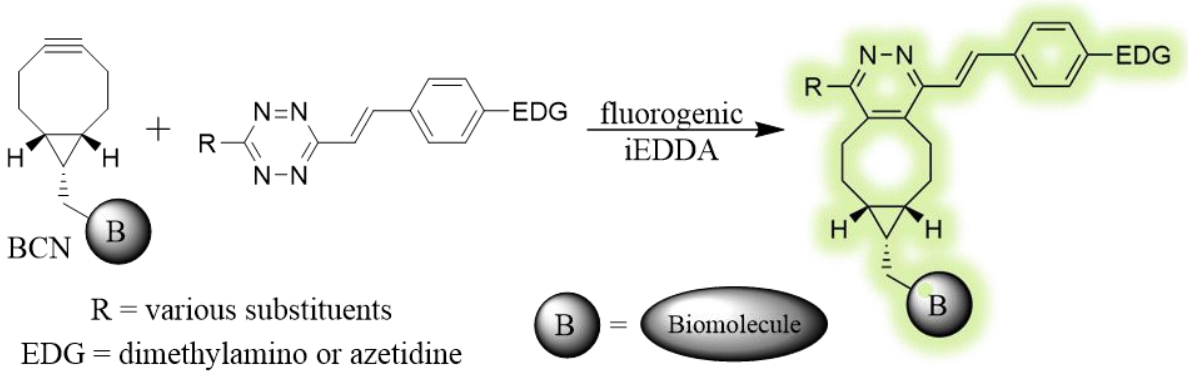


### 3.3.1 Background

In our previous work we showed that iEDDA reactions between 1,2,4,5-tetrazines bearing specific electron-donating dimethylamino or azetidine groups and various TCOs yield fluorescent 4,5-dihydropyridazine intermediates.[157] In this study we continued our work toward a more general strategy for such type of fluorogenic tetrazine ligations and discovered that these particular tetrazines also form fluorescent products in iEDDA reactions with BCN derivatives. Furthermore, we speculated that this new fluorogenic BCN-tetrazine cycloaddition should be orthogonal to the recently discovered formation of fluorescent 4,5-dihydropyridazine intermediates,[157] which employs the same class of tetrazines and various TCOs. Indeed, we were able to show that combination of both methods allows for a one-step two-color labeling activated by only a single tetrazine.

### 3.3.2 Declaration of contribution

Together with *Dr. Juraj Galeta,* I prepared the 1,2,4,5-tetrazines and BCN derivatives used in this study. In collaboration with *Dr. Martin Dračínský* I carried out the isolation and detailed NMR and HPLC-MS analysis of the fluorescent pyridazine product formed upon the

cycloaddition between BCN and one of the specific 1,2,4,5-tetrazines. Furthermore, I verified by HPLC-MS experiments the formation of the corresponding pyridazine products from the reactions with all other tested tetrazines and determined the respective second-order rate constants. I measured the photophysical properties of the fluorescent products obtained during this study and performed the fluorescence experiments in order to study the solvatochromic character of the compounds. *Dr. Rastislav Dzijak* carried out the cell labeling experiments and the toxicity studies. The two-color labeling experiments on the bilayer Tentagel resin beads were performed by *Dr. Juraj Galeta*, *Dr. Rastislav Dzijak* and *Dr. Milan Vrábel*. I also actively participated in writing the manuscript.

ChemPubSoc Europe

DOI: 10.1002/cplu.201900176

CHEMPLUSCHEM Communications

# Bioorthogonal Fluorescence Turn-On Labeling Based on Bicyclononyne–Tetrazine Cycloaddition Reactions that Form Pyridazine Products

Sebastian J. Siegl, Juraj Galeta, Rastislav Dzijak, Martin Dračínský, and Milan Vrabel*[a]

Fluorogenic bioorthogonal reactions enable visualization of biomolecules with excellent signal-to-noise ratio. A bicyclononyne–tetrazine ligation that produces fluorescent pyridazine products has been developed. In stark contrast to previous approaches, the formation of the dye is an inherent result of the chemical reaction and no additional fluorophores are needed in the reagents. The crucial structural elements that determine dye formation are electron-donating groups present in the starting tetrazine unit. The newly formed pyridazine fluorophores show interesting photophysical properties the fluorescence intensity increase in the reaction can reach an excellent 900-fold. Model imaging experiments demonstrate the application potential of this new fluorogenic bioorthogonal reaction.

Visualization of biomacromolecules involved in biological processes is an important part of biological research. The discovery and development of fluorescent proteins has revolutionized our ability to illuminate subcellular organization of enzymes and proteins and provided us with the unique possibility to study their structure and function in living systems.[1] Besides these genetically-encodable methods, the use of small-molecule fluorescent dyes has further advanced our understanding of biology and extended our possibility to examine biomolecules beyond proteins and enzymes.[2] Among the main advantages of using small-molecule fluorophores for bioimaging applications belong their superior and tunable photophysical properties and their small size.

A good signal-to-noise ratio is an important metric for determining the success of bioimaging experiments. Accordingly, the development of fluorogenic probes enabling turning-on of the fluorescence of the reporter molecule in response to a specific molecular event represents significant achievement in suppressing the undesired background signal.[3] In the last decades, the concept of fluorogenicity was successfully applied to various bioorthogonal reactions, which led to the development of chemically-activatable fluorogenic probes. These probes usually comprise specific structural features that lead to quenching of the fluorescence of the attached fluorophore. The fluorescence of the dye is then restored after the chemical reaction. This powerful concept was successfully utilized for numerous dyes and bioorthogonal reactions.[4]

Among other bioconjugations, the inverse electron-demand Diels-Alder reaction (iEDDA) of 1,2,4,5-tetrazines with strained dienophiles stands out due to expedient kinetics and excellent biocompatibility.[5] The inherent properties of the heterocyclic tetrazine core enabled development of fluorogenic tetrazine probes with tunable photophysical properties for bioimaging application.[6] In addition, we and others have shown that the iEDDA reaction of tetrazines with particular dienophiles can directly lead to formation of fluorescent dyes.[7] The latter approach represents an attractive alternative to the fluorophore-quenching concept as the only reaction products are the fluorescent species formed during the reaction and no additional fluorophores are required in the structure of reagents.

In our recent work we showed that 1,2,4,5-tetrazines decorated with vinylaniline or azetidine electron-donating groups produce in reaction with various *trans*-cyclooctenes (TCOs) fluorescent 4,5-dihydropyridazines.[8] We found that this class of tetrazines also forms fluorescent products in reaction with the bicyclononyne (BCN) dienophile. This unexpected observation prompted us to study this fluorogenic reaction in more detail.

Here we show that BCN yields fluorescent pyridazines in the reaction with 1,2,4,5-tetrazines bearing electron-donating groups (Figure 1). The increase in fluorescence intensity after the reaction can reach up to 900-fold, which is among the highest values reported for a bioorthogonal reaction to date. This new BCN–tetrazine reaction can be used in combination with the TCO–tetrazine cycloaddition for two-color fluorogenic imaging. In addition, the fluorogenicity is preserved in biological systems and enables the reaction to be used for bioimaging application.

We started our study with the reaction of the *p*-vinyldimethylaniline substituted tetrazine **1a** with BCN. The HPLC-MS analysis of the crude reaction mixture showed formation of the signal having the mass corresponding to the expected pyridazine **2a** (Figure S1 in the Supporting Information). The structure of the product was confirmed by NMR analysis (see the Supporting Information). The absorption maximum of the

[a] *MSc. S. J. Siegl, Dr. J. Galeta, Dr. R. Dzijak, Dr. M. Dračínský, Dr. M. Vrabel*
*Institute of Organic Chemistry*
*and Biochemistry of the Czech Academy of Sciences*
*Flemingovo nám. 2, 166 10, Prague (Czech Republic)*
*E-mail: vrabel@uochb.cas.cz*

Supporting information for this article is available on the WWW under https://doi.org/10.1002/cplu.201900176

This article is part of the "Early Career Series". To view the complete series, visit: http://chempluschem.org/earlycareer.

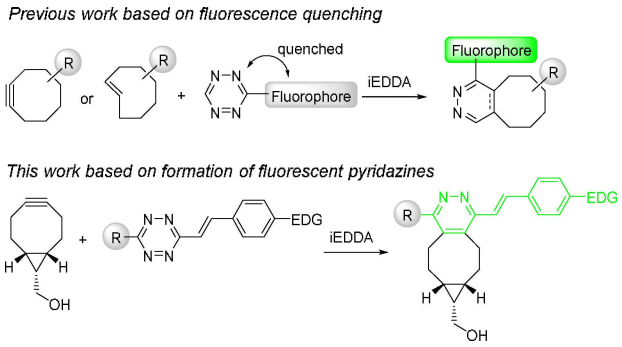


**Figure 1.** General concept of fluorogenic inverse electron-demand Diels-Alder reactions using strained dienophiles and 1,2,4,5-tetrazines. EDG = electron-donating group.

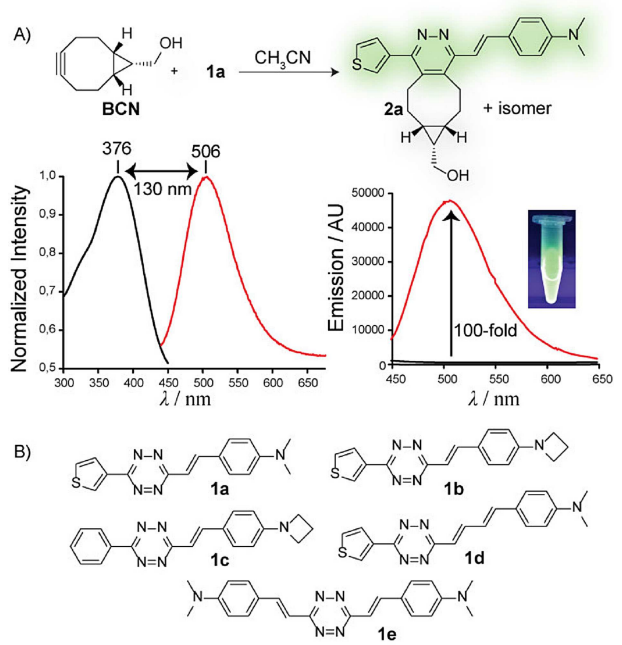


**Figure 2.** A) An example of the experiment showing formation of the fluorescent pyridazine product in the reaction of BCN with tetrazine **1a**. Shown are normalized absorption (black) and emission (red) spectra and the fluorescence enhancement after the reaction. Only one isomer (enantiomer) of the product is shown for clarity. B) Structures of tetrazines used in this study.

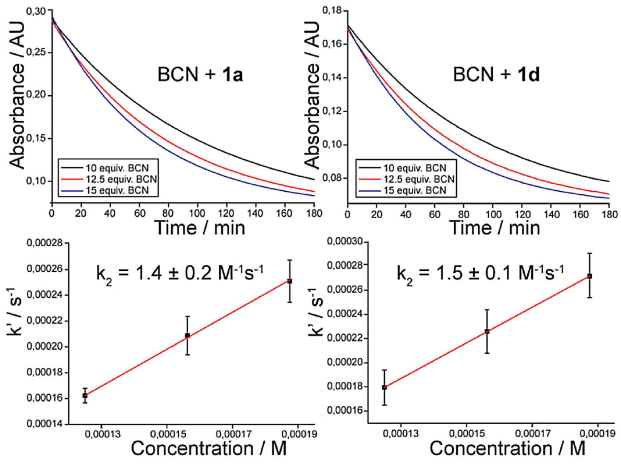


**Figure 3.** Second-order rate constant measurements of the reaction between tetrazines **1a** and **1d** with BCN. The reactions were performed in 1/1 mixture of $CH_3CN$ and $H_2O$ at room temperature (22°C) under pseudo-first-order conditions using an excess of BCN.

**Table 1.** Photophysical properties of the click products **2a**–**2e** formed in reaction of tetrazines **1a**–**1e** with BCN in $CH_3CN$.

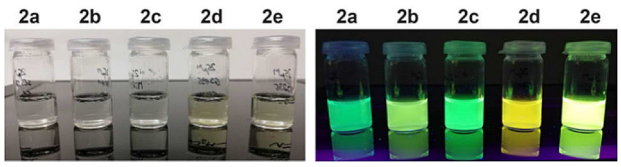


| Click product | $\lambda_{Abs}/\lambda_{Em}$ [nm][a] | Stokes shift [nm] | $\Phi$[b] | Fl. intensity increase |
|---|---|---|---|---|
| **2a** | 376/506 | 130 | 0.014 | 100-fold |
| **2b** | 370/513 | 143 | 0.010 | 185-fold |
| **2c** | 369/508 | 139 | 0.011 | 330-fold |
| **2d** | 392/562 | 170 | 0.038 | 10-fold |
| **2e** | 397/529 | 132 | 0.134 | 900-fold |

[a] Absorption and emission maxima in $CH_3CN$. [b] Fluorescence quantum yields were determined using quinine sulfate in 0.5 M $H_2SO_4$ as standard ($\Phi = 0.55$). For copies of absorption and emission spectra see Figure S3–S7.

product is at 376 nm and emission at 506 nm, respectively, giving a 130 nm Stokes shift in $CH_3CN$ (Figure 2A). The increase in the fluorescence signal after the reaction was 100-fold (starting tetrazine vs. the click product).

To study the effect of various substituents on the photophysical properties of the click products we next performed similar experiments with different tetrazines (Figure 2B, Table 1, Table S2). We did not find significant difference in the absorption and emission maxima when using tetrazine **1b**, which contains azetidine instead of the dimethylamino group. However, the enhancement of the fluorescent signal after the reaction increased to 185-fold. Tetrazine **1c** containing the phenyl substituent instead of the thiophene showed in the reaction a further increase in the fluorescence intensity which was 330-fold. In an attempt to shift the absorption and emission maxima by extending the conjugated π-system of the fluorophore we next introduced another double bond between the tetrazine core and the substituent bearing the electron-donating dimethylamino group. Indeed, the absorption and emission maxima of the click product formed in reaction of **1d** with BCN were 392 nm and 562 nm, respectively.

The above experimental data led us to hypothesize that the pyridazine core of the click product serves as an electron-poor part of the molecule. The presence of electron-donating substituents then leads to the formation of a push-pull-like system, which finally results in formation of the fluorophore. We therefore speculated that introducing the vinylaniline substituent from both sides of the tetrazine core could improve the photophysical properties of the click product. To test this hypothesis we prepared symmetric tetrazine **1e** and measured the photophysical properties of the click product formed after the reaction with BCN.

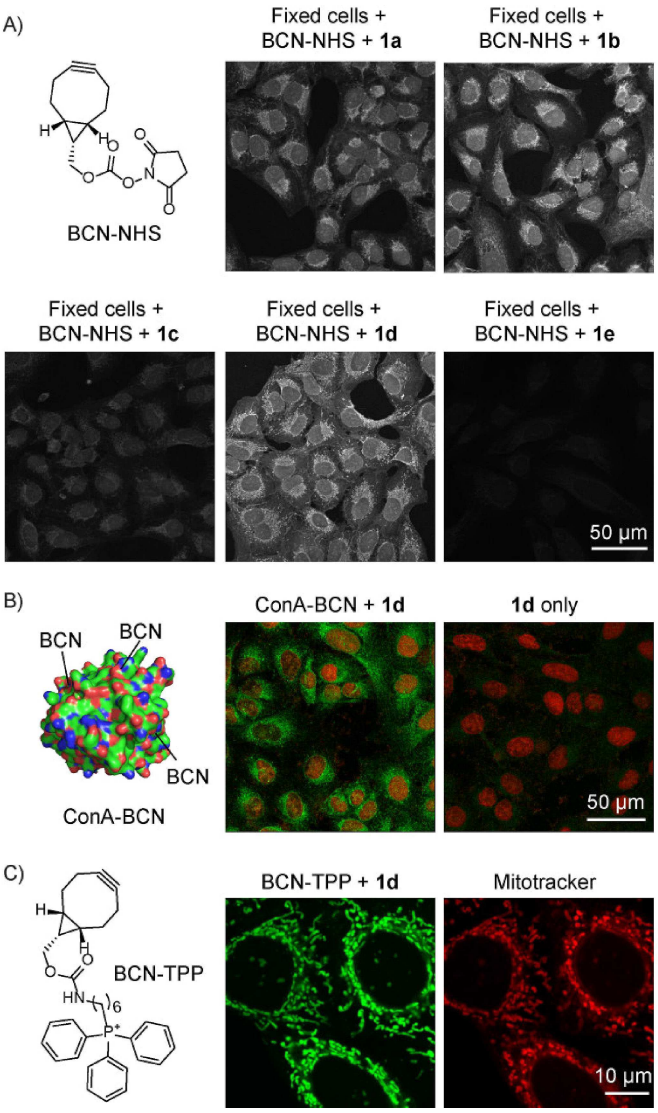


**Figure 4.** Images from confocal fluorescence microscope showing A) fluorogenic labeling of BCN-modified HeLa cells after addition of tetrazines **1a**–**1e**. Click product excitation: $\lambda = 405$ nm, emission: $\lambda = 517$–$587$ nm for **1a**, **1b**, **1c** and **1e** and $\lambda = 543$–$639$ nm window for **1d**. B) ConA–BCN modified U2OS cells after addition of **1d**. Nucleus was stained using commercially available DRAQ5 dye (Excitation: $\lambda = 633$ nm, Emission: $\lambda = 643$–$703$ nm window). C) fluorogenic labeling of live HeLa cells using BCN–TPP and **1d**. Mitotracker: Excitation: $\lambda = 633$ nm, Emission: $\lambda = 640$–$735$ nm window. The pictures are in pseudocolors.

Indeed, we found that **1e** yields a fluorescent product displaying interesting photophysical properties. The absorption and emission maxima of **2e** were 397 and 529 nm, respectively. Most importantly, the fluorescence enhancement in the reaction of this particular tetrazine with BCN reached an impressive 900-fold, which is the highest in the series. The fluorescence quantum yield of **2e** is also the highest among the click products (Table 1).

To simulate more biologically-relevant conditions we also measured the photophysical properties of the click products **2a–2e** in 1/1 mixture of $CH_3CN$ and $H_2O$ (Table S3 and Figure S8–S12). Interestingly, tetrazines **1a**, **1b** and **1d** showed even higher fluorescence turn-on in this solvent mixture, while for **1c** and **1e** the fluorescence intensity decreased. However, **2e** showed higher fluorescence in 1/1 mixture of $CH_3CN$ and PBS buffer (Figure S12). We also noticed that the absorption and emission maxima of the click products were shifted in $CH_3CN/H_2O$ mixture indicating that the pyridazine fluorophores are solvatochromic. We therefore determined the photophysical properties of the click product **2a** in different solvents. The experiment confirmed this assumption and the absorption and especially the emission maximum as well as the fluorescence quantum yields varied in different solvents (Table S4 and Figure S13–S17). These data indicate that the pyridazines could serve as useful fluorescent environment-sensitive probes.[9] In combination with the excellent fluorescence turn-on properties, these probes could find utility in various imaging applications, where a good signal-to-noise ratio is desirable.

The reactivity of 1,2,4,5-tetrazines with the BCN dienophile usually differs from that with the TCOs.[5c,10] To gain insight into the reactivity of our group of tetrazines with BCN we measured the second order rate constant for two representative deriva-

tives, namely for **1a** and **1d**. The second order rate constants were determined at room temperature (22°C) in a 1/1 mixture of $CH_3CN$ and $H_2O$ under pseudo first-order conditions using an excess of BCN by following the decay in the absorption of the starting tetrazine over time (Figure 3). The observed rate constants for each BCN concentration were finally plotted against BCN concentration and the second order rate constants were calculated from the slope of the plot (Table S5). The experiments were performed in triplicate. The determined second order rate constant for the reaction of tetrazine **1a** with BCN was $1.4 \pm 0.2\ M^{-1}s^{-1}$ and $1.5 \pm 0.1\ M^{-1}s^{-1}$ for tetrazine **1d**, respectively. These data show that there is no significant difference in reactivity of these two tetrazines.

For comparison, similar tetrazines react about ten-times faster with the equatorial *trans*-cyclooctenol as we determined in our previous work.[8] On the other hand, the determined reaction rate of the BCN–tetrazine cycloaddition is comparable to that of the reaction of tetrazines with, for example, norbornenes,[11] which are useful bioconjugation reagents and have been successfully used in bioimaging applications.[12]

We next studied the fluorogenic reaction of tetrazines **1a**–**1e** with BCN on HeLa cells. For this purpose, the cells were fixed and treated with the BCN active ester. We then added the individual tetrazines and inspected the cells on a confocal fluorescence microscope (Figure 4A and Figure S18). Addition of tetrazine **1e**, which we found superior regarding its photophysical properties (Table 1), led to formation of only a very weak fluorescent signal in the cells. Similarly **1c** also did not form significant labeling pattern. Tetrazines **1a** and **1b** performed similarly and gave rise to a visible fluorescent signal. Among the tetrazines tested, compound **1d** was found superior and we observed formation of clear visible fluorescent signal in the cells. Importantly, we did not observe any fluorescent signal in cells treated only with the tetrazines showing that formation of the fluorescent signal is a result of the reaction (Figure S18).

To further probe the fluorogenic reaction on cells we prepared concanavalin A modified with the BCN moiety (ConA–BCN). ConA is a lectin extensively used in studies of glycoconjugates.[13] After incubation of U2OS cells with ConA–BCN and addition of tetrazine **1d** we observed formation of a fluorescent signal indicating successful reaction, while cells treated only with the tetrazine were not fluorescent (Figure 4B).

To examine the fluorescence turn-on reaction in live cells we prepared BCN–triphenylphosphonium conjugate (BCN–TPP). The TPP moiety was used in order to target the BCN group to mitochondria.[14] Live HeLa cells were incubated with BCN–TPP and the fluorogenic reaction was subsequently initiated by addition of **1d**. Analysis of the cells by confocal microscopy showed formation of fluorescent signal inside mitochondria as confirmed by co-staining with commercially available mitotracker deep red dye (Figure 4C). Importantly, cells treated only with **1d** were not fluorescent. We obtained similar results with live U2OS cells (Figure S18).

We also evaluated the toxicity of **1a**–**1e** on HeLa and U2OS cells using XTT or crystal violet assay. Our results show that the tetrazines are not toxic up to 50 μM concentration after 24 hours of incubation (Figure S20).

Our recent discovery that various TCOs form 4,5-dihydropyridazine fluorophores in reaction with the same group of tetrazines[8] led us to speculate that we could use the BCN and the TCO moiety for two-color fluorogenic labeling using a single tetrazine as the activator. To test this on a model system, we prepared a topologically segregated bilayer Tentagel (TG) resin beads.[15] The outer layer of the beads was modified with the BCN moiety, while the inner part was functionalized by the TCO.

As the two fluorophores build from the two dienophiles (fully aromatic pyridazine from BCN and 4,5-dihydropyridazine from TCO) have distinct photophysical properties they should be distinguishable by using different excitation wavelength and emission filters.[8] Indeed, when we incubated the BCN–TCO-modified TG beads with tetrazine **1a** we observed clear formation of two fluorophores confirming a successful reaction and fluorescence turn-on corresponding to the reaction of the tetrazine with the two different dienophiles (Figure 5 and Figure S19). This model experiment demonstrates that the inherent fluorogenic nature of the TCO– and BCN–tetrazine click reaction can be utilized and combined on one system enabling two-color fluorogenic labeling after addition of a single tetrazine. However, the tautomerization of the 4,5-dihydropyridazine to the corresponding 1,4-dihydropyridazine as well as the propensity of both isomers to form oxidized pyridazines must be carefully considered in similar experiments as this may lead to changes in the fluorescence over time (Figure S21).[8,16]

In this study, we have shown that tetrazines decorated with electron-donating substituents connected via π-system yield in reaction with the strained bicyclononyne dienophile fluorescent pyridazine dyes. The fluorophores formed have large Stokes

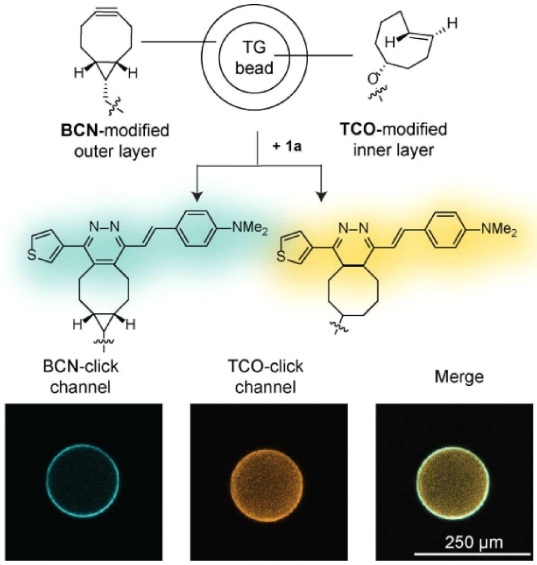


**Figure 5.** Confocal fluorescence microscope images showing two-color fluorogenic labeling of bilayer segregated Tentagel beads containing the BCN moiety on the outer layer and the TCO moiety in the inner part of the beads. BCN-click channel: Excitation at $\lambda = 458$ nm, Emission at $\lambda = 508$–556 nm window. TCO-click channel: Excitation at $\lambda = 561$ nm, Emission at $\lambda = 575$–645 nm window. The pictures are in pseudocolors.

shift, but rather low fluorescence quantum yield. The fluorescence turn-on in the reaction exceeded 100-fold in most cases and reached an impressive 900-fold when symmetric double-substituted tetrazine was used. The fluorogenic nature of the reaction is preserved in biological systems and provides application to bioimaging. In combination with the TCO–tetrazine cycloaddition, the reaction enables simultaneous two-color fluorogenic labeling using a single tetrazine as the activator.

## Acknowledgements

*This work was supported by the European Research Council (ERC) under the European Union's Horizon 2020 research and innovation programme (grants agreement No 677465). We gratefully acknowledge critical reading of the manuscript by Dr. Michael Downey.*

## Conflict of Interest

*The authors declare no conflict of interest.*

**Keywords:** cyclic alkynes · cycloaddition reactions · Diels-Alder reactions · fluorogenic probes · tetrazines

[1] a) P. Dedecker, F. C. De Schryver, J. Hofkens, *J. Am. Chem. Soc.* **2013**, *135*, 2387–2402; b) E. A. Rodriguez, R. E. Campbell, J. Y. Lin, M. Z. Lin, A. Miyawaki, A. E. Palmer, X. K. Shu, J. Zhang, R. Y. Tsien, *Trends Biochem. Sci.* **2017**, *42*, 111–129.

[2] a) E. A. Specht, E. Braselmann, A. E. Palmer, *Annu. Rev. Physiol.* **2017**, *79*, 93–117; b) T. Terai, T. Nagano, *Pflug. Arch. Eur. J. Phy.* **2013**, *465*, 347–359.

[3] a) C. Le Droumaguet, C. Wang, Q. Wang, *Chem. Soc. Rev.* **2010**, *39*, 1233–1239; b) A. Nadler, C. Schultz, *Angew. Chem. Int. Ed.* **2013**, *52*, 2408–2410; *Angew. Chem.* **2013**, *125*, 2466–2469.

[4] a) G. A. Lemieux, C. L. de Graffenried, C. R. Bertozzi, *J. Am. Chem. Soc.* **2003**, *125*, 4708–4709; b) K. Sivakumar, F. Xie, B. M. Cash, S. Long, H. N. Barnhill, Q. Wang, *Org. Lett.* **2004**, *6*, 4603–4606; c) P. Shieh, M. S. Siegrist, A. J. Cullen, C. R. Bertozzi, *Proc. Natl. Acad. Sci.* **2014**, *111*, 5456–5461; d) F. Friscourt, C. J. Fahrni, G. J. Boons, *Chem. Eur. J.* **2015**, *21*, 13996–14001; e) A. Herner, G. E. Girona, I. Nikic, M. Kallay, E. A. Lemke, P. Kele, *Bioconjugate Chem.* **2014**, *25*, 1370–1374; f) J. J. Shie, Y. C. Liu, J. C. Hsiao, J. M. Fang, C. H. Wong, *Chem. Commun.* **2017**, *53*, 1490–1493; g) O. Demeter, A. Kormos, C. Koehler, G. Mezo, K. Nemeth, E. Kozma, L. B. Takacs, E. A. Lemke, P. Kele, *Bioconjugate Chem.* **2017**, *28*, 1552–1559; h) E. Decuypere, M. Riomet, A. Sallustrau, S. Bregant, R. Thai, G. Pieters, G. Clavier, D. Audisio, F. Taran, *Chem. Commun.* **2018**, *54*, 10758–10761; i) W. Song, Y. Wang, J. Qu, M. M. Madden, Q. Lin, *Angew. Chem. Int. Ed.* **2008**, *47*, 2832–2835; *Angew. Chem.* **2008**, *120*, 2874–2877; j) E. Kozma, P. Kele, *Org. Biomol. Chem.* **2019**, *17*, 215–233.

[5] a) B. L. Oliveira, Z. Guo, G. J. L. Bernardes, *Chem. Soc. Rev.* **2017**, *46*, 4895–4950; b) A. C. Knall, C. Slugovc, *Chem. Soc. Rev.* **2013**, *42*, 5131–5142; c) R. Selvaraj, J. M. Fox, *Curr. Opin. Chem. Biol.* **2013**, *17*, 753–760.

[6] a) N. K. Devaraj, S. Hilderbrand, R. Upadhyay, R. Mazitschek, R. Weissleder, *Angew. Chem. Int. Ed.* **2010**, *49*, 2869–2872; *Angew. Chem.* **2010**, *122*, 2931–2934; b) H. X. Wu, J. Yang, J. Seckute, N. K. Devaraj, *Angew. Chem. Int. Ed.* **2014**, *53*, 5805–5809; *Angew. Chem.* **2014**, *126*, 5915–5919; c) E. Kozma, G. E. Girona, G. Paci, E. A. Lemke, P. Kele, *Chem. Commun.* **2017**, *53*, 6696–6699; d) A. Wieczorek, P. Werther, J. Euchner, R. Wombacher, *Chem. Sci.* **2017**, *8*, 1506–1510; e) Y. Lee, W. Cho, J. Sung, E. Kim, S. B. Park, *J. Am. Chem. Soc.* **2018**, *140*, 974–983; f) A. Wieczorek, T. Buckup, R. Wombacher, *Org. Biomol. Chem.* **2014**, *12*, 4177–4185; g) L. G. Meimetis, J. C. T. Carlson, R. J. Giedt, R. H. Kohler, R. Weissleder, *Angew. Chem. Int. Ed.* **2014**, *53*, 7531–7534; *Angew. Chem.* **2014**, *126*, 7661–7664; h) G. Knorr, E. Kozma, A. Herner, E. A. Lemke, P. Kele, *Chem. Eur. J.* **2016**, *22*, 8972–8979.

[7] a) X. Shang, X. Song, C. Faller, R. Lai, H. Li, R. Cerny, W. Niu, J. Guo, *Chem. Sci.* **2017**, *8*, 1141–1145; b) A. Vazquez, R. Dzijak, M. Dracinsky, R. Rampmaier, S. J. Siegl, M. Vrabel, *Angew. Chem. Int. Ed.* **2017**, *56*, 1334–1337; *Angew. Chem.* **2017**, *129*, 1354–1357; c) S. J. Siegl, A. Vazquez, R. Dzijak, M. Dracinsky, J. Galeta, R. Rampmaier, B. Klepetarova, M. Vrabel, *Chem. Eur. J.* **2018**, *24*, 2426–2432.

[8] S. J. Siegl, J. Galeta, R. Dzijak, A. Vazquez, M. Del Rio-Villanueva, M. Dracinsky, M. Vrabel, *ChemBioChem* **2019**, *20*, 886–890.

[9] A. S. Klymchenko, *Acc. Chem. Res.* **2017**, *50*, 366–375.

[10] D. Wang, W. Chen, Y. Zheng, C. Dai, K. Wang, B. Ke, B. Wang, *Org. Biomol. Chem.* **2014**, *12*, 3950–3955.

[11] a) M. Vrabel, P. Kolle, K. M. Brunner, M. J. Gattner, V. Lopez-Carrillo, R. de Vivie-Riedle, T. Carell, *Chem. Eur. J.* **2013**, *19*, 13309–13312; b) A. C. Knall, M. Hollauf, C. Slugovc, *Tetrahedron Lett.* **2014**, *55*, 4763–4766.

[12] a) T. Plass, S. Milles, C. Koehler, J. Szymanski, R. Mueller, M. Wiessler, C. Schultz, E. A. Lemke, *Angew. Chem. Int. Ed.* **2012**, *51*, 4166–4170; *Angew. Chem.* **2012**, *124*, 4242–4246; b) E. Kaya, M. Vrabel, C. Deiml, S. Prill, V. S. Fluxa, T. Carell, *Angew. Chem. Int. Ed.* **2012**, *51*, 4466–4469; *Angew. Chem.* **2012**, *124*, 4542–4545; c) K. Lang, L. Davis, J. Torres-Kolbus, C. J. Chou, A. Deiters, J. W. Chin, *Nat. Chem.* **2012**, *4*, 298–304.

[13] I. J. Goldstein, R. D. Poretz, in *The Lectins. Properties, Functions, and Applications in Biology and Medicine., Vol. 32* (Eds.: I.E. Liener, N. Sharon, I. J. Goldstein), Elsevier, **1986**, pp. 33–247.

[14] J. Zielonka, J. Joseph, A. Sikora, M. Hardy, O. Ouari, J. Vasquez-Vivar, G. Cheng, M. Lopez, B. Kalyanaraman, *Chem. Rev.* **2017**, *117*, 10043–10120.

[15] F. Bedard, A. Girard, E. Biron, *Int. J. Pept. Res. Ther.* **2013**, *19*, 13–23.

[16] a) J. C. T. Carlson, H. Mikula, R. Weissleder, *J. Am. Chem. Soc.* **2018**, *140*, 3603–3612; b) R. M. Versteegen, W. Ten Hoeve, R. Rossin, M. A. R. de Geus, H. M. Janssen, M. S. Robillard, *Angew. Chem. Int. Ed.* **2018**, *57*, 10494–10499.; *Angew. Chem.* **2018**, *130*, 10654-10659.

Manuscript received: March 19, 2019
Revised manuscript received: April 24, 2019
Accepted manuscript online: April 25, 2019

 

## 3.4 The discovery of pyridinium 1,2,4-triazines with enhanced performance in bioconjugation reactions

S.J. Siegl, R. Dzijak, A. Vázquez, R. Pohl, M. Vrabel, *Chem. Sci.* **2017**, 8, 3593-3598.
Copy of the publication with permission of the publisher; Published by The Royal Society of Chemistry.

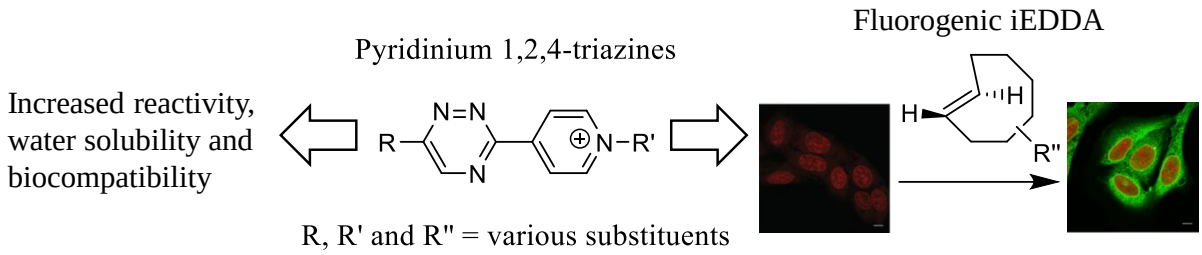


### 3.4.1 Background

Recently, 1,2,4-triazines were identified as a promising alternative to 1,2,4,5-tetrazines for bioorthogonal reactions with strained dienophiles.[139-140] However, their widespread utility for bioimaging is still limited due to considerably reduced reactivity, when compared to tetrazines. For this reason, our goal was to gain deeper insight into the reactivity of 1,2,4-triazines with TCOs by systematically studying the influence of the structure of both triazine and TCO on the reaction kinetics. We demonstrated that the substitution pattern of both starting materials significantly affects the reaction rates of the iEDDA reaction, which can vary by orders of magnitude. Furthermore, our study led to the discovery of a novel class of cationic *N*-alkyl pyridinium 1,2,4-triazines with excellent properties for bioconjugation applications. The most intriguing property of these pyridinium triazines was the formation of unprecedented fluorescent dihydropyridine products upon cycloaddition with various TCOs in a similar way to our previously described tetrazine ligations that form fluorescent dihydropyridazines.

### 3.4.2 Declaration of contribution

For this work, I synthesized all 1,2,4-triazines and, together with *Dr. Milan Vrábel*, the heterobifunctional 1,2,4-triazine derivatives. TCOs used in this study were prepared by *Dr. Arcadio Vázquez*. I measured the second-order rate constants for the click reactions between the 1,2,4-triazines and TCOs and verified the formation of the corresponding

dihydropyridine products by HPLC-MS measurements. Furthermore, I carried out the stability studies for the cationic pyridinium triazine by HPLC-MS and in collaboration with *Dr. Radek Pohl* by NMR experiments. I synthesized and isolated the dihydropyridine as well as the corresponding oxidized pyridine product of the click reaction between d-TCO and one of the cationic triazines, which was confirmed by HPLC-MS measurements performed by me and by NMR experiments performed by *Dr. Radek Pohl*. Additionally, I evaluated the stability of the reduced form of this click product under aqueous conditions and its susceptibility to oxidation in the presence of air by HPLC-MS analysis. The photophysical properties of this click product in different solvents I determined together with *Dr. Milan Vrábel*. Moreover, I performed the double click-labeling experiments of the azide-functionalized pyridinium triazine with d-TCO and BCN. Cell labeling experiments were carried out by *Dr. Rastislav Dzijak*. I also actively participated in writing the manuscript.

Chemical Science

EDGE ARTICLE

View Article Online
View Journal | View Issue



Cite this: *Chem. Sci.*, 2017, **8**, 3593

# The discovery of pyridinium 1,2,4-triazines with enhanced performance in bioconjugation reactions†

Sebastian J. Siegl, Rastislav Dzijak, Arcadio Vázquez, Radek Pohl and Milan Vrabel*

Received 13th December 2016
Accepted 1st March 2017

DOI: 10.1039/c6sc05442k

rsc.li/chemical-science

1,2,4-Triazines have recently been identified as versatile dienes participating in the inverse electron-demand Diels–Alder reaction with strained dienophiles. However, their widespread utility in bioconjugation reactions is still limited. Herein, we report a systematic study on the reactivity of various 1,2,4-triazines with *trans*-cyclooctenes showing that the structure of both the triazine and the dienophile significantly affect the reaction rate. Our kinetic study led to the discovery of novel cationic 1,2,4-triazines with superior properties for bioconjugation reactions. We have developed an efficient method that enables their late-stage functionalization and allows for easy access to various useful heterobifunctional scaffolds. In addition, these charged dienes form unprecedented fluorescent products upon reaction with *trans*-cyclooctenes and can be used for fluorogenic labeling of subcellular compartments in live cells.



## Introduction

Bioorthogonal reactions have become an invaluable tool for studying biomolecules in their native environment.[1] The success of these studies strongly depends on the inherent chemical properties of the reagents being employed in them. There has been an extensive effort to develop bioorthogonal probes which are inert to natural functional groups, are sufficiently water soluble, and which react selectively with high rates under strict biological conditions.[2] The improved design of reagents together with systematic kinetic studies has led to substantial advancements in this regard.[3]

The inverse electron-demand Diels–Alder reaction (IEDDA) of 1,2,4,5-tetrazines with strained alkenes is the reaction of choice when high reaction rates are desirable.[4] This particular cycloaddition has found numerous applications in biomolecule labeling, live cell labeling as well as in diagnostics.[5] Unfortunately, the exceptional reactivity of 1,2,4,5-tetrazines is often indispensably connected to their reduced stability toward biological nucleophiles.[5c,5f,6] 1,2,4-Triazines were recently identified as alternative heterodienes which participate in IEDDA reactions with *trans*-cyclooctene (TCO) and bicyclononyne (BCN) derivatives.[7] Although 1,2,4-triazines show remarkable stability under biological conditions[7b] their reactivity is considerably reduced when compared to 1,2,4,5-tetrazines. This hampers their broader utility in bioconjugation reactions.

To gain deeper insight into the reactivity of 1,2,4-triazines with TCOs, we decided to systematically investigate the influence of various substituents on the kinetics of the reaction. Our data show that the reaction rates can vary by orders of magnitude with the second-order rate constants ranging from 0.007 $M^{-1}$ $s^{-1}$ up to more than 20 $M^{-1}$ $s^{-1}$ depending on the structure of both the 1,2,4-triazine and the TCO. In addition, our study led to the discovery of a novel class of cationic pyridinium 1,2,4-triazines with enhanced performance in bioconjugation reactions. The advances provided by these charged heterodienes are manifold. Firstly, they are charged, which inherently improves their water solubility. Secondly, when compared to analogous derivatives bearing an unsubstituted pyridine moiety the reactivity of the pyridinium triazines increases significantly while their stability under biological conditions remains excellent. Thirdly, their structural features in combination with the developed synthetic methodology enable further derivatization of the scaffold and preparation of various useful heterobifunctional probes. The last advance presented herein is the formation of unprecedented fluorescent products upon reaction of the pyridinium 1,2,4-triazines with TCOs. This chemistry can be used for bioimaging as we demonstrate by fluorogenic cell labeling experiments.

## Results and discussion

Our study began with the synthesis of various 1,2,4-triazines. We first prepared 3,6-bisaryl substituted 1,2,4-triazines starting from the respective glyoxal derivatives in a sequence of reactions depicted in Scheme 1A.[8] It is worth mentioning that the success of the last dehydration–cyclization step strongly depends on the carboxaldehyde used. While 2- and 4-pyridyl derivatives led to the formation of the desired cyclized products, for example simple

*Institute of Organic Chemistry and Biochemistry of the Czech Academy of Sciences, Flemingovo nám. 2, 16610, Prague, Czech Republic. E-mail: vrabel@uochb.cas.cz*

† Electronic supplementary information (ESI) available: Experimental procedures; NMR; LC-MS; UV-Vis and fluorescence. See DOI: 10.1039/c6sc05442k

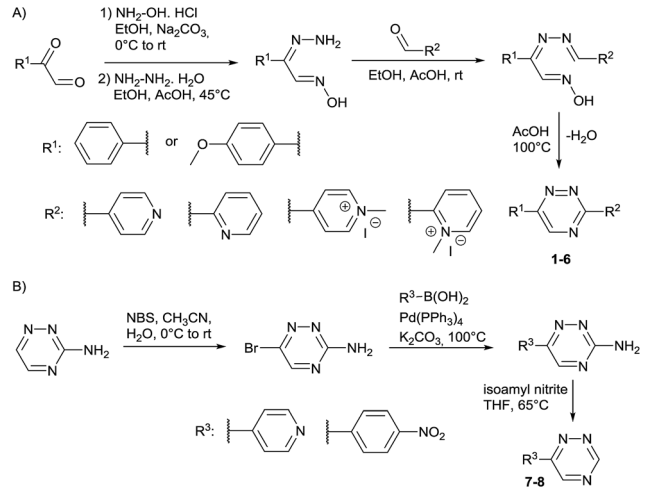


Scheme 1 Synthesis of mono- and bis-substituted 1,2,4-triazines.

benzaldehyde did not.[8b] On the other hand, reaction with 1-methylpyridinium 2- or 4-carboxaldehydes proceeded smoothly yielding a new type of charged pyridinium 1,2,4-triazines. For comparison, we also prepared monosubstituted 6-aryl 1,2,4-triazines starting from commercially available 3-amino 1,2,4-triazine utilizing a cross coupling–deamination reaction sequence reported previously (Scheme 1B).[7b]

To study the reactivity of 1,2,4-triazines in the IEDDA reaction we next synthesized a series of TCOs using the photochemical protocol developed by Fox and coworkers.[9] We determined the second-order rate constants in $CH_3CN/H_2O$ (1/1) at room temperature under pseudo first-order conditions using an excess of the corresponding TCO. Since the reactivity of various triazines as well as of TCOs differed significantly, we followed the progress of the reaction either by HPLC, for slower derivatives, or by UV/Vis spectroscopy, for faster derivatives (for details see ESI†). All experiments were performed in triplicate and the results are summarized in Table 1.

The data show that the presence of an electron donating *para*-methoxy substituent in **2** led to a slight decrease in reactivity, consistent with the inverse electron-demand nature of the cycloaddition. In contrast, the presence of the pyridinium group in **6** resulted in a greater than five-fold increase in reaction rate when compared to the analogous derivative bearing an unsubstituted pyridyl group (**3**). The position of the alkylation turned out to be very important. Triazine **5** bearing the alkyl group at the *para* position is about 30-times more reactive than the corresponding *ortho*-alkylated derivative **4**. This indicates that the electron withdrawing ability of the substituent is compromised by the increased steric demand in this case. Our data show that 3,6-bisaryl substituted 1,2,4-triazines (**1**–**6**) react with TCOs slower than the corresponding mono-substituted 6-aryl derivatives (**7**, **8**). Although the previously reported compound **8** (ref. 7b) was found to be the most reactive among the series, this particular derivative cannot be further modified and thus its utility in bioconjugation reactions is limited. It is reasonable to assume that alkylation of the pyridyl group of compound **7** could further increase its reactivity. Unfortunately, our attempts to prepare the corresponding derivative were unsuccessful.

The structure and configuration of the TCO also plays an important role. Simple *trans*-cyclooctene-ols are the slowest reaction partners (Table 1 and S2†). The dioxolane-fused TCO (d-TCO) is known for its improved reactivity in IEDDA reaction with 1,2,4,5-tetrazines.[10] This was also confirmed in our study and all triazines reacted with this dienophile about 10–20 times faster. A further increase in reactivity afforded the *trans*-bicyclononene derivative (s-TCO).[3b,10] This compound led to an impressive increase (2–4 orders of magnitude) in reaction rate when compared to TCO or BCN derivatives used in previous studies.[7] In fact, by reacting 1,2,4-triazines with d-TCO or s-TCO it is possible to reach reaction rates of the more reactive 1,2,4,5-tetrazines combined with less strained systems such as cyclopropene, norbornene or BCN derivatives, which are routinely employed in bioconjugation reactions.[3e–g,5d,11]

The excellent reactivity of pyridinium triazines drew our attention so we decided to study these compounds in more detail. We found that the pyridinium-modified 1,2,4-triazines are remarkably stable. Compound **6** was stable for over one week in PBS buffer at 37 °C even in the presence of an equimolar amount of L-cysteine (Fig. S5–S7†). In contrast, the most reactive 1,2,4,5-tetrazines are known to rapidly hydrolyze or degrade under similar conditions.[7b,9,11a,12] However, it should be noted that the stability of tetrazines also strongly depends on the substitution pattern.[6] The observed high reactivity of the presented 1,2,4-triazines is associated with the use of the most reactive TCOs (d-TCO or s-TCO) which isomerize to the much less reactive *cis* isomer more rapidly when compared to less strained TCOs.[10] This may become a problem for certain applications of the developed chemistry. It is therefore important to consider this particular limitation and accordingly design and plan the experiment. Further development of highly reactive and stable TCO derivatives would obviously provide an ideal solution to this obstacle. First attempts toward this direction has already been reported.[13]

We next aimed to exploit the structural features of the pyridinium 1,2,4-triazines for the synthesis of heterobifunctional probes. The possibility of further derivatization is an important step toward successful use of these compounds in bioconjugation reactions, where the attachment of an additional functionality is often desirable. We thought that a late-stage alkylation of the pyridyl group would provide an elegant approach in this sense. To investigate if the alkylation can proceed with sufficient selectivity on the pyridine nitrogen atom we reacted **3** with 5 equivalents of 3-iodopropionic acid. To our delight the reaction afforded the desired pyridinium compound **9** in 71% isolated yield without noticeable alkylation of the triazine heterocycle. Using this strategy, we synthesized a series of *N*-alkylated pyridinium 1,2,4-triazines depicted in Scheme 2.

The carboxyl group of **9** can be used for peptide coupling under standard conditions. The hydroxyl group of **10** can be converted to the corresponding active ester **14**. The terminal alkyne group of **11** can be employed in the Cu(I)-catalyzed azide–alkyne cycloaddition reaction with azides (Scheme 2 and ESI†).

Table 1 Second-order rate constants (in $M^{-1}\ s^{-1} \times 10^{-2}$) of the reaction between 1,2,4-triazines and TCOs[a]

| | Triazine/TCO | axial | syn/anti (12:1) | syn |
|---|---|---|---|---|
| 1 | 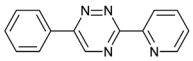 | 2.5 ± 0.1 | 56 ± 0.8 | 190 ± 3.0 |
| 2 | 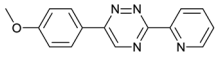 | 2.1 ± 0.2 | 36 ± 0.3 | 120 ± 1.0 |
| 3 | 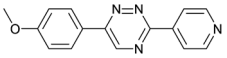 | 1.7 ± 0.4 | 35 ± 2.0 | 140 ± 3.0 |
| 4 | 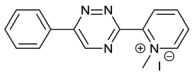 | 0.7 ± 0.1 | 8.3 ± 1.3 | 30 ± 1.0 |
| 5 | 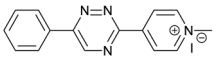 | 19.3 ± 0.2 | 260 ± 4.0 | 990 ± 30.0 |
| 6 | 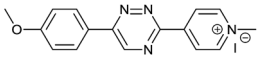 | 9.1 ± 0.3 | 190 ± 6.0 | 640 ± 20.0 |
| 7 | 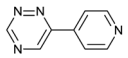 | 79.0 ± 5.0 | 940 ± 20.0 | 2020 ± 32.0 |
| 8 | 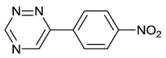 | 84.0 ± 7.0 | 1130 ± 50.0 | 2450 ± 70.0 |

[a] All reactions were performed in $H_2O/CH_3CN = 1/1$ at room temperature under pseudo first-order conditions using an excess of the corresponding TCO.

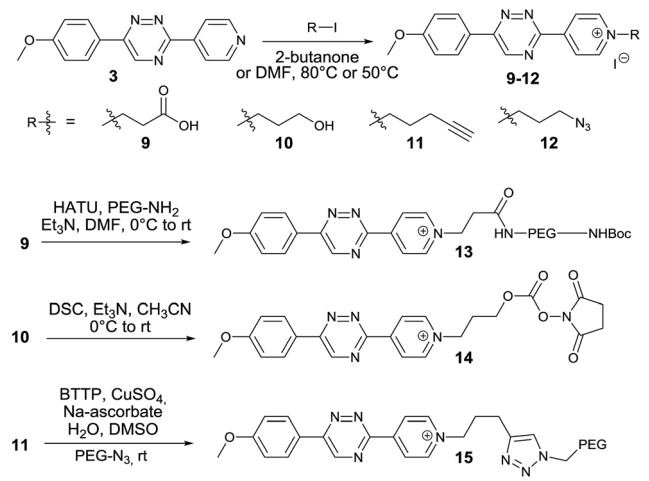


Scheme 2 Synthesis of heterobifunctional pyridinium 1,2,4-triazines.

The developed late-stage functionalization thus represents a simple and efficient synthetic methodology for preparation of various useful derivatives of 1,2,4-triazines.

We next speculated that the low reactivity of the triazine scaffold toward BCN[7a] should allow for its use in a one-pot double click-labeling reaction in combination with the strain-promoted azide–alkyne cycloaddition.[3a] To explore this, we synthesized compound **12**. The azido group of **12** could in principle also react with the olefinic bond of TCO in a 1,3-dipolar cycloaddition. However, the reported second-order rate constant for a similar reaction[14] was found to be ~0.02 $M^{-1}\ s^{-1}$ which is two orders of magnitude lower than the determined second-order rate constant of the reaction between **6** and *e.g.* d-TCO (1.9 $M^{-1}\ s^{-1}$). We hypothesized that the difference in reactivity will provide the required selectivity. Indeed, reaction of **12** with d-TCO afforded the respective Diels–Alder product as confirmed by HPLC-MS. The azido group of the intermediate was subsequently modified with BCN to give **16** (Fig. S8†). Similarly, reaction of **12** with BCN provided only the 1,3-dipolar cycloaddition adduct that was further reacted with d-TCO to afford the same doubly modified product **16** (Fig. S9†). Reaction of **12** with a mixture of d-TCO and BCN afforded the intended doubly-modified product **16** in a single step (Scheme 3 and Fig. S10†). This experiment demonstrates that the difference in reactivity of the two functional groups of **12** can be exploited for an efficient sequential and even single-step double labeling by two metal-free bioconjugation reactions. The 1,2,4-triazine and the azide group thus represent a new type of mutually orthogonal–bioorthogonal functional groups with potential utility in *e.g.* double-labeling of biomolecules,[15] simultaneous examination of multiple biological targets, or macromolecule assembly.[15b,16]

In the course of our study we discovered that the pyridinium substituted 1,2,4-triazines produce fluorescent products in Diels–Alder reaction with various TCOs. Such reagents are essential for the development of so-called fluorogenic reactions.[17] These reactions have great potential for bioimaging as they provide an improved signal-to-noise ratio.[18] By simply

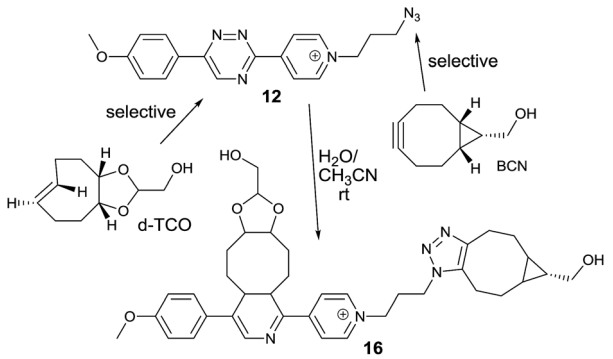


Scheme 3 Single-step double click labeling of azido functionalized 1,2,4-triazine. Only one regioisomer is shown.

mixing **6** with d-TCO in phosphate-buffered saline (PBS) a fluorescent product is formed with absorption and emission maxima at 405 nm and 650 nm respectively, yielding a new type of dye with an impressively large Stokes shift of 245 nm. We propose that the observed fluorescence results from the formation of a push–pull system arising from the initially formed dihydropyridine (Fig. 1). The structure of **17** was resolved by 1D and 2D NMR experiments (Fig. S11 and S12†). These experiments confirmed that it is the dihydropyridine and not the oxidized pyridine product that is fluorescent. As the starting triazine **6** is also not fluorescent one can conclude that the presence of a fully aromatic system abolishes the fluorescence even though a similar push–pull system can be drawn from these compounds as well.

We found that **17** is reasonably stable and only slowly started to oxidize/decompose over the course of a couple of days during incubation in PBS/$CH_3CN$ mixture at room temperature in the presence of air (Fig. S14†). We also found that **17** is a solvatochromic fluorophore with emissions ranging from 605 to 650 nm depending on the polarity of the solvent (Fig. 1D and S18†). In comparison to other commonly used fluorophores **17** has relatively low quantum yield. However, the strong increase in fluorescence upon the Diels–Alder reaction with TCOs (50-fold) together with the absorption maxima at 405 nm, which is a standard excitation wavelength used in *e.g.* confocal scanning microscopy, makes **17** a potential candidate for bioimaging applications. We therefore decided to investigate if the fluorogenic properties of the reaction will be preserved under biological conditions. We speculated that **6** as a positively charged and lipophilic molecule could be directly targeted to mitochondria.[19] To verify this, we incubated live U2OS cancer cells with **6** and then added d-TCO to initiate the fluorogenic reaction. We chose d-TCO instead of the more reactive s-TCO because of its improved stability under biological conditions.[10] When inspecting the cells under a confocal microscope, no fluorescence formed in cells treated only with **6**, while fluorescence was clearly visible in the live cells after addition of d-TCO (Fig. 2A-b and S19†). The targeting of **6** to mitochondria was confirmed by co-staining experiment using commercially available Mitotracker green (Fig. 2A and

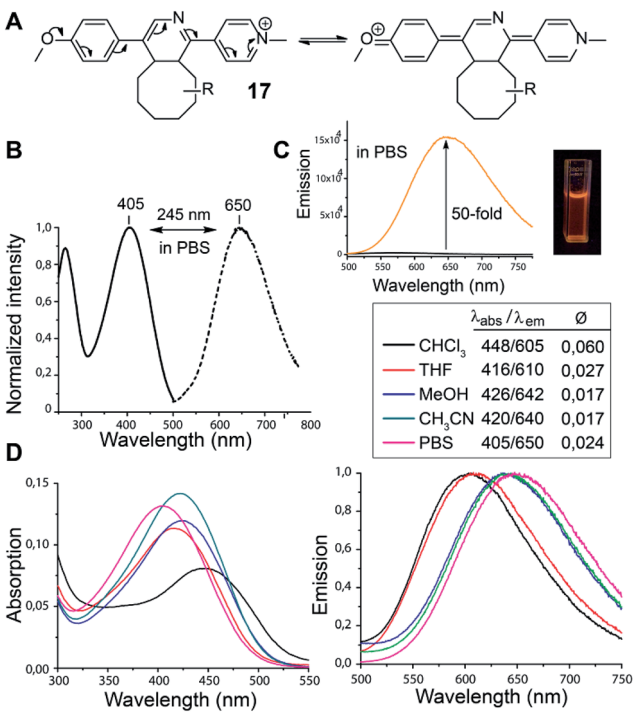


Fig. 1 (A) Proposed formation of the push–pull fluorescent click product. R = dioxolane moiety of d-TCO (as drawn for compound **16** in Scheme 3). (B) Normalized absorption (solid line) and emission spectra (dashed line) of the click product in PBS buffer. (C) Fluorescence intensity increase upon click reaction (black line for **6** and orange line for **6** + d-TCO). (D) Absorption and emission spectra of **17** in different solvents. The quantum yields were determined using Rhodamine 6G as standard (Ø = 0.94 in EtOH).

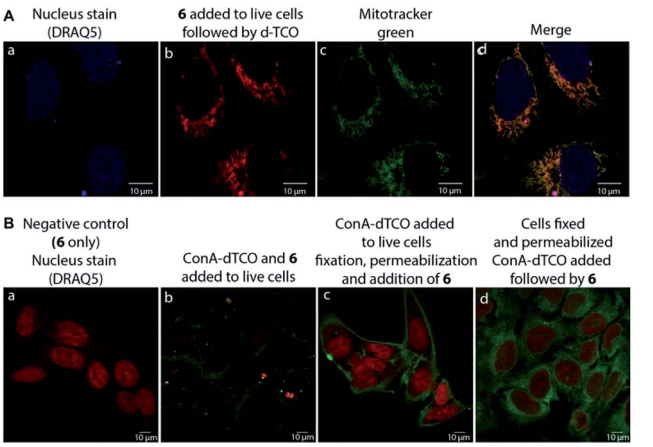


Fig. 2 Confocal microscope images of (A) fluorogenic click labeling of mitochondria in live U2OS cells treated with **6** and subsequently with d-TCO; targeting of **6** to mitochondria was confirmed by co-localization experiment using Mitotracker green (c and d); (B) fluorogenic labeling using α-D-mannose- and α-D-glucose-specific ConA-dTCO conjugate: (a) negative control (cells treated only with **6**, nucleus staining with DRAQ5), (b) live cells labelling with ConA-dTCO followed by addition of **6**, (c) live cells incubated with ConA-dTCO, then fixed, permeabilized and treated with **6**, (d) cells fixed, permeabilized and treated with ConA-dTCO followed by **6**. Click product (ex.: 405 nm, em.: 560–666 nm); DRAQ5 (ex.: 633 nm, em.: 653–732 nm); Mitotracker green (ex.: 496 nm, em.: 505–588 nm). Pictures were processed using LAS AF Lite program.

S20†). The inherent structural properties of **6** thus make this compound a new type of cell permeable, mitochondria-selective, chemically-activatable fluorogenic probe which may offer unique opportunities for dissecting the function of this vital cellular organelle.[20]

To further probe the potential of **6** for bioimaging, we conjugated the d-TCO moiety to concanavalin A (ConA-dTCO), a lectin with high specificity for α-D-mannose- and α-D-glucose-containing glycoconjugates.[21] We first added ConA-dTCO to live U2OS cells where it binds glycoconjugates on the cell membrane. Addition of **6** directly to live cells resulted into only a relatively weak fluorescent signal (Fig. 2B-b and S21†). However, after fixation and permeabilization, addition of **6** yielded a clear staining of the cellular membrane (Fig. 2B-c and S22†). In addition, when the cells were fixed and permeabilized first and subsequently incubated with ConA-dTCO, the addition of **6** resulted into perspicuous fluorescent staining of the internal glycosylated compartments (Fig. 2B-d and S23†). These experiments clearly express that the reaction proceeds efficiently under biological conditions and that the fluorogenic nature of the reaction can be used for bioimaging.

## Conclusions

In conclusion, our systematic study on the reactivity of various 1,2,4-triazines with TCOs in the IEDDA reaction shows that the reaction rates strongly depend on the substitution pattern of both the 1,2,4-triazine and the TCO. This study led to the discovery of novel *N*-alkyl pyridinium triazines with superb properties for use in bioconjugate chemistry. We have developed an efficient and modular synthetic strategy which enables the construction of various useful heterobifunctional probes based on the pyridinium 1,2,4-triazine scaffold. In addition, we describe the unprecedented fluorogenic nature of the reaction between these heterodienes and TCOs and demonstrate the potential of the chemistry for fluorogenic cell labeling. With this study, we have demonstrated pyridinium 1,2,4-triazines to be versatile and robust reagents with a prospective future in chemical biology and bioimaging. Further applications of these unique heterodienes for labeling of biomolecules as well as work toward improvement and modulation of their fluorogenic properties are currently underway.

## Acknowledgements

This work was supported by the Czech Science Foundation (P207/15-06020Y). We thank A. M. Downey for critical reading of the manuscript and P. Šimon for help with the synthesis of d-TCO.

## Notes and references

1 (*a*) Y. Takaoka, A. Ojida and I. Hamachi, *Angew. Chem., Int. Ed.*, 2013, **52**, 4088–4106; (*b*) C. S. McKay and M. G. Finn, *Chem. Biol.*, 2014, **21**, 1075–1101; (*c*) C. D. Spicer and B. G. Davis, *Nat. Commun.*, 2014, **5**, 4740.

2 (*a*) H. C. Kolb, M. G. Finn and K. B. Sharpless, *Angew. Chem., Int. Ed.*, 2001, **40**, 2004–2021; (*b*) E. M. Sletten and C. R. Bertozzi, *Angew. Chem., Int. Ed.*, 2009, **48**, 6974–6998; (*c*) M. F. Debets, J. C. M. van Hest and F. P. T. J. Rutjes, *Org. Biomol. Chem.*, 2013, **11**, 6439–6455; (*d*) M. King and A. Wagner, *Bioconjugate Chem.*, 2014, **25**, 825–839.

3 (*a*) J. Dommerholt, S. Schmidt, R. Temming, L. J. Hendriks, F. P. Rutjes, J. C. van Hest, D. J. Lefeber, P. Friedl and F. L. van Delft, *Angew. Chem., Int. Ed.*, 2010, **49**, 9422–9425; (*b*) M. T. Taylor, M. L. Blackman, O. Dmitrenko and J. M. Fox, *J. Am. Chem. Soc.*, 2011, **133**, 9646–9649; (*c*) G. de Almeida, E. M. Sletten, H. Nakamura, K. K. Palaniappan and C. R. Bertozzi, *Angew. Chem., Int. Ed.*, 2012, **51**, 2443–2447; (*d*) C. G. Gordon, J. L. Mackey, J. C. Jewett, E. M. Sletten, K. N. Houk and C. R. Bertozzi, *J. Am. Chem. Soc.*, 2012, **134**, 9199–9208; (*e*) W. Chen, D. Wang, C. Dai, D. Hamelberg and B. Wang, *Chem. Commun.*, 2012, **48**, 1736–1738; (*f*) M. Vrabel, P. Kolle, K. M. Brunner, M. J. Gattner, V. Lopez-Carrillo, R. de Vivie-Riedle and T. Carell, *Chem.–Eur. J.*, 2013, **19**, 13309–13312; (*g*) A. C. Knall, M. Hollauf and C. Slugovc, *Tetrahedron Lett.*, 2014, **55**, 4763–4766; (*h*) E. H. Leunissen, M. H. Meuleners, J. M. Verkade, J. Dommerholt, J. G. Hoenderop and F. L. van Delft, *ChemBioChem*, 2014, **15**, 1446–1451; (*i*) X. S. Wang, Y.-J. Lee and W. R. Liu, *Chem. Commun.*, 2014, **50**, 3176–3179; (*j*) Z. Yu and Q. Lin, *J. Am. Chem. Soc.*, 2014, **136**, 4153–4156.

4 (*a*) M. L. Blackman, M. Royzen and J. M. Fox, *J. Am. Chem. Soc.*, 2008, **130**, 13518–13519; (*b*) N. K. Devaraj, R. Weissleder and S. A. Hilderbrand, *Bioconjugate Chem.*, 2008, **19**, 2297–2299; (*c*) R. Selvaraj and J. M. Fox, *Curr. Opin. Chem. Biol.*, 2013, **17**, 753–760.

5 (*a*) G. Budin, K. S. Yang, T. Reiner and R. Weissleder, *Angew. Chem., Int. Ed.*, 2011, **50**, 9378–9381; (*b*) N. K. Devaraj, G. M. Thurber, E. J. Keliher, B. Marinelli and R. Weissleder, *Proc. Natl. Acad. Sci. U. S. A.*, 2012, **109**, 4762–4767; (*c*) D. S. Liu, A. Tangpeerachaikul, R. Selvaraj, M. T. Taylor, J. M. Fox and A. Y. Ting, *J. Am. Chem. Soc.*, 2012, **134**, 792–795; (*d*) J. Yang, J. Seckute, C. M. Cole and N. K. Devaraj, *Angew. Chem., Int. Ed.*, 2012, **51**, 7476–7479; (*e*) M. M. Herth, V. L. Andersen, S. Lehel, J. Madsen, G. M. Knudsen and J. L. Kristensen, *Chem. Commun.*, 2013, **49**, 3805–3807; (*f*) J. Seckute and N. K. Devaraj, *Curr. Opin. Chem. Biol.*, 2013, **17**, 761–767; (*g*) C. Denk, D. Svatunek, T. Filip, T. Wanek, D. Lumpi, J. Frohlich, C. Kuntner and H. Mikula, *Angew. Chem., Int. Ed.*, 2014, **53**, 9655–9659; (*h*) F. C. van de Watering, M. Rijpkema, M. Robillard, W. J. Oyen and O. C. Boerman, *Front. Med.*, 2014, **1**, 44.

6 M. R. Karver, R. Weissleder and S. A. Hilderbrand, *Bioconjugate Chem.*, 2011, **22**, 2263–2270.

7 (*a*) K. A. Horner, N. M. Valette and M. E. Webb, *Chem.–Eur. J.*, 2015, **21**, 14376–14381; (*b*) D. N. Kamber, Y. Liang, R. J. Blizzard, F. Liu, R. A. Mehl, K. N. Houk and J. A. Prescher, *J. Am. Chem. Soc.*, 2015, **137**, 8388–8391.

8 (*a*) V. N. Kozhevnikov, D. N. Kozhevnikov, O. V. Shabunina, V. L. Rusinov and O. N. Chupakhin, *Tetrahedron Lett.*, 2005, **46**, 1791–1793; (*b*) V. N. Kozhevnikov, O. V. Shabunina, D. S. Kopchuk, M. M. Ustinova, B. König and D. N. Kozhevnikov, *Tetrahedron*, 2008, **64**, 8963–8973.

9 M. Royzen, G. P. Yap and J. M. Fox, *J. Am. Chem. Soc.*, 2008, **130**, 3760–3761.
10 A. Darko, S. Wallace, O. Dmitrenko, M. M. Machovina, R. A. Mehl, J. W. Chin and J. M. Fox, *Chem. Sci.*, 2014, **5**, 3770–3776.
11 (*a*) J. Yang, Y. Liang, J. Seckute, K. N. Houk and N. K. Devaraj, *Chem.–Eur. J.*, 2014, **20**, 3365–3375; (*b*) D. M. Patterson, L. A. Nazarova, B. Xie, D. N. Kamber and J. A. Prescher, *J. Am. Chem. Soc.*, 2012, **134**, 18638–18643; (*c*) K. Lang, L. Davis, J. Torres-Kolbus, C. Chou, A. Deiters and J. W. Chin, *Nat. Chem.*, 2012, **4**, 298–304; (*d*) K. Lang, L. Davis, S. Wallace, M. Mahesh, D. J. Cox, M. L. Blackman, J. M. Fox and J. W. Chin, *J. Am. Chem. Soc.*, 2012, **134**, 10317–10320; (*e*) T. Plass, S. Milles, C. Koehler, J. Szymanski, R. Mueller, M. Wiessler, C. Schultz and E. A. Lemke, *Angew. Chem., Int. Ed.*, 2012, **51**, 4166–4170; (*f*) E. Kaya, M. Vrabel, C. Deiml, S. Prill, V. S. Fluxa and T. Carell, *Angew. Chem., Int. Ed.*, 2012, **51**, 4466–4469.
12 H. Wu, J. Yang, J. Seckute and N. K. Devaraj, *Angew. Chem., Int. Ed.*, 2014, **53**, 5805–5809.
13 R. Rossin, S. M. van den Bosch, W. Ten Hoeve, M. Carvelli, R. M. Versteegen, J. Lub and M. S. Robillard, *Bioconjugate Chem.*, 2013, **24**, 1210–1217.
14 S. S. Matikonda, D. L. Orsi, V. Staudacher, I. A. Jenkins, F. Fiedler, J. Chen and A. B. Gamble, *Chem. Sci.*, 2015, **6**, 1212–1218.
15 (*a*) D. N. Kamber, L. A. Nazarova, Y. Liang, S. A. Lopez, D. M. Patterson, H. W. Shih, K. N. Houk and J. A. Prescher, *J. Am. Chem. Soc.*, 2013, **135**, 13680–13683; (*b*) D. M. Patterson and J. A. Prescher, *Curr. Opin. Chem. Biol.*, 2015, **28**, 141–149.
16 D. M. Beal and L. H. Jones, *Angew. Chem., Int. Ed.*, 2012, **51**, 6320–6326.
17 P. Shieh and C. R. Bertozzi, *Org. Biomol. Chem.*, 2014, **12**, 9307–9320.
18 A. Nadler and C. Schultz, *Angew. Chem., Int. Ed.*, 2013, **52**, 2408–2410.
19 S. Rin Jean, D. V. Tulumello, S. P. Wisnovsky, E. K. Lei, M. P. Pereira and S. O. Kelley, *ACS Chem. Biol.*, 2014, **9**, 323–333.
20 (*a*) J. R. Friedman and J. Nunnari, *Nature*, 2014, **505**, 335–343; (*b*) S. Vyas, E. Zaganjor and M. C. Haigis, *Cell*, 2016, **166**, 555–566.
21 I. J. Goldstein and R. D. Poretz, Properties, Functions, and Applications in Biology and Medicine, in *The Lectins*, ed. I. E. Liener, N. Sharon and I. J. Goldstein, Elsevier, 1986, vol. 32, pp. 33–247.

# 3.5 Probing the Scope of the Amidine–1,2,3-triazine Cycloaddition as a Prospective Click Ligation Method

S.J. Siegl, M. Vrabel, *Eur. J. Org. Chem.* **2018**, 5081–5085.

Copy of the publication with permission of the publisher; Published by Wiley-VCH Verlag GmbH & Co. KGaA.

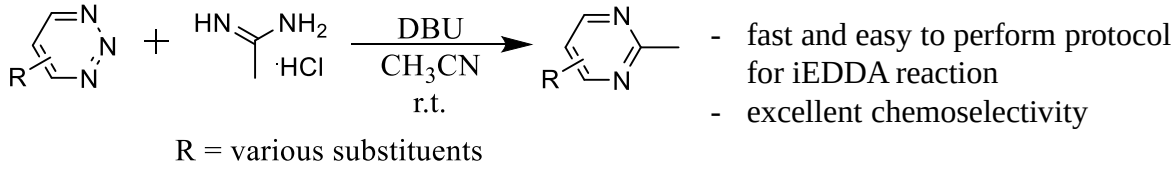


## 3.5.1 Background

Recently, it was reported that 1,2,3-triazines react quite selective in iEDDA cycloadditions with various dienophiles.[142a, 142b] Among those, amidines were shown to be especially reactive. This prompted us to study the cycloaddition between 1,2,3-triazines and amidines in more detail, and to evaluate its suitability for the use in bioconjugation applications. A potential limitation for a broader utility is the rather low stability of amidines in form of a free base. Amidines are usually stored as salts, which unfortunately do not form the desired pyrimidine products upon reaction with 1,2,3-triazines. Thus, amidine salts have to be transformed into the corresponding free amidine bases before the cycloaddition. This is usually done under rather harsh conditions by treatment of the salt with a strong base and subsequent extraction into organic solvents.[142a, 142b, 142d] Therefore, our first goal was to develop an optimized protocol for the *in situ* formation of the free amidine base under mild conditions to overcome this limitation. For this purpose, we screened several bases under different reaction conditions and identified diazabicyclo[5.4.0]undec-7-ene (DBU) as the most promising candidate enabling subsequent cycloaddition of the formed free amidine base with 1,2,3-triazines. Based on the optimized protocol, we further evaluated the potential of the 1,2,3-triazine-amidine cycloaddition for labeling applications. We speculated, for example, that the 1,2,3-triazine-amidine cycloaddition should be extremely chemoselective. Indeed, compatibility experiments demonstrated its remarkable orthogonality toward other common ligation methods like SPAAC and the cycloadditions between TCOs and 1,2,4,5-tetrazines or 1,2,4-triazines.

### 3.5.2 Declaration of contribution

For this study, I developed the optimized protocol for the *in situ* formation of free amidine bases and their subsequent cycloaddition with 1,2,3-triazines. I performed several small test reactions and HPLC-MS experiments in order to determine the optimal conditions and to study the origin of the side product of this cycloaddition arising in aqueous milieu. Furthermore, I isolated the pyrimidine product formed in the reaction between acetamidine hydrochloride and 5-phenyl-1,2,3-triazine under the optimized reaction conditions and confirmed its formation by NMR. I performed the stability studies of this click product and determined the second-order rate constants for the cycloaddition of acetamidine with different 1,2,3-triazines. Additionally, I carried out the competition experiment between acetamidine and the guanidine group of arginine as well as the compatibility experiments with other common ligation methods. I also actively participated in writing the manuscript.

ChemPubSoc Europe

DOI: 10.1002/ejoc.201800530

EurJOC European Journal of Organic Chemistry

Communication

Ligation Chemistry

SPECIAL ISSUE

# Probing the Scope of the Amidine–1,2,3-triazine Cycloaddition as a Prospective Click Ligation Method

Sebastian J. Siegl[a] and Milan Vrabel*[a]

**Abstract:** Despite recent achievements in the development of chemical reactions enabling selective modification of complex biomolecules, the demand for fast and efficient methodologies that allow the attachment of various functional groups to these systems is the subject of intense research. Here, we report on the study of the amidine–1,2,3-triazine cycloaddition reaction, which has the potential to address many of the challenges associated with the development of such chemistry. We describe an optimized protocol leading to the in situ formation of free amidine bases, which directly react in the cycloaddition reaction with 1,2,3-triazines. Our kinetic studies reveal the structural features determining the reaction rates. Finally, we show that the amidine–1,2,3-triazine cycloaddition is extraordinarily selective and orthogonal to other popular ligation reactions. The pros and cons of the methodology are presented.

## Introduction

Given the vast number of functional groups present within the structure of biomolecules, selective chemical modification of such complex systems represents an immense challenge for organic chemists.[1] Although a number of reactions targeting e.g. the functional groups of natural amino acids exist, these methodologies often suffer from the lack of control over the modification site.[2] This is simply because the naturally occurring functional groups are present in multiple copies within the structure. On the other hand, the desired high degree of selectivity can be achieved by embedding an orthogonal reacting group into structure of biomolecules. This reactive group is then used in the next step for attachment of the desired tag/modification via selective chemical reaction using the appropriate complementary reagent. These, so-called bioorthogonal reactions, already proved to be an extremely powerful way not only for modifying biomolecules, but also to study their delicate structure and understand their numerous functions.[3] In our continuous effort to identify chemical reactions having such attributes we became particularly interested in the inverse electron-demand Diels–Alder reaction of 1,2,3-triazines with amidines (Scheme 1). Our inspiration came from the pioneering studies of Boger who demonstrated the exquisite reactivity of 1,2,3-triazines with various dienophiles.[4] Especially intriguing is the regioselectivity of these chemical transformations, which proceed exclusively across C4/N1. This allows for excellent control over product formation giving well defined pyrimidines as sole reaction products. Another important feature of this [4+2] cycloaddition is the mild reaction conditions. Usually, the reaction proceeds at room temperature within minutes in solvents such as acetonitrile or dioxane giving good to excellent yields of the products. All of these attributes prompted us to explore the potential of the amidine–1,2,3-triazine cycloaddition in the context of bioorthogonal ligation methods.

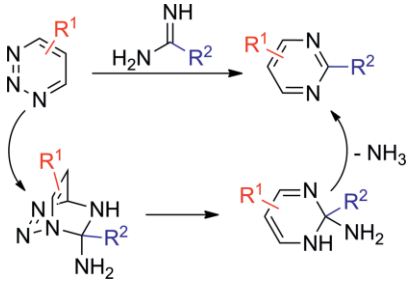


Scheme 1. Schematic presentation of the amidine–1,2,3-triazine cycloaddition reaction leading to substituted pyrimidine products.

## Results and Discussion

An essential prerequisite for successful reaction of 1,2,3-triazines with amidines is the presence of the amidine in the form of a free base.[4a] Indeed, our pilot experiments confirmed that acetamidine hydrochloride in reaction with 5-phenyl-1,2,3-triazine does not lead to the desired pyrimidine product. Usually, the free base of amidine is generated by treating the salt with a strong base, such as 1–2 N aqueous NaOH, followed by extraction into organic phase and immediate use in the cycloaddition step. These rather harsh conditions not only limit the substrate scope containing the amidine group, but also involve handling of the relatively unstable free base of amidine. Our first goal was therefore to find reaction conditions allowing us to avoid this limitation. An ideal method should enable deprotonation of the amidine group leading to the in situ formation of free

[a] Institute of Organic Chemistry and Biochemistry of the Czech Academy of Sciences,
Flemingovo nám. 2, 16610, Prague 6, Czech Republic
E-mail: vrabel@uochb.cas.cz
http://www.uochb.cz/web/structure/1360.html?lang=cz

Supporting information and ORCID(s) from the author(s) for this article are available on the WWW under https://doi.org/10.1002/ejoc.201800530.

amidine base, which can then undergo the cycloaddition reaction with 1,2,3-triazines. We used 5-phenyl-1,2,3-triazine **1a** and commercially available acetamidine hydrochloride **2** to optimize the reaction conditions. We first screened several bases for the in situ formation of the amidine free base. We used 1,1,3,3-tetramethylguanidine (TMG), 1,5,7-triazabicyclo[4.4.0]-dec-5-ene (TBD), diazabicyclo[5.4.0]undec-7-ene (DBU) and Proton Sponge in these experiments. In particular, four equivalents of the corresponding base were mixed with **2** in the respective solvent prior to addition of 5-phenyl-1,2,3-triazine solution. The formation of the desired 2-methyl-5-phenylpyrimidine **3a** was monitored by HPLC-MS analysis by comparing the reaction mixtures to a standard compound. The results are summarized in Table 1 (for details see Table S1 and Figure S1 in Supporting Information).

Table 1. Optimization of the amidine–1,2,3-triazine cycloaddition.[b]

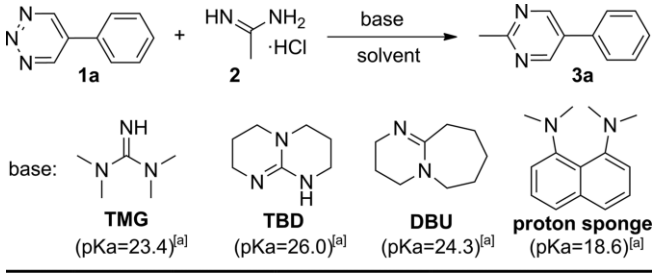


| Entry | Base | Solvent | Temperature | Results[c] |
|---|---|---|---|---|
| 1 | TMG | $CH_3CN$ | r. t. | 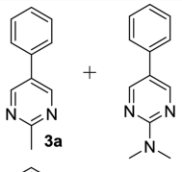 |
| 2 | TBD | $CH_3CN$ | r. t. | 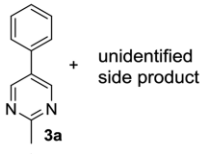 unidentified side product |
| 3 | DBU | $CH_3CN$ | r. t. | 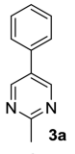 formed in 88% isolated yield |
| 4 | proton sponge | $CH_3CN$ | r. t. | 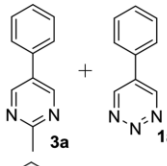 |
| 5 | DBU | $CH_3CN$ | 37°C | 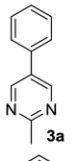 finished within 8 hours |
| 6 | DBU | $CH_3CN$/$H_2O$ (1:1) | r. t. | 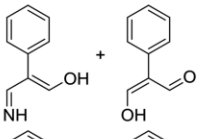 |
| 7 | TMG | $CH_3CN$/$H_2O$ (1:1) | r. t. | 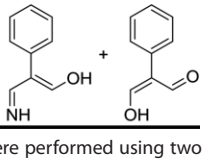 |

[a] p$K_a$ values in $CH_3CN$ from lit.[5] [b] All reactions were performed using two equivalents of acetamidine and four equivalents of the base. [c] Structures of side products are proposed from observed masses during HPLC-MS measurements (for details see Tables S1, S2 and Figures S1, S2 in Supporting Information).

The reaction in $CH_3CN$ using TMG as the base afforded the respective pyrimidine product **3a** accompanied by formation of a side product presumably arising from the cycloaddition reaction of the guanidine base with the phenyl triazine (judged from the observed MS spectrum) (entry 1 in Table 1 and Table S1 and Figure S1 in Supporting Information). Only traces of the desired product **3a** together with unidentified side products were formed in the presence of TBD base (entry 2). The reaction in the presence of Proton Sponge afforded only traces of **3a** and mostly the remaining starting material **1a** (entry 4). This can be attributed to the slightly lower p$K_a$ of Proton Sponge (12.3 in water)[6] when compared to acetamidine (12.5 in water)[7] which is unable to efficiently deprotonate the amidine salt. To our delight, the reaction with DBU provided very clean conversion to the desired product **3a** without formation of any side products. Under the optimized conditions **3a** formed in 88 % isolated yield (entry 3, for details see Supporting Information). As expected, the formation of the product was faster when we performed the reaction at elevated temperature (entry 5).

With the aim to explore the possibility of using the amidine–1,2,3-triazine cycloaddition on biomolecules we also tested the sensitivity of the reaction to aqueous conditions. Unfortunately, the reaction does not tolerate water. By increasing the water content to 50 % the reaction afforded mainly side products (entry 6 and 7 in Table 1, Table S1 and Figure S1 in Supporting Information). To better understand the formation of these side products under aqueous conditions we next performed a series of experiments. We found that 5-phenyl-1,2,3-triazine alone is stable in water (entry 1 in Table S2 and Figure S2 in Supporting Information). **1a** is also stable as a solution in $CH_3CN$ in the presence of DBU (entry 2 in Table S2 and Figure S2 in Supporting Information). However, the triazine **1a** decomposes in water when DBU is present (entry 3 in Table S2 and Figure S2 in Supporting Information). The same we observed by using TMG as the base (entry 4 and 5 in Table S2 and Figure S2 in Supporting Information). A proposed mechanism leading to the formation of side products (or decomposition of **1a**) under these conditions is shown in Scheme 2.

Based on these results we conclude that although strict anhydrous conditions are not required for successful reaction to take place (HPLC grade $CH_3CN$ is sufficient), the requirement for solely organic solvents limits utilization of the method to systems where these conditions are tolerated. Despite this restriction, our newly developed conditions enabling in situ formation of the reactive amidine free bases followed by cycloaddition of the 1,2,3-triazine may find broad utility. They provide an easy-to-perform alternative to the commonly used reaction conditions without the need for additional extraction steps and avoid handling of the unstable free amidine bases.

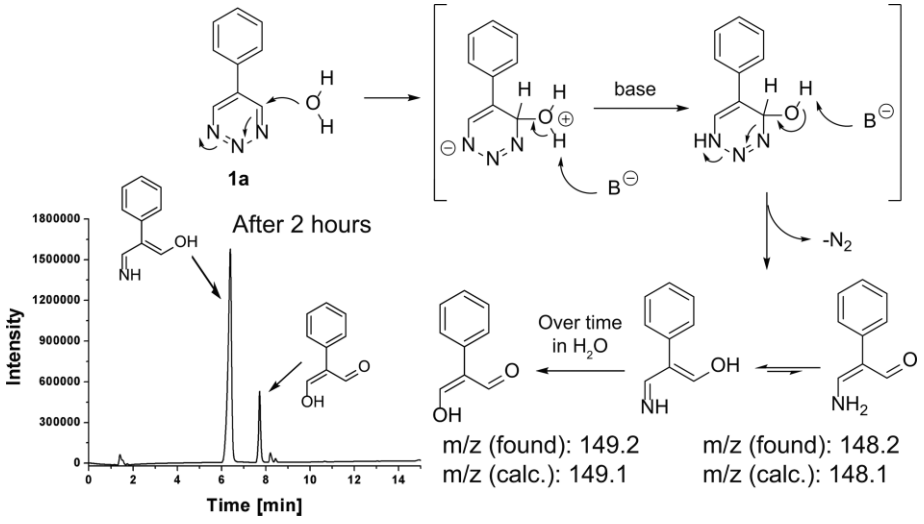


Scheme 2. Proposed reaction mechanism leading to formation of side products from **1a** in $CH_3CN/H_2O$ in the presence of the base. Bottom left is the HPLC chromatogram showing product distribution after 2 h.

Although the reactivity of various 1,2,3-triazines with amidines was previously experimentally compared,[4a–4c] to the best of our knowledge, no quantitative kinetic data are known from the literature. To get better insight into the reactivity of 1,2,3-triazines and to evaluate the generality of our optimized conditions, we next performed reaction kinetic experiments using a series of 1,2,3-triazines shown in Scheme 3. The second-order rate constants were determined using either HPLC or UV/Vis spectrophotometer (Table S3 in Supporting Information). Our data show that the reactivity of 1,2,3-triazines varies significantly and depends on the structure and substitution pattern. In general, the presence of electron withdrawing substituents increases the reactivity, which is in agreement with the inverse electron-demand nature of the reaction. The most electron poor 1,2,3-triazine **1d** bearing a methyloxycarbonyl substituent at C5 is the most reactive of the series. It exceeds in reactivity the corresponding C4 substituted triazine **1b** by two orders of magnitude and 5-phenyl-1,2,3-triazine **1a** by an impressive six orders of magnitude. The lower reactivity of **1b** when compared to **1d** indicates that the C4 substitution is much less activating even though the substituent is electron withdrawing. 4,6-disubstitution of **1c** increases its reactivity when compared to **1b** however still remains orders of magnitude below that of **1d**. The observed lower reactivity of **1b** and **1c** can be also possibly attributed to increased steric hindrance of substituents at C4 and C6 when compared to substituents at C5. It is known that other effects such as hydrogen bonding ability and the reaction mechanism itself also play an important role and influence the reactivity of 1,2,3-triazines.[8] A more comprehensive computational study would be needed to fully understand and explain the observed experimental data.

By comparison to other known bioorthogonal ligations, the determined second-order rate constant of 13.4 ± 0.15 $M^{-1}\,s^{-1}$ (for **1d**) reaches values of the reaction of 1,2,3,4-tetrazines with strained bicyclononyne (BCN).[9] The reaction of the most reactive 1,2,3-triazine **1d** with acetamidine is also an order of magnitude faster than the reaction of 1,2,3,4-tetrazines with norbornenes.[10] Considering the popularity of both of these reactions, the amidine–1,2,3-triazine cycloaddition holds great potential for applications where such exquisite reactivity is desirable.

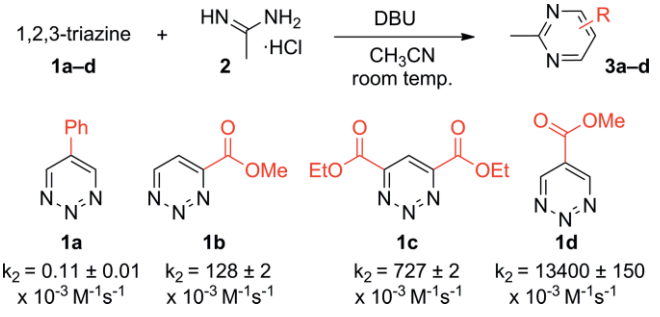


Scheme 3. Scheme showing conditions used during measurements of reaction kinetics. The determined second-order rate constants for individual 1,2,3-triazines are depicted below the structures.

Guanidine is, among other functional groups present in natural amino acids, structurally most similar to the amidine group. As already our reaction optimization experiments using different bases indicated, guanidines can react with 1,2,3-triazines to some extent (TMG base). This would be a potential obstacle for successful use of the 1,2,3-triazines for example selective peptide modification. To gain better insight into this "side" reaction we mixed *N*-benzoyl protected ethyl ester of arginine **4** with triazine **1a** under our optimized conditions (DBU as base, $CH_3CN$ as solvent). Indeed, HPLC-MS analysis of the reaction mixture confirmed the presence of the corresponding cycloaddition product **5a**. In addition, we observed also formation of cycloadduct **5b**, which forms when the amino acid part of the molecule eliminates during the last step of the reaction instead of ammonia (see mechanism in Scheme 1). To further evaluate if this side reactivity represents a serious obstacle for example peptide modification we performed a competitive experiment. We first mixed the ariginine amino acid **4** and acet-

amidine hydrochloride **2** with an excess of DBU in $CH_3CN$. These solutions were combined and **1a** was added. Under these conditions, the corresponding 2-methyl-5-phenylpyrimidine **3a** was formed predominantly. However, formation of small traces of **5a** together with **5b**, which both result from the reaction of the triazine with the double bond of the guanidine group, was observed as well (Scheme 4 and Figure S5, S6 in Supporting Information). These experiments confirmed that the amidine–1,2,3-triazine cycloaddition under these conditions competes with cycloaddition to guanidines, however, the latter is slower.

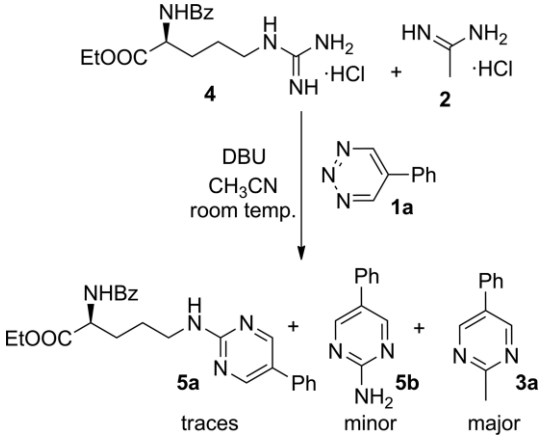


Scheme 4. Competition experiment of the cycloaddition between 5-phenyl-1,2,3-triazine and acetamidine or arginine respectively.

After validating the chemo-selectivity of the reaction toward guanidines we next turned our attention to explore the selectivity of the reaction in the context of other popular biocompatible ligations. In particular we were interested if the reaction between *trans*-cyclooctenes (TCO), one of the most reactive dienophiles known to date,[11] and 1,2,4,5-tetrazines is orthogonal to the amidine–1,2,3-triazine cycloaddition. To probe the selectivity, we reacted phenyl triazine **1a**, diphenyl-*s*-tetrazine **6**, TCO **7** (we used pure axial isomer) and acetamidine hydrochloride **2** (in both cases two equivalents of the dienophile were used) under our optimized reaction conditions (Scheme 5 and Figure S7 in Supporting Information). We followed the progress of the reaction by HPLC-MS analysis. As expected, the reaction between diphenyl-*s*-tetrazine and TCO was finished already during first analysis and gave the corresponding dihydropyridazine **8**. Most importantly, we found that the amidine–1,2,3-triazine reaction proceeds selectively under these conditions. We did not observe formation of any of the products that would arise from the cross-reaction between the reagents (TCO with 1,2,3-triazine or 1,2,4,5-tetrazine with acetamidine). In other words, the two inverse electron-demand cycloadditions are orthogonal to each other and can be performed in a one pot reaction setup.

Encouraged by these results, we decided to further probe the selectivity of the amidine–1,2,3-triazine cycloaddition and performed a series of other competition experiments. We first carried out the reaction in the presence of 3-azido-7-hydroxycoumarine **9** and bicyclononyne (BCN) **10** (Scheme 6A), and second, in the presence of 3-(2-pyridyl)-6-phenyl-1,2,4-triazine **12** and TCO **7** (Scheme 6B, for details and additional examples see Supporting Information Scheme S7–S9, Figures S10–S12).

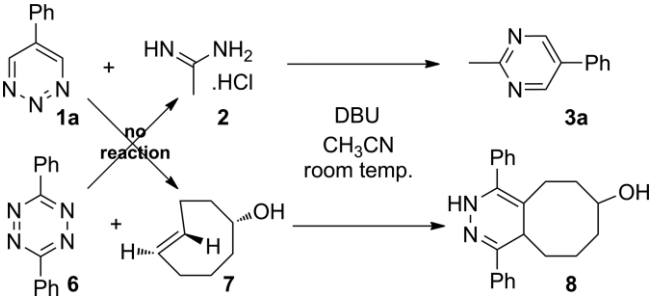


Scheme 5. Competition experiment between amidine–1,2,3-triazine and TCO–1,2,4,5-tetrazine cycloaddition.

We again observed selective formation of the desired products (**3a**, **11** and **13** respectively) in each case without formation of any of the side products which would result from cross reactions between the reagents (Scheme 6, Figure S8 and S9 in Supporting Information). These experiments show that the reaction between amidines and 1,2,3-triazines proceeds with excellent selectivity and that it is orthogonal to other popular cycloadditions such as the strain-promoted azide–alkyne cycloaddition (SPAAC),[12] TCO–1,2,4-triazine[13] and TCO–1,2,4,5-tetrazine cycloaddition.[14] Based on these results, we believe that the amidine–1,2,3-triazine cycloaddition may find application especially in experiments requiring attachment of various moieties to multifunctional scaffolds in a single step.[15]

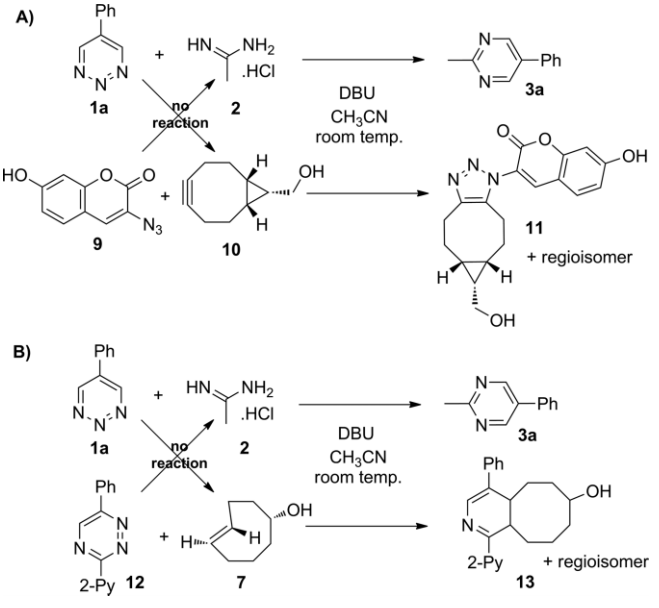


Scheme 6. Competition experiment between amidine–1,2,3-triazine and A) the strain promoted azide–alkyne cycloaddition or B) TCO–1,2,4-triazine cycloaddition.

## Conclusions

In conclusion, we describe our results from the evaluation of the amidine–1,2,3-triazine cycloaddition as a prospective click ligation method. Our optimized protocol for the in situ formation of free amidine bases, which directly participate in cycloaddition with various 1,2,3-triazines, represents a simplified and

straightforward synthetic route toward modified pyrimidines. Our analysis of the reaction kinetics reveals that the reactivity of 1,2,3-triazines with amidines can vary by orders of magnitude. The most reactive 1,2,3-triazines react with simple amidines with second-order rate constants reaching the values of some of the strain-promoted cycloaddition reactions. We show that the amidine–1,2,3-triazine cycloaddition is a powerful ligation method, which holds great potential for various applications. Despite the observed sensitivity to water, which limits the utility of this chemistry to systems compatible with organic solvents, the reaction proceeds with extraordinary chemo- and regio-selectivity. Under the conditions tested, we show that the reaction is orthogonal to some of the most popular ligation methods including the TCO–1,2,4,5-tetrazine, TCO–1,2,4-triazine as well as the strain-promoted azide–alkyne cycloaddition. We believe that the reported data will serve as valuable guidelines for future studies of the reaction and that the observed and described excellent orthogonality will find utility in multiple tagging/labeling experiments on complex systems.

## Experimental Section

**Optimization of the Amidine–1,2,3-triazine Cycloaddition:** A 20 mM solution of 5-phenyl-1,2,3-triazine was mixed at a ratio of 1:1 with a 40 mM solution of acetamidine hydrochloride containing 2 equiv. of a base (TMG, TBD, DBU or proton sponge). The solutions containing acetamidine hydrochloride and the base were incubated at room temperature for 20 min before mixing with the 5-phenyl-1,2,3-triazine to form the amidine free base. The reactions were performed either in $CH_3CN$ or in $CH_3CN/H_2O$ (1:1). The reaction mixtures were incubated at room temperature or at 37 °C and progress of the reaction was monitored by HPLC-MS analysis.

## *Acknowledgments*

This work was supported by the Institute of Organic Chemistry and Biochemistry of the Czech Academy of Sciences and by the Czech Science Foundation (P207/15-06020Y, for M. V.).

**Keywords:** Ligation · Click chemistry · Cycloaddition · Diels–Alder reactions · Nitrogen heterocycles

[1] a) L. W. Miller, V. W. Cornish, *Curr. Opin. Chem. Biol.* **2005**, *9*, 56–61; b) Y. Takaoka, A. Ojida, I. Hamachi, *Angew. Chem. Int. Ed.* **2013**, *52*, 4088–4106; *Angew. Chem.* **2013**, *125*, 4182; c) C. S. McKay, M. G. Finn, *Chem. Biol.* **2014**, *21*, 1075–1101; d) C. D. Spicer, B. G. Davis, *Nat. Commun.* **2014**, *5*, 4740; e) X. Chen, Y. W. Wu, *Org. Biomol. Chem.* **2016**, *14*, 5417–5439; f) O. Boutureira, G. J. L. Bernardes, *Chem. Rev.* **2015**, *115*, 2174–2195.

[2] a) E. Basle, N. Joubert, M. Pucheault, *Chem. Biol.* **2010**, *17*, 213–227; b) J. N. deGruyter, L. R. Malins, P. S. Baran, *Biochemistry* **2017**, *56*, 3863–3873; c) O. Koniev, A. Wagner, *Chem. Soc. Rev.* **2015**, *44*, 5495–5551.

[3] a) E. M. Sletten, C. R. Bertozzi, *Angew. Chem. Int. Ed.* **2009**, *48*, 6974–6998; *Angew. Chem.* **2009**, *121*, 7108; b) R. K. Lim, Q. Lin, *Chem. Commun.* **2010**, *46*, 1589–1600; c) M. F. Debets, J. C. van Hest, F. P. Rutjes, *Org. Biomol. Chem.* **2013**, *11*, 6439–6455; d) M. King, A. Wagner, *Bioconjugate Chem.* **2014**, *25*, 825–839; e) D. M. Patterson, L. A. Nazarova, J. A. Prescher, *ACS Chem. Biol.* **2014**, *9*, 592–605; f) T. Carell, M. Vrabel, M. Yang, Y. Yang, P. R. Chen, J. Dommerholt, F. P. Rutjes, F. L. van Delft, A. Herner, Q. Lin, H. Wu, N. K. Devaraj, S. Kath-Schorr, *Top. Curr. Chem.* **2016**, *374*, 15.

[4] a) E. D. Anderson, D. L. Boger, *Org. Lett.* **2011**, *13*, 2492–2494; b) E. D. Anderson, A. S. Duerfeldt, K. Zhu, C. M. Glinkerman, D. L. Boger, *Org. Lett.* **2014**, *16*, 5084–5087; c) C. M. Glinkerman, D. L. Boger, *Org. Lett.* **2015**, *17*, 4002–4005; d) E. D. Anderson, D. L. Boger, *J. Am. Chem. Soc.* **2011**, *133*, 12285–12292.

[5] a) I. Kaljurand, A. Kutt, L. Soovali, T. Rodima, V. Maemets, I. Leito, I. A. Koppel, *J. Org. Chem.* **2005**, *70*, 1019–1028; b) K. Kaupmees, A. Trummal, I. Leito, *Croat. Chem. Acta* **2014**, *87*, 385–395.

[6] R. W. Alder, P. S. Bowman, W. R. S. Steele, D. R. Winterman, *Chem. Commun.* **1968**, 723–724.

[7] A. Albert, R. Goldacre, J. Phillips, *J. Chem. Soc.* **1948**, 2240–2249.

[8] Y. F. Yang, P. Yu, K. N. Houk, *J. Am. Chem. Soc.* **2017**, *139*, 18213–18221.

[9] D. Wang, W. Chen, Y. Zheng, C. Dai, K. Wang, B. Ke, B. Wang, *Org. Biomol. Chem.* **2014**, *12*, 3950–3955.

[10] a) M. Vrabel, P. Kolle, K. M. Brunner, M. J. Gattner, V. Lopez-Carrillo, R. de Vivie-Riedle, T. Carell, *Chem. Eur. J.* **2013**, *19*, 13309–13312; b) A. C. Knall, M. Hollauf, C. Slugovc, *Tetrahedron Lett.* **2014**, *55*, 4763–4766.

[11] R. Selvaraj, J. M. Fox, *Curr. Opin. Chem. Biol.* **2013**, *17*, 753–760.

[12] J. Dommerholt, F. P. J. T. Rutjes, F. L. van Delft, *Top. Curr. Chem.* **2016**, *374*, 16.

[13] a) K. A. Horner, N. M. Valette, M. E. Webb, *Chem. Eur. J.* **2015**, *21*, 14376–14381; b) D. N. Kamber, Y. Liang, R. J. Blizzard, F. Liu, R. A. Mehl, K. N. Houk, J. A. Prescher, *J. Am. Chem. Soc.* **2015**, *137*, 8388–8391; c) S. J. Siegl, R. Dzijak, A. Vazquez, R. Pohl, M. Vrabel, *Chem. Sci.* **2017**, *8*, 3593–3598.

[14] a) A.-C. Knall, C. Slugovc, *Chem. Soc. Rev.* **2013**, *42*, 5131–5142; b) B. L. Oliveira, Z. Guo, G. J. L. Bernardes, *Chem. Soc. Rev.* **2017**, *46*, 4895–4950.

[15] a) D. M. Patterson, J. A. Prescher, *Curr. Opin. Chem. Biol.* **2015**, *28*, 141–149; b) M. K. Narayanam, Y. Liang, K. N. Houk, J. M. Murphy, *Chem. Sci.* **2016**, *7*, 1257–1261; c) S. Kolodych, E. Rasolofonjatovo, M. Chaumontet, M. C. Nevers, C. Creminon, F. Taran, *Angew. Chem. Int. Ed.* **2013**, *52*, 12056–12060; *Angew. Chem.* **2013**, *125*, 12278; d) A.-C. Knall, M. Hollauf, R. Saf, C. Slugovc, *Org. Biomol. Chem.* **2016**, *14*, 10576–10580.

Received: April 3, 2018

 

# 4. Conclusion and outlook

In the present thesis, I continued the work on the novel type of fluorescent iEDDA cycloadditions between various 1,2,4,5-tetrazines and axTCO-ol recently developed in our group. In order to further improve this methodology, new TCO derivatives and a more general approach were developed to expand the fluorophore-forming concept to a bigger range of TCOs.

First, the set of TCO dienophiles suitable for the formation of fluorescent products upon tetrazine ligation was extended by the design and synthesis of novel aziridine-fused TCOs. These TCO derivatives form fluorescent products upon cycloaddition with various 1,2,4,5-tetrazines and maintain their fluorogenic character even after functionalization with different groups. It was also shown that the use of aza-TCOs for the cycloaddition with tetrazines combines high reaction rates due to a highly strained "half-chair" conformation of aza-TCO with good to excellent stability of both reagent and product.

The development of an alternative strategy then extended this type of fluorogenic tetrazine ligations also to other TCO derivatives. It was found that 1,2,4,5-tetrazines containing specific electron-donating groups lead to the formation of fluorescent compounds through iEDDA reaction with various known TCOs, which did not show any fluorogenic behavior in reactions with other 1,2,4,5-tetrazines tested in previous studies. In continuation of the work, it was further demonstrated that also BCN derivatives form fluorescent products with interesting photophysical properties upon cycloaddition with this particular type of 1,2,4,5-tetrazines. The novel fluorogenic BCN-tetrazine cycloaddition was also combined with the aforementioned TCO-tetrazine cycloaddition for simultaneous two-color labeling using only a single tetrazine for the activation.

Finally, all these novel fluorogenic tetrazine ligation reactions were successfully applied to labeling of model biomolecules *in vitro* and to labeling of different compartments in live cells in order to confirm that their fluorogenic character is preserved under biological conditions.

Although the bioimaging applications were quite successful, there is still space for improving the photophysical properties of the fluorophores formed upon such cycloadditions. First, most of the obtained fluorescent products emit in the green to yellow spectral region. As excitation at longer wavelengths results in lower phototoxicity and deeper tissue penetration, shifting the emission wavelength of more fluorescent products to the orange or red spectral region would be desirable. Additionally, although the obtained fluorophores show large Stokes shifts and a

strong increase of the fluorescence intensity, they possess rather low fluorescence quantum yields. Currently our group is investigating the possibility to improve the quantum yields by making the fluorescent dihydropyridazines more rigid, which was already applied to other common fluorophores to enhance their stability and photophysical properties.[158] We plan to introduce various *ortho*-substituted aryl moieties to the 1,2,4,5-tetrazine core. These substituents should spontaneously form lactams after the iEDDA reaction in an intramolecular reaction with the obtained dihydropyridazine moiety and thus cause rigidification of the fluorescent structure. Preliminary experiments already indicated that this strategy is feasible.

Another goal of this thesis was to evaluate the prospect of 1,2,4- and 1,2,3-triazines as versatile alternative heterodienes for cycloadditions with various dienophiles. In case of 1,2,4-triazines, kinetic studies demonstrated that the structure of both heterodiene and dienophile strongly affect the reaction rate, which can vary by orders of magnitude. Furthermore, these studies led to the discovery of a novel class of cationic pyridinium 1,2,4-triazines with excellent performance in bioconjugation reactions. Besides enhanced reactivity, water solubility and biocompatibility, another interesting property of these cationic triazines is the unprecedented fluorogenic character of the reaction with various TCOs. It was shown that this fluorogenic nature maintains, even when the pyridinium moiety of the triazine is alkylated with diverse functional groups. Therefore, an efficient method for late-stage functionalization of the triazine compounds was developed to allow easy preparation of various useful heterobifunctional pyridinium triazines. Additionally, this type of fluorogenic bioorthogonal reaction was already successfully applied to cell labeling experiments.
Moreover, this part of the thesis includes the development of an optimized and simplified protocol for the cycloaddition of 1,2,3-triazines with amidines. Usually, amidines are only available as salts that do not react with 1,2,3-triazines. Standard protocols for the thus necessary formation of the free amidine bases before the cycloaddition usually employ rather harsh conditions and require an additional extraction step into organic solvents.[142a, 142b, 142d] In contrast, our new protocol allows the *in situ* formation of the free amidine bases under mild conditions without the need for additional extraction steps and handling of the unstable free base. Although the observed sensitivity of 1,2,3-triazines toward water under these reaction conditions limits this approach to non-aqueous systems, the extraordinary chemo- and regioselectivity of the reaction is worth the effort to further study its potential for various labeling applications. Compatibility experiments with some of the most popular ligation methods like SPAAC and the cycloadditions between TCOs and 1,2,4,5-tetrazines or

1,2,4-triazines, for example, demonstrated the excellent orthogonality of the 1,2,3-triazine-amidine cycloaddition toward other bioorthogonal reactions, which may find utility in multiple labeling experiments in more complex systems.

However, for both types of triazines more studies and research are needed. In the case of the cationic 1,2,4-triazines, further improvement and modulation of the fluorogenic properties like increased fluorescent quantum yields is desirable. Additionally, the development of further applications using heterobifunctional triazine derivatives may be promising for further research. In the case of the cycloaddition between 1,2,3-triazines and amidines, the reported data in this thesis could be a valuable guideline for future studies, for example, of the biocompatibility of the reagents, especially in regard to the observed sensitivity toward water. Additional experiments about the described orthogonality toward other bioorthogonal reactions, as well as applications in biological systems would be also of interest.

# 5. Abbreviations

| | |
|---|---|
| axTCO-ol | Axial *trans*-cyclooctene-5-ol |
| BCN | Bicyclo[6.1.0]nonyne |
| BirA | Biotin ligase |
| CuAAC | Copper-catalyzed azide-alkyne [3+2] cycloaddition |
| DhaA | Haloalkane dehalogenase |
| DNSC | Dansyl chloride |
| EGFP | Enhanced green fluorescent protein |
| eqTCO-ol | Equatorial *trans*-cyclooctene-5-ol |
| FGE | Formylglycine-generating enzyme |
| FP | Fluorescent protein |
| GFP | Green fluorescent protein |
| hAGT | human $O^6$-Alkylguanine-DNA alkyl transferase |
| HOMO | Highest occupied molecular orbital |
| HPLC-MS | High performance liquid chromatography-mass spectrometry |
| iEDDA | inverse-Electron-demand Diels-Alder |
| LplA | Lipoic acid ligase |
| LUMO | Lowest unoccupied molecular orbital |
| NHS | *N*-Hydroxysuccinimide |
| NMR | Nuclear magnetic resonance |
| PPTase | Phosphopantetheine transferase |
| SPAAC | Strain-promoted azide-alkyne cycloaddition |
| SPANC | Strain-promoted alkyne-nitrone cycloaddition |
| SPANOC | Strain-promoted alkyne-nitrile oxide cycloaddition |
| TCO | *trans*-Cyclooctene |
| TCO-ol | *trans*-Cyclooctene-5-ol |
| TGase | Trans-glutaminase |
| wtGFP | Wild-type green fluorescent protein |

# 6. Bibliography


[1] H. C. Hang, C. Yu, D. L. Kato, C. R. Bertozzi, *Proc. Natl. Acad. Sci. U.S.A.* **2003**, *100*, 14846-14851.

[2] a) C. R. Bertozzi, *Acc. Chem. Res.* **2011**, *44*, 651-653; b) J. A. Prescher, C. R. Bertozzi, *Nat. Chem. Biol.* **2005**, *1*, 13-21; c) E. M. Sletten, C. R. Bertozzi, *Angew. Chem. Int. Ed.* **2009**, *48*, 6974-6998; d) M. King, A. Wagner, *Bioconjugate Chem.* **2014**, *25*, 825-839; e) B. L. Oliveira, Z. Guo, G. J. L. Bernardes, *Chem. Soc. Rev.* **2017**, *46*, 4895-4950; f) R. D. Row, J. A. Prescher, *Acc. Chem. Res.* **2018**, *51*, 1073-1081.

[3] A. N. Glazer, *Annu. Rev. Biochem.* **1970**, *39*, 101-130.

[4] a) E. Basle, N. Joubert, M. Pucheault, *Chem. Biol.* **2010**, *17*, 213-227; b) O. Koniev, A. Wagner, *Chem. Soc. Rev.* **2015**, *44*, 5495-5551.

[5] A. Miseta, P. Csutora, *Mol. Biol. Evol.* **2000**, *17*, 1232-1239.

[6] a) J. M. Chalker, G. J. Bernardes, Y. A. Lin, B. G. Davis, *Chem. - Asian J.* **2009**, *4*, 630-640; b) C. D. Spicer, E. T. Pashuck, M. M. Stevens, *Chem. Rev.* **2018**, *118*, 7702-7743.

[7] M. W. Crankshaw, G. A. Grant, *Wiley* **1996**, *Unit 15.1, Modification at Cysteine*.

[8] S. B. Gunnoo, A. Madder, *ChemBioChem* **2016**, *17*, 529-553.

[9] D. R. Goddard, L. Michaelis, *J. Biol. Chem.* **1935**, *112*, 361-371.

[10] E. S. Boja, H. M. Fales, *Anal. Chem.* **2001**, *73*, 3576-3582.

[11] M. L. Nielsen, M. Vermeulen, T. Bonaldi, J. Cox, L. Moroder, M. Mann, *Nat. Methods* **2008**, *5*, 459-460.

[12] a) N. Lundell, T. Schreitmuller, *Anal. Biochem.* **1999**, *266*, 31-47; b) P. I. Clark, G. Lowe, *J. Chem. Soc. Chem. Commun.* **1977**, 923-924; c) P. I. Clark, G. Lowe, *Eur. J. Biochem.* **1978**, *84*, 293-299; d) E. T. Kaiser, D. S. Lawrence, *Science* **1984**, *226*, 505-511; e) N. J. Davis, S. L. Flitsch, *Tetrahedron Lett.* **1991**, *32*, 6793-6796; f) D. Macmillan, R. M. Bill, K. A. Sage, D. Fern, S. L. Flitsch, *Chem. Biol.* **2001**, *8*, 133-145; g) R. S. Swanwick, A. M. Daines, L. H. Tey, S. L. Flitsch, R. K. Allemann, *ChemBioChem* **2005**, *6*, 1338-1340.

[13] a) J. E. Moore, W. H. Ward, *J. Am. Chem. Soc* **1956**, *78*, 2414-2418; b) Y. Zhang, V. S. Bhatt, G. Sun, P. G. Wang, A. F. Palmer, *Bioconjugate Chem.* **2008**, *19*, 2221-2230; c) D. J. Betting, K. Kafi, A. Abdollahi-Fard, S. A. Hurvitz, J. M. Timmerman, *J. Immunol.* **2008**, *181*, 4131-4140.

[14] a) M. S. Masri, M. Friedman, *J. Protein Chem.* **1988**, *7*, 49-54; b) M. P. Lutolf, J. A. Hubbell, *Biomacromolecules* **2003**, *4*, 713-722.

[15] a) S. C. Alley, D. R. Benjamin, S. C. Jeffrey, N. M. Okeley, D. L. Meyer, R. J. Sanderson, P. D. Senter, *Bioconjugate Chem.* **2008**, *19*, 759-765; b) A. D. Baldwin, K. L. Kiick, *Bioconjugate Chem.* **2011**, *22*, 1946-1953; c) B. Q. Shen, K. Xu, L. Liu, H. Raab, S. Bhakta, M. Kenrick, K. L. Parsons-Reponte, J. Tien, S. F. Yu, E. Mai, D. Li, J. Tibbitts, J. Baudys, O. M. Saad, S. J. Scales, P. J. McDonald, P. E. Hass, C. Eigenbrot, T. Nguyen, W. A. Solis, R. N. Fuji, K. M. Flagella, D. Patel, S. D. Spencer, L. A. Khawli, A. Ebens, W. L. Wong, R. Vandlen, S. Kaur, M. X. Sliwkowski, R. H. Scheller, P. Polakis, J. R. Junutula, *Nat. Biotechnol.* **2012**, *30*, 184-189.

[16] a) D. P. Nair, M. Podgórski, S. Chatani, T. Gong, W. Xi, C. R. Fenoli, C. N. Bowman, *Chem. Mater.* **2014**, *26*, 724-744; b) S. Chatani, D. P. Nair, C. N. Bowman, *Polym. Chem.* **2013**, *4*, 1048-1055.

[17] G. J. Bernardes, J. M. Chalker, J. C. Errey, B. G. Davis, *J. Am. Chem. Soc.* **2008**, *130*, 5052-5053.
[18] T. H. Wright, B. J. Bower, J. M. Chalker, G. J. Bernardes, R. Wiewiora, W. L. Ng, R. Raj, S. Faulkner, M. R. Vallee, A. Phanumartwiwath, O. D. Coleman, M. L. Thezenas, M. Khan, S. R. Galan, L. Lercher, M. W. Schombs, S. Gerstberger, M. E. Palm-Espling, A. J. Baldwin, B. M. Kessler, T. D. Claridge, S. Mohammed, B. G. Davis, *Science* **2016**, *354*.
[19] a) G. L. Ellman, *Arch. Biochem. Biophys.* **1959**, *82*, 70-77; b) S. Bubenikova, I.-C. Stancu, L. Kalinovska, E. Schacht, E. Lippens, H. Declercq, M. Cornelissen, M. Santin, M. Amblard, J. Martinez, *Carbohydr. Polym.* **2012**, *88*, 1239-1250; c) Q. Xu, Z. Zhang, C. Xiao, C. He, X. Chen, *Biomacromolecules* **2017**, *18*, 1411-1418.
[20] A. Fontana, E. Scoffone, C. A. Benassi, *Biochemistry* **1968**, *7*, 980-986.
[21] a) B. G. Davis, M. A. T. Maughan, M. P. Green, A. Ullman, J. B. Jones, *Tetrahedron: Asymmetry* **2000**, *11*, 245-262; b) D. P. Gamblin, P. Garnier, S. J. Ward, N. J. Oldham, A. J. Fairbanks, B. G. Davis, *Org. Biomol. Chem.* **2003**, *1*, 3642-3644.
[22] D. P. Gamblin, P. Garnier, S. van Kasteren, N. J. Oldham, A. J. Fairbanks, B. G. Davis, *Angew. Chem. Int. Ed.* **2004**, *43*, 828-833.
[23] a) H. J. Creech, R. N. Jones, *J. Am. Chem. Soc.* **1941**, *63*, 1670-1673; b) L. Goodfriend, A. H. Sehon, *Can. J. Biochem. Physiol.* **1958**, *36*, 1177-1184.
[24] A. H. Coons, H. J. Creech, R. N. Jones, E. Berliner, *J. Immunol.* **1942**, *45*, 159-170.
[25] D. Podhradsky, L. Drobnica, P. Kristian, *Experientia* **1979**, *35*, 154-155.
[26] P. R. Banks, D. M. Paquette, *Bioconjugate Chem.* **1995**, *6*, 447-458.
[27] a) B. T. Miller, T. J. Collins, G. T. Nagle, A. Kurosky, *J. Biol. Chem.* **1992**, *267*, 5060-5069; b) B. T. Miller, *Biochem. Biophys. Res. Commun.* **1996**, *218*, 377-382; c) B. T. Miller, T. J. Collins, M. E. Rogers, A. Kurosky, *Peptides* **1997**, *18*, 1585-1595; d) W. C. Yang, H. Mirzaei, X. Liu, F. E. Regnier, *Anal. Chem.* **2006**, *78*, 4702-4708; e) F. E. Regnier, S. Julka, *Proteomics* **2006**, *6*, 3968-3979; f) M. D. Leavell, P. Novak, C. R. Behrens, J. S. Schoeniger, G. H. Kruppa, *J. Am. Soc. Mass Spectrom.* **2004**, *15*, 1604-1611; g) S. Kalkhof, A. Sinz, *Anal. Bioanal. Chem.* **2008**, *392*, 305-312; h) S. Mädler, C. Bich, D. Touboul, R. Zenobi, *J. Mass Spectrom.* **2009**, *44*, 694-706.
[28] a) J. V. Staros, *Biochemistry* **1982**, *21*, 3950-3955; b) J. B. Denny, G. Blobel, *Proc. Natl. Acad. Sci. U.S.A.* **1984**, *81*, 5286-5290; c) A. W. Yem, H. A. Zurcher-Neely, K. A. Richard, N. D. Staite, R. L. Heinrikson, M. R. Deibel, Jr., *J. Biol. Chem.* **1989**, *264*, 17691-17697; d) J. V. Staros, R. W. Wright, D. M. Swingle, *Anal. Biochem.* **1986**, *156*, 220-222.
[29] a) R. F. Borch, M. D. Bernstein, H. D. Durst, *J. Am. Chem. Soc.* **1971**, *93*, 2897-2904; b) G. R. Gray, *Arch. Biochem. Biophys.* **1974**, *163*, 426-428.
[30] J. M. McFarland, M. B. Francis, *J. Am. Chem. Soc.* **2005**, *127*, 13490-13491.
[31] G. Weber, *Biochem. J.* **1952**, *51*, 155-167.
[32] a) C. Gros, B. Labouesse, *Eur. J. Biochem.* **1969**, *7*, 463-470; b) C. Lefevre, H. C. Kang, R. P. Haugland, N. Malekzadeh, S. Arttamangkul, R. P. Haugland, *Bioconjugate Chem.* **1996**, *7*, 482-489.
[33] a) B. S. Hartley, V. Massey, *Biochim. Biophys. Acta* **1956**, *21*, 58-70; b) D. J. Herzig, A. W. Rees, R. A. Day, *Biopolymers* **1964**, *2*, 349-360; c) J. K. Lin, J. Y. Chang, *Anal. Chem.* **1975**, *47*, 1634-1638; d) A. Andreoni, G. Bottiroli, A. Colasanti, M. C. Giangare, P. Riccio, G. Roberti, P. Vaghi, *J. Biochem. Biophys. Methods* **1994**, *29*, 157-172.
[34] M. J. Hunter, M. L. Ludwig, *J. Am. Chem. Soc.* **1962**, *84*, 3491-3504.

[35] a) R. R. Traut, A. Bollen, T. T. Sun, J. W. Hershey, J. Sundberg, L. R. Pierce, *Biochemistry* **1973**, *12*, 3266-3273; b) R. Jue, J. M. Lambert, L. R. Pierce, R. R. Traut, *Biochemistry* **1978**, *17*, 5399-5406.
[36] a) J. M. Antos, M. B. Francis, *J. Am. Chem. Soc.* **2004**, *126*, 10256-10257; b) J. M. Antos, J. M. McFarland, A. T. Iavarone, M. B. Francis, *J. Am. Chem. Soc.* **2009**, *131*, 6301-6308.
[37] a) N. S. Joshi, L. R. Whitaker, M. B. Francis, *J. Am. Chem. Soc.* **2004**, *126*, 15942-15943; b) J. M. McFarland, N. S. Joshi, M. B. Francis, *J. Am. Chem. Soc.* **2008**, *130*, 7639-7644; c) D. W. Romanini, M. B. Francis, *Bioconjugate Chem.* **2008**, *19*, 153-157.
[38] S. D. Tilley, M. B. Francis, *J. Am. Chem. Soc.* **2006**, *128*, 1080-1081.
[39] a) O. Shimomura, F. H. Johnson, Y. Saiga, *J. Cell. Comp. Physiol.* **1962**, *59*, 223-239; b) F. H. Johnson, O. Shimomura, Y. Saiga, L. C. Gershman, G. T. Reynolds, J. R. Waters, *J. Cell. Comp. Physiol.* **1962**, *60*, 85-103.
[40] D. C. Prasher, V. K. Eckenrode, W. W. Ward, F. G. Prendergast, M. J. Cormier, *Gene* **1992**, *111*, 229-233.
[41] a) M. Chalfie, Y. Tu, G. Euskirchen, W. W. Ward, D. C. Prasher, *Science* **1994**, *263*, 802-805; b) S. Inouye, F. I. Tsuji, *FEBS Lett.* **1994**, *341*, 277-280.
[42] a) R. Y. Tsien, *Annu. Rev. Biochem.* **1998**, *67*, 509-544; b) S. G. Olenych, N. S. Claxton, G. K. Ottenberg, M. W. Davidson, *Curr. Protoc. Cell. Biol.* **2007**, *Unit 21.5*, 1-34; c) N. C. Shaner, G. H. Patterson, M. W. Davidson, *J. Cell. Sci.* **2007**, *120*, 4247-4260; d) P. Dedecker, F. C. De Schryver, J. Hofkens, *J. Am. Chem. Soc.* **2013**, *135*, 2387-2402.
[43] a) R. Heim, A. B. Cubitt, R. Y. Tsien, *Nature* **1995**, *373*, 663-664; b) B. P. Cormack, R. H. Valdivia, S. Falkow, *Gene* **1996**, *173*, 33-38.
[44] a) R. Heim, D. C. Prasher, R. Y. Tsien, *Proc. Natl. Acad. Sci. U.S.A.* **1994**, *91*, 12501-12504; b) H. W. Ai, N. C. Shaner, Z. Cheng, R. Y. Tsien, R. E. Campbell, *Biochemistry* **2007**, *46*, 5904-5910.
[45] R. Heim, R. Y. Tsien, *Curr. Biol.* **1996**, *6*, 178-182.
[46] a) M. Ormö, A. B. Cubitt, K. Kallio, L. A. Gross, R. Y. Tsien, S. J. Remington, *Science* **1996**, *273*, 1392-1395; b) A. Miyawaki, O. Griesbeck, R. Heim, R. Y. Tsien, *Proc. Natl. Acad. Sci. U.S.A.* **1999**, *96*, 2135-2140.
[47] M. V. Matz, A. F. Fradkov, Y. A. Labas, A. P. Savitsky, A. G. Zaraisky, M. L. Markelov, S. A. Lukyanov, *Nat. Biotechnol.* **1999**, *17*, 969-973.
[48] a) R. E. Campbell, O. Tour, A. E. Palmer, P. A. Steinbach, G. S. Baird, D. A. Zacharias, R. Y. Tsien, *Proc. Natl. Acad. Sci. U.S.A.* **2002**, *99*, 7877-7882; b) N. C. Shaner, R. E. Campbell, P. A. Steinbach, B. N. Giepmans, A. E. Palmer, R. Y. Tsien, *Nat. Biotechnol.* **2004**, *22*, 1567-1572; c) L. Wang, W. C. Jackson, P. A. Steinbach, R. Y. Tsien, *Proc. Natl. Acad. Sci. U.S.A.* **2004**, *101*, 16745-16749.
[49] G. H. Patterson, J. Lippincott-Schwartz, *Science* **2002**, *297*, 1873-1877.
[50] a) D. M. Chudakov, V. V. Verkhusha, D. B. Staroverov, E. A. Souslova, S. Lukyanov, K. A. Lukyanov, *Nat. Biotechnol.* **2004**, *22*, 1435-1439; b) R. Ando, H. Hama, M. Yamamoto-Hino, H. Mizuno, A. Miyawaki, *Proc. Natl. Acad. Sci. U.S.A.* **2002**, *99*, 12651-12656; c) H. Tsutsui, S. Karasawa, H. Shimizu, N. Nukina, A. Miyawaki, *EMBO Rep.* **2005**, *6*, 233-238; d) J. Wiedenmann, S. Ivanchenko, F. Oswald, F. Schmitt, C. Rocker, A. Salih, K. D. Spindler, G. U. Nienhaus, *Proc. Natl. Acad. Sci. U.S.A.* **2004**, *101*, 15905-15910; e) G. U. Nienhaus, K. Nienhaus, A. Hölzle, S. Ivanchenko, F. Renzi, F. Oswald, M. Wolff, F. Schmitt, C. Röcker, B. Vallone, W. Weidemann, R. Heilker, H. Nar, J. Wiedenmann, *Photochem. Photobiol.* **2006**, *82*, 351-358; f) N. G. Gurskaya, V. V. Verkhusha, A. S. Shcheglov, D. B. Staroverov, T.

V. Chepurnykh, A. F. Fradkov, S. Lukyanov, K. A. Lukyanov, *Nat. Biotechnol.* **2006**, *24*, 461-465.

[51] a) D. M. Chudakov, V. V. Belousov, A. G. Zaraisky, V. V. Novoselov, D. B. Staroverov, D. B. Zorov, S. Lukyanov, K. A. Lukyanov, *Nat. Biotechnol.* **2003**, *21*, 191-194; b) R. Ando, H. Mizuno, A. Miyawaki, *Science* **2004**, *306*, 1370-1373; c) S. Habuchi, R. Ando, P. Dedecker, W. Verheijen, H. Mizuno, A. Miyawaki, J. Hofkens, *Proc. Natl. Acad. Sci. U.S.A.* **2005**, *102*, 9511-9516.

[52] a) M. Andresen, R. Schmitz-Salue, S. Jakobs, *Mol. Biol. Cell* **2004**, *15*, 5616-5622; b) C. Hoffmann, G. Gaietta, M. Bünemann, S. R. Adams, S. Oberdorff-Maass, B. Behr, J. P. Vilardaga, R. Y. Tsien, M. H. Ellisman, M. J. Lohse, *Nat. Methods* **2005**, *2*, 171-176.

[53] K. Afitska, A. Fucikova, V. V. Shvadchak, D. A. Yushchenko, *Biophys. J.* **2017**, *113*, 2182-2191.

[54] a) B. A. Griffin, S. R. Adams, R. Y. Tsien, *Science* **1998**, *281*, 269-272; b) S. R. Adams, R. E. Campbell, L. A. Gross, B. R. Martin, G. K. Walkup, Y. Yao, J. Llopis, R. Y. Tsien, *J. Am. Chem. Soc.* **2002**, *124*, 6063-6076.

[55] M. F. Langhorst, S. Genisyuerek, C. A. Stuermer, *Histochem. Cell Biol.* **2006**, *125*, 743-747.

[56] T. L. Halo, J. Appelbaum, E. M. Hobert, D. M. Balkin, A. Schepartz, *J. Am. Chem. Soc.* **2009**, *131*, 438-439.

[57] a) E. G. Guignet, R. Hovius, H. Vogel, *Nat. Biotechnol.* **2004**, *22*, 440-444; b) A. N. Kapanidis, Y. W. Ebright, R. H. Ebright, *J. Am. Chem. Soc.* **2001**, *123*, 12123-12125; c) S. Lata, A. Reichel, R. Brock, R. Tampe, J. Piehler, *J. Am. Chem. Soc.* **2005**, *127*, 10205-10215; d) C. T. Hauser, R. Y. Tsien, *Proc. Natl. Acad. Sci. U.S.A.* **2007**, *104*, 3693-3697; e) A. Ojida, K. Honda, D. Shinmi, S. Kiyonaka, Y. Mori, I. Hamachi, *J. Am. Chem. Soc.* **2006**, *128*, 10452-10459; f) H. Nonaka, S. Tsukiji, A. Ojida, I. Hamachi, *J. Am. Chem. Soc.* **2007**, *129*, 15777-15779; g) M. Nitz, K. J. Franz, R. L. Maglathlin, B. Imperiali, *ChemBioChem* **2003**, *4*, 272-276; h) K. J. Franz, M. Nitz, B. Imperiali, *ChemBioChem* **2003**, *4*, 265-271.

[58] A. Keppler, S. Gendreizig, T. Gronemeyer, H. Pick, H. Vogel, K. Johnsson, *Nat. Biotechnol.* **2003**, *21*, 86-89.

[59] A. E. Pegg, *Mutat. Res.* **2000**, *462*, 83-100.

[60] a) A. Keppler, H. Pick, C. Arrivoli, H. Vogel, K. Johnsson, *Proc. Natl. Acad. Sci. U.S.A.* **2004**, *101*, 9955-9959; b) S. Gendreizig, M. Kindermann, K. Johnsson, *J. Am. Chem. Soc.* **2003**, *125*, 14970-14971.

[61] A. Gautier, A. Juillerat, C. Heinis, I. R. Correa, Jr., M. Kindermann, F. Beaufils, K. Johnsson, *Chem. Biol.* **2008**, *15*, 128-136.

[62] G. V. Los, L. P. Encell, M. G. McDougall, D. D. Hartzell, N. Karassina, C. Zimprich, M. G. Wood, R. Learish, R. F. Ohana, M. Urh, D. Simpson, J. Mendez, K. Zimmerman, P. Otto, G. Vidugiris, J. Zhu, A. Darzins, D. H. Klaubert, R. F. Bulleit, K. V. Wood, *ACS Chem. Biol.* **2008**, *3*, 373-382.

[63] a) R. F. Ohana, L. P. Encell, K. Zhao, D. Simpson, M. R. Slater, M. Urh, K. V. Wood, *Protein Expr. Purif.* **2009**, *68*, 110-120; b) T. K. Neklesa, H. S. Tae, A. R. Schneekloth, M. J. Stulberg, T. W. Corson, T. B. Sundberg, K. Raina, S. A. Holley, C. M. Crews, *Nat. Chem. Biol.* **2011**, *7*, 538-543.

[64] a) I. Chen, M. Howarth, W. Lin, A. Y. Ting, *Nat. Methods* **2005**, *2*, 99-104; b) M. Howarth, K. Takao, Y. Hayashi, A. Y. Ting, *Proc. Natl. Acad. Sci. U.S.A.* **2005**, *102*, 7583-7588; c) S. A. Slavoff, I. Chen, Y. A. Choi, A. Y. Ting, *J. Am. Chem. Soc.* **2008**, *130*, 1160-1162.

[65] a) H. Sato, M. Ikeda, K. Suzuki, K. Hirayama, *Biochemistry* **1996**, *35*, 13072-13080; b) M. Taki, M. Shiota, K. Taira, *Protein. Eng. Des. Sel.* **2004**, *17*, 119-126; c) C. W. Lin, A. Y. Ting, *J. Am. Chem. Soc.* **2006**, *128*, 4542-4543.

[66] a) M. Fernandez-Suarez, H. Baruah, L. Martinez-Hernandez, K. T. Xie, J. M. Baskin, C. R. Bertozzi, A. Y. Ting, *Nat. Biotechnol.* **2007**, *25*, 1483-1487; b) H. Baruah, S. Puthenveetil, Y. A. Choi, S. Shah, A. Y. Ting, *Angew. Chem. Int. Ed.* **2008**, *47*, 7018-7021; c) C. Uttamapinant, K. A. White, H. Baruah, S. Thompson, M. Fernandez-Suarez, S. Puthenveetil, A. Y. Ting, *Proc. Natl. Acad. Sci. U.S.A.* **2010**, *107*, 10914-10919.

[67] a) I. S. Carrico, B. L. Carlson, C. R. Bertozzi, *Nat. Chem. Biol.* **2007**, *3*, 321-322; b) J. S. Rush, C. R. Bertozzi, *J. Am. Chem. Soc.* **2008**, *130*, 12240-12241.

[68] a) H. Mao, S. A. Hart, A. Schink, B. A. Pollok, *J. Am. Chem. Soc.* **2004**, *126*, 2670-2671; b) S. Samantaray, U. Marathe, S. Dasgupta, V. K. Nandicoori, R. P. Roy, *J. Am. Chem. Soc.* **2008**, *130*, 2132-2133; c) R. Parthasarathy, S. Subramanian, E. T. Boder, *Bioconjugate Chem.* **2007**, *18*, 469-476; d) M. W. Popp, J. M. Antos, G. M. Grotenbreg, E. Spooner, H. L. Ploegh, *Nat. Chem. Biol.* **2007**, *3*, 707-708; e) T. Tanaka, T. Yamamoto, S. Tsukiji, T. Nagamune, *ChemBioChem* **2008**, *9*, 802-807.

[69] a) N. George, H. Pick, H. Vogel, N. Johnsson, K. Johnsson, *J. Am. Chem. Soc.* **2004**, *126*, 8896-8897; b) J. Yin, F. Liu, X. Li, C. T. Walsh, *J. Am. Chem. Soc.* **2004**, *126*, 7754-7755; c) J. J. La Clair, T. L. Foley, T. R. Schegg, C. M. Regan, M. D. Burkart, *Chem. Biol.* **2004**, *11*, 195-201; d) L. Vivero-Pol, N. George, H. Krumm, K. Johnsson, N. Johnsson, *J. Am. Chem. Soc.* **2005**, *127*, 12770-12771; e) Z. Zhou, P. Cironi, A. J. Lin, Y. Xu, S. Hrvatin, D. E. Golan, P. A. Silver, C. T. Walsh, J. Yin, *ACS Chem. Biol.* **2007**, *2*, 337-346.

[70] S. T. Laughlin, C. R. Bertozzi, *Proc. Natl. Acad. Sci. U.S.A.* **2009**, *106*, 12-17.

[71] a) A. Salic, T. J. Mitchison, *Proc. Natl. Acad. Sci. U.S.A.* **2008**, *105*, 2415-2420; b) C. Y. Jao, A. Salic, *Proc. Natl. Acad. Sci. U.S.A.* **2008**, *105*, 15779-15784; c) A. B. Neef, N. W. Luedtke, *Proc. Natl. Acad. Sci. U.S.A.* **2011**, *108*, 20404-20409.

[72] J. T. Ngo, D. A. Tirrell, *Acc. Chem. Res.* **2011**, *44*, 677-685.

[73] H. C. Hang, J. P. Wilson, G. Charron, *Acc. Chem. Res.* **2011**, *44*, 699-708.

[74] D. Rideout, *Science* **1986**, *233*, 561-563.

[75] a) V. W. Cornish, K. M. Hahn, P. G. Schultz, *J. Am. Chem. Soc.* **1996**, *118*, 8150-8151; b) Z. Zhang, B. A. Smith, L. Wang, A. Brock, C. Cho, P. G. Schultz, *Biochemistry* **2003**, *42*, 6735-6746; c) S. Ulrich, D. Boturyn, A. Marra, O. Renaudet, P. Dumy, *Chem. Eur. J.* **2014**, *20*, 34-41.

[76] a) P. Agarwal, J. van der Weijden, E. M. Sletten, D. Rabuka, C. R. Bertozzi, *Proc. Natl. Acad. Sci. U.S.A.* **2013**, *110*, 46-51; b) P. Agarwal, R. Kudirka, A. E. Albers, R. M. Barfield, G. W. de Hart, P. M. Drake, L. C. Jones, D. Rabuka, *Bioconjugate Chem.* **2013**, *24*, 846-851.

[77] P. I. Kitov, D. F. Vinals, S. Ng, K. F. Tjhung, R. Derda, *J. Am. Chem. Soc.* **2014**, *136*, 8149-8152.

[78] J. Kalia, R. T. Raines, *Angew. Chem. Int. Ed.* **2008**, *47*, 7523-7526.

[79] a) A. Dirksen, T. M. Hackeng, P. E. Dawson, *Angew. Chem. Int. Ed.* **2006**, *45*, 7581-7584; b) A. Dirksen, S. Dirksen, T. M. Hackeng, P. E. Dawson, *J. Am. Chem. Soc.* **2006**, *128*, 15602-15603; c) Y. Zeng, T. N. Ramya, A. Dirksen, P. E. Dawson, J. C. Paulson, *Nat. Methods.* **2009**, *6*, 207-209.

[80] P. Crisalli, E. T. Kool, *J. Org. Chem.* **2013**, *78*, 1184-1189.

[81] P. Crisalli, E. T. Kool, *Org. Lett.* **2013**, *15*, 1646-1649.

[82] a) E. T. Kool, D. H. Park, P. Crisalli, *J. Am. Chem. Soc.* **2013**, *135*, 17663-17666; b) E. T. Kool, P. Crisalli, K. M. Chan, *Org. Lett.* **2014**, *16*, 1454-1457.

[83] W. P. Jencks, *J. Am. Chem. Soc.* **1959**, *81*, 475-481.
[84] P. Schmidt, L. Zhou, K. Tishinov, K. Zimmermann, D. Gillingham, *Angew. Chem. Int. Ed.* **2014**, *53*, 10928-10931.
[85] a) O. Dilek, Z. Lei, K. Mukherjee, S. Bane, *Chem. Commun.* **2015**, *51*, 16992-16995; b) C. J. Stress, P. J. Schmidt, D. G. Gillingham, *Org. Biomol. Chem.* **2016**, *14*, 5529-5533.
[86] a) L. K. Mahal, K. J. Yarema, C. R. Bertozzi, *Science* **1997**, *276*, 1125-1128; b) H. C. Hang, C. R. Bertozzi, *J. Am. Chem. Soc.* **2001**, *123*, 1242-1243.
[87] R. J. Griffin, *Prog. Med. Chem.* **1994**, *31*, 121-232.
[88] a) K. L. Kiick, E. Saxon, D. A. Tirrell, C. R. Bertozzi, *Proc. Natl. Acad. Sci. U.S.A.* **2002**, *99*, 19-24; b) S. F. van Dongen, R. L. Teeuwen, M. Nallani, S. S. van Berkel, J. J. Cornelissen, R. J. Nolte, J. C. van Hest, *Bioconjugate Chem.* **2009**, *20*, 20-23.
[89] E. Saxon, C. R. Bertozzi, *Science* **2000**, *287*, 2007-2010.
[90] H. Staudinger, J. Meyer, *Helv. Chim. Acta.* **1919**, *2*, 635-646.
[91] E. Saxon, J. I. Armstrong, C. R. Bertozzi, *Org. Lett.* **2000**, *2*, 2141-2143.
[92] B. L. Nilsson, L. L. Kiessling, R. T. Raines, *Org. Lett.* **2000**, *2*, 1939-1941.
[93] a) G. A. Lemieux, C. L. De Graffenried, C. R. Bertozzi, *J. Am. Chem. Soc.* **2003**, *125*, 4708-4709; b) M. J. Hangauer, C. R. Bertozzi, *Angew. Chem. Int. Ed.* **2008**, *47*, 2394-2397.
[94] F. L. Lin, H. M. Hoyt, H. van Halbeek, R. G. Bergman, C. R. Bertozzi, *J. Am. Chem. Soc.* **2005**, *127*, 2686-2695.
[95] a) E. Saxon, S. J. Luchansky, H. C. Hang, C. Yu, S. C. Lee, C. R. Bertozzi, *J. Am. Chem. Soc.* **2002**, *124*, 14893-14902; b) J. A. Prescher, D. H. Dube, C. R. Bertozzi, *Nature* **2004**, *430*, 873-877; c) D. H. Dube, J. A. Prescher, C. N. Quang, C. R. Bertozzi, *Proc. Natl. Acad. Sci. U.S.A.* **2006**, *103*, 4819-4824.
[96] D. J. Vocadlo, H. C. Hang, E. J. Kim, J. A. Hanover, C. R. Bertozzi, *Proc. Natl. Acad. Sci. U.S.A.* **2003**, *100*, 9116-9121.
[97] S. J. Luchansky, S. Argade, B. K. Hayes, C. R. Bertozzi, *Biochemistry* **2004**, *43*, 12358-12366.
[98] G. Charron, M. M. Zhang, J. S. Yount, J. Wilson, A. S. Raghavan, E. Shamir, H. C. Hang, *J. Am. Chem. Soc.* **2009**, *131*, 4967-4975.
[99] V. V. Rostovtsev, L. G. Green, V. V. Fokin, K. B. Sharpless, *Angew. Chem. Int. Ed.* **2002**, *41*, 2596-2599.
[100] C. W. Tornoe, C. Christensen, M. Meldal, *J. Org. Chem.* **2002**, *67*, 3057-3064.
[101] H. C. Kolb, M. G. Finn, K. B. Sharpless, *Angew. Chem. Int. Ed.* **2001**, *40*, 2004-2021.
[102] a) A. Michael, *J. Prakt. Chem.* **1893**, *48*, 94-95; b) R. Huisgen, *Angew. Chem. Int. Ed.* **1963**, *73*, 656-657.
[103] a) D. C. Kennedy, C. S. McKay, M. C. Legault, D. C. Danielson, J. A. Blake, A. F. Pegoraro, A. Stolow, Z. Mester, J. P. Pezacki, *J. Am. Chem. Soc.* **2011**, *133*, 17993-18001; b) V. Hong, N. F. Steinmetz, M. Manchester, M. G. Finn, *Bioconjugate Chem.* **2010**, *21*, 1912-1916.
[104] a) T. R. Chan, R. Hilgraf, K. B. Sharpless, V. V. Fokin, *Org. Lett.* **2004**, *6*, 2853-2855; b) V. Hong, S. I. Presolski, C. Ma, M. G. Finn, *Angew. Chem. Int. Ed.* **2009**, *48*, 9879-9883; c) D. Soriano Del Amo, W. Wang, H. Jiang, C. Besanceney, A. C. Yan, M. Levy, Y. Liu, F. L. Marlow, P. Wu, *J. Am. Chem. Soc.* **2010**, *132*, 16893-16899; d) C. Besanceney-Webler, H. Jiang, T. Zheng, L. Feng, D. Soriano del Amo, W. Wang, L. M. Klivansky, F. L. Marlow, Y. Liu, P. Wu, *Angew. Chem. Int. Ed.* **2011**, *50*, 8051-8056.
[105] a) A. T. Blomquist, L. H. Liu, *J. Am. Chem. Soc.* **1953**, *75*, 2153-2154; b) G. Wittig, A. Krebs, *Chem. Ber.* **1961**, *94*, 3260-3275.

[106] N. J. Agard, J. A. Prescher, C. R. Bertozzi, *J. Am. Chem. Soc.* **2004**, *126*, 15046-15047.
[107] a) J. M. Baskin, J. A. Prescher, S. T. Laughlin, N. J. Agard, P. V. Chang, I. A. Miller, A. Lo, J. A. Codelli, C. R. Bertozzi, *Proc. Natl. Acad. Sci. U.S.A.* **2007**, *104*, 16793-16797; b) X. Ning, J. Guo, M. A. Wolfert, G. J. Boons, *Angew. Chem. Int. Ed.* **2008**, *47*, 2253-2255; c) M. F. Debets, S. S. van Berkel, S. Schoffelen, F. P. Rutjes, J. C. van Hest, F. L. van Delft, *Chem. Commun.* **2010**, *46*, 97-99; d) A. Kuzmin, A. Poloukhtine, M. A. Wolfert, V. V. Popik, *Bioconjugate Chem.* **2010**, *21*, 2076-2085; e) J. C. Jewett, E. M. Sletten, C. R. Bertozzi, *J. Am. Chem. Soc.* **2010**, *132*, 3688-3690; f) J. Dommerholt, S. Schmidt, R. Temming, L. J. Hendriks, F. P. Rutjes, J. C. van Hest, D. J. Lefeber, P. Friedl, F. L. van Delft, *Angew. Chem. Int. Ed.* **2010**, *49*, 9422-9425; g) G. de Almeida, E. M. Sletten, H. Nakamura, K. K. Palaniappan, C. R. Bertozzi, *Angew. Chem. Int. Ed.* **2012**, *51*, 2443-2447.
[108] a) A. M. Jawalekar, E. Reubsaet, F. P. Rutjes, F. L. van Delft, *Chem. Commun.* **2011**, *47*, 3198-3200; b) B. C. Sanders, F. Friscourt, P. A. Ledin, N. E. Mbua, S. Arumugam, J. Guo, T. J. Boltje, V. V. Popik, G. J. Boons, *J. Am. Chem. Soc.* **2011**, *133*, 949-957; c) K. Gutsmiedl, C. T. Wirges, V. Ehmke, T. Carell, *Org. Lett.* **2009**, *11*, 2405-2408.
[109] a) C. S. McKay, J. Moran, J. P. Pezacki, *Chem. Commun.* **2010**, *46*, 931-933; b) X. Ning, R. P. Temming, J. Dommerholt, J. Guo, D. B. Ania, M. F. Debets, M. A. Wolfert, G. J. Boons, F. L. van Delft, *Angew. Chem. Int. Ed.* **2010**, *49*, 3065-3068; c) C. S. McKay, J. A. Blake, J. Cheng, D. C. Danielson, J. P. Pezacki, *Chem. Commun.* **2011**, *47*, 10040-10042.
[110] N. A. McGrath, R. T. Raines, *Chem. Sci.* **2012**, *3*, 3237-3240.
[111] S. Wallace, J. W. Chin, *Chem. Sci.* **2014**, *5*, 1742-1744.
[112] a) R. A. Carboni, R. V. Lindsey, *J. Am. Chem. Soc.* **1959**, *81*, 4342-4346; b) F. Thalhammer, U. Wallfahrer, J. Sauer, *Tetrahedron Lett.* **1990**, *31*, 6851-6854; c) J. Sauer, D. K. Heldmann, J. Hetzenegger, J. Krauthan, H. Sichert, J. Schuster, *Eur. J. Org. Chem.* **1998**, 2885-2896.
[113] a) N. K. Devaraj, R. Weissleder, S. A. Hilderbrand, *Bioconjugate Chem.* **2008**, *19*, 2297-2299; b) M. L. Blackman, M. Royzen, J. M. Fox, *J. Am. Chem. Soc.* **2008**, *130*, 13518-13519.
[114] a) M. R. Karver, R. Weissleder, S. A. Hilderbrand, *Bioconjugate Chem.* **2011**, *22*, 2263-2270; b) K. Lang, L. Davis, S. Wallace, M. Mahesh, D. J. Cox, M. L. Blackman, J. M. Fox, J. W. Chin, *J. Am. Chem. Soc.* **2012**, *134*, 10317-10320; c) J. Yang, M. R. Karver, W. Li, S. Sahu, N. K. Devaraj, *Angew. Chem. Int. Ed.* **2012**, *51*, 5222-5225; d) H. Wu, J. Yang, J. Seckute, N. K. Devaraj, *Angew. Chem. Int. Ed.* **2014**, *53*, 5805-5809; e) Y. Qu, F. X. Sauvage, G. Clavier, F. Miomandre, P. Audebert, *Angew. Chem. Int. Ed.* **2018**, *57*, 12057-12061.
[115] a) M. T. Taylor, M. L. Blackman, O. Dmitrenko, J. M. Fox, *J. Am. Chem. Soc.* **2011**, *133*, 9646-9649; b) A. Darko, S. Wallace, O. Dmitrenko, M. M. Machovina, R. A. Mehl, J. W. Chin, J. M. Fox, *Chem. Sci.* **2014**, *5*, 3770-3776.
[116] Y. Fang, H. Zhang, Z. Huang, S. L. Scinto, J. C. Yang, C. W. Am Ende, O. Dmitrenko, D. S. Johnson, J. M. Fox, *Chem. Sci.* **2018**, *9*, 1953-1963.
[117] a) J. Yang, J. Seckute, C. M. Cole, N. K. Devaraj, *Angew. Chem. Int. Ed.* **2012**, *51*, 7476-7479; b) D. M. Patterson, L. A. Nazarova, B. Xie, D. N. Kamber, J. A. Prescher, *J. Am. Chem. Soc.* **2012**, *134*, 18638-18643; c) D. N. Kamber, L. A. Nazarova, Y. Liang, S. A. Lopez, D. M. Patterson, H. W. Shih, K. N. Houk, J. A. Prescher, *J. Am. Chem. Soc.* **2013**, *135*, 13680-13683.

[118] a) K. Lang, L. Davis, J. Torres-Kolbus, C. Chou, A. Deiters, J. W. Chin, *Nat. Chem.* **2012**, *4*, 298-304; b) M. Vrabel, P. Kolle, K. M. Brunner, M. J. Gattner, V. Lopez-Carrillo, R. de Vivie-Riedle, T. Carell, *Chem. Eur. J.* **2013**, *19*, 13309-13312.
[119] S. B. Engelsma, L. I. Willems, C. E. van Paaschen, S. I. van Kasteren, G. A. van der Marel, H. S. Overkleeft, D. V. Filippov, *Org. Lett.* **2014**, *16*, 2744-2747.
[120] W. Chen, D. Wang, C. Dai, D. Hamelberg, B. Wang, *Chem. Commun.* **2012**, *48*, 1736-1738.
[121] E. Kaya, M. Vrabel, C. Deiml, S. Prill, V. S. Fluxa, T. Carell, *Angew. Chem. Int. Ed.* **2012**, *51*, 4466-4469.
[122] a) A. Borrmann, S. Milles, T. Plass, J. Dommerholt, J. M. Verkade, M. Wiessler, C. Schultz, J. C. van Hest, F. L. van Delft, E. A. Lemke, *ChemBioChem* **2012**, *13*, 2094-2099; b) T. Plass, S. Milles, C. Koehler, J. Szymanski, R. Mueller, M. Wiessler, C. Schultz, E. A. Lemke, *Angew. Chem. Int. Ed.* **2012**, *51*, 4166-4170.
[123] a) J. L. Seitchik, J. C. Peeler, M. T. Taylor, M. L. Blackman, T. W. Rhoads, R. B. Cooley, C. Refakis, J. M. Fox, R. A. Mehl, *J. Am. Chem. Soc.* **2012**, *134*, 2898-2901; b) R. J. Blizzard, D. R. Backus, W. Brown, C. G. Bazewicz, Y. Li, R. A. Mehl, *J. Am. Chem. Soc.* **2015**, *137*, 10044-10047.
[124] H. S. Han, N. K. Devaraj, J. Lee, S. A. Hilderbrand, R. Weissleder, M. G. Bawendi, *J. Am. Chem. Soc.* **2010**, *132*, 7838-7839.
[125] J. B. Haun, N. K. Devaraj, S. A. Hilderbrand, H. Lee, R. Weissleder, *Nat. Nanotechnol.* **2010**, *5*, 660-665.
[126] R. Rossin, P. R. Verkerk, S. M. van den Bosch, R. C. Vulders, I. Verel, J. Lub, M. S. Robillard, *Angew. Chem. Int. Ed.* **2010**, *49*, 3375-3378.
[127] a) T. Reiner, E. J. Keliher, S. Earley, B. Marinelli, R. Weissleder, *Angew. Chem. Int. Ed.* **2011**, *50*, 1922-1925; b) S. Liu, M. Hassink, R. Selvaraj, L. P. Yap, R. Park, H. Wang, X. Chen, J. M. Fox, Z. Li, P. S. Conti, *Mol. Imaging* **2013**, *12*, 121-128; c) F. Emmetiere, C. Irwin, N. T. Viola-Villegas, V. Longo, S. M. Cheal, P. Zanzonico, N. Pillarsetty, W. A. Weber, J. S. Lewis, T. Reiner, *Bioconjugate Chem.* **2013**, *24*, 1784-1789.
[128] a) C. M. Cole, J. Yang, J. Seckute, N. K. Devaraj, *ChemBioChem* **2013**, *14*, 205-208; b) F. Doll, A. Buntz, A. K. Späte, V. F. Schart, A. Timper, W. Schrimpf, C. R. Hauck, A. Zumbusch, V. Wittmann, *Angew. Chem. Int. Ed.* **2016**, *55*, 2262-2266.
[129] P. Agarwal, B. J. Beahm, P. Shieh, C. R. Bertozzi, *Angew. Chem. Int. Ed.* **2015**, *54*, 11504-11510.
[130] R. S. Erdmann, H. Takakura, A. D. Thompson, F. Rivera-Molina, E. S. Allgeyer, J. Bewersdorf, D. Toomre, A. Schepartz, *Angew. Chem. Int. Ed.* **2014**, *53*, 10242-10246.
[131] a) J. Schoch, M. Wiessler, A. Jaschke, *J. Am. Chem. Soc.* **2010**, *132*, 8846-8847; b) J. Schoch, M. Staudt, A. Samanta, M. Wiessler, A. Jaschke, *Bioconjugate Chem.* **2012**, *23*, 1382-1386.
[132] U. Rieder, N. W. Luedtke, *Angew. Chem. Int. Ed.* **2014**, *53*, 9168-9172.
[133] J. Schoch, S. Ameta, A. Jaschke, *Chem. Commun.* **2011**, *47*, 12536-12537.
[134] a) A. M. Pyka, C. Domnick, F. Braun, S. Kath-Schorr, *Bioconjugate Chem.* **2014**, *25*, 1438-1443; b) H. Wu, B. T. Cisneros, C. M. Cole, N. K. Devaraj, *J. Am. Chem. Soc.* **2014**, *136*, 17942-17945.
[135] a) L. I. Willems, N. Li, B. I. Florea, M. Ruben, G. A. van der Marel, H. S. Overkleeft, *Angew. Chem. Int. Ed.* **2012**, *51*, 4431-4434; b) A. A. Neves, H. Stockmann, Y. A. Wainman, J. C. Kuo, S. Fawcett, F. J. Leeper, K. M. Brindle, *Bioconjugate Chem.* **2013**, *24*, 934-941.
[136] a) A. Sachdeva, K. Wang, T. Elliott, J. W. Chin, *J. Am. Chem. Soc.* **2014**, *136*, 7785-7788; b) M. R. Karver, R. Weissleder, S. A. Hilderbrand, *Angew. Chem. Int. Ed.* **2012**,

*51*, 920-922; c) A. Niederwieser, A. K. Späte, L. D. Nguyen, C. Jungst, W. Reutter, V. Wittmann, *Angew. Chem. Int. Ed.* **2013**, *52*, 4265-4268; d) A. K. Späte, H. Busskamp, A. Niederwieser, V. F. Schart, A. Marx, V. Wittmann, *Bioconjugate Chem.* **2014**, *25*, 147-154.

[137] a) R. M. Versteegen, R. Rossin, W. ten Hoeve, H. M. Janssen, M. S. Robillard, *Angew. Chem. Int. Ed.* **2013**, *52*, 14112-14116; b) R. Rossin, S. M. van Duijnhoven, W. Ten Hoeve, H. M. Janssen, L. H. Kleijn, F. J. Hoeben, R. M. Versteegen, M. S. Robillard, *Bioconjugate Chem.* **2016**, *27*, 1697-1706.

[138] a) J. Li, S. Jia, P. R. Chen, *Nat. Chem. Biol.* **2014**, *10*, 1003-1005; b) G. Zhang, J. Li, R. Xie, X. Fan, Y. Liu, S. Zheng, Y. Ge, P. R. Chen, *ACS Cent. Sci.* **2016**, *2*, 325-331; c) X. Fan, Y. Ge, F. Lin, Y. Yang, G. Zhang, W. S. Ngai, Z. Lin, S. Zheng, J. Wang, J. Zhao, J. Li, P. R. Chen, *Angew. Chem. Int. Ed.* **2016**, *55*, 14046-14050.

[139] D. N. Kamber, Y. Liang, R. J. Blizzard, F. Liu, R. A. Mehl, K. N. Houk, J. A. Prescher, *J. Am. Chem. Soc.* **2015**, *137*, 8388-8391.

[140] K. A. Horner, N. M. Valette, M. E. Webb, *Chem. Eur. J.* **2015**, *21*, 14376-14381.

[141] a) L. Crespin, L. Biancalana, T. Morack, D. C. Blakemore, S. V. Ley, *Org. Lett.* **2017**, *19*, 1084-1087; b) J. Meng, M. Wen, S. Zhang, P. Pan, X. Yu, W. P. Deng, *J. Org. Chem.* **2017**, *82*, 1676-1687.

[142] a) E. D. Anderson, D. L. Boger, *Org. Lett.* **2011**, *13*, 2492-2494; b) E. D. Anderson, D. L. Boger, *J. Am. Chem. Soc.* **2011**, *133*, 12285-12292; c) E. D. Anderson, A. S. Duerfeldt, K. Zhu, C. M. Glinkerman, D. L. Boger, *Org. Lett.* **2014**, *16*, 5084-5087; d) C. M. Glinkerman, D. L. Boger, *Org. Lett.* **2015**, *17*, 4002-4005.

[143] a) C. Le Droumaguet, C. Wang, Q. Wang, *Chem. Soc. Rev.* **2010**, *39*, 1233-1239; b) A. Nadler, C. Schultz, *Angew. Chem. Int. Ed.* **2013**, *52*, 2408-2410; c) G. B. Cserép, A. Herner, P. Kele, *Methods Appl. Fluoresc.* **2015**, *3*, 042001.

[144] a) K. Sivakumar, F. Xie, B. M. Cash, S. Long, H. N. Barnhill, Q. Wang, *Org. Lett.* **2004**, *6*, 4603-4606; b) Z. Zhou, C. J. Fahrni, *J. Am. Chem. Soc.* **2004**, *126*, 8862-8863.

[145] a) F. Friscourt, C. J. Fahrni, G. J. Boons, *J. Am. Chem. Soc.* **2012**, *134*, 18809-18815; b) P. Shieh, M. S. Siegrist, A. J. Cullen, C. R. Bertozzi, *Proc. Natl. Acad. Sci. U.S.A.* **2014**, *111*, 5456-5461; c) O. Demeter, A. Kormos, C. Koehler, G. Mezo, K. Nemeth, E. Kozma, L. B. Takacs, E. A. Lemke, P. Kele, *Bioconjugate Chem.* **2017**, *28*, 1552-1559.

[146] a) N. K. Devaraj, S. Hilderbrand, R. Upadhyay, R. Mazitschek, R. Weissleder, *Angew. Chem. Int. Ed.* **2010**, *49*, 2869-2872; b) L. G. Meimetis, J. C. Carlson, R. J. Giedt, R. H. Kohler, R. Weissleder, *Angew. Chem. Int. Ed.* **2014**, *53*, 7531-7534; c) A. Wieczorek, T. Buckup, R. Wombacher, *Org. Biomol. Chem.* **2014**, *12*, 4177-4185; d) E. Kozma, G. Estrada Girona, G. Paci, E. A. Lemke, P. Kele, *Chem. Commun.* **2017**, *53*, 6696-6699; e) A. Wieczorek, P. Werther, J. Euchner, R. Wombacher, *Chem. Sci.* **2017**, *8*, 1506-1510; f) G. Knorr, E. Kozma, J. M. Schaart, K. Nemeth, G. Török, P. Kele, *Bioconjugate Chem.* **2018**, *29*, 1312-1318.

[147] T. Komatsu, K. Johnsson, H. Okuno, H. Bito, T. Inoue, T. Nagano, Y. Urano, *J. Am. Chem. Soc.* **2011**, *133*, 6745-6751.

[148] C. P. Ramil, Q. Lin, *Curr. Opin. Chem. Biol.* **2014**, *21*, 89-95.

[149] W. Song, Y. Wang, J. Qu, M. M. Madden, Q. Lin, *Angew. Chem. Int. Ed.* **2008**, *47*, 2832-2835.

[150] W. Song, Y. Wang, J. Qu, Q. Lin, *J. Am. Chem. Soc.* **2008**, *130*, 9654-9655.

[151] Z. Yu, T. Y. Ohulchanskyy, P. An, P. N. Prasad, Q. Lin, *J. Am. Chem. Soc.* **2013**, *135*, 16766-16769.

[152] a) Z. Yu, Y. Pan, Z. Wang, J. Wang, Q. Lin, *Angew. Chem. Int. Ed.* **2012**, *51*, 10600-10604; b) Z. Yu, Q. Lin, *J. Am. Chem. Soc.* **2014**, *136*, 4153-4156.
[153] X. S. Wang, Y. J. Lee, W. R. Liu, *Chem. Commun.* **2014**, *50*, 3176-3179.
[154] X. Shang, X. Song, C. Faller, R. Lai, H. Li, R. Cerny, W. Niu, J. Guo, *Chem. Sci.* **2017**, *8*, 1141-1145.
[155] A. Vazquez, R. Dzijak, M. Dracinsky, R. Rampmaier, S. J. Siegl, M. Vrabel, *Angew. Chem. Int. Ed.* **2017**, *56*, 1334-1337.
[156] S. J. Siegl, A. Vazquez, R. Dzijak, M. Dracinsky, J. Galeta, R. Rampmaier, B. Klepetarova, M. Vrabel, *Chem. Eur. J.* **2018**, *24*, 2426-2432.
[157] S. J. Siegl, J. Galeta, R. Dzijak, A. Vazquez, M. Del Rio-Villanueva, M. Dracinsky, M. Vrabel, *ChemBioChem* **2019**, *20*, 886-890.
[158] a) C.-F. Shu, W. J. Tsai, J.-Y. Chen, A. K.-Y. Jen, Y. Zhang, T.-A. Chen, *Chem. Commun.* **1996**, *19*, 2279-2280; b) C.-F. Shu, Y.-C. Shu, Z.-H. Gong, S.-M. Peng, G.-H. Lee, A. K.-Y. Jen, *Chem. Mater.* **1998**, *10*, 3284-3286; c) Y.-C. Shu, Z.-H. Gong, C.-F. Shu, E. M. Breitung, R. J. McMahon, G.-H. Lee, A. K.-Y. Jen, *Chem. Mater.* **1999**, *11*, 1628-1632; d) U. Mayerhöffer, B. Fimmel, F. Würthner, *Angew Chem Int Ed Engl* **2012**, *51*, 164-167; e) U. Mayerhöffer, M. Gsänger, M. Stolte, B. Fimmel, F. Würthner, *Chemistry* **2013**, *19*, 218-232; f) L. Viteva, T. Gospodovoa, J. Rashkova, I. Abrahams, I. Timtcheva, S. Simova, M. R. Mazieres, J. G. Wolf, *Eur. J. Org. Chem.* **2007**, *19*; g) K. C. Kreß, T. Fischer, J. Stumpe, W. Frey, M. Raith, O. Beiraghi, S. H. Eichhorn, S. Tussetschläger, S. Laschat, *ChemPlusChem* **2014**, *79*, 223-232; h) J. C. Haenle, K. Bruchlos, S. Ludwigs, A. Köhn, S. Laschat, *ChemPlusChem* **2017**, *82*, 1197-1210.

# 7. Appendix: Supplementary information to the publications

## 7.1 Supplementary information to chapter 3.1

S.J. Siegl*, A. Vázquez*, R. Dzijak, M. Dračínský, J. Galeta, R. Rampmaier, B. Klepetářová, M. Vrabel, *Chem. Eur. J.* **2018**, 24, 2426-2432.
"Design and Synthesis of Aza-Bicyclononene Dienophiles for Rapid Fluorogenic Ligations".
*: These authors contributed equally to this work.

The corresponding NMR spectra are not presented here and can be found in the original publication.

CHEMISTRY
A European Journal

Supporting Information

# Design and Synthesis of Aza-Bicyclononene Dienophiles for Rapid Fluorogenic Ligations

Sebastian J. Siegl[+], Arcadio Vázquez[+], Rastislav Dzijak, Martin Dračínský, Juraj Galeta, Robert Rampmaier, Blanka Klepetářová, and Milan Vrabel*[a]

chem_201705188_sm_miscellaneous_information.pdf

# Supporting Information

## Content

## General information

The chemicals were obtained from *Sigma Aldrich*, *Alfa Aesar*, *Acros Organics*, *ABCR* or *VWR* and were used without further purification. Reactions with air- and moisture-sensitive reactants were performed under nitrogen or argon atmosphere and in anhydrous solvents from *VWR*.
Solutions were concentrated on a rotary evaporator from *Heidolph* equipped with a PC3001 VARIOpro pump from *Vacuubrand*. Photochemical reactions were performed in a RPR-200 Rayonet reaction chamber equipped with 16 Hg-quartz iodine lamps (2537 Å) from *Southern New England Ultraviolet Company*. The continuous flow system during the photoreaction was produced by a STEPDOS 03 RC membrane-metering pump from *KNF*. Column chromatography was carried out on silica gel 60A (particle size: 40-60 µm) from *Acros Organics*. Solvents in the p.a. quality from *Lach-Ner* and *Penta* were used for elution. Mixtures of solvents are each stated as volume fractions. For flash column chromatography a Combi*Flash*® Rf+ from *Teledyne ISCO* was used. Thin-layer chromatography was performed on aluminum sheets from *Merck* (silica gel 60 F254, 20 × 20 cm). Chromatograms were visualized by UV light (λ = 254 nm/ 366 nm) or by staining with $KMnO_4$ solution. $^{1}H$- and $^{13}C$-NMR spectra were measured on a Bruker Avance III™ HD 400 MHz NMR system equipped with Prodigy cryo-probe or on a Bruker Avance III™ HD 500 MHz Cryo. $CDCl_3$ and DMSO-$d_6$ from *Sigma Aldrich* or *Eurisotop* were used as solvents. Chemical shifts δ are quoted in ppm in relation to the chemical shift of the residual non-deuterated solvent peak ($CDCl_3$: $\delta(^{1}H) = 7.26$, $\delta(^{13}C) = 77.2$; DMSO-$d_6$: $\delta(^{1}H) = 2.50$, $\delta(^{13}C) = 39.5$). High-resolution mass spectra were recorded on an *Agilent* 5975C MSD Quadrupol, Q-Tof micro from *Waters* or LTQ Orbitrap XL from *Thermo Fisher Scientific*. HPLC-MS measurements were performed on an LCMS-2020 system from *Shimadzu* equipped either with a Luna® C18(2) column (3µm, 100A, 100 × 4.6 mm) or a Kinetex® C18 column (2.6µm, 100A, 100 × 4.6 mm). UV/VIS spectroscopy was performed on a Cary 60 UV/Vis spectrophotometer from *Agilent Technologies* equipped with an SFA-20 rapid kinetics accessory from *Hi-Tech Scientific* for stopped flow kinetic measurements. Data from kinetic experiments were processed using OriginPro 9.1 software. Fluorescence measurements were performed on an LD-45 fluorescence spectrometer from *Perkin Elmer* equipped with a single cuvette reader. Click-labeling experiments on peptides were monitored on an M205 FA fluorescence stereomicroscope from *Leica* equipped with *p*E-300$^{white}$ LED light source and DFC3000 G grayscale camera. SDS-PAGE was performed on a Mini-PROTEAN Tetra Cell electrophoresis system from *Bio-Rad*. PageRuler$^{TM}$ Prestained Protein Ladder (10-180 kDa) from *Thermo Fisher Scientific* was used as a size standard in SDS-PAGE and colloidal coomassie (PageBlue$^{TM}$) from *Thermo Fisher Scientific* was used for staining the gels. Fluorescence imaging of the gels was performed either on a Typhoon FLA 9500 biomolecular imager (using blue LD laser, 473 nm) from *GE Healthcare* or on a G:BOX F3 gel doc system equipped with an UV transilluminator (302 nm) (using an orange emission filter, 572-625 nm) from *SynGene*.

## Synthetic procedures

The following compounds were prepared according to literature procedures.

**_trans_-Cyclooct-4-enol**[1]

**((2s,3a*R*,9a*S*,*E*)-3a,4,5,8,9,9a-Hexahydrocycloocta[*d*][1,3]dioxol-2-yl)methanol**[2]

**(*rel*-1*R*,8*S*,9*R*,4*E*)-Bicyclo[6.1.0]non-4-ene-9-yl-methanol**[3]

**(*E*)-3-Phenyl-6-styryl-1,2,4,5-tetrazine**[4]

**(*E*)-3-(4-Methoxystyryl)-6-phenyl-1,2,4,5-tetrazine**[5]

**(*E*)-3-Phenyl-6-(4-(trifluoromethyl)styryl)-1,2,4,5-tetrazine**[5]

**(*E*)-3-(Pyridin-4-yl)-6-styryl-1,2,4,5-tetrazine**[5]

**4-(6-(4-Methoxyphenyl)-1,2,4-triazin-3-yl)-1-methylpyridinium iodide**[6]

**6-(4-Nitrophenyl)-1,2,4-triazine**[6]

**4-Oxo-4-((6-(6-(pyridin-2-yl)-1,2,4,5-tetrazin-3-yl)pyridin-3-yl)amino)butanoic acid**[7]

**Cyclooctene monoepoxide (6)**[8]

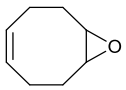


77% *m*-chloroperbenzoic acid (9.81 g, 46.2 mmol) was added in portions to a solution of 1,5-cyclooctadiene (5.00 g, 46.2 mmol) in DCM (100 mL) cooled in a water bath. After 19 h of stirring at room temperature the mixture was filtered and the filtrate was washed with sat. aq. $NaHCO_3$ (2 × 60 mL) and brine (100 mL), dried over $Na_2SO_4$ and concentrated *in vacuo*. The crude product was purified by silica gel column chromatography (PE/EtOAc 9:1) to provide **6** as colorless oil (3.55 g, 62%).
Analytical data matched with literature.[9]

**(*Z*)-8-Azidocyclooct-4-en-1-ol (7)**

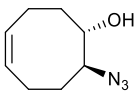


$NaN_3$ (4.45 g, 68.4 mmol) was added to a solution of epoxide **6** (1.70 g, 13.7 mmol) in $H_2O$ (100 mL). The reaction mixture was heated at 90 °C for 17 h and was afterwards extracted

with EtOAc (2 × 300 mL). The combined organic layers were washed with brine (150 mL), dried over $Na_2SO_4$ and concentrated *in vacuo*. Purification by silica gel column chromatography (PE/EtOAc 4:1) provided **7** as slightly yellow oil (1.62 g, 71%).
$^1$H NMR (401 MHz, $CDCl_3$): δ 5.69–5.63 (m, 1H), 5.60–5.53 (m, 1H), 3.78–3.66 (m, 2H), 2.55–2.39 (m, 2H), 2.27–2.11 (m, 4H), 1.82–1.67 (m, 2H).
$^{13}$C NMR (101 MHz, $CDCl_3$): δ 130.6, 127.6, 73.2, 67.0, 32.5, 29.8, 23.7, 23.2.
IR ($CHCl_3$, $cm^{-1}$): $\tilde{\nu}$ 3572 (m, OH), 3342 (w, 6r, OH), 1653 (w, C=C), 1054 (m, C-OH). $\tilde{\nu}_{as}$ = 3070 (vw, sh, =CH), 2938 (s, $CH_2$), 2104 (vs, -$N_3$). $\tilde{\nu}_s$ = 2865 (m, $CH_2$), 1259 (s, -$N_3$). β = 1409 (w, sh, =CH), 663 (m, -$N_3$). $\beta_s$ = 1482 (m, $CH_2$), 1468 (w, $CH_2$), 1448 (w, $CH_2$), 1430 (w, $CH_2$). γ = 559 (w, -$N_3$).

**(1*R*,8*S*,*Z*)-9-Azabicyclo[6.1.0]non-4-ene (8)**

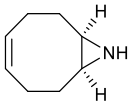


Triphenylphosphine (3.05 g, 11.6 mmol) was added to a solution of **7** (1.62 g, 9.69 mmol) in anhydrous THF (75 mL) under argon and the mixture was heated at 75 °C for 17 h. After concentration *in vacuo* the crude product was purified by silica gel column chromatography (PE/EtOAc/MeOH 1:4:0.1 (to remove triphenylphosphine oxide) → DCM/MeOH 10:1) to provide **8** as yellow oil (779 mg, 65%). The compound is slightly volatile and care should be taken especially during concentration of solutions under reduced pressure.
Analytical data matched with literature.[10]

**2-(Trimethylsilyl)ethyl-(1*R*,8*S*,*Z*)-9-azabicyclo[6.1.0]non-4-ene-9-carboxylate (9)**

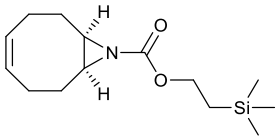


To a solution of **8** (600 mg, 4.87 mmol) in anhydrous DCM (30 mL) was added $NEt_3$ (1.70 mL, 12.2 mmol) followed by 1-[2-(trimethylsilyl)ethoxycarbonyloxy]pyrrolidin-2,5-dione (1.26 g, 4.87 mmol) under argon at 0 °C. The solution was stirred at room temperature under argon for 1 h. The crude product was diluted with DCM (100 mL), washed with $H_2O$ (70 mL) and brine (70 mL), dried over $Na_2SO_4$ and concentrated *in vacuo*. Purification by silica gel column chromatography (PE/$Et_2O$ 4:1) provided **9** as colorless oil (834 mg, 64%).
$^1$H NMR (401 MHz, $CDCl_3$): δ 5.57 (t, *J* = 3.9 Hz, 2H), 4.20–4.15 (m, 2H), 2.54–2.49 (m, 2H), 2.44–2.35 (m, 2H), 2.18–2.11 (m, 2H), 2.05–1.93 (m, 4H), 1.03–0.97 (m, 2H), 0.04 (s, 9H).
$^{13}$C NMR (101 MHz, $CDCl_3$): δ 164.7, 129.3, 64.7, 42.1, 28.4, 24.2, 17.6, -1.3.
HRMS (ESI): m/z calcd. for $C_{14}H_{25}NNaO_2Si$ $[M+Na]^+$ 290.1547, found 290.1548.

**2-(Trimethylsilyl)ethyl (1*R*,8*S*,*E*)-9-azabicyclo[6.1.0]non-4-ene-9-carboxylate (10)**

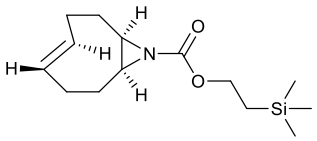

*Cis*-isomer **9** (834 mg, 3.12 mmol) and methyl benzoate (1.00 mL, 8.11 mmol) were dissolved in hexane/$Et_2O$ 4:1 (350 mL) and placed into a quartz-glass flask under argon and the mixture was irradiated in the UV reactor (254 nm, 6/10 lamps) for 7 h. During irradiation the reaction mixture was pumped through a silica gel column (10 w/w% $AgNO_3$ in silica on a thin layer of pure silica) via a continuous flow system with a flow rate of 50 mL/min. Flow system and column were then washed with $Et_2O$ (100 mL) and the column dried with compressed air. The dried silica was suspended in aq. $NH_4OH$ (50 mL) and extracted with $Et_2O$ (5 × 50 mL). The combined organic layers were washed with brine (80 mL), dried over $Na_2SO_4$ and concentrated *in vacuo*. The crude *trans*-isomer was purified by silica gel column chromatography (PE/$Et_2O$ 4:1) to provide **10** as colorless oil (577 mg, 69%).

$^1$H NMR (401 MHz, $CDCl_3$): δ 5.78–5.70 (m, 1H), 5.30–5.22 (dddd, *J* = 16.8, 10.5, 3.8, 1.1 Hz, 1H), 4.18–4.13 (m, 2H), 2.53–2.40 (m, 2H), 2.35–2.25 (m, 3H), 2.21–2.15 (ddd, *J* = 10.4, 6.3, 5.0 Hz, 1H), 2.11–1.96 (m, 2H), 1.18–1.10 (m, 1H), 1.02–0.96 (m, 2H), 0.95–0.85 (dddd, *J* = 14.1, 13.2, 10.4, 2.6 Hz, 1H), 0.03 (s, 9H).

$^{13}$C NMR (101 MHz, $CDCl_3$): δ 164.3, 137.3, 132.3, 64.8, 41.0, 40.3, 38.9, 31.9, 31.0, 25.8, 17.6, -1.3.

HRMS (ESI): m/z calcd. for $C_{14}H_{25}NNaO_2Si$ $[M+Na]^+$ 290.1547, found 290.1548.

**2-((1*R*,8*S*,*E*)-9-Azabicyclo[6.1.0]non-4-en-9-yl)ethan-1-ol (1a)**

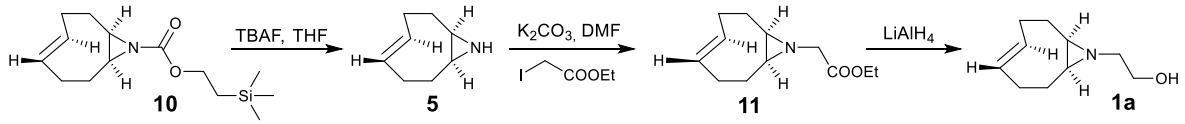


The following steps are best performed without isolation of intermediates in the reaction sequence as described below to prevent losses during work with volatile intermediates such as **5**.

Tetrabutylammonium fluoride (1 M in THF, 3.55 mL, 3.55 mmol) was added dropwise to a solution of **10** (475 mg, 1.78 mmol) in anhydrous THF (10 mL) under argon at 0 °C. The solution was shaded from light with aluminum foil and stirred under argon at 0 °C for 10 min and afterwards at room temperature for 2 h. The reaction mixture was diluted with $H_2O$ (10 mL) and the aqueous layer was extracted with $Et_2O$ (3 × 30 mL). The combined organic layers were dried over $Na_2SO_4$ and concentrated *in vacuo* (just partly at 910 mbar at 40–45 °C, to prevent evaporation of the volatile free aziridine **5**).

The partly concentrated solution of **5** was dissolved in anhydrous DMF (2 mL) and $K_2CO_3$ (368 mg, 2.66 mmol) was added. After the solution was stirred under argon at room temperature for 5 min, ethyl iodoacetate (252 µL, 2.13 mmol) was added and the reaction

mixture was stirred under argon at room temperature for another 30 min (TLC in DCM/MeOH 9:1). The mixture was diluted with $Et_2O$ (40 mL) and $H_2O$ (10 mL) and the aqueous layer was extracted with $Et_2O$ (3 × 40 mL). The combined organic layers were washed with brine (15 mL), dried over $Na_2SO_4$ and concentrated *in vacuo* (again just partly, not till dryness to prevent evaporation of the volatile ethyl ester **11**).

For the last step, $LiAlH_4$ (2.4 M in THF, 740 µL, 1.78 mmol) was added dropwise to the ethyl ester **11** dissolved in anhydrous THF (5 mL) under argon at 0 °C. The reaction mixture was stirred under these conditions for 30 min, quenched with sat. aq. $NH_4Cl$ (5 mL) at 0 °C, diluted with $Et_2O$ (40 mL) and filtered through celite. The filtrate was washed with brine (20 mL), dried over $Na_2SO_4$ and concentrated *in vacuo* (**1a** is not volatile). The crude product was purified by silica gel column chromatography (DCM/MeOH 20:1 → 9:1) to provide **1a** as yellow oil (205 mg, 69%).

To confirm the 'half-chair' conformation of **1a** the NMR spectra were measured at room temperature on spectrometers operating at 600.1 MHz for $^1H$ and at 150.9 MHz for $^{13}C$ or at 850.3 MHz for $^1H$ in $CDCl_3$ (2 mg of the compound were dissolved in 0.6 mL of the solvent). A combination of 1D and 2D experiments (COSY, HSQC, HMBC) was used for the assignment of all of the $^1H$ and $^{13}C$ resonances of compound **1a**.

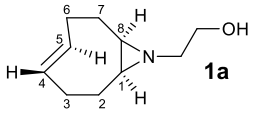

**1a**

$^1H$ NMR (850.3 MHz, $CDCl_3$): δ = 0.81 (dddd, 1H, $J_{gem}$ = 14.0, $J_{2en,3ex}$ = 13.3, $J_{2en,1}$ = 10.5, $J_{2en,3en}$ = 2.5, H-2endo), 1.07 (dtd, 1H, $J_{gem}$ = 12.3, $J_{7en,6ex}$ = $J_{7en,8}$ = 11.8, $J_{7en,6en}$ = 7.4, H-7endo), 1.19 (ddd, 1H, $J_{1,2en}$ = 10.4, $J_{1,8}$ = 6.5, $J_{1,2ex}$ = 5.0, H-1), 1.30 (ddd, 1H, $J_{8,7en}$ = 11.8, $J_{8,1}$ = 6.5, $J_{8,7ex}$ = 3.6, H-8), 1.98 (dddd, 1H, $J_{gem}$ = 13.0, $J_{6ex,7en}$ = 11.7, $J_{6ex,5}$ = 6.3, $J_{6ex,7ex}$ = 5.0, H-6exo), 2.02 (ddddd, 1H, $J_{gem}$ = 12.0, $J_{3ex,2en}$ = 13.3, $J_{3ex,4}$ = 10.5, $J_{3ex,2ex}$ = 2.2, $J_{l.r.}$ = 0.7, H-3exo), 2.27–2.31 (m, 2H, H-3endo and H-6endo), 2.34 (dm, 1H, $J_{gem}$ = 12.4, H-7exo), 2.37 (t, 1H, $J_{OH,CH2}$ = 5.9, OH), 2.41 (dm, 1H, $J_{gem}$ = 14.0, H-2exo), 2.48–2.54 (m, 2H, N-$CH_2$), 3.69–3.73 (m, 2H, O$CH_2$), 5.21 (dddd, 1H, $J_{4,5}$ = 16.8, $J_{4,3ex}$ = 10.5, $J_{4,3en}$ = 3.8, $J_{l.r.}$ = 1.2, H-4), 5.78 (ddd, 1H, $J_{5,4}$ = 16.8, $J_{5,6en}$ = 9.5, $J_{5,6ex}$ = 6.2, H-5).

$^{13}C$ NMR (150.9 MHz, $CDCl_3$): δ = 26.1 (C-6), 31.4 (C-3), 32.2 (C-2), 39.3 (C-7), 42.2 (C-8), 42.9 (C-1), 62.1 (O$CH_2$), 63.2 (N$CH_2$), 131.5 (C-4), 137.7 (C-5).

HRMS (ESI): m/z calcd. for $C_{10}H_{16}NO$ $[MH]^+$ 166.1232, found 166.1233.

**<u>Methyl 4-(((1*R*,8*S*,*E*)-9-azabicyclo[6.1.0]non-4-en-9-yl)methyl)benzoate</u> (14)**

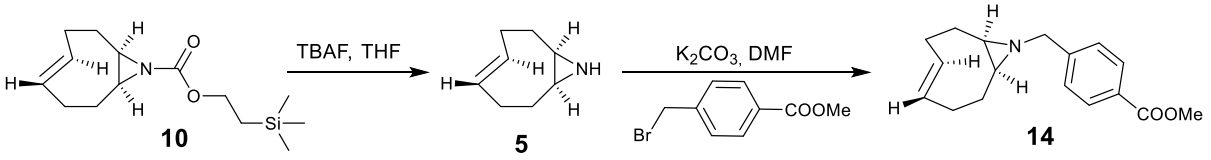


The following steps are best performed without isolation of intermediate **5** similarly as described for product **1a** synthesis above.

Tetrabutylammonium fluoride (1 M in THF, 1.50 mL, 1.50 mmol) was added dropwise to a solution of **10** (200 mg, 0.748 mmol) in anhydrous $Et_2O$ (5 mL) under argon at 0 °C. The

mixture was stirred in the dark under argon at room temperature for 4 h and it was then diluted with $Et_2O$ (30 mL) and $H_2O$ (10 mL). After extraction of the aqueous layer with $Et_2O$ (3 × 30 mL), the combined organic layers were washed with brine (10 mL), dried over $Na_2SO_4$ and concentrated *in vacuo* (910 mbar at 40-45 °C, to prevent evaporation of the volatile free aziridine **5**).

The partly concentrated solution of **5** was dissolved in anhydrous DMF (3 mL). $K_2CO_3$ (207 mg, 1.50 mmol) was added and the solution was stirred under argon at room temperature for 5 min. Then, methyl 4-(bromomethyl)benzoate (206 mg, 0.897 mmol) was added and the reaction mixture was stirred in the dark under argon at room temperature for 1.5 h. The solution was diluted with EtOAc (50 mL) and $H_2O$ (10 mL) and the aqueous layer was extracted once more with EtOAc (50 mL). The combined organic layers were washed with brine (20 mL), dried over $Na_2SO_4$ and concentrated *in vacuo*. The crude product was purified by silica gel column chromatography (PE → PE/$Et_2O$ 2:1) to provide the aza-TCO **14** as slightly yellow-green oil (138 mg, 68%).

$^1$H NMR (401 MHz, $CDCl_3$): δ 7.98 (d, *J* = 7.9 Hz, 2H), 7.39 (d, *J* = 7.9 Hz, 2H), 5.78 (ddd, *J* = 16.3, 9.5, 6.3 Hz, 1H), 5.21 (ddd, *J* = 16.7, 10.5, 3.7 Hz, 1H), 3.90 (s, 3H), 3.64–3.53 (m, 2H), 2.41–2.25 (m, 4H), 2.05–1.92 (m, 2H), 1.39–1.34 (m, 1H), 1.24 (dt, *J* = 11.1, 5.7 Hz, 1H), 1.13 (qd, *J* = 11.9, 7.4 Hz, 1H), 0.92–0.82 (m, 1H).

$^{13}$C NMR (101 MHz, $CDCl_3$): δ 167.2, 145.1, 137.8, 131.7, 129.8, 128.8, 127.7, 65.1, 52.2, 43.5, 42.8, 39.4, 32.2, 31.6, 26.3.

HRMS (ESI): m/z calcd. for $C_{17}H_{21}NO_2$ $[MH]^+$ 271.1572, found 271.1574.

**(4-(((1*R*,8*S*,*E*)-9-Azabicyclo[6.1.0]non-4-en-9-yl)methyl)phenyl)methanol (15)**

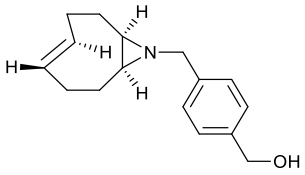


$LiAlH_4$ (2.4 M in THF, 135 µL, 0.324 mmol) was added dropwise to a solution of **14** (80 mg, 0.295 mmol) in anhydrous THF (3 mL) under argon at 0 °C. The reaction mixture was stirred in the dark under argon at 0 °C for 1.5 h, quenched with sat. aq. $NH_4Cl$ (5 mL) at 0 °C, diluted with $Et_2O$ (50 mL) and filtered through celite. The filtrate was washed with brine (30 mL), dried over $Na_2SO_4$ and concentrated *in vacuo*. The product **15** was isolated as yellowish oil (67 mg, 93%) after silica gel column chromatography (DCM/MeOH 10:1).

$^1$H NMR (401 MHz, $CDCl_3$): δ 7.26 (s, 4H), 5.77 (ddd, *J* = 16.2, 9.5, 6.2 Hz, 1H), 5.20 (dddd, *J* = 16.8, 10.5, 3.8, 1.1 Hz, 1H), 4.62 (s, 2H), 3.57–3.46 (m, 2H), 2.40–2.23 (m, 4H), 2.01–1.90 (m, 2H), 1.41–1.35 (m, 1H), 1.27 (s, 1H), 1.14–1.07 (m, 1H), 0.92–0.86 (m, 1H).

$^{13}$C NMR (101 MHz, $CDCl_3$): δ 139.9, 138.7, 137.7, 131.8, 128.1, 127.1, 64.98, 64.95, 43.4, 42.8, 39.2, 32.0, 31.6, 26.2.

HRMS (EI+): m/z calcd. for $C_{16}H_{21}NO$ $[MH]^+$ 243.1623, found 243.1624.

**Synthesis of compound (1b)**

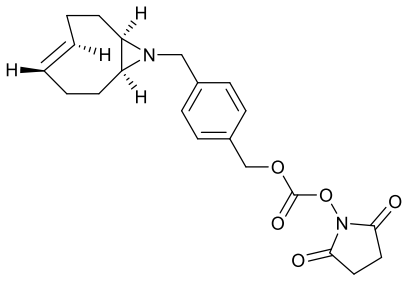

To a solution of **15** (67 mg, 0.275 mmol) in anhydrous $CH_3CN$ (3 mL) was added $NEt_3$ (153 µL, 1.10 mmol) followed by *N*,*N*′-disuccinimidyl carbonate (141 mg, 0.551 mmol) at 0 °C. The flask was purged with argon and the solution was stirred at room temperature for 1 h. For purification, the reaction mixture was loaded directly on a silica gel column (DCM → DCM/EtOAc 2:3 → 1:4) to provide **1b** as slightly yellow oil (66 mg, 62%).

$^1$H NMR (401 MHz, $CDCl_3$): δ 7.35 (s, 4H), 5.78 (ddd, *J* = 16.2, 9.4, 6.2 Hz, 1H), 5.29 (s, 2H), 5.22 (dddd, *J* = 16.9, 10.5, 3.8, 1.1 Hz, 1H), 3.62–3.50 (m, 2H), 2.83 (s, 4H), 2.42–2.25 (m, 4H), 2.05–1.93 (m, 2H), 1.42–1.37 (m, 1H), 1.29–1.27 (m, 1H), 1.18–1.11 (m, 1H), 0.88–0.86 (m, 1H).

$^{13}$C NMR (101 MHz, $CDCl_3$): δ 168.7, 151.7, 137.8, 131.9, 131.8, 128.9, 128.3, 127.2, 72.9, 64.9, 43.5, 42.8, 39.3, 32.1, 31.6, 26.3, 25.6.

HRMS (ESI): m/z calcd. for $C_{21}H_{25}N_2O_5$ $[MH]^+$ 385.1758, found 385.1759.

**Synthesis of compound (1c)**

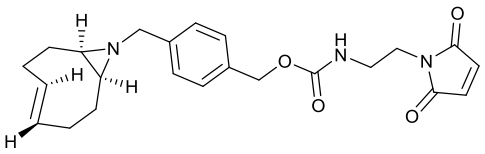

To a solution of the active ester **1b** (20 mg, 0.0520 mmol) in anhydrous DMF (1 mL) was added $NEt_3$ (21.8 µL, 0.156 mmol) followed by *N*-(2-aminoethyl)maleimide hydrochloride (10.1 mg, 0.0572 mmol) at 0 °C. The flask was purged with argon and the solution was stirred at room temperature for 1.5 h. For purification, the reaction mixture was loaded directly on a silica gel column (DCM → DCM/EtOAc 2:3 → DCM/EtOAc/MeOH 2:3:0.1) to provide **1c** as yellowish oil (9 mg, 42%).

$^1$H NMR (401 MHz, $CDCl_3$): δ 7.31–7.28 (m, 4H), 6.67 (s, 2H), 5.78 (ddd, *J* = 16.3, 9.5, 6.2 Hz, 1H), 5.21 (dddd, *J* = 16.8, 10.5, 3.8, 1.1 Hz, 1H), 5.04 (s, 2H), 3.68 (dd, *J* = 6.6, 4.6 Hz, 2H), 3.60–3.49 (m, 2H), 3.41 (q, *J* = 5.8 Hz, 2H), 2.37–2.24 (m, 4H), 2.04–1.91 (m, 2H), 1.41–1.35 (m, 1H), 1.28 (s, 1H), 1.16–1.09 (m, 1H), 0.88–0.83 (m, 1H).

$^{13}$C NMR (101 MHz, $CDCl_3$): δ 170.9, 156.6, 137.8, 134.3, 131.8, 128.3, 128.1, 66.8, 65.0, 43.5, 42.8, 40.2, 39.3, 37.9, 32.1, 31.6, 26.3, (2×CH=**C**($CH_2$)-CH not observed).

HRMS (ESI): m/z calcd. for $C_{23}H_{28}N_3O_4$ $[MH]^+$ 410.2074, found 410.2075.

**Synthesis of D-amino acid (1f)**

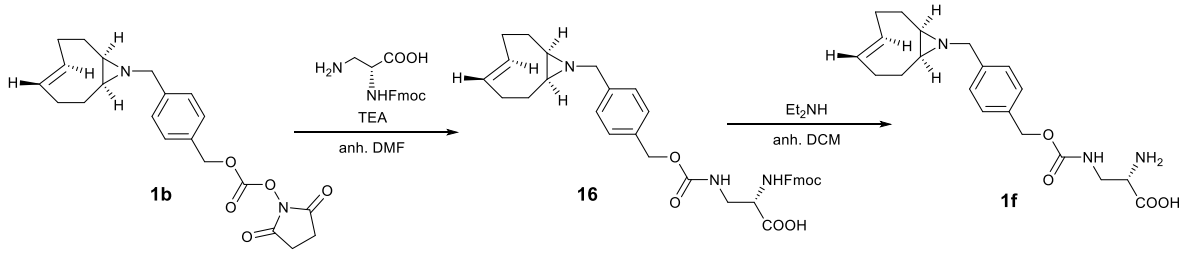


To a stirred solution of **1b** (146 mg, 0.380 mmol) in anhydrous DMF (7 mL) at 0°C under argon was added the Fmoc protected amino acid (161 mg, 0.494 mmol, 1.3 equiv.) (for synthesis see: *J. Org. Chem.* **1997**, *62*, 6918 and *Synlett* **2011**, 1917) followed by TEA (132 µL, 0.949 mmol, 2.5 equiv.). Then, the flask was left to heat up to RT and the solvent was evaporated after 3 h (formation of the product was verified by HPLC-MS). During the process the flask was kept in the dark. The crude product was separated by silica gel column chromatography (DCM/MeOH 10:1 + methanol contains 1% HCOOH; $R_f$ = 0.22). We obtained 225 mg (>99%) of **16** as a very viscous colorless oil which was directly used in the next step.

Compound **16** (265 mg, 0.445 mmol) was dissolved in anhydrous DCM (20 mL) and diethylamine (1 mL) was added at room temperature under argon. There was no starting material after 10 h and the solvent was evaporated (verified by HPLC-MS). The crude mixture was separated by flash chromatography on reverse phase silica. Since the product is UV-inactive, we performed small scale reactions (<100 µL) with commercially available 3,6-di-2-pyridyl-1,2,4,5-tetrazine from each fraction obtained after purification. By this way, we were easily able to distinguish between those containing the product and those, which do not (starting material – red-purple, product – yellow). Flash chromatography had to be repeated two more times to get reasonably pure product **1f** (48 mg, 29%) as a white powder after lyophilization.

$^1$H NMR (600.1 MHz, DMSO-$d_6$): δ 8.21 (s, NH), 7.30–7.26 (m, 4H), 5.76–5.69 (m, 1H), 5.18–5.10 (m, 1H), 5.01–4.97 (m, 2H), 3.48–3.39 (m, 3H), 3.32–3.29 (m, 1H), 3.28–3.23 (m, 1H), 2.28–2.22 (m, 1H), 2.20–2.12 (m, 3H), 1.98–1.87 (m, 2H), 1.36–1.30 (m, 1H), 1.24–1.18 (m, 1H), 1.03–0.96 (m, 1H), 0.76–0.68 (m, 1H).

$^{13}$C NMR (150.9 MHz, DMSO-$d_6$): δ 168.2, 156.2, 139.7, 137.5, 135.2, 131.3, 127.7, 127.6, 65.4, 63.9, 54.1, 42.3, 41.8, 41.5, 38.9, 31.7, 31.1, 25.8.

HRMS (ESI): m/z calcd. for $C_{20}H_{28}N_3O_4$ [$MH^+$] 374.2074, found 374.2081

**Synthesis of compound (12f)**

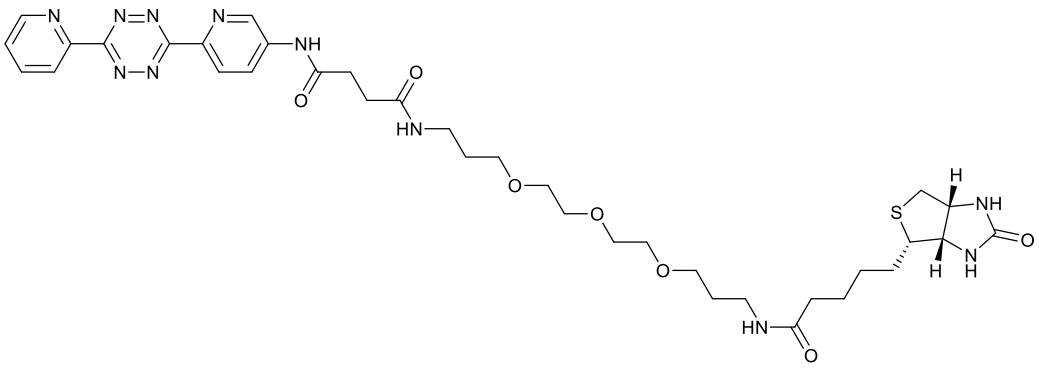

To a solution of 4-oxo-4-((6-(6-(pyridin-2-yl)-1,2,4,5-tetrazin-3-yl)pyridin-3-yl)amino)butanoic acid (300 mg, 0.854 mmol) and *N*-Boc-4,7,10-trioxa-1,13-tridecanediamine (342 mg, 1.07 mmol) in anhydrous DMF (10 mL) was under argon at 0 °C added HATU (406 mg, 1.07 mmol) followed by DIPEA (446 µL, 0.0793 mmol). The solution was stirred under argon at room temperature for 1 h, concentrated *in vacuo* and purified by silica gel column chromatography (DCM/MeOH 10:1) to provide the Boc-protected intermediate as colorless oil (530 mg, 80%) which was used directly in the next step.

Deprotection of the Boc-protected intermediate (150 mg, 0.229 mmol) was carried out in DCM (5 mL) by adding dropwise TFA (0.25 mL) and stirring the mixture at room temperature for 1 h. The deprotected intermediate was concentrated *in vacuo*, dried under high vacuum and used in the next step.

The deprotected intermediate was dissolved together with biotin (56.1 mg, 0.229 mmol) in anhydrous DMF (2.5 mL). Then HATU (96.0 mg, 0.252 mmol) and DIPEA (200 µL, 1.15 mmol) were added under argon at 5 °C and the solution was stirred at room temperature for 20 h. MeOH was added and the mixture was concentrated *in vacuo* and dried under high vacuum. The crude product was purified by silica gel column chromatography (DCM/MeOH 5:1). Remaining impurities were removed by reverse phase flash column chromatography ($CH_3CN/H_2O$ mixture) to provide **12f** as red semisolid (85 mg, 45%).

$^1$H NMR (401 MHz, DMSO-$d_6$): δ 10.63 (s, 1H), 9.05 (dd, $J$ = 2.6, 0.7 Hz, 1H), 8.93 (ddd, $J$ = 4.7, 1.8, 0.9 Hz, 1H), 8.62 (dd, $J$ = 8.7, 0.6 Hz, 1H), 8.59 (dt, $J$ = 8.0, 1.1 Hz, 1H), 8.41 (dd, $J$ = 8.7, 2.5 Hz, 1H), 8.15 (td, $J$ = 7.8, 1.8 Hz, 1H), 7.90 (t, $J$ = 5.6 Hz, 1H), 7.75–7.69 (m, 2H), 6.42–6.35 (m, 2H), 4.30 (ddt, $J$ = 7.6, 5.2, 1.1 Hz, 1H), 4.12 (ddd, $J$ = 7.5, 4.4, 2.0 Hz, 1H), 3.52–3.45 (m, 8H), 3.39 (dt, $J$ = 8.6, 6.4 Hz, 4H), 3.12–3.03 (m, 5H), 2.81 (dd, $J$ = 12.4, 5.1 Hz, 1H), 2.67 (t, $J$ = 7.0 Hz, 2H), 2.57 (d, $J$ = 12.4 Hz, 1H), 2.46 (t, $J$ = 7.0 Hz, 2H), 2.04 (t, $J$ = 7.4 Hz, 2H), 1.64–1.57 (m, 4H), 1.52–1.42 (m, 2H), 1.35–1.22 (m, 4H).

$^{13}$C NMR (101 MHz, DMSO-$d_6$): δ 171.9, 171.8, 170.9, 163.0, 162.8, 162.7, 150.6, 150.2, 143.7, 141.2, 138.6, 137.8, 126.6, 126.0, 124.9, 124.2, 69.8, 69.5, 68.10, 68.06, 61.1, 59.2, 55.4, 40.1, 35.9, 35.7, 35.2, 31.7, 30.0, 29.41, 29.39, 28.2, 28.0, 25.3.

HRMS (ESI): m/z calcd. for $C_{36}H_{50}N_{11}O_7S$ $[MH]^+$ 780.3610, found 780.3613 and m/z calcd. for $C_{36}H_{49}NaN_{11}O_7S$ $[M+Na]^+$ 802.3429, found 802.3432.

**Synthesis of compound (12g)**

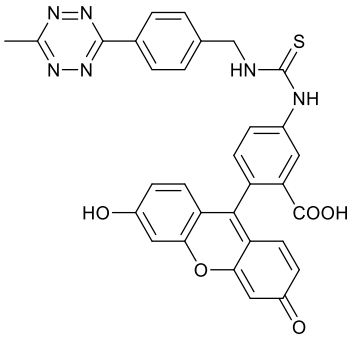

To a solution of 6-methyl-3-benzyl-tetrazine-amine (TFA salt, 10 mg, 0.0317 mmol) in anhydrous DMF (2.5 mL) was added DIPEA (13.8 µL, 0.0793 mmol) followed by fluorescein-5-isothiocyanate (12.4 mg, 0.0317 mmol). The reaction mixture was stirred in the dark at room temperature until the starting materials disappeared (TLC in DCM/MeOH 9:1) and then concentrated *in vacuo*. The crude product was purified by silica gel column chromatography (EtOAc → EtOAc/MeOH 20:1) to provide **12g** as red viscous oil which was re-dissolved in $CH_3CN/H_2O$ and lyophilized to give the title compound as red-orange solid (16 mg, 85%).

The formation of the product was verified by HPLC-MS (Figure S1) and HRMS.

HRMS (ESI): m/z calcd. for $C_{31}H_{23}N_6O_5S$ $[MH]^+$ 591.1445, found 591.1446.

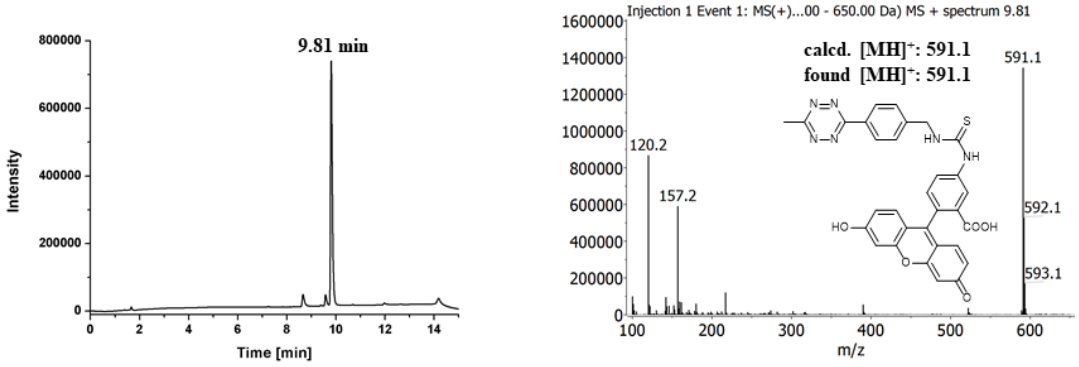


**Figure S1.** Exported HPLC-MS chromatograms of **12g** after purification (conditions used: solvent A: $H_2O$ + 0.05% HCOOH; solvent B: $CH_3CN$ + 0.05% HCOOH; gradient: 5% B → 95% B in 9 min, then 95% B for 2 min and back to 5% B). The product eluates at 9.81 min (on a Luna® C18(2) column (3µm, 100A, 100 × 4.6 mm) at 1 mL/min flow rate).

**Synthesis of compound (12h)**

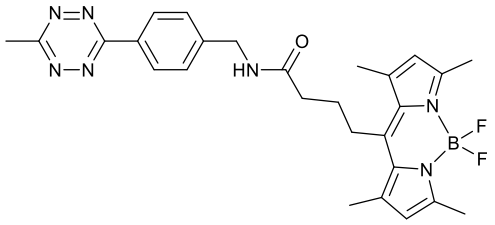

To a solution of 6-methyl-3-benzyl-tetrazine-amine (TFA salt, 22 mg, 0.070 mmol) in anhydrous DMF (2 mL) was added bodipy NHS active ester (15 mg, 0,035 mmol, for synthesis see: *J. Org. Chem.* **2006**, *71*, 1718) and DIPEA (61 µL, 0.351 mmol, 5 equiv.) at 0°C. The reaction mixture was stirred in the dark at room temperature until the starting materials disappeared (ca. 2 hours, verified by TLC in AcOEt/Hex/DCM 3:1:1). The reaction mixture was diluted with AcOEt (50 mL), washed with $H_2O$ and brine. The organic phase was dried over $MgSO_4$ and concentrated *in vacuo*. The crude product was purified by silica gel column chromatography (AcOEt/Hex/DCM 3:1:1) to provide **12h** as orange solid (10 mg, 56%).
HRMS (ESI): m/z calcd. for $C_{27}H_{30}N_7OBF_2$ $[M+Na]^+$ 540.2465, found 540.2466.

## Computational methods

**For aza-TCO**

Molecular modelling studies were performed using Hyperchem 8 (Hypercube) software.[11] The conjugate gradient method for energy minimizations was used to convergence (less than 0.01 kcal $Å^{-1}$ $mol^{-1}$ RMS force). Force field MM+ was used for all computations. General protocol for obtaining lowest-energy conformers by simulated annealing: optimized starting structure was subjected to dynamic run - 0.5 ps heating from 300 to 1000 °C, 0.7 ps equilibration and 1 ps cooling to 200 °C followed by energy minimization. Every next run started from the previously minimized structure. A set of 100 structures was so obtained for each compound.
The lowest-energy conformations and other conformations important for the proposed reactions were subjected to geometry optimization at DFT level using B3LYP functional,[12] standard 6-31+G(d,p) basis set and polarizable continuum model used for implicit acetonitrile solvation.[13] The Gaussian16 program package was used throughout this study.[14] The QST3 optimization method[15] was applied in the search for the transition state structures of the reaction, that is the structures of the reactant, product and estimated transition state were used as input for the TS search. The vibrational frequencies and free energies were calculated for all of the optimized structures and the stationary-point character (a minimum or a first-order saddle point) was thus confirmed.

**Formation of the fluorescent product with the dioxolane-fused TCO (d-TCO)**

For a comparison with current calculations of the energy barrier of formation of the 1,4-dihydropyridazine fluorophore in compound **1a** and with previous calculations for ax-TCO-ol, we performed the conformational analysis and transition-state search also for the dioxolane fused TCO (d-TCO) derivative (derivatives without the hydroxymethyl group in **1a** were used in these experiment to simplify the calculations as shown below). The conformational analysis revealed several low-energy conformers with short distances between the bridgehead hydrogen and dioxolane oxygen. However, the shortest distance (2.3 Å) was longer than that found in ax-TCO-ol (2.0 Å) and the transition state for the hydrogen migration in d-TCO (28 kcal/mol) was much more energetically demanding than that found for ax-TCO-ol derivative (15 kcal/mol) or **1a-II** (10 kcal/mol).

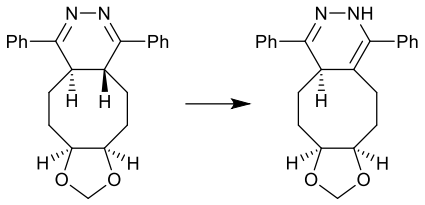

## Cartesian coordinates of ground-state and transition-state structures

**Table S1.** Atomic numbers, Cartesian coordinates (Å), electronic and free energies (a.u.) of the reactant, transition state and product of the IEDDA of compound **1a** with diphenyl-*s*-tetrazine.

| | reactant | | | | TS | | | | product | | |
|---|---|---|---|---|---|---|---|---|---|---|---|
| *Z* | *x* | *y* | *z* | *Z* | *x* | *y* | *z* | *Z* | *x* | *y* | *z* |
| 6 | 0.4966 | -0.5544 | 0.1345 | 6 | -0.2994 | -0.7200 | 0.2773 | 6 | -0.6253 | -0.6786 | 0.2379 |
| 6 | 0.3022 | 0.7678 | 0.2489 | 6 | 0.1525 | 0.5955 | 0.2077 | 6 | 0.0476 | 0.7111 | 0.2115 |
| 6 | 0.5289 | 1.4935 | 1.5496 | 6 | 0.7893 | 1.2283 | 1.4271 | 6 | 0.8421 | 1.0706 | 1.4843 |
| 6 | 1.2900 | -1.1050 | -1.0179 | 6 | 0.2344 | -1.7318 | -0.7086 | 6 | 0.0136 | -1.7222 | -0.7045 |
| 1 | 0.5055 | -1.1613 | 1.0422 | 1 | -0.4960 | -1.1156 | 1.2740 | 1 | -0.6154 | -1.0776 | 1.2580 |
| 1 | 0.3632 | 1.3725 | -0.6566 | 1 | 0.5753 | 0.9029 | -0.7466 | 1 | 0.7205 | 0.7679 | -0.6487 |
| 1 | 0.2458 | 2.5493 | 1.4770 | 1 | 1.0561 | 2.2686 | 1.2227 | 1 | 1.2833 | 2.0627 | 1.3433 |
| 1 | -0.0375 | 1.0576 | 2.3809 | 1 | 0.1074 | 1.2204 | 2.2843 | 1 | 0.1627 | 1.1465 | 2.3407 |
| 6 | 2.0590 | 1.3411 | 1.8380 | 6 | 2.0606 | 0.4059 | 1.7873 | 6 | 1.9617 | 0.0664 | 1.8234 |
| 6 | 2.7830 | -0.9020 | -0.6031 | 6 | 1.6559 | -2.1518 | -0.2351 | 6 | 1.3655 | -2.2809 | -0.2165 |
| 1 | 1.1087 | -2.1681 | -1.2062 | 1 | -0.3951 | -2.6243 | -0.7538 | 1 | -0.6737 | -2.5675 | -0.8009 |
| 1 | 1.0767 | -0.5572 | -1.9442 | 1 | 0.2856 | -1.3031 | -1.7163 | 1 | 0.1242 | -1.2943 | -1.7089 |
| 6 | 2.9233 | 1.5568 | 0.5998 | 6 | 2.9203 | 0.0976 | 0.5729 | 6 | 2.8476 | -0.2371 | 0.6336 |
| 6 | 3.2290 | 0.5541 | -0.4915 | 6 | 2.7163 | -1.0673 | -0.3585 | 6 | 2.5459 | -1.3335 | -0.3398 |
| 1 | 2.2408 | 0.3299 | 2.2150 | 1 | 1.7594 | -0.5331 | 2.2621 | 1 | 1.5379 | -0.8662 | 2.2084 |
| 1 | 2.3783 | 2.0387 | 2.6248 | 1 | 2.6550 | 0.9598 | 2.5252 | 1 | 2.5681 | 0.4850 | 2.6362 |
| 1 | 3.4349 | -1.4007 | -1.3341 | 1 | 1.9772 | -3.0141 | -0.8331 | 1 | 1.5927 | -3.1787 | -0.8054 |
| 1 | 2.9577 | -1.4007 | 0.3568 | 1 | 1.6039 | -2.4974 | 0.8030 | 1 | 1.2712 | -2.6162 | 0.8220 |
| 7 | 4.2325 | 0.9193 | 0.5160 | 7 | 3.8233 | -1.0528 | 0.6115 | 7 | 3.6415 | -1.4695 | 0.6348 |
| 1 | 2.8850 | 2.5855 | 0.2239 | 1 | 3.3221 | 0.9883 | 0.0818 | 1 | 3.3417 | 0.6388 | 0.2051 |
| 1 | 3.3637 | 1.0319 | -1.4682 | 1 | 3.0034 | -0.8567 | -1.3922 | 1 | 2.8545 | -1.1350 | -1.3690 |
| 6 | 5.3595 | 1.7465 | 0.0917 | 6 | 5.1743 | -0.8495 | 0.0845 | 6 | 5.0069 | -1.3631 | 0.1156 |
| 6 | 6.5264 | 0.8660 | -0.3388 | 6 | 5.8238 | -2.1928 | -0.2258 | 6 | 5.5338 | -2.7429 | -0.2600 |
| 8 | 7.5856 | 1.7332 | -0.7514 | 8 | 7.1415 | -1.9319 | -0.7275 | 8 | 6.8699 | -2.5769 | -0.7536 |
| 1 | 5.6736 | 2.3675 | 0.9384 | 1 | 5.7654 | -0.3277 | 0.8463 | 1 | 5.6411 | -0.9332 | 0.8998 |
| 1 | 5.0953 | 2.4252 | -0.7384 | 1 | 5.1770 | -0.2253 | -0.8251 | 1 | 5.0691 | -0.6997 | -0.7638 |
| 1 | 6.2137 | 0.2103 | -1.1652 | 1 | 5.2283 | -2.7349 | -0.9730 | 1 | 4.8929 | -3.1936 | -1.0302 |
| 1 | 6.8348 | 0.2322 | 0.5034 | 1 | 5.8693 | -2.8022 | 0.6860 | 1 | 5.5242 | -3.3968 | 0.6215 |
| 1 | 8.3568 | 1.2023 | -0.9844 | 1 | 7.5735 | -2.7757 | -0.9153 | 1 | 7.2236 | -3.4455 | -0.9866 |
| 6 | -2.1092 | -1.7903 | -0.0559 | 6 | -2.4896 | -0.5894 | -0.1238 | 6 | -2.1666 | -0.4595 | -0.0867 |
| 7 | -2.5160 | -1.2070 | 1.0933 | 7 | -2.8269 | 0.2214 | 0.9510 | 7 | -2.6530 | 0.4863 | 0.9578 |
| 7 | -2.9263 | 0.0354 | 1.0422 | 7 | -2.4108 | 1.4363 | 0.9172 | 7 | -2.1139 | 1.6060 | 0.9457 |
| 6 | -2.9379 | 0.6559 | -0.1577 | 6 | -1.6641 | 1.8120 | -0.1862 | 6 | -1.0812 | 1.7842 | -0.0960 |
| 6 | -1.5758 | -3.1670 | 0.0082 | 6 | -2.9357 | -2.0042 | -0.0628 | 6 | -3.0120 | -1.7150 | -0.0780 |
| 6 | -1.3339 | -3.7768 | 1.2514 | 6 | -3.1363 | -2.6250 | 1.1817 | 6 | -3.2891 | -2.3439 | 1.1455 |
| 6 | -0.8362 | -5.0781 | 1.3102 | 6 | -3.5540 | -3.9549 | 1.2486 | 6 | -4.0500 | -3.5143 | 1.1861 |
| 6 | -0.5778 | -5.7876 | 0.1331 | 6 | -3.7759 | -4.6834 | 0.0748 | 6 | -4.5453 | -4.0717 | 0.0027 |
| 6 | -0.8204 | -5.1871 | -1.1063 | 6 | -3.5741 | -4.0725 | -1.1668 | 6 | -4.2732 | -3.4498 | -1.2186 |
| 6 | -1.3155 | -3.8851 | -1.1720 | 6 | -3.1543 | -2.7426 | -1.2380 | 6 | -3.5104 | -2.2781 | -1.2608 |
| 6 | -3.2880 | 2.0897 | -0.2065 | 6 | -1.1415 | 3.2016 | -0.2298 | 6 | -0.5972 | 3.2154 | -0.1851 |
| 6 | -3.3323 | 2.7681 | -1.4371 | 6 | -0.5085 | 3.6792 | -1.3898 | 6 | 0.1388 | 3.6219 | -1.3084 |
| 6 | -3.6582 | 4.1231 | -1.4795 | 6 | -0.0112 | 4.9824 | -1.4374 | 6 | 0.6191 | 4.9297 | -1.4072 |
| 6 | -3.9446 | 4.8164 | -0.2992 | 6 | -0.1380 | 5.8258 | -0.3283 | 6 | 0.3691 | 5.8493 | -0.3833 |
| 6 | -3.9029 | 4.1460 | 0.9274 | 6 | -0.7641 | 5.3550 | 0.8303 | 6 | -0.3630 | 5.4500 | 0.7380 |
| 6 | -3.5771 | 2.7912 | 0.9772 | 6 | -1.2613 | 4.0513 | 0.8826 | 6 | -0.8437 | 4.1405 | 0.8386 |
| 1 | -1.5441 | -3.2258 | 2.1612 | 1 | -2.9692 | -2.0627 | 2.0942 | 1 | -2.9167 | -1.9148 | 2.0706 |
| 1 | -0.6524 | -5.5397 | 2.2759 | 1 | -3.7058 | -4.4220 | 2.2171 | 1 | -4.2567 | -3.9879 | 2.1414 |
| 1 | -0.1921 | -6.8019 | 0.1814 | 1 | -4.1014 | -5.7181 | 0.1280 | 1 | -5.1379 | -4.9813 | 0.0334 |
| 1 | -0.6261 | -5.7345 | -2.0240 | 1 | -3.7443 | -4.6306 | -2.0828 | 1 | -4.6537 | -3.8738 | -2.1432 |
| 1 | -1.5097 | -3.4165 | -2.1300 | 1 | -3.0024 | -2.2702 | -2.2018 | 1 | -3.3044 | -1.8014 | -2.2120 |
| 1 | -3.1130 | 2.2246 | -2.3491 | 1 | -0.4116 | 3.0300 | -2.2534 | 1 | 0.3311 | 2.9180 | -2.1122 |
| 1 | -3.6901 | 4.6382 | -2.4351 | 1 | 0.4750 | 5.3388 | -2.3406 | 1 | 1.1856 | 5.2292 | -2.2840 |
| 1 | -4.1990 | 5.8718 | -0.3351 | 1 | 0.2489 | 6.8398 | -0.3665 | 1 | 0.7412 | 6.8667 | -0.4599 |
| 1 | -4.1261 | 4.6787 | 1.8471 | 1 | -0.8672 | 6.0032 | 1.6955 | 1 | -0.5631 | 6.1564 | 1.5383 |
| 1 | -3.5464 | 2.2657 | 1.9248 | 1 | -1.7492 | 3.6900 | 1.7807 | 1 | -1.4118 | 3.8389 | 1.7109 |
| 7 | -2.7408 | 0.0002 | -1.3229 | 7 | -2.0189 | 1.2354 | -1.3981 | 7 | -1.6728 | 1.3602 | -1.3964 |
| 7 | -2.3225 | -1.2393 | -1.2710 | 7 | -2.4366 | 0.0211 | -1.3651 | 7 | -2.2163 | 0.2424 | -1.3862 |
| | E = -1279.737205 | | | | E = -1279.717784 | | | | E = -1279.760181 | | |
| | G = -1279.347890 | | | | G = -1279.302047 | | | | G = -1279.339783 | | |

**Table S2.** Atomic numbers, Cartesian coordinates (Å), electronic and free energies (a.u.) of the reactant, transition state and product of the nitrogen elimination reaction after IEDDA of compound **1a** with diphenyl-*s*-tetrazine.

| | reactant | | | | TS | | | | product | | |
|---|---|---|---|---|---|---|---|---|---|---|---|
| *Z* | *x* | *y* | *z* | *Z* | *x* | *y* | *z* | *Z* | *x* | *y* | *z* |
| 6 | -0.6253 | -0.6786 | 0.2379 | 6 | -0.6388 | -0.6865 | 0.1825 | 6 | -0.7104 | -0.5576 | 0.1272 |
| 6 | 0.0476 | 0.7111 | 0.2115 | 6 | 0.0659 | 0.6977 | 0.1943 | 6 | 0.1211 | 0.7593 | 0.1676 |
| 6 | 0.8421 | 1.0706 | 1.4843 | 6 | 0.8709 | 0.9988 | 1.4766 | 6 | 0.9394 | 0.9496 | 1.4694 |
| 6 | 0.0136 | -1.7222 | -0.7045 | 6 | 0.0090 | -1.7073 | -0.7934 | 6 | -0.1576 | -1.5607 | -0.9290 |
| 1 | -0.6154 | -1.0776 | 1.2580 | 1 | -0.6137 | -1.1178 | 1.1887 | 1 | -0.6453 | -1.0515 | 1.1028 |
| 1 | 0.7205 | 0.7679 | -0.6487 | 1 | 0.7613 | 0.7321 | -0.6516 | 1 | 0.8688 | 0.6891 | -0.6353 |
| 1 | 1.2833 | 2.0627 | 1.3433 | 1 | 1.3445 | 1.9789 | 1.3618 | 1 | 1.5270 | 1.8681 | 1.3771 |
| 1 | 0.1627 | 1.1465 | 2.3407 | 1 | 0.1980 | 1.0757 | 2.3381 | 1 | 0.2685 | 1.0940 | 2.3235 |
| 6 | 1.9617 | 0.0664 | 1.8234 | 6 | 1.9615 | -0.0431 | 1.7949 | 6 | 1.8998 | -0.2182 | 1.7749 |
| 6 | 1.3655 | -2.2809 | -0.2165 | 6 | 1.3478 | -2.3070 | -0.3207 | 6 | 1.1130 | -2.3185 | -0.4903 |
| 1 | -0.6737 | -2.5675 | -0.8009 | 1 | -0.6887 | -2.5388 | -0.9318 | 1 | -0.9240 | -2.3094 | -1.1458 |
| 1 | 0.1242 | -1.2943 | -1.7089 | 1 | 0.1292 | -1.2369 | -1.7776 | 1 | 0.0177 | -1.0237 | -1.8706 |
| 6 | 2.8476 | -0.2371 | 0.6336 | 6 | 2.8577 | -0.3223 | 0.6074 | 6 | 2.7945 | -0.5520 | 0.5994 |
| 6 | 2.5459 | -1.3335 | -0.3398 | 6 | 2.5475 | -1.3800 | -0.4042 | 6 | 2.4056 | -1.5190 | -0.4775 |
| 1 | 1.5379 | -0.8662 | 2.2084 | 1 | 1.5135 | -0.9793 | 2.1416 | 1 | 1.3513 | -1.1161 | 2.0749 |
| 1 | 2.5681 | 0.4850 | 2.6362 | 1 | 2.5649 | 0.3331 | 2.6305 | 1 | 2.5197 | 0.0563 | 2.6380 |
| 1 | 1.5927 | -3.1787 | -0.8054 | 1 | 1.5605 | -3.1872 | -0.9409 | 1 | 1.2546 | -3.1684 | -1.1714 |
| 1 | 1.2712 | -2.6162 | 0.8220 | 1 | 1.2422 | -2.6782 | 0.7043 | 1 | 0.9561 | -2.7552 | 0.5020 |
| 7 | 3.6415 | -1.4695 | 0.6348 | 7 | 3.6300 | -1.5684 | 0.5764 | 7 | 3.4162 | -1.8725 | 0.5272 |
| 1 | 3.3417 | 0.6388 | 0.2051 | 1 | 3.3724 | 0.5584 | 0.2145 | 1 | 3.4175 | 0.2818 | 0.2607 |
| 1 | 2.8545 | -1.1350 | -1.3690 | 1 | 2.8702 | -1.1551 | -1.4235 | 1 | 2.7915 | -1.2747 | -1.4718 |
| 6 | 5.0069 | -1.3631 | 0.1156 | 6 | 5.0025 | -1.4689 | 0.0751 | 6 | 4.8119 | -1.9213 | 0.0939 |
| 6 | 5.5338 | -2.7429 | -0.2600 | 6 | 5.5106 | -2.8452 | -0.3381 | 6 | 5.1789 | -3.3371 | -0.3342 |
| 8 | 6.8699 | -2.5769 | -0.7536 | 8 | 6.8541 | -2.6863 | -0.8138 | 8 | 6.5441 | -3.3120 | -0.7565 |
| 1 | 5.6411 | -0.9332 | 0.8998 | 1 | 5.6352 | -1.0745 | 0.8789 | 1 | 5.4475 | -1.6262 | 0.9364 |
| 1 | 5.0691 | -0.6997 | -0.7638 | 1 | 5.0854 | -0.7798 | -0.7825 | 1 | 5.0219 | -1.2279 | -0.7392 |
| 1 | 4.8929 | -3.1936 | -1.0302 | 1 | 4.8701 | -3.2613 | -1.1277 | 1 | 4.5214 | -3.6612 | -1.1548 |
| 1 | 5.5242 | -3.3968 | 0.6215 | 1 | 5.4817 | -3.5256 | 0.5227 | 1 | 5.0348 | -4.0228 | 0.5114 |
| 1 | 7.2236 | -3.4455 | -0.9866 | 1 | 7.1968 | -3.5535 | -1.0674 | 1 | 6.8214 | -4.2069 | -0.9873 |
| 6 | -2.1666 | -0.4595 | -0.0867 | 6 | -2.1284 | -0.5027 | -0.2057 | 6 | -2.1947 | -0.2933 | -0.1736 |
| 7 | -2.6530 | 0.4863 | 0.9578 | 7 | -2.6078 | 0.5686 | 1.2170 | 7 | -2.5967 | 0.3640 | 1.6620 |
| 7 | -2.1139 | 1.6060 | 0.9457 | 7 | -2.0693 | 1.6068 | 1.1964 | 7 | -2.3662 | 1.3685 | 2.0862 |
| 6 | -1.0812 | 1.7842 | -0.0960 | 6 | -0.9684 | 1.8026 | -0.1735 | 6 | -0.6921 | 1.9685 | -0.2817 |
| 6 | -3.0120 | -1.7150 | -0.0780 | 6 | -3.0315 | -1.6973 | -0.1274 | 6 | -3.1345 | -1.4689 | -0.1826 |
| 6 | -3.2891 | -2.3439 | 1.1455 | 6 | -3.0391 | -2.5058 | 1.0215 | 6 | -2.9898 | -2.5344 | 0.7201 |
| 6 | -4.0500 | -3.5143 | 1.1861 | 6 | -3.8865 | -3.6123 | 1.1086 | 6 | -3.8750 | -3.6138 | 0.7016 |
| 6 | -4.5453 | -4.0717 | 0.0027 | 6 | -4.7366 | -3.9329 | 0.0456 | 6 | -4.9207 | -3.6478 | -0.2242 |
| 6 | -4.2732 | -3.4498 | -1.2186 | 6 | -4.7356 | -3.1339 | -1.1017 | 6 | -5.0754 | -2.5905 | -1.1256 |
| 6 | -3.5104 | -2.2781 | -1.2608 | 6 | -3.8941 | -2.0220 | -1.1869 | 6 | -4.1947 | -1.5087 | -1.1028 |
| 6 | -0.5972 | 3.2154 | -0.1851 | 6 | -0.4794 | 3.2270 | -0.2000 | 6 | -0.0447 | 3.3193 | -0.3076 |
| 6 | 0.1388 | 3.6219 | -1.3084 | 6 | -0.0022 | 3.7500 | -1.4128 | 6 | 0.3358 | 3.8681 | -1.5416 |
| 6 | 0.6191 | 4.9297 | -1.4072 | 6 | 0.4874 | 5.0565 | -1.4808 | 6 | 0.9285 | 5.1311 | -1.6057 |
| 6 | 0.3691 | 5.8493 | -0.3833 | 6 | 0.5011 | 5.8621 | -0.3380 | 6 | 1.1353 | 5.8691 | -0.4376 |
| 6 | -0.3630 | 5.4500 | 0.7380 | 6 | 0.0251 | 5.3493 | 0.8719 | 6 | 0.7423 | 5.3379 | 0.7940 |
| 6 | -0.8437 | 4.1405 | 0.8386 | 6 | -0.4587 | 4.0396 | 0.9434 | 6 | 0.1603 | 4.0701 | 0.8602 |
| 1 | -2.9167 | -1.9148 | 2.0706 | 1 | -2.3922 | -2.2698 | 1.8605 | 1 | -2.1919 | -2.5247 | 1.4562 |
| 1 | -4.2567 | -3.9879 | 2.1414 | 1 | -3.8817 | -4.2221 | 2.0072 | 1 | -3.7481 | -4.4250 | 1.4127 |
| 1 | -5.1379 | -4.9813 | 0.0334 | 1 | -5.3930 | -4.7955 | 0.1117 | 1 | -5.6083 | -4.4885 | -0.2415 |
| 1 | -4.6537 | -3.8738 | -2.1432 | 1 | -5.3909 | -3.3745 | -1.9338 | 1 | -5.8855 | -2.6064 | -1.8493 |
| 1 | -3.3044 | -1.8014 | -2.2120 | 1 | -3.8979 | -1.4028 | -2.0762 | 1 | -4.3131 | -0.6812 | -1.7926 |
| 1 | 0.3311 | 2.9180 | -2.1122 | 1 | -0.0189 | 3.1314 | -2.3043 | 1 | 0.1519 | 3.3046 | -2.4514 |
| 1 | 1.1856 | 5.2292 | -2.2840 | 1 | 0.8542 | 5.4438 | -2.4269 | 1 | 1.2184 | 5.5412 | -2.5689 |
| 1 | 0.7412 | 6.8667 | -0.4599 | 1 | 0.8778 | 6.8793 | -0.3904 | 1 | 1.5903 | 6.8541 | -0.4870 |
| 1 | -0.5631 | 6.1564 | 1.5383 | 1 | 0.0282 | 5.9674 | 1.7649 | 1 | 0.8821 | 5.9128 | 1.7050 |
| 1 | -1.4118 | 3.8389 | 1.7109 | 1 | -0.8276 | 3.6580 | 1.8883 | 1 | -0.1619 | 3.6762 | 1.8188 |
| 7 | -1.6728 | 1.3602 | -1.3964 | 7 | -1.7832 | 1.5022 | -1.2568 | 7 | -1.8510 | 1.9135 | -0.8578 |
| 7 | -2.2163 | 0.2424 | -1.3862 | 7 | -2.3754 | 0.3461 | -1.2618 | 7 | -2.6019 | 0.7406 | -0.8557 |
| | E = -1279.760181 | | | | E = -1279.746879 | | | | E = -1279.826530 | | |
| | G = -1279.339783 | | | | G = -1279.329402 | | | | G = -1279.429021 | | |

**Table S3.** Atomic numbers, Cartesian coordinates (Å), electronic and free energies (a.u.) of the reactant, transition state and product of the proton migration leading to fluorescent product. Cationic pathway.

| reactant | | | | TS | | | | product | | | |
|---|---|---|---|---|---|---|---|---|---|---|---|
| *Z* | *x* | *y* | *z* | *Z* | *x* | *y* | *z* | *Z* | *x* | *y* | *z* |
| 6 | -0.9045 | -0.4409 | 0.0958 | 6 | 0.2385 | -0.0691 | 0.3846 | 6 | 0.7010 | -0.5341 | 0.3029 |
| 6 | 0.0425 | 0.7833 | 0.2818 | 6 | -1.2192 | -0.5554 | 0.1200 | 6 | 0.1913 | 0.8200 | -0.1729 |
| 6 | 0.7539 | 0.7723 | 1.6653 | 6 | -1.3345 | -1.7286 | -0.8953 | 6 | -0.6563 | 0.7623 | -1.4810 |
| 6 | -0.4461 | -1.3914 | -1.0519 | 6 | 0.7787 | -0.4206 | 1.7856 | 6 | 0.0398 | -1.2163 | 1.4788 |
| 1 | -0.8695 | -1.0386 | 1.0159 | 1 | 0.9771 | -0.9638 | -0.2945 | 1 | -0.4222 | 1.2558 | 0.6217 |
| 1 | 0.8284 | 0.6901 | -0.4725 | 1 | -1.6131 | -0.9153 | 1.0762 | 1 | -1.0441 | 1.7664 | -1.6882 |
| 1 | 1.4131 | 1.6432 | 1.7246 | 1 | -2.3805 | -1.8195 | -1.2036 | 1 | -0.0058 | 0.4969 | -2.3201 |
| 1 | 0.0115 | 0.8819 | 2.4641 | 1 | -0.7681 | -1.4855 | -1.8018 | 6 | -1.8248 | -0.2427 | -1.4570 |
| 6 | 1.5835 | -0.5087 | 1.8979 | 6 | -0.9014 | -3.0982 | -0.3464 | 6 | -1.3611 | -1.8320 | 1.2297 |
| 6 | 0.7344 | -2.2995 | -0.6475 | 6 | 0.8626 | -1.9413 | 2.0457 | 1 | 0.6811 | -2.0214 | 1.8458 |
| 1 | -1.2775 | -2.0395 | -1.3413 | 1 | 1.7655 | 0.0198 | 1.9267 | 1 | -0.0434 | -0.4916 | 2.3018 |
| 1 | -0.1975 | -0.7884 | -1.9336 | 1 | 0.1268 | 0.0216 | 2.5503 | 6 | -2.6787 | -0.0513 | -0.2258 |
| 6 | 2.5002 | -0.8196 | 0.7312 | 6 | 0.5960 | -3.3251 | -0.1874 | 6 | -2.4425 | -0.7872 | 1.0467 |
| 6 | 2.0861 | -1.6233 | -0.4672 | 6 | 1.4493 | -2.8049 | 0.9245 | 1 | -1.4368 | -1.2644 | -1.4957 |
| 1 | 0.9367 | -1.3692 | 2.0959 | 1 | -1.2716 | -3.8656 | -1.0330 | 1 | -2.4422 | -0.0976 | -2.3494 |
| 1 | 2.1810 | -0.3681 | 2.8068 | 1 | -1.4028 | -3.2861 | 0.6120 | 1 | -1.6344 | -2.4478 | 2.0928 |
| 1 | 0.8480 | -3.0652 | -1.4246 | 1 | -0.1333 | -2.3295 | 2.2889 | 1 | -1.3182 | -2.4998 | 0.3640 |
| 1 | 0.4767 | -2.8368 | 0.2716 | 1 | 1.4673 | -2.0971 | 2.9428 | 7 | -3.6264 | -1.1483 | 0.1861 |
| 7 | 2.9946 | -2.1842 | 0.5445 | 7 | 1.5529 | -2.2237 | -0.4444 | 1 | -3.1545 | 0.9215 | -0.1302 |
| 1 | 3.2246 | -0.0294 | 0.5168 | 1 | 0.9388 | -4.2663 | -0.6112 | 1 | -2.7597 | -0.2815 | 1.9546 |
| 1 | 2.5572 | -1.3153 | -1.4037 | 1 | 2.2965 | -3.4266 | 1.2016 | 6 | -5.0248 | -0.8826 | 0.6082 |
| 6 | 4.4057 | -2.3217 | 0.1751 | 6 | 2.6844 | -2.5817 | -1.3332 | 6 | -5.9514 | -0.7773 | -0.6011 |
| 6 | 4.6609 | -3.7017 | -0.4193 | 6 | 3.8765 | -1.6477 | -1.2929 | 8 | -7.2543 | -0.5620 | -0.0658 |
| 8 | 6.0511 | -3.7728 | -0.7623 | 8 | 4.4177 | -1.6434 | 0.0316 | 1 | -5.0314 | 0.0460 | 1.1818 |
| 1 | 5.0110 | -2.1979 | 1.0806 | 1 | 2.2899 | -2.6047 | -2.3538 | 1 | -5.3299 | -1.7028 | 1.2620 |
| 1 | 4.7243 | -1.5512 | -0.5471 | 1 | 3.0177 | -3.5949 | -1.0760 | 1 | -5.9158 | -1.7028 | -1.1908 |
| 1 | 4.0368 | -3.8487 | -1.3113 | 1 | 3.5948 | -0.6336 | -1.6036 | 1 | -5.6452 | 0.0571 | -1.2447 |
| 1 | 4.4016 | -4.4763 | 0.3138 | 1 | 4.6105 | -2.0256 | -2.0151 | 1 | -7.8813 | -0.4771 | -0.7969 |
| 1 | 6.2353 | -4.6483 | -1.1276 | 1 | 5.2961 | -1.2403 | 0.0108 | 6 | 1.8188 | -0.9970 | -0.3117 |
| 6 | -2.3555 | -0.0733 | -0.0086 | 6 | 0.5810 | 1.1752 | -0.2149 | 7 | 2.4904 | -0.1228 | -1.1829 |
| 7 | -2.6923 | 1.1874 | -0.0506 | 7 | -0.2972 | 1.7277 | -1.0738 | 7 | 2.4696 | 1.2308 | -0.9702 |
| 7 | -1.8779 | 2.3073 | -0.1524 | 7 | -1.6681 | 1.5846 | -1.0114 | 6 | 1.4062 | 1.7111 | -0.4021 |
| 6 | -0.6055 | 2.1226 | 0.0020 | 6 | -2.1227 | 0.5700 | -0.3550 | 6 | 2.4775 | -2.3152 | -0.1119 |
| 6 | -3.4291 | -1.0731 | -0.0346 | 6 | 1.8091 | 1.9722 | 0.0142 | 6 | 1.7733 | -3.5141 | -0.3149 |
| 6 | -3.3302 | -2.2492 | 0.7357 | 6 | 3.0647 | 1.3870 | 0.2593 | 6 | 2.4004 | -4.7490 | -0.1314 |
| 6 | -4.3705 | -3.1750 | 0.7311 | 6 | 4.1888 | 2.1847 | 0.4706 | 6 | 3.7442 | -4.8048 | 0.2508 |
| 6 | -5.5079 | -2.9534 | -0.0528 | 6 | 4.0831 | 3.5788 | 0.4548 | 6 | 4.4585 | -3.6182 | 0.4467 |
| 6 | -5.6062 | -1.7980 | -0.8346 | 6 | 2.8387 | 4.1737 | 0.2331 | 6 | 3.8318 | -2.3837 | 0.2637 |
| 6 | -4.5776 | -0.8589 | -0.8255 | 6 | 1.7124 | 3.3807 | 0.0143 | 6 | 1.4059 | 3.1498 | -0.0415 |
| 6 | 0.2281 | 3.3422 | -0.1200 | 6 | -3.5906 | 0.5249 | -0.1239 | 6 | 0.2131 | 3.8285 | 0.2706 |
| 6 | 1.5439 | 3.2868 | -0.6160 | 6 | -4.1936 | -0.5208 | 0.5991 | 6 | 0.2233 | 5.1876 | 0.5982 |
| 6 | 2.2968 | 4.4537 | -0.7528 | 6 | -5.5740 | -0.5381 | 0.8171 | 6 | 1.4250 | 5.8986 | 0.6211 |
| 6 | 1.7556 | 5.6883 | -0.3830 | 6 | -6.3799 | 0.4841 | 0.3130 | 6 | 2.6206 | 5.2359 | 0.3149 |
| 6 | 0.4510 | 5.7530 | 0.1198 | 6 | -5.7934 | 1.5300 | -0.4113 | 6 | 2.6123 | 3.8802 | -0.0069 |
| 6 | -0.3089 | 4.5923 | 0.2464 | 6 | -4.4180 | 1.5528 | -0.6243 | 1 | 0.7368 | -3.4781 | -0.6349 |
| 1 | -2.4641 | -2.4286 | 1.3625 | 1 | 3.1825 | 0.3119 | 0.2852 | 1 | 1.8417 | -5.6656 | -0.2959 |
| 1 | -4.2940 | -4.0688 | 1.3414 | 1 | 5.1507 | 1.7145 | 0.6494 | 1 | 4.2321 | -5.7647 | 0.3916 |
| 1 | -6.3120 | -3.6825 | -0.0594 | 1 | 4.9610 | 4.1947 | 0.6238 | 1 | 5.5016 | -3.6527 | 0.7469 |
| 1 | -6.4775 | -1.6325 | -1.4596 | 1 | 2.7386 | 5.2544 | 0.2398 | 1 | 4.3910 | -1.4677 | 0.4343 |
| 1 | -4.6481 | 0.0114 | -1.4709 | 1 | 0.7495 | 3.8643 | -0.1126 | 1 | -0.7379 | 3.3077 | 0.2495 |
| 1 | 1.9819 | 2.3438 | -0.9232 | 1 | -3.6008 | -1.3340 | 1.0008 | 1 | -0.7119 | 5.6880 | 0.8321 |
| 1 | 3.3055 | 4.3963 | -1.1495 | 1 | -6.0149 | -1.3550 | 1.3801 | 1 | 1.4331 | 6.9536 | 0.8782 |
| 1 | 2.3467 | 6.5935 | -0.4830 | 1 | -7.4525 | 0.4689 | 0.4811 | 1 | 3.5629 | 5.7760 | 0.3379 |
| 1 | 0.0279 | 6.7076 | 0.4172 | 1 | -6.4106 | 2.3309 | -0.8072 | 1 | 3.5424 | 3.3686 | -0.2280 |
| 1 | -1.3167 | 4.6403 | 0.6431 | 1 | -3.9693 | 2.3683 | -1.1793 | 1 | 3.3821 | -0.4316 | -1.5449 |
| 1 | -3.6751 | 1.4455 | -0.0500 | 1 | -0.0208 | 2.5252 | -1.6309 | 1 | -3.5105 | -2.0240 | -0.3251 |
| E = -1170.747431 | | | | E = -1170.722213 | | | | E = -1170.761896 | | | |
| G = -1170.322102 | | | | G = -1170.298408 | | | | G = -1170.335627 | | | |

**Table S4.** Atomic numbers, Cartesian coordinates (Å), electronic and free energies (a.u.) of the reactant, transition state and product of the proton migration leading to fluorescent product. Neutral pathway.

| reactant | | | | TS | | | | product | | | |
|---|---|---|---|---|---|---|---|---|---|---|---|
| *Z* | *x* | *y* | *z* | *Z* | *x* | *y* | *z* | *Z* | *x* | *y* | *z* |
| 6 | -0.9298 | -0.4061 | 0.0401 | 6 | 0.1761 | -0.0300 | 0.4062 | 6 | 0.7200 | -0.5018 | 0.3044 |
| 6 | 0.0346 | 0.7867 | 0.2791 | 6 | -1.2483 | -0.5566 | 0.1015 | 6 | 0.1029 | 0.8057 | -0.1754 |
| 6 | 0.7084 | 0.7418 | 1.6756 | 6 | -1.3268 | -1.7079 | -0.9401 | 6 | -0.7234 | 0.6851 | -1.4934 |
| 6 | -0.4604 | -1.3341 | -1.1132 | 6 | 0.6870 | -0.4144 | 1.8047 | 6 | 0.1030 | -1.2360 | 1.4740 |
| 1 | -0.9195 | -1.0225 | 0.9466 | 1 | 1.0323 | -1.0327 | -0.3321 | 1 | -0.5599 | 1.1753 | 0.6114 |
| 1 | 0.8439 | 0.6946 | -0.4522 | 1 | -1.6593 | -0.9616 | 1.0372 | 1 | -1.1820 | 1.6622 | -1.6927 |
| 1 | 1.3758 | 1.6043 | 1.7748 | 1 | -2.3673 | -1.8159 | -1.2665 | 1 | -0.0398 | 0.4864 | -2.3263 |
| 1 | -0.0534 | 0.8415 | 2.4585 | 1 | -0.7540 | -1.4340 | -1.8351 | 6 | -1.8134 | -0.4014 | -1.4780 |
| 6 | 1.5169 | -0.5549 | 1.9051 | 6 | -0.8705 | -3.0804 | -0.4160 | 6 | -1.2422 | -1.9563 | 1.2111 |
| 6 | 0.6890 | -2.2803 | -0.7027 | 6 | 0.8456 | -1.9419 | 2.0281 | 1 | 0.8135 | -1.9752 | 1.8553 |
| 1 | -1.2980 | -1.9563 | -1.4437 | 1 | 1.6383 | 0.0738 | 2.0152 | 1 | -0.0501 | -0.5102 | 2.2874 |
| 1 | -0.1709 | -0.7210 | -1.9767 | 1 | -0.0142 | -0.0527 | 2.5733 | 6 | -2.7132 | -0.3054 | -0.2648 |
| 6 | 2.4503 | -0.8631 | 0.7502 | 6 | 0.6287 | -3.2752 | -0.2396 | 6 | -2.4261 | -1.0277 | 1.0133 |
| 6 | 2.0487 | -1.6361 | -0.4714 | 6 | 1.4607 | -2.7662 | 0.8927 | 1 | -1.3533 | -1.3934 | -1.5127 |
| 1 | 0.8511 | -1.4076 | 2.0709 | 1 | -1.2102 | -3.8496 | -1.1169 | 1 | -2.4176 | -0.3074 | -2.3900 |
| 1 | 2.1015 | -0.4442 | 2.8270 | 1 | -1.3759 | -3.2943 | 0.5353 | 1 | -1.4565 | -2.6043 | 2.0715 |
| 1 | 0.8122 | -3.0367 | -1.4885 | 1 | -0.1339 | -2.3785 | 2.2560 | 1 | -1.1479 | -2.6159 | 0.3432 |
| 1 | 0.3951 | -2.8265 | 0.2009 | 1 | 1.4559 | -2.0993 | 2.9219 | 7 | -3.5131 | -1.4748 | 0.1304 |
| 7 | 2.9273 | -2.2336 | 0.5478 | 7 | 1.5672 | -2.1431 | -0.4632 | 1 | -3.2135 | 0.6601 | -0.1492 |
| 1 | 3.1932 | -0.0825 | 0.5640 | 1 | 1.0059 | -4.1890 | -0.6917 | 1 | -2.7412 | -0.5060 | 1.9201 |
| 1 | 2.5486 | -1.3174 | -1.3898 | 1 | 2.3240 | -3.3717 | 1.1544 | 6 | -4.8777 | -1.2098 | 0.5906 |
| 6 | 4.3424 | -2.3863 | 0.2028 | 6 | 2.7020 | -2.4389 | -1.3741 | 6 | -5.8500 | -1.2782 | -0.5811 |
| 6 | 4.5861 | -3.7538 | -0.4241 | 6 | 3.9037 | -1.5239 | -1.2656 | 8 | -7.1643 | -1.0145 | -0.0709 |
| 8 | 5.9820 | -3.8423 | -0.7407 | 8 | 4.4708 | -1.6634 | 0.0401 | 1 | -4.9703 | -0.2249 | 1.0796 |
| 1 | 4.9329 | -2.2975 | 1.1223 | 1 | 2.3060 | -2.3868 | -2.3929 | 1 | -5.1471 | -1.9727 | 1.3307 |
| 1 | 4.6890 | -1.6027 | -0.4923 | 1 | 3.0227 | -3.4699 | -1.1870 | 1 | -5.8062 | -2.2729 | -1.0430 |
| 1 | 3.9784 | -3.8649 | -1.3325 | 1 | 3.6275 | -0.4819 | -1.4646 | 1 | -5.5764 | -0.5334 | -1.3408 |
| 1 | 4.2977 | -4.5435 | 0.2815 | 1 | 4.6174 | -1.8374 | -2.0379 | 1 | -7.7955 | -1.0682 | -0.8005 |
| 1 | 6.1564 | -4.7091 | -1.1306 | 1 | 5.3138 | -1.1910 | 0.0668 | 6 | 1.8766 | -0.8670 | -0.3028 |
| 6 | -2.3773 | 0.0294 | -0.0836 | 6 | 0.5055 | 1.2200 | -0.2064 | 7 | 2.4752 | 0.0644 | -1.1759 |
| 7 | -2.7756 | 1.2559 | -0.1694 | 7 | -0.3142 | 1.8838 | -1.0409 | 7 | 2.3449 | 1.4110 | -0.9508 |
| 7 | -1.8515 | 2.3134 | -0.2810 | 7 | -1.6656 | 1.6297 | -0.9556 | 6 | 1.2403 | 1.7959 | -0.3873 |
| 6 | -0.5967 | 2.1272 | -0.0323 | 6 | -2.1401 | 0.5844 | -0.3475 | 6 | 2.6451 | -2.1234 | -0.1018 |
| 6 | -3.4549 | -1.0002 | -0.0444 | 6 | 1.7984 | 1.9490 | 0.0171 | 6 | 2.0316 | -3.3784 | -0.2590 |
| 6 | -3.3099 | -2.2078 | 0.6631 | 6 | 3.0067 | 1.3238 | 0.3761 | 6 | 2.7589 | -4.5572 | -0.0776 |
| 6 | -4.3487 | -3.1412 | 0.7038 | 6 | 4.1748 | 2.0631 | 0.5829 | 6 | 4.1160 | -4.5025 | 0.2553 |
| 6 | -5.5464 | -2.8936 | 0.0275 | 6 | 4.1705 | 3.4529 | 0.4391 | 6 | 4.7409 | -3.2603 | 0.4063 |
| 6 | -5.6995 | -1.7012 | -0.6891 | 6 | 2.9783 | 4.0946 | 0.0890 | 6 | 4.0131 | -2.0817 | 0.2270 |
| 6 | -4.6664 | -0.7652 | -0.7236 | 6 | 1.8126 | 3.3542 | -0.1139 | 6 | 1.1152 | 3.2303 | -0.0285 |
| 6 | 0.2670 | 3.3386 | -0.1225 | 6 | -3.6099 | 0.5352 | -0.1235 | 6 | -0.1261 | 3.7940 | 0.3217 |
| 6 | 1.5991 | 3.2737 | -0.5708 | 6 | -4.2300 | -0.5456 | 0.5358 | 6 | -0.2357 | 5.1499 | 0.6456 |
| 6 | 2.3750 | 4.4309 | -0.6726 | 6 | -5.6123 | -0.5699 | 0.7495 | 6 | 0.8916 | 5.9738 | 0.6262 |
| 6 | 1.8406 | 5.6720 | -0.3153 | 6 | -6.4165 | 0.4802 | 0.3029 | 6 | 2.1346 | 5.4267 | 0.2817 |
| 6 | 0.5200 | 5.7487 | 0.1415 | 6 | -5.8179 | 1.5615 | -0.3588 | 6 | 2.2458 | 4.0747 | -0.0359 |
| 6 | -0.2585 | 4.5952 | 0.2351 | 6 | -4.4410 | 1.5904 | -0.5642 | 1 | 0.9841 | -3.4277 | -0.5381 |
| 1 | -2.3953 | -2.4240 | 1.2046 | 1 | 3.0590 | 0.2506 | 0.4976 | 1 | 2.2674 | -5.5172 | -0.2059 |
| 1 | -4.2195 | -4.0613 | 1.2659 | 1 | 5.0910 | 1.5474 | 0.8575 | 1 | 4.6822 | -5.4189 | 0.3930 |
| 1 | -6.3502 | -3.6233 | 0.0545 | 1 | 5.0786 | 4.0260 | 0.6033 | 1 | 5.7934 | -3.2076 | 0.6693 |
| 1 | -6.6224 | -1.5032 | -1.2265 | 1 | 2.9520 | 5.1756 | -0.0178 | 1 | 4.5058 | -1.1231 | 0.3662 |
| 1 | -4.7811 | 0.1555 | -1.2845 | 1 | 0.8884 | 3.8556 | -0.3745 | 1 | -1.0221 | 3.1834 | 0.3347 |
| 1 | 2.0360 | 2.3254 | -0.8650 | 1 | -3.6416 | -1.3843 | 0.8901 | 1 | -1.2065 | 5.5592 | 0.9097 |
| 1 | 3.3970 | 4.3601 | -1.0327 | 1 | -6.0570 | -1.4173 | 1.2638 | 1 | 0.8067 | 7.0265 | 0.8796 |
| 1 | 2.4475 | 6.5696 | -0.3881 | 1 | -7.4901 | 0.4599 | 0.4656 | 1 | 3.0209 | 6.0550 | 0.2705 |
| 1 | 0.0982 | 6.7070 | 0.4304 | 1 | -6.4292 | 2.3880 | -0.7114 | 1 | 3.2128 | 3.6539 | -0.2885 |
| 1 | -1.2799 | 4.6523 | 0.5946 | 1 | -3.9836 | 2.4341 | -1.0680 | 1 | 3.3960 | -0.1655 | -1.5231 |
| E = -1170.296339 | | | | E = -1170.242224 | | | | E = -1170.390914 | | | |
| G = -1169.885977 | | | | G = -1169.833679 | | | | G = -1169.898670 | | | |

## X-Ray crystallography

Crystals suitable for X-ray analysis were obtained from a solution of **4** in a mixture of $Et_2O$/hexane and slow evaporation of the solvent in the dark. Compound **4** crystalized as a mixture of two enantiomers in 6:4 ratio (Figure S2).

### Data collection

The crystal data were collected on an Xcalibur PX diffractometer equipped with Onyx CCD detector and a Cu Kα sealed tube (λ = 1.54178 Å) with an enhanced monochromator using combined φ and ω scans at 180 K. CrysAlisProCCD (CrysAlisPro, Oxford Diffraction, 2002) was used for data collection, cell refinement and data reduction. The structure was solved by direct methods with SIR92 (*J. Appl. Cryst.* **1994,** *27*, 435) and refined by full-matrix least-squares on F with CRYSTALS (*J. Appl. Cryst.* **2003**, *36*, 1487). The positional and anisotropical thermal parameters of all non-hydrogen atoms were refined. All hydrogen atoms were found from a Fourier difference map and then recalculated into idealized positions and refined with riding constraints.

### Crystal data (0.20 × 0.41 × 0.59 mm):

$C_{15}H_{19}N_1O_2S_1$, triclinic, space group *P*-1, $a$ = 7.53182(18) Å, $b$ = 8.8685(2) Å, $c$ = 11.5315(2) Å, α = 100.2646(19)°, β = 90.4516(18)°, γ = 103.102(2)°, $V$ = 1386.6(9) Å$^3$, $V$ = 737.26(3) Å$^3$, $Z$ = 2, $M$ = 277.39, 18359 reflections measured, 2988 independent reflections. Final $R$ = 0.036, $wR$ = 0.027, $GoF$ = 1.238 for 2846 reflections with $I > 2\sigma(I)$ and 191 parameters. CCDC 1553867.

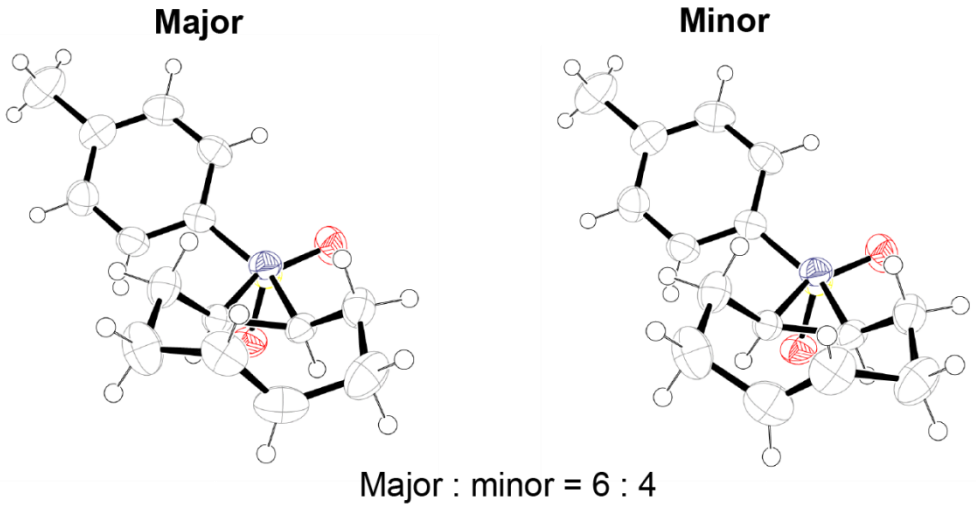


**Figure S2.** An ORTEP (*J. Appl. Cryst.* **2012**, *45*, 849) view of compound **4**, displacement ellipsoids shown with 50% probability.

## Click reactions of *trans*-cyclooctenes (TCO) with 1,2,4,5-tetrazines and 1,2,4-triazines

Click reactions with tetrazines: 300 µL of a 1.25 mM solution of the tetrazine in $CH_3CN$ + 5% $H_2O$ were added to 300 µL of a 2.5 mM solution of the appropriate TCO in $CH_3CN$ + 10% MeOH. The final concentration of all tetrazines was 0.625 mM in $CH_3CN$ containing 5% MeOH and 2.5% $H_2O$ using 2 equiv. of TCO.
Click reactions with triazines: 30 µL of a 1.25 mM solution of the triazine in $CH_3CN/H_2O$ 1:4 were added to 30 µL of a 1.875 mM or 2.5 mM solution of **1a** in $CH_3CN/H_2O$ 1:4. The final concentration of all triazines was 0.625 mM in $CH_3CN/H_2O$ 1:4 using 1.5 equiv. or 2 equiv. of **1a**.
The solutions were incubated at room temperature for 5-30 min and then measured by HPLC-MS to verify the formation of the corresponding click products. HPLC-MS measurements were performed on a Luna® C18(2) column (3µm, 100A, 100 × 4.6 mm) using a linear gradient of $CH_3CN$ + 0.05% HCOOH (5 → 95% in 9 min) in $H_2O$ + 0.05% HCOOH at a flow rate of 1.0 mL/min. All low-resolution masses found during these measurements are summarized in Table S5 and S6.
For absorbance measurements these stock solutions were diluted with $CH_3CN$ to a concentration of 25 µM and for fluorescence measurements further to 1.25 µM.

**Table S5.** Calculated and observed masses of the click products $[M+H]^+$ arising from the reaction between 3,6-diphenyl-*s*-1,2,4,5-tetrazine and various TCOs[a].

| **Tetrazine** | 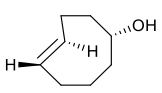 axial | | 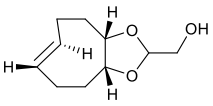 syn:anti 12:1 | | 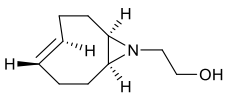 | | 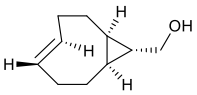 syn | |
|---|---|---|---|---|---|---|---|---|
| | calcd. | found | calcd. | found | calcd. | found | calcd. | found |
| 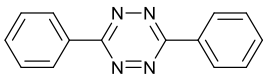 | 333.2 | 333.2 | 391.2 | 391.2 | 374.2 | 374.2 | 359.2 | 359.2 |

a) all reactions were performed in $CH_3CN$ containing 5% MeOH and 2.5% $H_2O$ at room temperature using an excess of the TCO.

**Table S6.** Calculated and observed masses of the click products $[M+H]^+$ arising from the reaction between **1a** and various 1,2,4,5-tetrazines and 1,2,4-triazines[a].

| **Tetrazine/Triazine** | 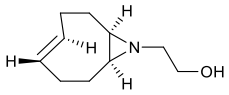 | |
|---|---|---|
| | calcd. | found |
| 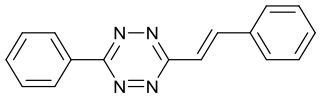 | 400.2 | 400.2 |
| 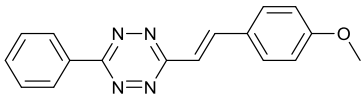 | 430.2 | 430.2 |
| 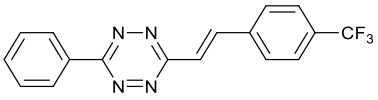 | 468.2 | 468.2 |
| 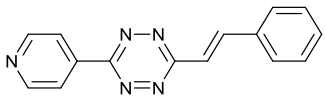 | 401.2 | 401.2[b] |
| 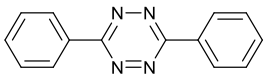 | 374.2 | 374.2 |
| 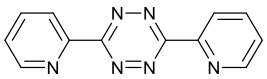 | 376.2 | 376.2[b] |
| 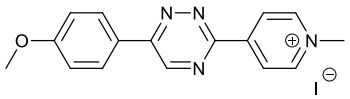 | 418.2 | 418.2 |
| 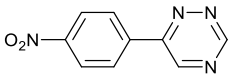 | 342.2 | 342.2 |

a) all reactions were performed in $CH_3CN$ containing 5% MeOH and 2.5% $H_2O$ (click with tetrazines) or in $CH_3CN/H_2O$ 1:4 (click with triazines) at room temperature using an excess of **1a**, b) these click reactions were diluted 1:4 with $H_2O$ before measurement on HPLC-MS and the measurement was performed on a Kinetex® C18 column (2.6µm, 100A, 100 × 4.6 mm) using the same linear gradient and flow rate as above.

## HPLC chromatograms and low-resolution mass spectra of the click products

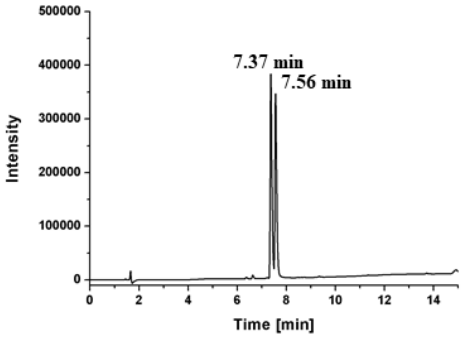


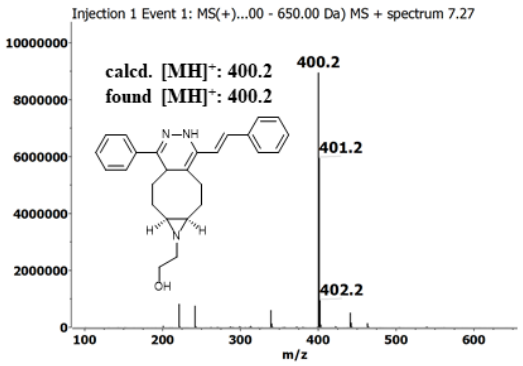


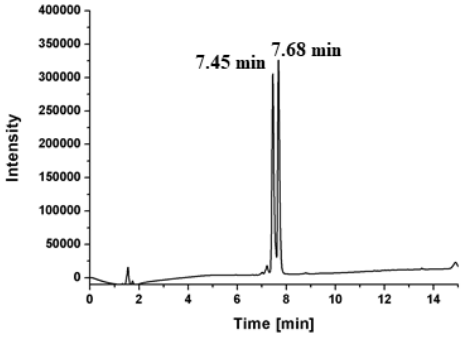


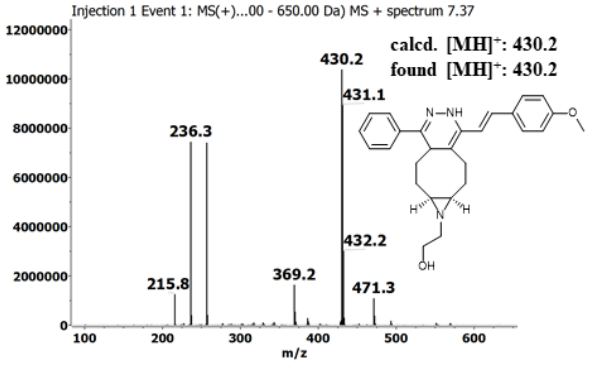

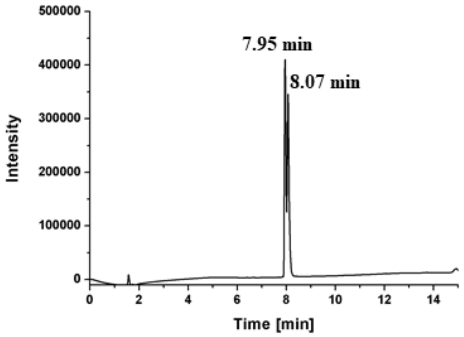
7.95 min
8.07 min
Intensity
Time [min]

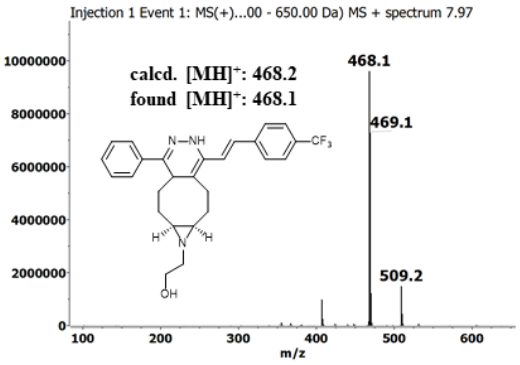
Injection 1 Event 1: MS(+)...00 - 650.00 Da) MS + spectrum 7.97
calcd. [MH]+: 468.2
found [MH]+: 468.1
468.1
469.1
509.2
m/z

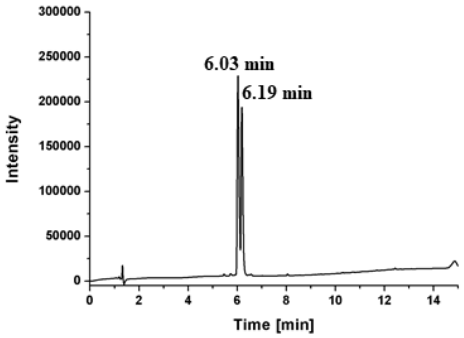
6.03 min
6.19 min
Intensity
Time [min]

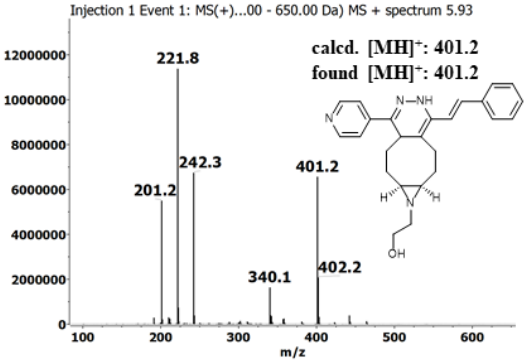
Injection 1 Event 1: MS(+)...00 - 650.00 Da) MS + spectrum 5.93
calcd. [MH]+: 401.2
found [MH]+: 401.2
221.8
242.3
201.2
401.2
340.1
402.2
m/z

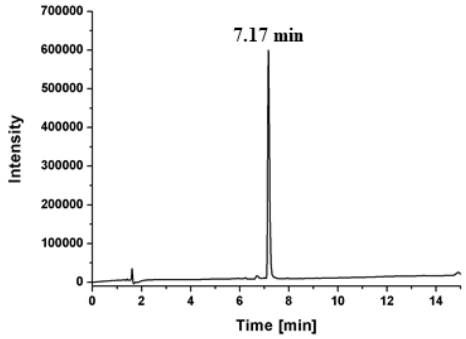
7.17 min
Intensity
Time [min]

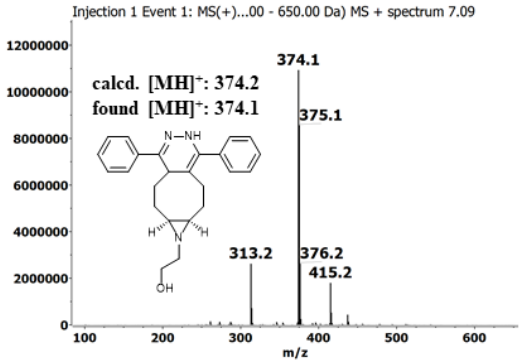
Injection 1 Event 1: MS(+)...00 - 650.00 Da) MS + spectrum 7.09
calcd. [MH]+: 374.2
found [MH]+: 374.1
374.1
375.1
313.2
376.2
415.2
m/z

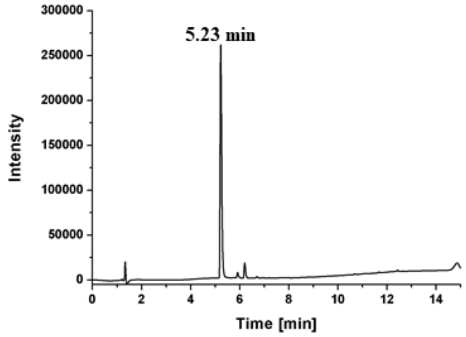
5.23 min
Intensity
Time [min]

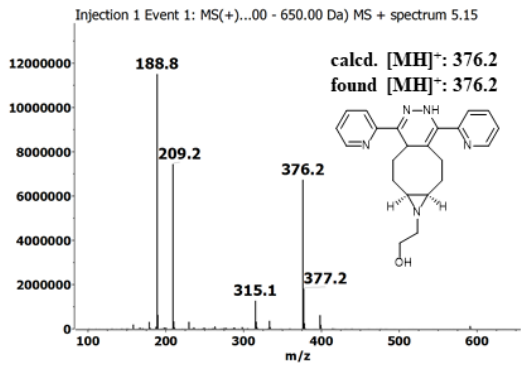
Injection 1 Event 1: MS(+)...00 - 650.00 Da) MS + spectrum 5.15
calcd. [MH]+: 376.2
found [MH]+: 376.2
188.8
209.2
376.2
315.1
377.2
m/z

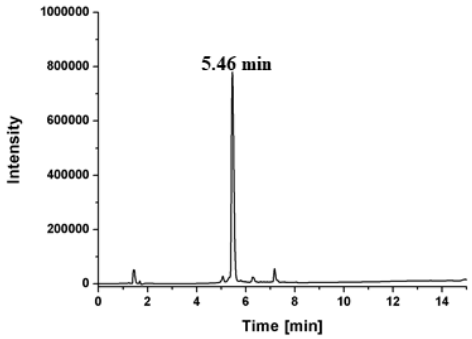
5.46 min
Intensity
Time [min]

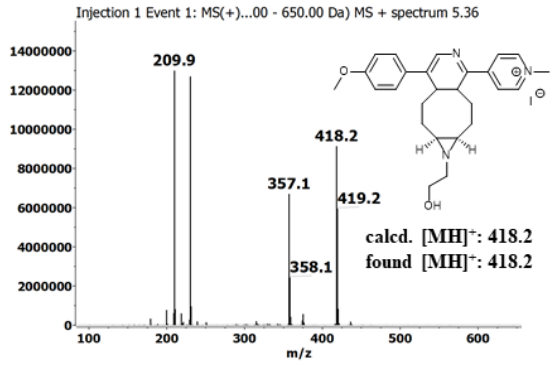
Injection 1 Event 1: MS(+)...00 - 650.00 Da) MS + spectrum 5.36
209.9
418.2
357.1
419.2
358.1
calcd. [MH]+: 418.2
found [MH]+: 418.2
m/z

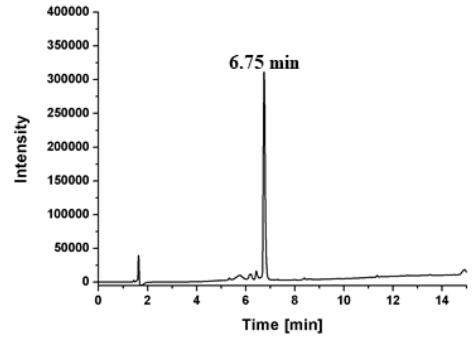
6.75 min
Intensity
Time [min]

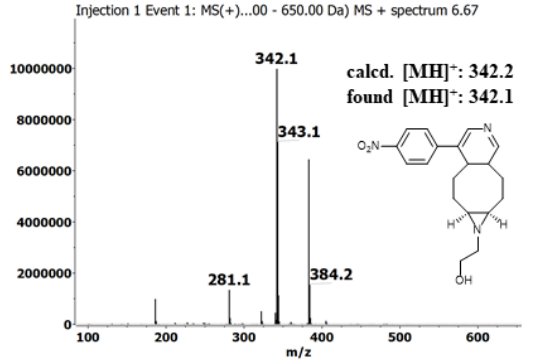
Injection 1 Event 1: MS(+)...00 - 650.00 Da) MS + spectrum 6.67
342.1
343.1
calcd. [MH]+: 342.2
found [MH]+: 342.1
281.1
384.2
m/z

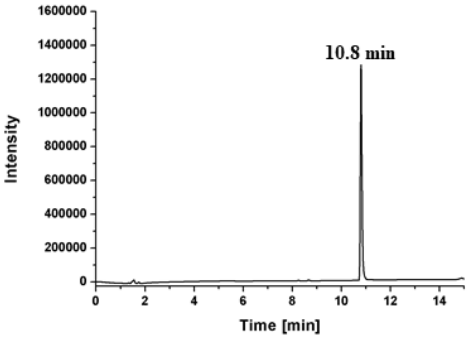
10.8 min
Intensity
Time [min]

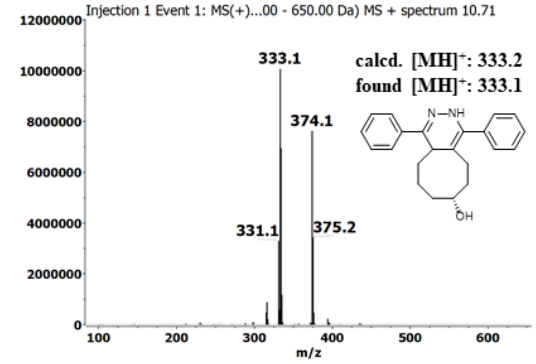
Injection 1 Event 1: MS(+)...00 - 650.00 Da) MS + spectrum 10.71
333.1
374.1
calcd. [MH]+: 333.2
found [MH]+: 333.1
331.1
375.2
m/z

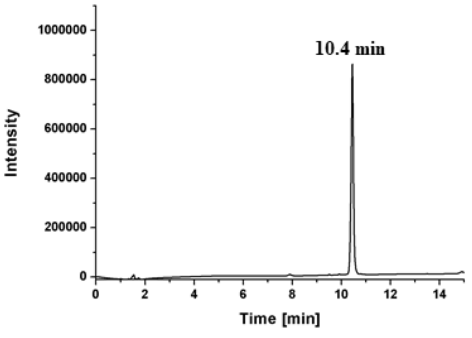
10.4 min
Intensity
Time [min]

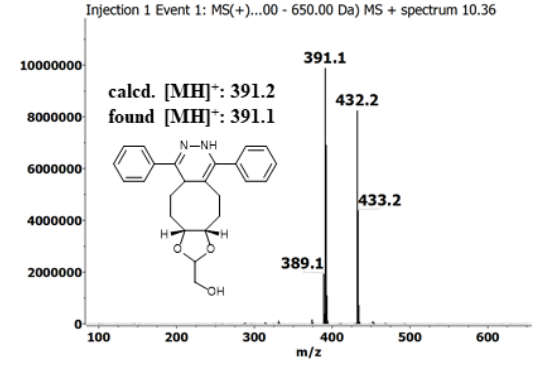
Injection 1 Event 1: MS(+)...00 - 650.00 Da) MS + spectrum 10.36
391.1
432.2
calcd. [MH]+: 391.2
found [MH]+: 391.1
433.2
389.1
m/z

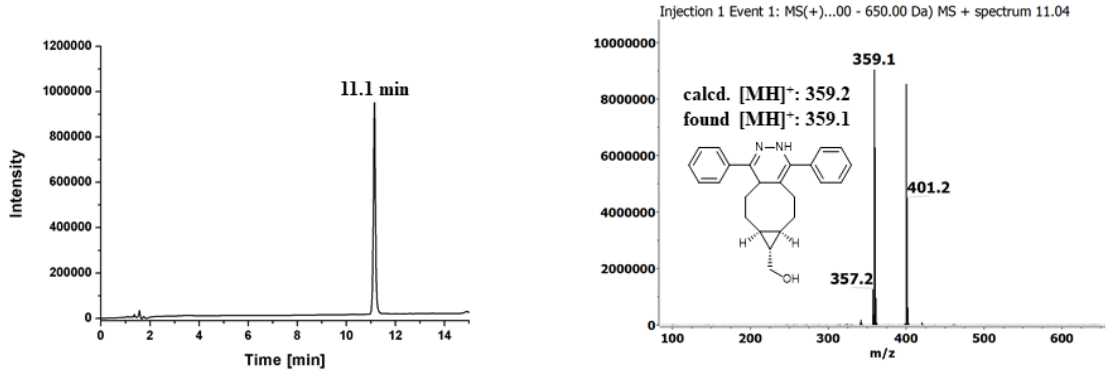


**Figure S3.** HPLC chromatograms and low-resolution mass spectra of the click products of different TCOs with various 1,2,4,5-tetrazines and 1,2,4-triazines performed in $CH_3CN$ containing 5% MeOH and 2.5% $H_2O$ (click with tetrazines) or in $CH_3CN/H_2O$ 1:4 (click with triazines) at room temperature using an excess of the TCO. Please note that peaks in the MS spectra with a mass of the product + 41 are artefacts arising from the adduct of $CH_3CN$ which is used as eluent in the HPLC experiments (solvent A: $H_2O$ + 0.05% HCOOH; solvent B: $CH_3CN$ + 0.05% HCOOH; gradient: 5% B → 95% B in 9 min, then 95% B for 2 min and back to 5% B; column: Luna® C18(2) column (3µm, 100A, 100 × 4.6 mm) or Kinetex® C18 column (2.6µm, 100A, 100 × 4.6 mm) at a flow rate of 1 mL/min).

## Identification and confirmation of the fluorescent species formed upon reaction of aza-TCOs with 1,2,4,5-tetrazines

The following experiments were performed to confirm the identity of fluorophores formed upon reaction of aza-TCOs with 1,2,4,5-tetrazines. These experiments confirmed that it is the 1,4-dihydropyridazine structure which is fluorescent and not the fully aromatic pyridazine.

Calculations:
The UV-Vis absorption spectra of compounds **1a-1** and the corresponding aromatic pyridazine were calculated using a TD-DFT method (*Chem. Soc. Rev.* **2013,** *42*, 845-856 and *Phys. Chem. Chem. Phys.* **2014,** *16*, 14334-14356).

The excitation wavelengths, oscillator strengths and transition dipole moments are summarised in Table S7. The most intensive absorption bands of compound **1a-1** were found at 360, 320 and 267 nm, which is in good agreement with experiment (318 and ~250 nm, see below). The aromatic pyridazine product does not absorb in visible range, the first intensive absorption band is found at 260 nm. Geometry optimization of first excited-state structures of compound **1a-1** and its emission spectra were also calculated using TD-DFT. The most intensive emission band was found at 482 nm (oscillator strength 0.32, transition dipole moment 5.06 AU), which is in excellent agreement with the experiment (emission at 463 nm).

**Table S7.** The calculated (TD-B3LYP/6-31+g(d,p)/PCM) electronic transitions of compounds **1a-1** and the corresponding pyridazine.

| Compound | Transition | $\lambda_{max}$ / nm | Oscillator strength | Transition dipole moment / AU |
|---|---|---|---|---|
| **1a-1** | 1 | 360 | 0.36 | 4.25 |
| | 2 | 320 | 0.14 | 1.45 |
| | 3 | 295 | 0.00 | 0.03 |
| | 4 | 286 | 0.10 | 0.10 |
| | 5 | 267 | 0.29 | 2.52 |
| | 6 | 260 | 0.04 | 0.36 |
| **Pyridazine** | 1 | 327 | 0.01 | 0.12 |
| | 2 | 296 | 0.00 | 0.00 |
| | 3 | 275 | 0.02 | 0.17 |
| | 4 | 274 | 0.01 | 0.07 |
| | 5 | 260 | 0.75 | 6.42 |
| | 6 | 257 | 0.01 | 0.08 |

Synthesis of the oxidized pyridazine product

Aza-TCO **1a** (18,4 mg, 0.11 mmol, 0.1 equiv.) was combined with di-phenyl-s-tetrazine (diPhTet, 23.4 mg, 0.1 mmol) in DMF (2 mL) and the reaction mixture was stirred at room temperature for couple of minutes (discoloration indicates the reaction is complete). TLC in DCM/MeOH = 5/0.25 (fluorescent spot under 365 nm UV lamp). Then 27 mg of DDQ were added to the reaction mixture and stirring continued for 1h at room temperature. The solvent was removed under reduced pressure and the residue was loaded onto silica gel column. The product was isolated as white-yellow powder after chromatography using DCM/MeOH = 5/0.25 as eluent. The product was further purified by RP-HPLC to give 2.5 mg of white powder after lyophilization. Purity of the product was finally verified by HPLC/MS.

$^1$H NMR (MeOD-*d*3, 401 MHz): δ 9.11 (m, 10H), 5.26 (t, 2H), 4.56 (m, 2H), 4.40 (m, 2H), 4.18 (t, 2H), 4.05 (m, 2H), 3.75 (m, 2H), 3.22 (m, 2H).

HRMS (ESI): m/z calcd. for $C_{24}H_{26}N_3O$ $[MH]^+$ 372.20704, found: 372.20708.

To directly compare the photophysical properties of the pyridazine product with the respective 1,4-dihydropyridazine **1a-1** (for synthesis and characterization see the stability studies below) a 10 mM stock solutions of both compounds were prepared in $CH_3CN/H_2O$ mixture = 1/1. For absorbance measurements the solution was further diluted with $CH_3CN$ to final 25 µM. For fluorescence measurements, these solutions were further diluted with $CH_3CN$ to final 2.5 µM. All spectra as well as HPLC chromatograms are summarized in Figure S4.

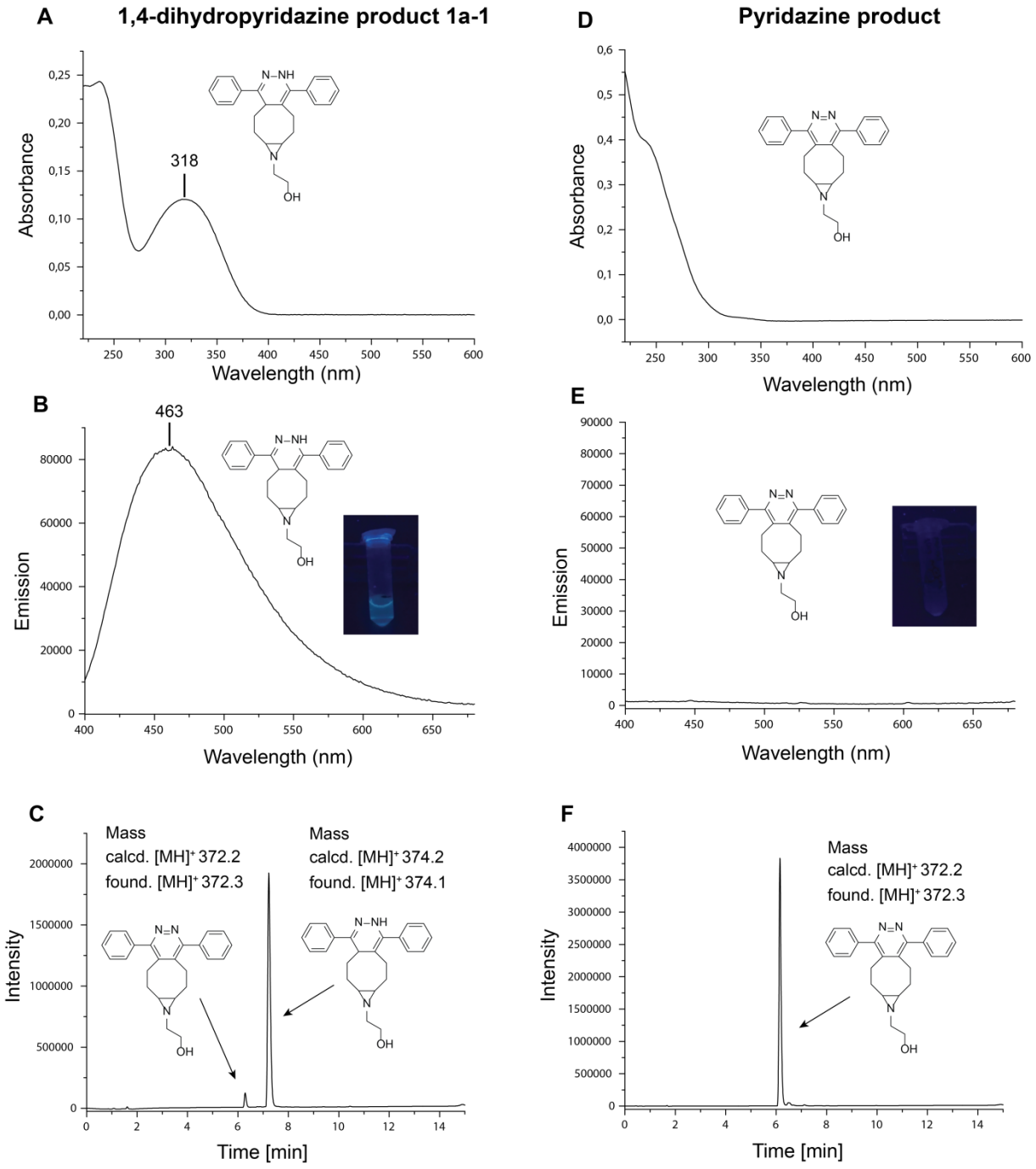


**Figure S4.** Comparison of the absorption, fluorescence spectra and HPLC chromatograms of the 1,4-dihydropyridazine **1a-1** (A, B and C) and the aromatic pyridazine (D, E, F) formed upon reaction of diPhTet with aza-TCO and subsequent oxidation using DDQ. All experiments were performed under identical conditions side-by-side. 25 µM solutions ($CH_3CN$) were used for UV-Vis and 2.5 µM solutions for fluorescence measurements (excitation 350 nm). HPLC experiments (solvent A: $H_2O$ + 0.05% HCOOH; solvent B: $CH_3CN$ + 0.05% HCOOH; gradient: 5% B → 95% B in 9 min, then 95% B for 2 min and back to 5% B; column: Luna® C18(2) column (3µm, 100A, 100 × 4.6 mm).

These experiments confirm that it is the 1,4-dihydropyridazine structure which is responsible for the fluorescence. No fluorescence was observed for the fully aromatic pyridazine product.

Measurements of excitation spectra of the product formed upon reaction of diPyTet with aza-TCO.

The experiment was performed on FluoroMax 4 spectrofluorometer (Jobin Yvon, Horiba) equipped with a 450 W xenon lamp. The settings were as follows: Emission wavelength 474 nm, slit 3.0 nm; Excitation 250-468 nm, increment 1.0 nm, slit 3.0 nm and data algebra formula S1c/R1c. For comparison, the respective absorption spectrum (25 µM in $CH_3CN$) and fluorescence are included as well.

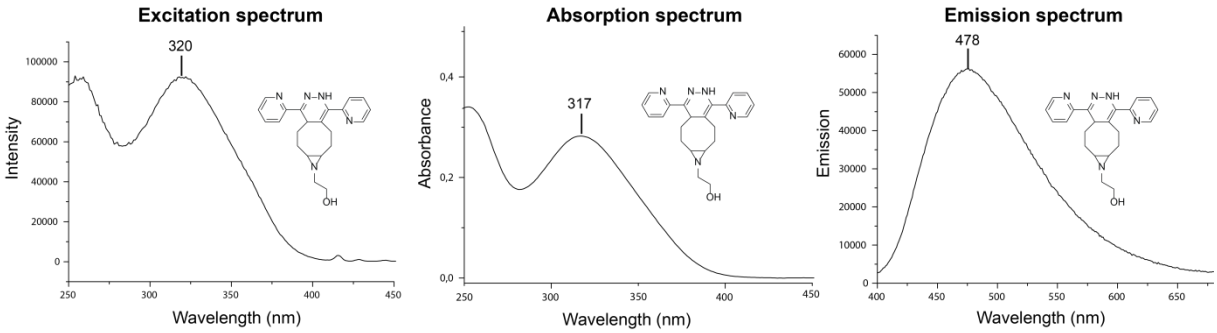


**Figure S5.** Comparison of the excitation, absorption and fluorescence of the product formed upon reaction of diPyTet with aza-TCO.

These experiments further confirm that it is the 1,4-dihydropyridazine structure which gets excited and is responsible for the fluorescence.

The reaction of diPyTet with bicyclo[6.1.0]nonyne (BCN) was performed on preparative scale and the product was isolated by flash column chromatography.

Briefly: BCN (40 mg, 0,266 mmol, 1.25 equiv.) was dissolved/suspended in 3 mL of $CH_3CN/H_2O$=1/1. To this mixture was in portions added diPyTet (50 mg, 0,213 mmol) as a solid. After discoloration of the solution the reaction mixture was evaporated to dryness under reduced pressure and the crude product was purified by normal phase silica gel flash column chromatography using gradient of DCM/MeOH (0 to 15% of MeOH in DCM over 20 min). The product was isolated as white solid 60 mg (78%).

$^1$H NMR (methanol-*d*4, 401 MHz): δ 8.75 (m, 2H), 8.06 (m, 2H), 7.81 (m, 2H), 7.58 (m, 2H), 3.67 (d, 2H), 3.35 (s, 1H), 3.00 (m, 4H), 2.22 (m, 2H), 1.70 (bs, 2H), 1.05 (m, 3H).

$^{13}$C NMR (methanol-*d*4, 101 MHz): δ 161.1, 157.3, 150.0, 144.6, 138.8, 126.1, 125.3, 91.4, 28.7, 24.8, 23.0, 19.8.

HRMS (ESI): m/z calcd. for $C_{22}H_{23}N_4O$ $[MH]^+$ 359.18664, found: 359.18693.

The settings for fluorescence measurements were as follows: Excitation wavelength 350 nm, slit 3.0 nm; Emission 400-680 nm, increment 1.0 nm, slit 3.0 nm and data algebra formula S1c/R1c.

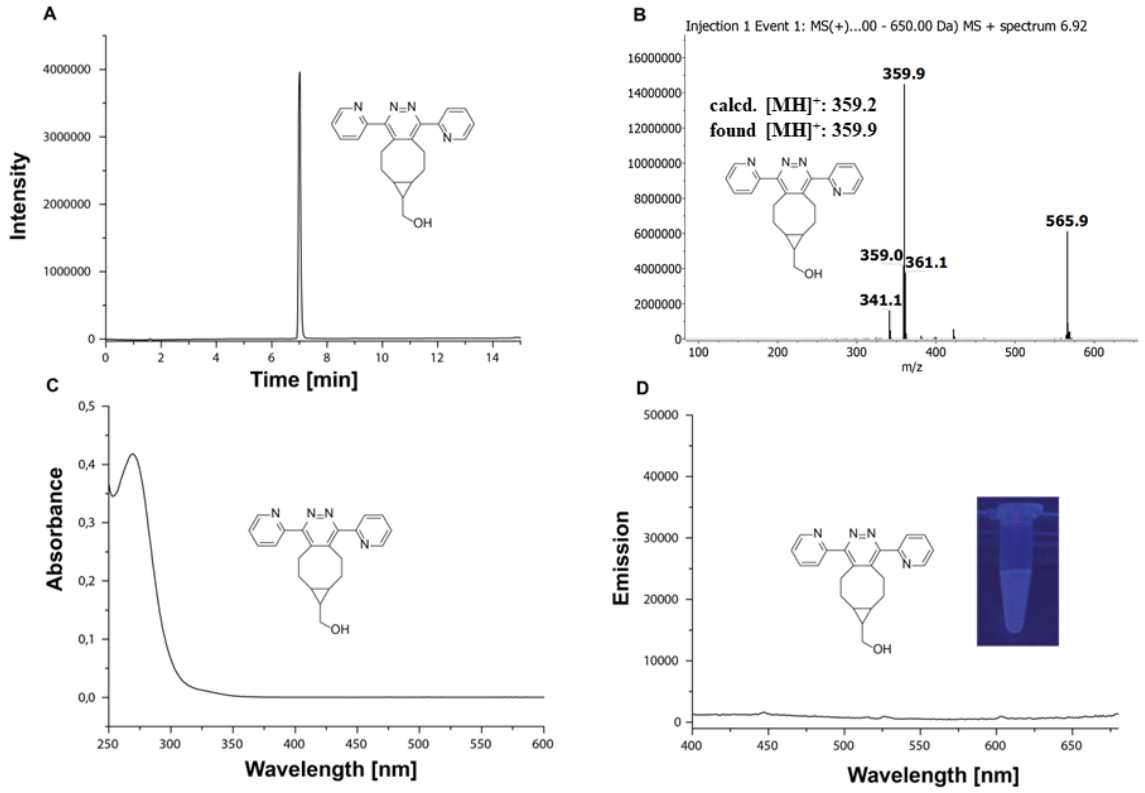


**Figure S6.** A) HPLC chromatogram of the product formed upon reaction of diPyTet with BCN (solvent A: $H_2O$ + 0.05% HCOOH; solvent B: $CH_3CN$ + 0.05% HCOOH; gradient: 5% B → 95% B in 9 min, then 95% B for 2 min and back to 5% B; column: Luna® C18(2) column (3µm, 100A, 100 × 4.6 mm). B) low resolution MS signal of the product. C) Absorption (measured at 25 µM in $CH_3CN$) and D) emission spectra of the product (measured at 2.5 µM in $CH_3CN$, excitation 350 nm, emission 400-680 nm).

# Photophysical properties of the click products of aza-TCO 1a with various 1,2,4,5-tetrazines

## Determination of fluorescence quantum yields

Quantum yields of click products were measured at 22 °C in $CH_3CN$ (1.25 µM final concentration) using a 1 cm quartz cuvette. The experiment was performed on FluoroMax 4 spectrofluorometer (Jobin Yvon, Horiba) equipped with a 450 W xenon lamp using Quinine Sulfate (solution in 0.5 M $H_2SO_4$) as reference ($\phi_{QS}$ = 0.55). The settings were as follows: Excitation wavelength 350 nm, slit 3.0 nm; Emission 400-680 nm, increment 1.0 nm, slit 3.0 nm and data algebra formula S1c/R1c. The fluorescence quantum yields were calculated using the following equation:

$$\phi_{sample} = \phi_{ref} \frac{F_{sample}}{F_{ref}} \times \frac{(1-10^{-abs})_{ref}}{(1-10^{-abs})_{sample}} \times \frac{n^2_{sample}}{n^2_{ref}}$$

Where:

$\phi_{ref}$ is 0.55 (Quantum yield of Quinine sulfate in 0.5 M $H_2SO_4$)[16]

**F** are the integrated intensities (areas) of standard and the sample fluorescence spectra (integrals calculated using OriginPro software)

**abs** is the absorbance of standard and sample at the excitation wavelength (350 nm)

***n*** are the refractive indices for standard (1.333) and the sample solution (1.3404)

## Table of photophysical properties of the click products using aza-TCO 1a

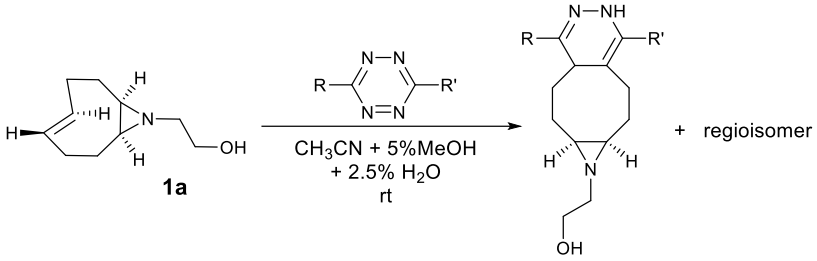


**Table S8.** Photophysical properties of the click products of **1a** with various 1,2,4,5-tetrazines[a].

| Starting tetrazine | Click product | $\lambda_{Abs}/\lambda_{Em}$ [b] [nm] | Stokes shift [nm] | $\phi$ [c] | Fl. intensity increase [d] | $\varepsilon_{max}$ ($\times 10^3$ $M^{-1}$ $cm^{-1}$) |
|---|---|---|---|---|---|---|
| 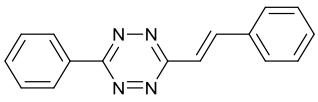 | 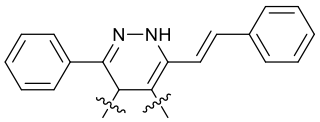 | 333/501 | 168 | 0.07 | 60-fold | 21.3 |
| 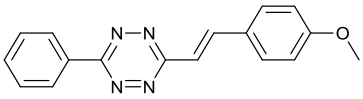 | 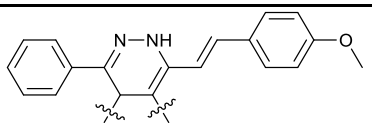 | 321/475 | 154 | 0.15 | 55-fold | 15.7 |
| 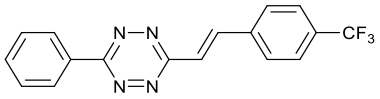 | 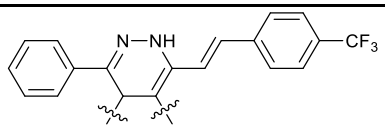 | 337/540 | 203 | 0.04 | 40-fold | 22.6 |
| 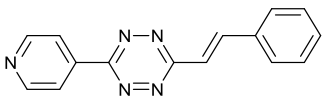 | 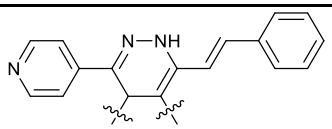 | 335/489 | 154 | 0.11 | 70-fold | 16.6 |
| 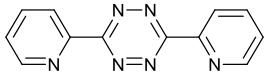 | 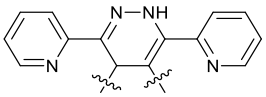 | 317/476 | 159 | 0.06 | 20-fold | 11.5 |

a) all reactions were performed in $CH_3CN$ containing 5% MeOH and 2.5% $H_2O$ at room temperature using an excess of the TCO, b) absorption and emission maxima were measured in $CH_3CN$, c) quantum yields were determined by using quinine sulfate in 0.5 M $H_2SO_4$ as standard ($\phi$ = 0.55), d) calculated as the integral of the fluorescence of the click product divided by the integral of the fluorescence of the starting tetrazine.

## Absorption and emission spectra of the click products and starting tetrazines

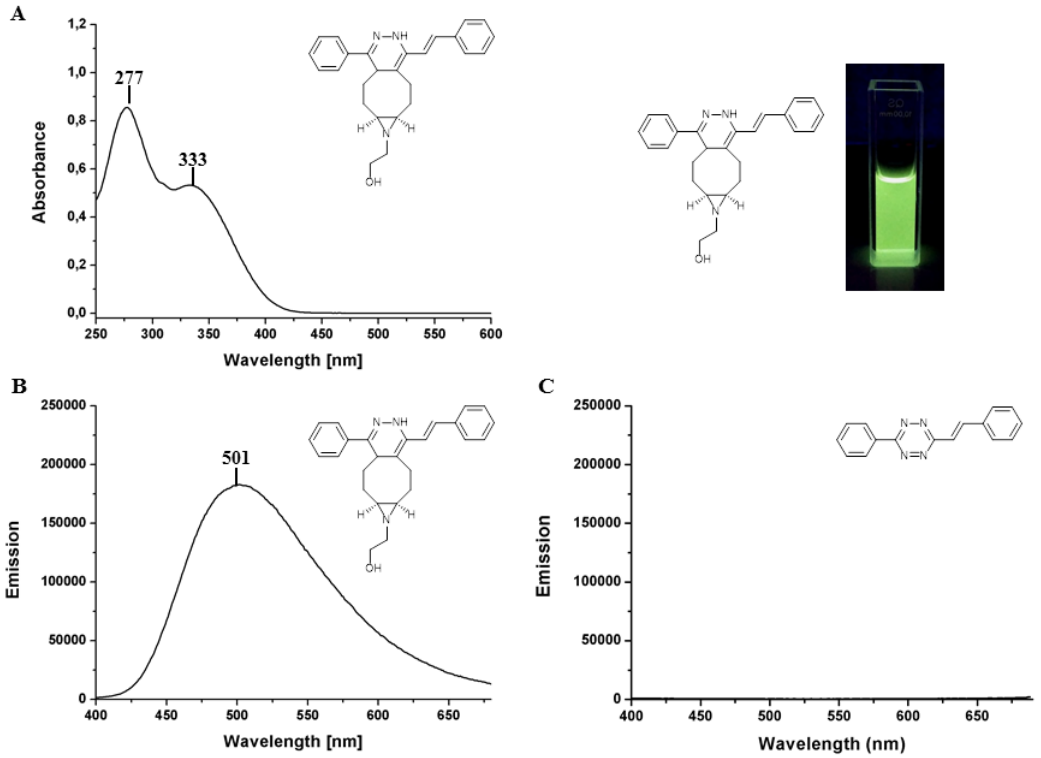


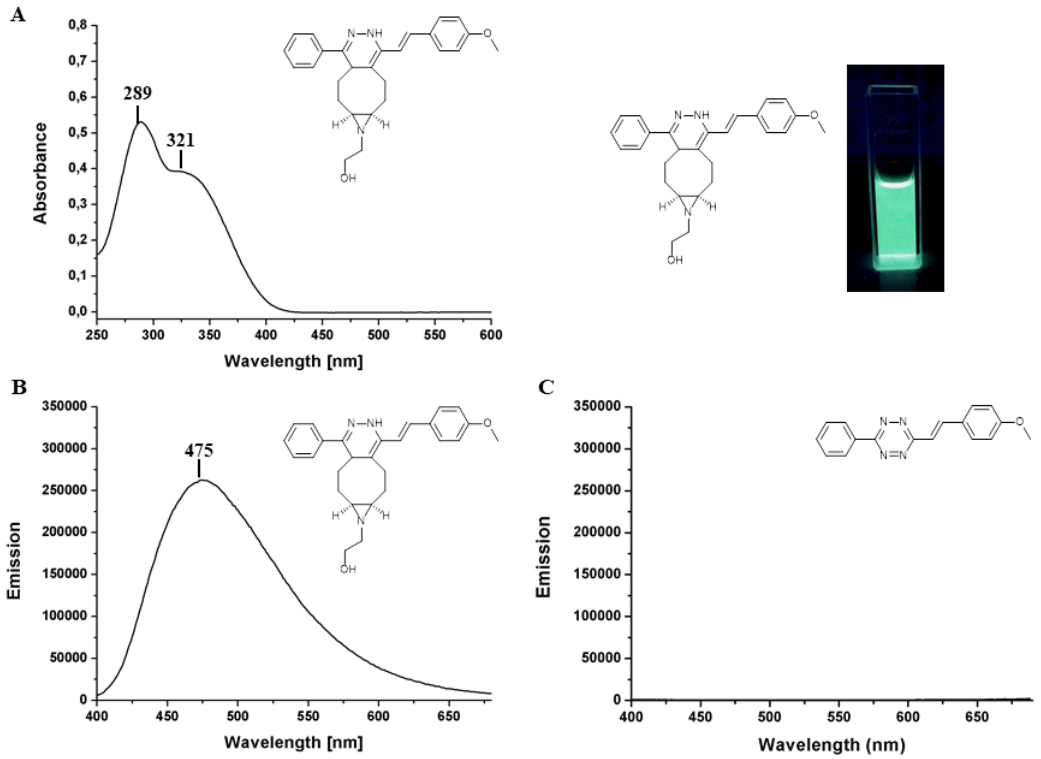

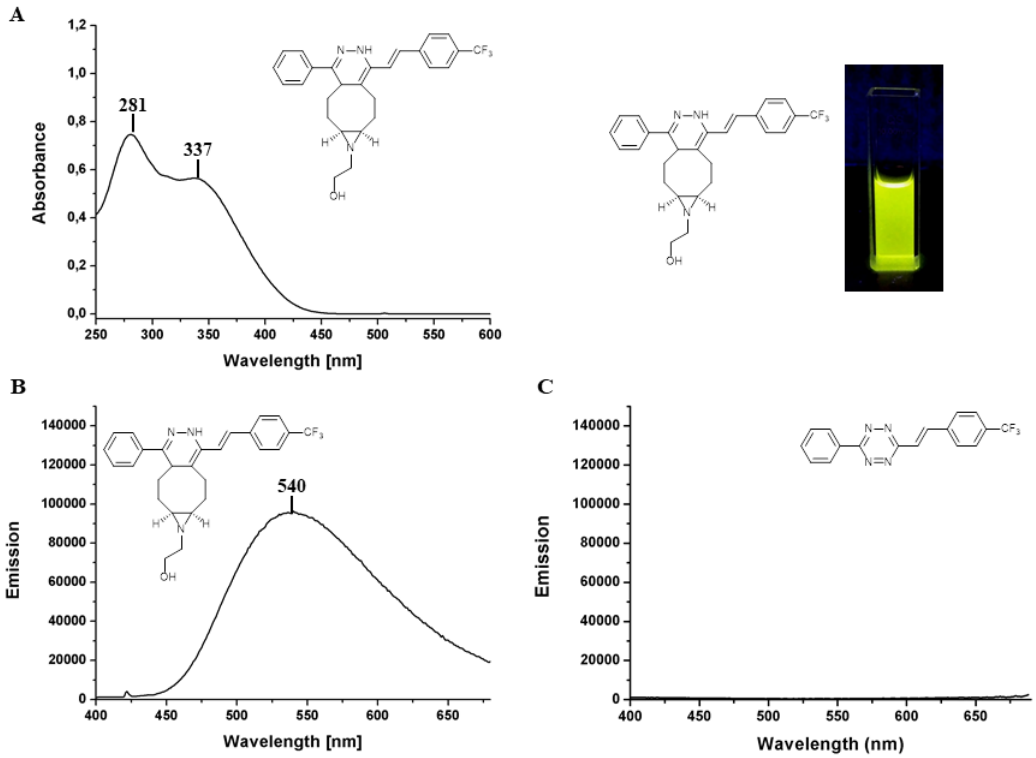
A
Absorbance
Wavelength [nm]
281
337
B
Emission
Wavelength [nm]
540
C
Emission
Wavelength (nm)

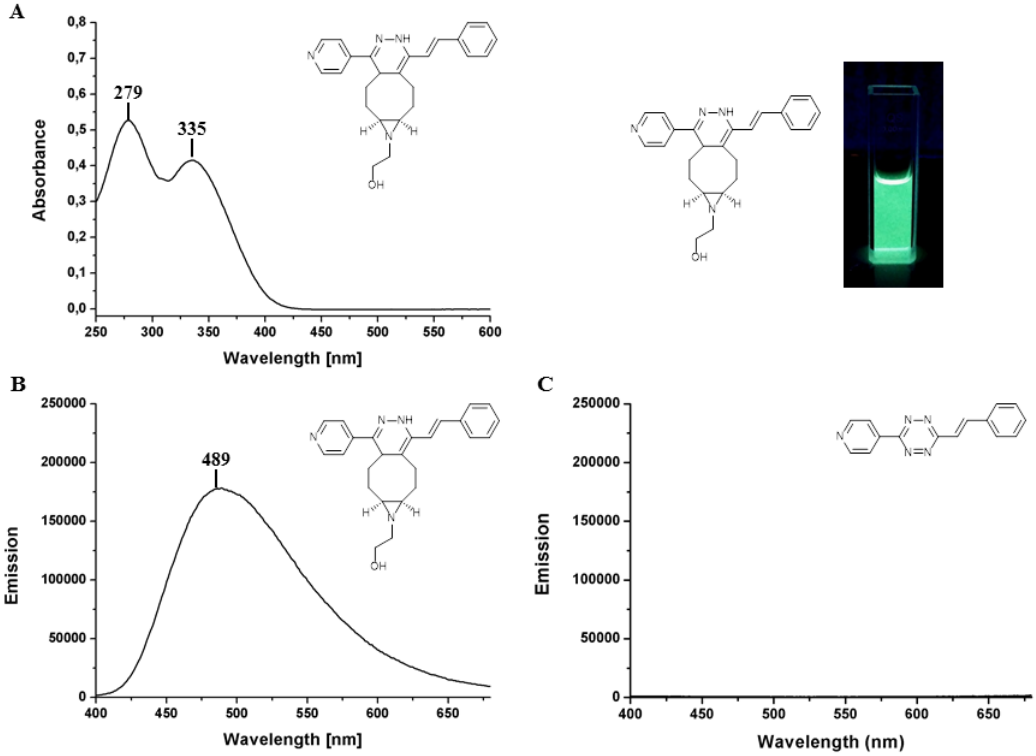
A
Absorbance
Wavelength [nm]
279
335
B
Emission
Wavelength [nm]
489
C
Emission
Wavelength (nm)

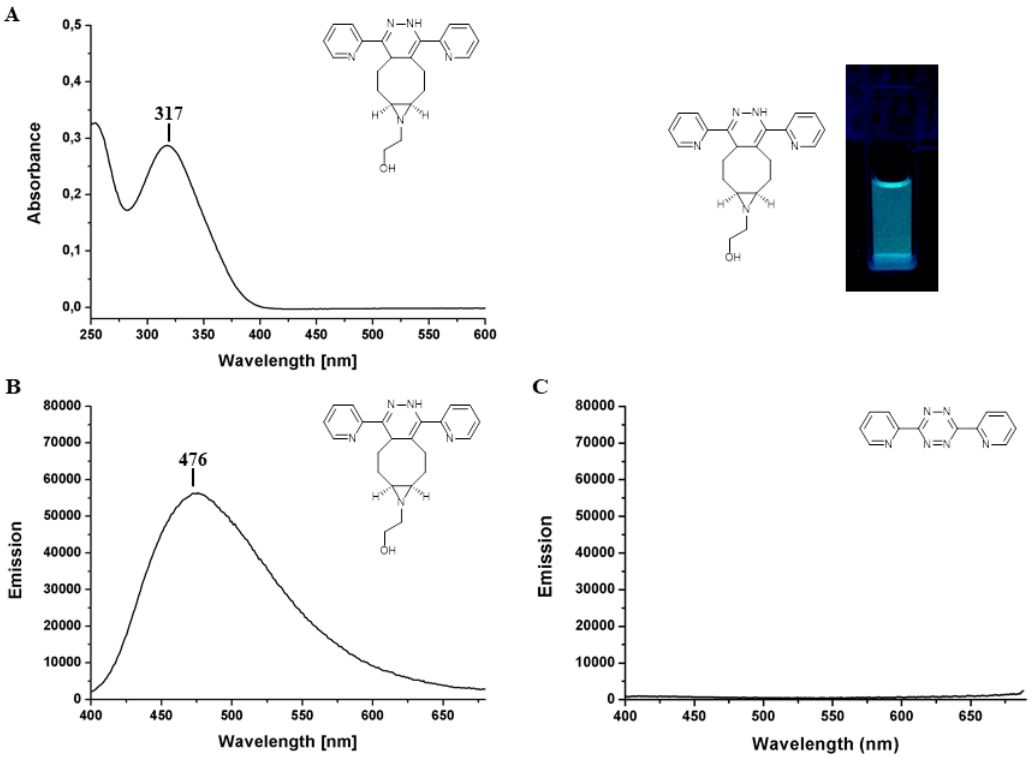


**Figure S7.** Absorption and emission spectra of the click products of **1a** with various 1,2,4,5-tetrazines (A and B, respectively) and emission spectra of the 1,2,4,5-tetrazines alone (C) measured in $CH_3CN$ at room temperature (25 µM for absorbance and 1.25 µM for fluorescence measurements).

## Comparison of the fluorogenic properties of the click reaction of di-Py-Tet with different TCOs and BCN

For TCOs:

100 µL of a 5 mM solution of 3,6-di(2-pyridyl)-1,2,4,5-tetrazine in $CH_3CN$ were added to 250 µL of a 5 mM solution of the appropriate TCO in $CH_3CN/H_2O$ 1:1 and diluted with $CH_3CN$ and $H_2O$. The final concentration of the tetrazine was 1 mM in $CH_3CN/H_2O$ 1:1 using 2.5 equiv. of TCO. The solutions were incubated at room temperature for 15 min and then measured by HPLC-MS (diluted 1:4 with $H_2O$) to verify the formation of the corresponding click products. HPLC-MS measurements were performed on a Luna® C18(2) column (3µm, 100A, 100 × 4.6 mm) using a linear gradient of $CH_3CN$ + 0.05% HCOOH (5 → 95% in 9 min) in $H_2O$ + 0.05% HCOOH at a flow rate of 1.0 mL/min.

For absorbance measurements these stock solutions were diluted with $CH_3CN$ to a concentration of 25 µM and for fluorescence measurements further to 1.25 µM.

The data are summarized in Figure S8.

**Absorption and emission spectra, HPLC chromatograms and low-resolution mass spectra of the click products**

1) aza-TCO + 3,6-di(2-pyridyl)-1,2,4,5-tetrazine:

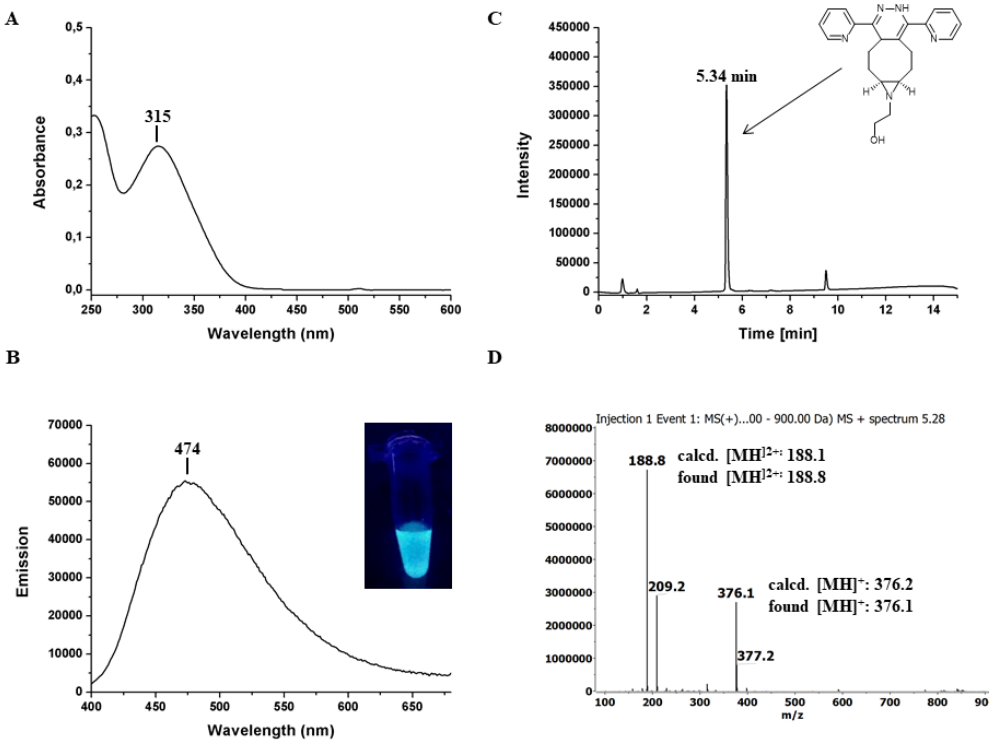


2) d-TCO + 3,6-di(2-pyridyl)-1,2,4,5-tetrazine:

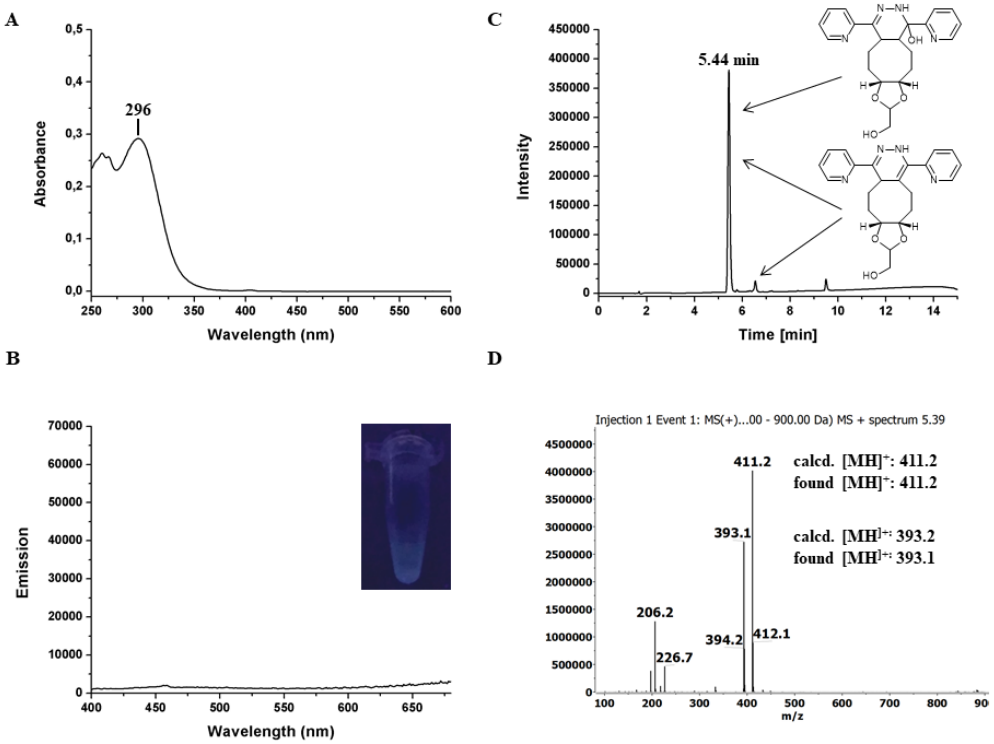

3) s-TCO + 3,6-di(2-pyridyl)-1,2,4,5-tetrazine:

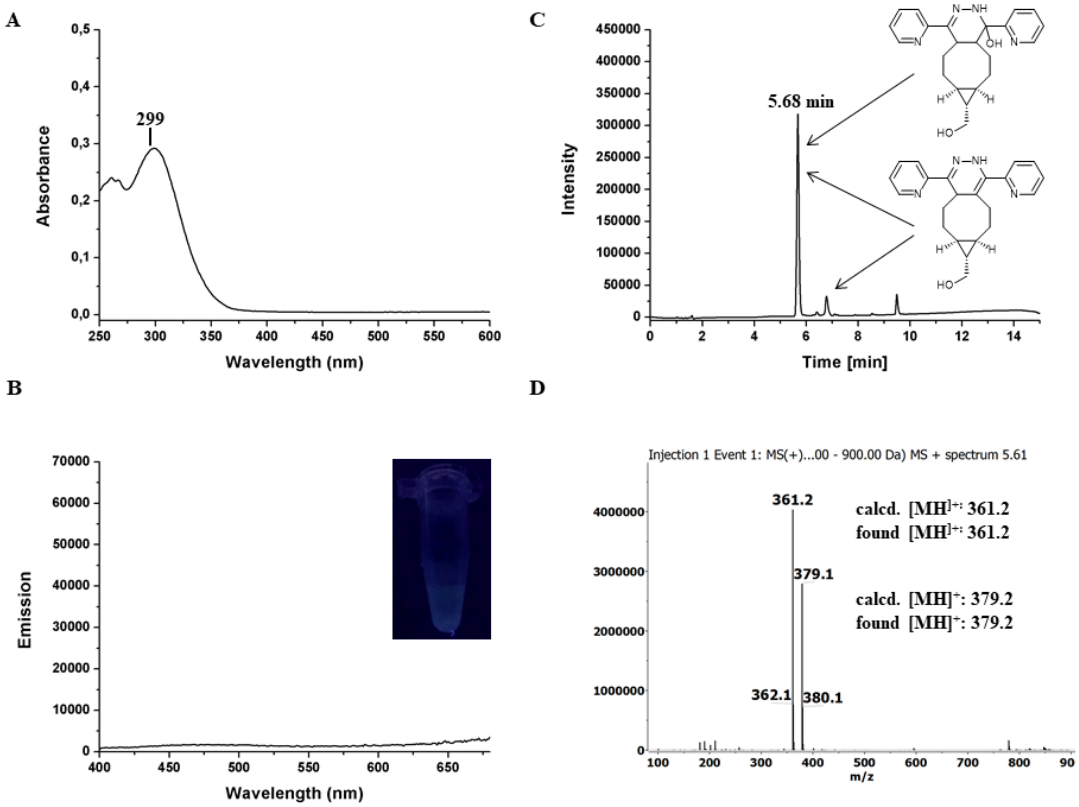


**Figure S8.** Absorption (A) and emission (B) spectra, HPLC chromatograms (C) and corresponding low-resolution mass spectra (D) of the click products of 3,6-di(2-pyridyl)-1,2,4,5-tetrazine with 1) aza-TCO, 2) d-TCO and 3) s-TCO performed in $CH_3CN/H_2O$ 1:1 at room temperature using an excess of the TCO. A and B were each measured in $CH_3CN$ at room temperature (25 µM for absorbance and 1.25 µM for fluorescence measurements). For C and D the samples were diluted 1:4 with $H_2O$ for the HPLC-MS measurements (solvent A: $H_2O$ + 0.05% HCOOH; solvent B: $CH_3CN$ + 0.05% HCOOH; gradient: 5% B → 95% B in 9 min, then 95% B for 2 min and back to 5% B; column: Luna® C18(2) column (3µm, 100A, 100 × 4.6 mm). Note: signals in HPLC-MS having the mass of the product +18 (for d-TCO and s-TCO) also gave signal of the product alone in MS probably as a result of fragmentation in the MS detector. Pictures of fluorescent products in polypropylene tubes were captured using hand-held UV lamp (365 nm irradiation).

## Determination of second-order rate constants

Second order rate constants of the reactions between *trans*-cyclooctenes (TCO) and 1,2,4,5-tetrazines or 1,2,4-triazines were determined by following the decay in the concentration of the starting tetrazine or triazine over time. The concentration decrease was monitored by UV/VIS spectroscopy using a manual stopped-flow device connected to the UV/VIS spectrophotometer for measurements with tetrazines (faster kinetics). The measurements were performed either in MeOH (for tetrazines) or in $CH_3CN/H_2O$ 1:1 (for triazines) at room temperature under pseudo first-order conditions using an excess of the corresponding TCO. All measurements were performed at least three times.

To compare the reactivity of various TCOs with diPhTet we performed the measurements using 25 µM solution of diPhTet in MeOH (final concentration) and an excess of TCO (5 equiv., 7.5 equiv and 10 equiv.) The observed rate constants were plotted against concentration of the TCO and finally the second order rate constants were calculated from the slope of this plot. The results are summarized in Table S9.

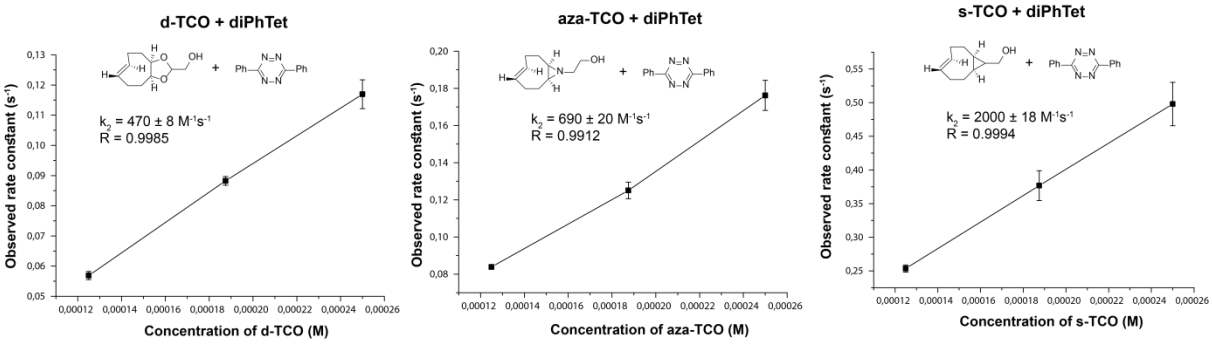


**Table S9.** Second-order rate constants (in $M^{-1}$ $s^{-1}$) of the reaction between 3,6-diphenyl-1,2,4,5-tetrazine and various TCOs[a].

| **Tetrazine** | 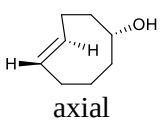 axial | 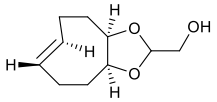 syn:anti 12:1 | 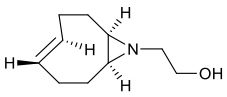 | 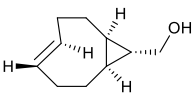 syn |
|---|---|---|---|---|
| 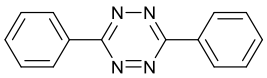 | 38 ± 3 | 470 ± 8 | 690 ± 20 | 2000 ± 18 |

a) all reactions were performed in MeOH at room temperature using a manual stopped-flow device connected to the UV/Vis spectrophotometer under pseudo first-order conditions using an excess of the corresponding TCO. The rate constants were determined at 294 nm.

Rate determination with other tetrazines: A 50 µM solution of the respective tetrazine in MeOH was mixed with a 250 µM solution of the appropriate TCO in MeOH by manual stopped-flow device in flow cell to give a final tetrazine concentration of 25 µM using 5 eq. of TCO.

Rate determination with triazines: A 25 mM solution of the respective triazine in $CH_3CN/H_2O$ 1:1 and a 25 mM solution of **1a** in $CH_3CN/H_2O$ 1:1 were added to $CH_3CN/H_2O$ 1:1 to give a final volume of 3 mL. The mixture had a final triazine concentration of 50 µM using 10 equiv. of **1a** and was immediately measured on the UV/VIS spectrophotometer.

The measurements were performed at the corresponding absorption maxima of the tetrazines or triazines, which were determined by UV/VIS spectroscopy before the measurement (see Table S10). The measured intensity of the absorption was plotted against time. Fitting the curves with single exponential equation ($y = y_0 + Ae^{-k/t}$) provided the observed rate constants. The second order rate constants were calculated by dividing the observed rate constants by the initial concentration of the TCO. All data were processed using Origin or Excel software and are summarized in Table S10.

The formation of the corresponding click products was verified by HPLC-MS measurements on a Luna® C18(2) column (3µm, 100A, 100 × 4.6 mm) using a linear gradient of $CH_3CN$ + 0.05% HCOOH (5 → 95% in 9 min) in $H_2O$ + 0.05% HCOOH at a flow rate of 1.0 mL/min. All found low-resolution masses are summarized in Table S5 and S6.

**Table S10.** Absorption maxima of 1,2,4,5-tetrazines and 1,2,4-triazines used during kinetic measurements and the corresponding second-order rate constants (in $M^{-1}$ $s^{-1}$) of the reactions with **1a**.

| **Triazine/Tetrazine** | **$\lambda_{Abs}$ [nm]**[a] | 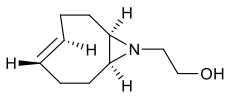 |
|---|---|---|
| 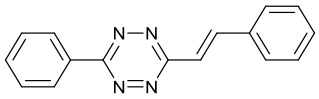 | 328 | 318 ± 3[b] |
| 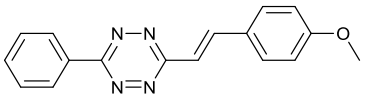 | 354 | 255 ± 7[b] |
| 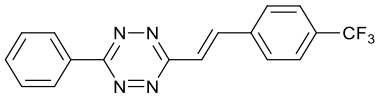 | 320 | 316 ± 2[b] |
| 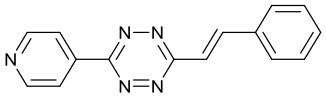 | 332 | 740 ± 25[b] |
| 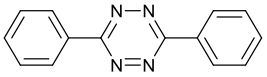 | 294 | 680 ± 12[b] |
| 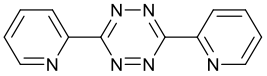 | 295 | 6360 ± 90[b] |
| 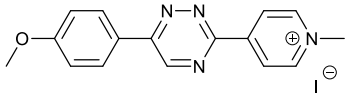 | 357 | 2.00 ± 0.09[c] |
| 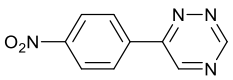 | 289 | 9.34 ± 0.85[c] |

a) absorption maxima were determined in MeOH (for tetrazines) or in $CH_3CN/H_2O$ 1:1 (for triazines) at room temperature using a 25 mM solution of the respective tetrazine or triazine b) determined in MeOH at room temperature using a manual stopped-flow device connected to the UV/Vis spectrophotometer under pseudo first-order conditions using an excess of **1a**, c) determined in $CH_3CN/H_2O$ 1:1 at room temperature under pseudo first-order conditions using an excess of **1a**.

## Stability studies

### Stability of 1a in $CD_3OD$

**1a** (5 mg) was dissolved in methanol-*d4* (0.6 mL) and the sample was measured at indicated time points. The NMR spectra were acquired at room temperature on a spectrometer operating at 401 MHz. Meanwhile the sample was stored at room temperature covered with aluminum foil.

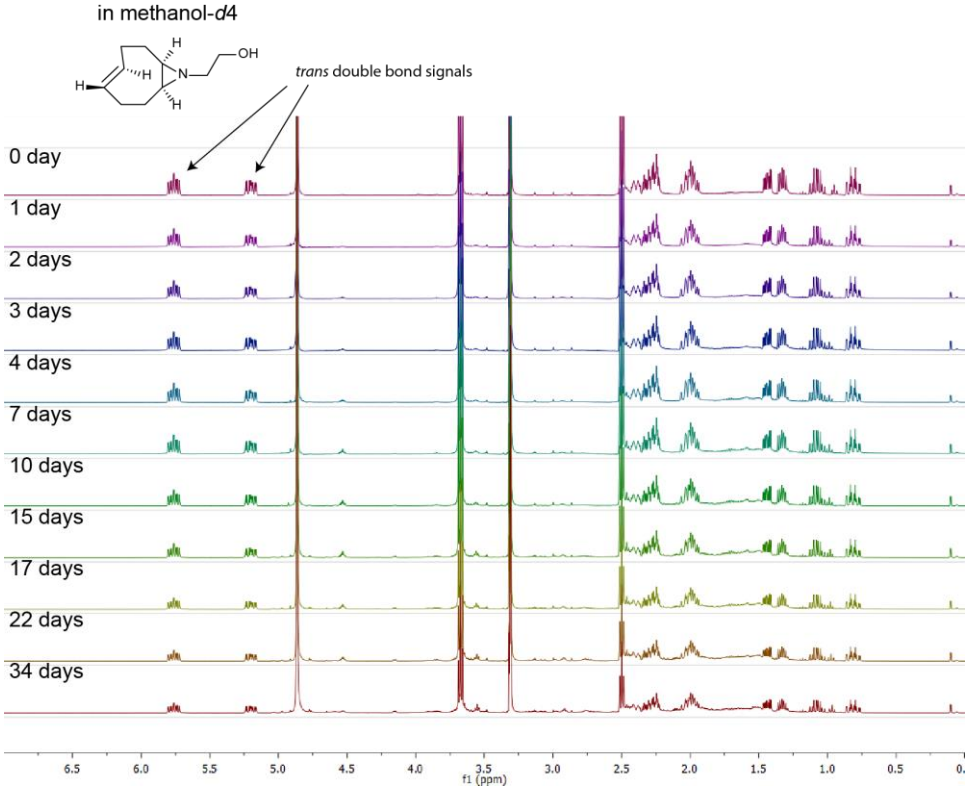


**Figure S9.** Stability of **1a** in $CD_3OD$ as determined by NMR spectroscopy.

### Stability of 1a in the presence of L-cysteine

To a solution of **1a** (1 mg, 0.006 mmol) in 50 mM deuterated phosphate buffer (500 µL, pD 7.4) and $CD_3CN$ (100 µL) was added L-cysteine (2.7 mg, 0.022 mmol). The solution was monitored by $^1H$ NMR spectroscopy to observe the *trans* to *cis* isomerization of **1a**.Waterfall plot from the measurements is shown in Figure S10.

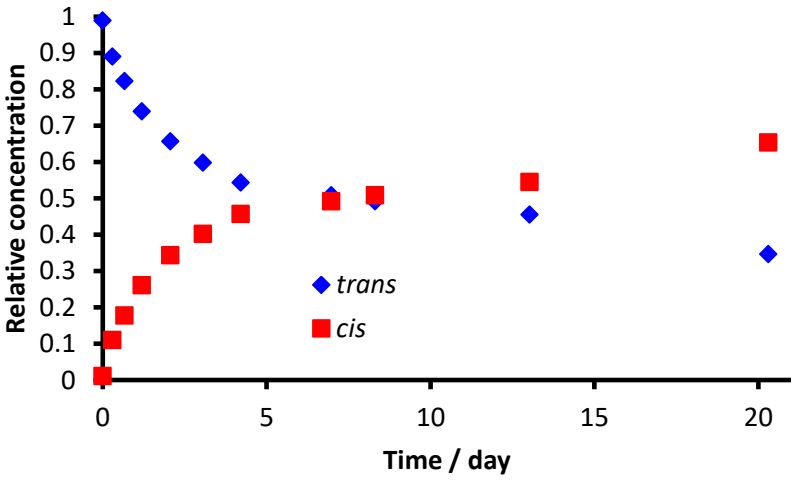


**Figure S10**. The *trans* to *cis* isomerization of compound **1a** in the presence of 3.5 equivalents of L-cysteine.

## Stability of the click products

### Reaction of 1a with diphenyl-*s*-tetrazine and dipyridyl-*s*-tetrazine

To a solution of **1a** (18.4 mg, 1.1 equiv.) in $CH_3CN/H_2O$ 4:1 (5 ml) was in portions added diphenyl-*s*-tetrazine (23.4 mg, 1 equiv.) or dipyridyl-*s*-tetrazine (23.6 mg, 1 equiv.) as a solid. The reaction mixture was stirred at room temperature until the red color of the tetrazine disappeared. The crude reaction mixture was concentrated under reduced pressure and was purified by silica gel column chromatography using DCM/MeOH 20:1 as the eluent. Further purification by semi-preparative RP-HPLC (gradient of $CH_3CN$ in $H_2O$, 5 to 90% in 30 min) afforded 30 mg (80%) of **1a-1** and 31 mg (80%) of **1a-2** respectively.

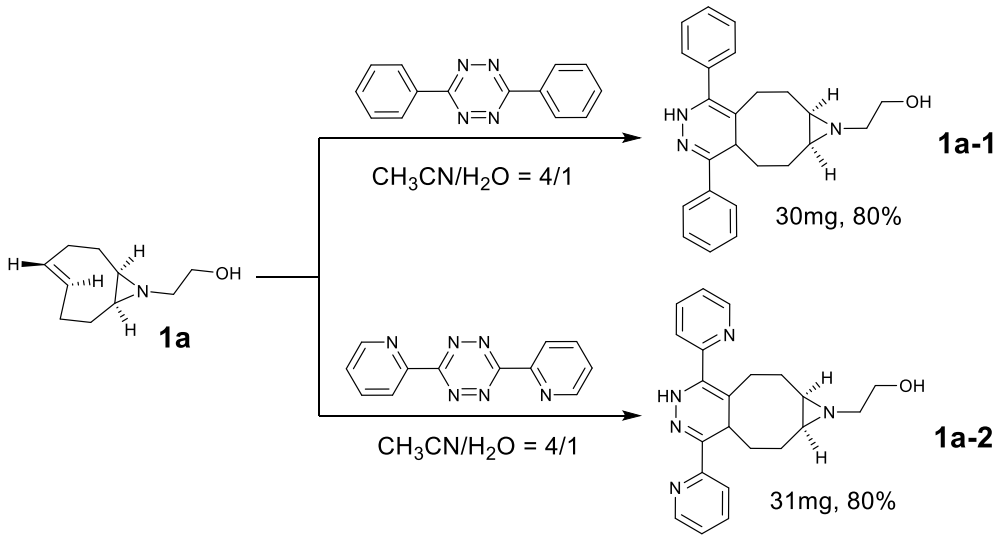


**1a-1:**

$^1$H NMR (DMSO-*d*6, 401 MHz): δ 9.80 (s, 1H), 7.82 (d, 2H), 7.49–7.30 (m, 8H), 4.43 (m, 1H), 3.82 (m, 1H), 3.53 (q, 2H), 2.39 (m, 2H), 2.24 (d, 2H), 1.82 (m, 1H), 1.69–1.52 (m, 3H), 1.47–1.15 (m, 4H).

$^{13}$C NMR (DMSO-*d*6, 101 MHz): δ 138.5, 136.3, 136.2, 134.9, 129.2, 128.5, 128.3, 128.2, 127.8, 125.4, 103.25, 79.2, 62.4, 60.9, 41.7, 41.6, 36.2, 30.9, 29.1, 24.2, 22.5.
HRMS (ESI): m/z calcd. for $C_{24}H_{28}N_3O$ $[MH]^+$ 374.2227, found: 374.2227.

**1a-2:**
$^1$H NMR (methanol-*d*4, 401 MHz): δ 8.65 (d, 1H), 8.54 (d, 1H), 8.11 (d, 1H), 7.90 (m, 1H), 7.79 (m, 1H), 7,53 (d, 1H), 7.41 (m, 1H), 7.32 (m, 1H), 4.34 (m, 1H), 3.79 (t, 2H), 2.82 (t, 2H), 2.72 (m, 1H), 2.52 (m, 1H), 2.40 (m, 2H), 2.04 (m, 1H), 1.87 (m, 1H), 1.75–1.40 (m, 4H).
$^{13}$C NMR (methanol-*d*4, 101 MHz): δ 146.2, 144.1, 141.0, 140.1, 133.0, 128.9, 128.4, 127.9, 116.2, 115.2, 114.7, 113.0, 99.8, 51.8, 51.4, 36.4, 36.3, 27.5, 20.2, 19.8, 15.2, 13.0.
HRMS (ESI): m/z calcd. for $C_{22}H_{26}N_5O$ $[MH]^+$ 376.2133, found: 376.2132.

The compounds were then incubated at 37 °C in a mixture of $CH_3CN$/phosphate buffer (PBS, pH 7.4) 1:1 and analyzed by HPLC-MS over time (Figure S11A and S11B).
Additionally, the stability of click product **1a-2** was also measured in PBS (pH 7.4) only as well as in fetal bovine serum/$H_2O$ 1:1. For these stability studies, 80 µL of a 12.5 mM solution of dipyridyl-*s*-tetrazine in MeOH were mixed with 80 µL of a 25 mM solution of **1a** (2 equiv.) in MeOH and diluted with either PBS or fetal bovine serum/$H_2O$ 1:1 to a final volume of 1 mL. The reaction mixtures were incubated at 37 °C and analyzed over time by HPLC-MS (Figure S11C and S11D).
We observed the formation of the fully aromatic pyridazines as the major side-product in all cases. Waterfall plots were generated from the raw HPLC-MS data using OriginPro software (Figure S8).

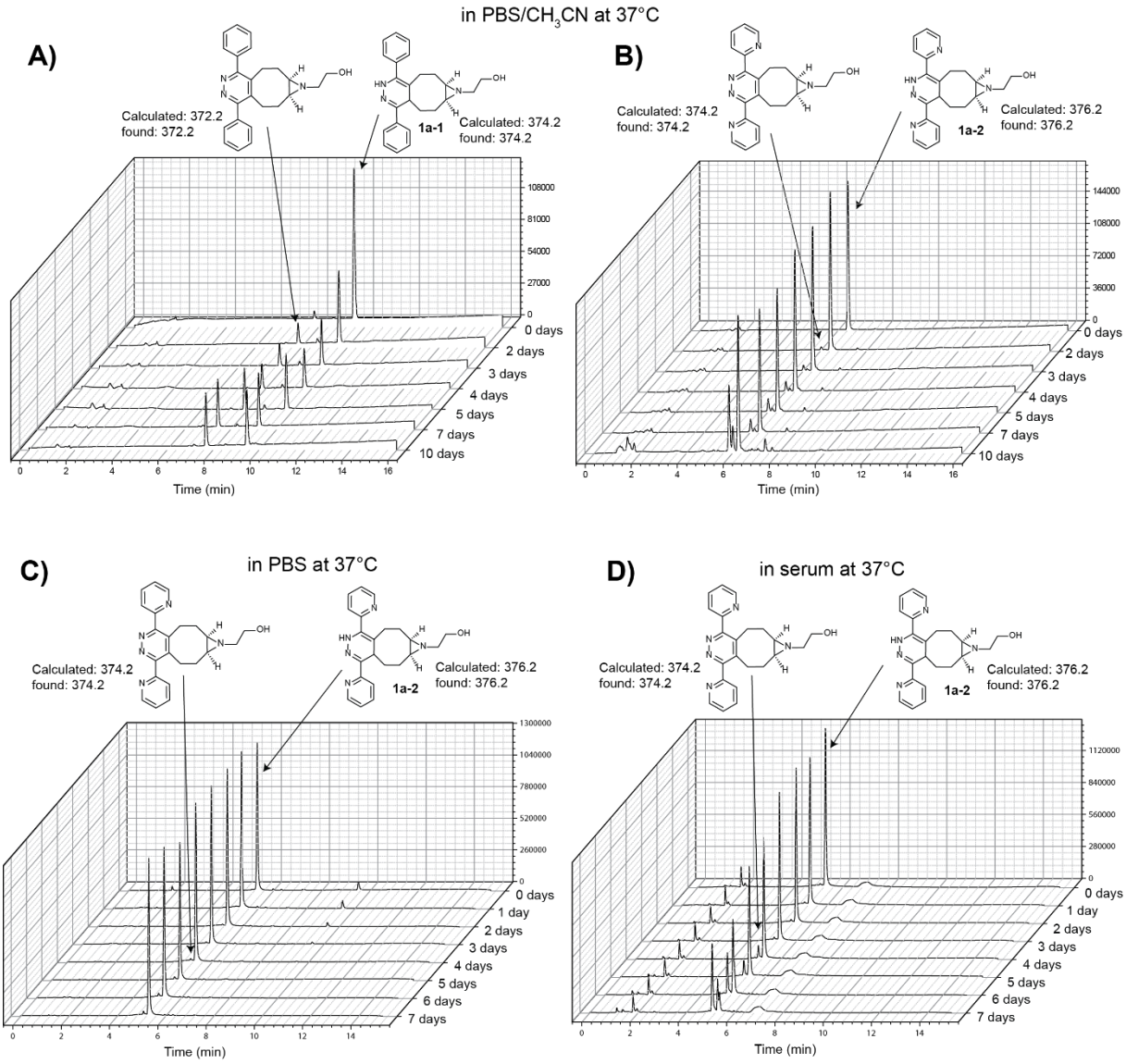


**Figure S11.** Stability measurements: Stability of A) **1a-1** in PBS/$CH_3CN$ 1:1 at 37 °C, B) **1a-2** in PBS/$CH_3CN$ 1:1 at 37 °C, C) **1a-2** in PBS at 37 °C and D) **1a-2** in fetal bovine serum/$H_2O$ 1:1 at 37 °C as measured by HPLC-MS. The corresponding signals of the products are indicated by arrows.

# Fluorogenic click-labeling of model peptide KYHWYGYTPQNVI

## Synthesis of KYHWYGYTPQNVI model peptide

YHWYGYTPQNVI peptide was synthesized on TentaGel S-OH resin (particle size 130 µm; from *Iris Biotech GmbH*) using standard Fmoc chemistry on a PS3 peptide synthesizer from *Protein Technologies Inc.*. The first amino acid was manually attached to the resin as a symmetrical anhydride (generated in situ using 10 equiv. of amino acid and 5 equiv. of DIC in DCM at 0 °C), further coupling steps used 3.3 equiv. of amino acid and HBTU in DMF containing 0.2 M N-methylmorpholine (NMM) for 20 min. After removal of the Fmoc

protecting group (20% piperidine (v/v) in DMF, 3 × 5 min) the N-terminal lysine was added manually (6.6 equiv. of amino acid and HBTU, 45 min) and the N-terminus was capped with acetic anhydride (7.5% $Ac_2O$ and 7.5% NMM (v/v) in DMF, 1 h).

## Fluorogenic click-labeling of aza-TCO-KYHWYGYTPQNVI peptide on Tentagel resin with various tetrazines

30 mg of the model peptide on Tentagel S-OH resin were washed with DCM (5 × 2 mL) and dried *in vacuo*. The side-chain protecting groups were removed by shaking the beads in a mixture of TFA/TIPS/$H_2O$ 95:2.5:2.5 (300 µL) for 1 h at room temperature. Afterwards the beads were filtered and washed with DCM (5 × 2 mL) and DMF (5 × 2 mL) and dried *in vacuo*. A small amount of the resin (ca. 3 mg) was taken for cleaving of the peptide from the resin to verify the formation of the peptide by HPLC-MS (conditions see below, Figure S10).
A solution of TCO active ester **1b** (3 mg) in DMF (250 µL) was added to the rest of the resin beads, followed by DIPEA (5 µL). The reaction mixture was shaken at room temperature for 2 h in the dark and the beads were washed with DMF (5 × 2 mL) and DCM (5 × 2 mL). The modification of the peptide with aza TCO (Scheme S1) was verified by taking a small amount of the resin (ca. 3 mg), cleaving the modified peptide from the beads and analysis by HPLC-MS (conditions see below, Figure S11).

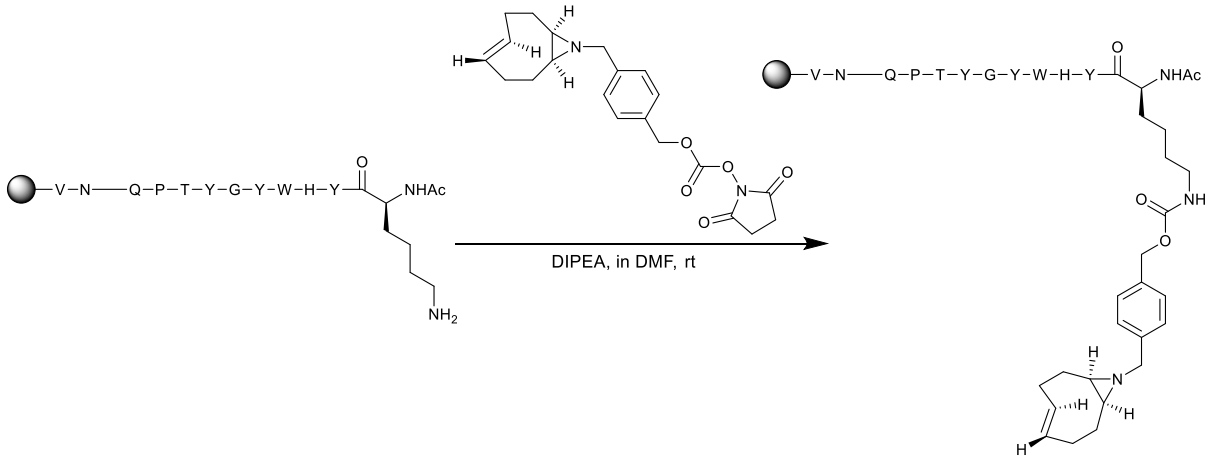


**Scheme S1.** Peptide KYHWYGYTPQNVI modified with TCO active ester **1b**.

The remaining resin was divided up into 3 PP vials and each was suspended in DMSO/$H_2O$ 1:1 (100 µL). Then to each vial was added a different tetrazine (5 mg, Scheme S2 and Figure S12) dissolved in DMF (200 µL) until the reddish color of the tetrazine persisted (excess of the tetrazine). The beads were shaken at room temperature for 30 min and washed with $CH_3CN$ (3 × 200 µL) and DMF (2 × 200 µL). After taking another small amount (ca. 3 mg) of each vial for cleaving and analysis by HPLC-MS (conditions see below, Figure S15-S17) to verify the success of click reactions, the beads were transferred to a glass slide and were inspected under a fluorescence stereomicroscope. The pictures were captured by a DFC3000 G grayscale camera using UV excitation (350 nm) and later processed by LAS AF software (Figure S12).

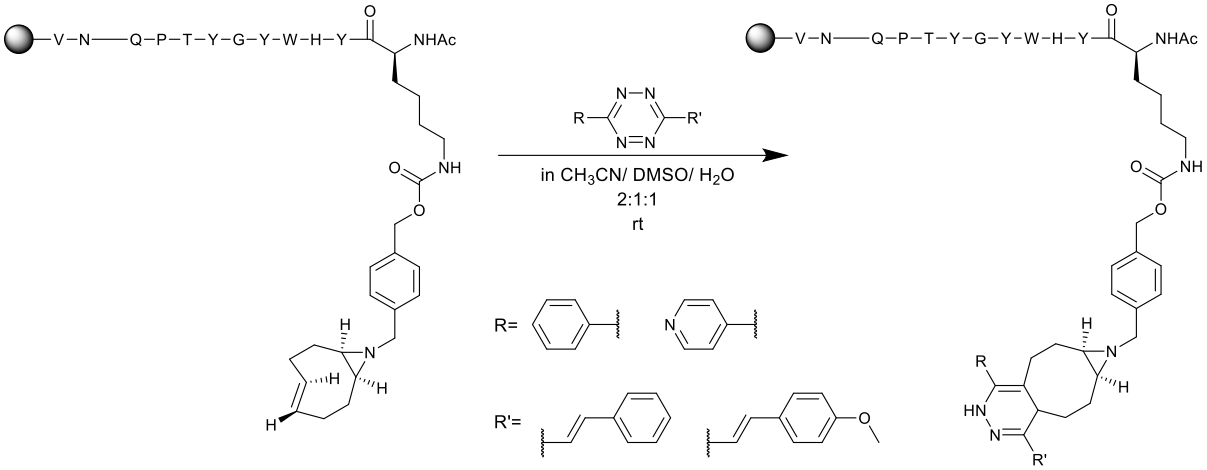


**Scheme S2.** Click-labeling of the aza-TCO modified peptide KYHWYGYTPQNVI with different 1,2,4,5-tetrazines.

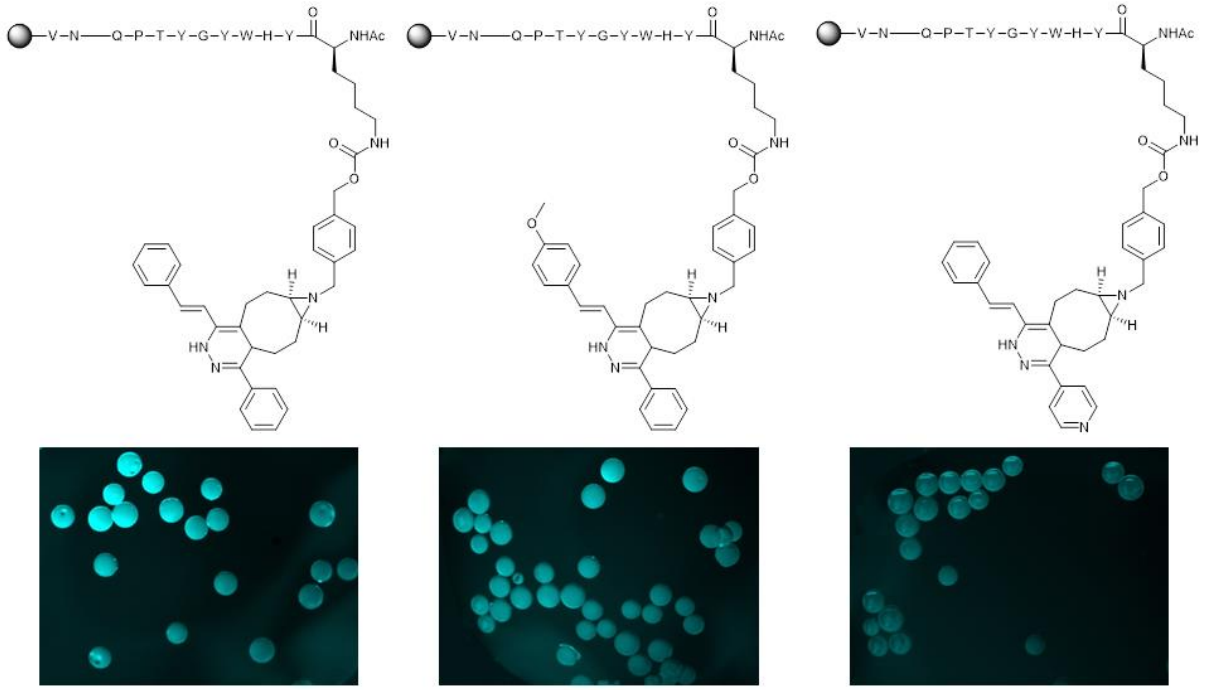

**Figure S12.** aza-TCO modified model peptide on Tentagel S-OH resin after click-labeling with various 1,2,4,5-tetrazines. The pictures were captured under a fluorescence stereomicroscope using UV-excitation (350 nm). The color of the beads was adjusted using LAS AF Lite program.

**Conditions for cleavage**: 100 mM NaOH (30 µL) was added to the resin taken for cleavage. The suspension was shaken at room temperature for 1.5 h and neutralized with 1 M HCl (3 µL, 1 equiv.). The beads were filtered through a small column consisting of Empore™ Octadecyl C18 (47 mm) Extraction Disks from *Supelco* and washed with $H_2O$ + 0.1% formic acid (100 µL). Before adding the resin the column was conditioned with MeOH (100 µL), $CH_3CN$ + 0.1% formic acid (100 µL) and $H_2O$ + 0.1% formic acid (2 × 100 µL). The cleaved peptide was eluted from the column by $CH_3CN$ + 0.1% formic acid (50 µL) and dried on a SpeedVac. For HPLC-MS measurements the residue was dissolved in $CH_3CN/H_2O$ 1:5.

Please note that the formed carbamate linker between the TCO active ester **1b** and the peptide is not completely stable toward the cleaving procedure (100 mM NaOH). Therefore partial cleavage of the TCO moiety is observed providing in the HPLC measurements a peak corresponding to the click product without the peptide and for the peptide itself.

Conditions for HPLC-MS:
solvent A: $H_2O$ + 0.05% HCOOH; solvent B: $CH_3CN$ + 0.05% HCOOH; gradient: 5% B → 50% B in 7 min, 50% B → 95% B in 1.5 min, then 95% B for 2.5 min and back to 5% B; column: Luna® C18(2) column (3µm, 100A, 100 × 4.6 mm), flow rate: 1 mL/min.

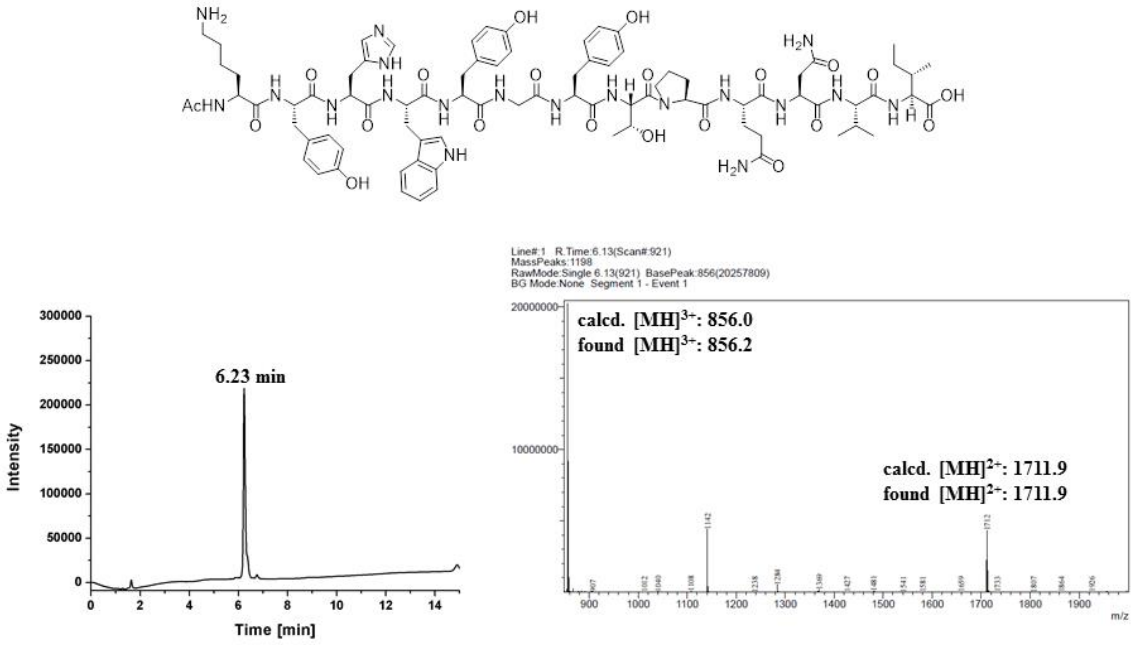


**Figure S13.** HPLC chromatogram and low-resolution mass spectra of the starting peptide KYHWYGYTPQNVI.

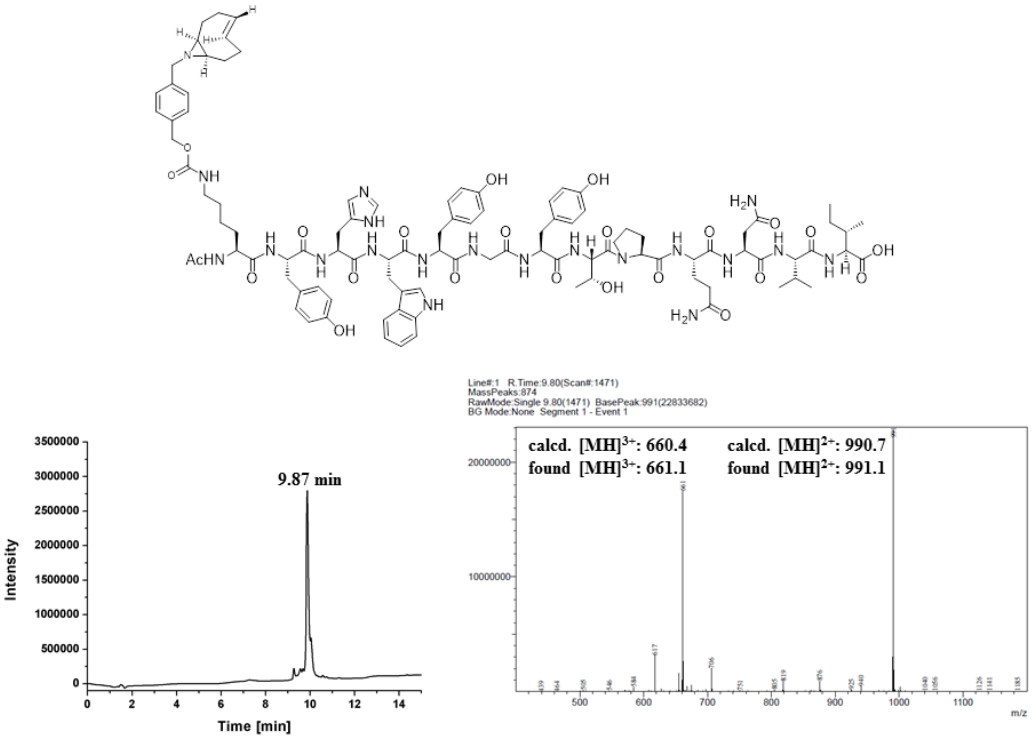


**Figure S14.** HPLC chromatogram and low-resolution mass spectra of the aza-TCO **1b** modified peptide.

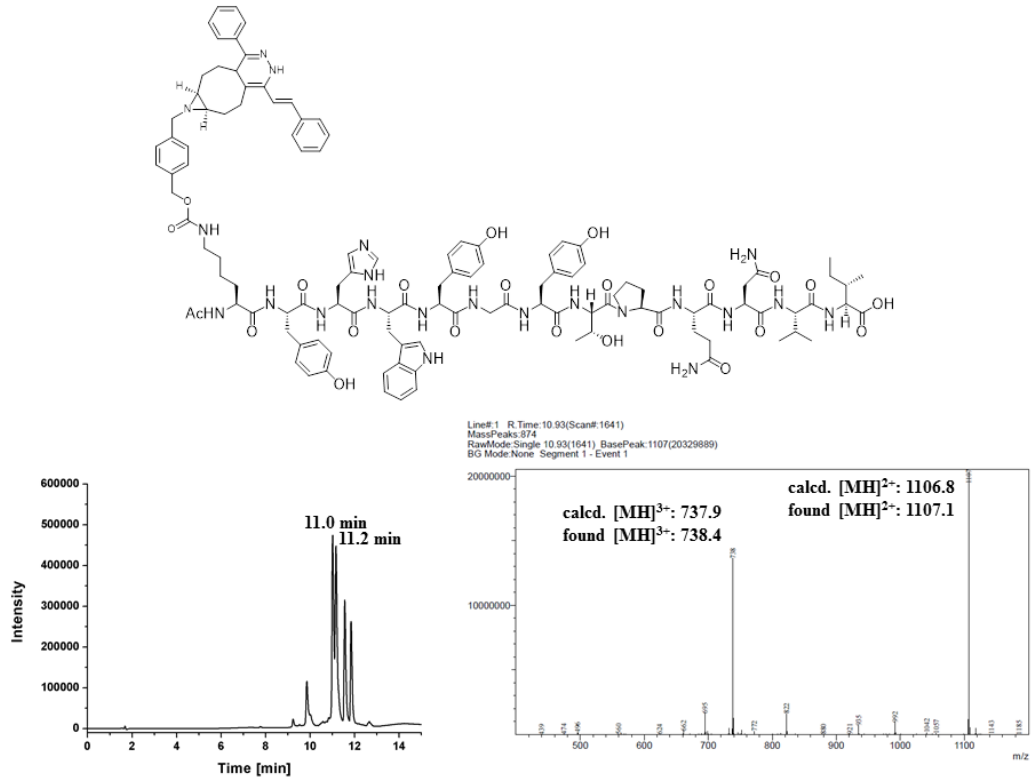


**Figure S15.** HPLC chromatogram and low-resolution mass spectra of the aza-TCO **1b** modified peptide after labeling with tetrazine **12b**. The smaller peaks at 11.6 min and 11.8 min correspond to the click product without the peptide (result of the carbamate linker cleavage) and the small peak at 9.85 min to unmodified peptide.

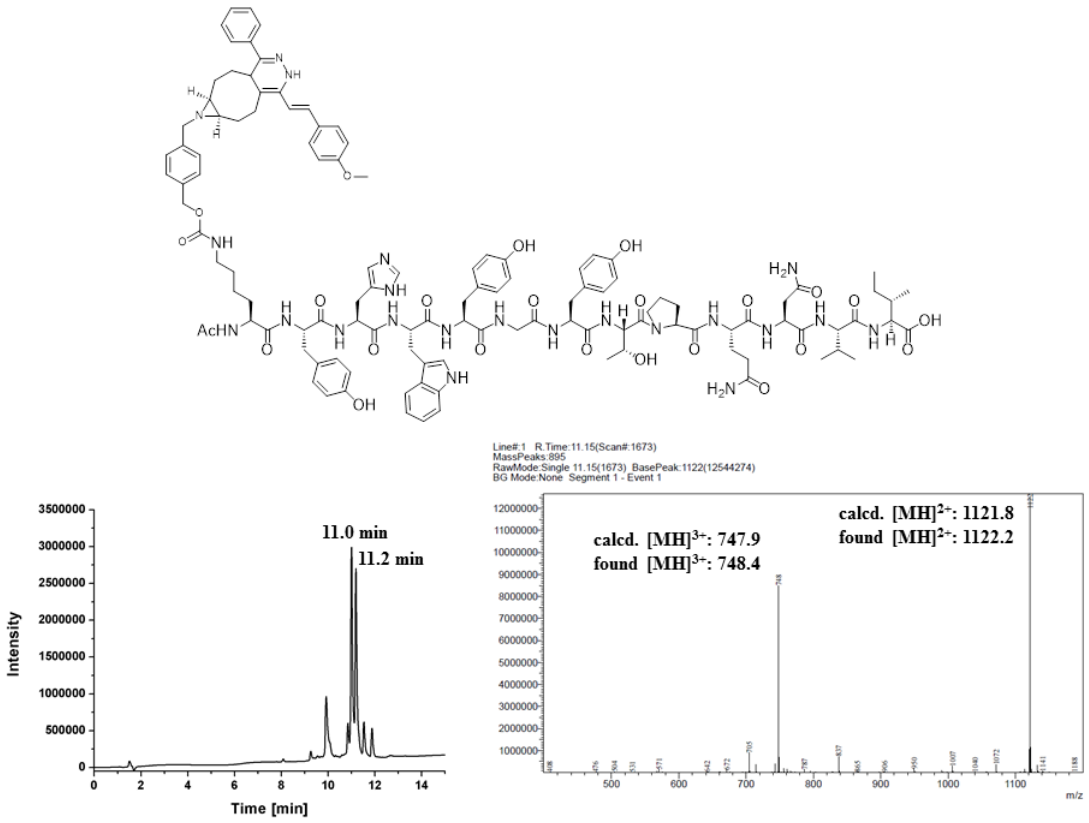


**Figure S16.** HPLC chromatogram and low-resolution mass spectra of the aza-TCO **1b** modified peptide after labeling with tetrazine **12c**. The smaller peaks at 11.5 min and 11.9 min correspond to the click product without the peptide (result of the carbamate linker cleavage) and the small peak at 9.85 min to unmodified peptide.

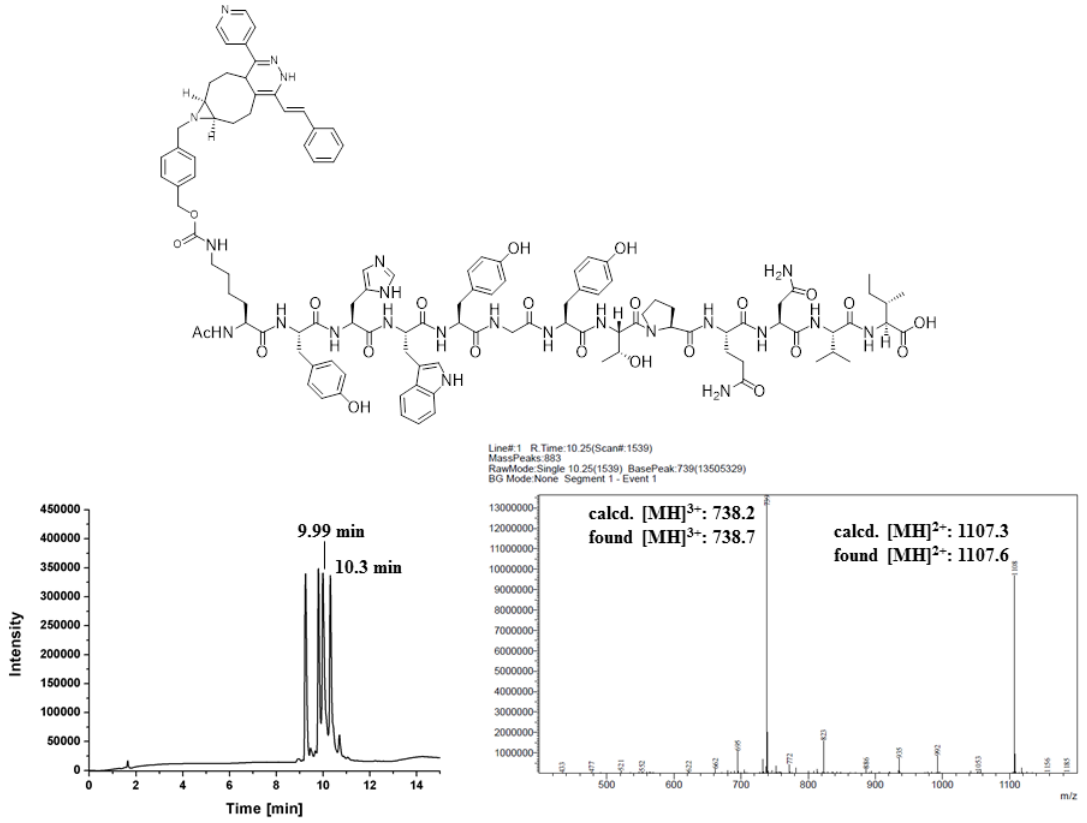


**Figure S17.** HPLC chromatogram and low-resolution mass spectra of the aza-TCO **1b** modified peptide after labeling with tetrazine **12e**. The peak at 9.25 min corresponds to the click product without the peptide (result of the carbamate linker cleavage) and the peak at 9.85 min to unmodified peptide.

# Fluorogenic click-labeling of model proteins

## Labeling of aza-TCO modified human carbonic anhydrase II (hCAII) with 1,2,4,5-tetrazines

A 0.8 mg/mL solution of hCAII in TRIS ·$H_2SO_4$, pH 7.8 was used as stock solution. First 3 mL of the solution were dialyzed against 200 mM NaCl, 10 mM HEPES pH 8.3. 250 µL of the dialyzed solution were separated to a PP vial. Then 2.76 µL of a 25 mM solution of TCO active ester **1b** in DMF/DMSO/$H_2O$ 2:1:1 (10× molar excess to the protein) were added to the vial and incubated at 4 °C for 2 h.

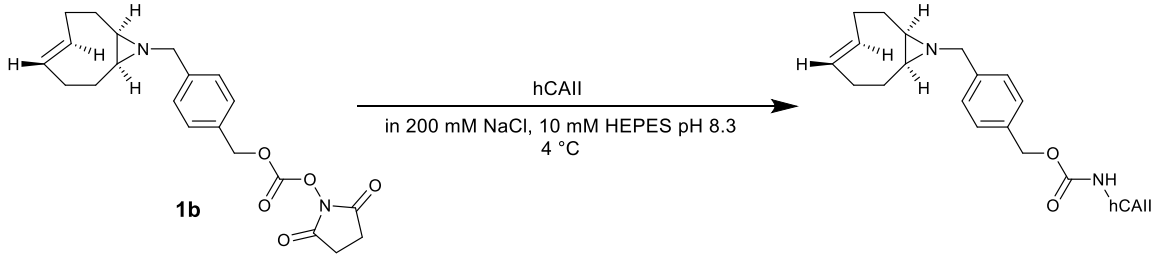


**Scheme S3.** hCAII modified with TCO active ester **1b**.

The solution with the aza-TCO modified protein (Scheme S3) was dialyzed against 200 mM NaCl, 20 mM HEPES pH 7.4. 160 µL of the dialyzed mixture were divided up into 2 PP vials. To each vial were added 10 µL of a 5 mM solution of a different tetrazine in DMSO (2.3 equiv. relative to the active ester **1b**, Scheme S4). After incubation in the dark at room temperature for 1.5 h, the mixtures were filtered using Zeba$^{TM}$ spin desalting columns (7K MWCO, 0.5 mL) from *Thermo Fisher Scientific* preconditioned with 200 mM NaCl, 20 mM HEPES pH 7.4 to remove excess of reagents.

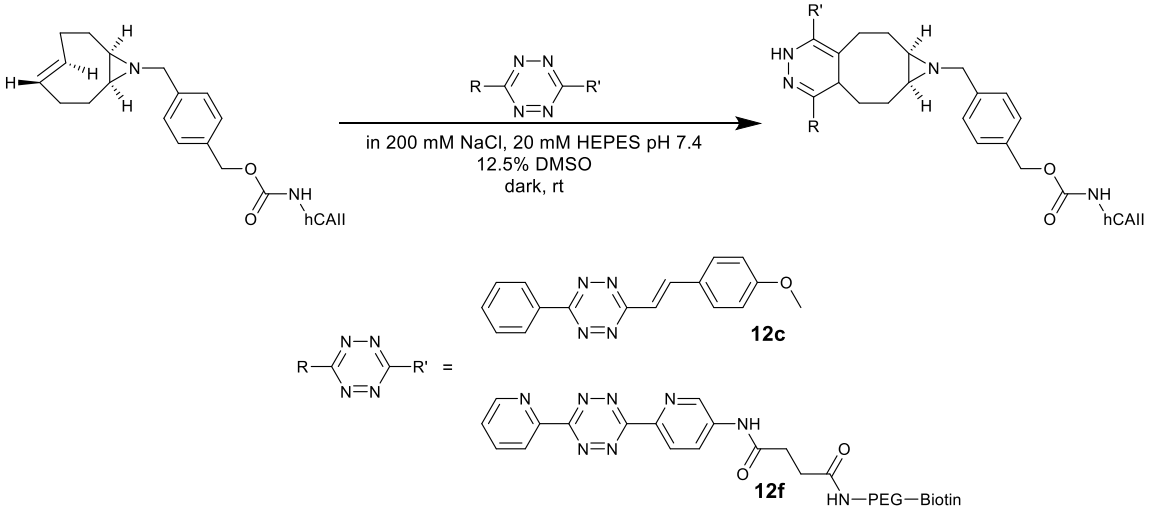


**Scheme S4.** Click-labeling of aza-TCO modified hCAII with different 1,2,4,5-tetrazines.

For SDS-PAGE analysis (12% Tris-glycine gel), the samples were diluted 2:3 with $H_2O$, mixed with 2× SDS-PAGE sample loading buffer containing dithiothreitol (DTT) and heated at 95 °C for 10 min. After electrophoreses, the gel was first analyzed by fluorescence spectrophotometry using a G:BOX F3 gel doc system equipped with an UV transilluminator (302 nm) using an orange emission filter (572-625 nm) (Figure S18B). Proteins were then visualized by staining the gel in colloidal coomassie (PageBlue$^{TM}$) (Figure S18A). Additionally, the same procedure was repeated except for the coomassie gel staining step to confirm the presence of the biotin moiety by western blot analysis. After blotting the proteins, the nitrocellulose membrane was washed in PBS and incubated in a BSA-solution containing 5% PBS at 4 °C overnight. Next, the membrane was washed 3× with PBS containing 0.005% Tween20 and incubated in the dark in a fluorescein-conjugated streptavidin solution at room temperature for 1 h. After washing 3× in PBS containing 0.005% Tween20, the membrane was analyzed by fluorescence spectrophotometry using a Typhoon FLA 9500 biomolecular imager (blue LD laser, 473 nm) (Figure S18C).

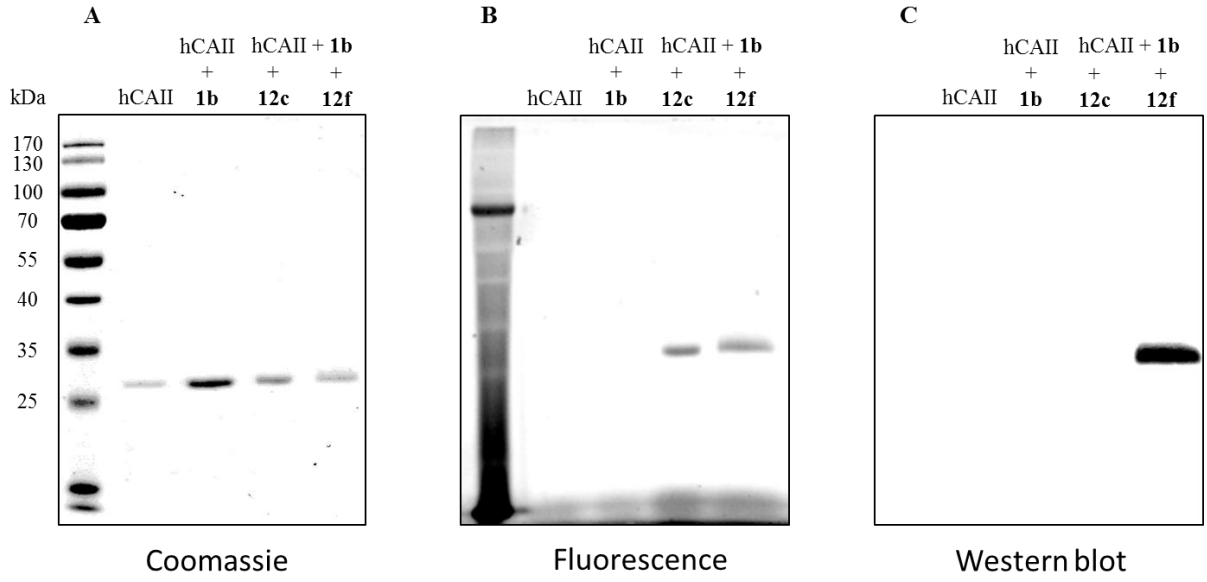


**Figure S18.** Fluorogenic labeling of aza-TCO modified hCAII with different 1,2,4,5-tetrazines. The protein samples were denaturated by heating at 95 °C and analyzed by SDS-PAGE. Shown are pictures of the Coomassie Blue stained gel (A), a fluorescent image captured before Coomassie blue treatment on a G:BOX F3 gel doc system (UV transilluminator (302 nm) and orange emission filter (572-625 nm)) (B) and a picture of the nitrocellulose membrane after western blot and treatment with fluorescein-conjugated streptavidin captured on a Typhoon FLA 9500 biomolecular imager (blue LD laser, 473 nm) (C).

## Labeling of aza-TCO modified ADP-ribosylation factor 1 (Arf1) with 1,2,4,5-tetrazines

A 5.7 mg/mL solution of Arf1 protein in 50 mM NaCl, 0.2 mM TCEP, 20 mM TRIS, pH 7.4 stock solution was used. 2.75 µL of a 100 mM solution of TCO maleimide **1c** in DMSO (10× molar excess to the protein) were added to 100 µL of the protein solution. The mixture was diluted with DMSO (22.25 µL) and incubated at room temperature for 2 h.

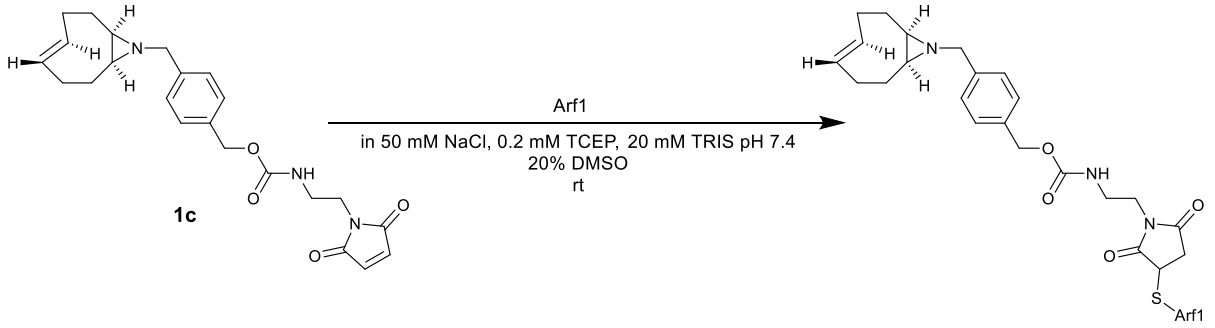


**Scheme S5.** Arf1 modified with TCO maleimide **1c**.

Next, the solution with the aza-TCO modified protein (Scheme S5) was filtered using a Zeba™ spin desalting column (7K MWCO, 0.5 mL) from *Thermo Fisher Scientific* preconditioned with 150 mM NaCl, 20 mM TRIS pH 7.5. 50 µL of the filtrate were mixed with 11 µL of a 5 mM solution of tetrazine **12c** in DMSO (5 equiv. relative to the starting protein, Scheme S6). Another 10 µL of the filtrate were mixed with 4.41 µL of a 2.5 mM

solution of tetrazine **12g** in DMSO (5 equiv. relative to the starting protein) as a positive control (Scheme S6). Both samples were diluted with 150 mM NaCl, 20 mM TRIS pH 7.5 to a final volume of 100 µL. After incubation in the dark at room temperature for 2 h, the mixtures were filtered using Zeba$^{TM}$ spin desalting columns (7K MWCO, 0.5 mL) from *Thermo Fisher Scientific* preconditioned with 150 mM NaCl, 20 mM TRIS pH 7.5.

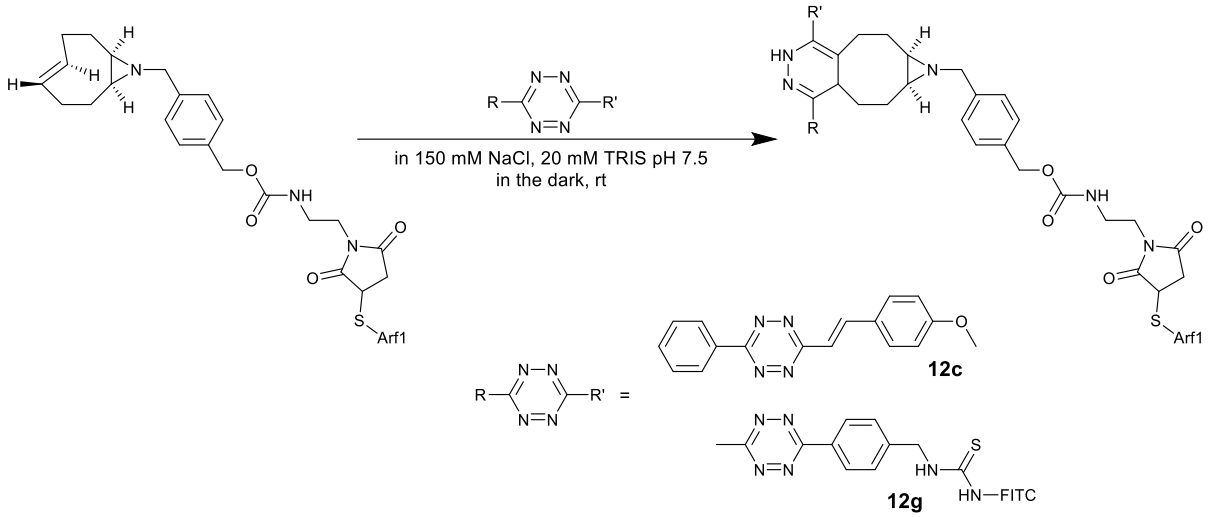


**Scheme S6.** Click-labeling of aza-TCO modified Arf1 with tetrazines **12c** and **12g**.

Additionally, the starting unmodified Arf1 solution (5.7 mg/mL) in 50 mM NaCl, 0.2 mM TCEP, 20 mM TRIS pH 7.4 was mixed with each of the tetrazines alone as a negative control (Scheme S7). For that purpose 50 µL of the protein solution were mixed with 12.5 µL of a 10 mM solution of tetrazine **12c** or **12g** in DMSO. The samples were incubated at room temperature for 2 h and filtered using Zeba$^{TM}$ spin desalting columns (7K MWCO, 0.5 mL) from *Thermo Fisher Scientific* preconditioned with 150 mM NaCl, 20 mM TRIS pH 7.5.

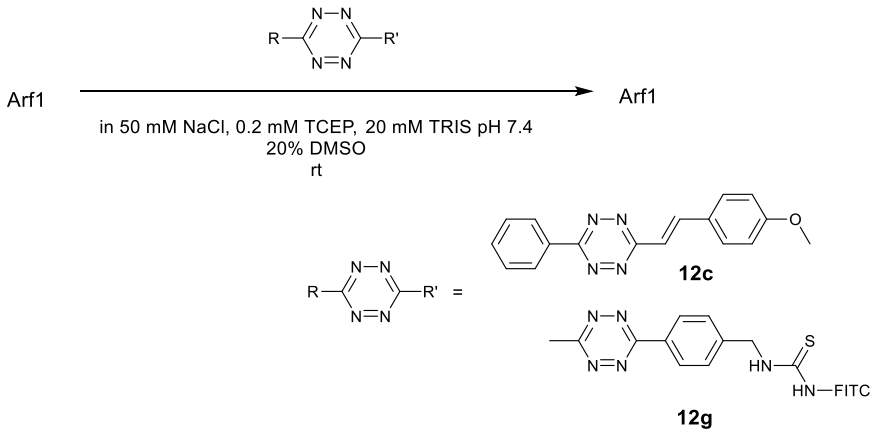


**Scheme S7.** Negative control: click-labeling of unmodified Arf1 with tetrazines **12c** and **12g**.

For SDS-PAGE analysis using a 14% Tris-glycine gel, the samples were mixed with 2× SDS-PAGE sample loading buffer containing DTT and heated at 95 °C for 10 min. After the electrophoresis the gel was incubated for 10 min in a fixing solution containing 50% MeOH

and 10% $CH_3COOH$. The fixed gel was then analyzed by fluorescence spectrophotometry using a Typhoon FLA 9500 biomolecular imager (blue LD laser, 473 nm) (Figure S19B) and a G:BOX F3 gel doc system (UV transilluminator (302 nm) and orange emission filter (572-625 nm)) (Figure S19C). Proteins were visualized by staining the gel in a Coomassie staining solution (2.5% Coomassie R-250, 50% MeOH and 10% $CH_3COOH$) (Figure S19A).

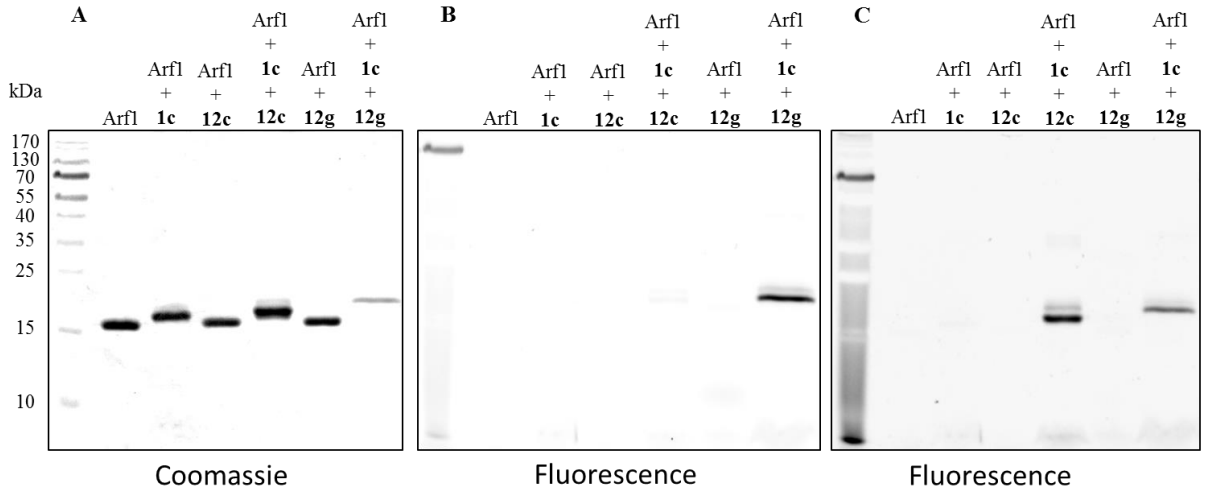


**Figure S19.** Fluorogenic labeling of aza-TCO modified Arf1 with different 1,2,4,5-tetrazines. The protein samples were denaturated by heating at 95 °C and analyzed by SDS-PAGE. Shown are a picture of the Coomassie Blue stained gel (A) and fluorescent images captured before Coomassie blue treatment on a Typhoon FLA 9500 biomolecular imager (blue LD laser, 473 nm) (B) and on a G:BOX F3 gel doc system (UV transilluminator (302 nm) and orange emission filter (572-625 nm)) (C).

## Cell labeling experiments

### Labeling of Concanavalin A by TCOs

2.5 mg of Concanavalin A (*Sigma* #C2010) were dissolved in 1 ml of 150 mM NaCl, 50 mM HEPES pH 8.3 (to obtain a 2.5 mg/ml solution). 250 µL (0.625 mg, approx. 6 nmol of the tetramer) of this solution were combined with 6 µL of a 10 mM solution of TCO NHS active ester **1b**, **1d** or **1e** (approx. 10× molar excess) in anhydrous DMSO (Figure S20). The reaction mixture was incubated at room temperature for 1 h with constant shaking. After one hour any precipitated material was spun at 25000 rpm for 10 min. Clean supernatant was split and 2× 130 µL were loaded onto two Zeba™ spin desalting columns (7K MWCO, 0.5 mL, Thermo) preconditioned with 150 mM NaCl, 50 mM TRIS pH 7.4.

### SDS PAGE

2 µl of a 2.5 µg/µl solution of a given ConA were mixed with 2 µl of a 250 µM solution of tetrazine **12c** or **12g** in DMSO. The reaction was incubated for 10 min at room temperature and then diluted in 20 µl of water. 4 µl of 5× SDS sample loading buffer (without DTT) were added to the mixture and heated at 95 °C for 5 min. 10 µl were loaded onto a 15%

polyacrylamide gel and resolved at 35 mA (constant current) for 50 min. Fluorescence of the proteins was photographed on a SynGene documentation system using UV illumination (302 nm) and an orange emission filter (572-625 nm) (Figure S20). The gel was subsequently stained with colloidal coomassie (PageBlue, Thermo) (Figure S20).

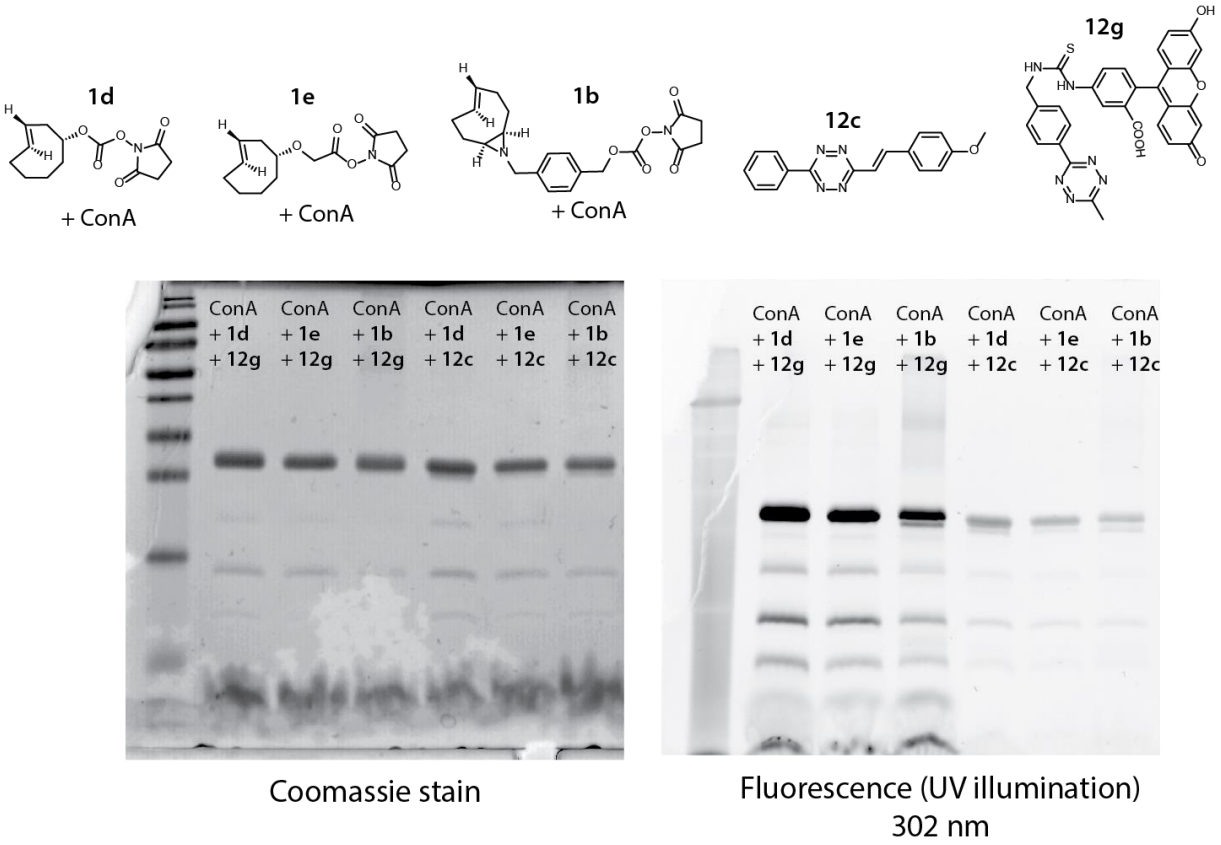


**Figure S20.** Fluorogenic labeling of TCO **1d**, **1e** or **1b** modified ConA with different 1,2,4,5-tetrazines. The protein samples were denaturated by heating at 95 °C and analyzed by SDS-PAGE. Shown are pictures of the Coomassie Blue stained gel and a fluorescent image captured before Coomassie blue treatment on a G:BOX F3 gel doc system (UV transilluminator (302 nm excitation) and orange emission filter (572-625 nm)).

## Labeling of U2OS cells using ConA-aza-TCO conjugate

Osteosarcoma U2OS cells grown on coverslips, were fixed with 4% formaldehyde solution (WVR) for 10 min at room temperature and permeabilized for 10 min with 0.1% Triton X-100 (Sigma) in PBS. After washing (3× PBS/0.005% Tween20) the cells were incubated with Concanavalin A-TCO conjugate (0.25 µg/µl in PBS with 0.5 mM $CaCl_2$ and 0.005% Tween20) at room temperature for 1h. After that, the cells were washed 3× with PBS/Tween20 to remove unbound Concanavalin A. The coverslips were incubated with 0.25 mM tetrazine in PBS/Tween20 for 10 min and then washed once in PBS/Tween20 and once in PBS/Tween20 containing 5 µM DRAQ5 DNA stain (Thermo). The coverslips were mounted on a glass slide using ProlongDiamond without DAPI (Thermo) and sealed with a nail polish. Pictures were taken approximately 2 h after the click reaction using a Zeiss LSM780 confocal microscope equipped with 63 1.4 Oil DIC M27 objective (Figure S21). The

click product with tetrazine **12c** was excited with a 405 nm laser (intensity 1.2%) and the fluorescence was collected in a 447-525 nm interval. The click product with tetrazine FITC **12g** was excited with a 458 nm laser and the fluorescence was collected in interval 490-552 nm. DRAQ5 was excited with a 633 nm laser (intensity 2.2%) and the fluorescence was collected in a 642-735 nm window. Pictures were processed using ImageJ software.

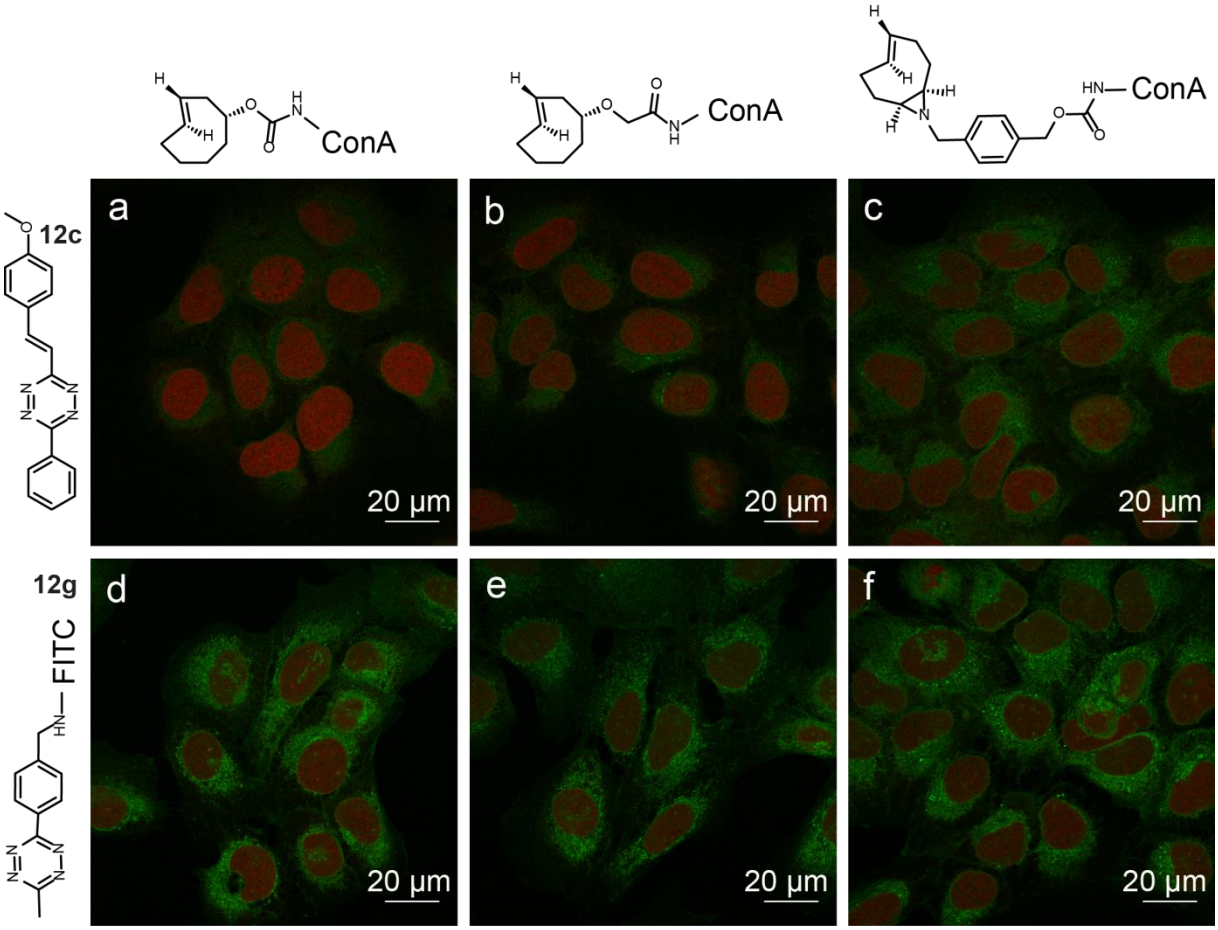


**Figure S21**. Cell labeling experiments using ConA modified with TCOs **1d**, **1e** or **1b**. Tetrazine **12c** click products a), b) and c) were excited using a 405 nm laser (intensity 1.2%) and fluorescence was collected in a 447-525 nm interval. Tetrazine FITC **12g** click products d), e) and f) were excited by a 458 nm laser and fluorescence was collected in interval 490-552 nm. DRAQ5 was excited by a 633 nm laser (intensity 2.2%) and fluorescence was collected in a 642-735 nm window. Scale bar 20µM.

## Labeling of the bacterial cell wall using aza-TCO D-amino acid 1f

**1f** was dissolved in 100mM NaOH and added to the media to a final 1mM concentration (Note: **1f** is best stored as a suspension in sterile water at -20°C and should be diluted just before the experiment with 100 mM NaOH to get clear solution. For long term storage we recommend to store **1f** as a solid at -20°C or -80°C). Wild-type B. subtilis 168 was inoculated into 2ml of LB media and cultivated for 2 hours at 37 °C in the presence of 1mM **1f**. 1ml of culture was spun for 5min at 4000 rcf, pellet was resuspended in 1ml of PBS buffer and centrifuged again. Pellet was resuspended in 100µL of PBS containing 25 µM **12h** and

incubated for 15 min at room temperature. Cells were washed in 1ml of PBS, fixed with 70% ethanol, washed again with PBS containing 100µg/ml DAPI and mounted on agarose pads. E. coli strain ER2738 was diluted 100× from overnight culture into LB media. Cells were incubated for 2, 6 or 12 hours at 37°C with constant shaking. At indicated time points cells were spun for 2 minutes at 25000rcf and washed twice with 1×TBS. After the second wash cells were incubated with 25 µM **12h** for 15 min at room temperature. Cells were spun for 2 min at 25000rcf and washed once in 1x TBS and fixed with 70% ethanol/water. After fixation cells were spun for 2 min at 25000rcf and resuspended in 1×TBS. DRAQ5 was added to a final concentration of 50 µM, the cells were mounted on an agarose pad and covered with coverslips and sealed with a nail polish. Pictures were acquired sequentially. Bodipy fluorescence was excited with 458 nm (laser intensity 1%) and collected in 499-569 nm interval. DRAQ5 was excited with a 633 nm laser (intensity 2.5%) and the fluorescence was collected in a 642-735 nm window. Pictures were processed using ImageJ software.

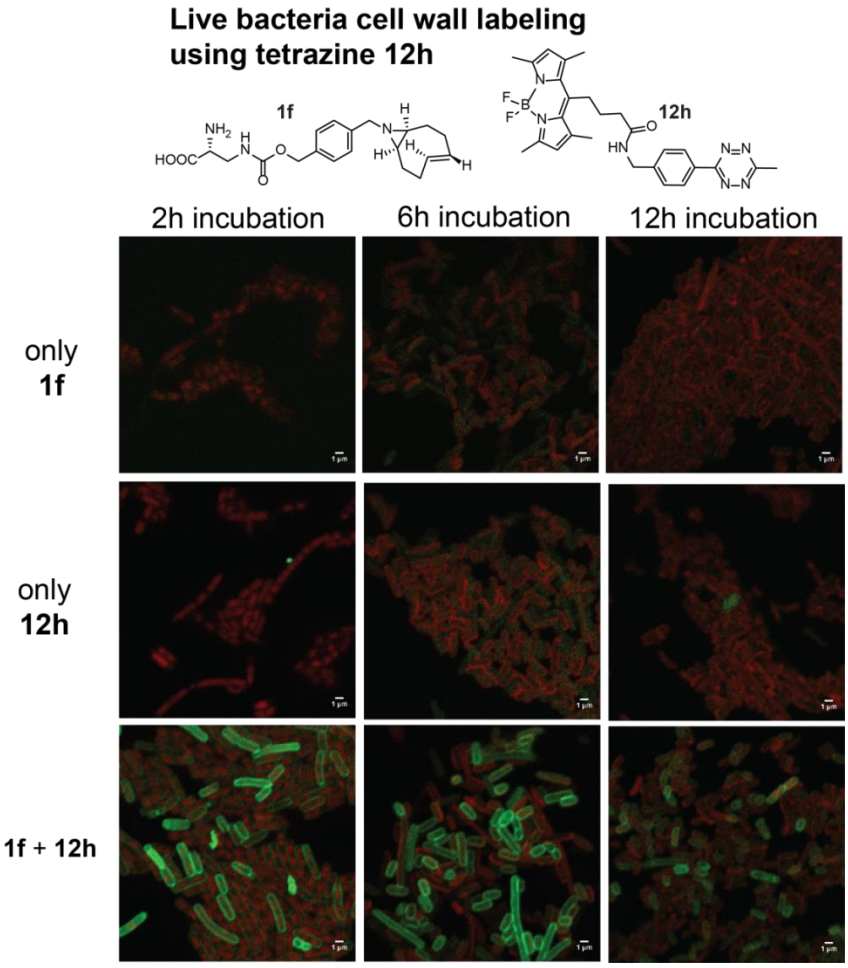


**Figure S22**. E. coli cell wall labeling using aza-TCO modified D-amino acid **1f** and bodipy tetrazine **12h**. Live E. coli were incubated with **1f** (1 mM) for 2, 6 or 12 hours or with **12h** only (negative controls). After washing, the reaction was initiated by addition of **12h** (25 µM, for 15 min). DNA was stained with 50 µM DRAQ5. After washing the cells were inspected under confocal microscope and the click products (green) were excited using a 458 nm laser (intensity 1%) and collected in 499-569 nm interval. DRAQ5 was excited by a 633 nm laser (intensity 2%) and fluorescence was collected in a 642-735 nm window. Scale bar 1 µM.

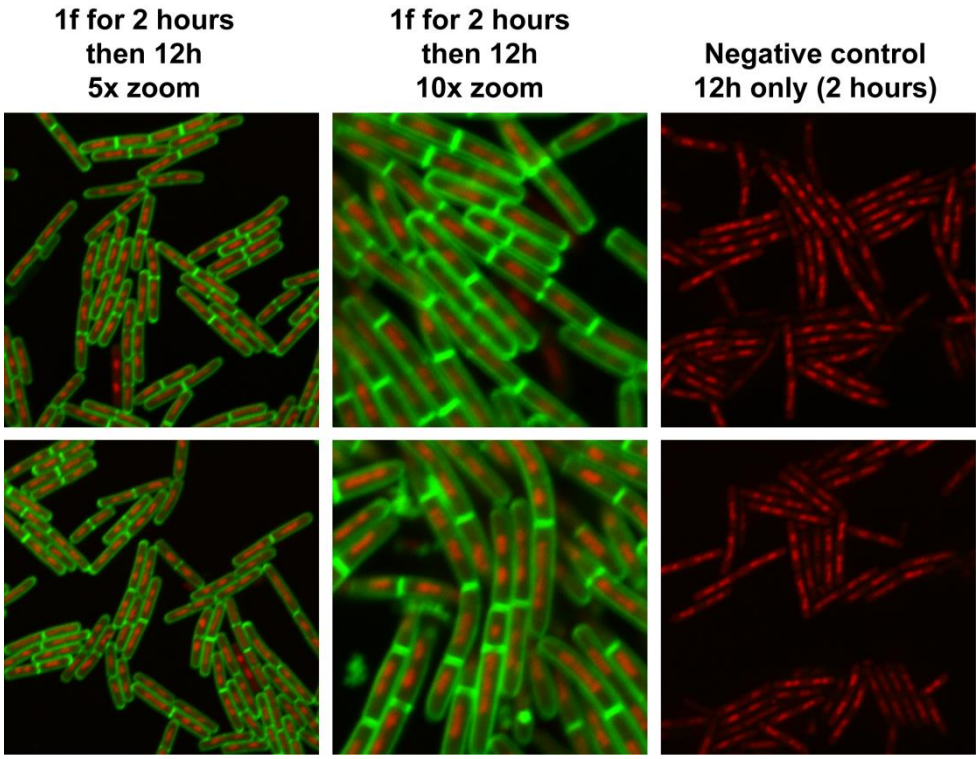


**Figure S23**. B. subtilis cell wall labeling using aza-TCO modified D-amino acid **1f** and bodipy tetrazine **12h**. Live B. subtilis were incubated with **1f** (1 mM) for 2 hours or with **12h** only (negative control). After washing, the reaction was initiated by addition of **12h** (25 μM, for 15 min). DNA was stained with 100μg/ml DAPI. After washing the cells were inspected under confocal microscope.

# References


1. Royzen, M.; Yap, G. P.; Fox, J. M. *J. Am. Chem. Soc.* **2008**, *130*, 3760-3761.
2. Darko, A.; Wallace, S.; Dmitrenko, O.; Machovina, M. M.; Mehl, R. A.; Chin, J. W.; Fox, J. M. *Chem. Sci.* **2014**, *5*, 3770-3776.
3. Taylor, M. T.; Blackman, M. L.; Dmitrenko, O.; Fox, J. M. *J. Am. Chem. Soc.* **2011**, *133*, 9646-9649.
4. Wu, H.; Yang, J.; Seckute, J.; Devaraj, N. K. *Angew. Chem., Int. Ed.* **2014**, *53*, 5805-5809.
5. Vazquez, A.; Dzijak, R.; Dracinsky, M.; Rampmaier, R.; Siegl, S. J.; Vrabel, M. *Angew. Chem., Int. Ed.* **2017**, *56*, 1334-1337.
6. Siegl, S. J.; Dzijak, R.; Vazquez, A.; Pohl, R.; Vrabel, M. *Chem. Sci.* **2017**, *8*, 3593-3598.
7. Oliveira, B. L.; Guo, Z.; Boutureira, O.; Guerreiro, A.; Jimenez-Oses, G.; Bernardes, G. J. *Angew. Chem., Int. Ed.* **2016**, *55*, 14683-14687.
8. Hillmyer, M. A.; Laredo, W. R.; Grubbs, R. H. *Macromolecules* **1995**, *28*, 6311-6316.
9. Clark, P. G.; Guidry, E. N.; Chan, W. Y.; Steinmetz, W. E.; Grubbs, R. H. *J. Am. Chem. Soc.* **2010**, *132*, 3405-3412.
10. Hoesch, L.; Egger, N.; Dreiding, A. S. *Helv. Chim. Acta* **1978**, *61*, 795-814.
11. *HyperChem 8.0.3*, Hypercube Inc.: Gainesville, **2007**.
12. (a) Becke, A. D. *J. Chem. Phys.* **1993**, *98*, 5648-5652; (b) Lee, C. T.; Yang, W. T.; Parr, R. G. *Phys. Rev. B* **1988**, *37*, 785-789.
13. (a) Barone, V.; Cossi, M. *J. Phys. Chem. A* **1998**, *102*, 1995-2001; (b) Cossi, M.; Rega, N.; Scalmani, G.; Barone, V. *J. Comput. Chem.* **2003**, *24*, 669-681.
14. Frisch, M. J.; Trucks, G. W.; Schlegel, H. B.; Scuseria, G. E.; Robb, M. A.; Cheeseman, J. R.; Scalmani, G.; Barone, V.; Petersson, G. A.; Nakatsuji, H.; Li, X.; Caricato, X.; Marenich, A. V.; Bloino, J.; Janesko, B. G.; Gomperts, R.; Mennucci, B.; Hratchian, H. P.; Ortiz, J. V.; Izmaylov, A. F.; Sonnenberg, J. L.; Williams-Young, D.; Ding, F.; Lipparini, F.; Egidi, F.; Goings, J.; Peng, B.; Petrone, A.; Henderson, T.; Ranasinghe, D.; Zakrzewski, V. G.; Gao, J.; Rega, N.; Zheng, G.; Liang, W.; Hada, M.; Ehara, M.; Toyota, K.; Fukuda, R.; Hasegawa, J.; Ishida, M.; Nakajima, T.; Honda, Y.; Kitao, O.; Nakai, H.; Vreven, T.; Throssell, K.; Montgomery, Jr., J. A.; Peralta, J. E.; Ogliaro, F.; Bearpark, M. J.; Heyd, J. J.; Brothers, E. N.; Kudin, K. N.; Staroverov, V. N.; Keith, T. A.; Kobayashi, R.; Normand, J.; Raghavachari, K.; Rendell, A. P.; Burant, J. C.; Iyengar, S. S.; Tomasi, J.; Cossi, M.; Millam, J. M.; Klene, M.; Adamo, C.; Cammi, R.; Ochterski, J. W.; Martin, R. L.; Morokuma, K.; Farkas, O.; Foresman, J. B.; Fox, D. J. Gaussian, Inc., Wallingford CT, **2016**.
15. (a) Peng, C.; Ayala, P. Y.; Schlegel, H. B.; Frisch, M. J. *J. Comput. Chem.* **1996**, *17*, 49-56; (b) Peng, C.; Schlegel, H. B. *Israel J. Chem.* **1994**, *33*, 449-454.
16. Eaton, D. F. *J. Photochem. Photobiol. B* **1988**, *2*, 523-531.

## 7.2 Supplementary information to chapter 3.2

S.J. Siegl, J. Galeta, R. Dzijak, A. Vázquez, M. Del Río-Villanueva, M. Dračínský, M. Vrabel, *ChemBioChem* **2019**, 20, 886– 890.
"An Extended Approach for the Development of Fluorogenic *trans*-Cyclooctene-Tetrazine Cycloadditions".

The corresponding NMR spectra are not presented here and can be found in the original publication.

CHEMBIOCHEM

Supporting Information

# An Extended Approach for the Development of Fluorogenic *trans*-Cyclooctene–Tetrazine Cycloadditions

Sebastian J. Siegl, Juraj Galeta, Rastislav Dzijak, Arcadio Vázquez, Miguel Del Río-Villanueva, Martin Dračínský, and Milan Vrabel*[a]

cbic_201800711_sm_miscellaneous_information.pdf

## Content

## General information

The chemicals were obtained from commercial suppliers and were used without further purification. Reactions with air- and moisture-sensitive reactants were performed in anhydrous solvents under nitrogen or argon atmosphere. Photochemical reactions (synthesis of TCOs) were performed in a RPR-200 Rayonet reaction chamber equipped with 16 Hg-quartz iodine lamps (2537 Å) from *Southern New England Ultraviolet Company*. The continuous flow system during the photoreaction was produced by a STEPDOS 03 RC membrane-metering pump from *KNF*. Column chromatography was carried out on silica gel 60A (particle size: 40-60 µm) from *Acros Organics*. Mixtures of solvents are each stated as volume fractions. For flash column chromatography a Combi*Flash*® Rf+ from *Teledyne ISCO* was used. Thin-layer chromatography was performed on aluminum sheets from *Merck* (silica gel 60 F254, 20 × 20 cm). Chromatograms were visualized by UV light (λ = 254 nm/ 366 nm) or by staining with $KMnO_4$ solution. $^{1}H$- and $^{13}C$-NMR spectra were measured on a Bruker Avance III™ HD 400 MHz NMR system equipped with Prodigy cryo-probe. Chemical shifts δ are quoted in ppm in relation to the chemical shift of the residual non-deuterated solvent peak ($CDCl_3$: $\delta(^{1}H) = 7.26$, $\delta(^{13}C) = 77.16$). High-resolution mass spectra were recorded on an *Agilent* 5975C MSD Quadrupol, Q-Tof micro from *Waters* or LTQ Orbitrap XL from *Thermo Fisher Scientific*. HPLC-MS measurements were performed on an LCMS-2020 system from *Shimadzu* equipped either with a Luna® C18(2) column (3µm, 100A, 100 × 4.6 mm) or a Kinetex® C18 column (2.6µm, 100A, 100 × 4.6 mm). UV/VIS spectroscopy was performed on a Cary 60 UV/Vis spectrophotometer from *Agilent Technologies*. Data from kinetic experiments were processed using OriginPro 9.1 software. Fluorescence measurements were performed on a FluoroMax 4 spectrofluorometer (Jobin Yvon, Horiba) from *Perkin Elmer* equipped with a 450 W xenon lamp and a single cuvette reader using the dye nile red in MeOH as standard for determination of fluorescence quantum yields.

## Synthetic procedures

The synthesis of tetrazines **1a-c** has been published in one of our earlier publications.[1]

### General procedure for the synthesis of 1d-f

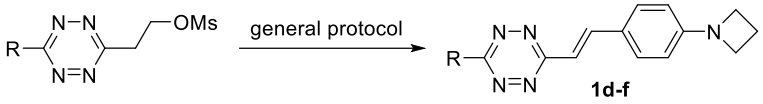


To a Schlenk vessel we added mesilated starting tetrazine[1] (50 mg), P(*o*-Tol)$_3$ (40 mol%), $Pd_2(dba)_3$ (10 mol%) and 1-(4-bromophenyl)azetidine (1.5 equiv). The vessel was purged with argon and 5 mL of degassed anhydrous 1,4-dioxane was added via syringe followed by $Cy_2NMe$ (3 equiv). The reaction mixture was vigorously stirred at 70 °C and cooled to RT after 20 h. Water (10 mL) was added and the mixture was extracted with DCM (3 × 5 mL), the combined extracts were dried over $Na_2SO_4$, filtered and evaporated.

1-(4-Bromophenyl)azetidine

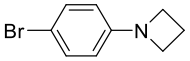


To a dry flask under an argon atmosphere was added azetidine hydrochloride (100 mg, 1.07 mmol), 1-bromo-4-iodobenzene (454 mg, 1.60 mmol, 1.5 equiv), Xantphos (62 mg, 0.107 mmol, 10 mol%), $Pd_2(dba)_3$ (50 mg, 0.053 mmol, 5 mol%) and *t*BuONa (308 mg, 3.204 mmol, 3 equiv). Then, anhydrous degassed 1,4-dioxane was added (10 mL) and the mixture was stirred at 95 °C for 12 h. Then, it was cooled to RT, brine (10 mL) and water (20 mL) were added and the mixture was extracted with $Et_2O$ (2 × 50 mL). Collected extracts were dried over $Na_2SO_4$, filtered and evaporated.

PURIFICATION: flash chromatography, gradient PE → PE/EA 9:1
YIELD: 70 mg (31%)
$^1$H NMR (400 MHz, $CDCl_3$): δ 7.25 – 7.30 (m, 2H), 6.29 – 6.33 (m, 2H), 3.85 (t, *J* = 7.2, 4H), 2.36 (pent, *J* = 7.2, 2H).
$^{13}$C NMR (101 MHz, $CDCl_3$): δ 151.2, 131.7, 113.1, 109.3, 52.6, 17.0.
HRMS (EI+) calcd. for $C_9H_{10}N_{Br}^+$ $[M]^+$: 210.9997, found 210.9995

(*E*)-3-(4-Azetidin-1-yl)styryl-6-phenyl-1,2,4,5-tetrazine **1d**

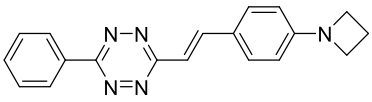


PURIFICATION: column chromatography, PE/DCM 1:4
YIELD: 32 mg (57%)
$^1$H NMR (400 MHz, $CDCl_3$): δ 8.56 – 8.61 (m, 2H), 8.29 (d, *J* = 16.1, 1H), 7.54 – 7.61 (m, 5H), 7.26 (d, *J* = 16.1, 1H), 6.42 – 6.47 (m, 2H), 3.99 (t, *J* = 7.3, 4H), 2.42 (pent, *J* = 7.3, 2H).

$^{13}$C NMR (101 MHz, $CDCl_3$): δ 165.4, 162.6, 153.1, 142.0, 132.4, 132.2, 129.9, 129.3, 127.7, 124.2, 115.4, 111.1, 52.0, 16.8.
HRMS (APCI+) calcd. for $C_{19}H_{18}N_5^+$ $[M+H]^+$: 316.1557, found 316.1557.

(*E*)-3-(4-Azetidin-1-yl)styryl)-6-(pyridin-4-yl)-1,2,4,5-tetrazine **1e**

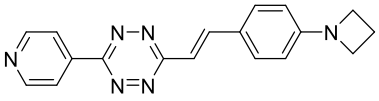

PURIFICATION: column chromatography, PE/EA 1:2 to 1:4
YIELD: 18 mg (32%)
$^1$H NMR (400 MHz, $CDCl_3$ / $CD_3OD$ 10:1): δ 8.77 – 8.81 (m, 2H), 8.38 – 8.42 (m, 2H), 8.31 (d, *J* = 16.0, 1H), 7.52 – 7.56 (m, 2H), 7.22 (d, *J* = 16.0, 1H), 6.38 – 6.42 (m, 2H), 3.97 (t, *J* = 7.3, 4H), 2.39 (pent, *J* = 7.3, 2H).
$^{13}$C NMR (101 MHz, $CDCl_3$ + $CD_3OD$ 10:1): δ 166.1, 161.0, 153.4, 150.6, 144.0, 140.2, 130.3, 123.6, 121.1, 114.4, 110.9, 51.8, 16.6.
HRMS (APCI+) calcd. for $C_{18}H_{17}N_6^+$ $[M+H]^+$: 317.1509, found 317.1510.

(*E*)-3-(4-Azetidin-1-yl)styryl)-6-(thiophen-3-yl)-1,2,4,5-tetrazine **1f**

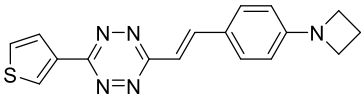

PURIFICATION: column chromatography (DCM)
YIELD: 42 mg (75%)
$^1$H NMR (400 MHz, $CDCl_3$ + $CD_3OD$ 10:1): δ 8.54 (dd, *J* = 3.1, 1.2, 1H), 8.24 (d, *J* = 16.0, 1H), 8.04 (dd, *J* = 5.1, 1.2, 1H), 8.54 (dd, *J* = 3.1, 1.2, 1H), 7.54 – 7.58 (m, 2H), 7.50 (dd, *J* = 5.1, 3.1, 1H), 7.23 (d, *J* = 16.0, 1H), 6.42 – 6.46 (m, 2H), 3.99 (t, *J* = 7.3, 4H), 2.42 (pent, *J* = 7.3, 2H).
$^{13}$C NMR (101 MHz, $CDCl_3$ + $CD_3OD$ 10:1): δ 164.9, 160.3, 153.1, 141.7, 135.3, 129.9, 129.1, 127.4, 126.5, 124.1, 115.3, 111.0, 52.0, 16.7.
HRMS (APCI+) calcd. for $C_{17}H_{16}N_5S^+$ $[M+H]^+$: 322.1121, found 317.1122.

## Synthesis of TPP-TCO

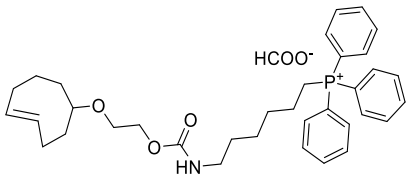

To a solution of TPP amine[2] 35.5 mg (1.25 equiv) in 500 µL of dry $CH_3CN$ was added 20 mg NHS-TCO active ester (major equatorial isomer)[1, 3] dissolved in 500 µL of dry $CH_3CN$ followed by addition of 28 µL (2.5 equiv) of DIPEA. The progress of the reaction was followed by HPLC/MS. After 30 min the reaction mixture was concentrated under reduced pressure and the residue purified by flash chromatography using gradient of MeOH in DCM (2 to 10%). Isolated after freeze-drying as white hygroscopic powder: 31 mg (79%).

$^{1}$H NMR (400 MHz, $CDCl_3$) δ 7.88 – 7.74 (m, 10H), 7.69 (m, 6H), 5.76 – 5.35 (m, 2H), 5.24 – 5.10 (m, 1H), 4.11 (q, *J* = 5.2, 2H), 3.86 – 3.65 (m, 3H), 3.65 – 3.49 (m, 2H), 3.43 – 3.28 (m, 1H), 3.21 – 3.06 (m, 3H), 2.41 – 2.26 (m, 1H), 2.26 – 1.21 (m, 14H).
$^{13}$C NMR (101 MHz, $CDCl_3$) δ 156.8, 135.1, 133.9, 133.8, 132.1, 130.7, 130.1, 129.6, 119.0, 118.1, 81.1, 80.3, 66.7, 64.2, 54.1, 42.4, 40.7, 34.2, 33.5, 31.2, 30.0, 29.8, 29.5, 28.5, 26.1, 25.9, 25.7, 25.6, 22.9, 22.7, 22.7, 22.4, 18.8, 17.5, 12.2.
(ESI+) HRMS $[M]^+$ m/z calculated. for $[C_{35}H_{45}O_3NP]^+$ = 558.3132, found 558.3124.

## The reaction progress of eqTCO 2a with 1c monitored by HPLC-MS and by NMR

### HPLC-MS

The progress of the reaction of eqTCO **2a** with tetrazine **1c** was followed by HPLC/MS. The time dependent formation of the 4,5-dihydropyridazine intermediate **3c** and the 1,4-dihydropyridazine **3c'** was measured using pH neutral $NH_4OAc$ since the tautomerization is sensitive to pH.[4] Monitoring at 380 nm was found most suitable due to differences in absorption maxima of **3c** and **3c'**. Formation of double peaks presumably corresponds to the formation of two different dihydropyridazine regioisomers in the IEDDA reaction.

Stock solutions: **1c**: 1 mM in DMSO, eqTCO **2a**: 50 mM in $CH_3CN/H_2O$ = 1/1
Procedure: 4 µL of eqTCO stock solution (10 equiv, 2 mM final concentration) was mixed with 26 µL $CH_3CN/H_2O$ = 1/1. To this solution was added 20 µL of **1c** stock solution (200 µM final concentration). This solution was further diluted with 50 µL $CH_3CN/H_2O$ = 1/1 and injected into LC/MS (10 µL injection) at different time points (Figure S1).

Gradient: (solvent A = 20 mM $NH_4OAc$ in water, solvent B = 10 mM $NH_4OAc$ of 90% $CH_3CN$ in water) 5 to 95 % B in 10 min and back to 5% B.

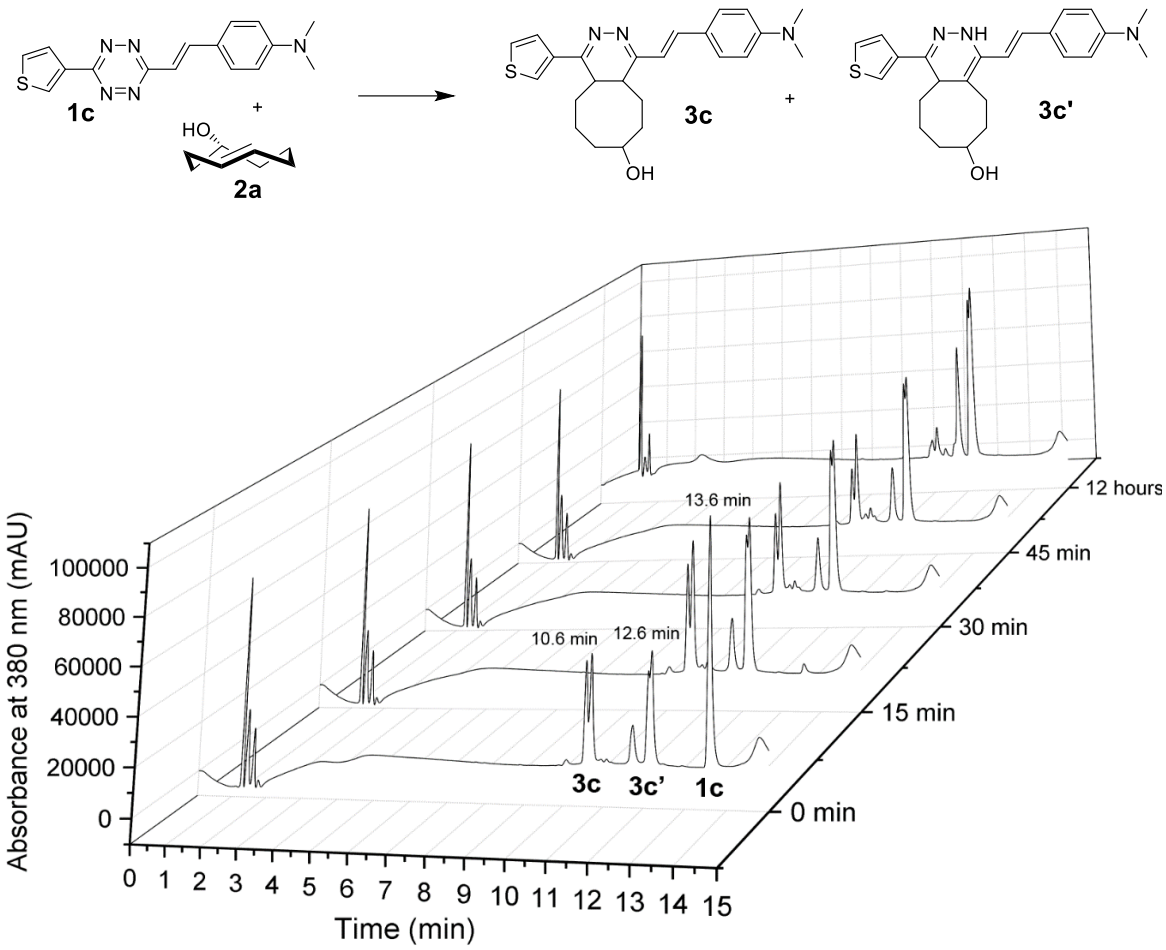


**Figure S1**: HPLC chromatogram showing progress of the reaction between **1c** and eqTCO **2a**. The double peak eluting at 10.6 min was ascribed to the 4,5-dihydropyridazine intermediate **3c** (observed mass 408.2), which is slowly converted to the 1,4-dihydropyridazine **3c'** (observed mass 408.2) eluting at 12.6 min. Signal at 13.6 min corresponds to the starting tetrazine **1c** (observed mass 310.1). Monitored at 380 nm. Note: We also observed formation of the oxidized pyridazine product after 12 hours. However, the product is detectable only by the MS detector and no significant signal was observed in the DAD detector.

## NMR experiment

For the NMR monitoring of eqTCO reaction with compound **1c**, the studied eqTCO (ca 5 mg) was dissolved in $CD_3CN$ (250 µL) and $D_2O$ (250 µL) solvent mixture. After acquisition of $^1H$ NMR spectrum, a suspension of tetrazine **1c** (15.4 mg) in DMSO-$d_6$ (500 µL) was added to the solution and NMR experiments were acquired periodically, and the reaction progress was monitored. A combination of 1D ($^1H$ and $^{13}C$) experiments with 2D correlation experiments (H,H-COSY, H,C-HSQC, H,C-HMBC) was used to determine the structure of the final products. Unfortunately, the structure of the intermediates could not be confirmed unequivocally because of the complexity of the reaction mixture and difficult solubility of **1c**.

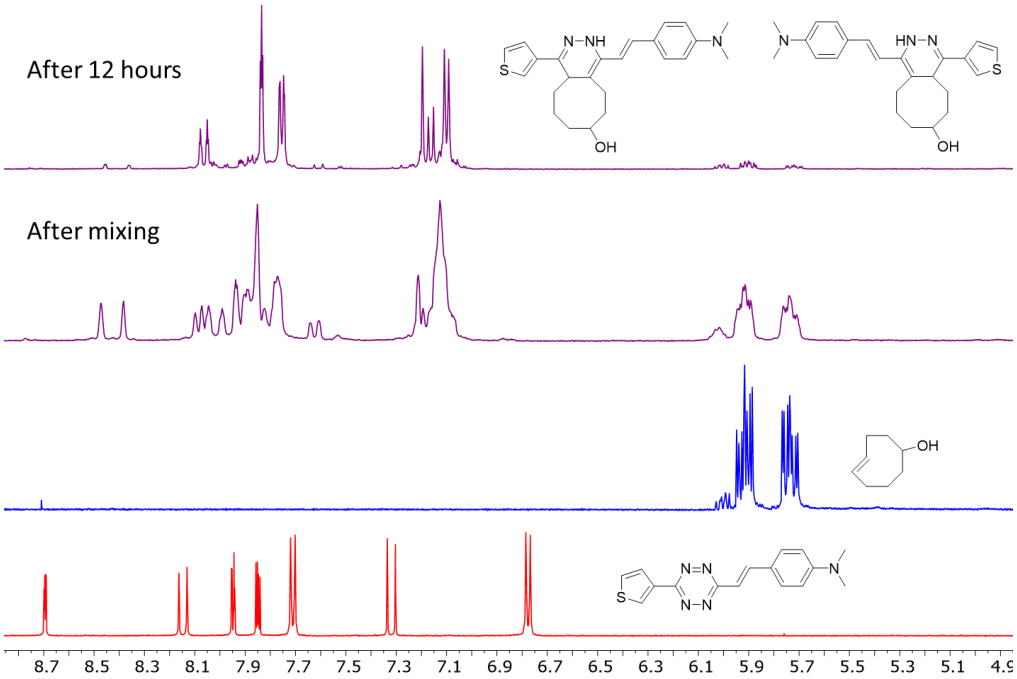


**Figure S2**. The double-bond and aromatic region of $^{1}$H NMR spectra of **1c**, TCO **2a**, the reaction mixture immediately after mixing and after 12 hours.

## Determination of second-order rate constants

Second-order rate constants of the reactions of *trans*-cyclooctenes (TCO) **2a** and **2b** with 1,2,4,5-tetrazines **1a-1f** were determined by following the decay in the concentration of the starting tetrazine over time. The concentration decrease was monitored by scanning kinetics measurements on a UV/VIS spectrophotometer. The measurements were performed in $CH_3CN/H_2O$ 1:1 at room temperature under pseudo first-order conditions using an excess of the corresponding TCO. All measurements were performed at least three times.

Conditions: A 50 µM solution of the respective tetrazine in $CH_3CN/H_2O$ 1:1 containing 5% of DMSO was mixed with a 500 µM solution of the appropriate TCO in $CH_3CN/H_2O$ 1:1. The mixture was further diluted with $CH_3CN/H_2O$ 1:1 to give a final tetrazine concentration of 12.5 µM using 10 equiv of TCO and was immediately measured on the UV/VIS spectrophotometer.

The absorption of the mixtures was followed by scanning kinetics measurements over 4 min. The measured intensity of the absorption at the corresponding absorption maxima of the starting tetrazine (see Table S1) was plotted against time. Fitting the curves with single exponential equation ($y = y_0 + Ae^{-k/t}$) provided the observed rate constants. The second order rate constants (summarized in Table S1) were calculated by dividing the observed rate constants by the initial concentration of the TCO.

The second order rate constants of the click-reactions using tetrazine **1c** were additionally determined by measuring pseudo first order rate constants at different TCO concentrations (10 equiv., 15 equiv. and 20 equiv. of TCO **2a** and 5 equiv., 7.5 equiv. and 10 equiv. of TCO **2b**). The measurements were performed in $CH_3CN/H_2O$ 1:1 at room temperature using a final tetrazine concentration of 12.5 µM. The observed rate constants were plotted against the concentration of the

TCO in order to obtain the second order rate constants (see Table S1) from the slope of the resulting plot.

**Table S1.** Absorption maxima of 1,2,4,5-tetrazines used during kinetic measurements and the corresponding second-order rate constants (in $M^{-1}$ $s^{-1}$) of the reactions with TCOs **2a** and **2b**.

| Tetrazine | $\lambda_{Abs}$ [nm][a] | $k_2$ [$M^{-1}$ $s^{-1}$][b] | |
|---|---|---|---|
| | | 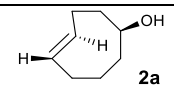 **2a** | 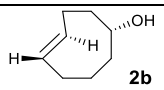 **2b** |
| | | equatorial | axial |
| 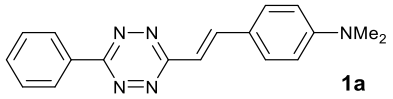 **1a** | 430 | 7.8 ± 0.3 | 35.7 ± 0.5 |
| 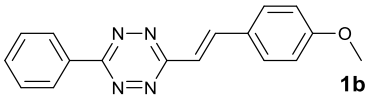 **1b** | 355 | 5.4 ± 0.2 | 66.9 ± 0.8 |
| 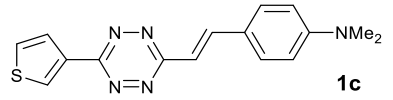 **1c** | 425 | 7.9 ± 0.5[c] | 27.3 ± 0.6[c] |
| 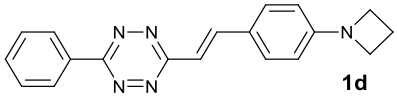 **1d** | 415 | 6.8 ± 0.4 | 39.2 ± 0.5 |
| 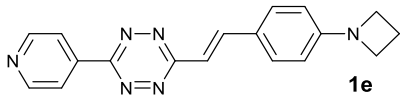 **1e** | 445 | n.m.[d] | 136 ± 3.0 |
| 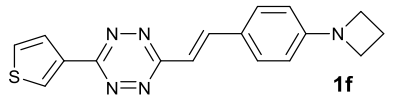 **1f** | 415 | 8.0 ± 1.5 | 30.9 ± 1.1 |

a) Absorption maxima of the starting tetrazines were determined in $CH_3CN/H_2O$ 1:1 at room temperature using a 25 µM solution of the respective tetrazine, b) second-order rate constants were determined in $CH_3CN/H_2O$ 1:1 at room temperature under pseudo first-order conditions using an excess of TCO, c) second order rate constant for derivative **1c** were additionally determined using three different TCO concentrations (10, 15 and 20 equiv. for eqTCO and 5, 7.5 and 10 equiv. of axTCO). The determined $k_2$ were 6.5 $M^{-1}$ $s^{-1}$ and 36.3 $M^{-1}$ $s^{-1}$ respectively, d) not measured; decay of the tetrazine was not traceable due to overlapping of the absorption maximum of the tetrazine and the absorption maximum of the corresponding click product.

## Photophysical properties of the click products of tetrazines 1a-1f with equatorial TCO 2a

Conditions for the following absorption and emission measurements:
A 1 mM solution of the respective tetrazine in DMSO was mixed with a 50 mM solution of the appropriate TCO in $CH_3CN/H_2O$ 1:1 and further diluted with $CH_3CN/H_2O$ 1:1 to give a final tetrazine concentration of 500 µM using 2 equiv of TCO. The reaction mixtures were incubated at room temperature in the dark for 5 min and then further diluted to a tetrazine concentration of 25 µM for absorption measurements and to a concentration of 2.5 µM for emission measurements.

### Determination of fluorescence quantum yields

Quantum yields of click products were measured at room temperature (22 °C) in $CH_3CN/H_2O$ 1:1 (2.5 µM final concentration) using a 1 cm quartz cuvette. The settings were as follows: Excitation wavelength 550 nm, slit 5.0 nm; Emission 575-750 nm, increment 1.0 nm, slit 5.0 nm and data algebra formula S1c/R1c. The fluorescence quantum yields were calculated using the following equation:

$$\phi_{sample} = \phi_{ref} \frac{F_{sample}}{F_{ref}} \times \frac{(1\text{-}10^{-abs})_{ref}}{(1\text{-}10^{-abs})_{sample}} \times \frac{n^2_{sample}}{n^2_{ref}}$$

Where:

$\phi_{ref}$ is 0.38 (fluorescence quantum yield of nile red in MeOH)[5]

**F** are the integrated intensities (areas) of the standard and the sample fluorescence spectra (integrals calculated using OriginPro software)

**abs** is the absorbance of standard and sample at the excitation wavelength (550 nm)

***n*** are the refractive indices for standard (MeOH: 1.327) and sample solution ($CH_3CN/H_2O$ (1:1): 1.3478)[6]

**Table S2.** Photophysical properties of the click products of TCO **2a** with tetrazines **1a-f**[a].

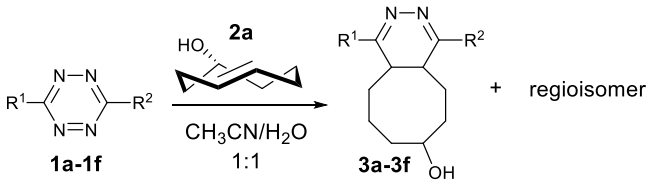


| Tetr. | $R^1$ | $R^2$ | $\lambda_{Abs}/\lambda_{Em}$ [b] [nm] | Stokes shift [nm] | $\phi$ [c] | $\varepsilon_{max}$ ($\times 10^3$ $M^{-1}$ $cm^{-1}$) | Fl. intensity increase[d] |
|---|---|---|---|---|---|---|---|
| **1a** | 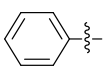 | 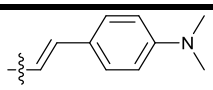 | 545/628 | 83 | 0.005 | 6.4 | 13-fold |
| **1b** | 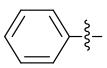 | 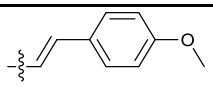 | 295/- | - | - | - | - |
| **1c** | 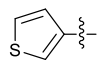 | 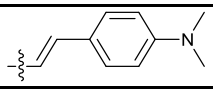 | 546/626 | 80 | 0.005 | 11.5 | 18-fold |
| **1d** | 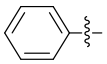 | 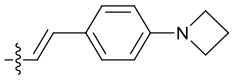 | 546/626 | 80 | 0.004 | 5.3 | 10-fold |
| **1e** | 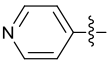 | 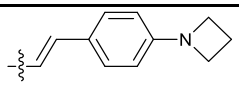 | 566/643 | 77 | 0.002 | 4.5 | 3-fold |
| **1f** | 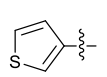 | 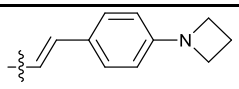 | 549/626 | 77 | 0.005 | 9.5 | 12-fold |

a) All reactions were performed in $CH_3CN/H_2O$ 1:1 at room temperature using an excess of the TCO, b) absorption and emission (at 550 nm excitation) maxima were measured in $CH_3CN/H_2O$ 1:1 at room temperature, c) quantum yields were determined by using nile red in MeOH as standard ($\phi$ = 0.38), d) calculated as the integral of the fluorescence of the click product divided by the integral of the fluorescence of the starting tetrazine.

## Absorption and emission spectra of the click products and starting tetrazines

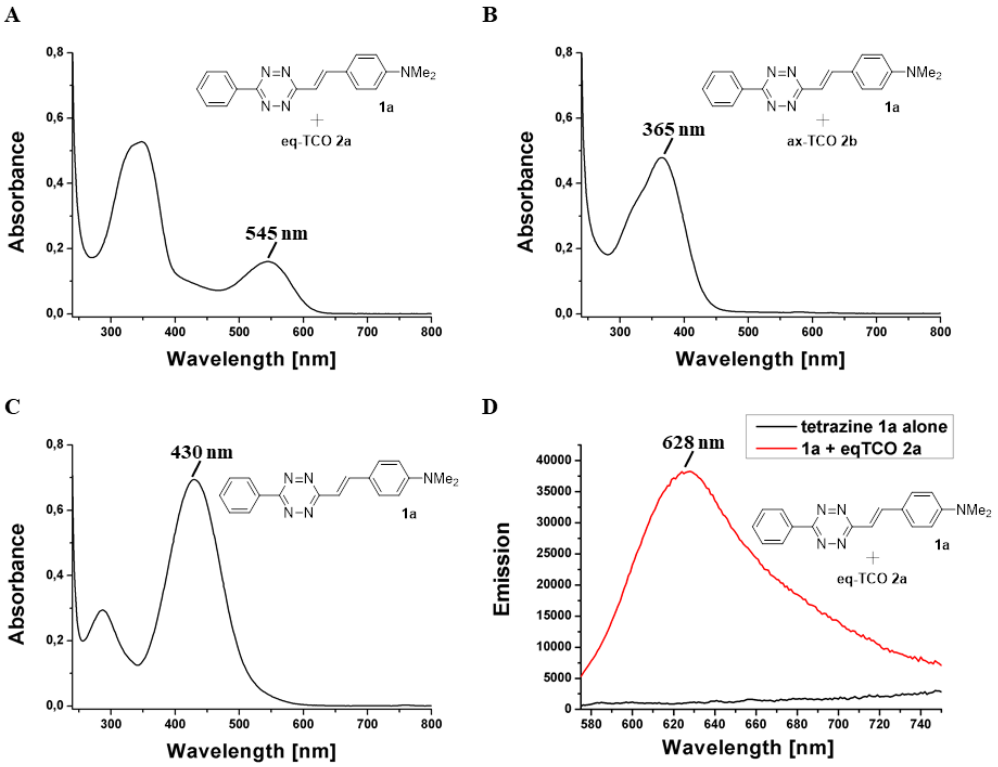


**Figure S3.** Absorption and emission spectra of click product formed in reaction of **1a** with **2a** (A and D), absorption spectrum of the click product of **1a** with axial TCO **2b** (B) and absorption and emission spectra of **1a** (C and D). All spectra were measured in $CH_3CN/H_2O$ 1:1 at room temperature using a tetrazine concentration of 25 µM for absorption measurements and 2.5 µM for emission measurements.

**Figure S4.** Absorption and emission spectra of click product formed in reaction of **1b** with **2a** (A and D), absorption spectrum of the click product of **1b** with axial TCO **2b** (B) and absorption and emission spectra of **1b** (C and D). All spectra

were measured in $CH_3CN/H_2O$ 1:1 at room temperature using a tetrazine concentration of 25 µM for absorption measurements and 2.5 µM for emission measurements.

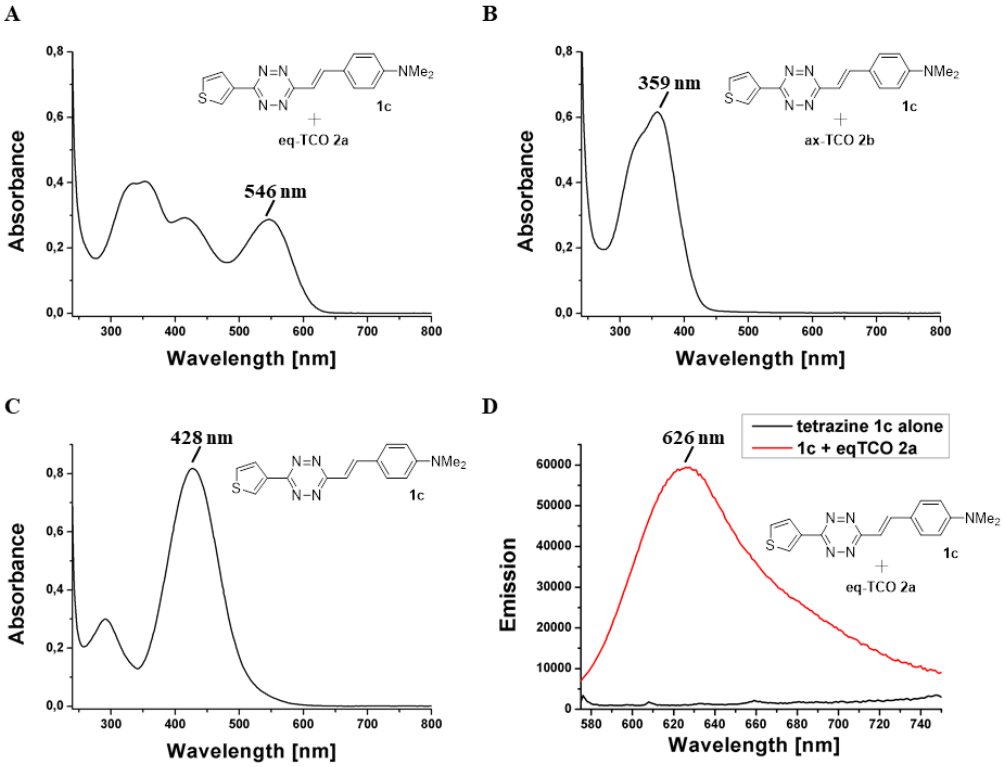


**Figure S5.** Absorption and emission spectra of click product formed in reaction of **1c** with **2a** (A and D), absorption spectrum of the click product of **1c** with axial TCO **2b** (B) and absorption and emission spectrum of **1c** (C and D). All spectra were measured in $CH_3CN/H_2O$ 1:1 at room temperature using a tetrazine concentration of 25 µM for absorption measurements and 2.5 µM for emission measurements.

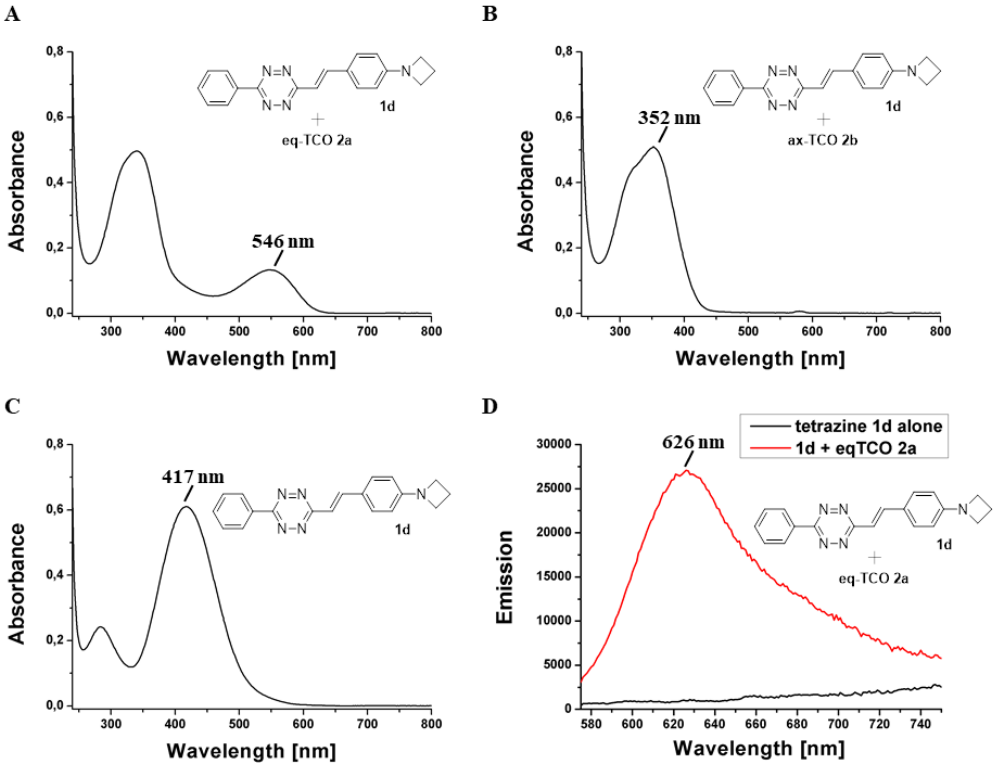


**Figure S6.** Absorption and emission spectra of click product formed in reaction of **1d** with **2a** (A and D), absorption spectrum of the click product of **1d** with axial TCO **2b** (B) and absorption and emission spectrum of **1d** (C and D). All spectra

were measured in $CH_3CN/H_2O$ 1:1 at room temperature using a tetrazine concentration of 25 µM for absorption measurements and 2.5 µM for emission measurements.

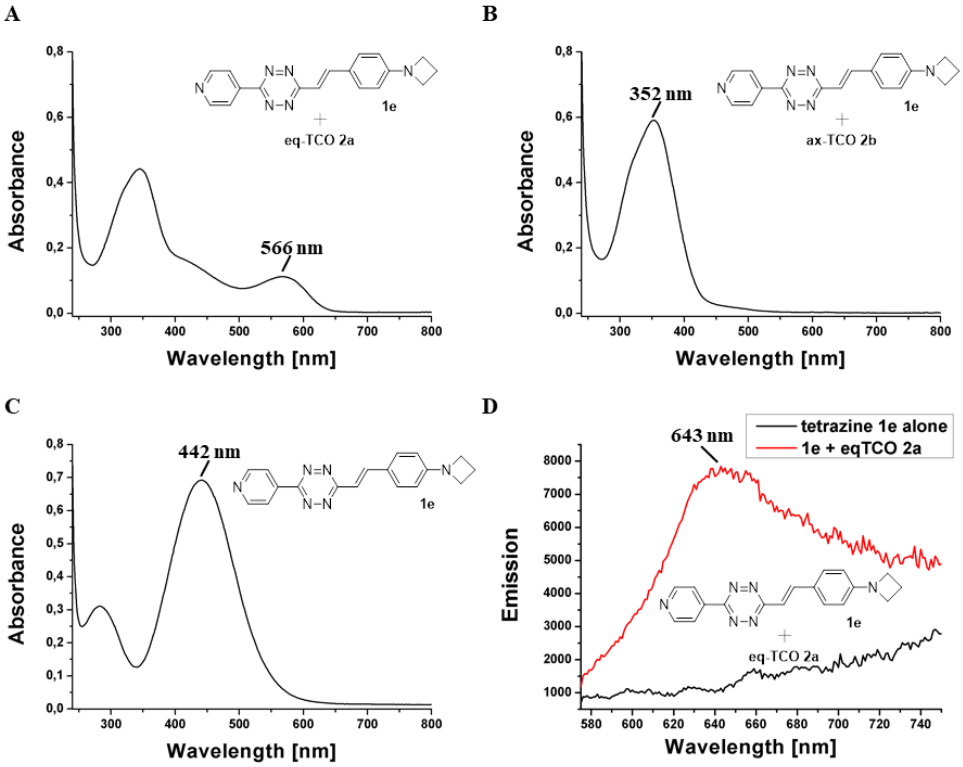


**Figure S7.** Absorption and emission spectra of click product formed in reaction of **1e** with **2a** (A and D), absorption spectrum of the click product of **1e** with axial TCO **2b** (B) and absorption and emission spectra of **1e** (C and D). All spectra were measured in $CH_3CN/H_2O$ 1:1 at room temperature using a tetrazine concentration of 25 µM for absorption measurements and 2.5 µM for emission measurements.

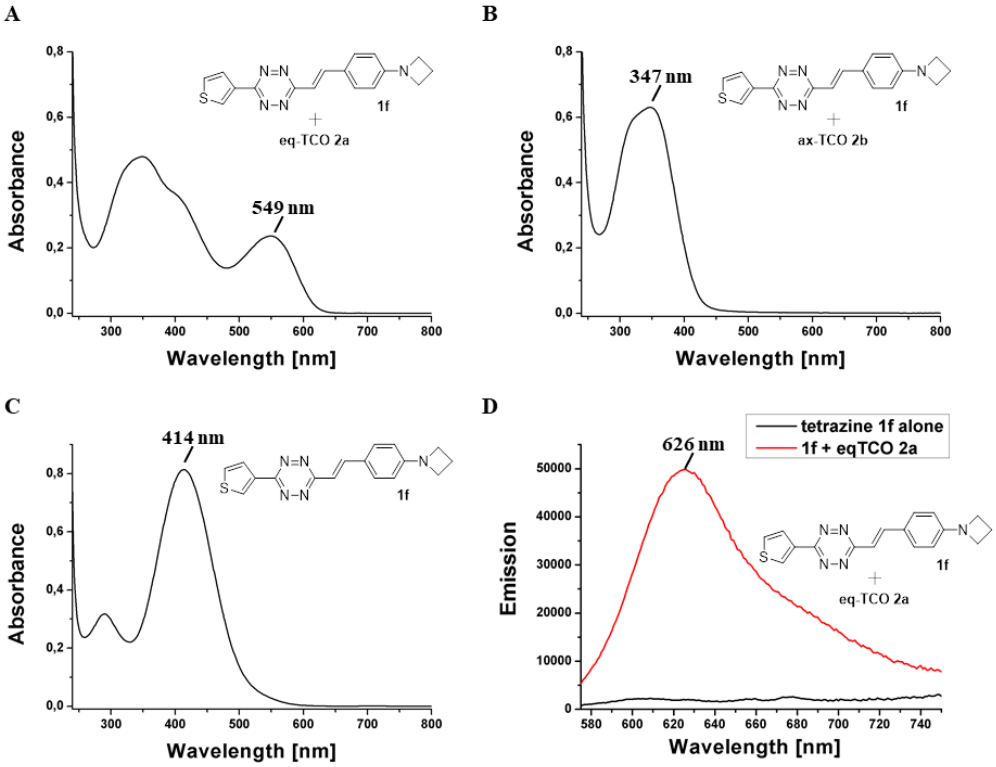


**Figure S8.** Absorption and emission spectra of click product formed in reaction of **1f** with **2a** (A and D), absorption spectrum of the click product of **1f** with axial TCO **2b** (B) and absorption and emission spectra of **1f** (C and D). All spectra were

measured in $CH_3CN/H_2O$ 1:1 at room temperature using a tetrazine concentration of 25 µM for absorption measurements and 2.5 µM for emission measurements.

## The fluorescence decay of the thiophene containing click products 3c and 3f over time

Conditions for the emission measurements:
A 1 mM solution of the respective tetrazine in DMSO was mixed with a 50 mM solution of TCO **2a** in $CH_3CN/H_2O$ 1:1 and further diluted with $CH_3CN/H_2O$ 1:1 to give a final tetrazine concentration of 500 µM using 2 equiv of TCO. The reaction mixtures were incubated at room temperature in the dark for 5 min and then further diluted to a tetrazine concentration of 2.5 µM for the emission measurements. The diluted solutions were measured at indicated time points (Figure S9 and S10). The settings were as follows: Excitation wavelength 550 nm, slit 5.0 nm; Emission 575-750 nm, increment 1.0 nm, slit 5.0 nm and data algebra formula S1c/R1c.
Or: Excitation wavelength 350 nm, slit 5.0 nm; Emission 400-680 nm, increment 1.0 nm, slit 5.0 nm and data algebra formula S1c/R1c.

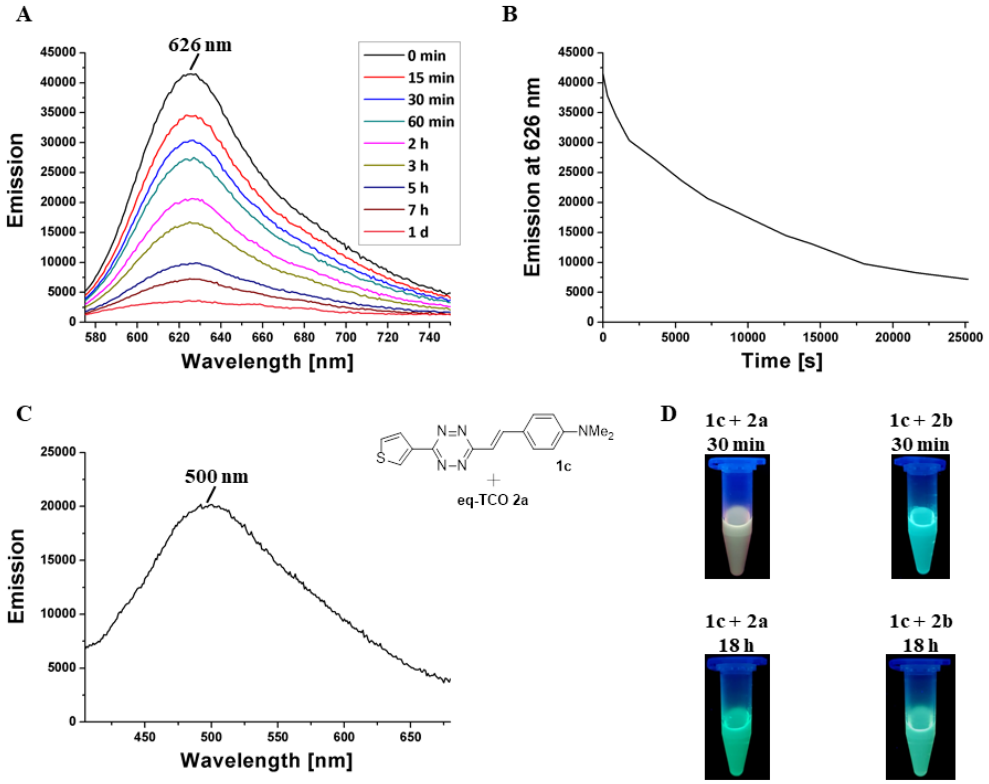


**Figure S9.** Emission spectra of click product formed in reaction of **1c** with **2a** excited at 550 nm at different time points (A), corresponding decay of the emission maximum at 626 nm over time (B), emission spectrum of click product formed in reaction of **1c** with **2a** after 1 d of incubation at 350 nm excitation (C) and fluorescence pictures of click products formed in the reactions of **1c** with **2a** and **2b** taken after 30 min and 18 h respectively (captured under UV-Vis lamp, 354 nm) (D). All spectra were measured in $CH_3CN/H_2O$ 1:1 at room temperature using a tetrazine concentration of 2.5 µM.

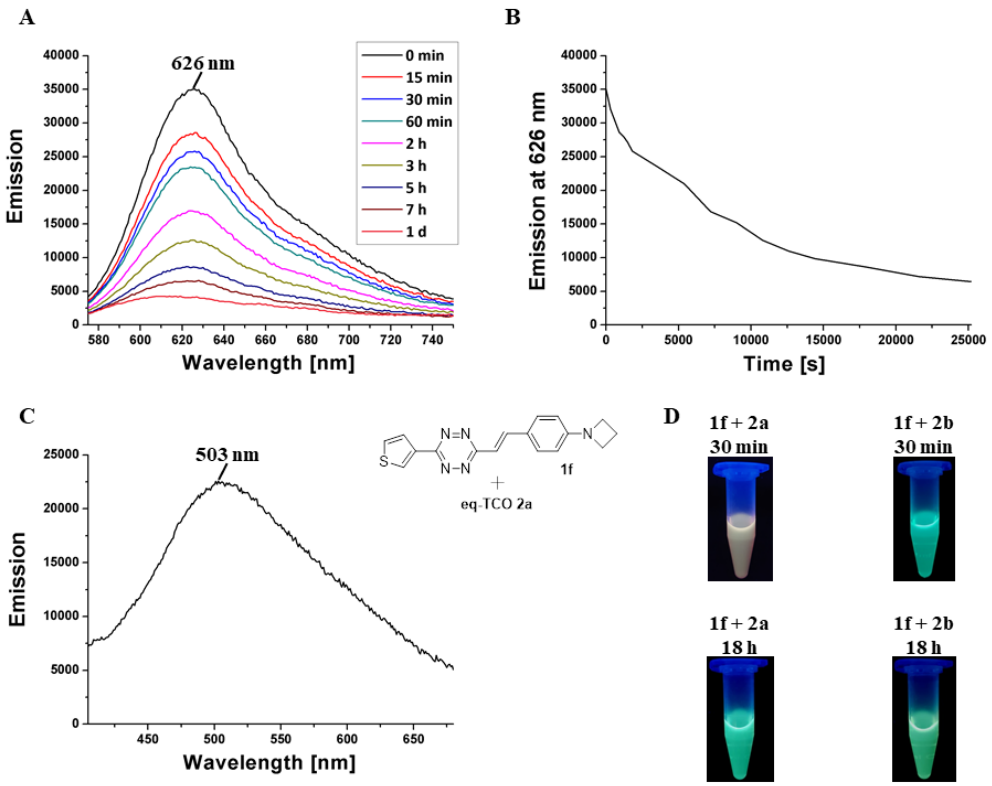


**Figure S10.** Emission spectra of click product formed in reaction of **1f** with **2a** excited at 550 nm at different time points (A), corresponding decay of the emission maximum at 626 nm over time (B), emission spectrum of click product formed in reaction of **1f** with **2a** after 1 d of incubation at 350 nm excitation (C) and fluorescence pictures of click products formed in the reactions of **1f** with **2a** and **2b** taken after 30 min and 18 h respectively (captured under UV-Vis lamp, 354 nm) (D). All spectra were measured in $CH_3CN/H_2O$ 1:1 at room temperature using a tetrazine concentration of 2.5 µM.

## The fluorescence comparison of the thiophene containing tetrazines 1c and 1f with different TCOs

Conditions for the absorption and emission measurements:

A 1 mM solution of the respective tetrazine in DMSO was mixed with a 50 mM solution of the appropriate TCO in $CH_3CN/H_2O$ 1:1 and further diluted with $CH_3CN/H_2O$ 1:1 to give a final tetrazine concentration of 500 µM using 2 equiv of TCO. The reaction mixtures were incubated at room temperature in the dark for 5 or 30 min and then further diluted to a tetrazine concentration of 25 µM for absorption measurements and 2.5 µM for emission measurements. The settings for emission measurements were as follows: Excitation wavelength 550 nm, slit 5.0 nm; Emission 575-750 nm, increment 1.0 nm, slit 5.0 nm and data algebra formula S1c/R1c. Quantum yields were determined by using nile red in MeOH as standard ($\phi$ = 0.38).

**Table S3.** Photophysical properties of the click products of tetrazine **1c** with various TCOs.

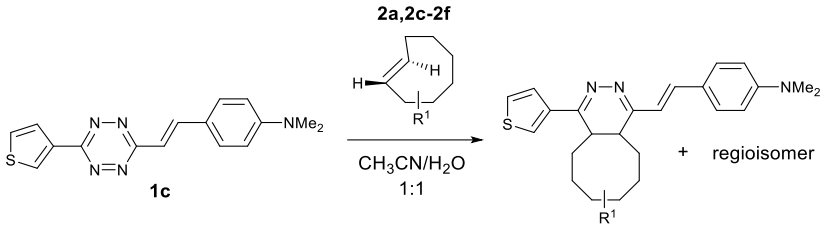


| TCO | $\lambda_{Abs}/\lambda_{Em}$ [a] [nm] | Stokes shift [nm] | $\phi$ | $\varepsilon_{max}$ ($\times 10^3$ $M^{-1}$ $cm^{-1}$) | Fl. intensity increase [b] |
|---|---|---|---|---|---|
| 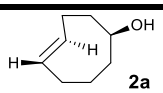 **2a** equatorial | 546/626 | 80 | 0.005 | 11.5 | 18-fold |
| **2c** 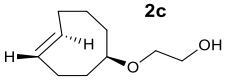 | 547/627 | 80 | 0.004 | 11.5 | 13-fold |
| 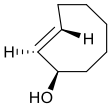 **2d** | 550/627 | 77 | 0.004 | 14.4 | 14-fold |
| 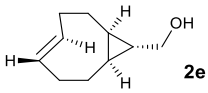 **2e** | 547/631 | 84 | 0.003 | 12.2 | 11-fold |
| 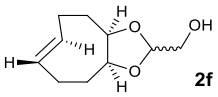 **2f** | 558/638 | 80 | 0.002 | 7.8 | 6-fold |

a) Absorption and emission maxima were measured in $CH_3CN/H_2O$ 1:1 at room temperature, b) calculated as the integral of the fluorescence of the click product divided by the integral of the fluorescence of the starting tetrazine.

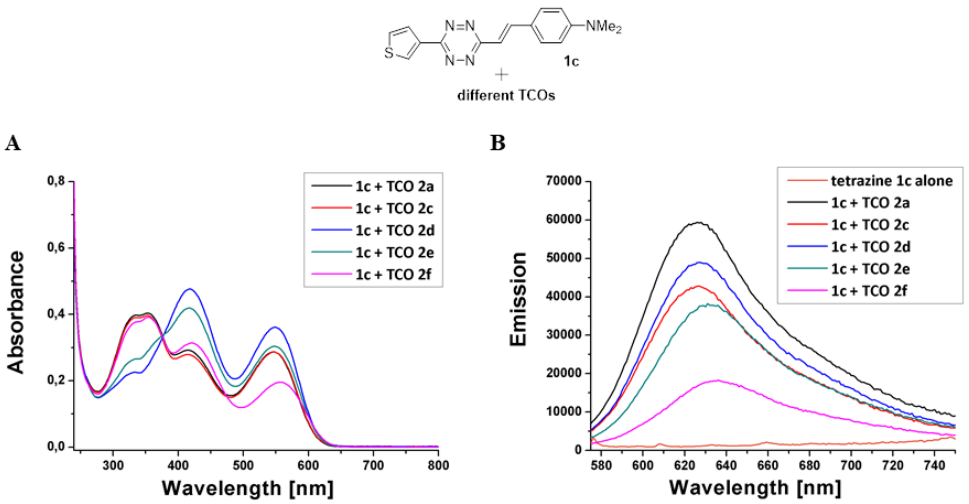


**Figure S11.** Absorption (A) and emission (B) spectra of the click products of **1c** with various TCOs. The spectra were measured after 5 min (for click reactions with TCO **2a, 2e** and **2f**) or after 30 min (for click reactions with TCO **2c** and **2d**) of incubation.

**Table S4.** Photophysical properties of the click products of tetrazine **1f** with various TCOs.

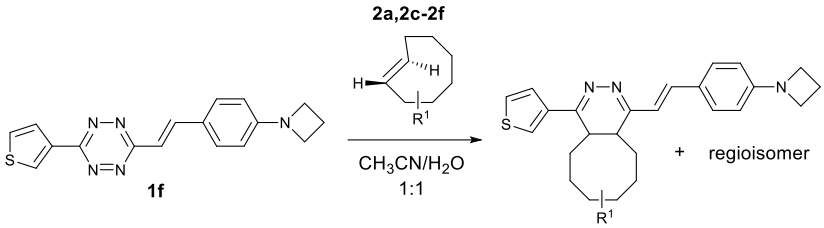


| TCO | $\lambda_{Abs}/\lambda_{Em}$ [b] [nm] | Stokes shift [nm] | $\phi$ [c] | $\varepsilon_{max}$ ($\times 10^3$ $M^{-1}$ $cm^{-1}$) | Fl. intensity increase [d] |
|---|---|---|---|---|---|
| 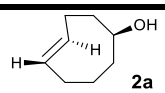 **2a** equatorial | 549/626 | 77 | 0.005 | 9.5 | 12-fold |
| 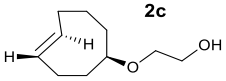 **2c** | 550/627 | 77 | 0.004 | 9.5 | 9-fold |
| 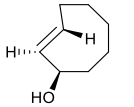 **2d** | 550/627 | 77 | 0.003 | 11.6 | 9-fold |
| 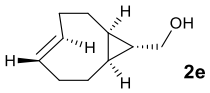 **2e** | 550/631 | 81 | 0.003 | 10.1 | 8-fold |
| 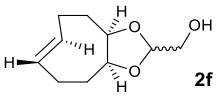 **2f** | 551/631 | 80 | 0.002 | 6.4 | 4-fold |

a) Absorption and emission maxima were measured in $CH_3CN/H_2O$ 1:1 at room temperature, b) calculated as the integral of the fluorescence of the click product divided by the integral of the fluorescence of the starting tetrazine.

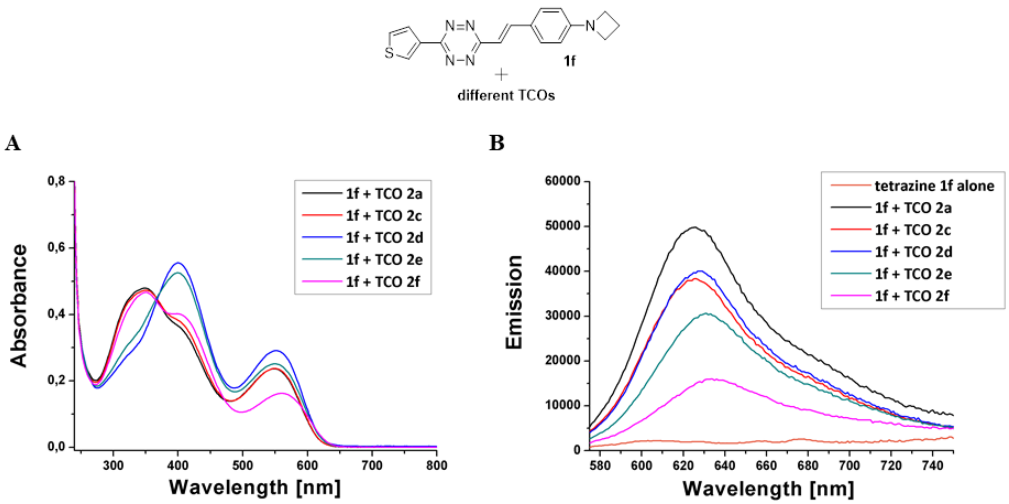


**Figure S12.** Absorption (A) and emission (B) spectra of the click products of **1f** with various TCOs. The spectra were measured after 5 min (for click reactions with TCO **2a, 2e** and **2f**) or after 30 min (for click reactions with TCO **2c** and **2d**) of incubation.

## Cell labeling experiments

### Preparation of ConA-TCO

100 µl of 5 mg/ml solution of concanavalin A (4.7 nmol of tetramer) in 1 M NaCl, 50 mM HEPES-NaOH (pH 8.3), 3 mM $CaCl_2$, 3 mM $MnCl_2$ was combined with 2.3 µL of 10 mM NHS TCO ester[1, 3] (5× molar excess of active ester dissolved in dry DMSO). Reaction was incubated at room temperature for 1 h with constant shaking. After one hour, 10 µL of 1 M Tris-HCl (pH 6.8) was added to neutralize the remaining NHS ester and incubated for another 10 min. at room temperature. TCO excess was removed by desalting using Zeba (Thermo) spin columns into 1 M NaCl, 20 mM Tris-HCl (pH 6.8), 3 mM $CaCl_2$, 3 mM $MnCl_2$.

### Cell experiments

HeLa cells were maintained in high glucose DMEM (Sigma) supplemented with 10% FBS (Thermo) and 0.1 mg/mL of penicillin-streptomycin (Sigma) at 37 °C/5% $CO_2$. One day before the experiment $2\times10^4$ cells were seeded at the 96 well plate cultivation dishes with a coverglass in the bottom (CellVis).

Cells were incubated with the TCO-TPP or ConA-TCO compounds in complete media for the indicated time points at 37 °C. Cells were then washed three times with 100 µL of Leibovitz's L15 media (Thermo) containing 1% BSA. After the last wash, cells were incubated with 100 µL of tetrazine (**1c**)-containing Leibovitz's L15 (1% BSA) in final concentration 5 µM with the addition of either 0.5 µM DRAQ 5 (Thermo), or 10 nM Mitotracker deep red (Thermo).

### Microscopy

Pictures of live cells were taken using Leica TCS SP5 Tandem confocal microscope equipped with a HCX PL APO 63x/1.30 GLYC CORR. 37 °C objective. Excitation for the click products was 561 nm. Emission was collected sequentially using Hyd detector in BrightR mode, with a AOBS window set to λ = 568-620 nm. DRAQ5 for nuclei staining was excited with a 633 nm laser and collected in a 643-703 nm window. Mitotracker: excitation 633 nm, emission window 643-703 nm. Brightness of the raw images was adjusted using Adobe Photoshop.

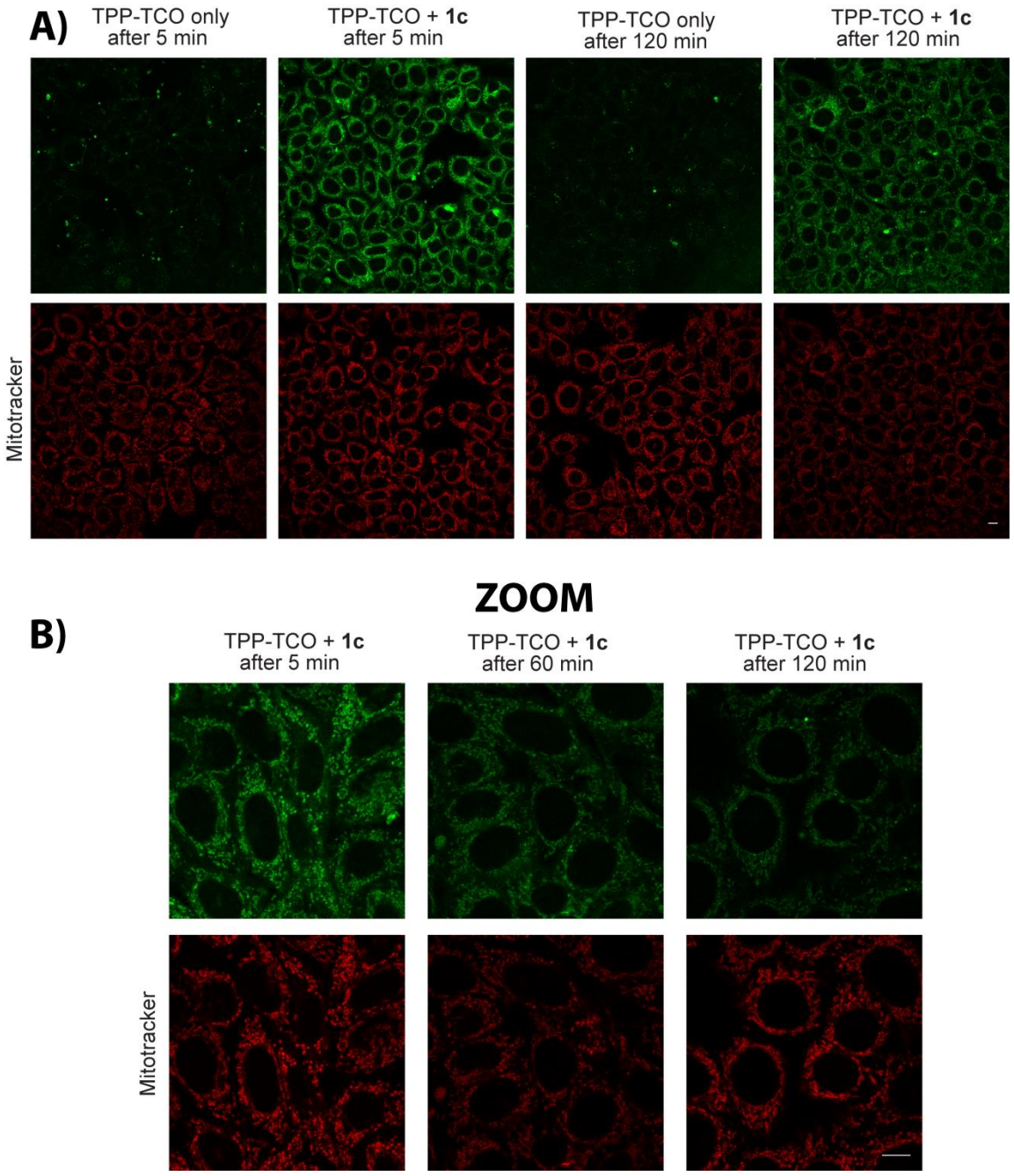


**Figure S13.** HeLa cells were incubated for 15 min with 5 µM TPP-TCO in Leibowitz L15 media containing 1% BSA + 10 nM Mitotracker deep red. Washed 3× with Leibowitz L15 media with 1% BSA. Incubated for 5-120 min with 5 µM (final) concentration of **1c** and imaged at indicated time points using Leica SP5 confocal microscope equipped with 63× glycerol immersion objective. For the click products, a λ = 561 nm laser was used for excitation (intensity 50%), emission was collected in a λ = 568-620 nm window. Mitotracker deep red was excited with laser λ = 633 nm, intensity 20%, emission was collected in a λ = 643-703 nm window. Scale bar 10 µm.

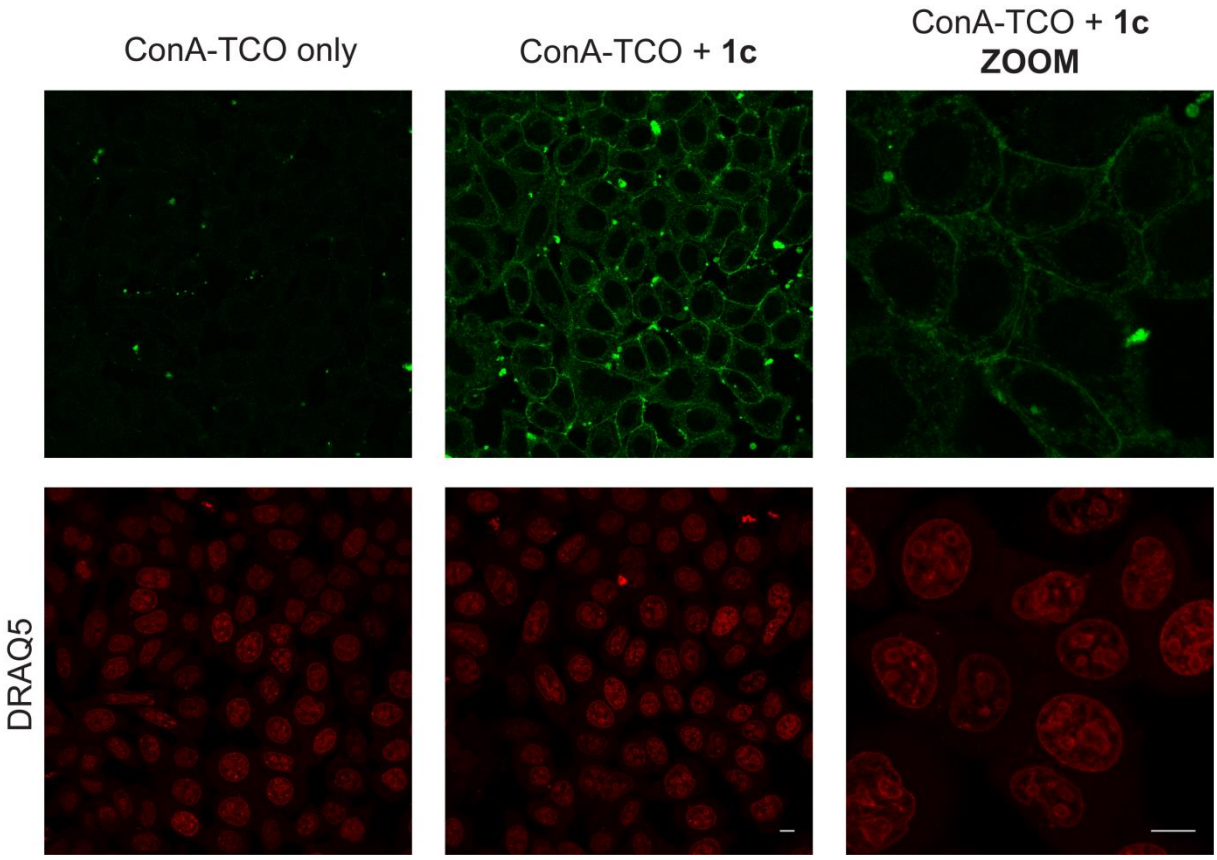


**Figure S14.** HeLa cells were incubated for 15 min with 1/10 dilution of ConA-TCO conjugate (0.5 mg/mL final concentration) in Leibowitz L15 media with 1% BSA + 0.5 µM DRAQ5. Washed 3× with Leibowitz L15 media with 1% BSA. Incubated for 1 h with 5 µM (final) concentration of **1c** and imaged on Leica SP5 confocal microscope, 63× glycerol immersion objective, excitation laser λ = 561 nm, intensity 50% emission λ = 568-620 nm window. DRAQ5 excitation laser λ = 633 nm, intensity 25%, emission λ = 643-703 nm window. Scale bar 10 µm.

## References


[1] A. Vázquez, R. Dzijak, M. Dračínský, R. Rampmaier, S. J. Siegl, M. Vrabel, *Angew. Chem. Int. Ed.* **2017**, *56*, 1334-1337.

[2] H. Ma, B. Song, Y. X. Wang, C. L. Liu, X. Wang, J. L. Yuan, *Dyes Pigments* **2017**, *140*, 407-416.

[3] Y. Kurra, K. A. Odoi, Y.-J. Lee, Y. Yang, T. Lu, S. E. Wheeler, J. Torres-Kolbus, A. Deiters, W. R. Liu, *Bioconjugate Chemistry* **2014**, *25*, 1730-1738.

[4] J. C. T. Carlson, H. Mikula, R. Weissleder, *J. Am. Chem. Soc.* **2018**, *140*, 3603-3612.

[5] a) J. Jose, K. Burgess, *J. Org. Chem.* **2006**, *71*, 7835-7839; b) M. La Deda, M. Ghedini, I. Aiello, T. Pugliese, F. Barigelletti, G. Accorsi, *J. Organomet. Chem.* **2005**, *690*, 857-861.

[6] J. E. Bertie, Z. D. Lan, *Journal of Physical Chemistry B* **1997**, *101*, 4111-4119.

## 7.3 Supplementary information to chapter 3.3

S.J. Siegl, J. Galeta, R. Dzijak, M. Dračínský, M. Vrabel, *ChemPlusChem* **2019**, 84, 493-497. "Bioorthogonal Fluorescence Turn-On Labeling Based on Bicyclononyne–Tetrazine Cycloaddition Reactions that Form Pyridazine Products".

The corresponding NMR spectra are not presented here and can be found in the original publication.

CHEMPLUSCHEM

Supporting Information



# Bioorthogonal Fluorescence Turn-On Labeling Based on Bicyclononyne–Tetrazine Cycloaddition Reactions that Form Pyridazine Products

Sebastian J. Siegl, Juraj Galeta, Rastislav Dzijak, Martin Dračínský, and Milan Vrabel*

## Content

## General information

The chemicals were obtained from commercial suppliers and were used without further purification. Reactions with air- and moisture-sensitive reactants were performed in anhydrous solvents under nitrogen or argon atmosphere. Column chromatography was carried out on silica gel 60A (particle size: 40-60 µm) from *Acros Organics*. Mixtures of solvents are each stated as volume fractions. For flash column chromatography a Combi*Flash*® Rf+ from *Teledyne ISCO* was used. Thin-layer chromatography was performed on aluminum sheets from *Merck* (silica gel 60 F254, 20 × 20 cm). Chromatograms were visualized by UV light (λ = 254 nm/ 366 nm) or by staining with $KMnO_4$ solution. $^{1}H$- and $^{13}C$-NMR spectra were measured on a Bruker Avance III™ HD 400 MHz NMR system equipped with Prodigy cryo-probe. Chemical shifts δ are quoted in ppm in relation to the chemical shift of the residual non-deuterated solvent peak ($CDCl_3$: $\delta(^{1}H) = 7.26$, $\delta(^{13}C) = 77.16$; DMSO-$d_6$: $\delta(^{1}H) = 2.50$, $\delta(^{13}C) = 39.52$). High-resolution mass spectra were recorded on an *Agilent* 5975C MSD Quadrupol, Q-Tof micro from *Waters* or LTQ Orbitrap XL from *Thermo Fisher Scientific*. HPLC-MS measurements were performed on an LCMS-2020 system from *Shimadzu* equipped with a Luna® C18(2) column (3µm, 100A, 100 × 4.6 mm). UV/VIS spectroscopy was performed on a Cary 60 UV/Vis spectrophotometer from *Agilent Technologies*. Data from kinetic experiments were processed using OriginPro 9.1 software. Fluorescence measurements were performed on a FluoroMax 4 spectrofluorometer (Jobin Yvon, Horiba) from *Perkin Elmer* equipped with a 450 W xenon lamp and a single cuvette reader using the dye quinine sulfate (solution in 0.5 M $H_2SO_4$) as standard for determination of fluorescence quantum yields.

## Synthetic procedures

The synthesis of tetrazines **1a**[1] and **1b**,**c**[2] has already been published in our earlier publications.

## Synthesis of tetrazines 1d, 1e and BCN-TPP

### *N*,*N*-Dimethyl-4-((1*E*,3*E*)-4-(6-(thiophen-3-yl)-1,2,4,5-tetrazin-3-yl)buta-1,3-dien-1-yl)aniline (1d)

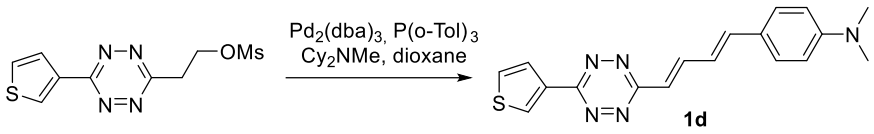


To a Schlenk vessel was added mesylated starting tetrazine[1] (100 mg, 0.349 mmol), P(*o*-Tol)$_3$ (43 mg, 0.140 mmol, 40 mol%), $Pd_2(dba)_3$ (32 mg, 0.0349 mmol, 10 mol%) and (*E*)-4-(2-iodovinyl)-*N*,*N*-dimethylaniline[3] (224 µL, 1.05 mmol, 1.5 equiv). The vessel was purged with argon and 10 mL of degassed anhydrous 1,4-dioxane was added via syringe followed by $Cy_2NMe$ (3 equiv). The reaction mixture was vigorously stirred at 90 °C and cooled to RT after 20 h. Water (10 mL) was added and the mixture was extracted with DCM (3 × 5 mL), the combined extracts were dried over $Na_2SO_4$, filtered and evaporated. Column chromatography (1. DCM; 2. DCM/PE 3:1) and subsequent sonication of the residue with acetone and decanting afforded 48 mg (41%) of a dark red tetrazine **1d**.

$^1$H NMR (400 MHz, $CDCl_3$): 8.54 (dd, 1H, *J* = 3.0, 1.2), 8.05–8.12 (m, 1H), 8.04 (dd, 1H, *J* = 5.1, 1.2), 7.50 (dd, 1H, *J* = 5.1, 3.0), 7.43 (d, 2H, *J* = 8.9), 6.93–6.96 (m, 2H), 6.90 (d, 1H, *J* = 15.4), 6.69 (d, 2H, *J* = 8.9), 3.02 (s, 6H).

$^{13}$C NMR (101 MHz, $CDCl_3$): 164.9, 160.2, 151.2, 142.6, 141.4, 135.5, 129.3, 129.0, 127.4, 126.6, 124.4, 123.3, 121.1, 112.2, 40.4.

HRMS (ESI): m/z calcd. for $C_{18}H_{18}N_5S$ $[MH]^+$ 336.1277, found 336.1278.

### 4,4'-((1*E*,1'*E*)-(1,2,4,5-Tetrazine-3,6-diyl)bis(ethene-2,1-diyl))bis(*N*,*N*-dimethylaniline) (1e)

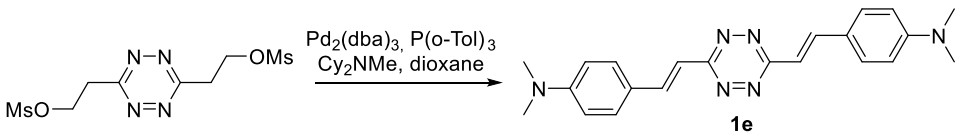


To a Schlenk vessel was added bis-mesylated tetrazine[4] (100 mg, 0.306 mmol), P(*o*-Tol)$_3$ (37 mg, 0.123 mmol, 40 mol%), $Pd_2(dba)_3$ (28 mg, 0.0306 mmol, 10 mol%) and 4-bromo-*N*,*N*-dimethylaniline (184 mg, 0.919 mmol, 3 equiv). The vessel was purged with argon and 10 mL of degassed anhydrous 1,4-dioxane was added via syringe followed by $Cy_2NMe$ (3 equiv). The reaction mixture was vigorously stirred at 90 °C and cooled to RT after 20 h. Water (10 mL) was added and the mixture was extracted with DCM (3 × 5 mL), the combined extracts were dried over $Na_2SO_4$, filtered and evaporated. Column chromatography (DCM → DCM/EA 10:1) and subsequent sonication of the residue with acetone and decanting afforded 33 mg (29%) of a very dark violet tetrazine **1e**.

HRMS (ESI): m/z calcd. for $C_{22}H_{25}N_6$ $[MH]^+$ 373.2141, found 373.2139.

Unfortunately the product showed poor solubility even in DMSO so that we were unable to get sufficiently concentrated solution to characterize it by NMR. To therefore confirmed its identity indirectly using HPLC/MS by reaction with the BCN dienophile. For this purpose, a suspension of tetrazine **1e** in DMSO was mixed with a solution of BCN in $CH_3CN$ at room temperature using an excess of BCN. The mixture was stirred in the dark for 19 h and then measured by HPLC-MS. HRMS (ESI): m/z calcd. for $C_{32}H_{39}N_4O$ $[MH]^+$ 495.3124, found 495.3128. For details and results of the measurement see Table S1 and Figure S2.

**(6-(((bicyclo[6.1.0]non-4-yn-9-ylmethoxy)carbonyl)amino)hexyl)triphenylphosphonium formate (BCN-TPP)**

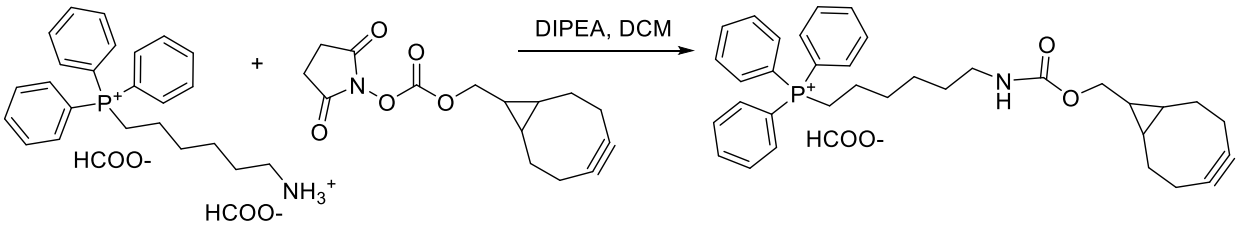


To a solution of BCN active ester (32 mg, 0.11 mmol) and TPP-amine (50 mg, 0.11 mmol, prepared as described in Dyes and Pigments, 2017, 407) in DCM (3 mL) was at 0°C dropwise added DIPEA (96 µL, 5 equiv.) The reaction mixture was stirred for 30-45 min at room temperature when HPLC/MS analysis showed that the reaction finished. After evaporation under reduced pressure, the crude reaction was purified by C-18 RP silica gel flash chromatography using a gradient of $CH_3CN$ in $H_2O$ as the eluent (5% to 80% over 10 min). Fractions containing the product were collected and the solvent was removed under reduced pressure giving the product as white foam (19 mg, 32%).

$^1$H NMR (400 MHz, Chloroform-*d*) δ 7.89 – 7.73 (m, 9H), 7.69 (ddd, *J* = 8.6, 6.9, 3.4 Hz, 6H), 4.08 (m, 2H), 3.81 (m, 2H), 3.12 (q, *J* = 6.4 Hz, 2H), 2.31 – 2.12 (m, 6H), 1.74 – 1.16 (m, 12H), 0.89 (ddd, *J* = 11.0, 6.1, 2.4 Hz, 2H).

$^{13}$C NMR (101 MHz, $CDCl_3$) δ 157.07, 135.09, 135.06, 133.85, 133.75, 130.64, 130.51, 118.92, 118.07, 98.98, 77.48, 77.36, 77.16, 76.84, 62.45, 53.56, 40.63, 30.00, 29.84, 29.58, 29.19, 26.17, 22.99, 22.63, 22.49, 21.55, 20.19, 17.94.

(ESI): m/z calcd. for $C_{35}H_{41}NO_2P$ $[M]^+$ 538.2869, found 538.2877.

## Isolation and confirmation of click product 2a

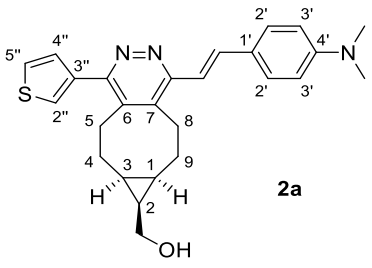

To a solution of tetrazine **1a** (30.0 mg, 0.0970 mmol) in $CH_3CN$ (3 mL) was added bicyclononyne (29.1 mg, 0.194 mmol). The reaction mixture was stirred for 18 h at room temperature until the starting materials disappeared (verified by TLC in DCM/EtOAc 1:1 or HPLC-MS, see Figure S1). The crude product was concentrated *in vacuo* and purified by flash column chromatography (0→40% EtOAc in DCM) to obtain an isomeric mixture of click product **2a** (44 mg). Separation by preparative TLC (eluting with DCM/EtOAc 4:1 + 5% MeOH and elution of the major product from the silica with DCM/MeOH 4:1) provided the main isomer of **2a** as yellow solid (27 mg, 64%).

As the occurrence of rotamers complicated the analysis of the cyclooctene moiety of **2a** at room temperature, the NMR measurements were performed in DMSO-$d_6$ at 80 °C.
$^1$H NMR (600.1 MHz, DMSO-$d_6$): δ 7.79 (d, 1H, $C^{1'}$-C**H**=CH, $J_{H\text{-}C=C\text{-}H}$ = 15.6), 7.70 (dd, 1H, $C^{2''}$**H**, $J_{2''\text{-}5''}$ = 2.9, $J_{2''\text{-}4''}$ = 1.3), 7.66 (dd, 1H, $C^{5''}$**H**, $J_{5''\text{-}4''}$ = 4.9, $J_{5''\text{-}2''}$ = 2.9), 7.57 (m, 2H, $C^{2'}$**H**), 7.36 (dd, 1H, $C^{4''}$**H**, $J_{4''\text{-}5''}$ = 4.9, $J_{4''\text{-}2''}$ = 1.3), 7.31 (d, 1H, $C^{1'}$-CH=C**H**, $J_{H\text{-}C=C\text{-}H}$ = 15.6), 6.76 (m, 2H, $C^{3'}$**H**), 3.49-3.55 (m, 2H, C**H$_2$**-OH), 3.09, 2.95-3.05, 2.89 (3x m, 4H, $C^5$**H$_2$** and $C^8$**H$_2$**), 2.97 (s, 6H, N-(C**H$_3$**)$_2$), 2.34, 2.10, 1.57-1.67 (3x m, 4H, $C^4$**H$_2$** and $C^9$**H$_2$**), 0.95 (m, 1H, $C^2$**H**), 0.71-0.78 (m, 2H, $C^1$**H** and $C^3$**H**).
$^{13}$C NMR (150.9 MHz, DMSO-$d_6$): δ 154.9 ($C^6$-**C**-N and $C^7$-**C**-N), 150.8 (**C**$^{4'}$), 139.2 (**C**$^6$), 138.8 ($C^7$ and $C^{3''}$), 135.5 ($C^{1'}$-**C**H=CH), 128.8 (**C**$^{4''}$), 128.6 (**C**$^{2'}$), 125.8 ($C^{5''}$), 125.4 ($C^{2''}$), 124.4 (**C**$^{1'}$), 116.6 ($C^{1'}$-CH=**C**H), 112.1 ($C^{3'}$), 57.1 (**C**H$_2$-OH), 39.8 (N-(**C**H$_3$)$_2$), 27.4 (**C**$^5$ or **C**$^8$), 25.5 (**C**$^5$ or **C**$^8$), 23.1 (**C**$^4$ or **C**$^9$), 22.2 (**C**$^4$ or **C**$^9$), 21.8 ($C^2$), 18.4 (**C**$^1$ and **C**$^3$) .
HRMS (ESI): m/z calcd. for $C_{26}H_{29}N_3OS$ $[MH]^+$ 432.2104, found 432.2102.

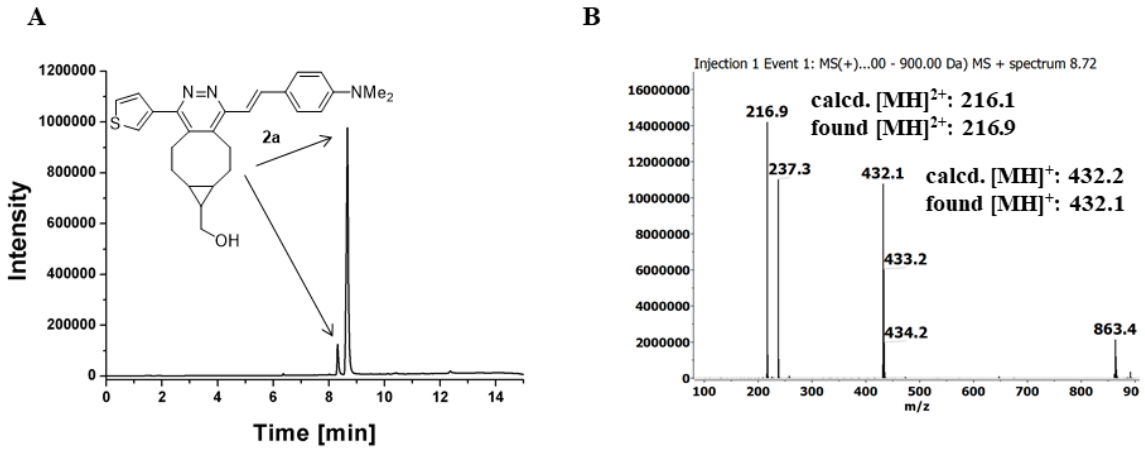


**Figure S1.** HPLC chromatogram and low-resolution mass spectrum of click product **2a** measured in $CH_3CN/H_2O$ 1:1 at room temperature (solvent A: $H_2O$ + 0.05% HCOOH; solvent B: $CH_3CN$ + 0.05% HCOOH; gradient: 5% B → 95% B in 9 min, then 95% B for 2 min and back to 5% B; column: Luna® C18(2) column (3µm, 100A, 100 x 4.6 mm) at a flow rate of 1 mL/min).

## Photophysical properties of the click products of BCN with tetrazines 1a-1e

Conditions for the following absorption and emission measurements:
A 1 mM solution of the respective tetrazine in DMSO was mixed with a 50 mM solution of BCN in the indicated solvent ($CH_3CN$, $CH_3CN/H_2O$ 1:1, $CHCl_3$, acetone, dioxane, *i*PrOH or MeOH) and further diluted with the corresponding solvent to give a final tetrazine concentration of 500 µM using 10 equiv of BCN. The reaction mixtures were incubated at room temperature in the dark for 19 h and then measured by HPLC-MS (Figure S2) to verify the formation of the corresponding click products.

HPLC-MS measurements were performed on a Luna® C18(2) column (3µm, 100A, 100 x 4.6 mm) using a linear gradient of $CH_3CN$ + 0.05% HCOOH (5→95% in 9 min) in $H_2O$ + 0.05% HCOOH at a flow rate of 1.0 mL/min. All low-resolution masses found during these measurements are summarized in Table S1. These stock solutions were further diluted to a tetrazine concentration of 25 µM for absorption measurements and to a concentration of 2.5 µM for emission measurements.

**Table S1.** Calculated and observed masses of click products **2a-2e**[a].

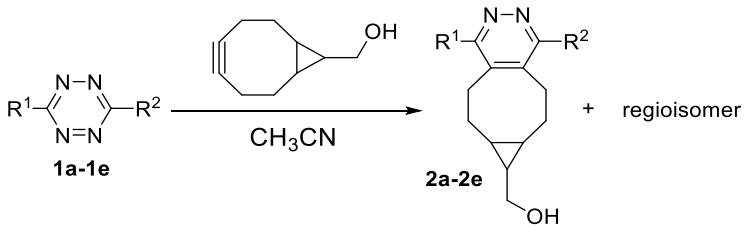


| Click-product | $R^1$ | $R^2$ | M [g/mol] | |
|---|---|---|---|---|
| | | | calcd. | found |
| **2a** |  | 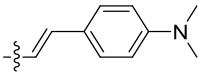 | 432.2 | 432.2 |
| **2b** |  | 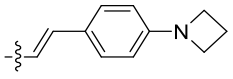 | 444.2 | 444.2 |
| **2c** | 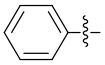 | 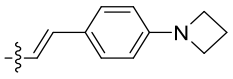 | 438.3 | 438.3 |
| **2d** |  | 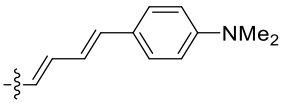 | 458.2 | 458.2 |
| **2e** | 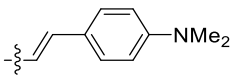 | | 495.3 | 495.3 |

a) All reactions were performed in $CH_3CN$ at room temperature using an excess of BCN and further diluted in 1:1 ratio with $CH_3CN$ for HPLC-MS measurements.

## HPLC chromatograms and low-resolution mass spectra of click products 2a-2e

A

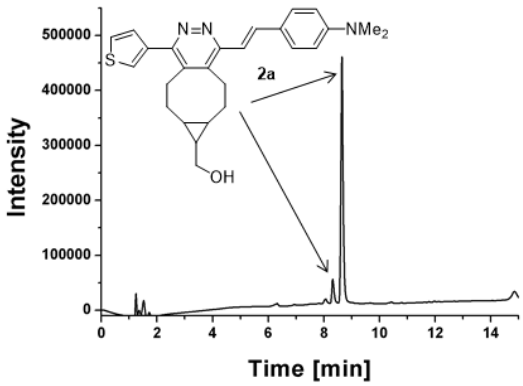
N=N
NMe2
S
OH
2a
Intensity
Time [min]

B

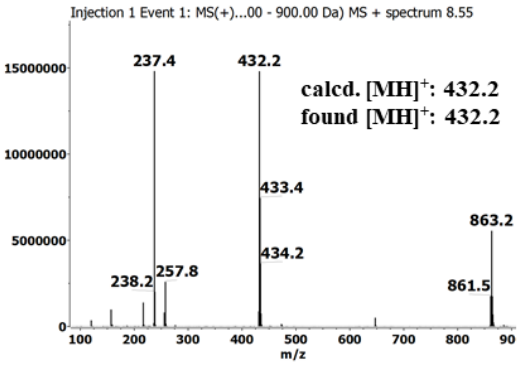
Injection 1 Event 1: MS(+)...00 - 900.00 Da) MS + spectrum 8.55
237.4
432.2
calcd. [MH]+: 432.2
found [MH]+: 432.2
433.4
863.2
434.2
238.2
257.8
861.5
m/z

A

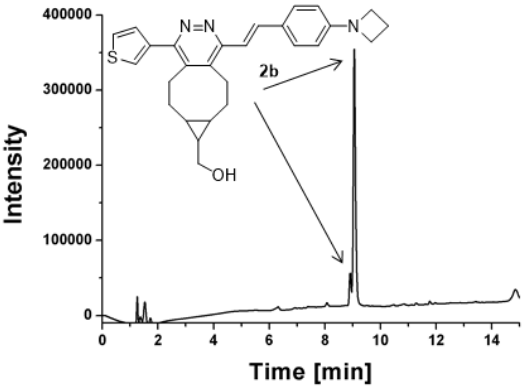
N=N
N
S
OH
2b
Intensity
Time [min]

B

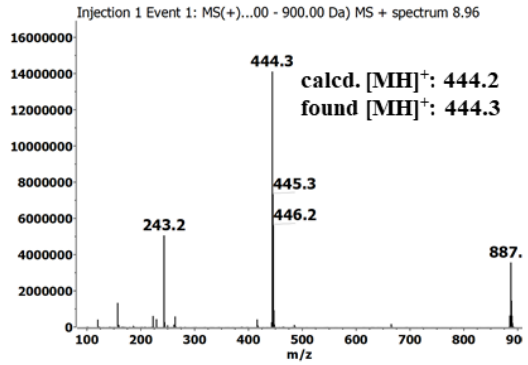
Injection 1 Event 1: MS(+)...00 - 900.00 Da) MS + spectrum 8.96
444.3
calcd. [MH]+: 444.2
found [MH]+: 444.3
445.3
446.2
243.2
887.
m/z

A

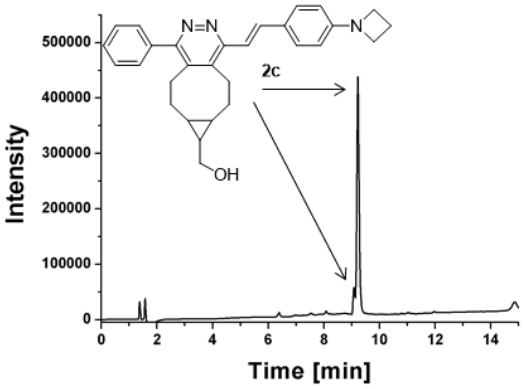
N=N
N
OH
2c
Intensity
Time [min]

B

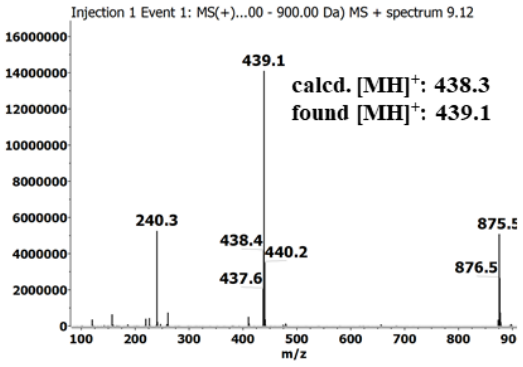
Injection 1 Event 1: MS(+)...00 - 900.00 Da) MS + spectrum 9.12
439.1
calcd. [MH]+: 438.3
found [MH]+: 439.1
240.3
875.5
438.4
440.2
437.6
876.5
m/z

A

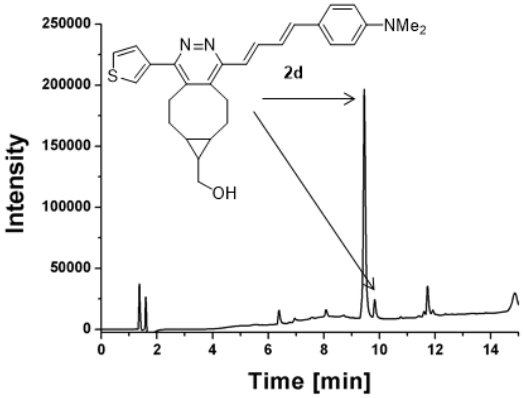
N=N
NMe2
S
OH
2d
Intensity
Time [min]

B

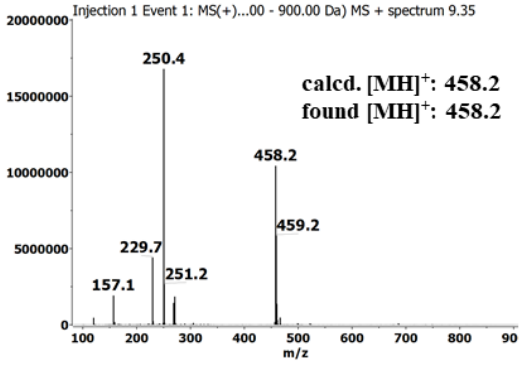
Injection 1 Event 1: MS(+)...00 - 900.00 Da) MS + spectrum 9.35
250.4
calcd. [MH]+: 458.2
found [MH]+: 458.2
458.2
459.2
229.7
251.2
157.1
m/z

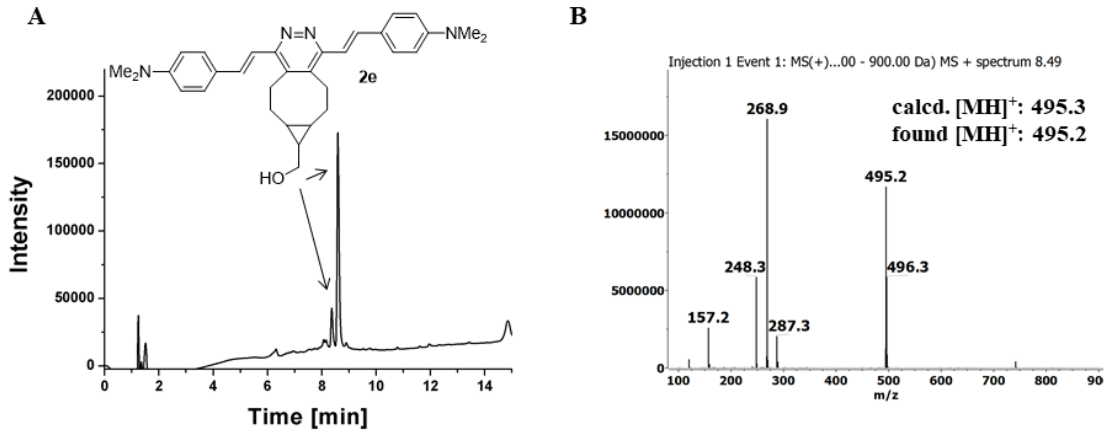


**Figure S2.** HPLC chromatograms (A's) and low-resolution mass spectra (B's) of click products **2a-2e** (solvent A: $H_2O$ + 0.05% HCOOH; solvent B: $CH_3CN$ + 0.05% HCOOH; gradient: 5% B → 95% B in 9 min, then 95% B for 2 min and back to 5% B; column: Luna® C18(2) column (3µm, 100A, 100 x 4.6 mm) at a flow rate of 1 mL/min).

## Determination of fluorescence quantum yields

Quantum yields of click products were measured at room temperature (22 °C) in the indicated solvents ($CH_3CN$, $CH_3CN/H_2O$ 1:1, $CHCl_3$, acetone, dioxane, *i*PrOH or MeOH) at 2.5 µM final concentration using a 1 cm quartz cuvette and quinine sulfate (solution in 0.5 M $H_2SO_4$) as reference ($\phi_{QS}$ = 0.55). The settings were as follows: Excitation wavelength 380 nm, slit 3.0 nm; Emission 400-700 nm, increment 1.0 nm, slit 3.0 nm and data algebra formula S1c/R1c. The fluorescence quantum yields were calculated using the following equation:

$$\phi_{sample} = \phi_{ref} \frac{F_{sample}}{F_{ref}} \times \frac{(1\text{-}10^{-abs})_{ref}}{(1\text{-}10^{-abs})_{sample}} \times \frac{n^2_{sample}}{n^2_{ref}}$$

Where:

$\phi_{ref}$ is 0.55 (fluorescence quantum yield of quinine sulfate in 0.5 M $H_2SO_4$)[5]

**F** are the integrated intensities (areas) of the standard and the sample fluorescence spectra (integrals calculated using OriginPro software)

**abs** are the absorptions of standard and sample at the excitation wavelength (380 nm)

***n*** are the refractive indices for standard (0.5 M $H_2SO_4$: 1.333) and sample solution ($CH_3CN$: 1.3404, $CH_3CN/H_2O$ (1:1): 1.3478)[6]

## Photophysical properties and absorption and emission spectra measured in $CH_3CN$

**Table S2.** Summary of photophysical properties of the click products of BCN with tetrazines **1a-1e** in $CH_3CN$[a].

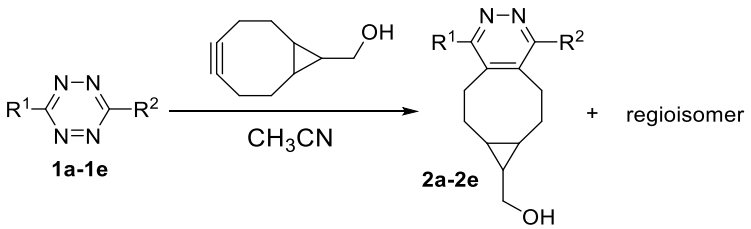

| Click-product | $R^1$ | $R^2$ | $\lambda_{Abs}/\lambda_{Em}$ [b] [nm] | Stokes shift [nm] | $\phi$ [c] | $\varepsilon_{max}$ ($\times 10^3$ $M^{-1}$ $cm^{-1}$) | Fl. intensity increase [d] |
|---|---|---|---|---|---|---|---|
| **2a** | 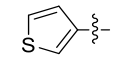 | 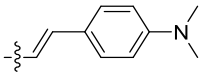 | 376/506 | 130 | 0.014 | 21.3 | 100-fold |
| **2b** | 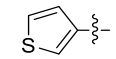 | 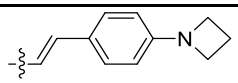 | 370/513 | 143 | 0.010 | 20.8 | 185-fold |
| **2c** | 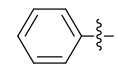 | 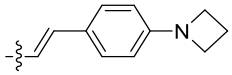 | 369/508 | 139 | 0.011 | 23.6 | 330-fold |
| **2d** | 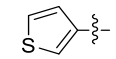 | 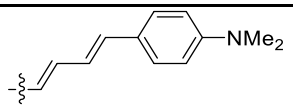 | 392/562 | 170 | 0.038 | 11.0 | 10-fold |
| **2e** | 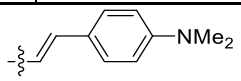 | | 397/529 | 132 | 0.134 | 13.8 | 900-fold |

a) All reactions were performed in $CH_3CN$ at room temperature using an excess of BCN, b) absorption and emission (at 380 nm excitation) maxima were measured in $CH_3CN$ at room temperature, c) quantum yields were determined by using quinine sulfate in 0.5 M $H_2SO_4$ as standard ($\phi$ = 0.55), d) calculated as the integral of the fluorescence of the click product divided by the integral of the fluorescence of the starting tetrazine.

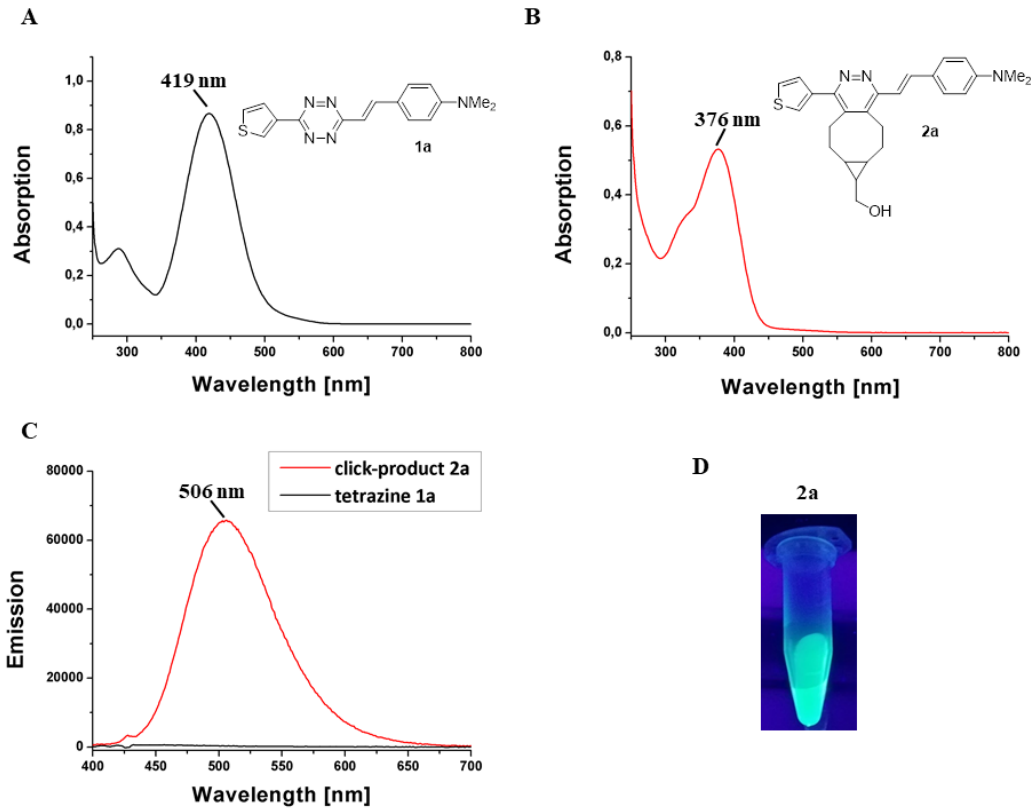


**Figure S3.** Absorption and emission spectra of tetrazine **1a** (A and C) and click product **2a** (B and C) and fluorescence picture of click product **2a** (D). All spectra were measured in $CH_3CN$ at room temperature using a tetrazine concentration of 25 µM for absorption measurements and 2.5 µM for emission measurements.

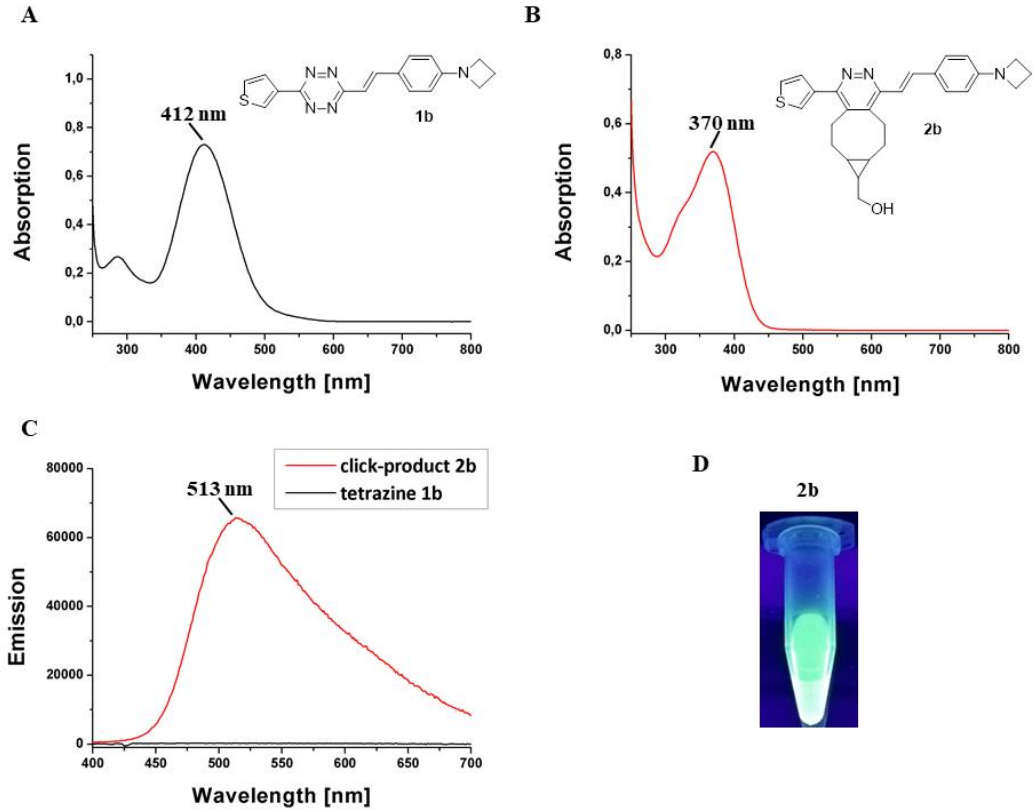


**Figure S4.** Absorption and emission spectra of tetrazine **1b** (A and C) and click product **2b** (B and C) and fluorescence picture of click product **2b** (D). All spectra were measured in $CH_3CN$ at room temperature using a tetrazine concentration of 25 µM for absorption measurements and 2.5 µM for emission measurements.

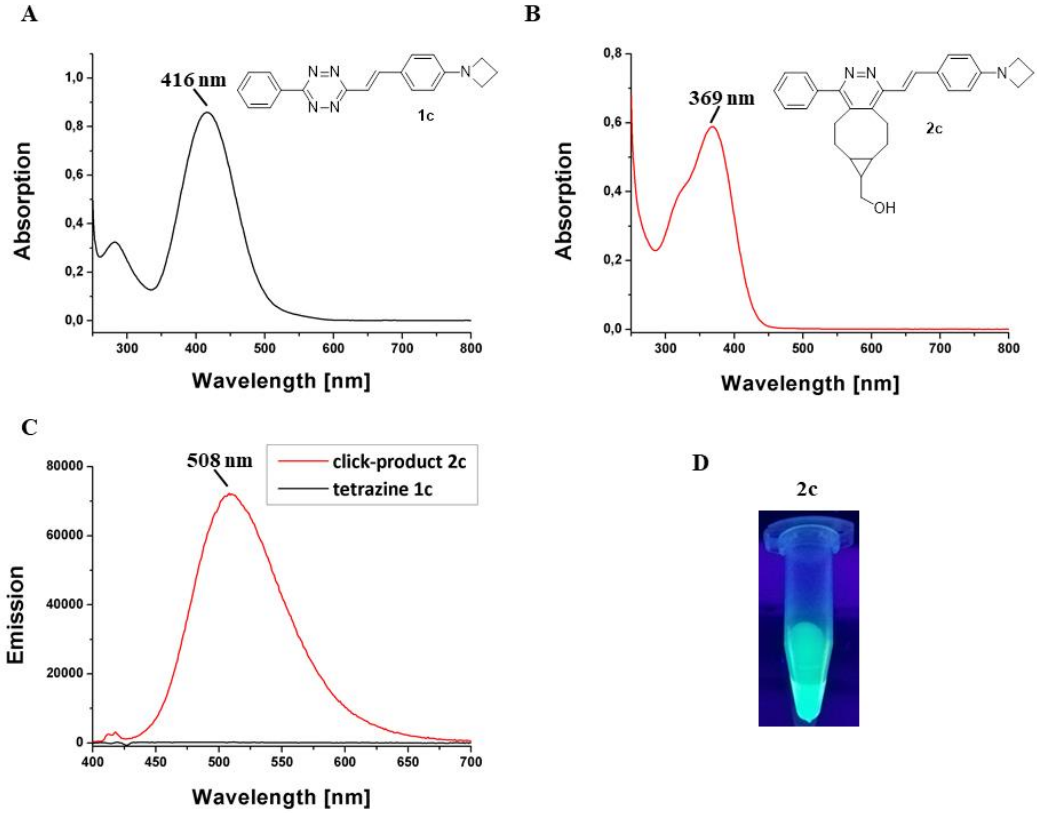


**Figure S5.** Absorption and emission spectra of tetrazine **1c** (A and C) and click product **2c** (B and C) and fluorescence picture of click product **2c** (D). All spectra were measured in $CH_3CN$ at room temperature using a tetrazine concentration of 25 µM for absorption measurements and 2.5 µM for emission measurements.

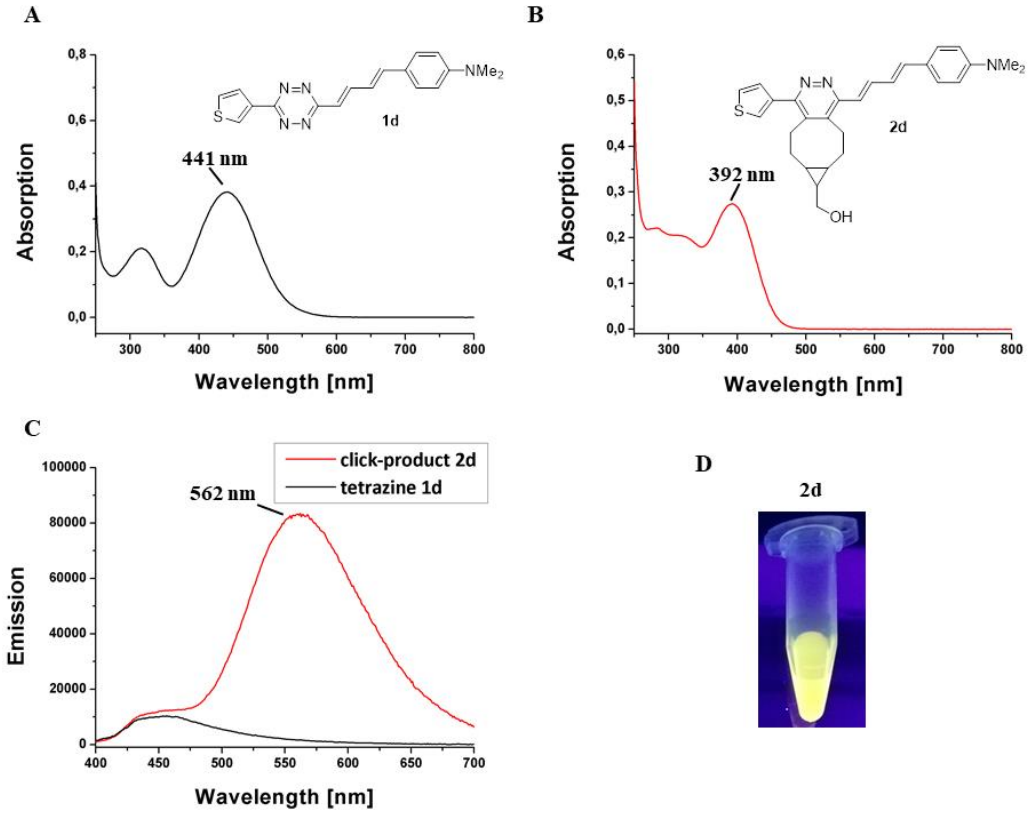


**Figure S6.** Absorption and emission spectra of tetrazine **1d** (A and C) and click product **2d** (B and C) and fluorescence picture of click product **2d** (D). All spectra were measured in $CH_3CN$ at room temperature using a tetrazine concentration of 25 µM for absorption measurements and 2.5 µM for emission measurements.

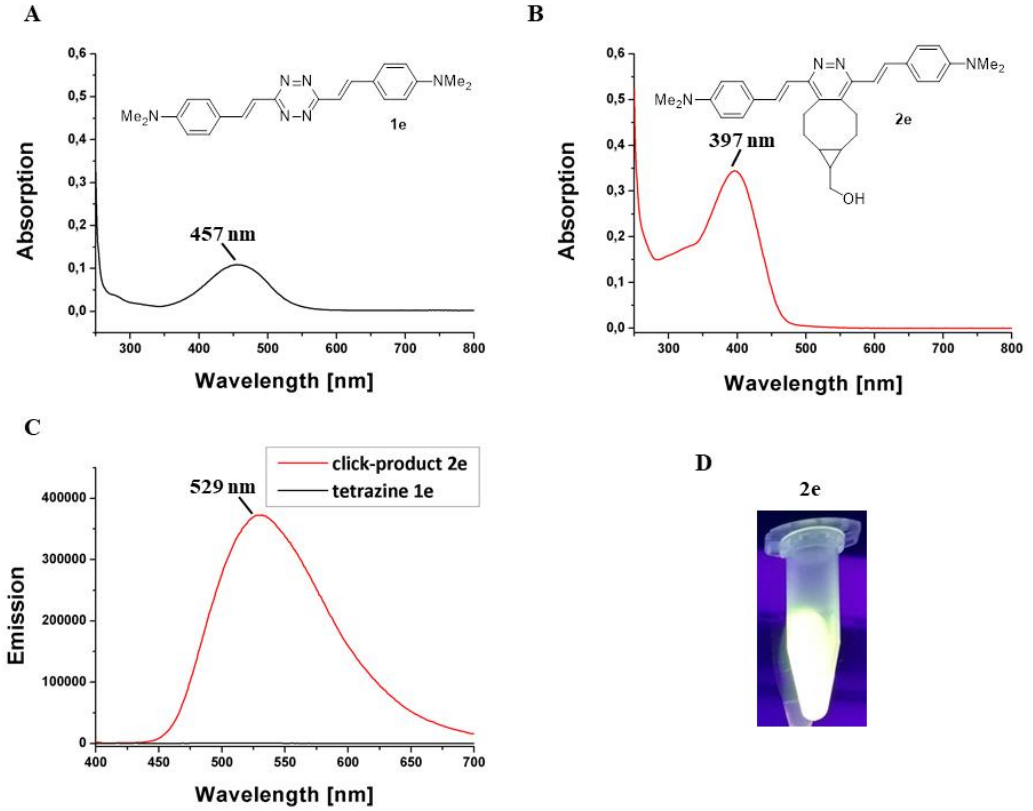


**Figure S7.** Absorption and emission spectra of tetrazine **1e** (A and C) and click product **2e** (B and C) and fluorescence picture of click product **2e** (D). All spectra were measured in $CH_3CN$ at room temperature using a tetrazine concentration of 25 µM for absorption measurements and 2.5 µM for emission measurements.

## Photophysical properties and absorption and emission spectra measured in $CH_3CN/H_2O$ 1:1

**Table S3.** Photophysical properties of the click products of BCN with tetrazines **1a-1e** in $CH_3CN/H_2O$ 1:1[a].

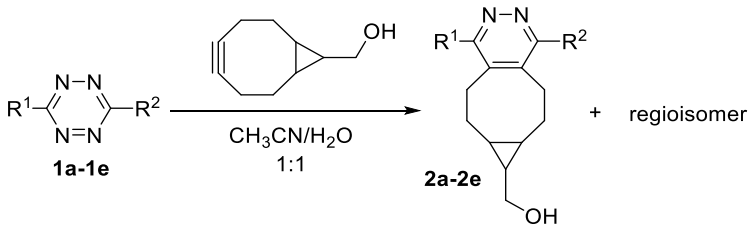


| Click-product | $R^1$ | $R^2$ | $\lambda_{Abs}/\lambda_{Em}$ [b] [nm] | Stokes shift [nm] | $\phi$ [c] | $\varepsilon_{max}$ ($\times 10^3$ $M^{-1}$ $cm^{-1}$) | Fl. intensity increase [d] |
|---|---|---|---|---|---|---|---|
| **2a** | 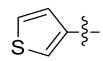 | 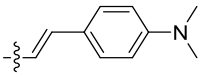 | 378/531 | 153 | 0.010 | 21.2 | 210-fold |
| **2b** | 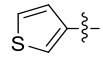 | 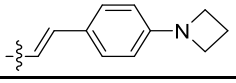 | 365/537 | 172 | 0.008 | 20.4 | 285-fold |
| **2c** | 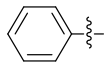 | 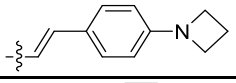 | 365/538 | 173 | 0.008 | 23.0 | 120-fold |
| **2d** | 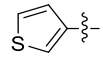 | 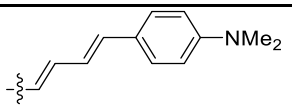 | 392/600 | 208 | 0.033 | 11.2 | 20-fold |
| **2e** | 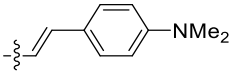 | | -[e]/553 | - | 0.011 | - | 20-fold |
| **2e** | 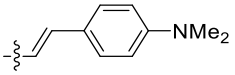 | | 396/558[f] | 162[f] | 0.019[f] | 2.2[f] | 70-fold[f] |

a) All reactions were performed in $CH_3CN/H_2O$ 1:1 at room temperature using an excess of BCN, b) absorption and emission (at 380 nm excitation) maxima were measured in $CH_3CN/H_2O$ 1:1 at room temperature, c) quantum yields were determined by using quinine sulfate in 0.5 M $H_2SO_4$ as standard ($\phi$ = 0.55), d) calculated as the integral of the fluorescence of the click product divided by the integral of the fluorescence of the starting tetrazine, e) no absorption maxima detectable in $CH_3CN/H_2O$ 1:1, f) reaction and measurements were performed in $CH_3CN$/PBS 1:1 at room temperature.

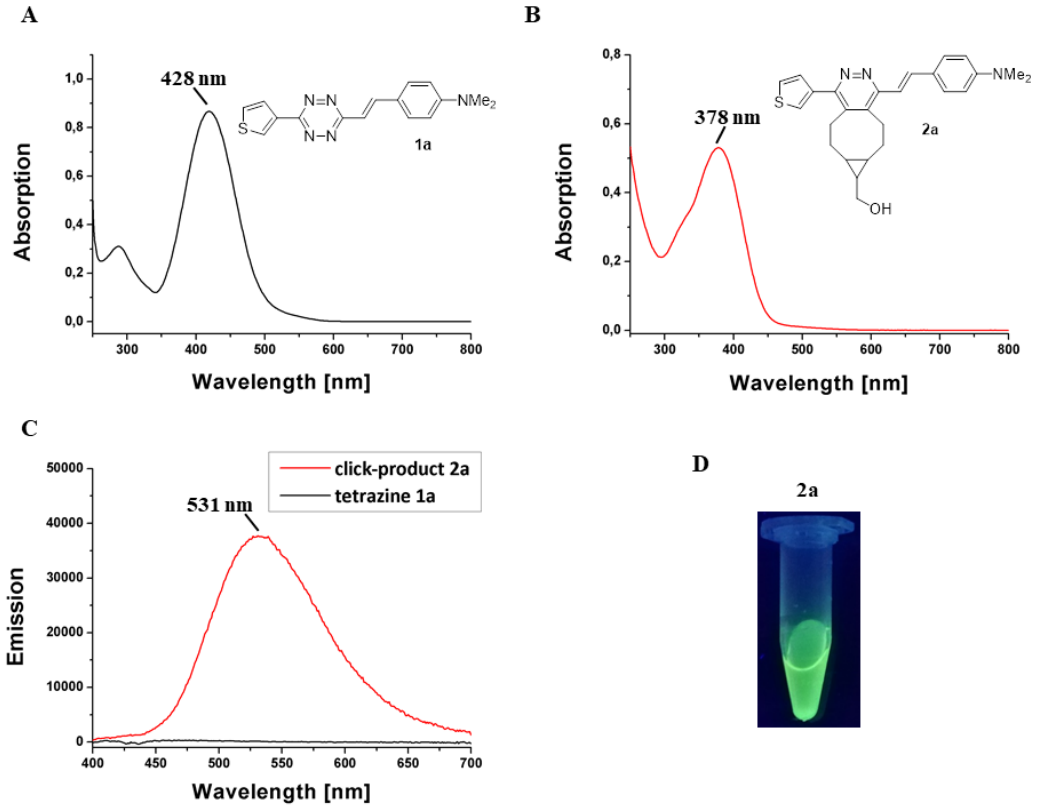


**Figure S8.** Absorption and emission spectra of tetrazine **1a** (A and C) and click product **2a** (B and C) and fluorescence picture of click product **2a** (D). All spectra were measured in $CH_3CN/H_2O$ 1:1 at room temperature using a tetrazine concentration of 25 µM for absorption measurements and 2.5 µM for emission measurements.

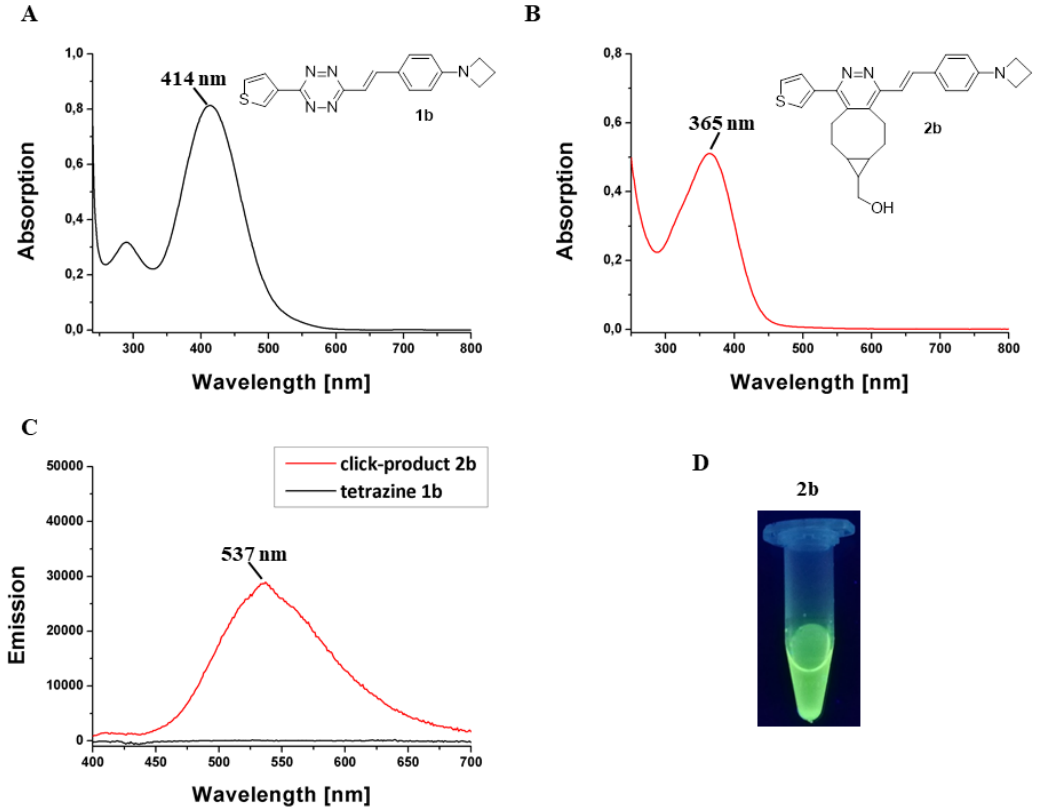


**Figure S9.** Absorption and emission spectra of tetrazine **1b** (A and C) and click product **2b** (B and C) and fluorescence picture of click product **2b** (D). All spectra were measured in $CH_3CN/H_2O$ 1:1 at room temperature using a tetrazine concentration of 25 µM for absorption measurements and 2.5 µM for emission measurements.

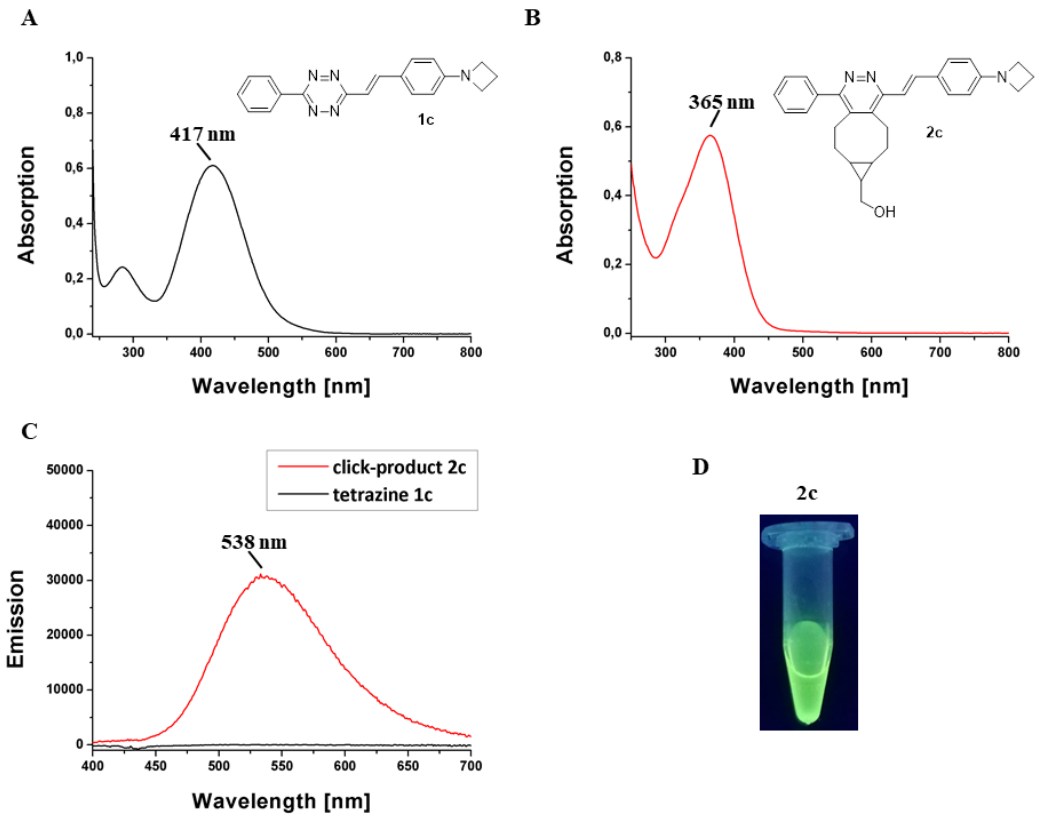


**Figure S10.** Absorption and emission spectra of tetrazine **1c** (A and C) and click product **2c** (B and C) and fluorescence picture of click product **2c** (D). All spectra were measured in $CH_3CN/H_2O$ 1:1 at room temperature using a tetrazine concentration of 25 µM for absorption measurements and 2.5 µM for emission measurements.

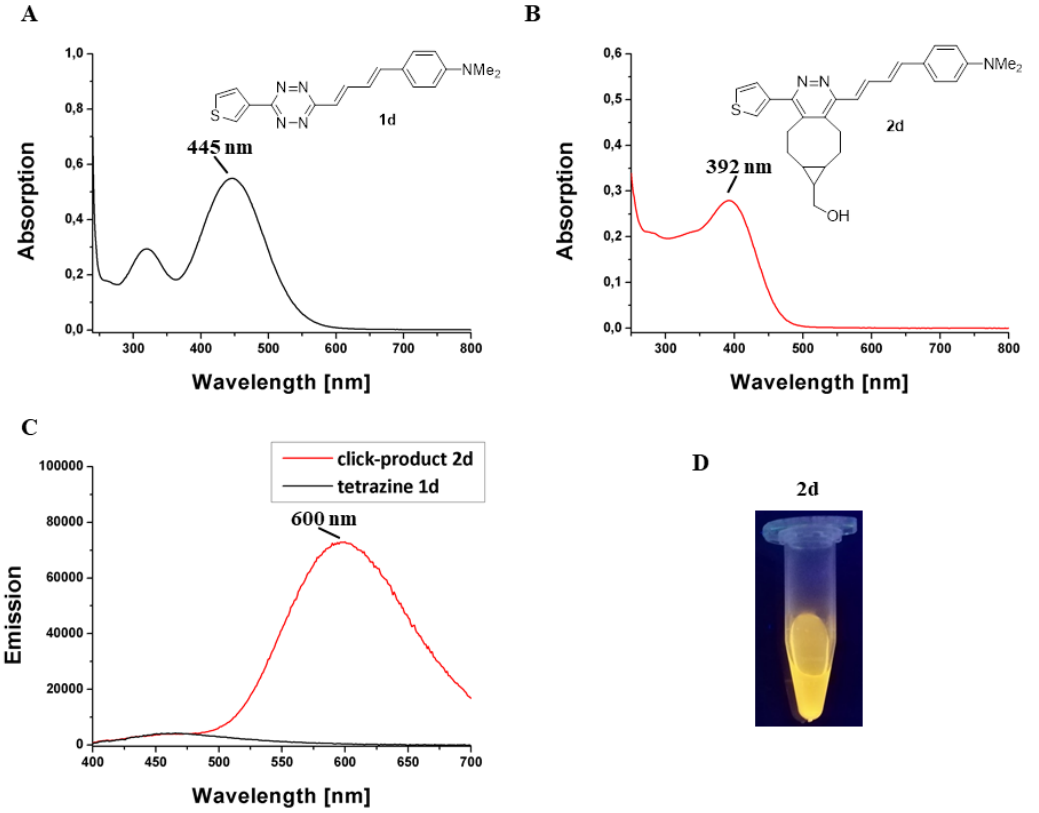


**Figure S11.** Absorption and emission spectra of tetrazine **1d** (A and C) and click product **2d** (B and C) and fluorescence picture of click product **2d** (D). All spectra were measured in $CH_3CN/H_2O$ 1:1 at room temperature using a tetrazine concentration of 25 µM for absorption measurements and 2.5 µM for emission measurements.

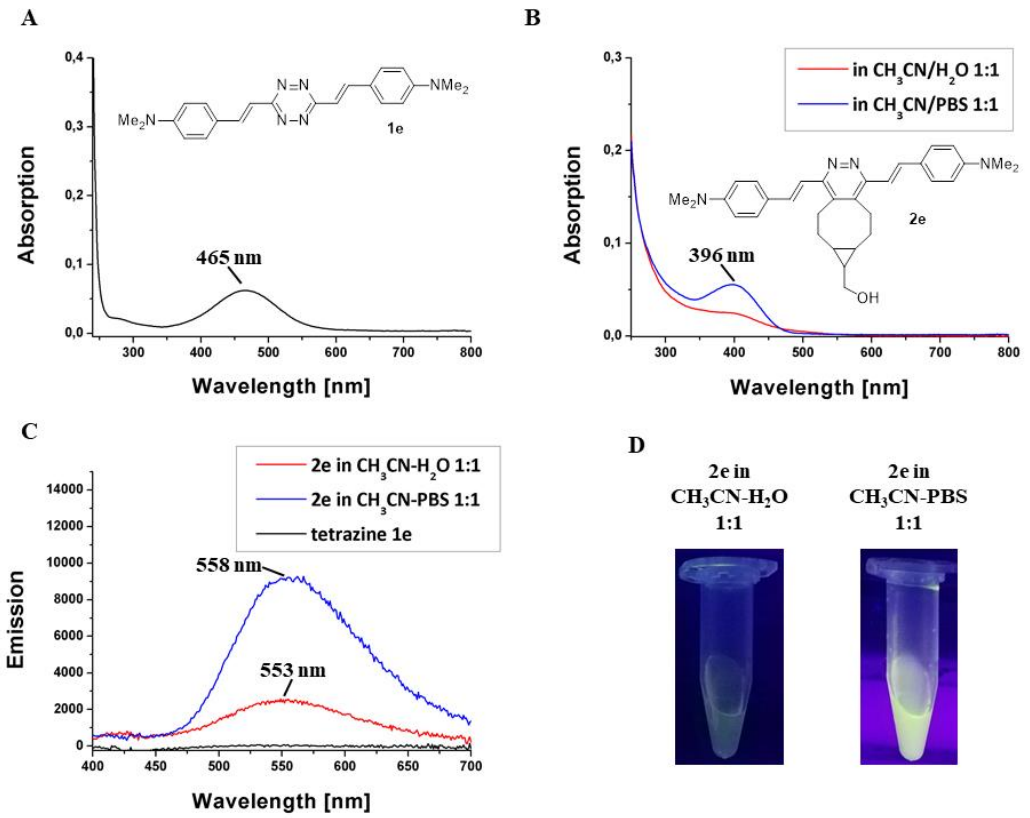


**Figure S12.** Absorption and emission spectra of tetrazine **1e** (A and C) and click product **2e** (B and C) and fluorescence pictures of click product **2e** (D). All spectra were measured in $CH_3CN/H_2O$ 1:1 or $CH_3CN$/PBS 1:1 at room temperature using a tetrazine concentration of 25 µM for absorption measurements and 2.5 µM for emission measurements.

## Photophysical properties, absorption and emission spectra of 2a in different solvents

**Table S4.** Photophysical properties of click product **2a** in different solvents[a].

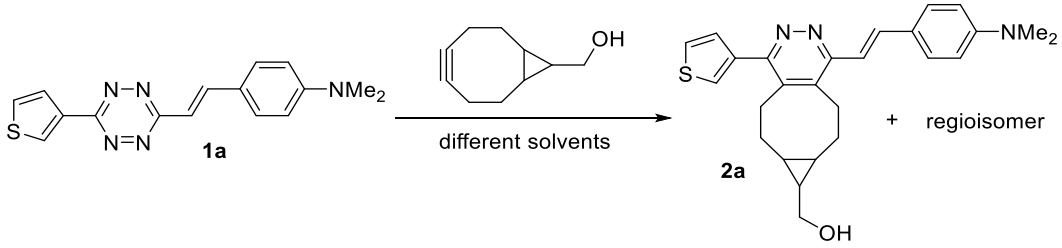

| solvent | $\lambda_{Abs}/\lambda_{Em}$ [b] [nm] | Stokes shift [nm] | $\phi$ [c] | $\varepsilon_{max}$ ($\times 10^3$ $M^{-1}cm^{-1}$) | Fl. intensity increase [d] |
|---|---|---|---|---|---|
| $CHCl_3$ | 383/476 | 93 | 0.004 | 21.2 | 50-fold |
| Acetone | 377/493 | 116 | 0.008 | 25.0 | 45-fold |
| Dioxane | 377/463 | 86 | 0.002 | 26.5 | 13-fold |
| *i*PrOH | 381/499 | 118 | 0.010 | 22.5 | 40-fold |
| MeOH | 381/518 | 137 | 0.010 | 25.6 | 55-fold |
| $CH_3CN$ | 376/506 | 130 | 0.014 | 21.3 | 100-fold |
| $CH_3CN/H_2O$ 1:1 | 378/531 | 153 | 0.010 | 21.2 | 210-fold |

a) The click-reaction was performed in the indicated solvents ($CHCl_3$, acetone, dioxane, iPrOH, MeOH, $CH_3CN$ or $CH_3CN/H_2O$ 1:1) at room temperature using an excess of BCN, b) absorption and emission (at 380 nm excitation) maxima were measured in the corresponding solvent at room temperature, c) quantum yields were determined by using quinine sulfate in 0.5 M $H_2SO_4$ as standard ($\phi$ = 0.55), d) calculated as the integral of the fluorescence of the click product divided by the integral of the fluorescence of the starting tetrazine.

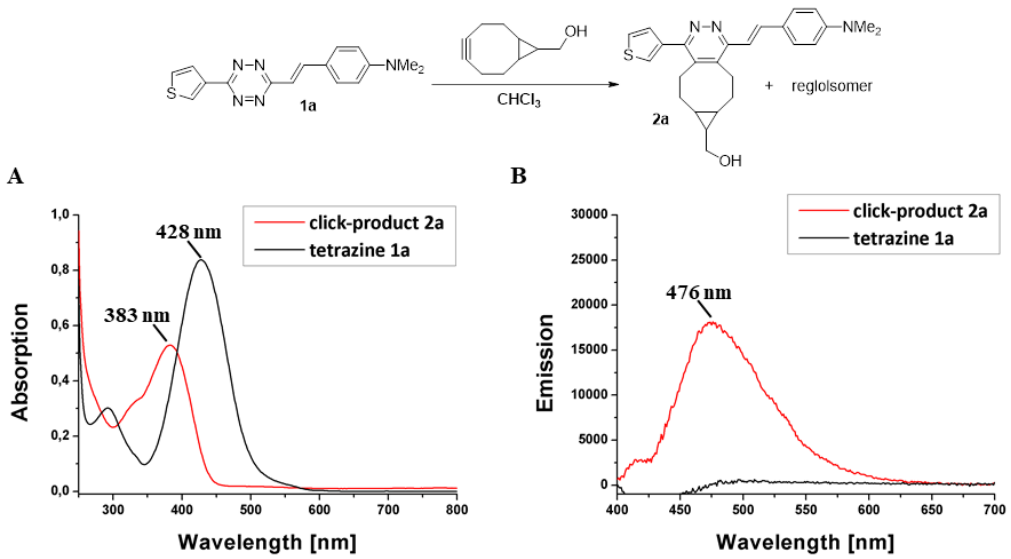


**Figure S13.** Absorption (A) and emission (B) spectra of tetrazine **1a** and click product **2a** in $CHCl_3$. All spectra were measured at room temperature using a tetrazine concentration of 25 µM for absorption measurements and 2.5 µM for emission measurements.

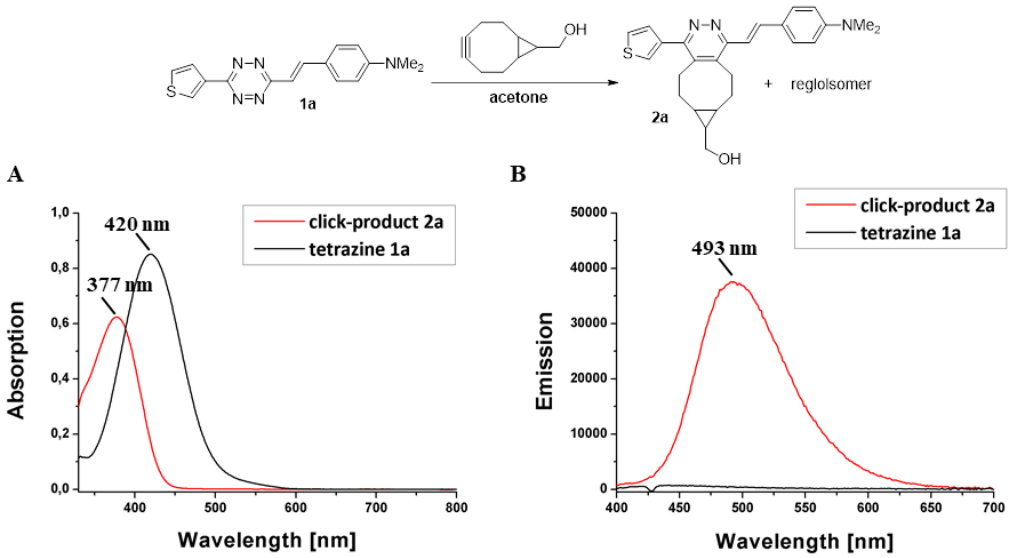


**Figure S14.** Absorption (A) and emission (B) spectra of tetrazine **1a** and click product **2a** in acetone. All spectra were measured at room temperature using a tetrazine concentration of 25 µM for absorption measurements and 2.5 µM for emission measurements.

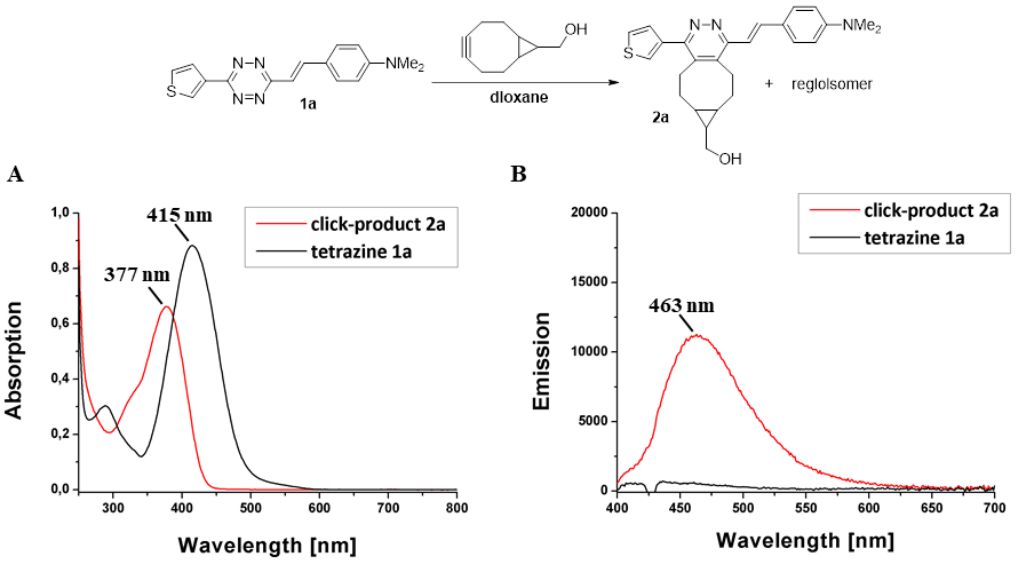


**Figure S15.** Absorption (A) and emission (B) spectra of tetrazine **1a** and click product **2a** in dioxane. All spectra were measured at room temperature using a tetrazine concentration of 25 µM for absorption measurements and 2.5 µM for emission measurements.

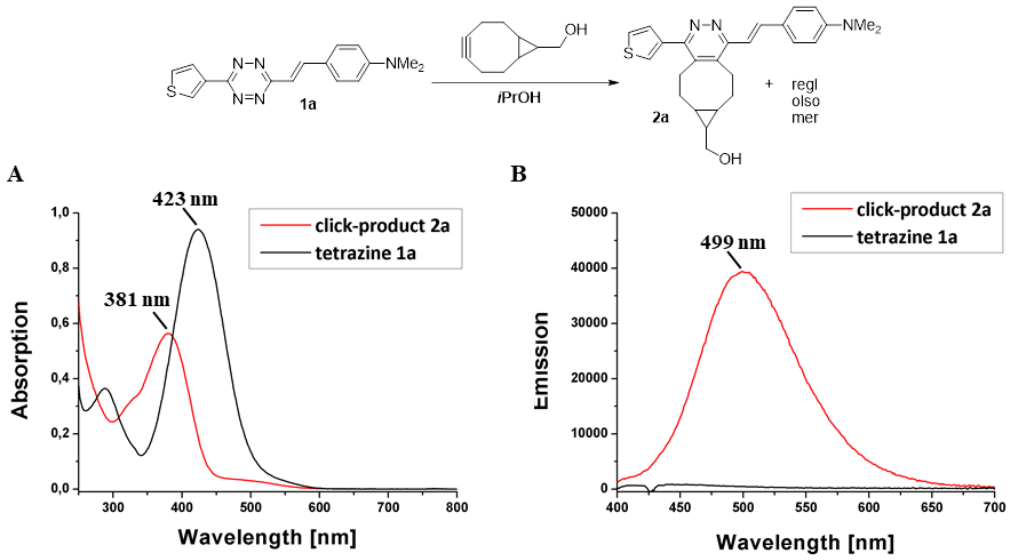


**Figure S16.** Absorption (A) and emission (B) spectra of tetrazine **1a** and click product **2a** in *i*PrOH. All spectra were measured at room temperature using a tetrazine concentration of 25 µM for absorption measurements and 2.5 µM for emission measurements.

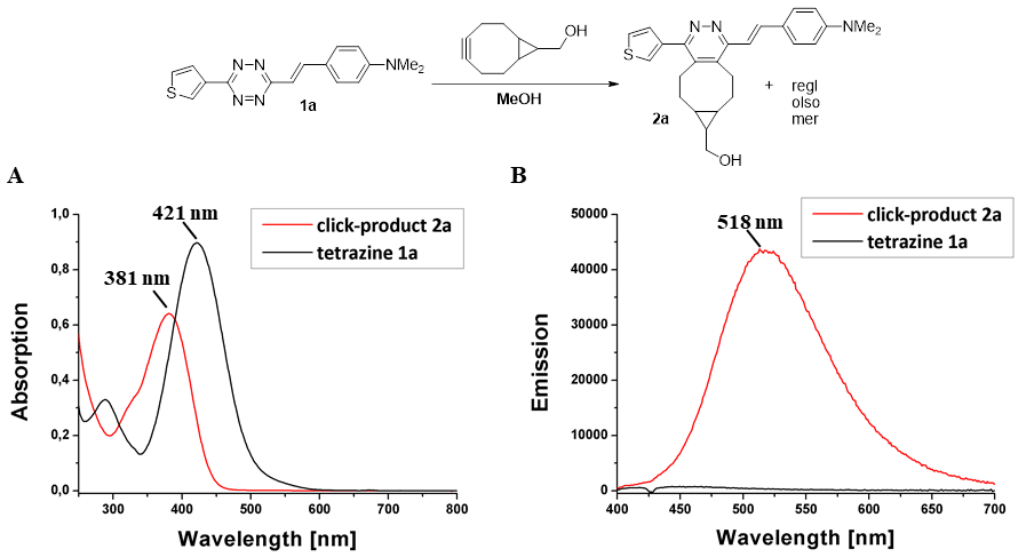


**Figure S17.** Absorption (A) and emission (B) spectra of tetrazine **1a** and click product **2a** in MeOH. All spectra were measured at room temperature using a tetrazine concentration of 25 µM for absorption measurements and 2.5 µM for emission measurements.

## Determination of second-order rate constants

Second-order rate constants of the reactions of bicyclononyne (BCN) with 1,2,4,5-tetrazines **1a** and **1d** were determined by following the decay in the concentration of the starting tetrazine over time. The rate constants were calculated from the pseudo first order rate constants of the concentration decrease measured at different BCN concentrations (10 equiv, 12.5 equiv and 15 equiv) by UV/VIS spectroscopy. The measurements were performed in $CH_3CN/H_2O$ 1:1 at room temperature using a final tetrazine concentration of 12.5 µM. All measurements were performed at least three times.

Conditions: A 50 µM solution of the respective tetrazine in $CH_3CN/H_2O$ 1:1 containing 5% of DMSO was mixed with a 500 µM solution of BCN in $CH_3CN/H_2O$ 1:1. The mixture was further diluted with $CH_3CN/H_2O$ 1:1 to give a final tetrazine concentration of 12.5 µM and was immediately measured on the UV/VIS spectrophotometer.
The time-dependent measurements were performed at the corresponding absorption maxima of the tetrazines used, which were determined by UV/VIS spectroscopy before the measurement (Table S5). The measured intensity of the absorption was plotted against time. Fitting the curves with single exponential equation ($y = y_0 + Ae^{-k/t}$) provided the observed rate constants. Finally, the observed rate constants were plotted against the concentration of BCN in order to obtain the second order rate constants (Table S5) from the slope of the resulting plot.

**Table S5.** Absorption maxima of 1,2,4,5-tetrazines used during kinetic measurements and the corresponding second-order rate constants $k_2$ of the reactions with BCN.

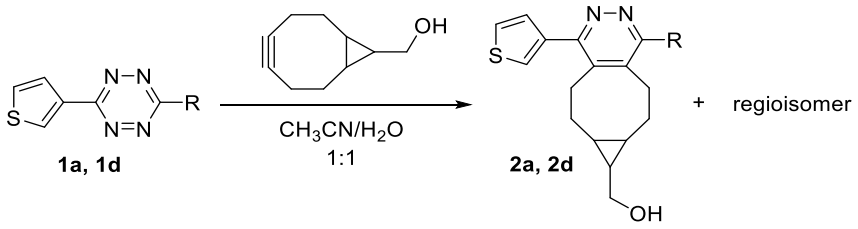


| Tetrazine | $\lambda_{Abs}$ [nm][a] | $k_2$ [$M^{-1}$ $s^{-1}$][b] |
|---|---|---|
| 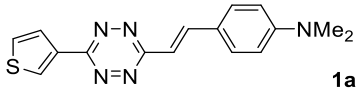 1a | 428 | 1.4 ± 0.2 |
| 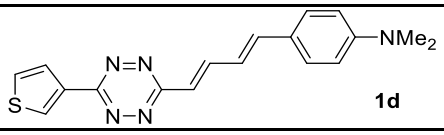 1d | 445 | 1.5 ± 0.1 |

a) Absorption maxima of the starting tetrazines were determined in $CH_3CN/H_2O$ 1:1 at room temperature using a 25 µM solution of the respective tetrazine, b) second-order rate constants were determined from pseudo first order rate constants measured in $CH_3CN/H_2O$ 1:1 at room temperature using three different BCN concentrations (10, 12.5 and 15 equiv).

## Fluorogenic cell labeling

HeLa cells fixed with methanol were rehydrated in 0.05% Tween in PBS and incubated with 100 µM BCN-NHS for 1 hour. The cells were then washed three-times with 0.05% Tween in PBS, incubated with 20 µM tetrazines for 4 hours and the nucleus was stained using commercially available DRAQ5. The cells were again washed three-times with 0.05% Tween in PBS and inspected on confocal microscope.

**ConA-BCN preparation**

100 µl of 5 mg/ml solution of concanavalin A (4.7 nmol of tetramer) in 1 M NaCl, 50 mM HEPES-NaOH (pH 8.3), 3 mM $CaCl_2$, 3 mM $MnCl_2$ was combined with 2.3 µL of 10 mM NHS BCN ester (5× molar excess of active ester dissolved in dry DMSO). Reaction was incubated at room temperature for 1 h with constant shaking. After one hour, 10 µL of 1 M Tris-HCl (pH 6.8) was added to neutralize the remaining NHS ester and incubated for another 10 min. at room temperature. BCN excess was removed by desalting using Zeba (Thermo) spin columns into 1 M NaCl, 20 mM Tris-HCl (pH 6.8), 3 mM $CaCl_2$, 3 mM $MnCl_2$.

**Live cell labeling**

$2x10^4$ HeLa (or U2OS) cells were seeded on glass bottom 96 well plate (Cellvis) one day prior experiment. The cells were incubated with 5 µM BCN-TPP for 15 min, washed 3x with medium and incubated with 20 µM **1d** for 45 min. Medium was replaced with Leibowitz's L15 containing 10 nM mitotracker deep red and the cells were incubated for 15 min. Pictures were taken using Zeiss confocal microscope equipped with 40x C-Apochromat 40x/1.20 W Korr FCS M27 objective. Set-up: click product: excitation at 405 nm, emission at 508-604 nm window, laser intensity 1%. Mitotracker: excitation at 633 nm, emission at 640-735 nm window, laser intensity 3%.

A)

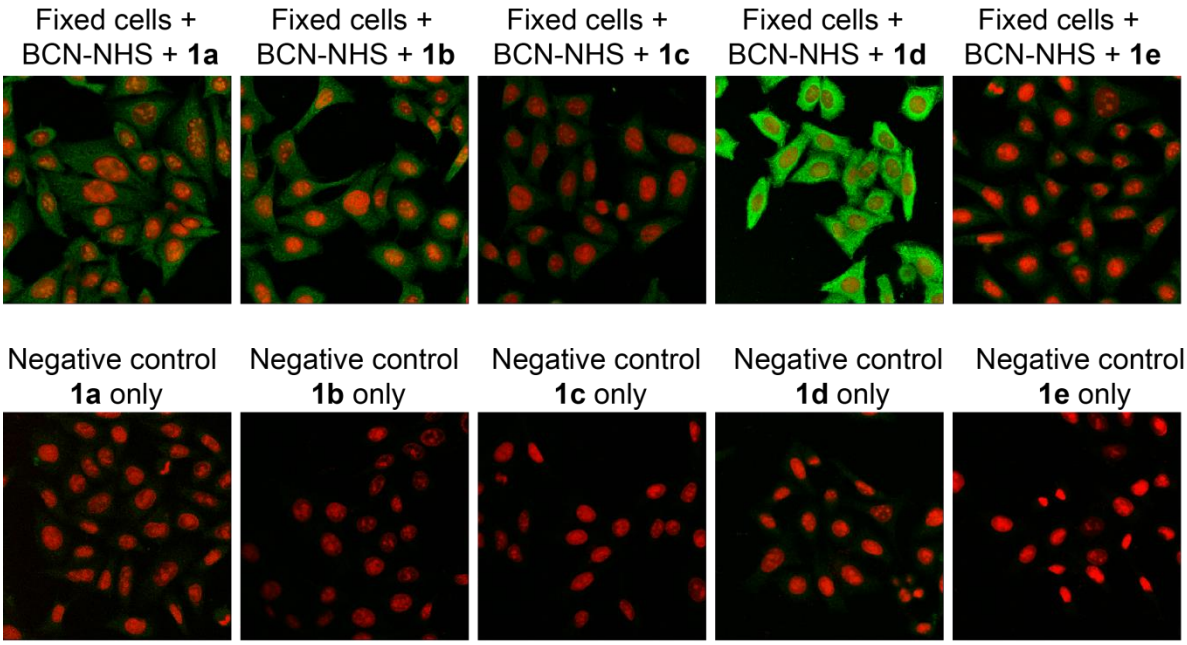


B)

Click products formed in the reaction of **1a** and **1d** with BCN can be excited also by 458 nm and partially by 488 nm laser

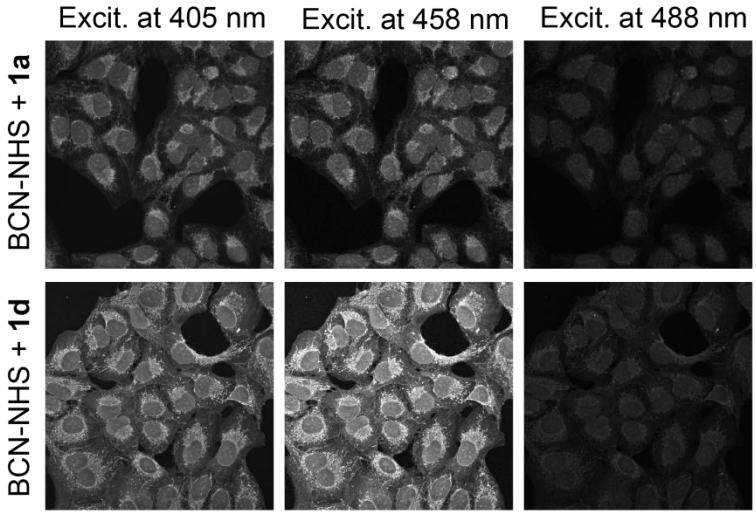


C)

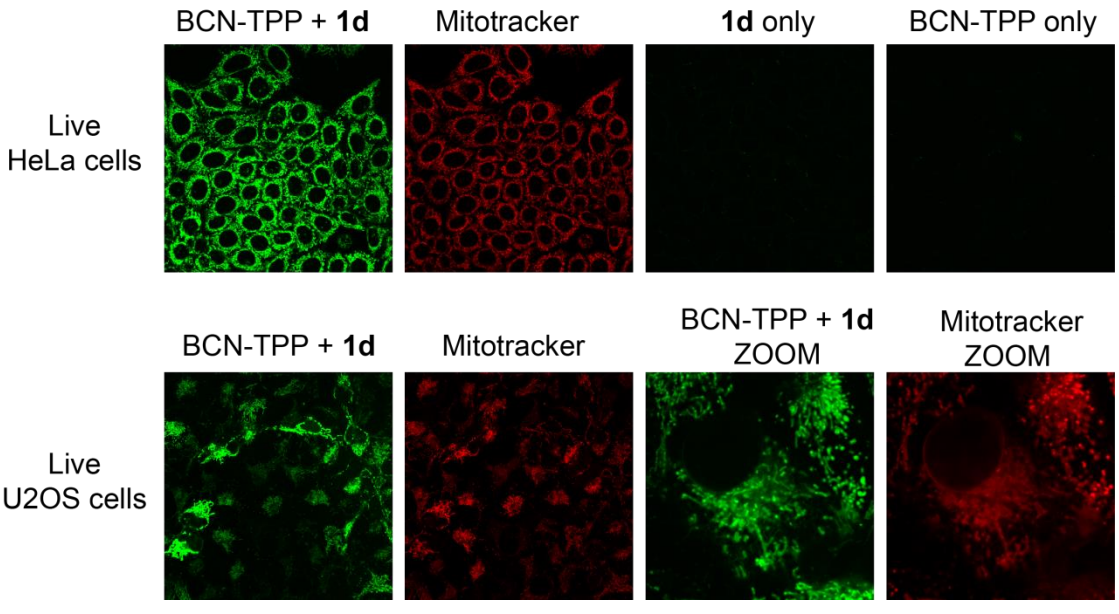

**Figure S18.** Fluorogenic labeling of cells. A) Shown are confocal microscope images of HeLa cells modified with BCN-NHS active ester after addition of tetrazines **1a**-**1e**. Negative controls are HeLa cells treated only with tetrazines **1a**-**1e**. DRAQ5 was used as nuclear specific dye (Excitation: $\lambda$ = 633 nm, Emission: $\lambda$ = 643-703 nm window). Click product excitation $\lambda$ = 458 nm, emission $\lambda$ = 517-587 nm for **1a**, **1b**, **1c** and **1e** and $\lambda$ = 543-639 window for **1d.** B) Click products **2a** and **2d** can be excited using both 405 nm and 458 nm laser. Emission: $\lambda$ = 517-587 nm window for **1a** and $\lambda$ = 543-639 window for **1d**. This experiment was performed on U2OS cancer cells. C) Live cell (HeLa and U2OS) labeling using BCN-TPP and **1d**.

## Two-color fluorogenic labeling of segregated bilayer TG beads

The segregated bilayer Tentagel beads were prepared by following literature procedure.[7]
Briefly: Tentagel $NH_2$ resin (25 mg, 130 µm beads) was swollen in dd$H_2O$ (2 mL) for 20 hours. After decantation the beads were briefly centrifuged, access water was pipetted off and the beads were briefly washed with DCM/$Et_2O$ = 55/45 mixture (2 mL). A solution of BCN-NHS active ester (2.1 mg) in DCM/$Et_2O$ = 55/45 mixture (2 mL) was added to the beads followed by DIPEA (2.5 µL) and the beads were rotated in a plastic tube for 30 min to modify the outer bead layer. The resin beads were then washed with DCM/$Et_2O$ = 55/45 mixture, DCM and DMF (5-times). To modify the inner part of the beads a solution of TCO-NHS active ester (2.25 mg) in DMF (2 mL) was added to the beads followed by DIPEA (2.5 µL). The beads were rotated in a plastic tube for 1.5 hours and were then washed with DMF. For labeling with tetrazine **1a**: A small portion (ca 2-3 mg) of the beads was transferred to a plastic tube and $CH_3CN/H_2O$ = 1/1 mixture (25 µL) was added followed by a solution of **1a** in DMSO (10 µL of 1 mM stock). After rotating the mixture for ca. 15-20 min the beads were washed with DMF and inspected on confocal microscope.
We have also prepared Tentagel beads modified only with BCN or TCO moiety respectively by the reaction of TG $NH_2$ beads with the BCN/TCO active esters (1 equiv.) in DMF using DIPEA (2 equiv.) as the base.
The BCN-NHS active ester is commercially available. TCO-NHS ester used in this experiment was prepared as previously described.[1] Structures of the NHS esters are shown below.

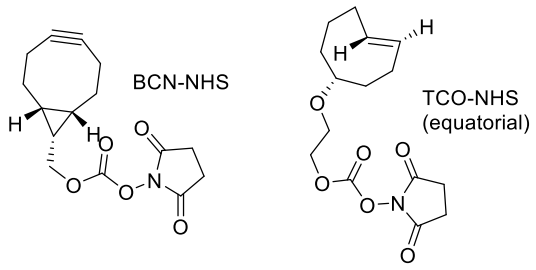

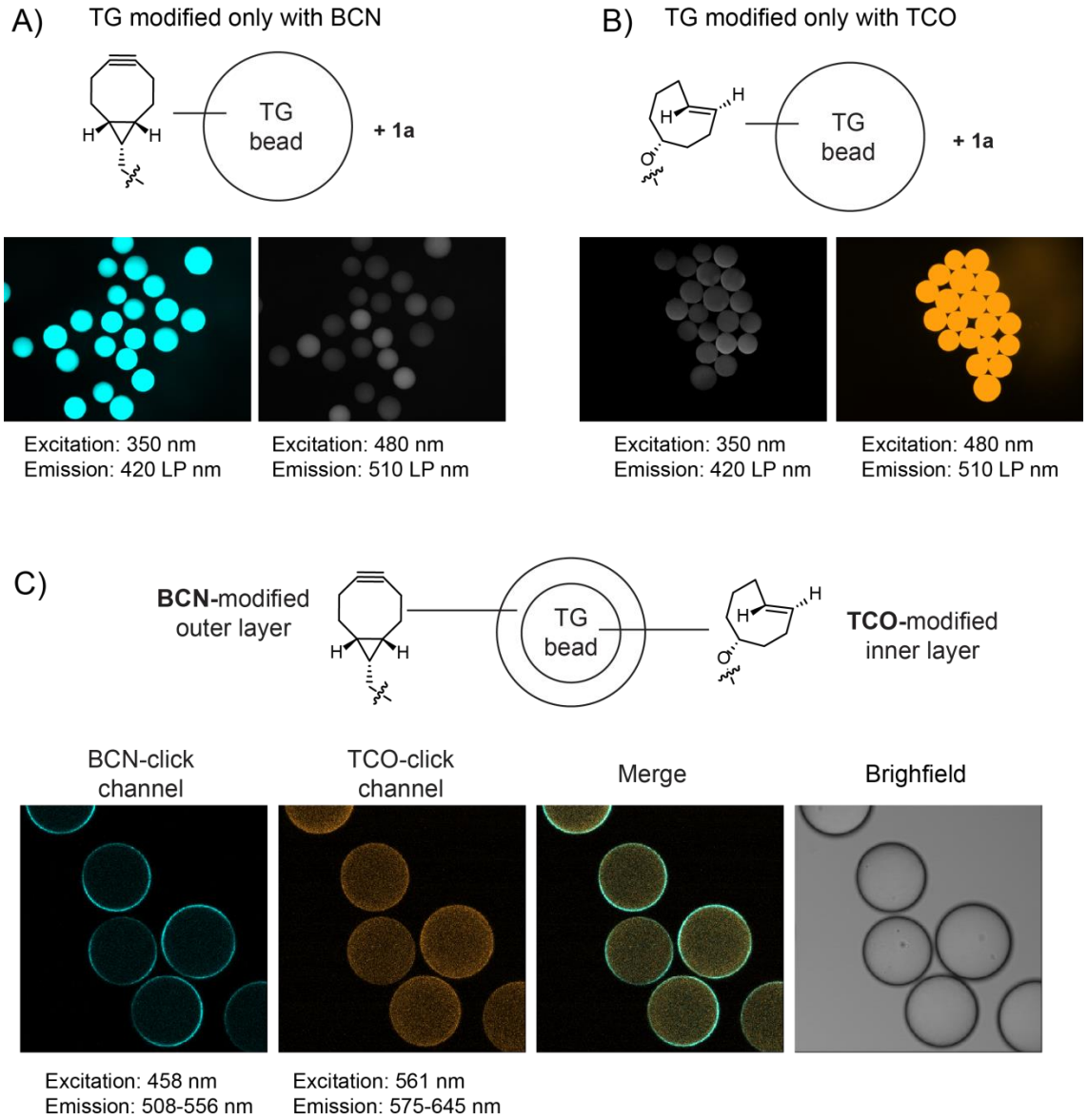


**Figure S19.** Fluorogenic labeling of TG beads modified with BCN and TCO dienophiles. A) Fluorescent stereomicroscope images of TG beads modified with BCN-NHS ester after addition of tetrazine **1a**. B) Fluorescent stereomicroscope images of TG beads modified with TCO-NHS ester after addition of tetrazine **1a**. C) Fluorescent confocal microscope images of segregated TG beads modified with BCN in the outer layer and TCO in the inner part after reaction with tetrazine **1a**. The images were captured by gray-scale camera and are in pseudocolors.

## Toxicity studies

$2x10^4$ HeLa (or U2OS) cells were seeded on glass bottom 96 well plate (Cellvis) one day prior experiment. The cells were incubated with various concentrations of tetrazines **1e-1e** for 24 hours. The tetrazines showed no toxicity up to 50 µM concentration. Compound **1d** showed toxicity at 100 µM, the highest concentration tested. The toxicity was determined using XTT assay or by using crystal violet (Figure S20). The experiments were performed in triplicate.

Briefly: Cells were cultivated for 24h with indicated concentrations of compounds. After 24h 50 µL of XTT(+PMS) was added to cell medium. Absorbance (difference 450-620 nm) was measured 1h after addition of XTT.

XTT (Thermo) was dissolved in DMEM (high glucose no serum) to give concentration 1mg/ml, PMS (phenmetrazine sulfate, Sigma) was dissolved in PBS to final concentration 0.383 mg/ml (1.25mM) solutions were combined in ratio 50:1 and added to cell culture medium. Total absorbane was calculated as absorbance measured at 450 nm subtracted by absorbance value measured at 620 nm.

Crystal violet:
Cells grown on 96 well plate were fixed with 100µl of 100% methanol for 10 minutes, rinsed 2x with water and incubated with 50 µl of 0.1% crystal violet solution. After 15 minutes of incubation crystal violet was removed, cells were washed 2x with water. Crystal violet adsorbed on cells was dissolved in 50 µl of 100% methanol. Absorbance was measured at 595 nm using plate reader.

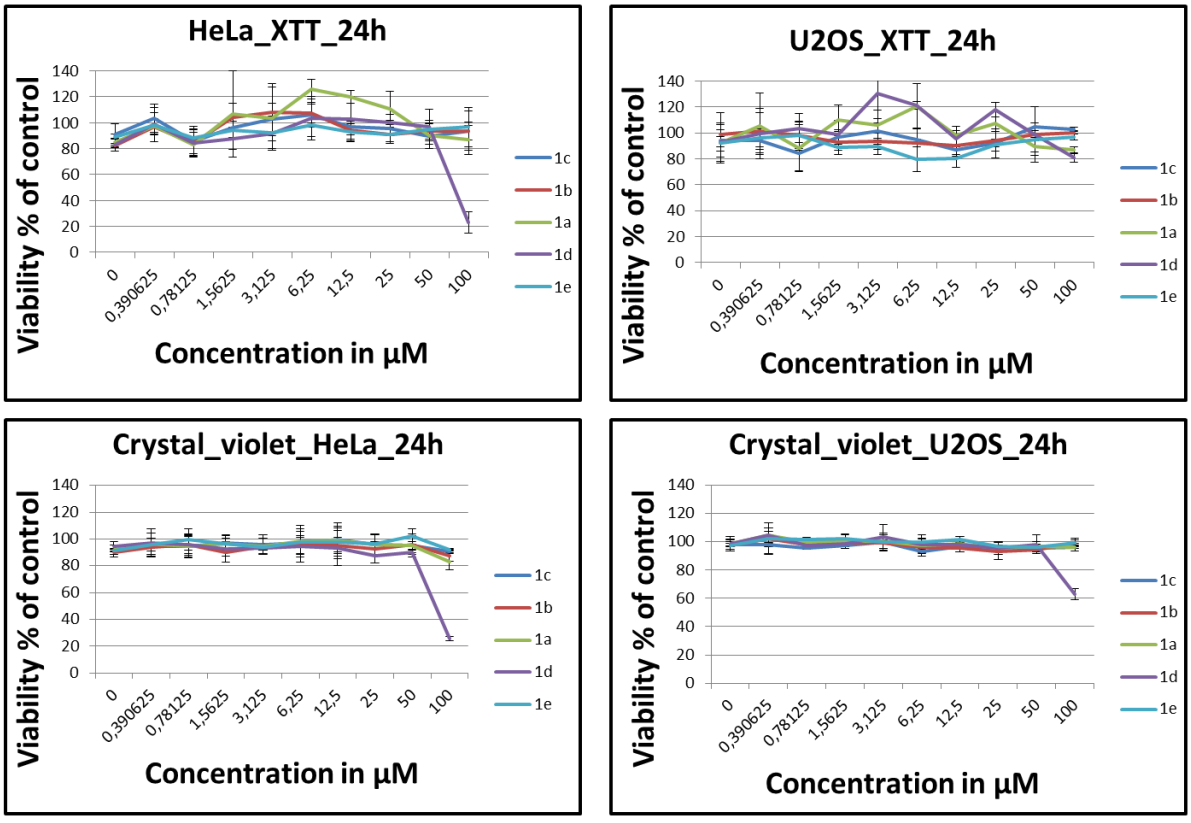


**Figure S20.** Toxicity of the tetrazines determined by XTT or crystal violet on HeLa or U2OS cells. Viability was calculated as % of control (DMSO).

## Time-lapse labeling of BCN- and TCO-modified TG beads

TG beads modified with BCN or TCO (prepared as described above) were reacted with tetrazines **1a**, **1d** and **1e** as follows: To small portion of the beads (ca. 5 mg) was added $CH_3CN/H_2O$ = 1/1 mixture (50 µL) and solution of the tetrazine in DMSO (10 µL of 1 mM stock). After 15 min, the reactions were inspected under UV-hand held lamp (365 nm) to confirm formation of the fluorophores. The beads were then washed twice with DMF, twice with $CH_3CN$/PBS= 1/1 mixture and finally were incubated at 37°C in 75 µL $CH_3CN$/PBS = 1/1 mixture for 24 hours. Small portion of the beads was pipetted off and the beads were inspected under fluorescence stereomicroscope at different time points (Leica M205 fluorescent stereomicroscope equipped with pE-300$^{white}$ LED light source and DFC3000 G grayscale camera). Set-up on the microscope was as follows: UV: Ex. 350 nm, Em. 420 nm (long pass), intensity: 30%, gain: 8, exposure: 1.25 s. GFP: 480 nm, Em. 510 nm (long pass), intensity: 20%, gain: 8, exposure: 1.25 s. RFP: 546 nm, Em. 590 nm (long pass), intensity: 50%, gain: 8, exposure: 1.25 s.
The results are shown in Figure S21 below.

**Figure S21.** Fluorogenic labeling of TG beads modified with BCN and TCO dienophiles. Tautomeriztaion of the 4,5-dihydropyridazine formed in the reaction of the tetrazines with TCO and/or oxidation to the corresponding pyridazine leads to changes in the fluorescence over time. Based on our previous study (ChemBioChem, 2019, 20, 886-890) the half-life of the 4,5-dihydropyridazine is about 2 hours. This may vary depending on the structure of the tetrazine used.

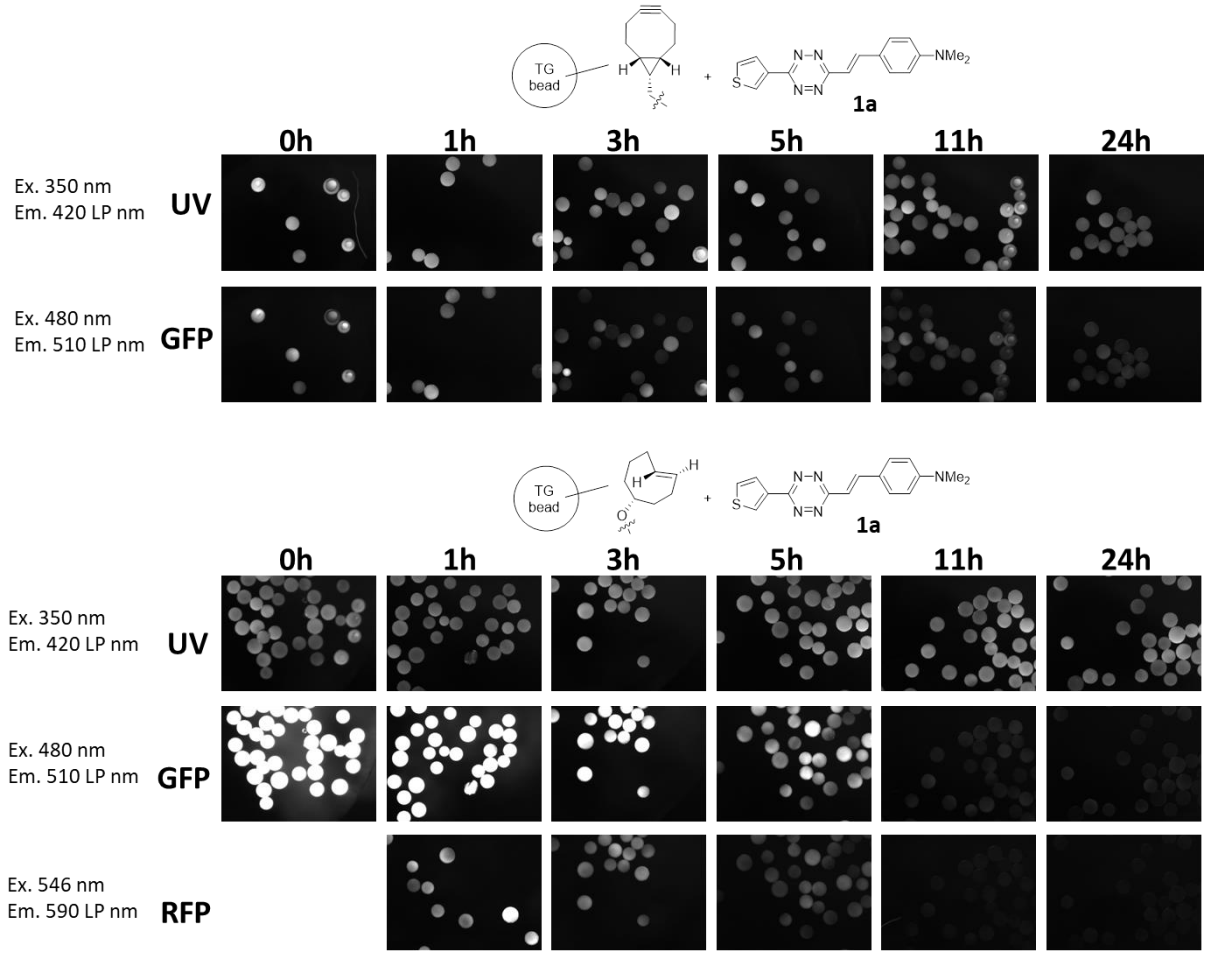

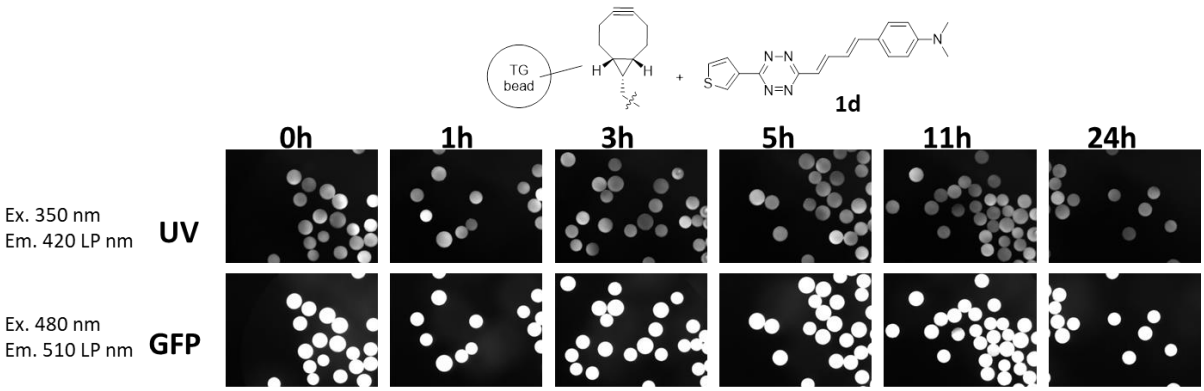
TG bead
1d
0h
1h
3h
5h
11h
24h
Ex. 350 nm
Em. 420 LP nm
UV
Ex. 480 nm
Em. 510 LP nm
GFP

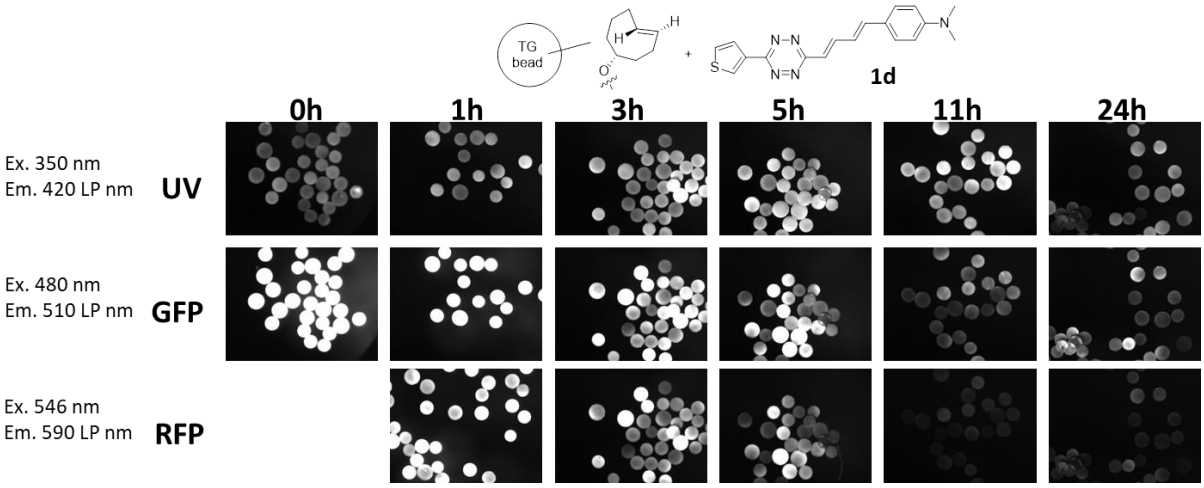
TG bead
1d
0h
1h
3h
5h
11h
24h
Ex. 350 nm
Em. 420 LP nm
UV
Ex. 480 nm
Em. 510 LP nm
GFP
Ex. 546 nm
Em. 590 LP nm
RFP

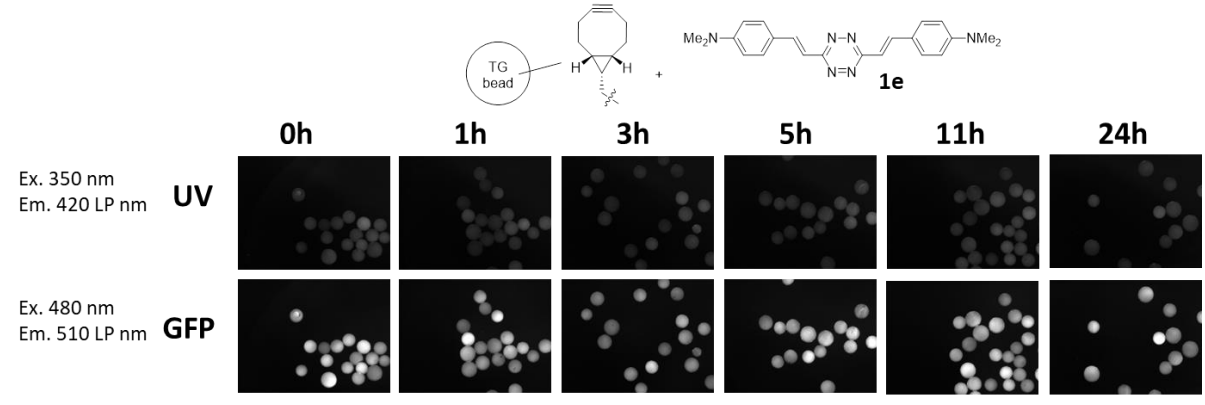
TG bead
1e
0h
1h
3h
5h
11h
24h
Ex. 350 nm
Em. 420 LP nm
UV
Ex. 480 nm
Em. 510 LP nm
GFP

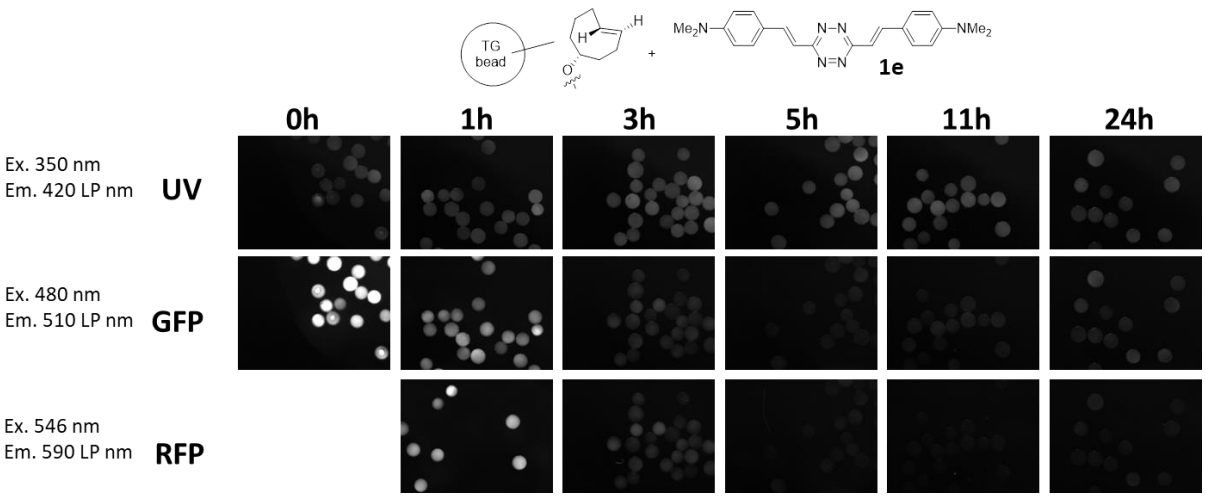
TG bead
1e
0h
1h
3h
5h
11h
24h
Ex. 350 nm
Em. 420 LP nm
UV
Ex. 480 nm
Em. 510 LP nm
GFP
Ex. 546 nm
Em. 590 LP nm
RFP

## References


[1] A. Vazquez, R. Dzijak, M. Dracinsky, R. Rampmaier, S. J. Siegl, M. Vrabel, *Angew. Chem. Int. Ed.* **2017**, *56*, 1334-1337.

[2] S. J. Siegl, J. Galeta, R. Dzijak, A. Vazquez, M. Del Río-Villanueva, M. Dracinsky, M. Vrabel, *ChemBioChem*.

[3] M. Beshai, B. Dhudshia, R. Mills, A. N. Thadani, *Tetrahedron Lett* **2008**, *49*, 6794-6796.

[4] H. X. Wu, J. Yang, J. Seckute, N. K. Devaraj, *Angew. Chem. Int. Ed.* **2014**, *53*, 5805-5809.

[5] D. F. Eaton, *J Photochem Photobiol B* **1988**, *2*, 523-531.

[6] J. E. Bertie, Z. D. Lan, *J Phys Chem B* **1997**, *101*, 4111-4119.

[7] F. Bedard, A. Girard, E. Biron, *Int. J. Pept. Res. Ther.* **2013**, *19*, 13-23.

## 7.4 Supplementary information to chapter 3.4

S.J. Siegl, R. Dzijak, A. Vázquez, R. Pohl, M. Vrabel, *Chem. Sci.* **2017**, 8, 3593-3598.
"The discovery of pyridinium 1,2,4-triazines with enhanced performance in bioconjugation reactions".

The corresponding NMR spectra are not presented here and can be found in the original publication.

# The Discovery of Pyridinium 1,2,4-Triazines with Enhanced Performance in Bioconjugation Ractions

Sebastian J. Siegl, Rastislav Dzijak, Arcadio Vázquez, Radek Pohl and Milan Vrabel

Institute of Organic Chemistry and Biochemistry of the Czech Academy of Sciences

vrabel@uochb.cas.cz

# Supporting Information

## Content

## General information

All chemicals were obtained from *Sigma Aldrich, Alfa Aesar, Acros Organics, ABCR* or *VWR* and were used without further purification. Reactions with air- and moisture-sensitive reactants were performed under nitrogen- or argon- atmosphere and in anhydrous solvents from *VWR*.

Solutions were concentrated on a rotary evaporator from *Heidolph* equipped with a PC3001 VARIOpro pump from *Vacuubrand*. Photochemical reactions were performed in a RPR-200 Rayonet reaction chamber equipped with 16 Hg-quartz iodine lamps (2537 Å) from *Southern New England Ultraviolet Company*. The continuous flow system during the photoreaction was produced by a STEPDOS 03 RC membrane-metering pump from *KNF*. Column chromatography was carried out on silica gel 60A (particle size: 40-60 μm) from *Acros Organics*. Solvents in the p.a. quality from *Lech-Ner* and *Penta* were used for elution. Mixtures of solvents are each stated as volume fractions. For flash column chromatography a Combi*Flash*® Rf+ from *Teledyne ISCO* was used. Thin-layer chromatography was performed on aluminium sheets from *Merck* (silica gel 60 F254, 20x20 cm). Chromatograms were visualized by UV light (λ = 254 nm/ 366 nm) or by staining with $KMnO_4$ or anisaldehyde solutions. $^1$H- and $^{13}$C-NMR spectra were measured on a Bruker Avance III™ HD 400 MHz NMR system equipped with Prodigy cryo-probe or on a Bruker Avance III™ HD 500 MHz Cryo. $CDCl_3$, MeOH-$d_4$ and DMSO-$d_6$ from *Sigma Aldrich* or *Eurisotop* were used as solvents. Chemical shifts δ are quoted in ppm in relation to the chemical shift of the residual non-deuterated solvent peak ($CDCl_3$: δ($^1$H) = 7.26, δ($^{13}$C) = 77.2; MeOH-$d_4$: δ($^1$H) = 3.31, δ($^{13}$C) = 49.0; DMSO-$d_6$: δ($^1$H) = 2.50, δ($^{13}$C) = 39.5). High-resolution mass spectra were recorded on an *Agilent* 5975C MSD Quadrupol, Q-Tof micro from *Waters* or LTQ Orbitrap XL from *Thermo Fisher Scientific*. UV/VIS spectroscopy was performed on a Cary 60 UV/Vis spectrophotometer from *Agilent Technologies*. HPLC-MS measurements were performed on a LCMS-2020 system from *Shimadzu* equipped with a Luna® C18 column (3u, 100A, 100 x 4.6 mm). The samples were eluted using a linear gradient of $CH_3CN$ + 0.05% HCOOH (5→95% in 9 min) in $H_2O$ + 0.05% HCOOH at a flow rate of 1.0 mL/min. Data from kinetic experiments were processed using OriginPro 9.1 software.

## Synthetic procedures

The following compounds were prepared according to literature procedures.

**_trans_-cyclooct-4-enol**[1]

**((2s,3a*R*,9a*S*,*E*)-3a,4,5,8,9,9a-hexahydrocycloocta[*d*][1,3]dioxol-2-yl)methanol**[2]

**(*rel*-1*R*,8*S*,9*R*,4*E*)-Bicyclo[6.1.0]non-4-ene-9-yl-methanol**[3]

**4-methoxyphenylglyoxal**[4]

**2-oxo-2-(4-methoxyphenyl)acetaldehyde oxime**[5]

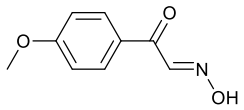


To a solution of 4-methoxyphenylglyoxal (1.73 g, 10.5 mmol) in EtOH (25 mL) $H_2O$ (10 mL), hydroxylamine hydrochloride (879 mg, 12.6 mmol) and anhydrous sodium carbonate (670 mg, 6.32 mmol) were added at 0 °C. After one hour at room temperature the mixture was diluted with brine (50 mL) and then extracted with EtOAc (2x 100 mL). The combined organic layers were washed with sat. aq. $NaHCO_3$ (70 mL), dried over $Na_2SO_4$ and concentrated *in vacuo*. The crude oxime (1.63 g) was used directly in the next step without further purification.

**2-hydrazono-2-(4-methoxyphenyl)acetaldehyde oxime**[6]

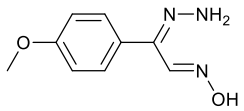


To a solution of 2-oxo-2-(4-methoxyphenyl)acetaldehyde oxime (1.63 g, 9.10 mmol) in EtOH (25 mL) hydrazine monohydrate (758 µL, 10.0 mmol) and a few drops of acetic acid were added at 45 °C. The solution was stirred at 45 °C for 15 h. After the starting material has disappeared, the crude product was concentrated *in vacuo* and purified by flash column chromatography (eluting with 0-25% EtOAc in $CH_2Cl_2$ + 1% MeOH) to provide the oximinohydrazone as an orange solid (1.02 mg, 58%).
The identity of the purified product was verified by HPLC-MS on a Luna® C18 column (3u, 100A, 100 x 4.6 mm) using a linear gradient of $CH_3CN$ (5-95% in 9 min and 1mL/min flow) in $H_2O$ + 0.05% HCOOH. The purification provided two isomers of the oximinohydrazone eluting at 6.42 min and 8.06 min, respectively (Figure S1).
MS (ESI): m/z calcd. for $C_9H_{12}N_3O_2$ $[MH]^+$ 194.1, found 194.1.

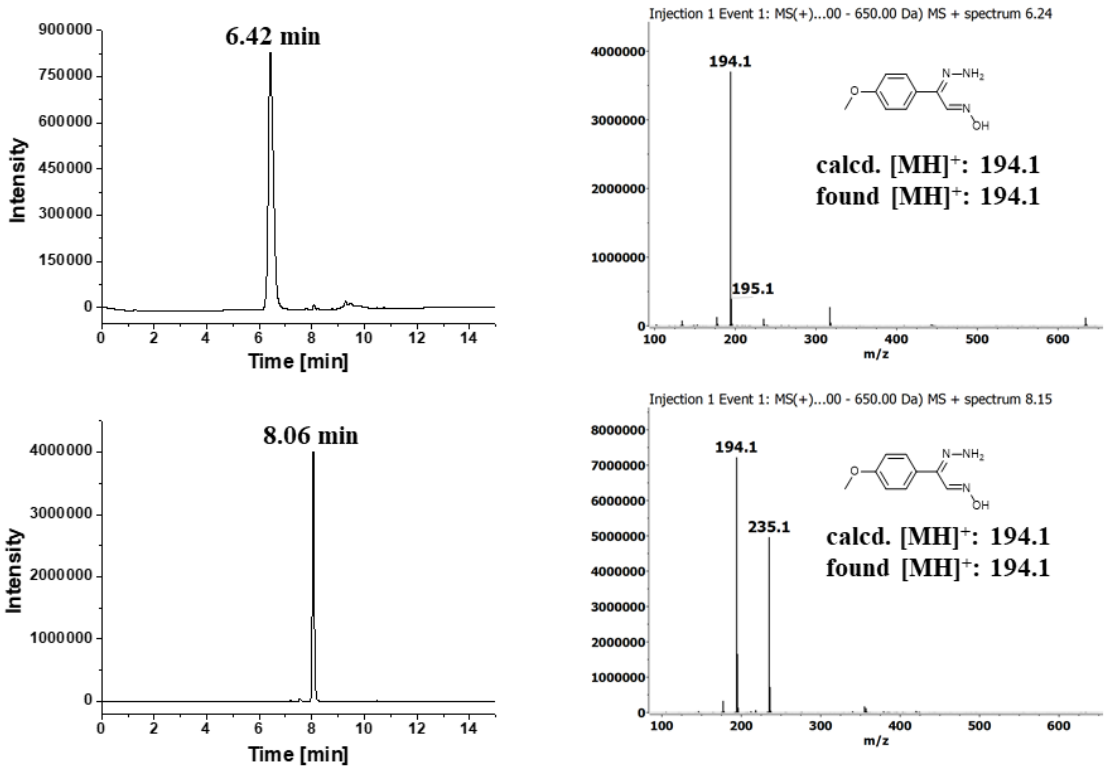


**Figure S1**. HPLC-MS analysis of the two isomers of 2-hydrazono-2-(4-methoxyphenyl)acetaldehyde oxime obtained after purification by flash column chromatography.

## 2-hydrazono-2-phenylacetaldehyde oxime[6]

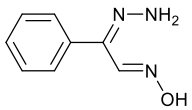

2-Isonitrosoacetophenone (2.50 g, 16.8 mmol) and a few drops of acetic acid were added to a solution of hydrazine monohydrate (1.27 mL, 16.8 mmol) in EtOH (25 mL) at 45 °C. The mixture was stirred at 45 °C for 20 h. After the starting material has disappeared, the crude product was concentrated *in vacuo* and purified by flash column chromatography (eluting with 0-20% EtOAc in $CH_2Cl_2$ + 1% MeOH) to provide the oximinohydrazone as a yellow solid (2.26 g, 82%).
Analytical data matched with literature.[7]

## 3-(2-pyridyl)-6-phenyl-1,2,4-triazine (1)[6]

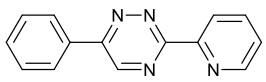

To a solution of 2-hydrazono-2-phenylacetaldehyde oxime (167 mg, 1.02 mmol) in EtOH (7 mL) a few drops of acetic acid and 2-pyridinecarboxaldehyde (117 µL, 1.23 mmol) were added. The solution was stirred at room temperature for 21 h. The formed bisaryl substituted intermediate was concentrated *in vacuo*, dissolved in acetic acid (2 mL) and heated at 100 °C under reflux for 1 h. After the complete intermediate was cyclized (verified by HPLC-MS),

the mixture was concentrated *in vacuo*, diluted with $H_2O$ (10 mL) and the pH was adjusted to ~8 by addition of sat. aq. $NaHCO_3$. The suspension was extracted with $CH_2Cl_2$ (3x 60 mL) and the combined organic layers were washed with brine (70 mL), dried over $Na_2SO_4$ and concentrated *in vacuo*. The crude triazine was purified by flash column chromatography (eluting with 0-30% MeOH in $CH_2Cl_2$) and further by recrystallization from EtOAc to provide **1** as a light-brown solid (154 mg, 64%).
HRMS (EI+): m/z calcd. for $C_{14}H_{10}N_4$ $[MH]^+$ 234.0905, found 234.0904. Spectral data matched with literature.[6]

**3-(2-pyridyl)-6-(4-methoxyphenyl)-1,2,4-triazine (2)**[6]

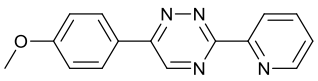

A few drops of acetic acid and 2-pyridinecarboxaldehyde (292 µL, 3.07 mmol) were added to a solution of 2-hydrazono-2-(4-methoxyphenyl)acetaldehyde oxime (362 mg, 1.87 mmol) in EtOH (10 mL). The solution was stirred at room temperature for 20 h. The formed bisaryl substituted intermediate was concentrated *in vacuo*, dissolved in acetic acid (5 mL) and heated at 100 °C under reflux for 1 h. After the complete intermediate was cyclized (verified by HPLC-MS), the mixture was concentrated *in vacuo*, diluted with $H_2O$ (10 mL) and the pH was adjusted to ~8 by addition of sat. aq. $NaHCO_3$. The suspension was extracted with $CH_2Cl_2$ (3x 60 mL) and the combined organic layers were washed with brine (70 mL), dried over $Na_2SO_4$ and concentrated *in vacuo*. The crude product was purified by flash column chromatography (eluting with 0-90% EtOAc in $CH_2Cl_2$ + 1% MeOH) and recrystallization from EtOAc to provide **2** as a brown solid (339 mg, 69%).
HRMS (EI+): m/z calcd. for $C_{15}H_{12}N_4O$ $[MH]^+$ 264.1011, found 264.1009. Spectral data matched with literature.[6]

**3-(4-pyridyl)-6-(4-methoxyphenyl)-1,2,4-triazine (3)**

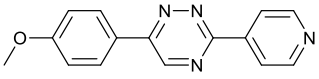

To a solution of 2-hydrazono-2-(4-methoxyphenyl)acetaldehyde oxime (420 mg, 2.17 mmol) in EtOH (15 mL) were added a few drops of acetic acid and 4-pyridinecarboxaldehyde (205 µL, 2.17 mmol). The solution was stirred at room temperature for 28 h. The formed bisaryl substituted intermediate was concentrated *in vacuo*, dissolved in acetic acid (6 mL) and heated at 100 °C under reflux for 1 h. After the complete intermediate was cyclized (verified by HPLC-MS), the mixture was concentrated *in vacuo*, diluted with $H_2O$ (10 mL) and the pH was adjusted to ~8 by addition of sat. aq. $NaHCO_3$. The suspension was extracted with $CH_2Cl_2$ (3x 60 mL) and the combined organic layers were washed with brine (70 mL), dried over $Na_2SO_4$ and concentrated *in vacuo*. The crude triazine was purified by flash column chromatography (eluting with 0-65% EtOAc in $CH_2Cl_2$ + 1% MeOH) to provide **3** as a yellow solid (316 mg, 55%).

$^{1}$H NMR (401 MHz, $CDCl_3$): δ 9.06 (s, 1H), 8.88 -8.79 (m, 2H), 8.42-8.35 (m, 2H), 8.20-8.08 (m, 2H), 7.16-7.04 (m, 2H), 3.91 (s, 3H).
$^{13}$C NMR (101 MHz, $CDCl_3$): δ 162.56, 160.27, 155.82, 150.90, 146.13, 142.25, 128.57, 125.20, 121.62, 115.12, 55.65.
HRMS (EI+): m/z calcd. for $C_{15}H_{12}N_4O$ $[MH]^+$ 264.1011, found 264.1009.

**2-formyl-1-methylpyridinium iodide**[8]

**4-formyl-1-methylpyridinium iodide**[8]

**1-methyl-2-(6-phenyl-1,2,4-triazin-3-yl)pyridinium iodide (4)**

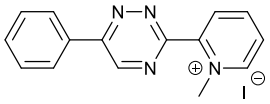

2-formyl-1-methylpyridinium iodide (382 mg, 1.53 mmol) and acetic acid (250 µL) were added to a solution of 2-hydrazono-2-phenylacetaldehyde oxime (250 mg, 1.53 mmol) in EtOH (10 mL). The solution was stirred at room temperature for 23 h. The formed bisaryl substituted intermediate was concentrated *in vacuo*, dissolved in acetic acid (3 mL) and heated at 100 °C under reflux for 3 h. After the complete intermediate was cyclized (verified by HPLC-MS), the mixture was concentrated *in vacuo*, diluted with $H_2O$ (10 mL) and the pH was adjusted to ~8 by addition of sat. aq. $NaHCO_3$. The suspension was extracted with *i*PrOH/$CH_2Cl_2$ (2:1) (3x 60 mL) and the combined organic layers were washed with brine (70 mL), dried over $Na_2SO_4$ and concentrated *in vacuo*. The crude triazine was purified twice by flash column chromatography (first eluting with 10% $H_2O$ in $CH_3CN$ and second with 5-60% MeOH in $H_2O$ on a reversed phase C18 column) to provide **4** as a yellow solid (61 mg, 11%).
$^{1}$H NMR (401 MHz, MeOH-$d_4$): δ 9.60 (s, 1H), 9.20 (d, $J$ = 6.2 Hz, 1H), 8.83 (td, $J$ = 7.8, 1.4 Hz, 1H), 8.76 (dd, $J$ = 8.1, 1.7 Hz, 1H), 8.40-8.33 (m, 2H), 8.30 (ddd, $J$ = 7.8, 6.1, 1.7 Hz, 1H), 7.72-7.63 (m, 3H), 4.70 (s, 3H).
$^{13}$C NMR (101 MHz, MeOH-$d_4$): δ 159.58, 158.14, 150.44, 149.90, 148.90, 147.48, 133.69, 133.26, 132.26, 130.79, 130.70, 130.12, 128.79.
HRMS (ESI): m/z calcd. for $C_{15}H_{13}N_4$ $[MH]^+$ 249.1135, found 249.1135.

**1-methyl-4-(6-phenyl-1,2,4-triazin-3-yl)pyridinium iodide (5)**

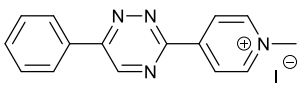

To a solution of 2-hydrazono-2-phenylacetaldehyde oxime (250 mg, 1.53 mmol) in EtOH (10 mL) were added a few drops of acetic acid and 4-formyl-1-methylpyridinium iodide (382 mg, 1.53 mmol). After stirring the solution at room temperature for 9 h, additional acetic acid (250 µL) was added and the mixture was stirred again at room temperature for 19 h. The mixture was concentrated *in vacuo*, diluted with $H_2O$ (10 mL) and the pH was adjusted to ~8

by addition of sat. aq. $NaHCO_3$. The suspension was extracted with *i*PrOH/$CH_2Cl_2$ (2:1) (3x 60 mL) and the combined organic layers were washed with brine (70 mL), dried over $Na_2SO_4$ and concentrated *in vacuo*. Purification by flash column chromatography (eluting with 10% $H_2O$ in $CH_3CN$ on normal phase silica gel) provided **5** as a yellow solid (226 mg, 39%).

$^1$H NMR (401 MHz, MeOH-$d_4$): δ 9.54 (s, 1H), 9.15 (d, $J$ = 6.9 Hz, 2H), 9.09 (d, $J$ = 7.0 Hz, 2H), 8.36-8.29 (m, 2H), 7.69-7.61 (m, 3H), 4.54 (s, 3H).

$^{13}$C NMR (101 MHz, MeOH-$d_4$): δ 159.35, 158.56, 151.61, 149.22, 147.78, 133.89, 133.10, 130.64, 128.65, 126.54.

HRMS (ESI): m/z calcd. for $C_{15}H_{13}N_4$ $[MH]^+$ 249.1135, found 249.1136.

**4-(6-(4-methoxyphenyl)-1,2,4-triazin-3-yl)-1-methylpyridinium iodide (6)**

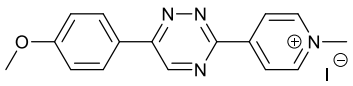

To a solution of 2-hydrazono-2-(4-methoxyphenyl)acetaldehyde oxime (300 mg, 1.55 mmol) in EtOH (10 mL) were added a few drops of acetic acid and 4-formyl-1-methylpyridinium iodide (387 mg, 1.55 mmol). After stirring the solution at room temperature for 20 h, additional acetic acid (250 µL) was added and the mixture was stirred again at room temperature for 23 h. The mixture was concentrated *in vacuo*, diluted with $H_2O$ (10 mL) and the pH was adjusted to ~8 by addition of sat. aq. $NaHCO_3$. The suspension was extracted with *i*PrOH/$CH_2Cl_2$ (2:1) (3x 60 mL) and the combined organic layers were washed with brine (70 mL), dried over $Na_2SO_4$ and concentrated *in vacuo*. The crude triazine was purified by flash column chromatography (eluting with 10% $H_2O$ in $CH_3CN$ on normal phase silica gel) to provide **6** as a yellow-brown solid (264 mg, 42%).

$^1$H NMR (401 MHz, DMSO-$d_6$): δ 9.67 (s, 1H), 9.24 (dd, $J$ = 6.4, 1.1 Hz, 2H), 8.97-8.88 (m, 2H), 8.38-8.27 (m, 2H), 7.25-7.14 (m, 2H), 4.48 (s, 3H), 3.88 (s, 3H).

$^{13}$C NMR (101 MHz, DMSO-$d_6$): δ 162.52, 157.27, 155.88, 148.97, 147.70, 146.81, 129.31, 124.74, 124.53, 115.13, 55.70, 48.04.

HRMS (ESI): m/z calcd. for $C_{16}H_{15}N_4O$ $[MH]^+$ 279.1240, found 279.1241.

**3-amino-6-bromo-1,2,4-triazine**

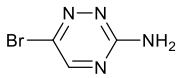

3-amino-6-bromo-1,2,4-triazine was prepared according to a slightly modified literature procedure with an additional purification step by flash column chromatography (eluting with 0-90% EtOAc in $CH_2Cl_2$ + 1% MeOH) at the end.[9]

Analytical data matched with literature.[10]

**6-(4-nitrophenyl)-1,2,4-triazine (8)**

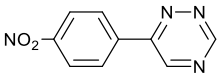

6-(4-nitrophenyl)-1,2,4-triazine was prepared according to a slightly modified literature procedure.[10]
Following the literature procedure, conditions of the Suzuki coupling were modified as follows: the reaction was performed in DMF/$H_2O$ (4:1) mixture and $K_2CO_3$ was used as base instead of $Cs_2CO_3$.
Analytical data matched with literature.[10]

**6-(4-pyridyl)-1,2,4-triazine (7)**

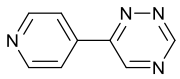

Following the literature procedure,[10] 3-amino-6-bromo-1,2,4-triazine (500 mg, 2.86 mmol), 4-pyridinyl-boronic acid (421 mg, 3.43 mmol) and $Pd(PPh_3)_4$ (165 mg, 0,143 mmol) were used. Unlike in the literature, the Suzuki coupling was performed in DMF/$H_2O$ (4:1) (25 mL) and $K_2CO_3$ (592 mg, 4.29 mmol) was used as base instead of $Cs_2CO_3$. The extracted intermediate was purified by flash column chromatography (eluting with 0-10% MeOH in $CH_2Cl_2$). In the second step 7.5 eq. of isopentyl nitrite (1.84 mL, 13.7 mmol) were added step by step over several hours until the intermediate has disappeared (verified by HPLC-MS). The crude product was purified by flash column chromatography (eluting with 0-10% MeOH in $CH_2Cl_2$) to provide **7** as an orange solid (53 mg, 19%).
$^1$H NMR (401 MHz, $CDCl_3$): δ 9.76 (s, 1H), 9.09 (s, 1H), 8.88-8.85 (m, 2H), 8.03-7.99 (m, 2H).
$^{13}$C NMR (101 MHz, $CDCl_3$): δ 157.35, 156.07, 151.20, 146.81, 140.52, 120.85.
HRMS (EI+): m/z calcd. for $C_8H_6N_4$ $[MH]^+$ 158.0592, found 158.0591.

**1-(2-carboxyethyl)-4-(6-(4-methoxyphenyl)-1,2,4-triazin-3-yl)pyridinium formate (9)**

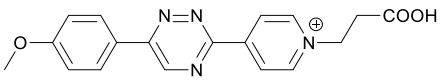

To a suspension of **3** (50 mg, 0.19 mmol) in 2-butanone (2.5 mL) was added 3-iodo-propionic acid (189 mg, 0.95 mmol, 5 eq.) and the reaction mixture was stirred at 80 °C overnight. The solvent was removed *in vacuo* and the product was isolated by normal phase silica gel column chromatography (eluting with $CH_3CN/H_2O$ (4:1) → $CH_3CN/H_2O$ (4:1) + 0.25% HCOOH). The product was isolated as yellow powder and as salt of formic acid (51 mg, 71%).
$^1$H NMR (400 MHz, $CD_3CN/D_2O$ (1:1)): δ 9.35 (s, 1H), 9.00 (d, $J$ = 6.8 Hz, 2H), 8.88 (d, $J$ = 6.7 Hz, 2H), 8.19 (d, $J$ = 8.9 Hz, 2H), 7.15 (d, $J$ = 8.9 Hz, 2H), 4.79 (t, $J$ = 6.6 Hz, 3H), 3.85 (s, 2H), 2.87 (t, $J$ = 6.6 Hz, 2H).

$^{13}$C NMR (100 MHz, $CD_3CN/D_2O$ (1:1)): δ 172.5, 162.8, 157.2, 156.4, 150.3, 147.7, 146, 129.2, 125.3, 124.4, 115.1, 56.9, 55.4, 34.2.
HRMS (ESI): m/z calcd. for $C_{18}H_{17}O_3N_4$ $[MH]^+$ 337.1295, found 337.1296.

**1-(3-hydroxypropyl)-4-(6-(4-methoxyphenyl)-1,2,4-triazin-3-yl)pyridinium chloride (10)**

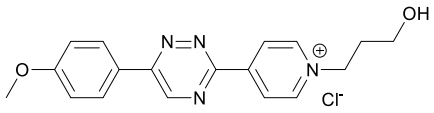


To a suspension of **3** (25 mg, 0.095 mmol) in 2-butanone (1 mL) was added 4-iodo-propanol (45 µL, 0.47 mmol, 5 eq.) and the reaction mixture was stirred at 100 °C for 1 h and then at 80 °C overnight. The solvent was removed under vacuum and the product was isolated by normal phase silica gel column chromatography (eluting with $CH_3CN/H_2O$ (10:1) + 0.1% of sat. aq. $NH_4PF_6$). Fractions containing the product were collected, evaporated and the solid was transferred into 2 mL polypropylene tube. The solid was repeatedly washed with $H_2O$ (3x 1mL) to remove excess of $NH_4PF_6$. After each washing step the tube was centrifuged and the liquid discarded. This product (as $PF_6^-$ salt) was further purified by second silica gel column (eluting with DCM/MeOH = 9:1). The product was isolated as a yellow powder (33 mg, 75%). The $PF_6^-$ salt (soluble in $CH_3CN$ or DCM) can be easily converted to the corresponding water soluble $Cl^-$ salt by passing the product through short column of Dowex 50 1X2 in $Cl^-$ form (elution with $H_2O$) and lyophilization.
$^1$H NMR (400 MHz, $CD_3CN/D_2O$ (1:1)): δ 9.33 (s, 1H), 8.98 (d, *J* = 6.7 Hz, 2H), 8.88 (d, *J* = 7.0 Hz, 2H), 8.28 (d, *J* = 9.1 Hz, 2H), 7.18 (d, *J* = 9.0 Hz, 2H), 4.83-4.65 (m, 2H), 3.61 (q, *J* = 5.5 Hz, 2H), 2.91 (t, *J* = 4.9 Hz, 2H), 2.18 (m, 2H).
$^{13}$C NMR (100 MHz, $CD_3CN/D_2O$ (1:1)): δ 164.0, 158.2, 157.5, 151.5, 148.1, 146.6, 130.2, 126.3, 125.6, 116.0, 60.3, 58.4, 56.3, 33.9.
HRMS (ESI): m/z calcd. for $C_{18}H_{19}O_2N_4$ $[MH]^+$ 323.1503, found 323.1503.

**4-(6-(4-methoxyphenyl)-1,2,4-triazin-3-yl)-1-(pent-4-yn-1-yl)pyridinium iodide (11)**

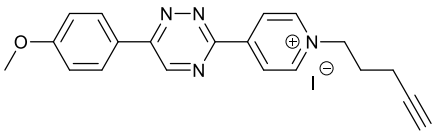


To a Schlenk tube containing a solution of triazine **3** (50 mg, 0.189 mmol) in anhydrous DMF (4 mL) was added step by step over several hours 5-iodo-1-pentyne (312 mg, 1.61 mmol) until the starting material has disappeared (verified by HPLC-MS). The reaction was performed under argon and at 50 °C. The crude product was concentrated *in vacuo* and purified by silica gel column chromatography (eluting with $CH_2Cl_2$/MeOH (20:1) → (10:1) → (5:1)) to provide the alkylated triazine **11** as an orange solid (58 mg, 67%).

$^1$H NMR (401 MHz, DMSO-$d_6$): δ 9.69 (s, 1H), 9.29 (d, $J$ = 7.0 Hz, 2H), 8.99 (d, $J$ = 6.9 Hz, 1H), 8.40-8.33 (m, 2H), 7.25-7.18 (m, 2H), 4.78 (t, $J$ = 7.1 Hz, 2H), 3.89 (s, 3H), 2.88 (t, $J$ = 2.6 Hz, 1H), 2.35 (td, $J$ = 6.9, 2.4 Hz, 2H), 2.21 (p, $J$ = 7.0 Hz, 2H).
$^{13}$C NMR (101 MHz, DMSO-$d_6$): δ 162.48, 157.16, 155.82, 149.45, 147.63, 146.10, 129.23, 125.09, 124.44, 115.06, 82.43, 72.51, 60.05, 55.62, 29.22, 14.85.
HRMS (ESI): m/z calcd. for $C_{20}H_{19}N_4O$ $[MH]^+$ 331.1553, found 331.1554.

**1-azido-3-iodopropane**

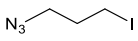

1-azido-3-iodopropane was prepared according to a slightly modified literature procedure.[11] Following the literature procedure, the crude product was purified by silica gel column chromatography (eluting with petroleum ether/EtOAc (4:1)) instead of distillation under reduced pressure.
Analytical data matched with literature.[11]

**1-(3-azidopropyl)-4-(6-(4-methoxyphenyl)-1,2,4-triazin-3-yl)pyridinium iodide (12)**

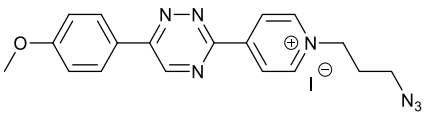

To a Schlenk tube containing a solution of triazine **3** (50 mg, 0.189 mmol) in anhydrous DMF (4 mL) was added 1-azido-3-iodopropane (200 mg, 0.946 mmol). The tube was flushed with argon and heated at 50 °C for 77 h. The crude product was concentrated *in vacuo* and purified by flash column chromatography (eluting with 0-10% MeOH in $CH_2Cl_2$) to provide the alkylated triazine **12** as an orange brown solid (75 mg, 83%).
$^1$H NMR (401 MHz, $CDCl_3$): δ 9.55-9.49 (m, 1H), 9.21 (s, 1H), 9.09-9.04 (m, 1H), 8.17 (d, $J$ = 8.9 Hz, 1H), 7.07 (d, $J$ = 9.0 Hz, 1H), 5.12 (t, $J$ = 7.2 Hz, 1H), 3.89 (s, 2H), 3.64 (t, $J$ = 6.2 Hz, 1H), 2.50-2.39 (m, 1H).
$^{13}$C NMR (101 MHz, $CDCl_3$): δ 163.34, 156.90, 156.57, 150.58, 146.55, 145.94, 129.34, 125.77, 124.14, 115.37, 59.51, 55.74, 48.08, 30.83.
HRMS (ESI): m/z calcd. for $C_{18}H_{18}N_7O$ $[MH]^+$ 348.1567, found 348.1569.

**Synthesis of compound 13**

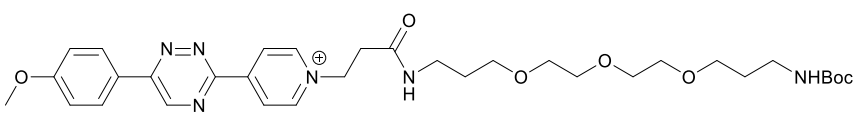

To an ice-water bath cooled suspension of **9** (10 mg, 0.026 mmol) in dry DMF (0.5 mL) was added *N*-Boc-4,7,10-trioxa-1,13-tridecanediamine (12.5 mg, 1.5 eq.) under argon followed by solid HATU (11 mg, 1.2 eq.) and DIPEA (11 µL, 2.5 eq.). The reaction mixture was stirred at room temperature under argon overnight. DMF was removed under vacuum and the residue

was purified by silica gel column chromatography (eluting with DCM/MeOH (9:1) → (5:1)). The product was isolated as yellow viscous oil (10 mg, 56%).
HRMS (ESI): m/z calcd. for $C_{33}H_{47}O_7N_6$ $[MH]^+$ 639.3501, found 639.3502.

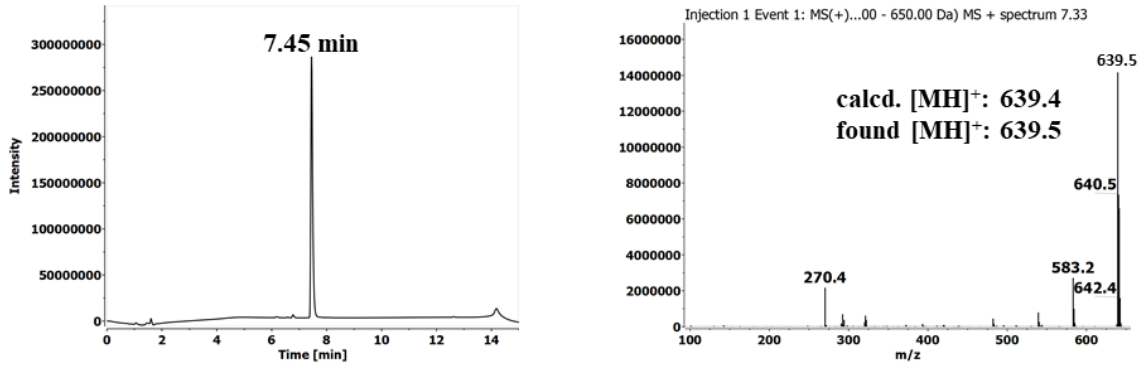


**Figure S2**. Exported HPLC-MS chromatograms of **13** (solvent A: $H_2O$ + 0.05% HCOOH; solvent B: $CH_3CN$ + 0.05% HCOOH; gradient: 5% B → 95% B in 9 min, then 2 min 95% B and back to 5% B). The product **13** eluates at 7.45 min (Luna® C18 column, 3u, 100A, 100 x 4.6 mm, 1 mL/min flow rate).

## Synthesis of compound 14

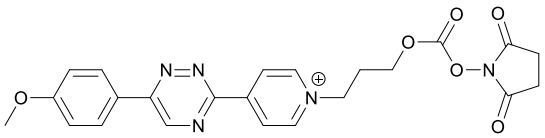

To an ice-cold solution of **10** (as $PF_6^-$ salt, 15 mg, 0.032 mmol) in dry DMF (1 mL) was added solid disuccinimidyl carbonate (DSC, 16.4 mg, 2 eq.) under argon followed by $Et_3N$ (18 µL, 4 eq.). The reaction mixture was stirred at room temperature until starting material disappeared (3 h, TLC in DCM/MeOH (9:1) and/or HPLC-MS). Our attempts to isolate the active ester by column chromatography led to partial decomposition of the product back to the starting material. However, the crude reaction mixture could be used directly in the next reaction step. The yield was ca. 80% (based on integrated peak area, Figure S3).

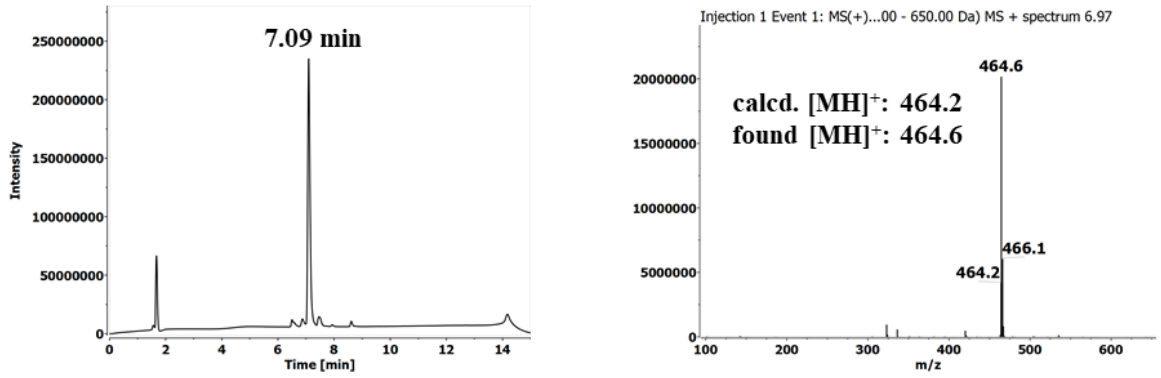


**Figure S3**. Exported HPLC-MS chromatograms of the crude reaction mixture after 3 h (solvent A: $H_2O$ + 0.05% HCOOH; solvent B: $CH_3CN$ + 0.05% HCOOH; gradient: 5% B → 95% B in 9 min, then 2 min 95% B and back to 5% B). Starting alcohol eluates at 6.35 min and product **14** at 7.1 min (Luna® C18 column, 3u, 100A, 100 x 4.6 mm, 1 mL/min flow rate).

## Synthesis of compound 15

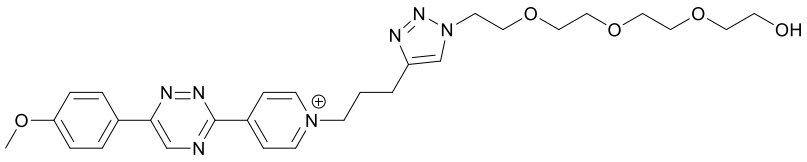

2-(2-(2-(2-azidoethoxy)ethoxy)ethoxy)ethan-1-ol (6 mg, 2.5 eq.) was added to a suspension of **11** (5 mg, 0.011 mmol) in $H_2O$/DMSO (3:2) (300 µL). In a separate tube aqueous Na-ascorbate solution (0.43 mg in 5 µL of $H_2O$, 20 mol%,) was added to a mixture of Cu-ligand BTTP[12] (1 mg, 20 mol%) and $CuSO_4$ .5 $H_2O$ (0.3 mg, 10 mol%) in 10 µL of $H_2O$/DMSO (1:1). The colorless activated solution of the catalyst was added to the suspension of the alkyne and azide reagents and the reaction mixture was stirred at room temperature. The progress of the reaction was followed by HPLC-MS. After 2.5 h the reaction mixture did not change any longer giving 76% of the product (based on integrated peak area, Figure S4).
The formation of product was verified by HPLC-MS and HRMS.
HRMS (ESI): m/z calcd. for $C_{28}H_{36}O_5N_7$ $[M]^+$ 550.27724, found 550.27740.

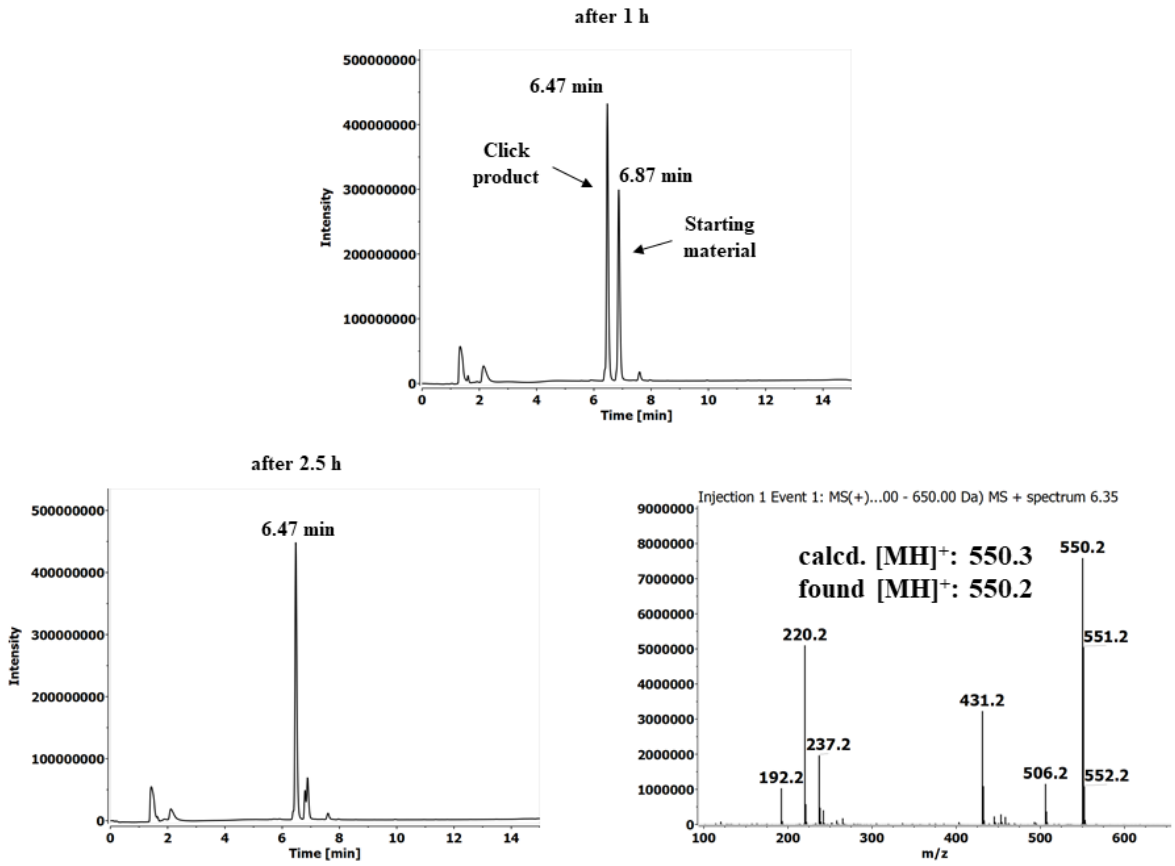


**Figure S4**. HPLC-MS chromatograms of the crude reaction mixture showing the formation of **15** after 1 h and 2.5 h respectively (solvent A: $H_2O$ + 0.05% HCOOH; solvent B: $CH_3CN$ + 0.05% HCOOH; gradient: 5% B → 95% B in 9 min, then 2 min 95% B and back to 5% B). Starting alkyne eluates at 6.9 min and the product **15** at 6.5 min (Luna® C18 column, 3u, 100A, 100 x 4.6 mm, 1 mL/min flow rate).

## Determination of the second-order rate constants

Second order rate constants of the reactions between triazines and *trans*-cyclooctenes (TCO) were determined by following the decrease in the concentration of the starting 1,2,4-triazine over time. The concentration decrease was monitored either by HPLC (for slower derivatives) or by UV/VIS spectroscopy (for faster derivatives). The measurements were performed in a mixture of $CH_3CN/H_2O$ (1:1) at room temperature under pseudo first-order conditions using an excess of the corresponding TCO. All runs were conducted at least three times.

For rate determination using HPLC: 20 µL of a 10 mM solution of the triazine in $CH_3CN/H_2O$ (1:1) (10 µL for **6** + TCO-ol and 5 µL for **4** + d-TCO) were added to 80 µL of a 25 mM solution of the appropriate TCO (for **6** + TCO-ol to 90 µL of a 10 mM solution and for **4** + d-TCO to 20 µL of a 25 mM solution diluted with 75 µL of $H_2O$). The final

concentration of all triazines was 2 mM using 10 eq. of TCO (1 mM of triazine using 9 eq. of TCO for **6** + TCO-ol and 0.5 mM of triazine using 10 eq. of TCO for **4** + d-TCO). The measurements were performed on a Luna® C18 column (3u, 100A, 100 x 4.6 mm) using a linear gradient of $CH_3CN$ + 0.05% HCOOH in $H_2O$ + 0.05% HCOOH (5→95% in 9 min) at a flow rate of 1.0 mL/min. The MS device was disconnected from the HPLC during measurements. The integral of the absorption of the triazine at 254 nm was measured over 105 or 360 min in 15 or 45 min intervals. By using a calibration curve, the measured integrals were converted into the corresponding concentrations of the triazine, which were plotted against time to provide the observed rate constant from the slope of this plot (fitted with single exponential function: $y = y_0 + Ae^{-k/t}$). The second order rate constants were calculated by dividing the observed rate constants with initial concentration of the TCO.

For UV/VIS-measurements: a solution of the triazine in $CH_3CN/H_2O$ (1:1) (135 µM, 10 mM or 50 mM) and 50 mM solution of the appropriate TCO in $CH_3CN/H_2O$ (1:1) was added to $CH_3CN/H_2O$ (1:1) to a give a final volume of 3 mL and immediately measured on the UV/VIS spectrophotometer. The final concentration of all triazines was either 45 µM or 50 µM using either 5 eq. or 10 eq. of TCO. The decrease in the absorption of the triazine was followed over 5-120 min in intervals of 0.25, 0.5, 1, 2 or 5 min. The time-dependent measurements were performed at the corresponding absorption maxima of the triazine used, which was determined by UV/VIS spectroscopy before the measurement. The measured intensity of the absorption was plotted against time. Fitting the curves with single exponential equation ($y = y_0 + Ae^{-k/t}$ ) provided the observed rate constants. The second order rate constants were calculated by dividing the observed rate constants with initial concentration of the TCO. All data were processed using Origin or Excel software and are summarized in table S2.

**Calculated and found low-resolution masses of the click-products from rate studies.**

The following experiments were performed to verify the formation of the corresponding click products during kinetic studies.

30 µL of a 10 mM solution of triazine in $CH_3CN/H_2O$ (1:1) were added to 15 µL of a 25 mM solution of the appropriate TCO in $CH_3CN/H_2O$ (1:1). The mixture was diluted with $CH_3CN/H_2O$ (1:1) to a final volume of 150 µL. The final concentration of all triazines was 1 mM using 1.25 eq. of TCO. The solution was incubated at room temperature for 30 min and then measured by HPLC-MS on a Luna® C18 column (3u, 100A, 100 x 4.6 mm) using a linear gradient of $CH_3CN$ + 0.05% HCOOH (5→95% in 9 min) in $H_2O$ + 0.05% HCOOH at a flow rate of 1.0 mL/min.

During the kinetic measurement we have observed in some cases also the formation of the corresponding oxidized pyridine products together with the dihydropyridine product. These particular cases are indicated in Table S1.

**Table S1**. Calculated and observed masses of the click products arising from the reaction between 1,2,4-triazines and various TCOs.

| **Triazine\TCO** | 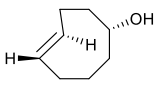 axial | | 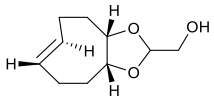 syn:anti 12:1 | | 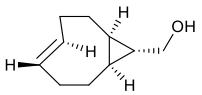 syn | |
|---|---|---|---|---|---|---|
| | calcd. | found | calcd. | found | calcd. | found |
| 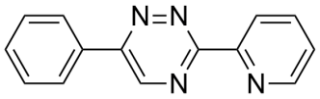 **1** | 333.2 | 333.2 [a] | 391.2 | 391.2[a] | 359.2 | 359.2 |
| 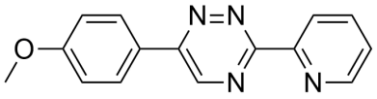 **2** | 363.2 | 363.2 [a] | 421.2 | 421.2[a] | 389.2 | 389.2 |
| 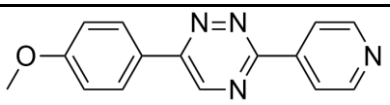 **3** | 363.2 | 363.2 [a] | 421.2 | 421.2 | 389.2 | 389.2 |
| 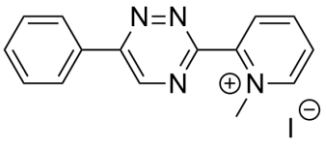 **4** | 347.2 | 347.2 [a] | 405.2 | 405.2 | 373.2 | 373.2 |
| 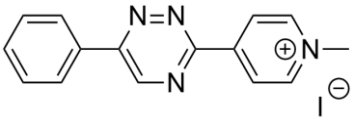 **5** | 347.2 | 347.2 [a] | 405.2 | 405.2 | 373.2 | 373.2 |
| 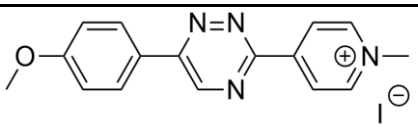 **6** | 377.2 | 377.2 [a] | 435.2 | 435.2 | 403.2 | 403.2 |
| 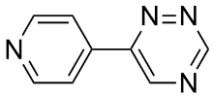 **7** | 257.2 | 257.2 [a] | 315.2 | 315.2 | 283.2 | 283.2 |
| 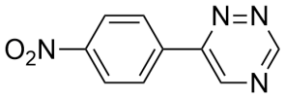 **8** | 299.1 | 299.2[b] | 359.2 | 359.2[a] | 327.2 | 327.2 |

a) for these compounds the mass of the oxidized form of the click-product was found as well, b) for this compound only the mass of the oxidized form of click-product was found.

**Table S2**. Second-order rate constants (in $M^{-1}$ $s^{-1}$) of the reaction between 1,2,4-triazines and various TCOs[a].

| **Triazine/TCO** | 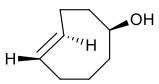 equatorial[b] | 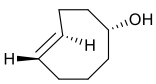 axial[b] | 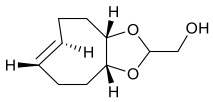 syn:anti 12:1 | 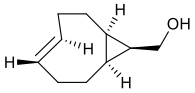 anti | 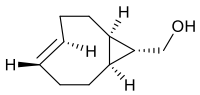 syn |
|---|---|---|---|---|---|
| 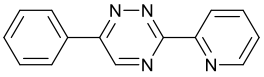 **1** | 0.67 ± 0.02 | 2.5 ± 0.04 | 0.56 ± 0.008 | 1.6 ± 0.05 | 1.9 ± 0.3 |
| 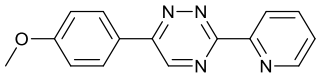 **2** | n.m. | 2.1 ± 0.2 | 0.36 ± 0.003 | n.m. | 1.2 ± 0.005 |
| 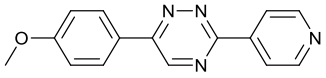 **3** | n.m. | 1.7 ± 0.4 | 0.35 ± 0.02 | n.m. | 1.4 ± 0.03 |
| 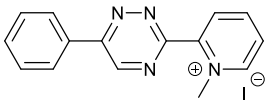 **4** | n.m. | 0.66 ± 0.08 | 0.083 ± 0.013 | n.m. | 0.30 ± 0.005 |
| 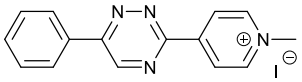 **5** | n.m. | 19 ± 2 | 2.6 ± 0.04 | n.m. | 9.9 ± 0.3 |
| 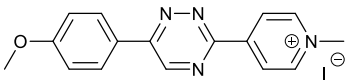 **6** | n.m. | 9.1 ± 0.3 | 1.9 ± 0.06 | n.m. | 6.4 ± 0.2 |
| 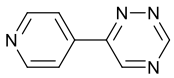 **7** | n.m. | 79 ± 5 | 9.4 ± 0.2 | n.m. | 20 ± 3 |
| 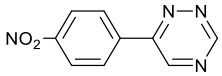 **8** | n.m. | 84 ± 7 | 11 ± 0.5 | n.m. | 24 ± 0.7 |

a) all reactions were performed in $CH_3CN/H_2O$ (1:1) at room temperature under pseudo first-order conditions using an excess of the corresponding TCO, b) these rate constants are in $M^{-1}$ $s^{-1}$ $x10^{-2}$, n.m.: not measured

## Stability studies of compound 6

The stability studies for triazine **6** were performed in $CH_3CN$/PBS (1:2) in the absence as well as in the presence of L-cysteine and were monitored by HPLC-MS on a Luna® C18 column (3u, 100A, 100 x 4.6 mm) (solvent A: $H_2O$ + 0.05% HCOOH; solvent B: $CH_3CN$ + 0.05% HCOOH; gradient: 5% B → 95% B in 9 min, then 2 min 95% B and back to 5% B; flow rate: 1.0 mL/min).

For the stability study without L-cysteine, 0.4 mL of a 15 mM solution of triazine **6** in $CH_3CN$/PBS (1:1) were diluted with PBS to a final volume of 0.6 mL. For the stability study with L-cysteine, 0.2 mL of a 30 mM solution of L-cysteine in PBS were added to 0.4 mL of a 15 mM solution of triazine **6** in $CH_3CN$/PBS (1:1). The final concentration of all reactants in both studies was 10 mM. In both cases the samples were incubated at 37 °C for 209 h and measured several times on the HPLC-MS (Figure S5 and S6).

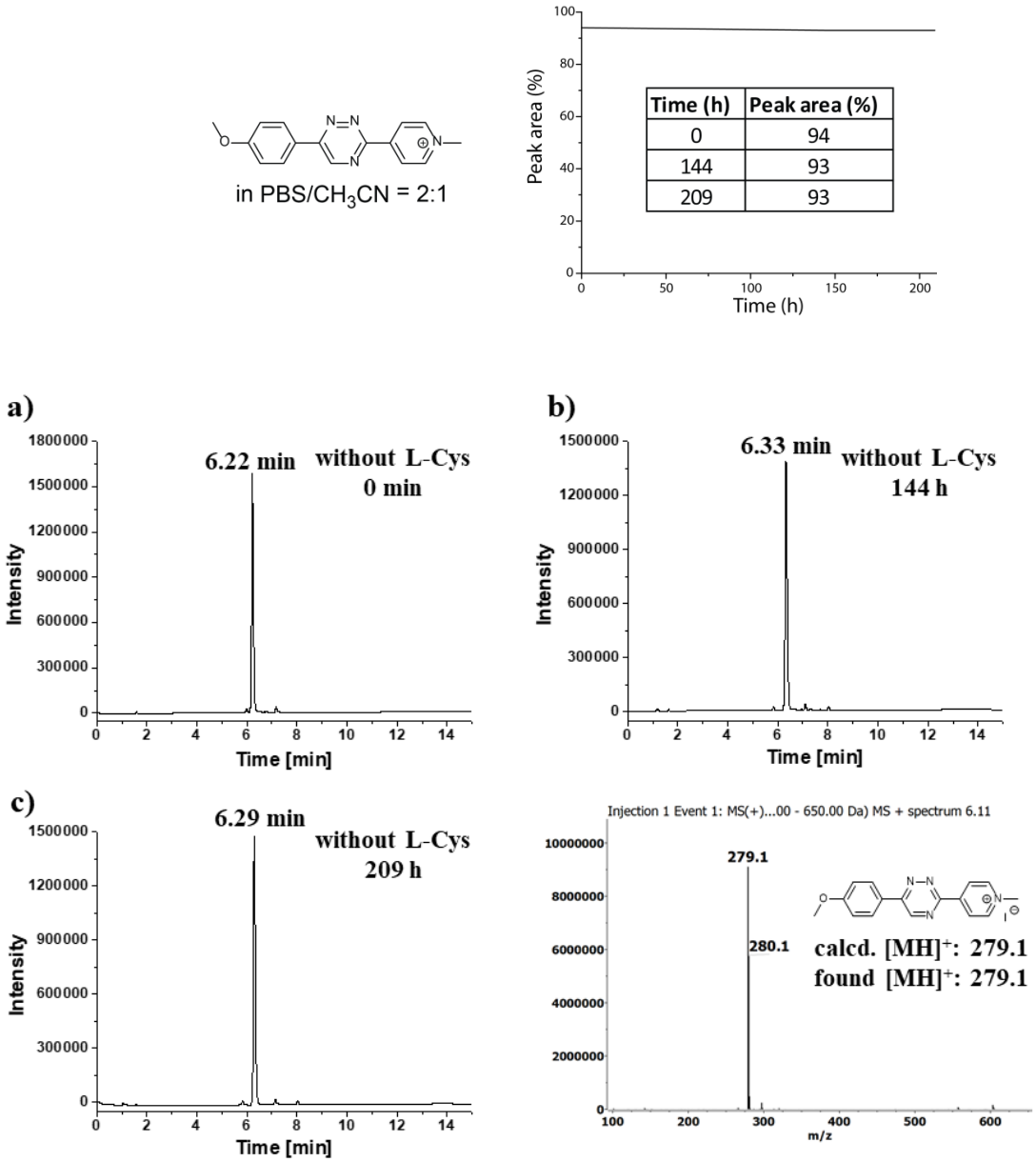


**Figure S5**. HPLC-MS analysis of **6** in $CH_3CN$/PBS (1:2) at 37°C after a) 0 min, b) 144 h and c) 209 h. Triazine **6** is stable under these conditions.

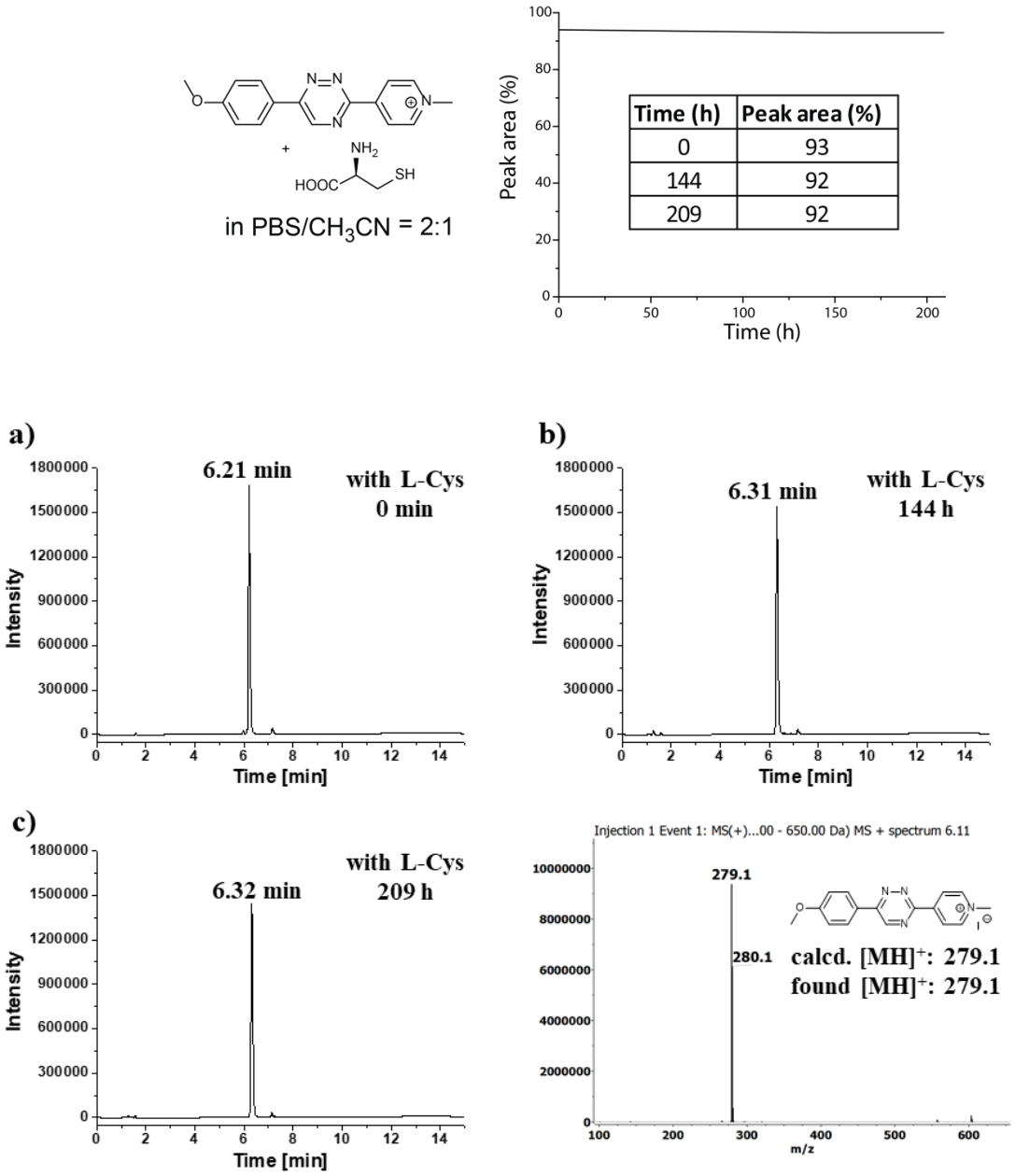


**Figure S6**. HPLC-MS analysis of **6** in $CH_3CN$/PBS (1:2) in the presence of L-cysteine at 37°C after a) 0 min, b) 144 h and c) 209 h. Triazine **6** is stable under these conditions.

In addition, the stability of **6** in the presence of L-cysteine was examined in $CD_3CN/D_2O$ (1:1) and followed by NMR spectroscopy. Conditions: 0.4 mL of a 80 mM solution of triazine **6** in $CD_3CN/D_2O$ (1:1) were added to 0.4 mL of a 80 mM solution of L-cysteine in $CD_3CN/D_2O$ (1:1) in order to get 40 mM final concentration of both triazine and L-cysteine. The reaction mixture was incubated at room temperature for 96 h in total. During that time the sample was measured several times by $^1$H-NMR (Figure S7).

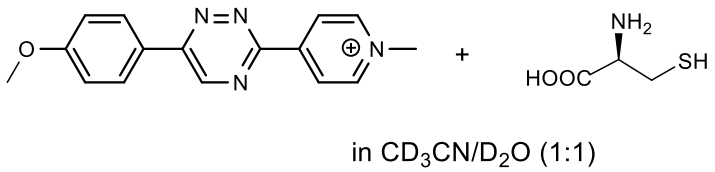


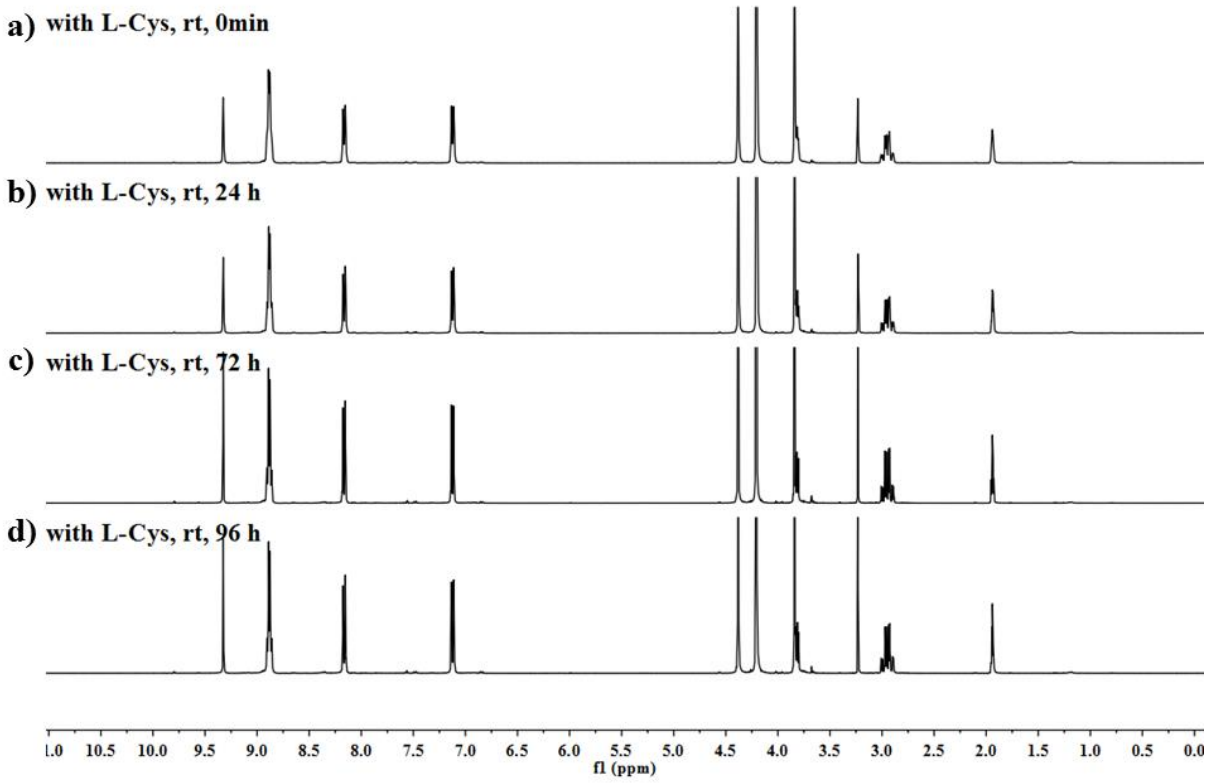


**Figure S7**. $^{1}$H-NMR analysis of **6** in $CD_3CN/D_2O$ (1:1) at room temperature in the presence of L-cysteine after a) 0 min, b) 24 h, c) 72 h and d) 96 h. The measurement further confirmed that **6** is stable in presence of L-cysteine.

## Double click-labeling of 12 by two orthogonal metal-free bioconjugations.

**A**) 50 µL of a 4 mM solution of **12** in $CH_3CN/H_2O$ (1:1) were added to 12 µL of a 25 mM solution of d-TCO in $CH_3CN/H_2O$ (1:1) and diluted with $CH_3CN/H_2O$ (1:1) to a final volume of 100 µL. The final concentration of triazine was 2 mM using 1.5 eq. of d-TCO. The mixture was incubated at room temperature for 1 h and measured by HPLC-MS. After the starting material has disappeared, a 25 mM solution of BCN (2.5 eq. of BCN) in $CH_3CN/H_2O$ (1:1) was added and the mixture was diluted with $CH_3CN/H_2O$ (1:1) to a final concentration of 1.33 mM (based on starting **12**). The mixture was incubated at room temperature for 2.5 h and measured by HPLC-MS (Figure S8).

All HPLC-MS measurements were performed on a Luna® C18 column (3u, 100A, 100 x 4.6 mm) using a linear gradient of $CH_3CN$ + 0.05% HCOOH (5→95% in 9 min) in $H_2O$ + 0.05% HCOOH at a flow rate of 1.0 mL/min.

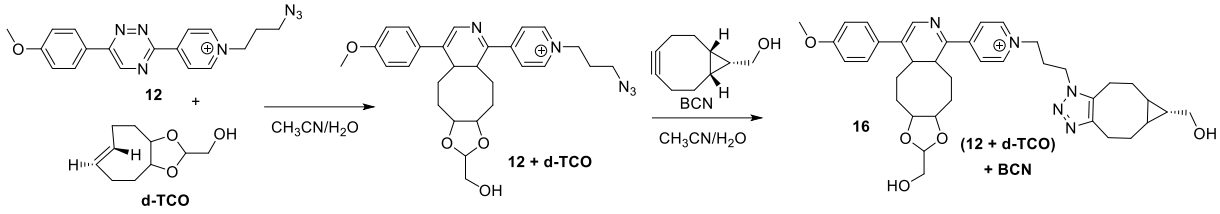


**Scheme S1**. Sequential double click-labeling of **12** using d-TCO and subsequently BCN.

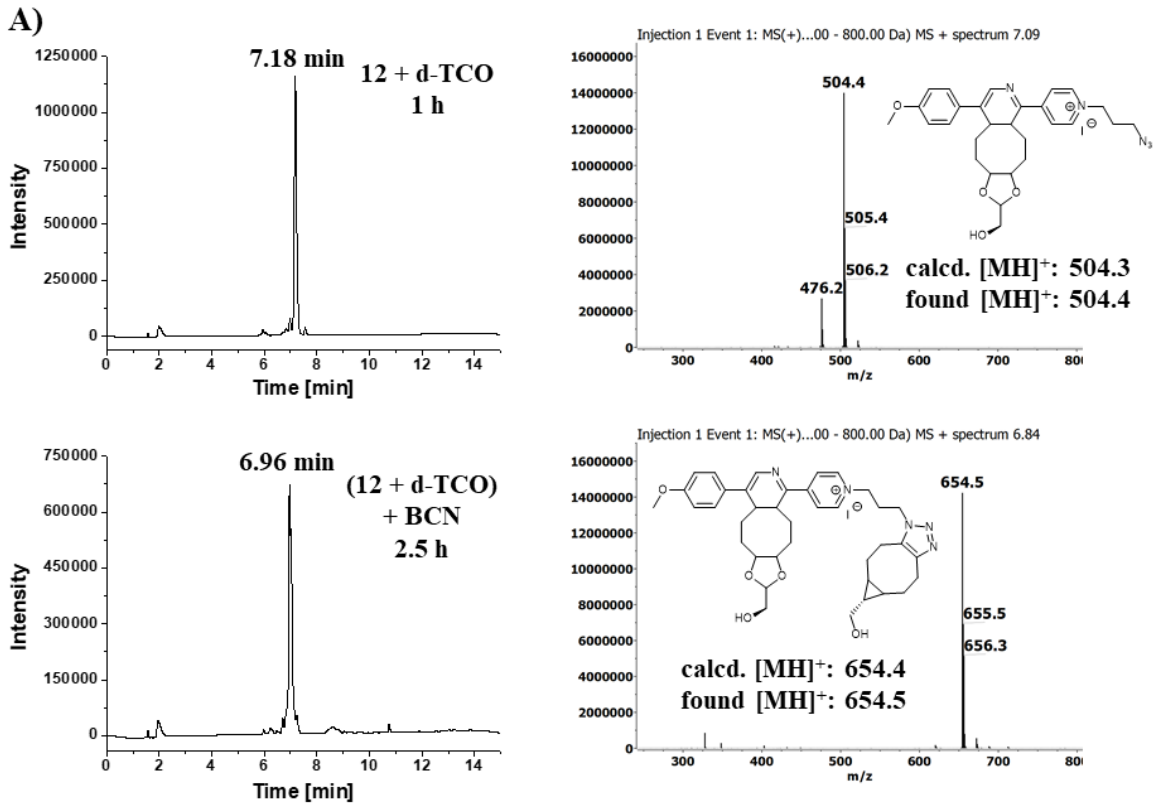


**Figure S8**. HPLC-MS analysis of sequential double click labeling of **12** incubated first with 1.5 eq. of d-TCO and subsequently with BCN (2.5 eq.) in $CH_3CN/H_2O$ (1:1). The analysis shows that both reactions proceed cleanly and selectively on the respective functional groups.

**B**) 50 µL of a 4 mM solution of **12** in $CH_3CN/H_2O$ (1:1) were added to 20 µL of a 25 mM solution of BCN in $CH_3CN/H_2O$ (1:1) and diluted with $CH_3CN/H_2O$ (1:1) to a final volume of 100 µL. The final concentration of triazine was 2 mM using 2.5 eq. of BCN. The mixture was incubated at room temperature for 2.5 h and measured by HPLC-MS. After the starting material has disappeared, a 25 mM solution of d-TCO (2.5 eq. of d-TCO) in $CH_3CN/H_2O$ (1:1) was added and the mixture and was diluted with $CH_3CN/H_2O$ (1:1) to a final concentration of 1.33 mM (based on starting **12**). The mixture was incubated at room temperature for 30 min and measured by HPLC-MS (Figure S9).

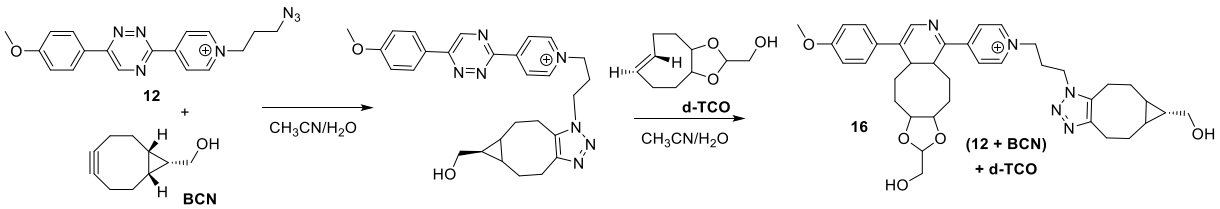


**Scheme S2**. Sequential double click-labeling of **12** using BCN and subsequently d-TCO.

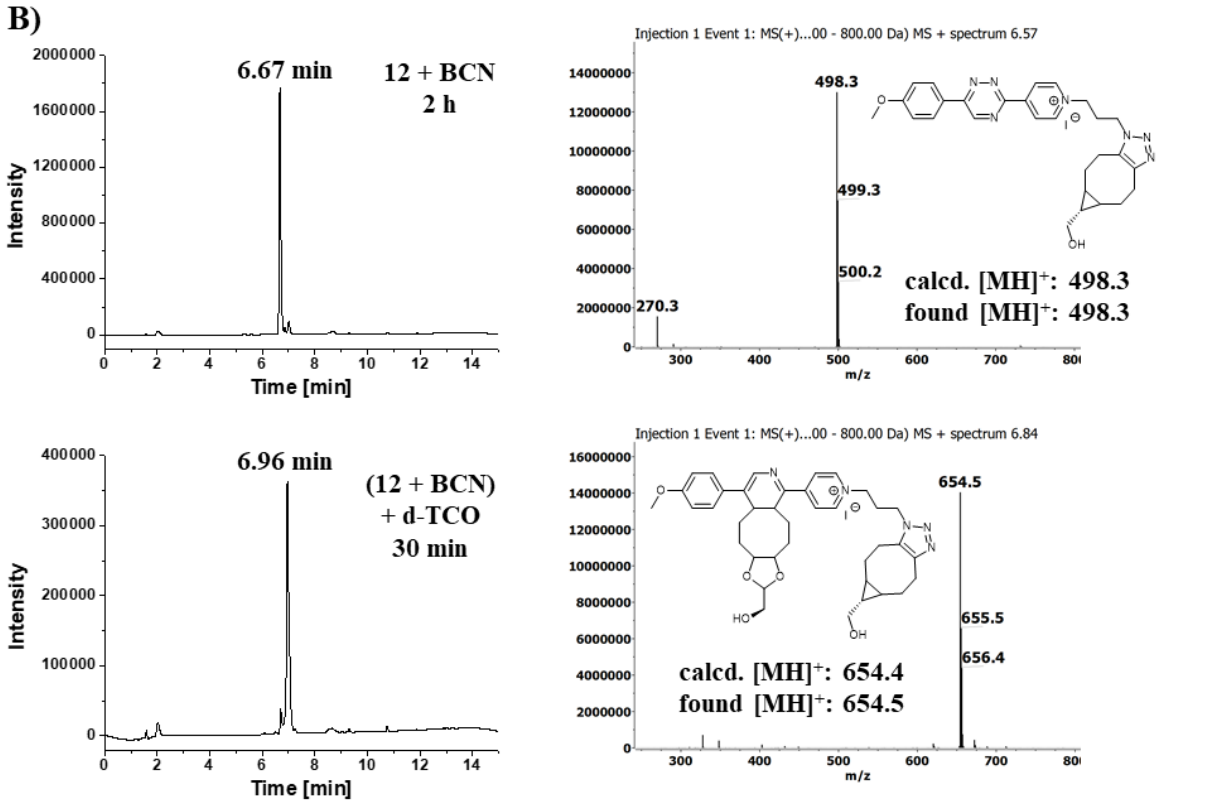


**Figure S9**. HPLC-MS analysis of sequential double click labeling of **12** incubated first with 2.5 eq. of BCN and subsequently with d-TCO (2.5 eq.) in $CH_3CN/H_2O$ (1:1).

**C**) 50 µL of a 4 mM solution of **12** in $CH_3CN/H_2O$ (1:1) were added to a mixture of 12 µL of a 25 mM solution of d-TCO in $CH_3CN/H_2O$ (1:1) and 20 µL of a 25 mM solution of BCN in $CH_3CN/H_2O$ (1:1). The mixture was diluted with $CH_3CN/H_2O$ (1:1) to a final volume of 150 µL. The final concentration of triazine was 1.33 mM using 1.5 eq. of d-TCO and 2.5 eq. of BCN. The mixture was incubated at room temperature for 3 h and monitored by HPLC-MS at 30 min, 1.5 h and 3 h (Figure S10).

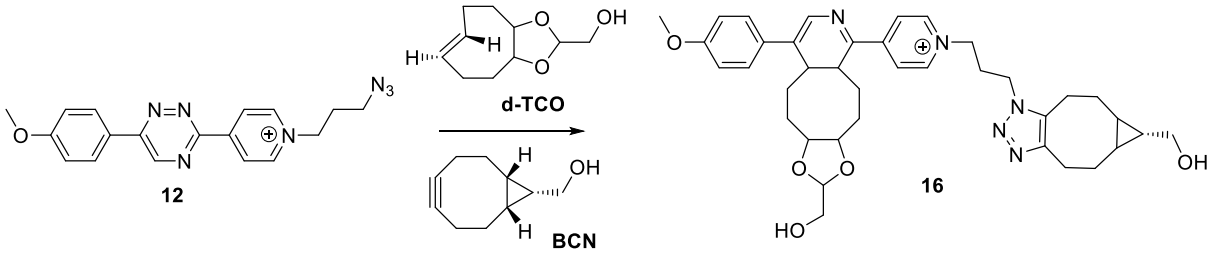


**Scheme S3**. One-pot double click-labeling of **12** using BCN and d-TCO.

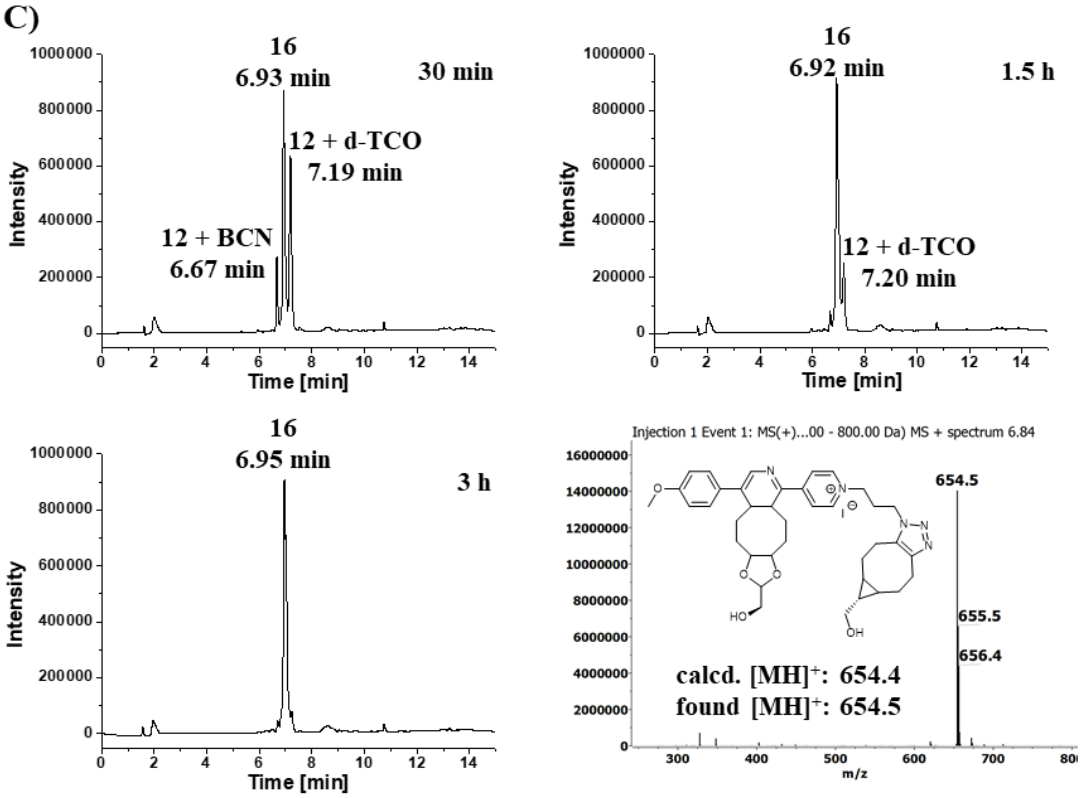


**Figure S10**. HPLC-MS analysis of the single-step double labeling of **12** with BCN (2.5 eq.) and d-TCO (1.5 eq.) in $CH_3CN/H_2O$ (1:1). The analysis shows that both reactions proceed cleanly and selectively on the respective functional groups.

## Synthesis and characterization of the click product 17

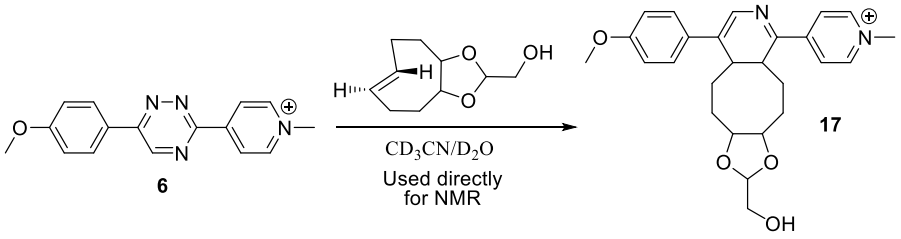


**Scheme S4**. Reaction scheme for the preparation of **17**.

Solution of d-TCO (5.10 mg, 0.0277 mmol) dissolved in $CD_3CN/D_2O$ (1:1) (500 µL) was added to Triazine **6** (7.5 mg, 0.0185 mmol) dissolved in $CD_3CN/D_2O$ (1:1) (500 µL). The mixture was stirred under argon at room temperature for 1 h. Formation of the click product **17** was verified by HPLC-MS and the crude reaction mixture was directly used for characterization by NMR (Figure S11 and S12).

**17** is formed as a mixture of diastereomers (4 in total). Two major diastereomers were assigned based on ROESY experiment. The two minor diastereomers are formed from the anti d-TCO isomer (starting d-TCO was used as an inseparable mixture of syn/anti = 12:1).

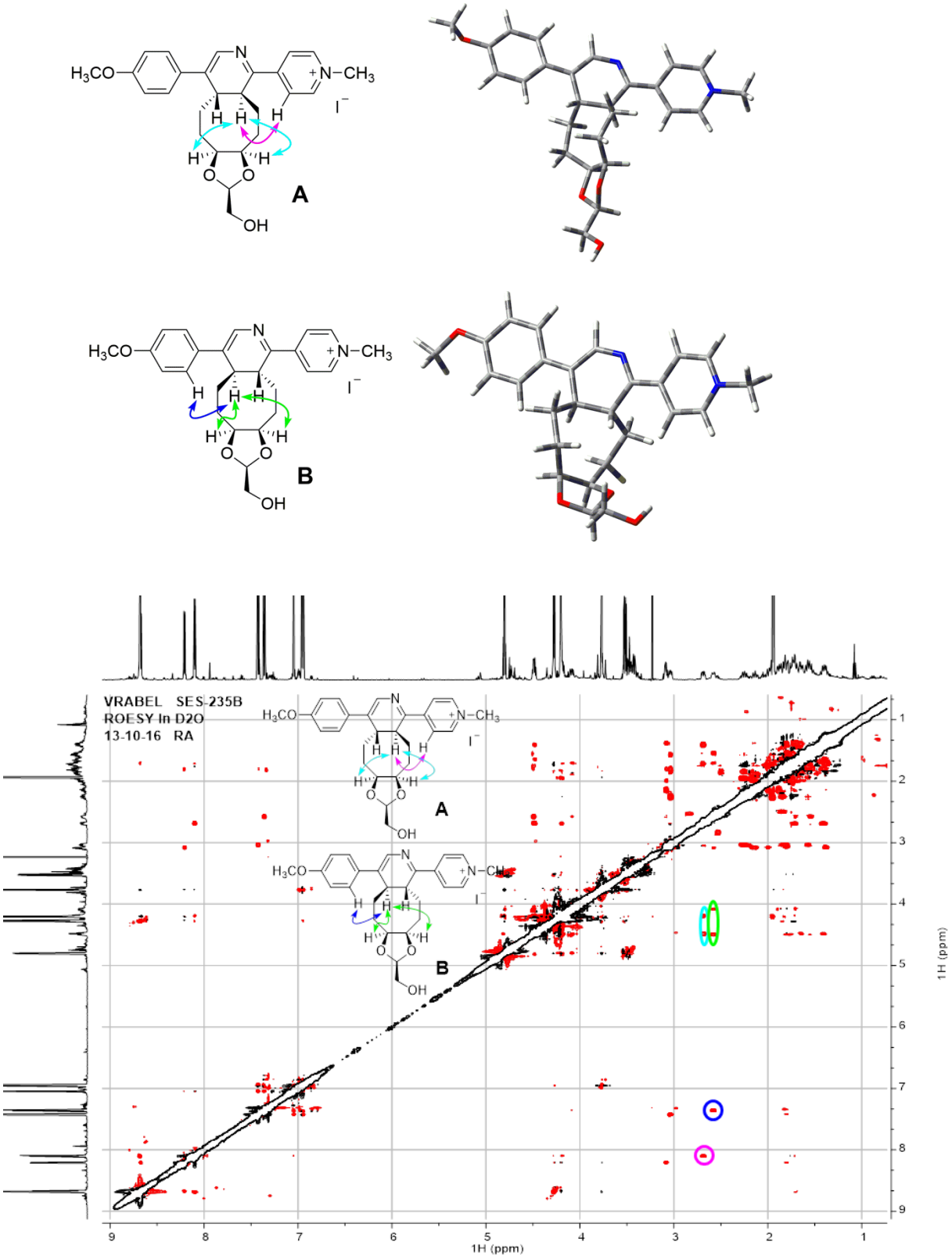


**Figure S11**. Shown are the key H-H interactions used for the assignment of the two major diastereomers formed upon reaction of **6** with d-TCO.

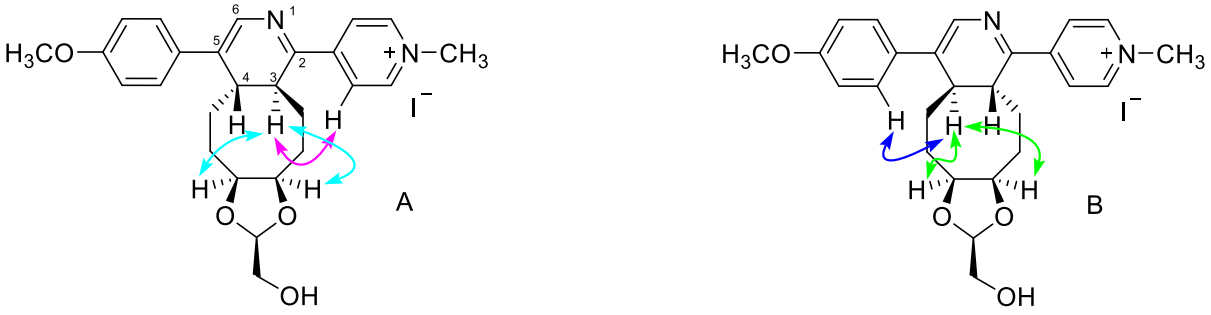


Major NOE signals observed. A mixture of two major diastereoisomers of **17** A:B ~ 5:4.

$^{1}$H NMR (600.1 MHz, $CD_3CN+D_2O$ (1:1 v/v)): 1.34 – 2.30 (m, 16H, OCHC**H$_2$**C**H$_2$**CH-cyclooct-A,B); 2.57 (m, 1H, H-4-B); 2.69 (ddd, 1H, *J* = 13.8, 6.5, 3.4, H-3-A); 3.04 (ddt, 1H, *J* = 8.7, 6.5, 2.0, H-4-A); 3.09 (m, 1H, H-3-B); 3.50, 3.52 (2 × dd, 2 × 1H, *J* = 12.0, 3.4, C**H$_2$**OH-B); 3.52, 3.54 (2 × dd, 2 × 1H, *J* = 12.2, 3.7, C**H$_2$**OH-A); 3.766 (s, 3H, $CH_3O$-A); 3.771 (s, 3H, $CH_3O$-B); 4.09 (m, 1H, OC**H**$CH_2CH_2$CH-cyclooct-B); 4.19 (m, 1H, OC**H**$CH_2CH_2$CH-cyclooct-A); 4.27 (s, 3H, $CH_3N$-B); 4.28 (s, 3H, $CH_3N$-A); 4.46 – 4.51 (m, 2H, OC**H**$CH_2CH_2$CH-cyclooct-A,B); 4.80 (t, 1H, *J* = 3.4, OCHO-B); 4.81 (t, 1H, *J* = 3.7, OCHO-A); 6.95 (m, 2H, H-*m*-$C_6H_4$OMe-A); 6.96 (m, 2H, H-*m*-$C_6H_4$OMe-B); 7.04 (s, 1H, H-6-B); 7.05 (s, 1H, H-6-A); 7.36 (m, 2H, H-*o*-$C_6H_4$OMe-B); 7.43 (m, 2H, H-*o*-$C_6H_4$OMe-A); 8.10 (m, 2H, H-3,5-pyr-A); 8.21 (m, 2H, H-3,5-pyr-B); 8.66 – 8.69 (m, 4H, H-2,6-A,B).

$^{13}$C NMR (150.9 MHz, $CD_3CN+D_2O$ (1:1 v/v)): 22.68 (OCH**C**$H_2CH_2$CH-cyclooct-B); 23.49, 23.74 (OCH**C**$H_2CH_2$CH-cyclooct-A); 24.39 (OCH**C**$H_2CH_2$CH-cyclooct-B); 29.66 (OCHC$H_2$**C**$H_2$CH-cyclooct-A); 30.73, 33.64 (OCHC$H_2$**C**$H_2$CH-cyclooct-B); 34.50 (OCHC$H_2$**C**$H_2$CH-cyclooct-A); 37.05 (CH-4-A); 37.93 (CH-3-B); 38.20 (CH-4-B); 39.28 (CH-3-A); 48.66 ($CH_3N$-B); 48.72 ($CH_3N$-A); 56.16 ($CH_3O$-A); 56.17 ($CH_3O$-B); 62.57 ($CH_2O$-B); 62.89 ($CH_2O$-A);79.77 (O**C**H$CH_2CH_2$CH-cyclooct-A); 80.14 (O**C**H$CH_2CH_2$CH-cyclooct-B); 80.37 (O**C**H$CH_2CH_2$CH-cyclooct-A); 80.62 (O**C**H$CH_2CH_2$CH-cyclooct-B); 101.44 (OCHO-B); 101.45 (OCHO-A); 115.24 (CH-*m*-$C_6H_4$OMe-A); 115.28 (CH-*m*-$C_6H_4$OMe-B); 125.97 (CH-3,5-pyr-B); 126.07 (CH-3,5-pyr-A); 128.82 (CH-*o*-$C_6H_4$OMe-A); 128.87 (CH-*o*-$C_6H_4$OMe-B); 129.77 (CH-6-B); 129.89 (CH-6-A); 130.27 (C-*i*-$C_6H_4$OMe-B); 130.50 (C-*i*-$C_6H_4$OMe-A); 133.34 (C-5-B); 133.64 (C-5-A); 146.22 (CH-2,6-pyr-B); 146.32 (CH-2,6-pyr-A); 153.98 (C-4-pyr-A); 154.10 (C-4-pyr-B); 160.72 (C-*p*-$C_6H_4$OMe-A); 160.77 (C-*p*-$C_6H_4$OMe-B); 161.88 (C-2-B); 161.94 (C-2-A).

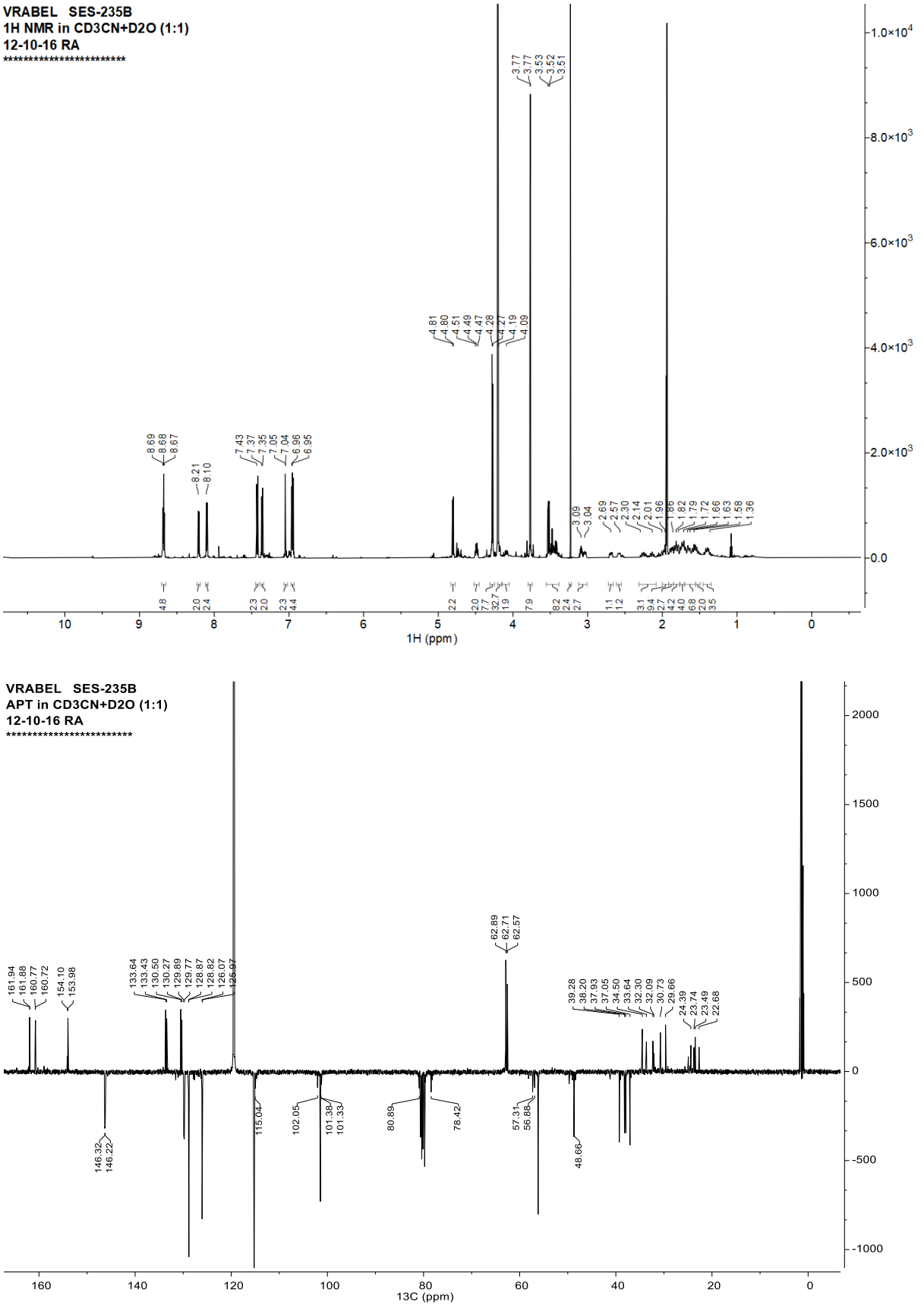


**Figure S12**. $^{1}H$ and $^{13}C$ NMR spectra of the diastereomeric mixture of **17**.

**Formation of the oxidized product 17ox during preparative TLC**

Our attempt to purify the click product **17** by preparative TLC (eluting with $CH_3CN/H_2O$ (4:1) and washing the silica with $CH_3CN/H_2O$ (4:1) + 0.5% HCOOH led to isolation of the corresponding oxidation click product **17ox**. The identity of the oxidized product was confirmed by HPLC-MS (Figure S13) and NMR.

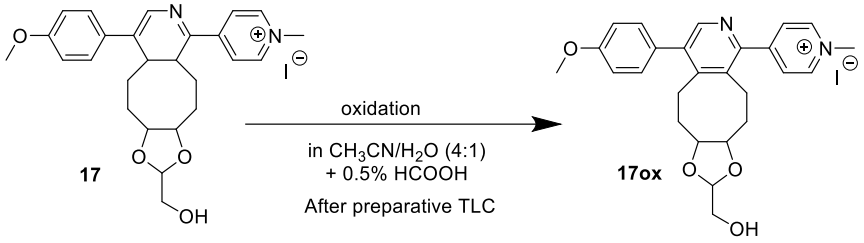


**Scheme S5**. Formation of **17ox** in $CH_3CN/H_2O$ (4:1) + 0.5% HCOOH during purification by preparative TLC.

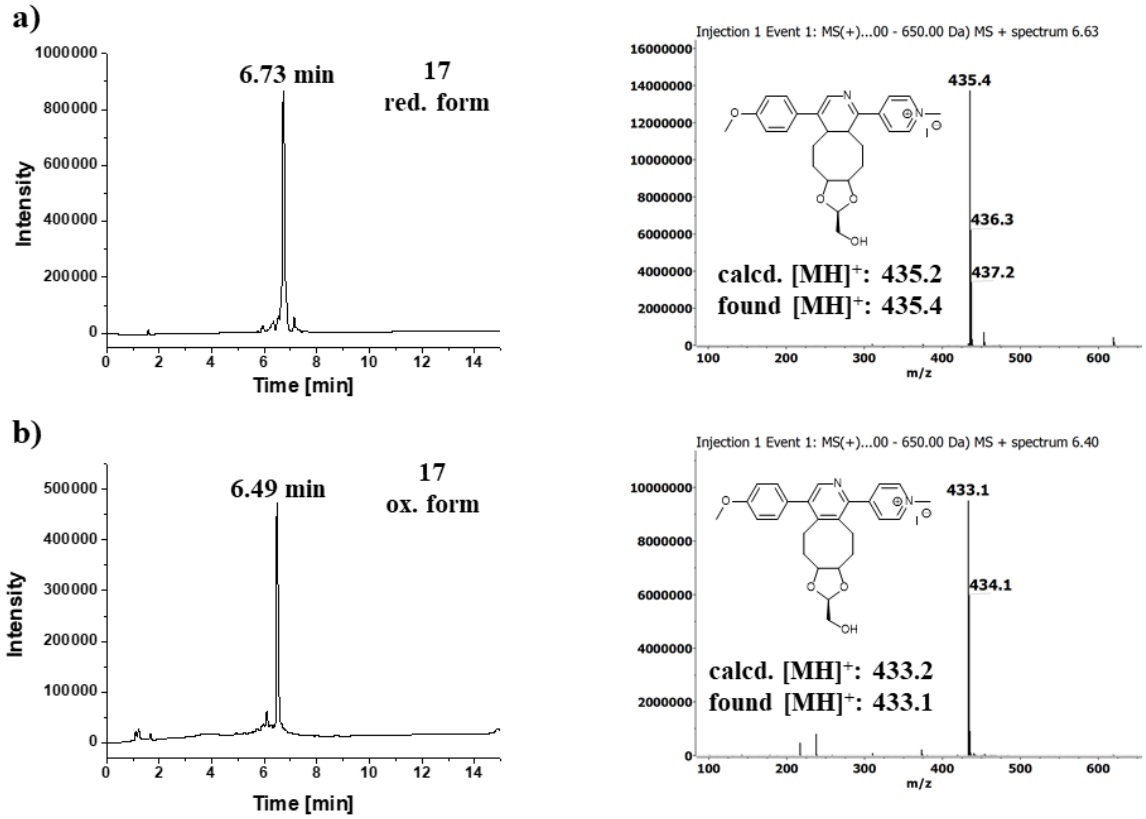


**Figure S13**. HPLC-MS analysis of a) the crude reaction mixture of compound **17** and b) the oxidized form **17ox**. Conditions: Luna® C18 column (3u, 100A, 100 x 4.6 mm) using a linear gradient of $CH_3CN$ + 0.05% HCOOH (5→95% in 9 min) in $H_2O$ + 0.05% HCOOH at a flow rate of 1.0 mL/min

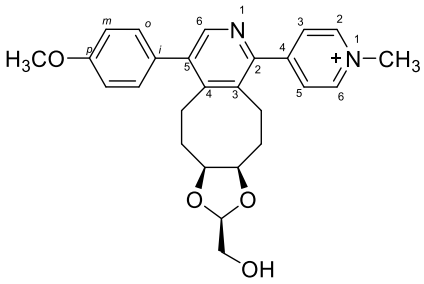

Major diastereomer:

$^{1}$H NMR (500.0 MHz, DMSO-$d_6$): 1.91 – 2.12 (m, 4H, OCHC$H_2$C$H_2$C-cyclooct.); 2.55 – 2.62, 2.78 – 2.87 (2 × m, 2 × 2H, OCHC$H_2$C$H_2$C-cyclooct.); 3.39 (d, 2H, $J$ = 4.0, C$H_2$OH); 3.82 (s, 3H, C$H_3$O); 4.17 – 4.29 (m, 2H, OCHC$H_2$C$H_2$C-cyclooct.); 4.45 (s, 3H, C$H_3$N); 4.75 (t, 1H, $J$ = 4.0, OCHO); 7.10 (m, 2H, H-*m*-$C_6H_4$OMe); 7.29 (m, 2H, H-*o*-$C_6H_4$OMe); 8.18 (d, 2H, $J$ = 5.3, H-3,5-pyr); 8.42 (s, 1H, H-6); 9.16 (d, 1H, $J$ = 5.3, H-2,6-pyr).

$^{13}$C NMR (125.7 MHz, DMSO-$d_6$): 23.47, 23.71 (OCHC$H_2$C$H_2$C-cyclooct.); 30.47 (OCHC$H_2$C$H_2$C-cyclooct.); 47.77 (C$H_3$N); 55.45 (C$H_3$O); 62.60 (C$H_2$OH); 78.20 (br, OCHC$H_2$C$H_2$C-cyclooct.); 102.55 (OCHO); 114.34 (CH-*m*-$C_6H_4$OMe); 127.68 (CH-3,5-pyr); 129.53 (C-*i*-$C_6H_4$OMe); 130.58 (CH-*o*-$C_6H_4$OMe); 136.07 (C-3); 138.03 (C-5); 145.75 (CH-2,6-pyr); 147.92 (CH-6); 150.23 (C-4); 151.72 (C-2); 155.70 (C-4-pyr); 159.27 (C-*p*-$C_6H_4$OMe).

## Stability of the click product 17

The stability studies of the click product **17** were performed in $CH_3CN/H_2O$ (1:1) at room temperature under exposure to air and were monitored by HPLC-MS on a Luna® C18 column (3u, 100A, 100 x 4.6 mm) using a linear gradient of $CH_3CN$ + 0.05% HCOOH (5→95% in 9 min) in $H_2O$ + 0.05% HCOOH at a flow rate of 1.0 mL/min.

0.5 mL of a 10 mM solution of **6** in $CH_3CN/H_2O$ (1:1) were added to 0.3 mL of a 25 mM solution of d-TCO in $CH_3CN/H_2O$ (1:1). The mixture was diluted with $CH_3CN/H_2O$ (1:1) to a final volume of 1 mL in order to get 5 mM final concentration of **6** using 1.5 eq of d-TCO. The solution was stirred at room temperature until starting material has disappeared (5 h, monitored by HPLC-MS, indicated time 0 min in Figure S13). For stability study, the click-product **17** was stirred at room temperature for 97 h in total under exposure to air. During that time the reaction mixture was measured several times by HPLC-MS (Figure S14).

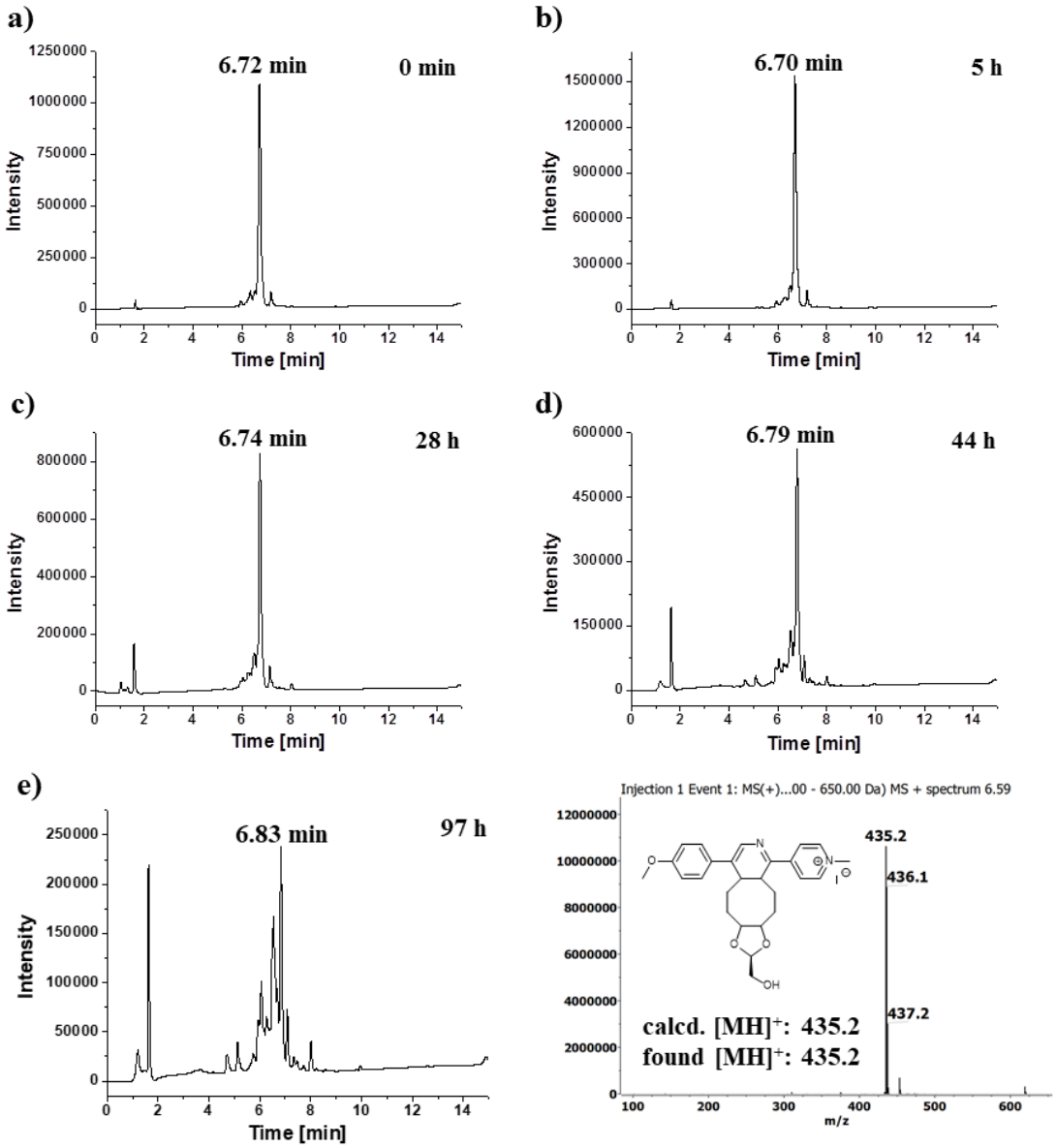


**Figure S14**. HPLC-MS analysis of **17** in $CH_3CN/H_2O$ (1:1) at room temperature under exposure to air after a) 0 min, b) 5 h, c) 28 h, d) 44 h and e) 97 h.

## Photophysical properties of the click product 17

A freshly prepared solution of **17** was used in the following experiments. Conditions: To 50 µL of a solution of **6** in $CH_3CN/H_2O$ (1:1) (stock: 50 mM) were added 50 µL of d-TCO solution in $CH_3CN/H_2O$ (1:1) (stock: 100 mM, 2 equiv.) giving a 25 mM final concentration of **6** and **17** respectively. The reaction mixture was incubated at room temperature in the dark for 0.5 h and then analyzed by HPLC-MS to verify the formation of the click product (Figure S15). This solution was further diluted in different solvents and used as such for absorbance measurements the quantum yield determination measurements (Figure S16-S18).

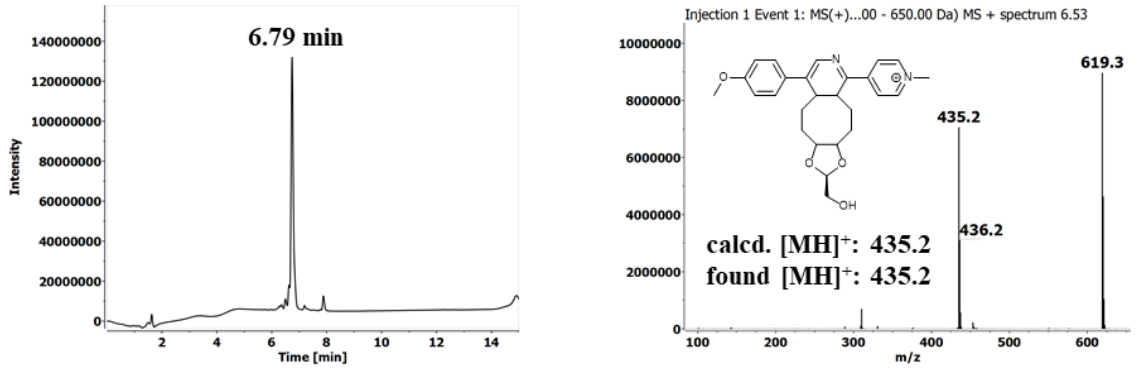


**Figure S15**. HPLC chromatogram of the reaction mixture between **6** and d-TCO showing the formation of **17** after 0.5 h and the corresponding MS spectra. (solvent A: $H_2O$ + 0.05% HCOOH; solvent B: $CH_3CN$ + 0.05% HCOOH; gradient: 5% B → 95% B in 9 min, then 2 min 95% B and back to 5% B). The product eluates at 6.8 min (Luna® C18 column, 3u, 100A, 100 x 4.6 mm, 1 mL/min flow rate).

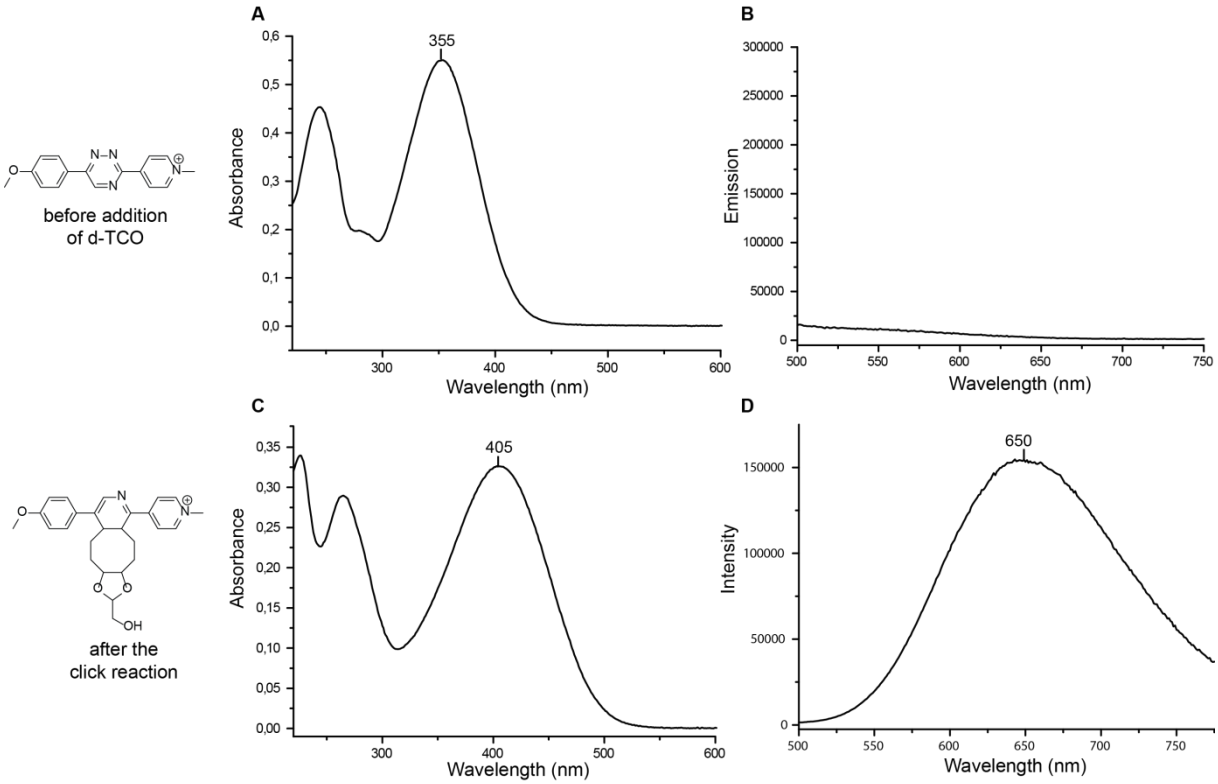


**Figure S16**. Absorption and emission spectra of **6** (A and B respectively) and of the click product **17** (C and D respectively). Measured in 1x PBS buffer (pH 7.4) at room temperature (25 µM for absorbance and 2.5 µM for fluorescence).

Quantum yield of the click product **17** in different solvents was measured at 22°C in 1 cm quartz cuvette using 5µM final concentration of **17**. The experiment was performed on FluoroMax 4 spectrofluorometer (Jobin Yvon, Horiba) equipped with a 450 W xenon lamp using Rhodamine 6G (solution in EtOH) as reference ($\phi_{QS}$ = 0.94). The settings were as follows: Excitation wavelength 405 nm, slit 5.0 nm; Emission 500 – 750 nm, increment 1.0 nm, slit 5.0 nm and data algebra formula S1c/R1c. The fluorescence quantum yields were calculated using the following equation:

$$\phi_{sample} = \phi_{ref} \frac{F_{sample}}{F_{ref}} \times \frac{(1\text{-}10^{-abs})_{ref}}{(1\text{-}10^{-abs})_{sample}} \times \frac{n^2_{sample}}{n^2_{ref}}$$

Where:

$\boldsymbol{\phi_{ref}}$ is 0,94 (Quantum yield of Rhodamine 6G in EtOH)[13]

**F** are the integrated intensities (areas) of standard and the sample fluorescence spectra (integrals calculated using OriginPro software)

**abs** is the absorbance of standard and sample at the excitation wavelength (405 nm)

***n*** are the refractive indices for standard (EtOH: 1.3616) and the sample solution ($CH_3CN$: 1.3441; PBS: 1.3284; MeOH: 1.327; THF: 1.4072; $CHCl_3$: 1.4441)

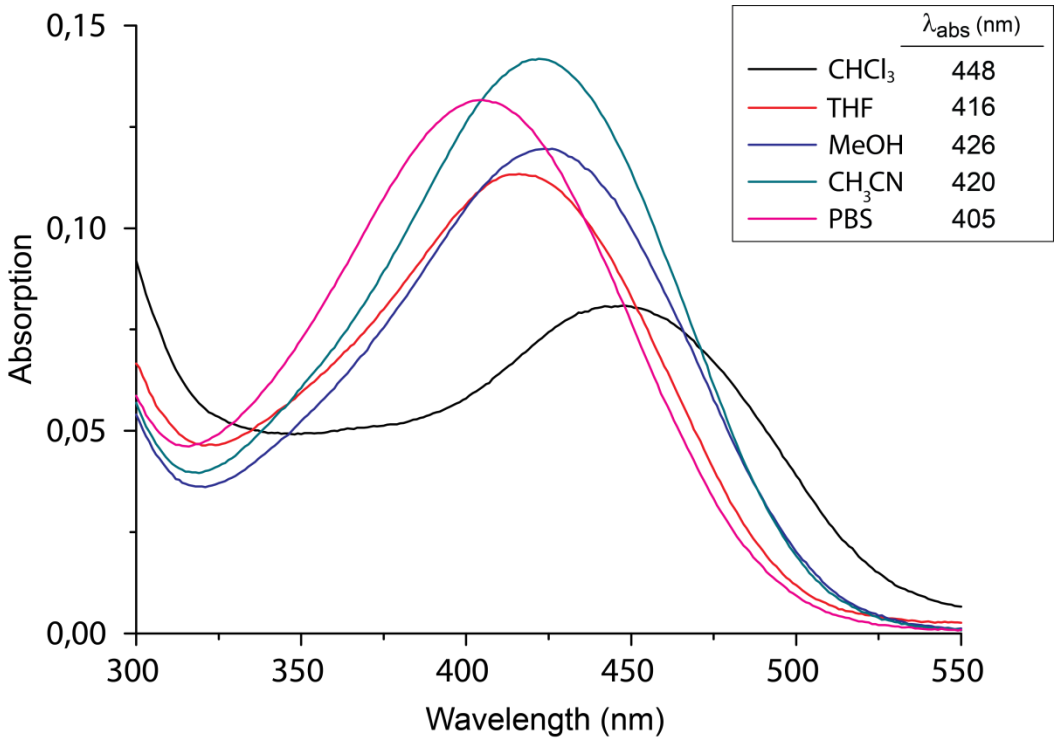


**Figure S17**. Absorption spectra of the click product **17** in different solvents.

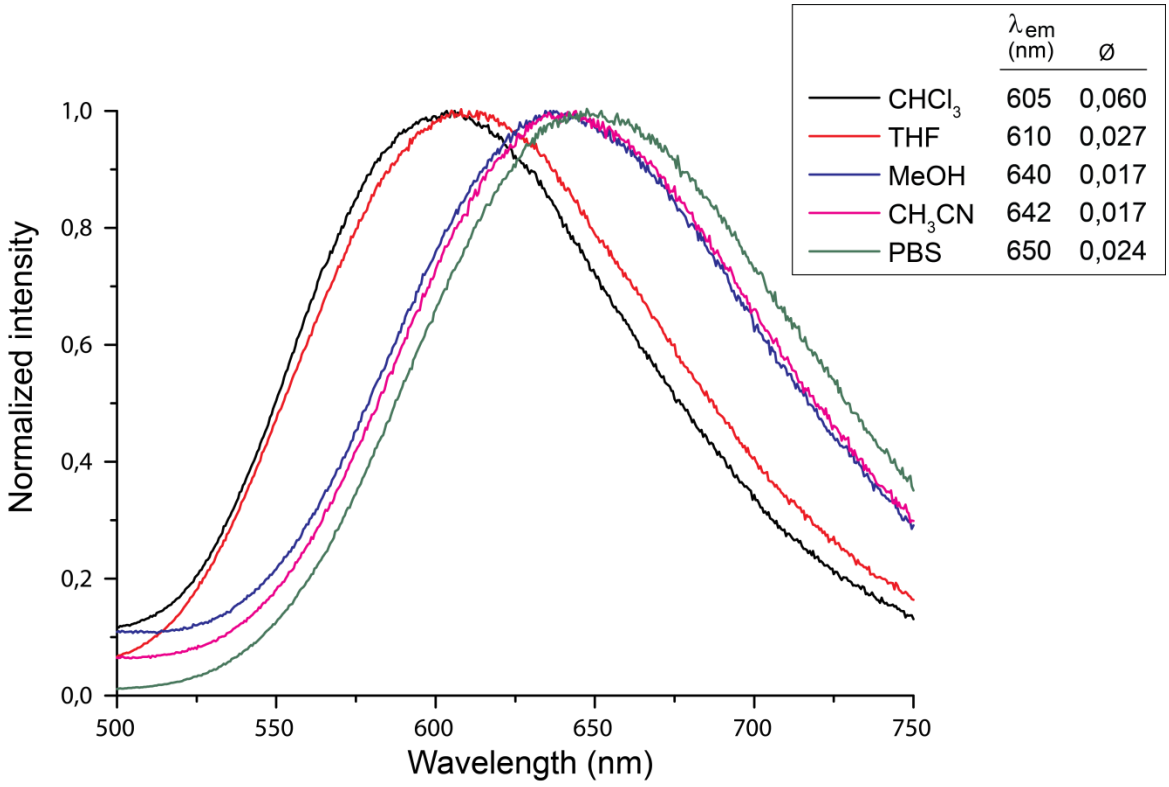


**Figure S18**. Emission spectra and quantum yield of the click product **17** in different solvents.

## Cell labeling experiments

U2OS cells were maintained in high glucose DMEM (*Sigma*) supplemented with 10% FBS (*Biosera*) and antibiotics at 37 °C/5% $CO_2$. One day before experiment cells were seeded at density $0.3x10^6$ at the glass bottom dishes (*SPL Life Sciences* 3.5 cm diameter). Triazine **6** was dissolved in DMSO/$H_2O$ = 1/1 (5 mM) and further diluted before experiments. d-TCO stock solution was in DMSO (50 mM).

Images were acquired on *Zeiss* LSM 780 or Leica TCS SP5 confocal scanning microscopes and raw pictures were processed by *FIJI* software.[14]

Excitation: 405nm, emission window: 525–648 nm for click products). The nucleus was stained with DRAQ5 (excitation: 633 nm, emission window: 667–748 nm).

### Mitochondria labeling in live U2OS cells

U2OS Cells were incubated with 5 µM (final) concentration of **6** in complete media for 3 h/37 °C. Cells were washed once with the media, and incubated for further 30 min in complete DMEM medium without phenol red containing 500 nM DRAQ5 dye (*Thermo Fisher*). The cells were then incubated with d-TCO (25 µM final concentration) for 15 min at 37 °C prior to imaging (Figure S19).

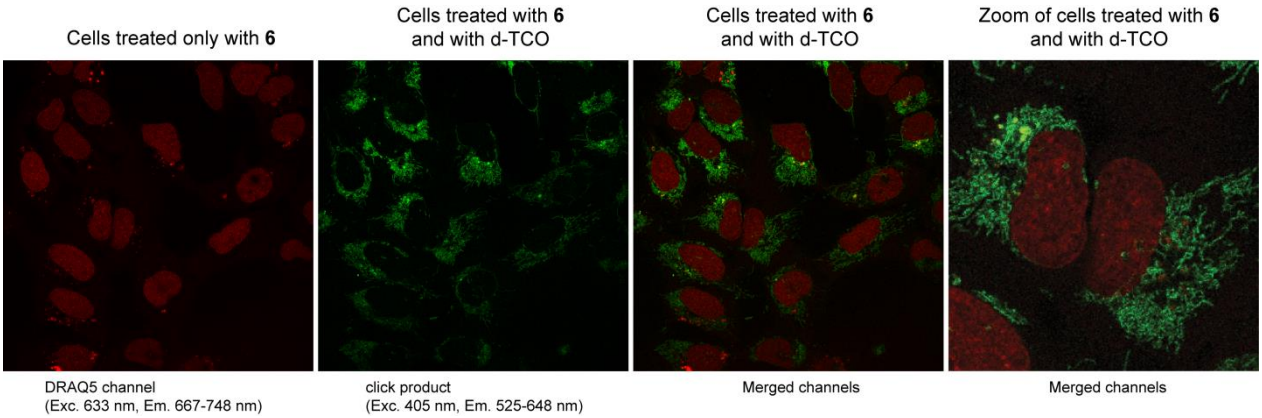


**Figure S19**. U2OS cell labeling experiment using triazine **6** and d-TCO**.**

### Colocalization experiment of 6 + dTCO and Mitotracker green

U2OS Cells were incubated with 25 µM (final) concentration of **6** in complete media for 2 h/37 °C. Cells were washed once with the media, and incubated for 15 min with d-TCO (25 µM final concentration). Then a 100 nM Mitotracker green (*Thermo Fisher*) and 500 nM DRAQ5 (*Thermo Fisher*) solutions were added. The cells were incubated for 10 min at 37 °C, washed several times with DMEM medium, and mounted to the confocal microscope for imaging (Figure S20). The images were acquired sequentially using the following filter set-up: Click product: excitation 405 nm, emission 560-666 nm; Mitotracker green: excitation

496 nm, emission 505-588 nm; DRAQ5 channel: excitation 633 nm, emission 667-748 nm. Laser intensity was set up to 10%.

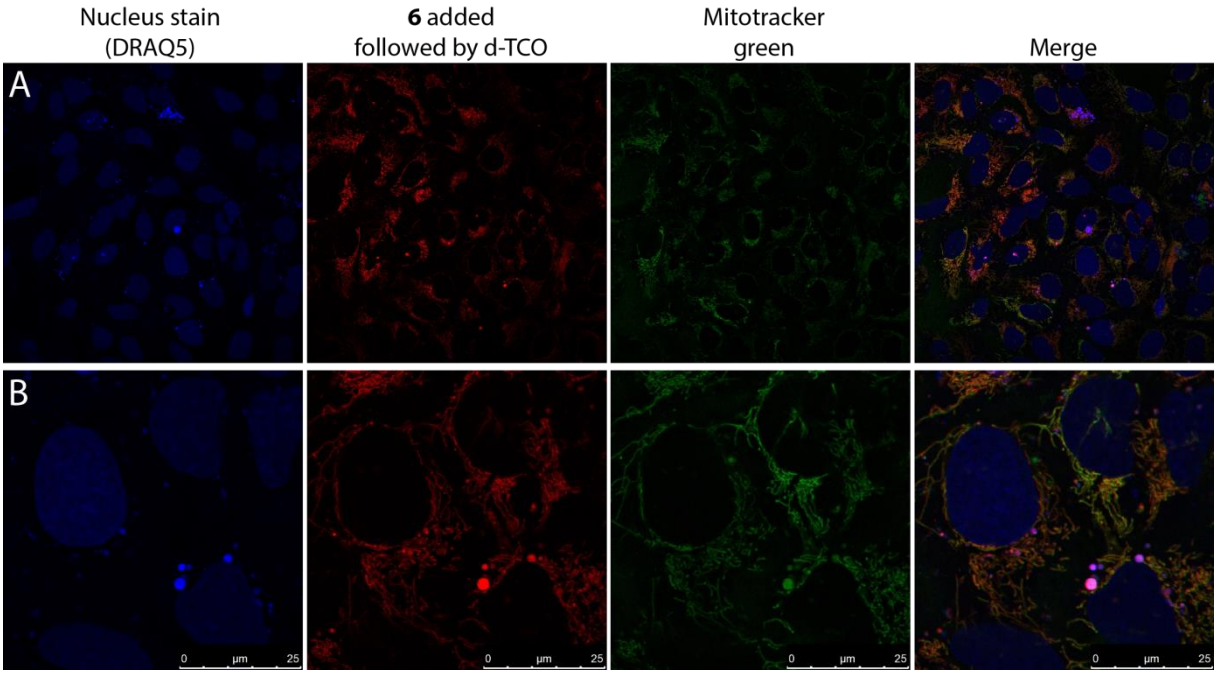


**Figure S20**. Colocalization experiment using U2OS cells treated with triazine **6** (25 µM)**,** d-TCO (25 µM) and with mitotracker green (100 nM)**.** B) is a zoom of pictures A. The experiment confirms that **6** is targeted to mitochondria where it can be labeled with d-TCO. The pictures were processed using LAS AS Lite and FIJI software. Filter set up: Click product: ex. 405 nm, em. 560-666 nm; Mitotracker green: ex. 496 nm, em. 505-588 nm. DRAQ5 channel: ex. 633 nm, em. 667-748 nm.

## Preparation of concanavalin A d-TCO conjugate (ConA-dTCO)

2.5 mg of Concanavalin A (*Sigma* #C2010) were dissolved in 1 ml of 150 mM NaCl, 50 mM HEPES pH 8.3 (to obtain a 2.5 mg/ml solution). 250 µL (0.625 mg) of this solution were combined with 3.6 µL of 100 mM d-TCO NHS active ester (10x molar excess dissolved in dry DMSO). The reaction mixture was incubated at room temperature for one hour with constant shaking. After one hour precipitated material was spun at 25000 rpm for 10 min. Clean supernatant was split and 2x 130 µL was loaded onto two Zeba desalting columns preconditioned with 150 mM NaCl, 50 mM TRIS pH 7.4 (in total 2 columns were used).
Note: The d-TCO active ester partially precipitated when added to ConA but after one hour the solution became clear again.

## ConA-dTCO Experiment 1 on live cells

Live U2OS cells were incubated for 10 min with ConA-dTCO (100x diluted) in Dulbeccos PBS (DPBS, with $Ca^{2+}$ and $Mg^{2+}$). After washing with DPBS cells were incubated with 50 µM **6** in DPBS with 500 nM DRAQ5 for 15 min. Pictures of living cells were taken at

405 nm excitation. Emission was collected at 525-648 nm. DRAQ channel: Exc. 633 nm, Em. 667-748 nm (Figure S21).

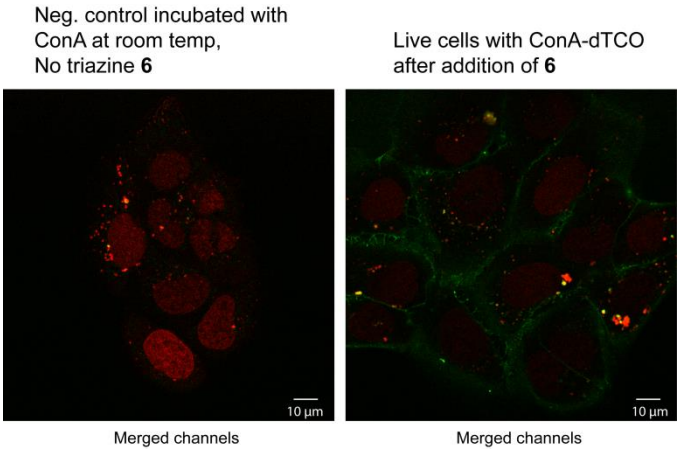


**Figure S21**. U2OS live cell labeling experiment using ConA-dTCO conjugate and triazine **6**. Only weak signal has been observed when the experiment was performed on live cells.

## ConA-dTCO Experiment 2

Live U2OS cells were incubated for 10 min with ConA-dTCO (100x diluted) in Dulbeccos PBS (DPBS, with $Ca^{2+}$ and $Mg^{2+}$). After fixation with 4% formaldehyde for 10 min and permeabilization with 0.1% Triton X100 in PBS for another 10 min cells were washed with DPBS and incubated with 50 µM **6** in PBST and with 500 nM DRAQ5 for 15 min. Pictures of fixed cells were taken at 405 nm excitation. Emission was collected at 525-648 nm. DRAQ channel: Exc. 633 nm, Em. 667-748 nm (Figure S22).

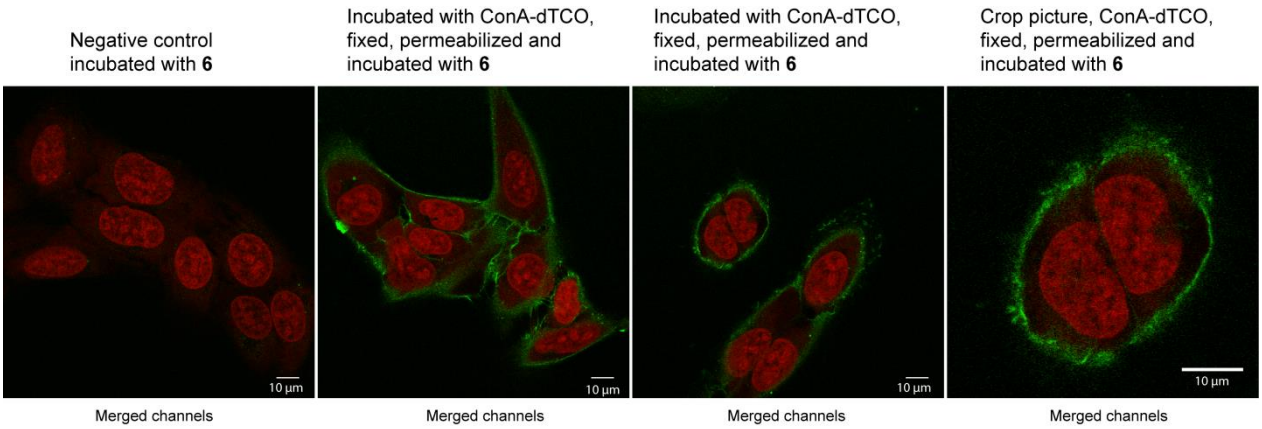


**Figure S22**. U2OS cell membrane labeling experiment using ConA-dTCO conjugate and triazine **6**.

## ConA-dTCO Experiment 3

U2OS cells were fixed with 4% formaldehyde for 10 min. After permeabilization with 0.1% Triton X100 in PBS cells and 3x washing with PBS 0.05% TWEEN20 (PBST) cells were incubated for 10 min with ConA-dTCO (100x diluted) in PBST. After washing 3x with PBST cells were incubated with 50 µM **6** in PBST containing 500 nM DRAQ5 for 15 min. Pictures

of fixed cells were taken at 405 nm or 458 nm excitation. Emission was collected at 525-648 nm. DRAQ5 channel: Exc. 633 nm, Em. 667-748 nm (Figure S23).

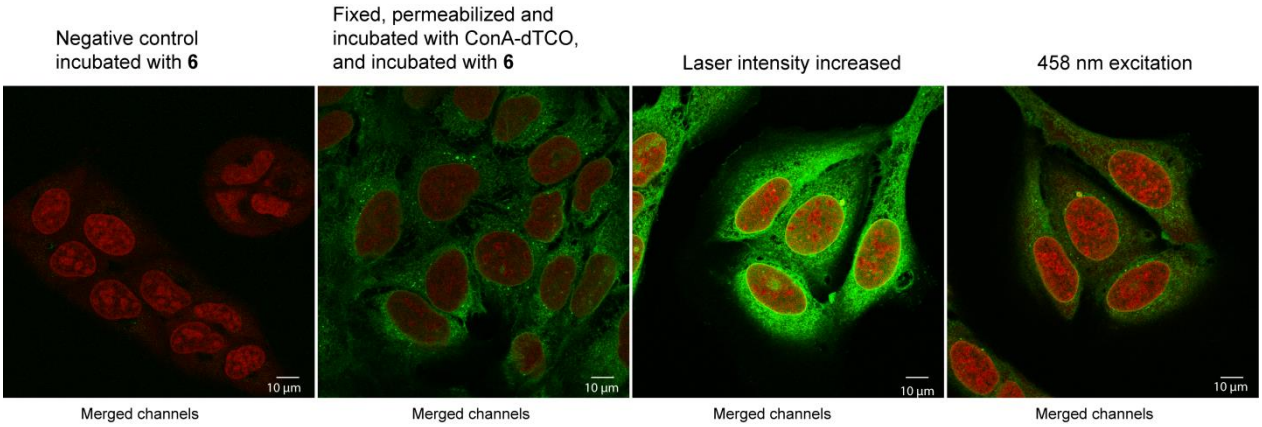


**Figure S23**. Fixed and permeabilized U2OS cell labeling experiment using ConA-dTCO conjugate and triazine **6**.

# References


[1] M. Royzen, G. P. Yap, J. M. Fox, *J. Am. Chem. Soc.* **2008**, *130*, 3760-3761.

[2] A. Darko, S. Wallace, O. Dmitrenko, M. M. Machovina, R. A. Mehl, J. W. Chin, J. M. Fox, *Chem. Sci.* **2014**, *5*, 3770-3776.

[3] M. T. Taylor, M. L. Blackman, O. Dmitrenko, J. M. Fox, *J. Am. Chem. Soc.* **2011**, *133*, 9646-9649.

[4] *according to Patent: WO2004/85408 A1, 2004*.

[5] *according to Patent: WO2006/033551 A1, 2006*.

[6] V. N. Kozhevnikov, O. V. Shabunina, D. S. Kopchuk, M. M. Ustinova, B. König, D. N. Kozhevnikov, *Tetrahedron* **2008**, *64*, 8963-8973.

[7] N. T. Coogan, M. A. Chimes, J. Raftery, P. Mocilac, M. A. Denecke, *J. Org. Chem.* **2015**, *80*, 8684-8693.

[8] J. Cabal, F. Hampl, F. Liska, J. Patocka, F. Riedl, K. Sevcikova, *Collect. Czech. Chem. Commun.* **1998**, *63*, 1021-1030.

[9] *according to Patent: US2011/212967 A1, 2011*.

[10] D. N. Kamber, Y. Liang, R. J. Blizzard, F. Liu, R. A. Mehl, K. N. Houk, J. A. Prescher, *J. Am. Chem. Soc.* **2015**, *137*, 8388-8391.

[11] P. C. Conrad, P. L. Kwiatkowski, P. L. Fuchs, *J. Org. Chem.* **1987**, *52*, 586-591.

[12] W. Wang, S. Hong, A. Tran, H. Jiang, R. Triano, Y. Liu, X. Chen, P. Wu, *Chem. Asian J.* **2011**, *6*, 2796-2802.

[13] D. F. Eaton, *J. Photochem. Photobiol. B* **1988**, *2*, 523-531.

[14] J. Schindelin, I. Arganda-Carreras, E. Frise, V. Kaynig, M. Longair, T. Pietzsch, S. Preibisch, C. Rueden, S. Saalfeld, B. Schmid, J. Y. Tinevez, D. J. White, V. Hartenstein, K. Eliceiri, P. Tomancak, A. Cardona, *Nat. Methods* **2012**, *9*, 676-682.

## 7.5 Supplementary information to chapter 3.5

S.J. Siegl, M. Vrabel, *Eur. J. Org. Chem.* **2018**, 5081–5085.

"Probing the Scope of the Amidine–1,2,3-triazine Cycloaddition as a Prospective Click Ligation Method".

The corresponding NMR spectra are not presented here and can be found in the original publication.

*Eur. J. Org. Chem.* · ISSN 1099–0690

https://doi.org/10.1002/ejoc.201800530

## ***SUPPORTING INFORMATION***

***Title:*** Probing the Scope of the Amidine–1,2,3-triazine Cycloaddition as a Prospective Click Ligation Method

***Author(s):*** Sebastian J. Siegl, Milan Vrabel*

# Content

## General information

The chemicals were obtained from *Sigma Aldrich*, *Alfa Aesar*, *Acros Organics*, *ABCR* or *VWR* and were used without further purification. $CH_3CN$ used for click reactions was of HPLC grade from *VWR*.
Solutions were concentrated on a rotary evaporator from *Heidolph* equipped with a PC3001 VARIOpro pump from *Vacuubrand*. Column chromatography was carried out on silica gel 60A (particle size: 40-60 µm) from *Acros Organics*. Solvents in the p.a. quality from *Lach-Ner* and *Penta* were distilled and used for elution. Mixtures of solvents are each stated as volume fractions. For flash column chromatography a Combi*Flash*® Rf+ from *Teledyne ISCO* was used. Thin-layer chromatography was performed on aluminum sheets from *Merck* (silica gel 60 F254, 20 × 20 cm). Chromatograms were visualized by UV light (λ = 254 nm). $^{1}$H- and $^{13}$C-NMR spectra were measured on a Bruker Avance III™ HD 400 MHz NMR system equipped with Prodigy cryo-probe or on a Bruker Avance III™ HD 500 MHz Cryo. $CD_3OD$ from *Sigma Aldrich* or *Eurisotop* was used as solvent. Chemical shifts δ are quoted in ppm in relation to the chemical shift of the residual non-deuterated solvent peak ($CD_3OD$: $\delta(^{1}H) = 3.31$, $\delta(^{13}C) = 49.0$). High-resolution mass spectra were recorded on an *Agilent* 5975C MSD Quadrupol, Q-Tof micro from *Waters* or LTQ Orbitrap XL from *Thermo Fisher Scientific*. HPLC-MS measurements were performed on an LCMS-2020 system from *Shimadzu* equipped with a Luna® C18(2) column (3µm, 100A, 100 × 4.6 mm). UV/VIS spectroscopy was performed on a Cary 60 UV/Vis spectrophotometer from *Agilent Technologies*. Data from kinetic experiments were processed using OriginPro 9.1 software.

## Synthetic procedures

The following compounds were prepared according to literature procedures.

***trans*-Cyclooct-4-enol**[1] **(pure axial isomer was used in this study)**

**3-(2-Pyridyl)-6-phenyl-1,2,4-triazine**[2]

**6-(4-Nitrophenyl)-1,2,4-triazine**[3]

## Optimization of click conditions for the reaction between acetamidine and 5-phenyl-1,2,3-triazine

Small test reactions were performed to determine the best conditions for the click reaction between acetamidine and 5-phenyl-1,2,3-triazine. For these test reactions, a 20 mM solution of 5-phenyl-1,2,3-triazine was mixed at a ratio of 1:1 with a 40 mM solution of acetamidine hydrochloride containing 2 eq. of a base (TMG, TBD, DBU or Proton Sponge). The solutions containing acetamidine hydrochloride and the base were incubated at room temperature for

20 min before mixing with the 5-phenyl-1,2,3-triazine to form the amidine free base. The reactions were performed either in $CH_3CN$ (HPLC grade) or in $CH_3CN/H_2O$ 1:1. The reaction mixtures were incubated at room temperature or at 37 °C and the progress of the reaction was monitored by HPLC-MS analysis at indicated time points (Figure S1). The samples for HPLC-MS measurements were diluted at a ratio of 1:4 with $CH_3CN$. Exact conditions for the test reactions and results from the HPLC-MS measurements are summarized in Table S1.

**Table S1.** Tested conditions and results for the optimization of the click reaction between 5-phenyl-1,2,3-triazine and acetamidine[a].

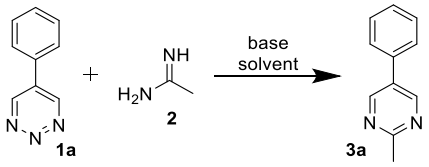


| entry | base | solvent | temperature | results[b] | products[b] |
|---|---|---|---|---|---|
| 1 | TMG | $CH_3CN$ | r.t. | product;<br>traces of side product<br>(presumably from<br>cycloaddition between TMG<br>and 1,2,3-triazine) | 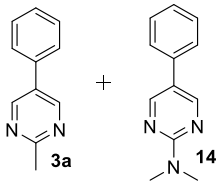 <br>major minor |
| 2 | TBD | $CH_3CN$ | r.t. | only traces of product;<br>mostly unidentified side<br>product;<br>starting material consumed | 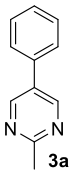 + unidentified side product 15<br>traces major |
| 3 | DBU | $CH_3CN$ | r.t. | product;<br>no side products | 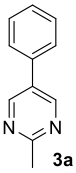 |
| 4 | proton<br>sponge | $CH_3CN$ | r.t. | only traces of product;<br>mostly remaining starting<br>material | 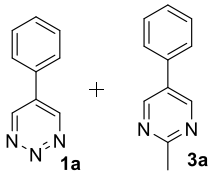 <br>major traces |
| 5 | DBU | $CH_3CN$ | 37 °C | product;<br>no side products;<br>slightly faster than at r.t. | 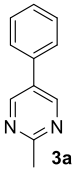 |

| | | | | | |
|---|---|---|---|---|---|
| 6 | DBU | $CH_3CN/H_2O$ 1:1 | r.t. | only traces of product; mostly side product (see Figure S2 and Scheme S1) | side products **16** and **17** major + 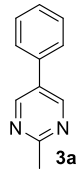 **3a** traces |
| 7 | TMG | $CH_3CN/H_2O$ 1:1 | r.t. | only traces of product; mostly side product (see Figure S2 and Scheme S1) | side products **16** and **17** major + 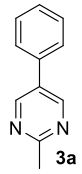 **3a** traces |

a) all reactions were performed using 2 eq. of acetamidine and 4 eq. of base. b) judged from the observed HPLC-MS spectra.

## HPLC chromatograms and low-resolution mass spectra of the optimization test reactions

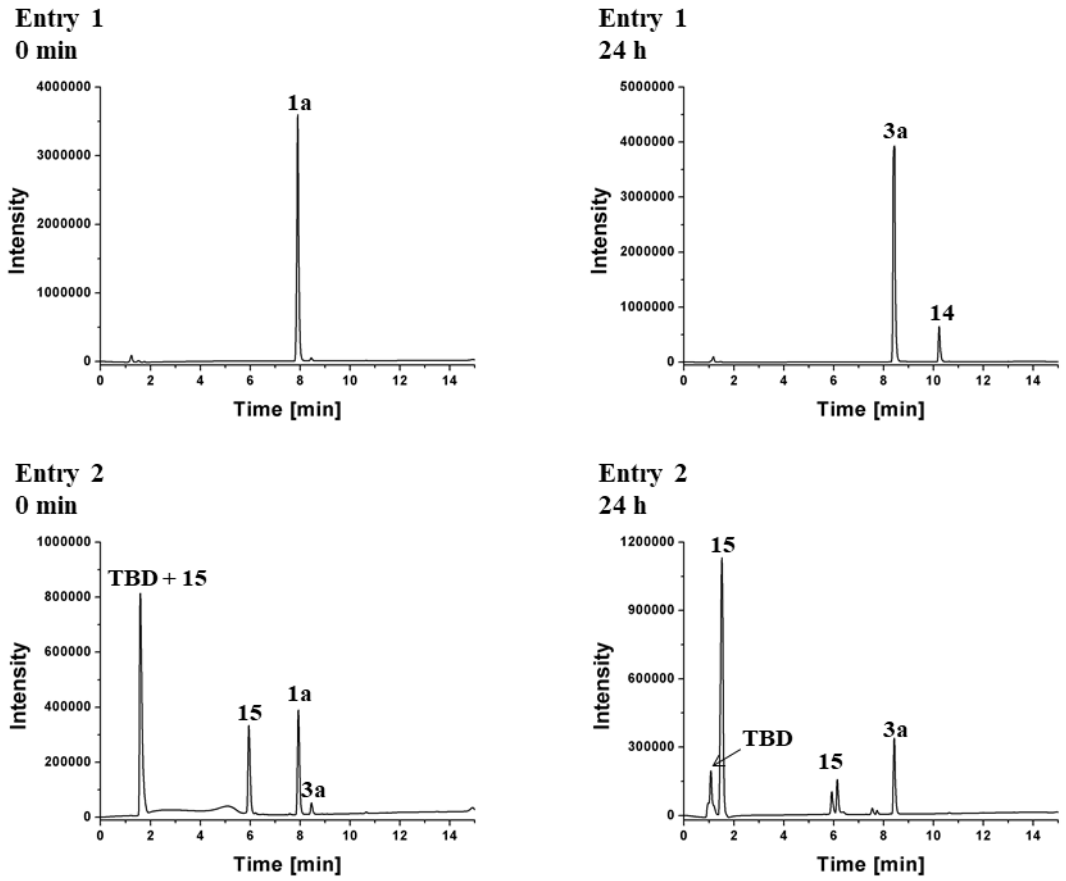

**Entry 3**
**0 min**

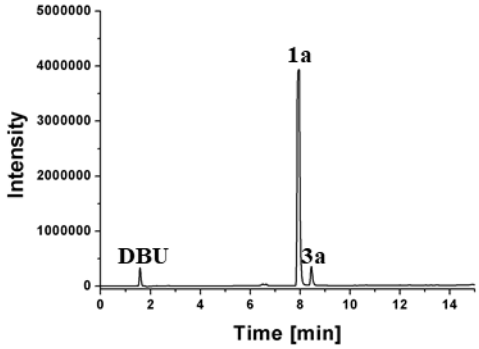


**Entry 3**
**24 h**

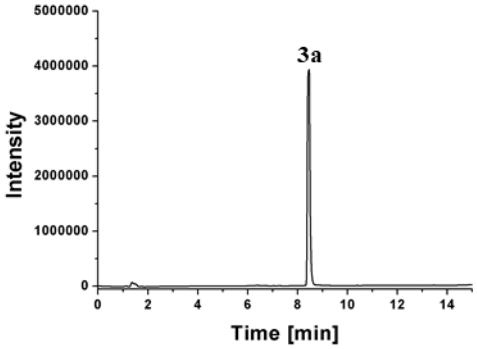


**Entry 4**
**0 min**

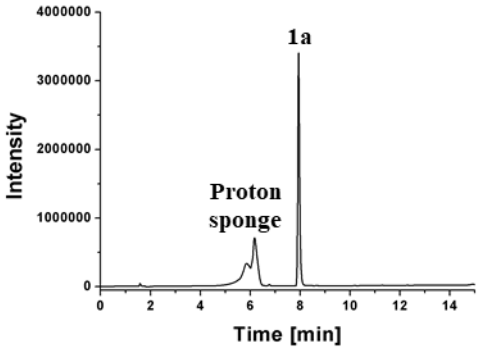


**Entry 4**
**24 h**

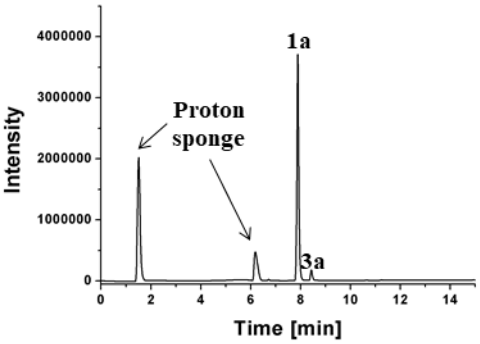


**Entry 5**
**0 min**

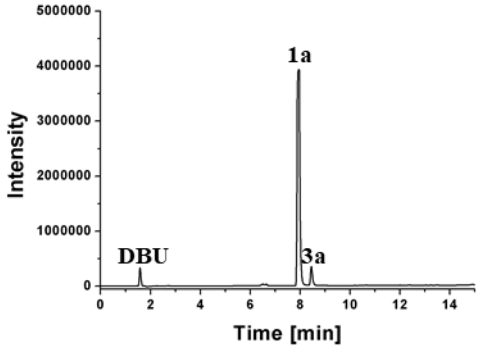


**Entry 5**
**8 h**

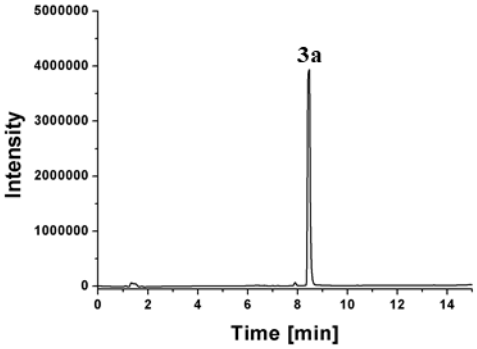


**Entry 6**
**0 min**

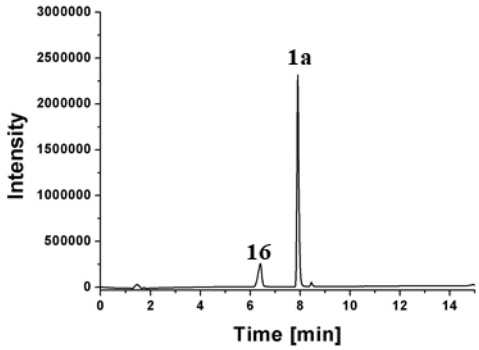


**Entry 6**
**5 h**

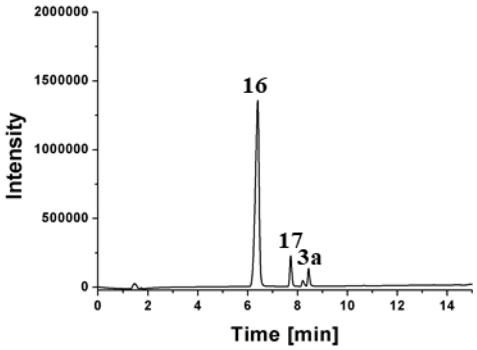

**Entry 7**
**0 min**

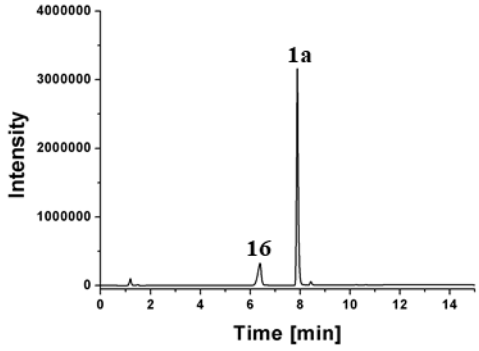


**Entry 7**
**5 h**

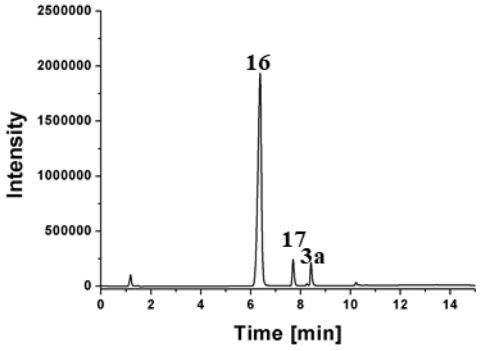


**1a**

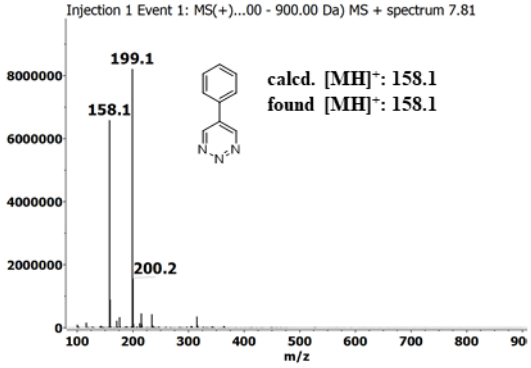


**3a**

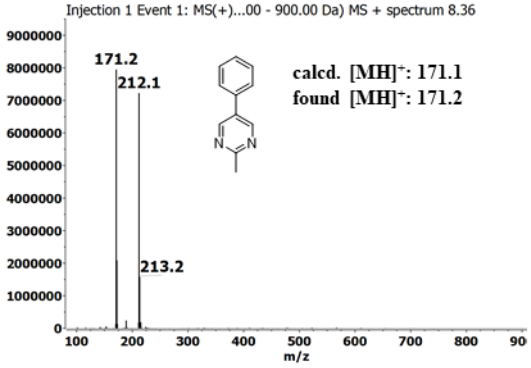


**TBD**

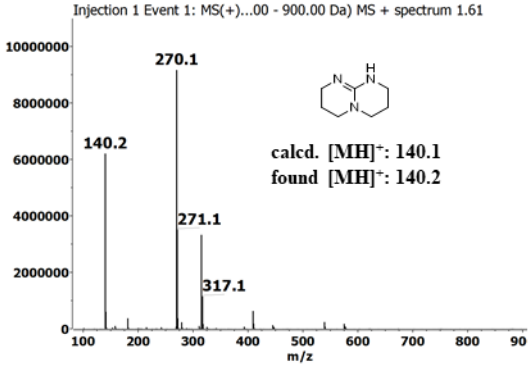


**DBU**

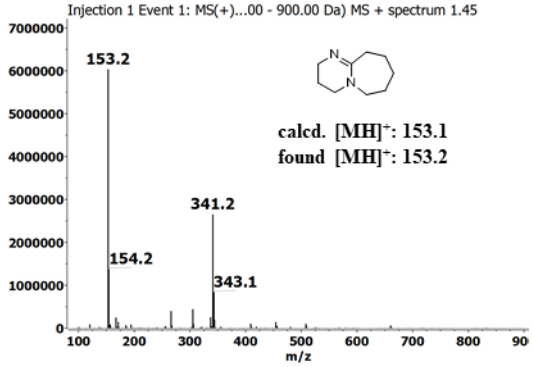


**Proton sponge**

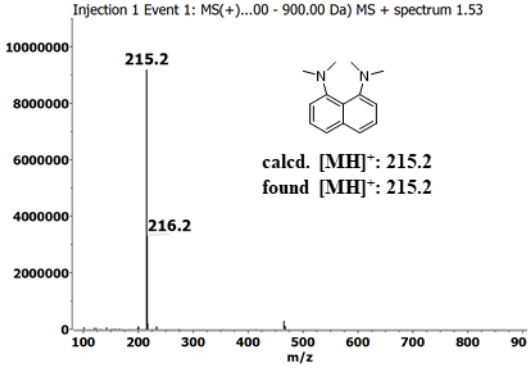


**14**

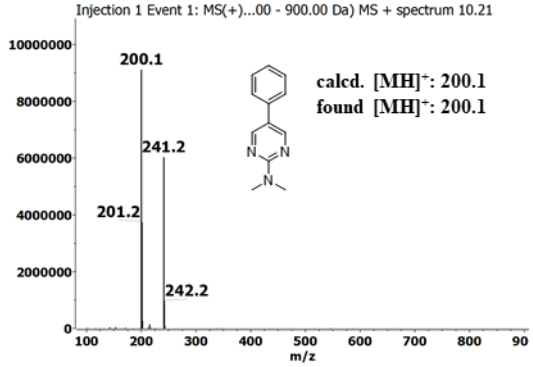

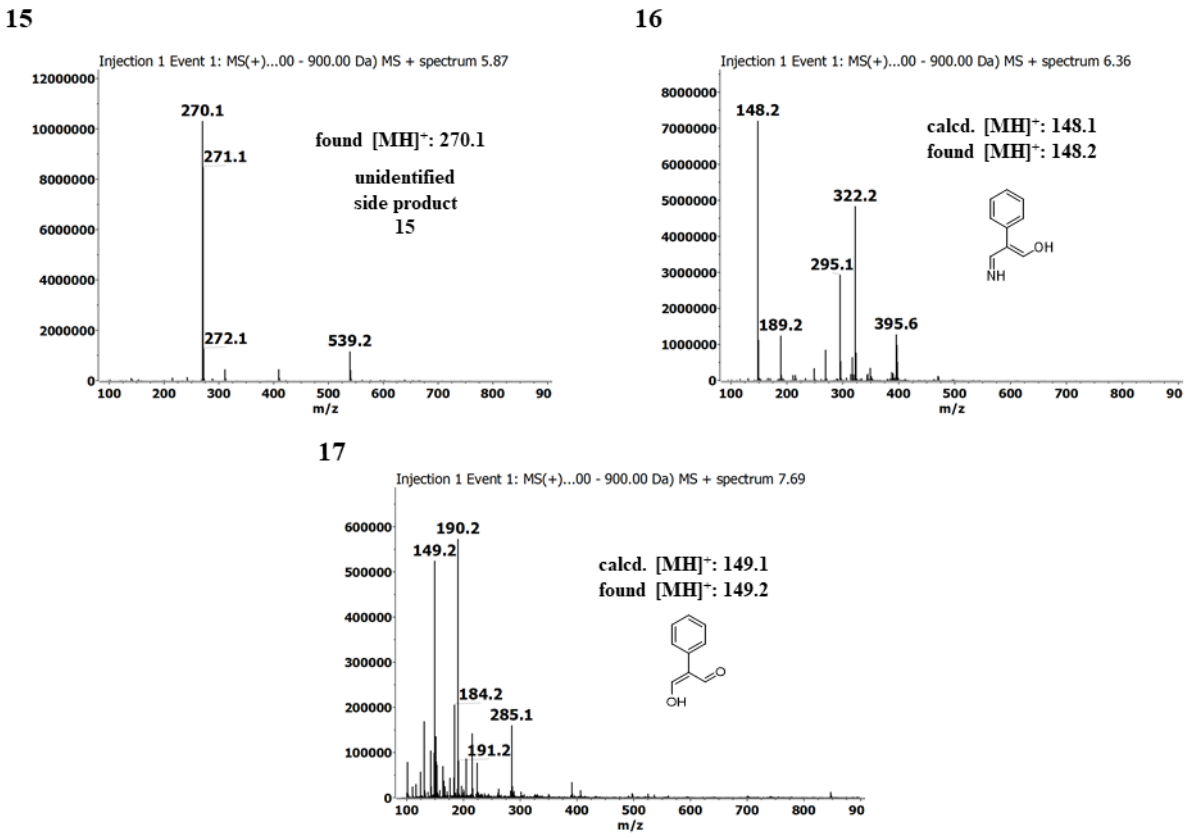


**Figure S1.** HPLC chromatograms (up) and corresponding low-resolution mass spectra (below) of the optimization reactions between 5-phenyl-1,2,3-triazine and acetamidine using 2 eq. of acetamidine and 4 eq. of base. Please note that peaks in the MS spectra with a mass of the product + 41 are artefacts arising from the adduct of $CH_3CN$ which is used as eluent in the HPLC experiments (solvent A: $H_2O$ + 0.05% HCOOH; solvent B: $CH_3CN$ + 0.05% HCOOH; gradient: 5% B → 95% B in 9 min, then 95% B for 2 min and back to 5% B; column: Luna® C18(2) column (3µm, 100A, 100 × 4.6 mm) at a flow rate of 1 mL/min).

Additionally, test reactions in absence of the amidine were performed to determine the origin of the side product arising in aqueous solutions. A 10 mM solution of 5-phenyl-1,2,3-triazine either in $CH_3CN$ or in $CH_3CN/H_2O$ 1:1 containing 4 eq. of a base (TMG or DBU) was incubated at room temperature and measured on HPLC-MS at indicated time points (Figure S2). The samples for HPLC-MS measurements were diluted at a ratio of 1:4 with $CH_3CN$. Exact conditions for the test reactions and results from the HPLC-MS measurements are summarized in Table S2. For a proposed mechanism leading to the observed side products **16** and **17** in aqueous solutions see Scheme S1.

**Table S2.** Tested conditions and results of the test reactions with 5-phenyl-1,2,3-triazine in absence of an amidine[a].

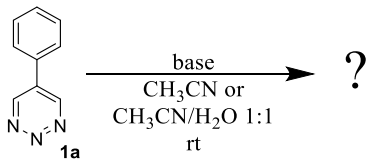


| entry | base | solvent | results[b] | products[b] |
|---|---|---|---|---|
| 1 | without base | $CH_3CN/H_2O$ 1:1 | only remaining starting material; no products | 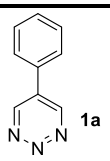 |
| 2 | DBU | $CH_3CN$ | only remaining starting material; no products | 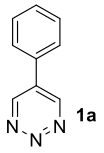 |
| 3 | DBU | $CH_3CN/H_2O$ 1:1 | starting material consumed; side product | 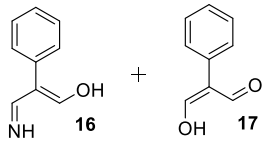 |
| 4 | TMG | $CH_3CN$ | only remaining starting material; no products | 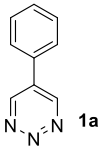 |
| 5 | TMG | $CH_3CN/H_2O$ 1:1 | starting material consumed; side product | 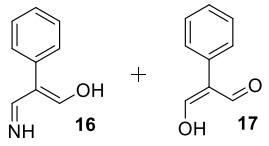 |

a) all reactions were performed at room temperature in absence of the amidine using 4 eq. of base. b) judged from the observed HPLC-MS spectra.

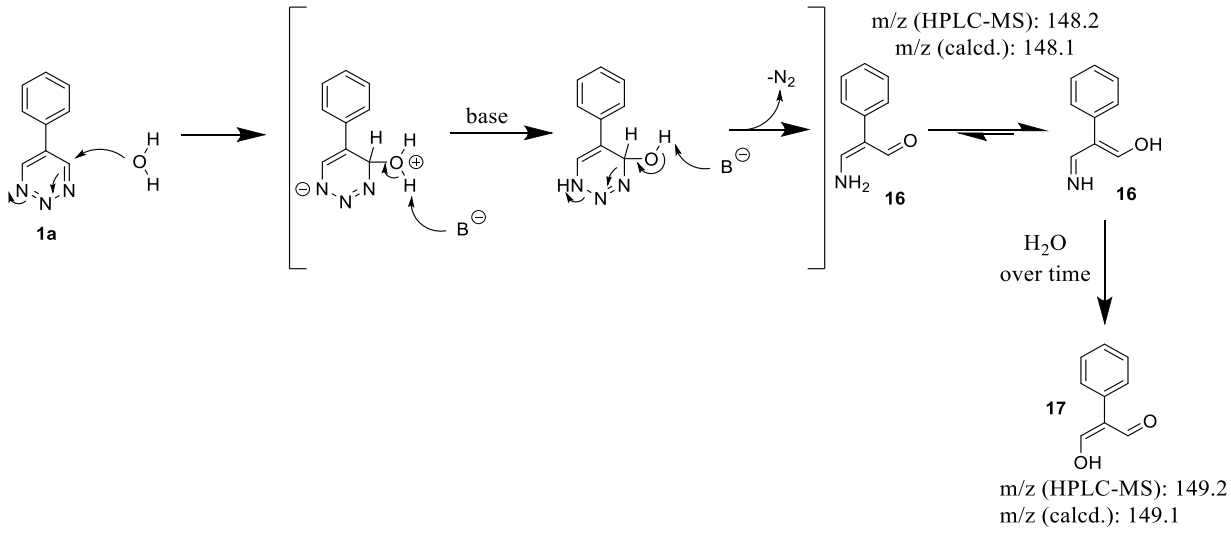


**Scheme S1.** Proposed mechanism leading to the observed side products **16** and **17** in aqueous solutions.

**HPLC chromatograms and low-resolution mass spectra of the test reactions with 5-phenyl-1,2,3-triazine in absence of an amidine**

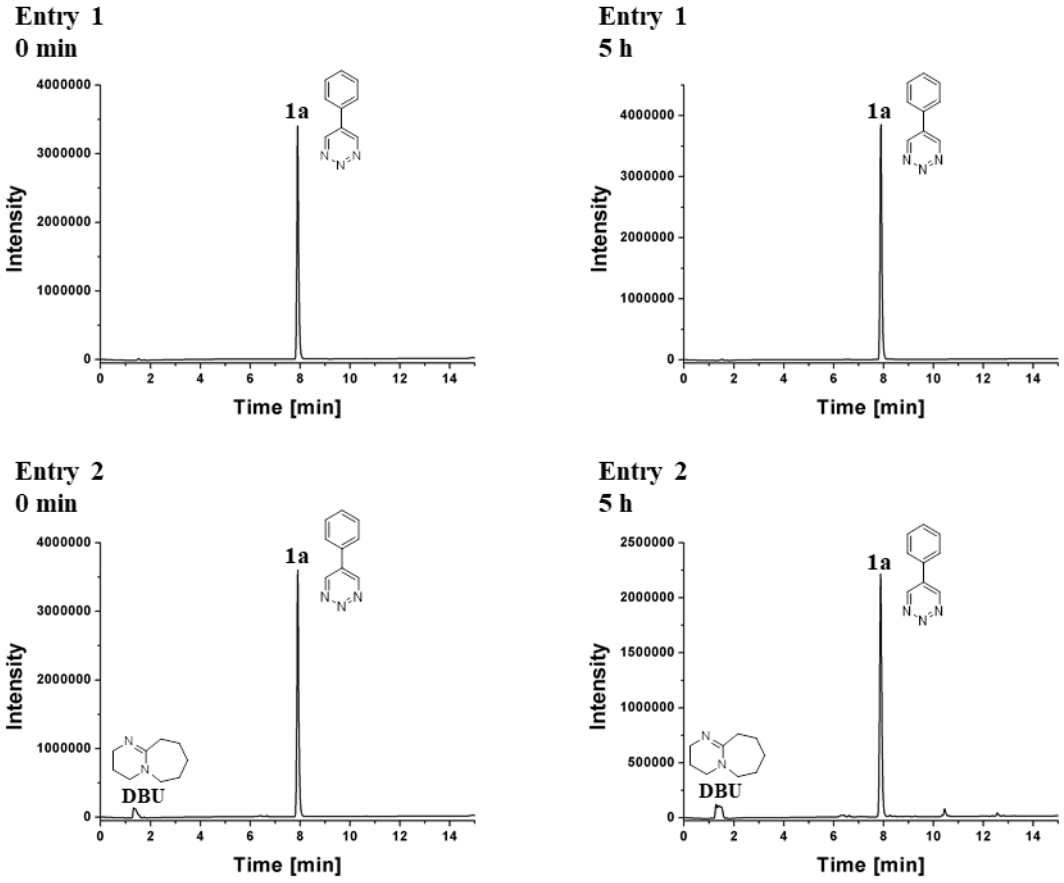

**Entry 3**
**0 min**

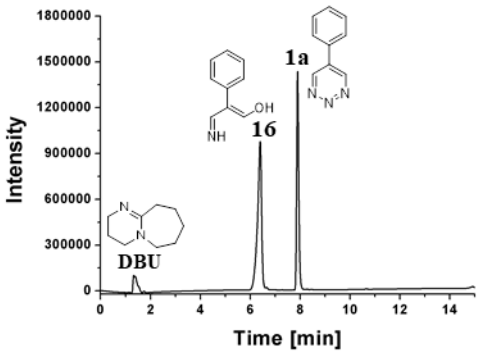


**Entry 3**
**2 h**

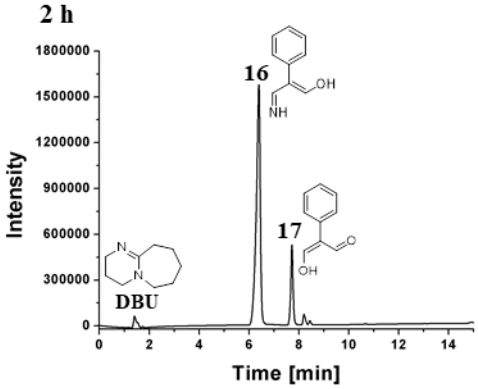


**Entry 3**
**24 h**

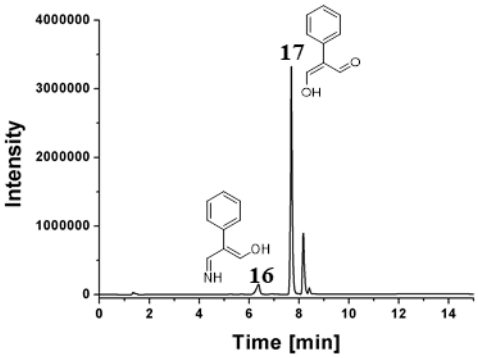


**Entry 4**
**0 min**

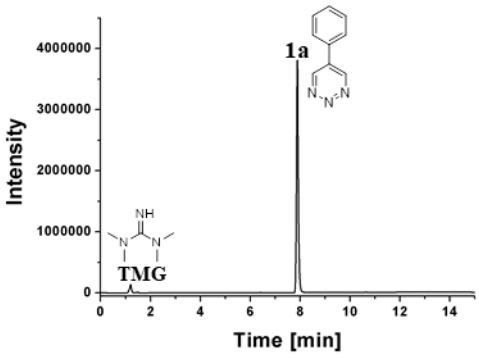


**Entry 4**
**5 h**

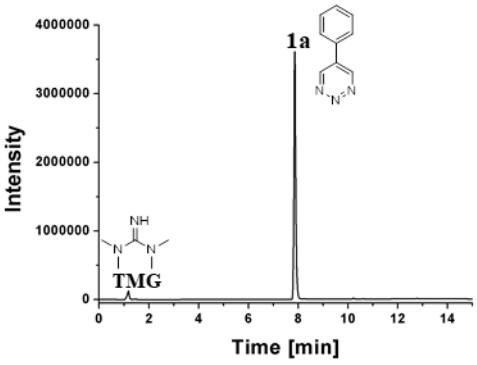


**Entry 5**
**0 min**

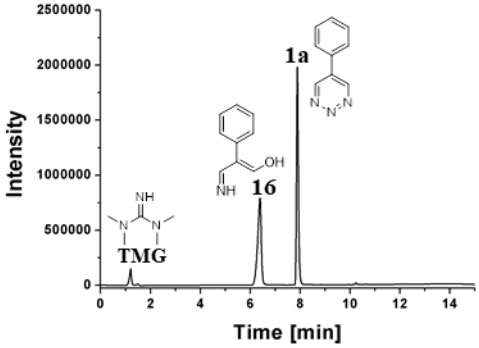


**Entry 5**
**2 h**

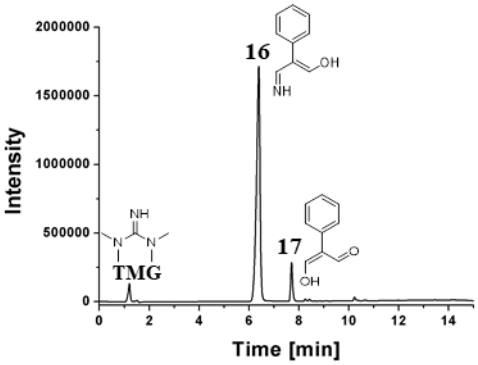

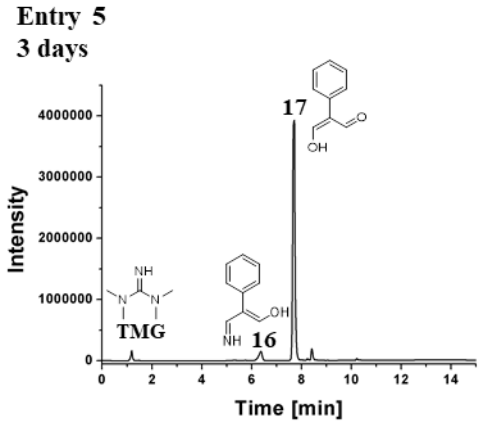


**Figure S2.** HPLC chromatograms of the test reactions with 5-phenyl-1,2,3-triazine in absence of an amidine using 4 eq. of base. For corresponding low-resolution mass spectra (**1a**, **16** and **17**) see Figure S1 (solvent A: $H_2O$ + 0.05% HCOOH; solvent B: $CH_3CN$ + 0.05% HCOOH; gradient: 5% B → 95% B in 9 min, then 95% B for 2 min and back to 5% B; column: Luna® C18(2) column (3µm, 100A, 100 × 4.6 mm) at a flow rate of 1 mL/min).

## Isolation and confirmation of click product 3a formed under the optimized conditions

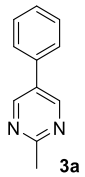


DBU (76.0 µL, 0.509 mmol) was added to a solution of acetamidine hydrochloride (24.1 mg, 0.254 mmol) in $CH_3CN$ (300 µL). After 20 min of stirring at room temperature a solution of 5-phenyl-1,2,3-triazine (20 mg, 0.127 mmol) in $CH_3CN$ (200 µL) was added and the reaction mixture was stirred for 16 h until the starting materials disappeared (verified by TLC in DCM/MeOH 10:1 or HPLC-MS). The crude product was concentrated *in vacuo* and purified by flash column chromatography (0→20% MeOH in DCM) to provide **3a** as slightly yellow solid (19 mg, 88%).

$^1$H NMR (401 MHz, $CD_3OD$): δ 8.94 (s, 2H), 7.70–7.66 (m, 2H), 7.54–7.50 (m, 2H), 7.46–7.43 (m, 1H), 2.73 (s, 3H).

$^{13}$C NMR (101 MHz, $CD_3OD$): δ 167.5, 156.2, 135.3, 132.9, 130.5, 130.0, 127.9, 25.1.

HRMS (CI+): m/z calcd. for $C_{11}H_{11}N_2$ $[MH]^+$ 171.0922, found 171.0924.

## Stability of click product 3a under the optimized reaction conditions

A 20 mM solution of 5-phenyl-1,2,3-triazine in $CH_3CN$ was mixed at a ratio of 1:1 with a 40 mM solution of acetamidine hydrochloride in $CH_3CN$ containing 2 eq. of DBU. The solution containing acetamidine hydrochloride and DBU was incubated at room temperature for 20 min before mixing with the 5-phenyl-1,2,3-triazine to form the amidine free base. The

reaction mixture was incubated at room temperature as well as at 37 °C for several days. After the starting materials disappeared (after 1 d, verified by HPLC-MS) the stability of the formed click product under the optimized reaction conditions was monitored by HPLC-MS analysis at indicated time points. The samples for HPLC-MS measurements were diluted at a ratio of 1:4 with $CH_3CN$. Waterfall plots were generated from the raw HPLC-MS data using OriginPro software (Figure S3).

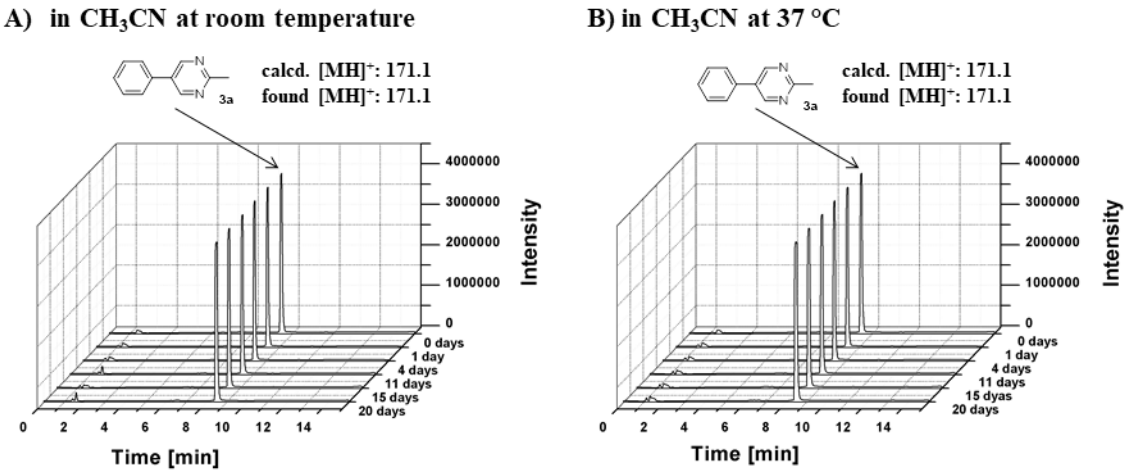


**Figure S3.** Stability measurements: Waterfall plots of the click product between 5-phenyl-1,2,3-triazine and acetamidine in presence of DBU in $CH_3CN$ A) at room temperature and B) at 37 °C as measured by HPLC-MS at indicated time points (solvent A: $H_2O$ + 0.05% HCOOH; solvent B: $CH_3CN$ + 0.05% HCOOH; gradient: 5% B → 95% B in 9 min, then 95% B for 2 min and back to 5% B; column: Luna® C18(2) column (3µm, 100A, 100 × 4.6 mm) at a flow rate of 1 mL/min).

## Determination of second-order rate constants

Second order rate constants of the reactions between acetamidine and 1,2,3-triazines were determined by following either the decay in the concentration of the starting triazine or the increase in the concentration of the emerging click product over time. The concentration decrease or increase was monitored either by HPLC (for the slowest derivative; 5-phenyl-1,2,3-triazine) or by UV/VIS spectroscopy (for faster derivatives). The measurements were performed in $CH_3CN$ at room temperature under pseudo first-order conditions using an excess of the acetamidine. All measurements were performed at least three times.

Rate determination by HPLC: A 5 mM solution of 5-phenyl-1,2,3-triazine in $CH_3CN$ was mixed with a 50 mM solution of acetamidine hydrochloride in $CH_3CN$ containing 2 eq. of DBU. The solution of acetamidine hydrochloride and DBU in $CH_3CN$ was incubated for 20 min to form the amidine free base before addition to the triazine. The mixture had a final triazine concentration of 2.5 mM using 10 eq. of acetamidine hydrochloride and 20 eq. of DBU. The measurement was performed on a Luna® C18 column (3u, 100A, 100 x 4.6 mm) using a linear gradient of $CH_3CN$ + 0.05% HCOOH in $H_2O$ + 0.05% HCOOH (5→95% in 9 min) at a flow rate of 1.0 mL/min. The MS device was disconnected from the HPLC during measurements. The integral of the absorption of the triazine at 254 nm was measured over

189 min in intervals of 21 min. The measured integrals were plotted against time to provide the observed rate constant from the slope of this plot (fitted with single exponential function: $y = y_0 + Ae^{-k/t}$). The second order rate constant was calculated by dividing the observed rate constant by the initial concentration of the acetamidine.

Rate determination by UV/VIS: A 10 mM solution of the respective triazine in $CH_3CN$ and a 50 mM solution of acetamidine hydrochloride in $CH_3CN$ containing 2 eq. of DBU were added to $CH_3CN$ to give a final volume of 3 mL. The solution of acetamidine hydrochloride and DBU in $CH_3CN$ was incubated for 20 min to form the amidine free base before addition to the triazine. The mixture had a final triazine concentration of 500 µM using 5 eq. of acetamidine hydrochloride and 10 eq. of DBU and was immediately measured on the UV/VIS spectrophotometer. As the absorption maxima of the triazines and the maxima of the corresponding click products partly overlap, it was not possible to perform the kinetic measurements at the relevant maxima. Wavelengths, suitable for following either the decay in the concentration of the starting triazine or the increase in the concentration of the emerging click product over time, were determined by scanning kinetics measurements on the UV/VIS spectrophotometer. The wavelengths used for the kinetic measurements are summarized in Table S3. The measured intensity of the absorption was plotted against time. Fitting the curves with single exponential equation ($y = y_0 + Ae^{-k/t}$) provided the observed rate constants. The second order rate constants were calculated by dividing the observed rate constants by the initial concentration of the acetamidine.

All data were processed using Origin or Excel software and are summarized in Table S3.

**Table S3.** Absorption wavelengths used during kinetic measurements and the corresponding second-order rate constants (in $M^{-1}\ s^{-1}\ x\ 10^{-3}$) of the reaction between acetamidine and various 1,2,3-triazines[a].

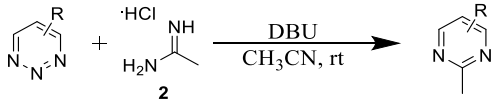


| **1,2,3-triazine** | 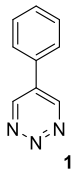 1a | 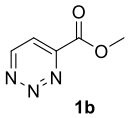 1b | 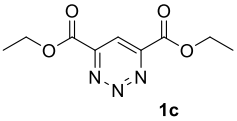 1c | 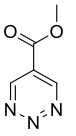 1d |
|---|---|---|---|---|
| **$\lambda_{Abs}$ [nm]** | [b] | 355 | 393 | 340 |
| **$k_2$ [$M^{-1}\ s^{-1}\ x\ 10^{-3}$]** | 0.106 ± 0.014 | 128 ± 2 | 727 ± 2 | 13392 ± 152 |

a) the reactions were performed in HPLC gradient $CH_3CN$ at room temperature under pseudo first-order conditions using 5 equiv. of acetamidine and 10 equiv. of DBU. Absorption wavelengths for the kinetic measurements were determined in $CH_3CN$ at room temperature by scanning kinetic measurements on a UV/VIS spectrophotometer using the same concentrations as for the kinetic measurements. b) the rate constant for this click reaction was determined by HPLC-MS at 254 nm using 10 equiv. of acetamidine and 20 equiv. of DBU.

The formation of the corresponding click products was verified by HPLC-MS measurements (Figure S4) on a Luna® C18(2) column (3µm, 100A, 100 × 4.6 mm) using a linear gradient of $CH_3CN$ + 0.05% HCOOH (5 → 95% in 9 min) in $H_2O$ + 0.05% HCOOH at a flow rate of 1.0 mL/min. All found low-resolution masses are summarized in Table S4.

**Table S4.** Calculated and observed masses of the click products $[M+H]^+$ arising from the reaction between acetamidine and various 1,2,3-triazines[a].

| **1,2,3-Triazine** | | 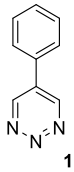 1a | 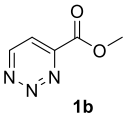 1b | 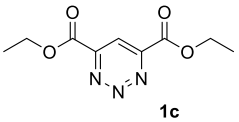 1c | 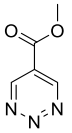 1d |
|---|---|---|---|---|---|
|  2 | **calcd.** | 171.1 | 153.1 | 239.1 | 153.1 |
| | **found** | 171.1 | 153.2 | 239.1 | 153.2 |

a) all reactions were performed in $CH_3CN$ at room temperature using 2 eq. of acetamidine and 4 eq. of DBU.

## HPLC chromatograms and low-resolution mass spectra of the click products

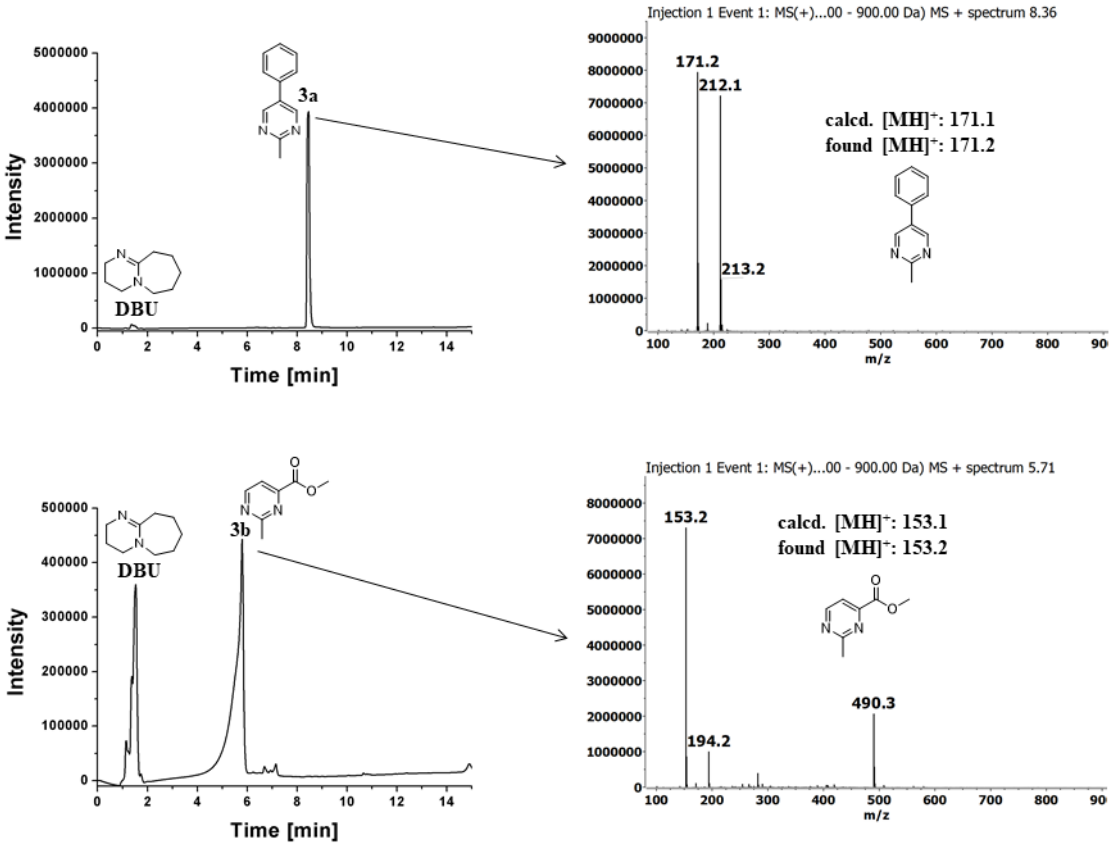

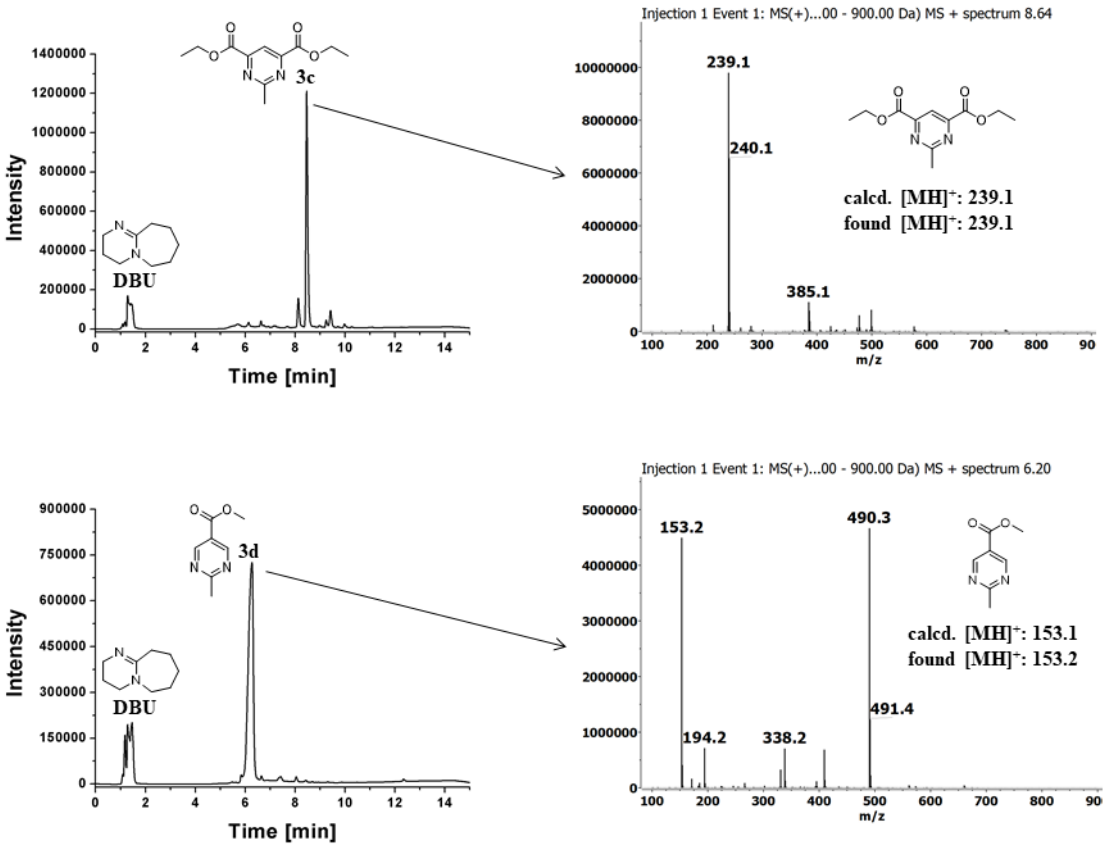


**Figure S4.** HPLC chromatograms and low-resolution mass spectra of the click products of acetamidine with various 1,2,3-triazines performed in $CH_3CN$ at room temperature using 2 eq. of acetamidine and 4 eq. of DBU. Please note that peaks in the MS spectra with a mass of the product + 41 are artefacts arising from the adduct of $CH_3CN$ which is used as eluent in the HPLC experiments (solvent A: $H_2O$ + 0.05% HCOOH; solvent B: $CH_3CN$ + 0.05% HCOOH; gradient: 5% B → 95% B in 9 min, then 95% B for 2 min and back to 5% B; column: Luna® C18(2) column (3µm, 100A, 100 × 4.6 mm) at a flow rate of 1 mL/min).

## Competition experiment between acetamidine and $N_\alpha$-Bz-L-Arg ethyl ester with 5-phenyl-1,2,3-triazine

First a possible cycloaddition between 1,2,3-triazines and the guanidine group of arginine was tested by mixing 5-phenyl-1,2,3-triazine with $N_\alpha$-Bz-L-Arg ethyl ester under the optimized click conditions (Scheme S2).

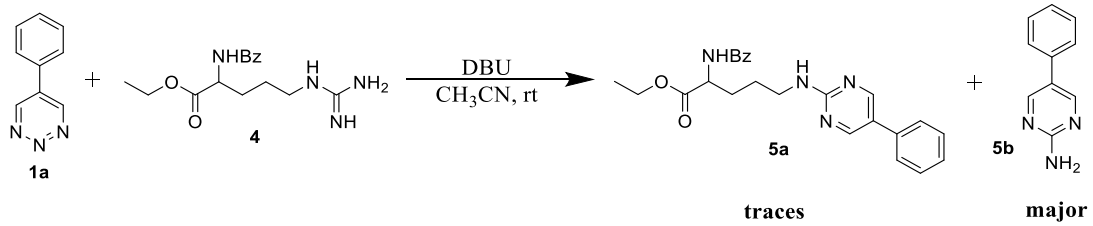


**Scheme S2.** Possible competing cycloaddition between 5-phenyl-1,2,3-triazine and *Nα*-Bz-L-Arg ethyl ester.

A 20 mM solution of the HCl-salt of $N_\alpha$-Bz-L-Arg ethyl ester in $CH_3CN$ containing 2 eq. of DBU was first incubated at room temperature for 20 min and then mixed at a ratio of 1:1 with a 10 mM solution of 5-phenyl-1,2,3-triazine in $CH_3CN$. The reaction mixture was diluted with $CH_3CN$ to a final triazine concentration of 2.5 mM using 2 eq. of $N_\alpha$-Bz-L-Arg ethyl ester and 4 eq. of DBU and incubated at room temperature until the starting materials disappeared. During the incubation the solution was analyzed by HPLC-MS at indicated time points (Figure S5). The samples for HPLC-MS measurements were diluted at a ratio of 1:1 with $CH_3CN$.

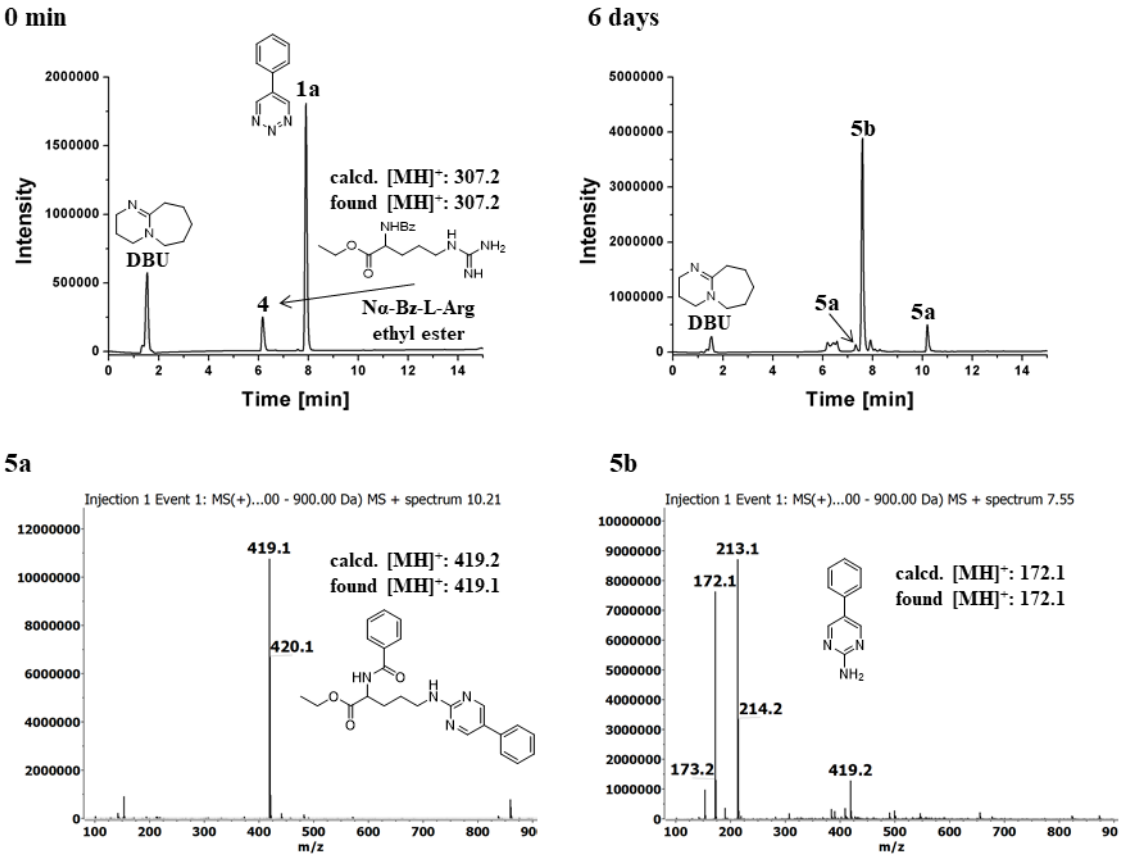


**Figure S5.** HPLC chromatograms and low-resolution mass spectra of the reaction between 5-phenyl-1,2,3-triazine and *Nα*-Bz-L-Arg ethyl ester in $CH_3CN$ at room temperature using 2 eq. of the arginine and 4 eq. of DBU. Please note that peaks in the MS spectra with a mass of the product + 41 are artefacts arising from the adduct of $CH_3CN$ which is used as eluent in the HPLC experiments (solvent A: $H_2O$ + 0.05% HCOOH; solvent B: $CH_3CN$ + 0.05% HCOOH; gradient: 5% B → 95% B in 9 min, then 95% B for 2 min and back to 5% B; column: Luna® C18(2) column (3µm, 100A, 100 × 4.6 mm) at a flow rate of 1 mL/min).

The observed reactivity between arginine and 1,2,3-triazines was afterwards compared to the reactivity between amidines and 1,2,3-triazines by mixing 5-phenyl-1,2,3-triazine with $N_\alpha$-Bz-L-Arg ethyl ester and acetamidine simultaneously in a one pot reaction under the optimized click conditions (Scheme S3).

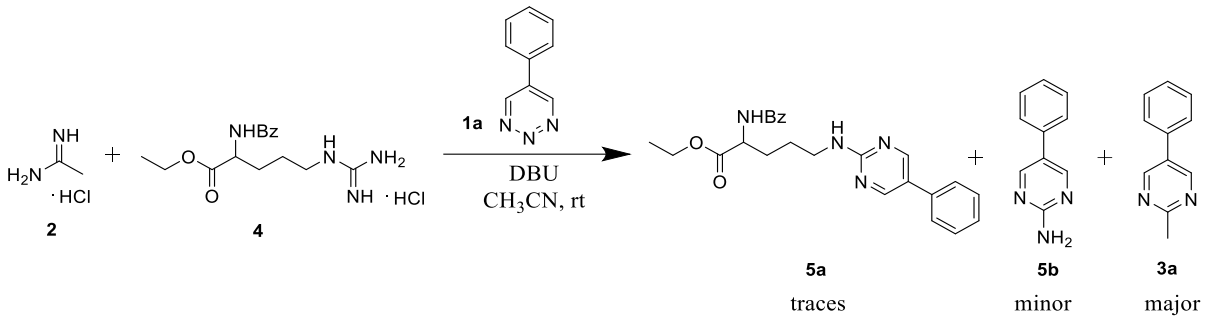


**Scheme S3.** Competition experiment of the cycloaddition between 5-phenyl-1,2,3-triazine and acetamidine or *Nα*-Bz-L-Arg ethyl ester respectively.

A 20 mM solution of the HCl-salt of $N_\alpha$-Bz-L-Arg ethyl ester in $CH_3CN$ containing 2 eq. of DBU and a 20 mM solution of acetamidine hydrochloride in $CH_3CN$ containing 2 eq. of DBU were first separately incubated at room temperature for 20 min. Then both solutions were mixed at a ratio of 1:1:1 together with a 10 mM solution of 5-phenyl-1,2,3-triazine in $CH_3CN$. The reaction mixture was diluted with $CH_3CN$ to a final triazine concentration of 2.5 mM using 2 eq. of $N_\alpha$-Bz-L-Arg ethyl ester, 2 eq. of acetamidine and 4 eq. of DBU. The solution was incubated at room temperature until the starting materials disappeared. During the incubation the solution was analyzed by HPLC-MS at indicated time points (Figure S6). The samples for HPLC-MS measurements were diluted at a ratio of 1:1 with $CH_3CN$.

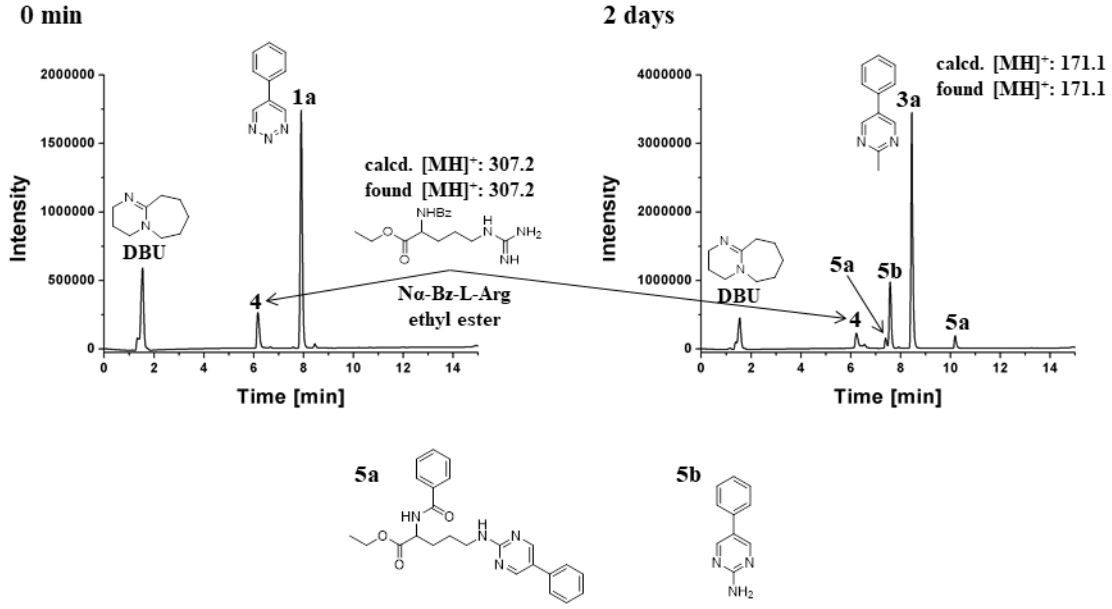


**Figure S6.** HPLC chromatograms of the competition reaction between *Nα*-Bz-L-Arg ethyl ester and acetamidine with 5-phenyl-1,2,3-triazine in $CH_3CN$ at room temperature using 2 eq. of the arginine, 2 eq. of acetamidine and 4 eq. of DBU. For corresponding low-resolution mass spectra (**5a** and **5b**) see Figure S5 (solvent A: $H_2O$ + 0.05% HCOOH; solvent B: $CH_3CN$ + 0.05% HCOOH; gradient: 5% B → 95% B in 9 min, then 95% B for 2 min and back to 5% B; column: Luna® C18(2) column (3µm, 100A, 100 × 4.6 mm) at a flow rate of 1 mL/min).

## Competition experiments between the amidine - 1,2,3-triazine cycloaddition and various other ligation methods

### Competition experiment with the *trans*-cyclooctene (TCO) – 1,2,4,5-tetrazine cycloaddition

The selectivity between amidine - 1,2,3-triazine and TCO - 1,2,4,5-tetrazine cycloaddition was tested by mixing 5-phenyl-1,2,3-triazine with acetamidine and diphenyl-*s*-tetrazine with *trans*-cyclooct-4-enol (TCO) simultaneously in a one pot reaction under the optimized reaction conditions for the amidine-1,2,3-triazine cycloaddition.

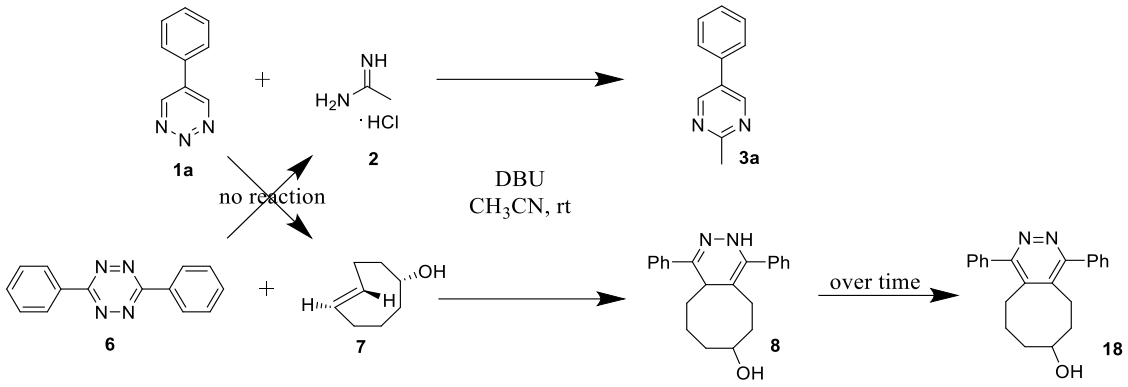


**Scheme S4.** Competition experiment between amidine - 1,2,3-triazine and TCO - 1,2,4,5-tetrazine cycloaddition.

A 20 mM solution of acetamidine hydrochloride in $CH_3CN$ containing 2 eq. of DBU was first incubated at room temperature for 20 min to form the amidine free base. Then the solution was mixed at a ratio of 1:1 with a 10 mM solution of 5-phenyl-1,2,3-triazine, a 20 mM solution of the TCO and a 10 mM solution of diphenyl-*s*-tetrazine all in $CH_3CN$ in a one pot reaction. The reaction mixture had a final triazine as well as a final tetrazine concentration of 2.5 mM using 2 eq. of TCO, 2 eq. of acetamidine and 4 eq. of DBU. The solution was incubated at room temperature until the starting materials disappeared. The progress of the reactions was monitored by HPLC-MS analysis at indicated time points (Figure S7). The samples for HPLC-MS measurements were diluted at a ratio of 1:1 with $CH_3CN$.

**competition experiment**
**0 min**

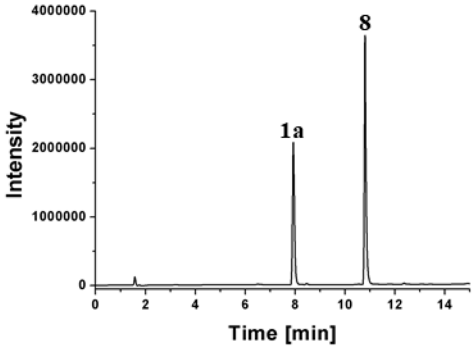


**competition experiment**
**5 days**

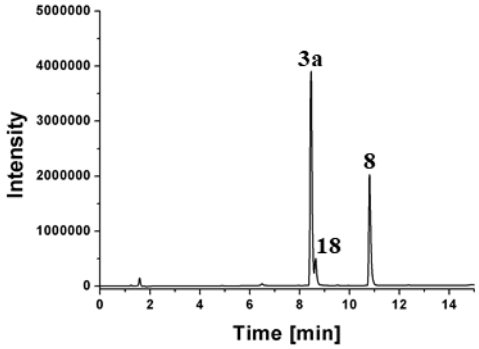


**TCO - 1,2,4,5-tetrazine cycloaddition alone**
**0 min**

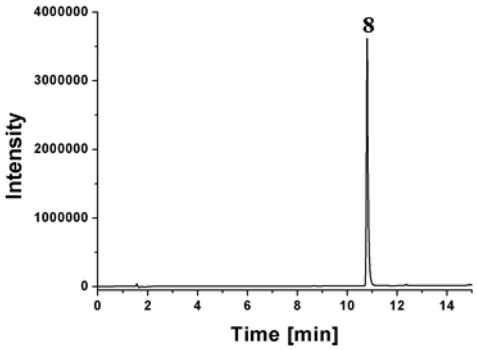


**TCO - 1,2,4,5-tetrazine cycloaddition alone**
**1 day**

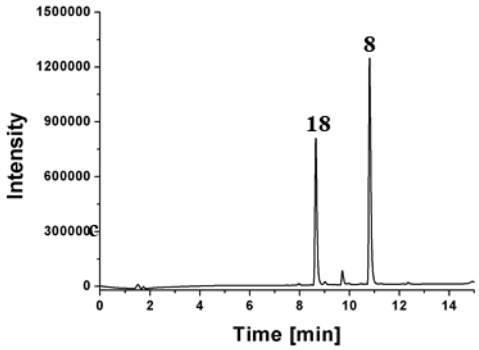


**1a**

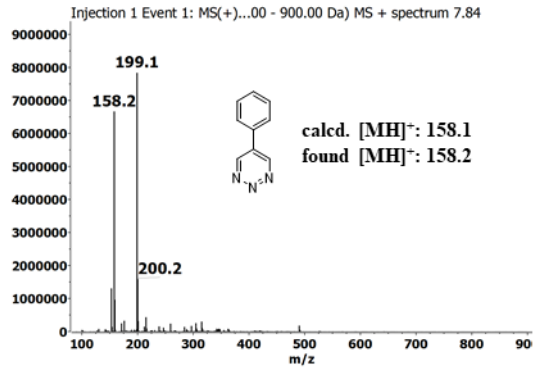


**3a**

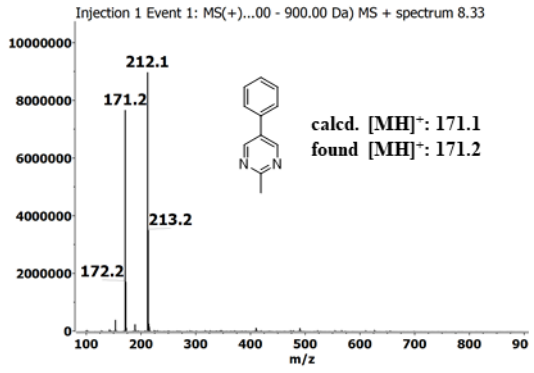


**8**

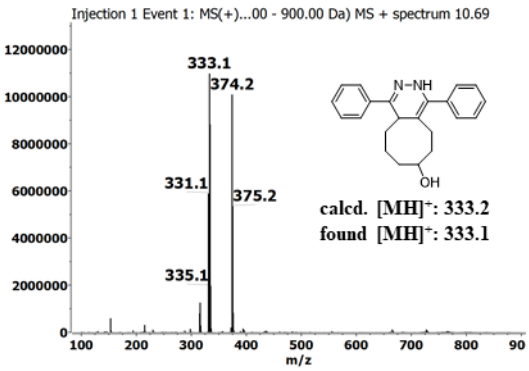


**18**

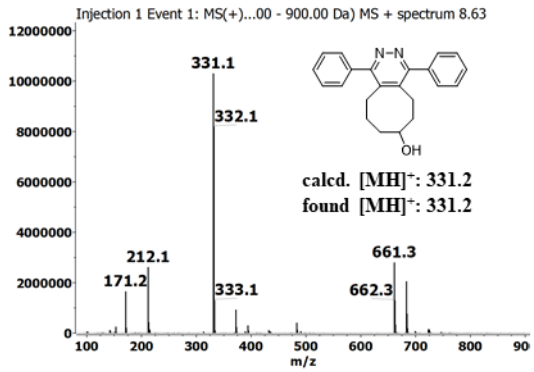

**Figure S7.** HPLC chromatograms and low-resolution mass spectra of the one pot competition reaction between amidine - 1,2,3-triazine and TCO - 1,2,4,5-tetrazine cycloaddition in $CH_3CN$ at room temperature using 2 eq. of TCO, 2 eq. of acetamidine and 4 eq. of DBU. Please note that peaks in the MS spectra with a mass of the product + 41 are artefacts arising from the adduct of $CH_3CN$ which is used as eluent in the HPLC experiments (solvent A: $H_2O$ + 0.05% HCOOH; solvent B: $CH_3CN$ + 0.05% HCOOH; gradient: 5% B → 95% B in 9 min, then 95% B for 2 min and back to 5% B; column: Luna® C18(2) column (3µm, 100A, 100 × 4.6 mm) at a flow rate of 1 mL/min).

## Competition experiment with the strain-promoted azide-alkyne cycloaddition (SPAAC)

The selectivity between amidine–1,2,3-triazine cycloaddition and SPAAC was tested by mixing 5-phenyl-1,2,3-triazine with acetamidine and 3-azido-7-hydroxycoumarine with bicyclononyne (BCN) simultaneously in a one pot reaction under the optimized reaction conditions for the amidine-1,2,3-triazine cycloaddition.

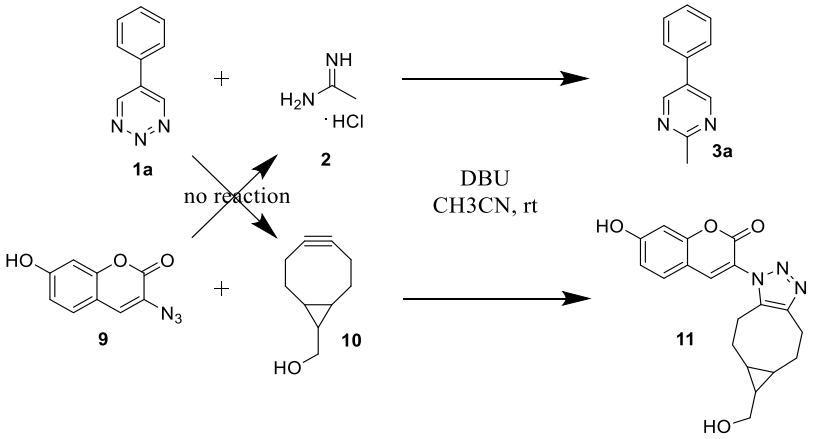


**Scheme S5.** Competition experiment between amidine - 1,2,3-triazine cycloaddition and SPAAC.

A 20 mM solution of acetamidine hydrochloride in $CH_3CN$ containing 2 eq. of DBU was first incubated at room temperature for 20 min to form the amidine free base. Then the solution was mixed at a ratio of 1:1 with a 10 mM solution of 5-phenyl-1,2,3-triazine, a 20 mM solution of BCN and a 10 mM solution of 3-azido-7-hydroxycoumarine all in $CH_3CN$ in a one pot reaction. The reaction mixture had a final triazine as well as a final 3-azido-7-hydroxycoumarine concentration of 2.5 mM using 2 eq. of BCN, 2 eq. of acetamidine and 4 eq. of DBU. The solution was incubated at room temperature until the starting materials disappeared. During the incubation the progress of the reactions was monitored by HPLC-MS analysis at indicated time points (Figure S8). The samples for HPLC-MS measurements were diluted at a ratio of 1:1 with $CH_3CN$.

**competition experiment**
**0 min**

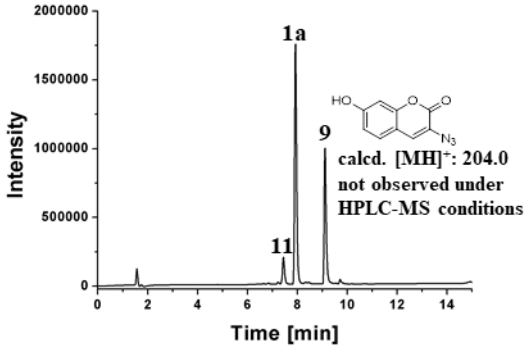


**competition experiment**
**4 days**

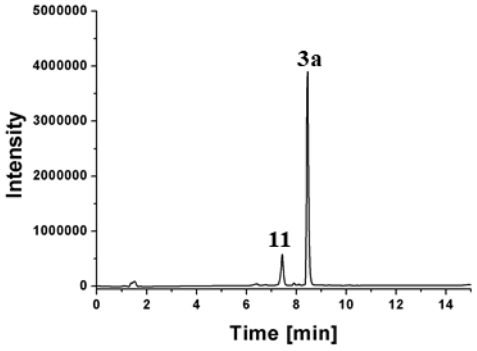


**SPAAC alone**
**0 min**

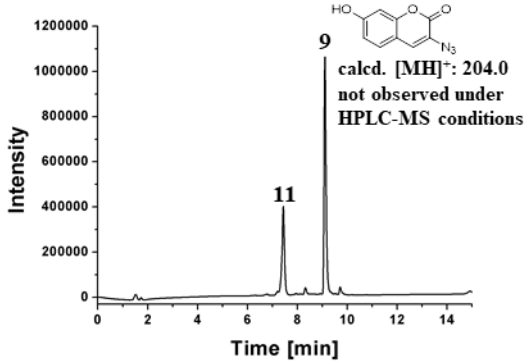


**SPAAC alone**
**5 h**

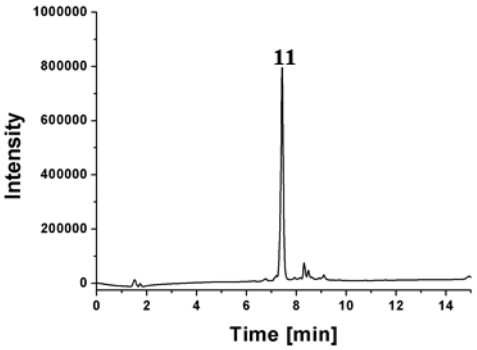


**1a**

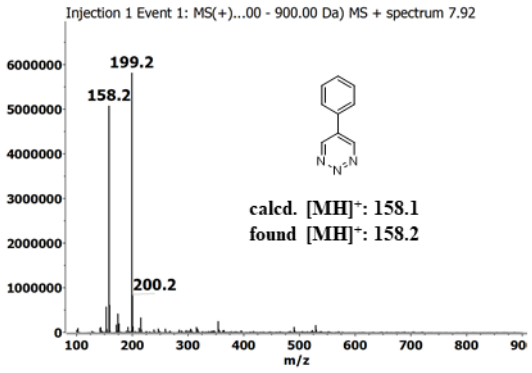


**3a**

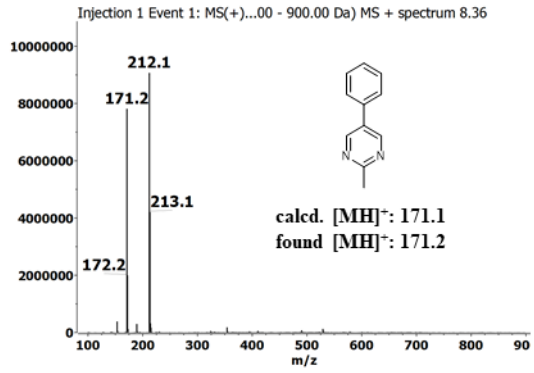


**11**

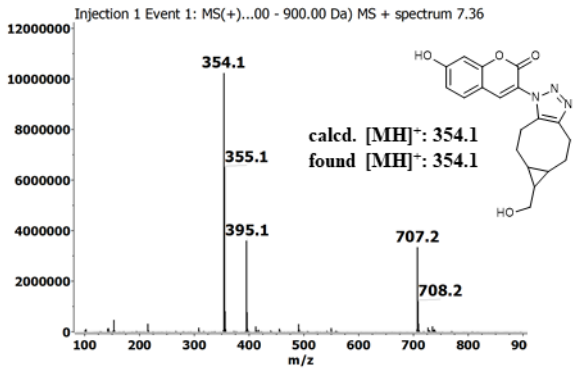

**Figure S8.** HPLC chromatograms and low-resolution mass spectra of the one pot competition reaction between amidine - 1,2,3-triazine cycloaddition and SPAAC in $CH_3CN$ at room temperature using 2 eq. of BCN, 2 eq. of acetamidine and 4 eq. of DBU. Please note that peaks in the MS spectra with a mass of the product + 41 are artefacts arising from the adduct of $CH_3CN$ which is used as eluent in the HPLC experiments (solvent A: $H_2O$ + 0.05% HCOOH; solvent B: $CH_3CN$ + 0.05% HCOOH; gradient: 5% B → 95% B in 9 min, then 95% B for 2 min and back to 5% B; column: Luna® C18(2) column (3µm, 100A, 100 × 4.6 mm) at a flow rate of 1 mL/min).

## Competition experiment with the TCO – 1,2,4-triazine cycloaddition

The selectivity between amidine - 1,2,3-triazine and TCO - 1,2,4-triazine cycloaddition was tested by mixing 5-phenyl-1,2,3-triazine with acetamidine and 3-(2-pyridyl)-6-phenyl-1,2,4-triazine with *trans*-cyclooct-4-enol (TCO) simultaneously in a one pot reaction under the optimized reaction conditions for the amidine-1,2,3-triazine cycloaddition.

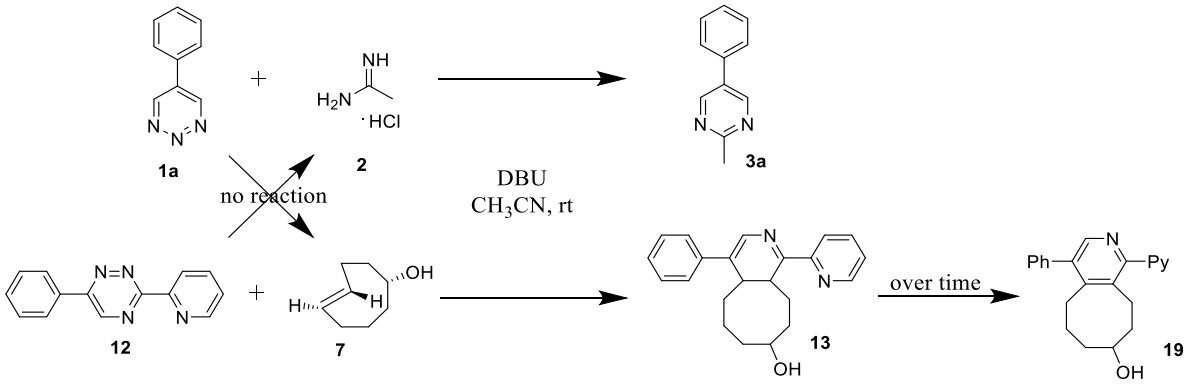


**Scheme S6.** Competition experiment between amidine - 1,2,3-triazine and TCO - 1,2,4-triazine cycloaddition using 3-(2-pyridyl)-6-phenyl-1,2,4-triazine.

A 20 mM solution of acetamidine hydrochloride in $CH_3CN$ containing 2 eq. of DBU was first incubated at room temperature for 20 min to form the amidine free base. Then the solution was mixed at a ratio of 1:1 with a 10 mM solution of 5-phenyl-1,2,3-triazine, a 20 mM solution of the TCO and a 10 mM solution of 3-(2-pyridyl)-6-phenyl-1,2,4-triazine all in $CH_3CN$ in a one pot reaction. The reaction mixture had a final 1,2,3-triazine as well as a final 1,2,4-triazine concentration of 2.5 mM using 2 eq. of TCO, 2 eq. of acetamidine and 4 eq. of DBU. The solution was incubated at room temperature until the starting materials disappeared. During the incubation the progress of the reactions was monitored by HPLC-MS analysis at indicated time points (Figure S9). The samples for HPLC-MS measurements were diluted at a ratio of 1:1 with $CH_3CN$.

**competition experiment**
**0 min**

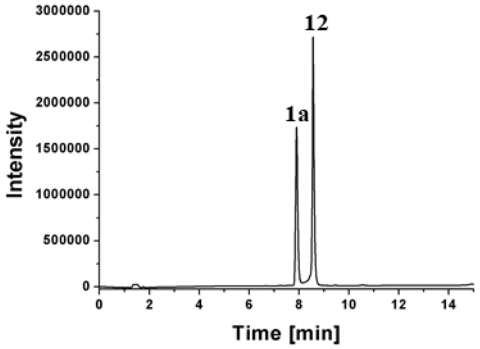


**competition experiment**
**7 days**

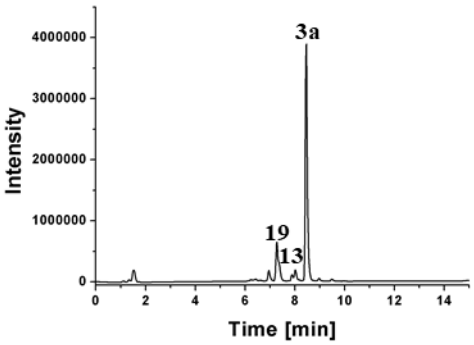


**TCO - 1,2,4-triazine cycloaddition alone**
**0 min**

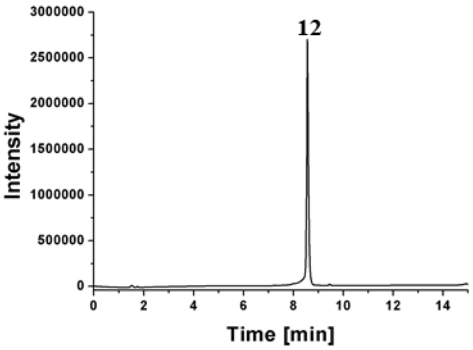


**TCO - 1,2,4-triazine cycloaddition alone**
**7 days**

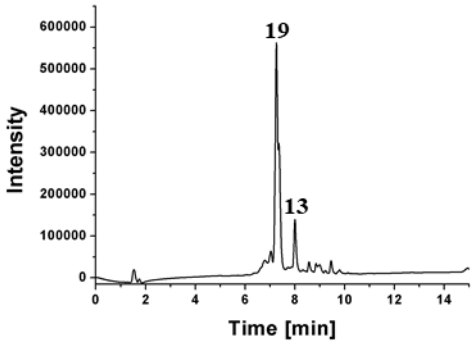


**1a**

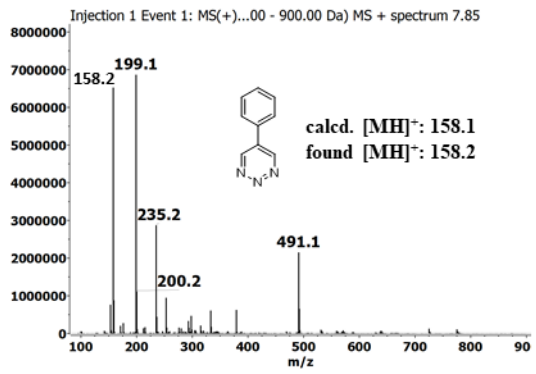


**3a**

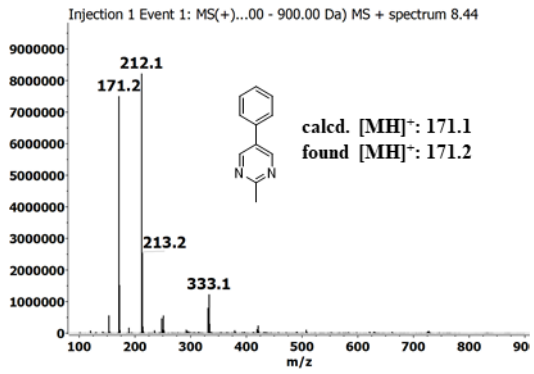


**12**

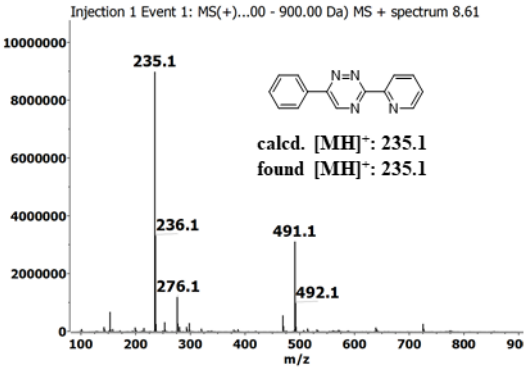


**13**

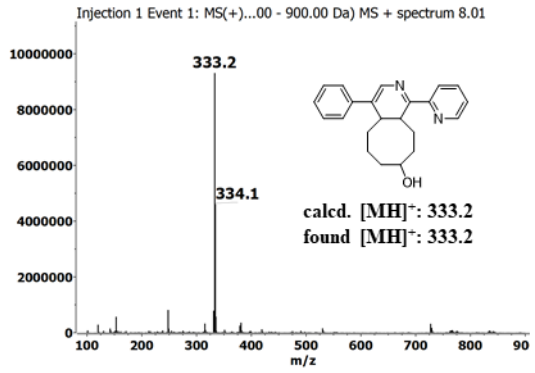

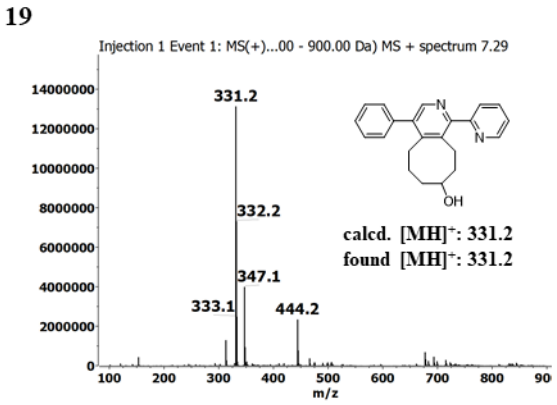


**Figure S9.** HPLC chromatograms and low-resolution mass spectra of the one pot competition reaction between amidine - 1,2,3-triazine and TCO - 1,2,4-triazine cycloaddition using 3-(2-pyridyl)-6-phenyl-1,2,4-triazine. The reaction was performed in $CH_3CN$ at room temperature using 2 eq. of TCO, 2 eq. of acetamidine and 4 eq. of DBU. Please note that peaks in the MS spectra with a mass of the product + 41 are artefacts arising from the adduct of $CH_3CN$ which is used as eluent in the HPLC experiments (solvent A: $H_2O$ + 0.05% HCOOH; solvent B: $CH_3CN$ + 0.05% HCOOH; gradient: 5% B → 95% B in 9 min, then 95% B for 2 min and back to 5% B; column: Luna® C18(2) column (3µm, 100A, 100 × 4.6 mm) at a flow rate of 1 mL/min).

The orthogonality of these two cycloadditions was additionally tested with 6-(4-nitrophenyl)-1,2,4-triazine, a more reactive 1,2,4-triazine in cycloaddition reactions with TCOs[2-3] under the same conditions as above.

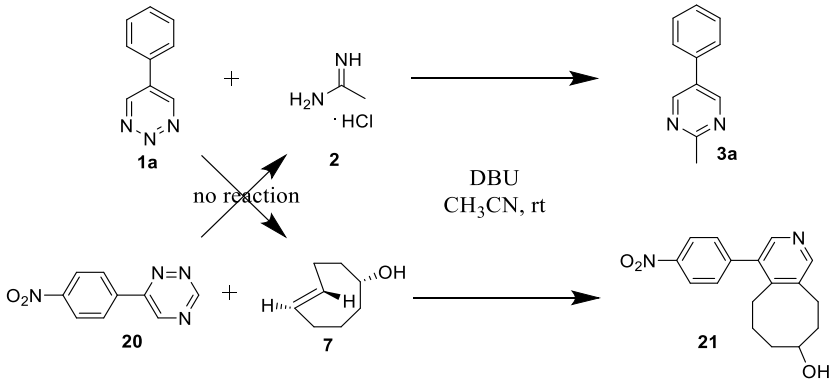


**Scheme S7.** Competition experiment between amidine–1,2,3-triazine and TCO–1,2,4-triazine cycloaddition using 6-(4-nitrophenyl)-1,2,4-triazine.

**competition experiment**
**0 min**

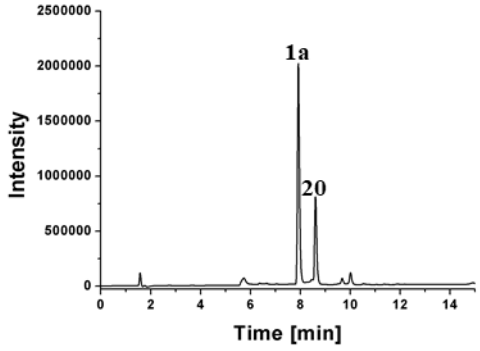


**competition experiment**
**5 days**

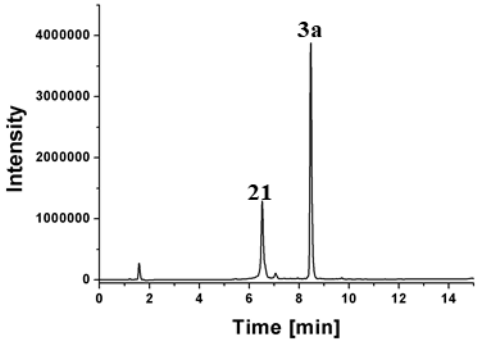


**TCO - 1,2,4-triazine cycloaddition alone**
**0 min**

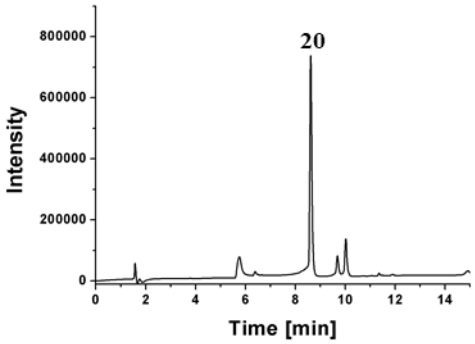


**TCO - 1,2,4-triazine cycloaddition alone**
**5 days**

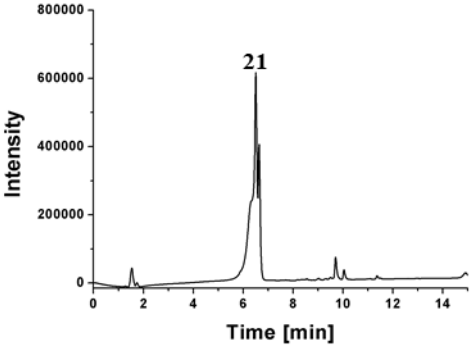


**1a**

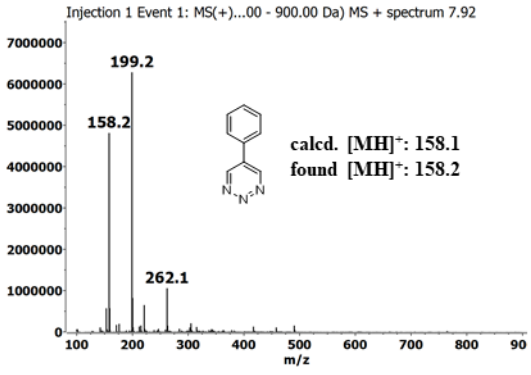


**3a**

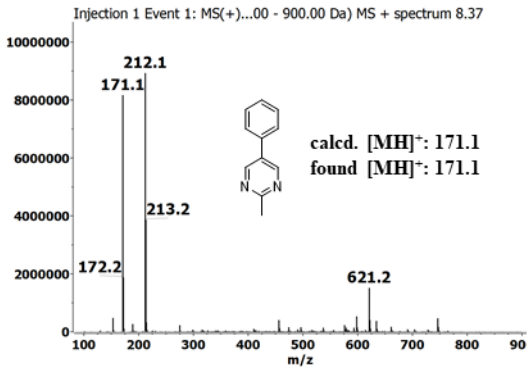


**20**

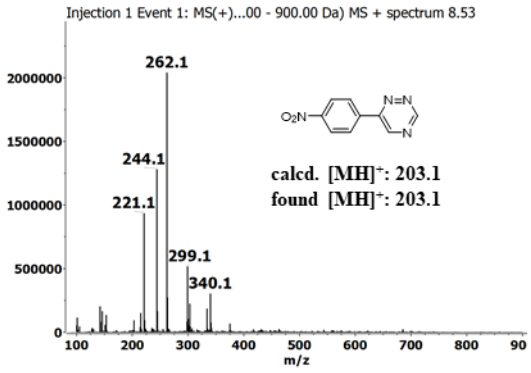


**21**

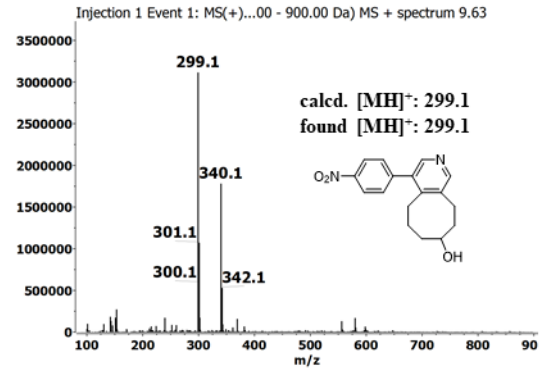

**Figure S10.** HPLC chromatograms and low-resolution mass spectra of the one pot competition reaction between amidine - 1,2,3-triazine and TCO - 1,2,4-triazine cycloaddition using 6-(4-nitrophenyl)-1,2,4-triazine. The reaction was performed in $CH_3CN$ at room temperature using 2 eq. of TCO, 2 eq. of acetamidine and 4 eq. of DBU. Please note that peaks in the MS spectra with a mass of the product + 41 and with a mass of the product + 18 are artefacts arising from the adducts of $CH_3CN$ and $H_2O$ respectively which are used as eluents in the HPLC experiments (solvent A: $H_2O$ + 0.05% HCOOH; solvent B: $CH_3CN$ + 0.05% HCOOH; gradient: 5% B → 95% B in 9 min, then 95% B for 2 min and back to 5% B; column: Luna® C18(2) column (3µm, 100A, 100 × 4.6 mm) at a flow rate of 1 mL/min).

## Competition experiment with SPAAC and the TCO – 1,2,4-triazine cycloaddition simultaneously

Finally, the selectivity of the amidine–1,2,3-triazine cycloaddition was tested towards two other ligation methods at the same time. 5-phenyl-1,2,3-triazine was reacted with acetamidine, 3-azido-7-hydroxycoumarine with bicyclononyne (BCN) and 3-(2-pyridyl)-6-phenyl-1,2,4-triazine with *trans*-cyclooct-4-enol (TCO) simultaneously in a one pot reaction under the optimized reaction conditions for the amidine - 1,2,3-triazine cycloaddition.

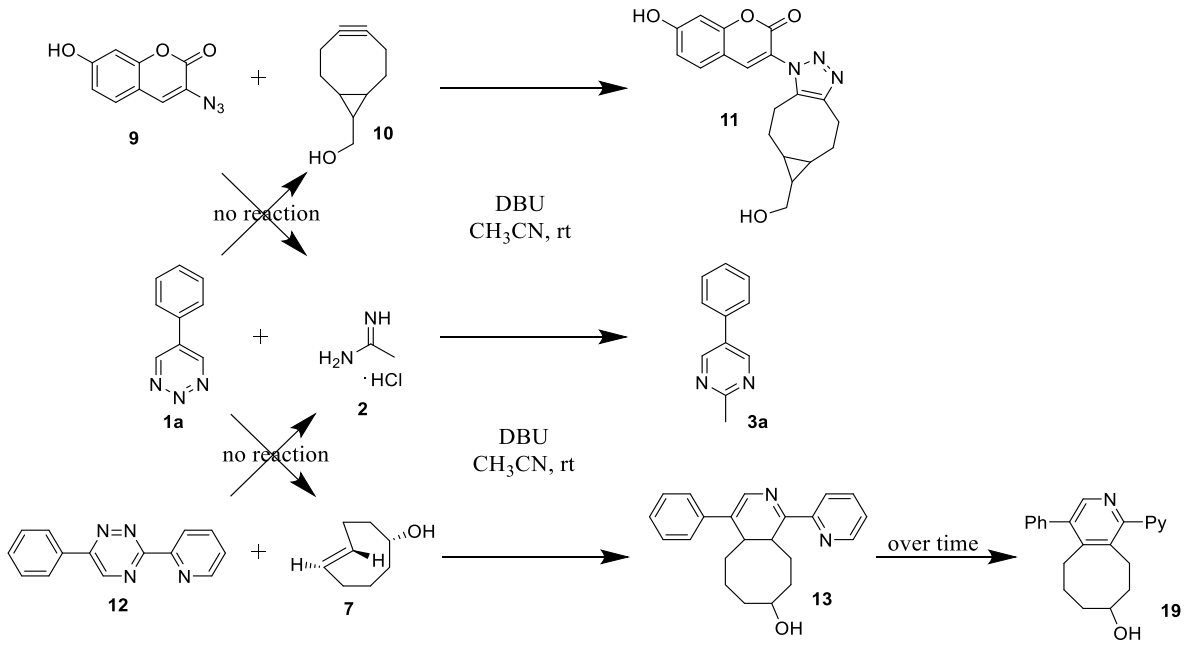


**Scheme S8.** Competition experiment between amidine–1,2,3-triazine cycloaddition, TCO–1,2,4-triazine cycloaddition and SPAAC using 3-(2-pyridyl)-6-phenyl-1,2,4-triazine.

A 20 mM solution of acetamidine hydrochloride in $CH_3CN$ containing 2 eq. of DBU was first incubated at room temperature for 20 min to form the amidine free base. Then the solution was mixed at a ratio of 1:1 with a 10 mM solution of 5-phenyl-1,2,3-triazine, a 20 mM solution of the TCO, a 10 mM solution of 3-(2-pyridyl)-6-phenyl-1,2,4-triazine, a 20 mM solution of BCN and a 10 mM solution of 3-azido-7-hydroxycoumarine all in $CH_3CN$ in a one pot reaction. The reaction mixture had a final concentration of 1,2,3-triazine as well as of 1,2,4-triazine and 3-azido-7-hydroxycoumarine of 1.67 mM using 2 eq. of TCO, 2 eq. of BCN, 2 eq. of acetamidine and 4 eq. of DBU. The solution was incubated at room temperature until the starting materials

disappeared. During the incubation the progress of the reactions was monitored by HPLC-MS analysis at indicated time points (Figure S11). The samples for HPLC-MS analysis were measured undiluted.

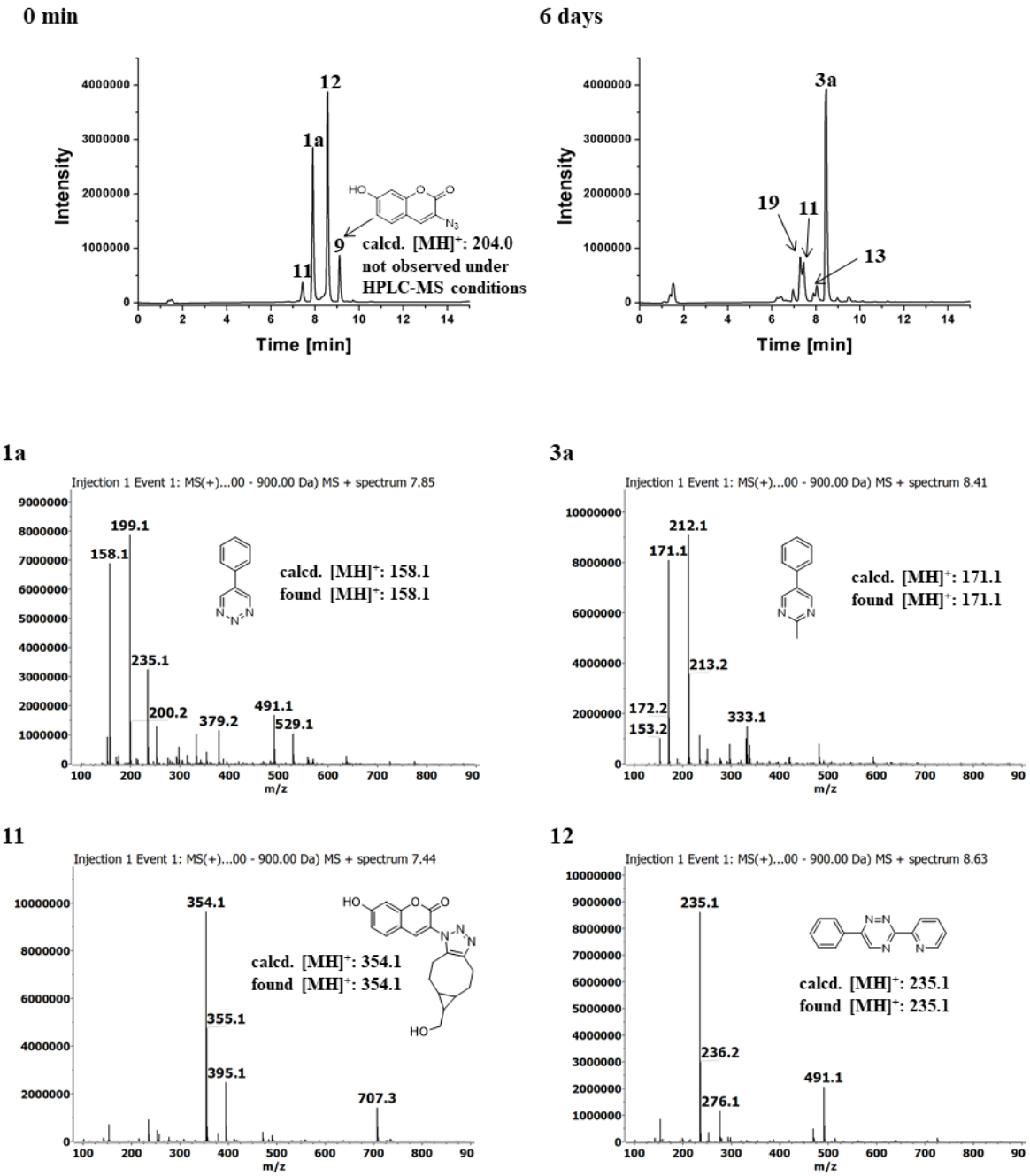

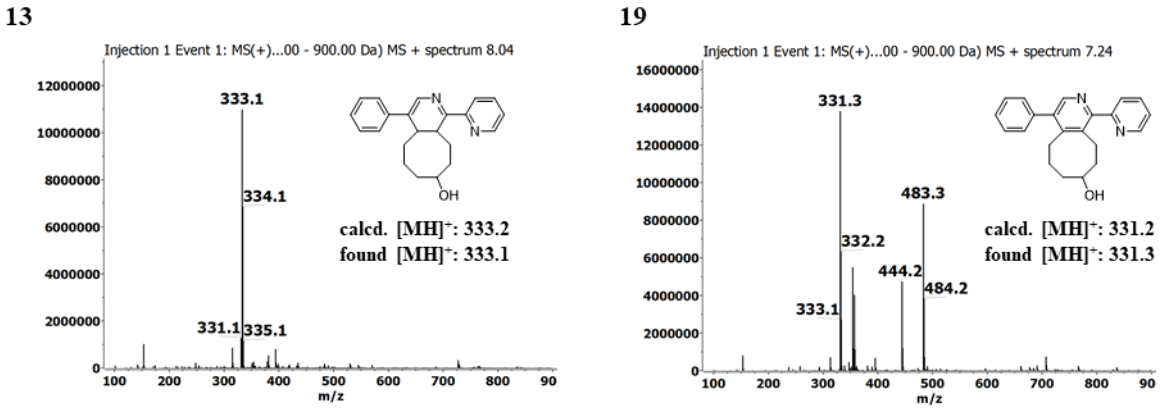


**Figure S11.** HPLC chromatograms and low-resolution mass spectra of the one pot competition reaction between amidine–1,2,3-triazine cycloaddition, TCO–1,2,4-triazine cycloaddition and SPAAC using 3-(2-pyridyl)-6-phenyl-1,2,4-triazine. The reaction was performed in $CH_3CN$ at room temperature using 2 eq. of TCO, 2 eq. of BCN, 2 eq. of acetamidine and 4 eq. of DBU. Please note that peaks in the MS spectra with a mass of the product + 41 are artefacts arising from the adduct of $CH_3CN$ which is used as eluent in the HPLC experiments (solvent A: $H_2O$ + 0.05% HCOOH; solvent B: $CH_3CN$ + 0.05% HCOOH; gradient: 5% B → 95% B in 9 min, then 95% B for 2 min and back to 5% B; column: Luna® C18(2) column (3µm, 100A, 100 × 4.6 mm) at a flow rate of 1 mL/min).

The orthogonality of these three cycloadditions was also tested with 6-(4-nitrophenyl)-1,2,4-triazine as 1,2,4-triazine under the same conditions as above. In this case cross reactivity between the 1,2,4-triazine and BCN was observed. Small traces of side product **22** arising from the cycloaddition between triazine **20** and BCN **10** were found by HPLC-MS analysis (Scheme S9 and Figure S12). However, the amidine - 1,2,3-triazine cycloaddition still remained orthogonal to both of the other ligation methods.

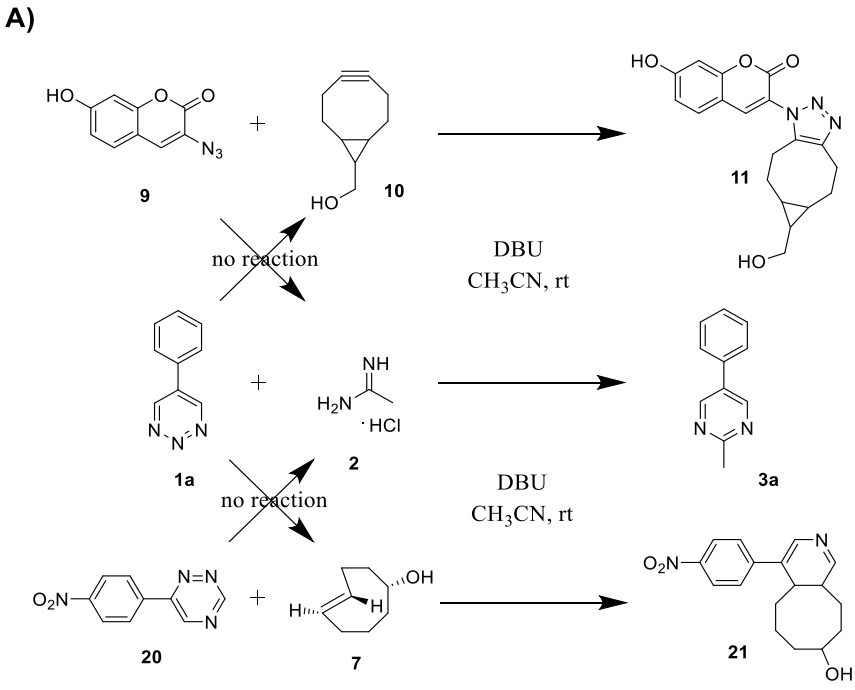

**B)**

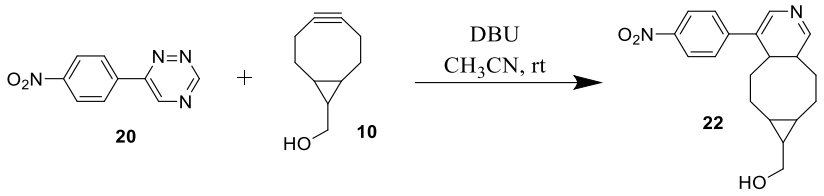


**Scheme S9.** A) Competition experiment between amidine–1,2,3-triazine cycloaddition, TCO–1,2,4-triazine cycloaddition and SPAAC using 6-(4-nitrophenyl)-1,2,4-triazine and B) cross reaction between triazine **20** and BCN **10** leading to side product **22** under these conditions.

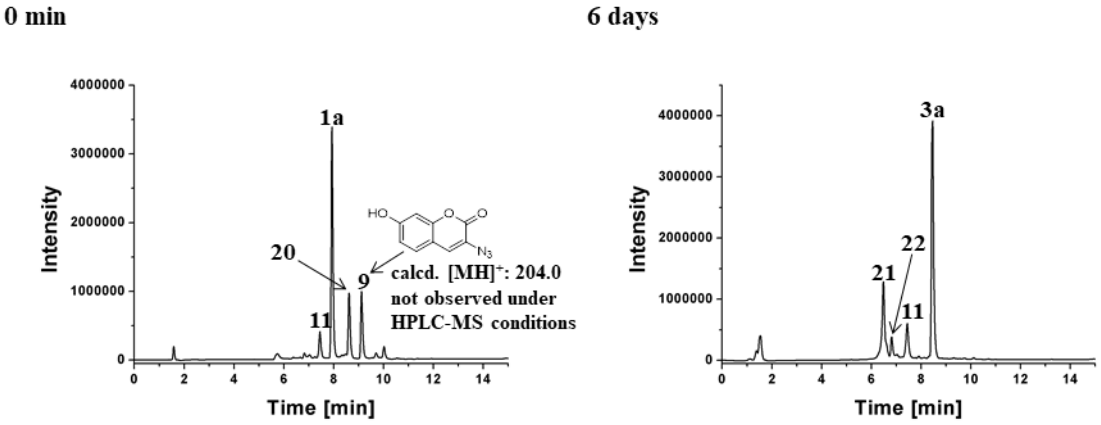

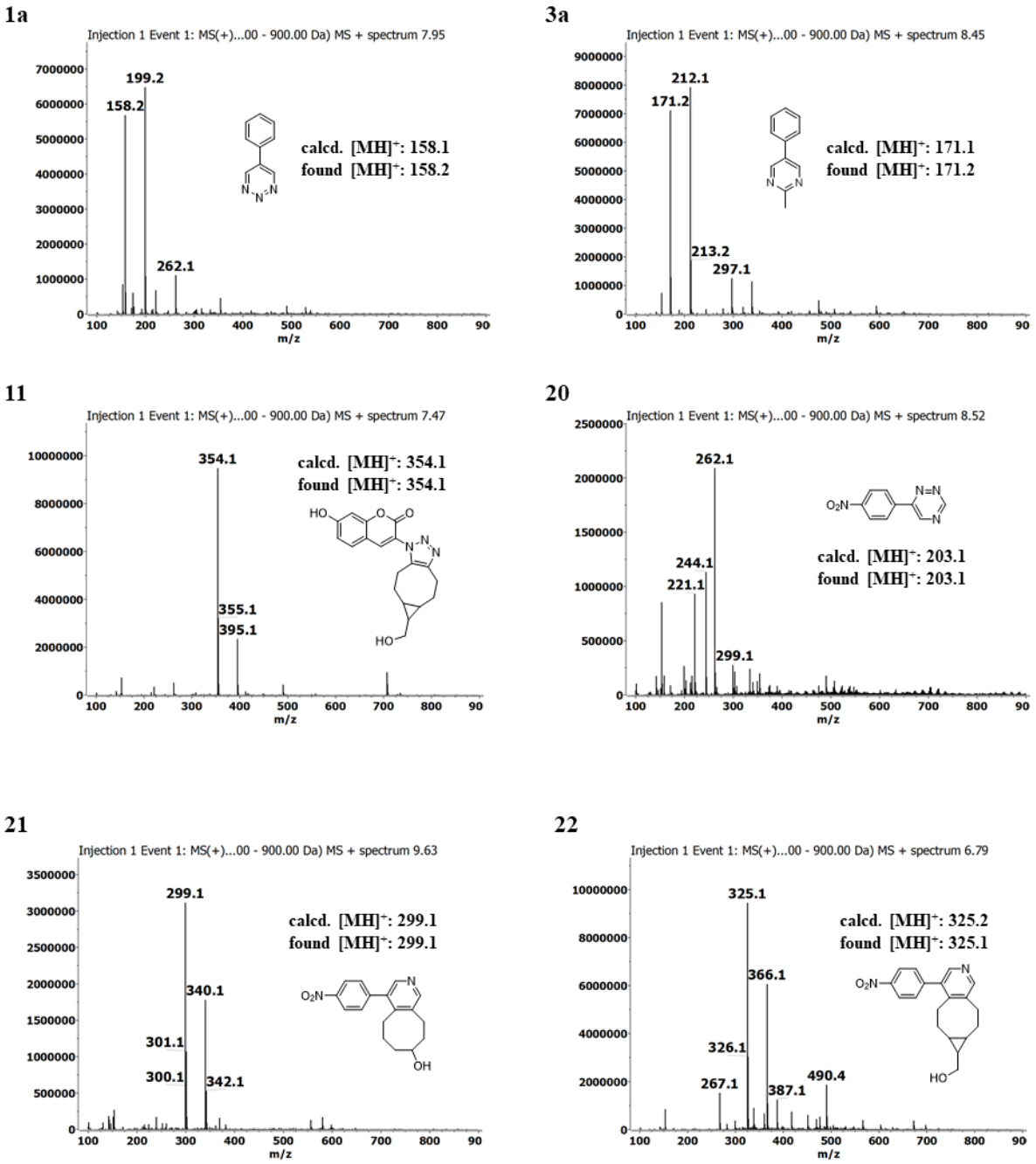


**Figure S12.** HPLC chromatograms and low-resolution mass spectra of the one pot competition reaction between amidine–1,2,3-triazine cycloaddition, TCO–1,2,4-triazine cycloaddition and SPAAC using 6-(4-nitrophenyl)-1,2,4-triazine. The reaction was performed in $CH_3CN$ at room temperature using 2 eq. of TCO, 2 eq. of BCN, 2 eq. of acetamidine and 4 eq. of DBU. Please note that peaks in the MS spectra with a mass of the product + 41 and with a mass of the product + 18 are artefacts arising from the adducts of $CH_3CN$ and $H_2O$ respectively which are used as eluents in the HPLC experiments (solvent A: $H_2O$ + 0.05% HCOOH; solvent B: $CH_3CN$ + 0.05% HCOOH; gradient: 5% B → 95% B in 9 min, then 95% B for 2 min and back to 5% B; column: Luna® C18(2) column (3µm, 100A, 100 × 4.6 mm) at a flow rate of 1 mL/min).

## References


[1] M. Royzen, G. P. Yap, J. M. Fox, *J Am Chem Soc* **2008**, *130*, 3760-3761.

[2] S. J. Siegl, R. Dzijak, A. Vazquez, R. Pohl, M. Vrabel, *Chem Sci* **2017**, *8*, 3593-3598.

[3] D. N. Kamber, Y. Liang, R. J. Blizzard, F. Liu, R. A. Mehl, K. N. Houk, J. A. Prescher, *J Am Chem Soc* **2015**, *137*, 8388-8391.